Multiproxy reconstructions of recent environmental change: understanding the ecological response of shallow lakes within the Selenga River basin, southeast Siberia, to anthropogenic and natural disturbances

Thesis submitted for the degree of

Doctor of Philosophy

UCL

Jennifer Karen Adams

Department of Geography

University College London

January 2018

I, Jennifer Karen Adams, confirm that the work presented in this thesis is my own. Where information has been derived from other sources, I confirm that this has been indicated in the thesis.

Jennifer Adams

Acknowledgements

I would like to thank first and foremost my supervisors, Anson Mackay and Neil Rose, whose guidance, knowledge, and wit were instrumental in forming this thesis. Thank you for always providing me with the inspiration and motivation to push further.

I am very thankful to my fieldwork companions - Sasha, Vania, Svetlana, and Dustin - thank you for always being optimistic, easygoing, and enthusiastic, and for making the weeks spent in Siberia fun and memorable.

Thank you to the people who contributed their knowledge and expertise to the making of this thesis. To Lena Vologina for providing me with the magnetic susceptibility data and physical descriptions for my sediment cores, and for giving me an office to set up shop in, as I whiled away the hours and days in Irkutsk following field seasons. Thank you to César Martins for undertaking the POPs analysis on two of my sediment cores, which provided a novel and insightful contribution to this thesis. Thank you to Gary Tarbuck and Simon Turner for help with water chemistry analyses. To Daria and Eftesum, for your wonderful and invaluable contributions to the Selenga datasets. To Carl Sayer for guidance on many things macrofossil and macrophyte related. Thank you to Sarah Roberts, for showing me the ropes in the pigments lab, and for always being free to help with any pigment, R, or other question I may ever have. Thank you to Miles Irving and Katie Penney for help with creating my maps, and rescuing me from my feeble attempts with ArcGIS.

To the many unforgettable people in the geography lab, microscope room, and ECRC, thank you for the memorable years of advice, conversations, and, at times, much needed distractions, but most importantly, thank you for making this Canadian feel at home in the UK.

Of course, thank you to my family and friends in Canada, for your excitement from the outset, encouragement along the way, and for always making me feel at least a little homesick. Finally, to Wojtek, who in everyway supports me and encourages me to follow my passions. Thank you for always inspiring me to keep going.

This thesis was funded by various funding bodies, without whom much of this work could not have taken place: UCL Overseas Research Scholarship, Natural Sciences and Engineering Research Council of Canada, Canadian Centennial Scholarship, UCL Graduate Fund, NERC, Royal Geographical Society, and Quaternary Research Association.

Abstract

Floodplain delta wetlands are highly productive and critical ecosystems between terrestrial uplands and large, aquatic systems. The largest inland freshwater floodplain delta in the world is the Selenga Delta. The Selenga Delta serves a crucial function between UNESCO World Heritage Site Lake Baikal, and the lake's primary inflow, the Selenga River, and its tributaries. The Selenga River flows approximately 950 km through northern Mongolia and southern Siberia prior to reaching the Selenga Delta, and within the Selenga River basin, numerous anthropogenic activities, including industry, urban settlements, agriculture, and mining, have the potential to cause ecological damage to the Selenga River and its tributaries. The aims of this thesis were to assess the extent of current and historical contamination in Selenga River basin shallow lakes, investigate the primary environmental drivers of variability in ecological structure and function of shallow lakes within the basin, and understand the ecological responses and sensitivity to disturbance. Multiproxy palaeolimnological investigstions of three shallow lakes with the Selenga River basin (two from within the Selenga Delta and one from a more heavily industrialized region), were chosen to undertake a multiproxy palaeolimnological approach to addressing these aims. Investigations on shallow lakes across the Selenga Delta revealed that variability and composition of contemporary ecological communities are determined by degree of connectivity, trophic interactions, and physical landscape parameters such as lake surface area and depth. The greatest period of contamination of shallow lakes (by trace metals and persistent organic pollutants) occurred in the mid-20th century, closely linked with periods of economic development in Russia. However the main drivers of ecological variability since the 19th century have been natural and anthropogenically-induced changes in hydrological regimes, and nutrient pollution, which resulted in significant ecological shifts across multiple trophic levels in shallow lakes.

Contents

List of figures

List of tables

Table 8.5. Summary of main ecological characteristics of dominant diatom species from BRYT02 sediment core.

Chapter 1 Introduction

1.1 Introduction

This study focuses on determining ecological response and sensitivity of shallow lake ecosystems to natural and anthropogenic disturbances since the 19th century. The focus is placed upon one primary location: the Selenga River basin, which provides over 50% of the water supply to Lake Baikal, and comprises approximately 80% of the Lake Baikal watershed (Figure 1.1 and Figure 1.2; Nadmitov *et al*., 2015). Within the Selenga River basin, two localized study regions were chosen. The first, the Selenga Delta, is a floodplain wetland and a designated Ramsar site (Figure 1.2), chosen for this study due to its importance in the Selenga River-Lake Baikal system, controlling the passage of approximately 60% of the water flowing into the UNESCO World Heritage Site, Lake Baikal, and the transport and transformation of related geochemical components (Chalov *et al*., 2016), and for the critical habitat it provides for spawning fish, waterfowl, and species endemic to Lake Baikal (Ramsar, 2015). The second locale is the Lake Gusinoye Region (Figure 1.2), southwest of Lake Baikal and the Selenga Delta, chosen as a more heavily industrialized region within the Selenga River basin (e.g. Naganawa 2012). Shallow lake ecosystems within the Selenga River basin may differ in their sensitivity and ecological response to disturbances, based on the relative importance of different drivers of environmental change. Hydrological regime and climate are the two primary drivers controlling variability in floodplain delta wetlands (Mitsch and Gosselink, 2007), which may override the potential impact of other anthropogenic stressors.

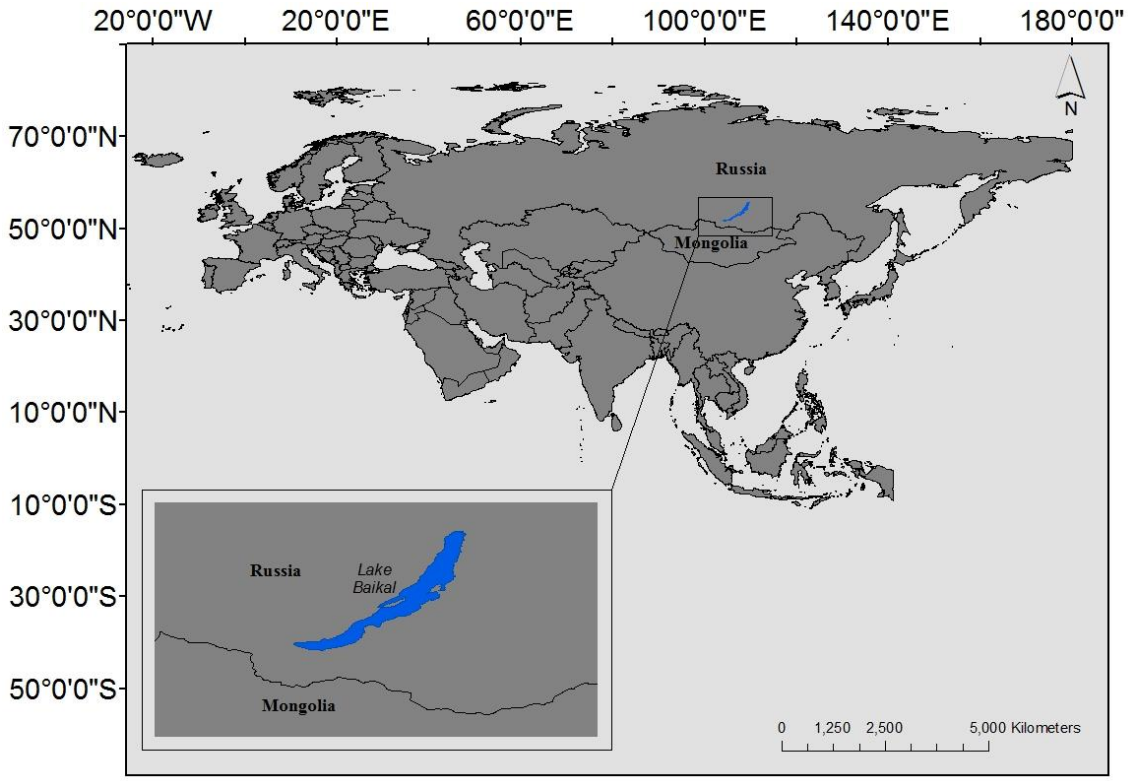

Figure 1.1. Map of Europe and Asia, with the southeast Siberian location of Lake Baikal highlighted. Map created in ArcGIS. Sources: TM_World_Borders, and North American Cartographic Information Society.

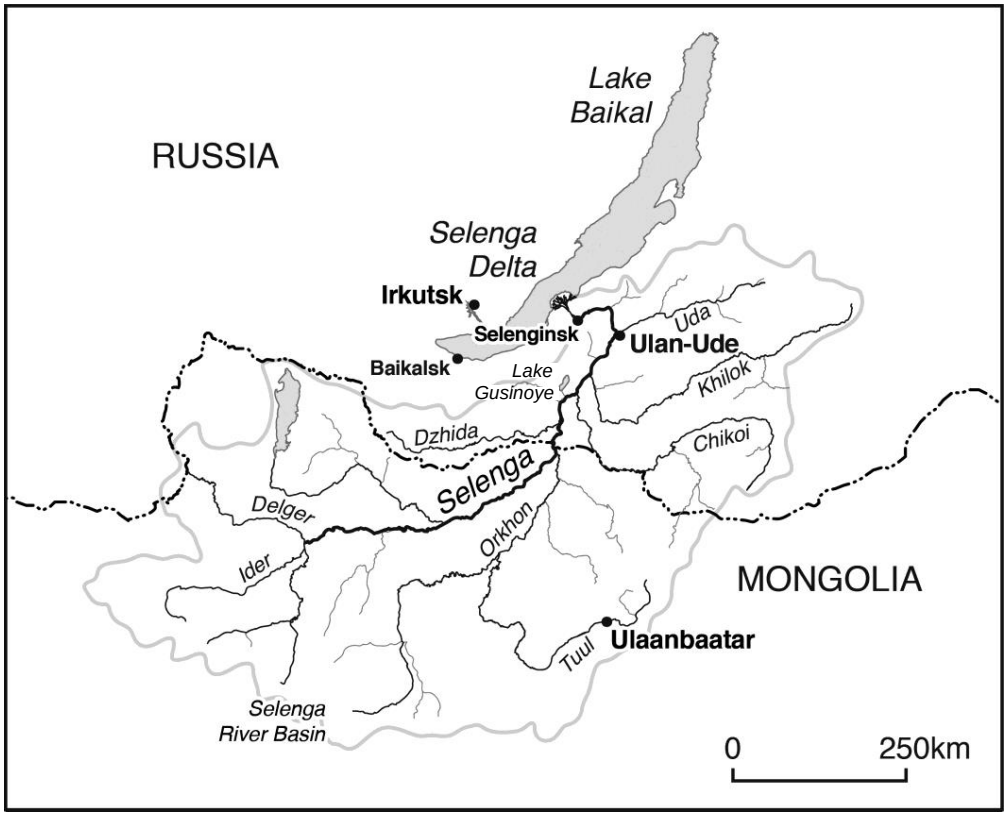

Figure 1.2. Map of the Selenga River basin (grey line delineated) in southeast Siberia and northern Mongolia, with major river tributaries, cities, and Lake Gusinoye labelled. Dashed line indicates the boundary between Mongolia and Russia. Map compiled by M. Irving, UCL.

The shallow lake systems of the Selenga River basin are of critical importance to maintaining the ecosystem health of Lake Baikal, and may act as sentinels for recent environmental change. Little is known about the ecology of these systems, and even less regarding the ecological sensitivity and response to perturbations. Nineteenth and 20th century developments within the Selenga River basin have had the potential to alter ecological structure and function of the shallow lakes, however primary drivers for ecological change, both contemporary and historical, are unknown. Therefore, this study aims to determine how sensitive these shallow lake ecosystems are to natural and anthropogenic disturbances, and determine the key drivers responsible for causing ecological shifts.

1.2 Freshwater Environments

1.2.1 Freshwater wetlands

Freshwater wetlands are some of the most diverse and productive systems on Earth, most prevalent in cool and wet climates, and occurring most extensively in regions where precipitation exceeds evapotranspiration (Mitsch and Gosselink, 2007). Wetlands are often located between a dry, terrestrial system and a permanently flooded, deep, aquatic system, and tend to possess higher productivity than the ecosystems surrounding them. However, peat wetlands have low productivity. Due to the situation of wetlands on the landscape, they are often important transitions between terrestrial and aquatic ecosystems. Nutrient cycling in wetlands differs from terrestrial and aquatic ecosystems on both temporal and spatial scales, and the unique soil characteristics of wetlands augments their biogeochemical role as that of a source, sink, and/or transformer (Mitsch and Gosselink, 2007). The ability of a wetland to perform this role is dependent on wetland type, hydrologic conditions, and length of time the wetland has been subjected to chemical loadings (June *et al*., 2013). Wetlands are frequently coupled to adjacent ecosystems through chemical exchanges that significantly affect both systems. For example, upstream systems are often significant sources to wetlands whereas downstream systems benefit either from the ability of wetlands to retain certain chemicals or from export of organic material.

At the ecosystem level, wetlands provide flood control by accumulating excess water in the wet season and slowly releasing it to the groundwater. Moreover, wetlands protect coastlines from storm surges such as hurricanes and tsunamis, and reduce erosion (Mitsch and Gosselink,

2007). Freshwater wetlands provide vital habitat for both terrestrial and aquatic organisms, and most significantly, provide crucial habitat for waterfowl migration and fish spawning. Wetlands also improve water quality through buffering of runoff and river discharge with the removal or adsorption of elements, chemicals and nutrients, due to the change in water velocity from river to wetland, presence of both anaerobic and aerobic processes in close proximity, high rate of productivity, and high diversity of decomposers. Globally, wetlands are important components of the biogeochemical cycling of carbon, nitrogen, and sulphur. Wetlands are an important global emitter of methane (CH_4), producing approximately 25% of global CH_4 emissions, but have the best capacity of any ecosystem for carbon dioxide (CO_2) sequestration, and 20-30% of all carbon stored in the Earth's soils is in wetlands (MEA, 2005; Mitsch and Gosselink, 2007; Junk *et al*., 2013). Wetland services provided through the view of the human population are mainly related to hunting and fishing; extraction of resources such as timber and mining of peat; food supply including rice paddies that feed approximately half the global population, cranberries in North America, wild rice in China, and animal grazing and hay production in Europe (Mitsch and Gosselink, 2007).

1.2.2 Floodplain delta wetlands

Floodplain freshwater delta wetlands are one major type of wetland ecosystem found throughout the world. The floodplain delta is a wetland-river-upland complex, located where a river forms distributaries as it merges with a large body of water (Mitsch and Gosselink, 2007). Floodplain delta wetlands are characterized by regularly flooded land, a highly connective landscape, and shallow lakes of varying degrees of connectivity (Mitsch and Gosselink, 2007). Climate and hydrology are the primary controls on the properties of the floodplain delta environment. The hydroperiod of a wetland (permanency of flooded lands) can vary from year to year, resulting in fluctuating water levels. Hydroperiod is influenced by physical features of terrain and proximity to other bodies of water. The hydrology of a wetland controls sediment and nutrient (and pollution) transport to/through wetlands; primary productivity is often enhanced by flowing conditions and a pulsing hydroperiod (Mitsch and Gosselink, 2007). Hydrology and geomorphology of a wetland combine to influence the physicochemical properties of wetland, and control nutrient cycling and availability, pH, toxicity (Mitsch and Gosselink, 2007). Macrophyte diversity and presence in Dowd Morass, a Southeastern Australian Ramsar

floodplain wetland, is primarily dictated by the length of the dry period, as deeper and longer inundated areas experienced decreased species richness and foliage protective cover relative to shallow and frequently exposed sites (Raulings *et al*., 2010). Current precipitation regimes of a region combined with annual temperatures control the water quality and quantity of lakes and ponds in the wetlands of Southern Australia. Precipitation and temperature in this region control the occurrence of droughts, as well as the quantity of water runoff and river flow regimes, and ultimately, lake-water levels, habitat structure and species distributions (Nielsen and Brock, 2009).

1.2.3 Shallow lake ecosystems

Shallow lakes are an important component of the floodplain delta wetland, and are generally formed on alluvial fan sediment. Shallow lakes constitue varying proportions of the floodplain wetland environment, but can comprise upwards of 50% of the total delta surface area (Brock *et al*., 2007). Important drivers of ecological variability within shallow lakes of floodplain wetlands would primarily be those of greatest impact to the floodplain wetland itself, including hydrological regime and climate (Mitsch and Gosselink, 2007), both of which can influence biodiversity and ecosystem functioning, and influence ecological structure within the shallow lakes of the system (Ward *et al*., 1999; Bailey and Guimond, 2009). Climatic variability, primarily in terms of changes in precipitation and temperature (observed as changes in rates of evapotranspiration) drive chemistry and nutrient levels within these shallow lakes (Mitsch and Gosselink, 2007). For example, annual precipitation-regime was determined to be an important driver of ecological status of shallow lakes in the Boreal forest zone of Alberta, Canada. Precipitation levels greatly influenced total phosphorus and ion levels through dilution, as well as phytoplankton biomass, and water depth (Cobbaert *et al*., 2014). Presence and diversity of submerged macrophyte communities are often very important factors influencing shallow lake ecological structure and function. Submerged macrophytes provide important habitat, refugia, and food supply for biota (Jeppesen *et al*., 2000; Sondergaard *et al*., 2010; Davidson *et al*., 2011; Davidson *et al*., 2013; Levi *et al.*, 2014), and are heavily involved in nutrient cycling, and sediment stability (Jeppesen *et al*., 1998). Moreover, macrophyte species composition, biomass, and density can influence structure and concentrations of algal and invertebrate communities (Vermaire *et al*., 2013), and macrophyte species richness in shallow lakes has

been positively correlated with species richness at other trophic levels (Korhonen *et al*., 2011). Nutrient concentrations will often influence primary producers in shallow lakes, with increasing nutrient concentrations (i.e. eutrophication) leading to destabilization of submerged macrophyte communities, and rapid and sustained shifts to phytoplankton-dominated (i.e. pelagic) primary producer communities (Scheffer, 1998; Körner, 2002; Zhou *et al*., 2006). Variations in algal primary producer diversity and abundance within the shallow lake community may be influenced by top-down community changes, including changes in grazing pressure and trophic structure, and bottom-up changes in resource availability (e.g. nutrient concentrations) (Leavitt and Hodgson, 2001; Sokal *et al*., 2008; McGowan *et al*., 2011; Bennion *et al*., 2012).

1.3 Ecological response to environmental change in shallow lakes and wetlands

1.3.1 Threats to freshwater environments

Despite the importance of maintaining critically important freshwater wetlands, many of these ecosystems are threatened, or have been completely destroyed due to various human induced pressures. Until the late-20th century, wetland environments were not considered to be distinct ecosystems from the adjacent upland terrestrial ecosystems and downstream deepwater aquatic systems (Junk *et al*., 2013). Prior to the 1970s, common practice was the draining and dredging of wetlands to clear land for agricultural fields, commercial, or residential developments (Mitsch and Gosselink, 2007). As a consequence, millions of hectares of wetlands have been lost (Junk *et al*., 2013). The most threatening forms of environmental degradation to freshwater ecosystems occur due to nutrient and pollution enrichment from urban and agricultural sources, introduction and establishment of non-indigenous species, land development, human modification to hydrological controls from the construction of dams, dykes, or levees, filling for solid-waste disposal, stream channelization and dredging for flood control, and groundwater withdrawal (Mitsch and Gosselink, 2007). Several natural environmental stressors can lead to the loss or degradation of wetland environments, including subsidence, sea-level rise for coastal wetlands, drought, hurricanes and other storms, and erosion (MEA, 2005; Mitsch and Gosselink, 2007).

Climate change will exacerbate many of the natural causes of wetland degradation, as it will lead to the alteration of the hydrologic cycle due to changes in regional precipitation and

temperature (Marin *et al*., 2009; Junk *et al*., 2013). While increased frequency of both drought events and increased precipitation are expected to occur in different regions, widespread increases in temperatures are expected to lead to increased rates of evapotranspiration. Changes in temperature and precipitation regimes will likely be the biggest stressors of freshwater wetlands in the future (Mitsch and Gosselink, 2007). Coastal wetlands can be threatened by sea-level rise, which will occur as a result of contemporary climate change and will be exacerbated by attempts to protect terrestrial upland systems from sea-level change by constructing coastal dykes and levees, which tends to degrade coastal wetlands (Mitsch and Gosselink, 2007).

In 1971, the International Convention on Wetlands was signed in Ramsar, Iran, leading the way for modern-day wetland conservation and management. The Ramsar Convention aims to conserve and use all wetlands wisely through local and national actions and international cooperation, leading to sustainable development of wetlands throughout the world (Ramsar, 2015). Currently there are over 2,200 Ramsar-designated sites, in 169 countries around the world, with over 2.1 million km^2 of protected lands (Ramsar, 2015). Despite the current degree of protection on many globally important wetlands, contemporary degradation of freshwater environments remains an issue, and causes of ecological change in freshwater wetland and shallow lakes environments can be biological, geochemical, or physical (Smol *et al*., 2005; Luoto *et al*., 2014).

1.3.2 Ecological change in freshwater shallow lakes and wetland systems

Hydrological controls are often very important drivers of ecological variability within freshwater wetlands, and changes to the hydrological regime of a system often results in subsequent ecological changes. Water depth is a significant variable influencing algal and macrophyte distributions in shallow wetland lakes, which may be related to changes in hydrological regimes (Moser *et al*., 2000; Michelutti *et al*., 2001a). Moreover, small fluctuations in water levels in shallow lake systems may have a large influence on dilution/evapoconcentration and light penetration (Cobbaert *et al*., 2014). Brock *et al*. (2011) observed that following the construction of the Peace River hydroelectric dam, flood regimes were altered downstream along the Slave River, resulting in increased flood frequency and higher water levels in shallow lakes in the Slave River Delta, altering the macrophyte and

diatom (single-celled algae) communities. Similarly, McGowan *et al*. (2011) observed increases in algal biomass in shallow lakes within the Peace-Athabasca Delta, Canada, through the investigation of photosynthetic pigments, related to increased macrophyte abundance during periods of low-water levels due to hydrological regulation and decreased flood frequency.

Climate-induced changes in the hydrological regime of freshwater delta wetlands are often attributed to changes in precipitation levels, which can result in complete shifts in the ecological structure of the shallow lakes within the delta wetland due to the strong influence of hydrology on these systems (Cobbaert *et al*., 2014). Altered precipitation and temperature regimes in climatically sensitive regions such as the Canadian High Arctic have proven disastrous for shallow lakes, as water bodies that were permanent structures for millennia are now ephemeral wetlands due to increased evaporation/precipitation ratios likely due to climate warming (Smol *et al*., 2005; Smol and Douglas, 2007). The ecological impacts of such a dramatic shift are seen throughout the food-web at these sites, with changes to phytoplankton, zooplankton, and benthic invertebrate communities (Smol and Douglas, 2007). Changes in precipitation and temperature regimes due to predicted climate change in Australia are likely to alter the salinity of wetland ecosystems through increased drought occurrence and declines in water runoff, leading to decreased water levels in lakes and ponds and a shift in community structure (Nielsen and Brock, 2009).

The occurrence of anthropogenic land conversion - either for urbanization or agriculture - has the potential to alter current ecological regimes. Land development in watersheds exerts strong impacts on wetland and shallow lake communities through stressors such as pollution, nutrient loading and sediment discharge (O'Dwyer *et al*., 2013; Kovalenko *et al*., 2014). Low regime-shift thresholds are known to exist for most taxonomic groups across wetland communities, including macrophytes, diatoms, zooplankton, benthic invertebrates, fish and birds. Kovalenko *et al*. (2014) observed that many of these groups experienced the crossing of ecological thresholds at as low as 1-5% land conversion in wetlands of the Laurentian Great Lakes, which are congruent with other sources mentioned therein, although this would be very dependent on land use type and location. Pollution increases such as nutrient enrichment could eventually lead to increased productivity of lakes and ponds and eventual eutrophication of the system (O'Dwyer *et al*., 2013; Luoto *et al*., 2014). Inputs of phosphorus and nitrogen are the

principal causes of eutrophication in freshwater ecosystems, which often stem from agricultural runoff, sewage, or industrial waste, but can also be released from soils during increased periods of sedimentation and erosion (O'Dwyer *et al*., 2013; Hobbs *et al*., 2016).

The potential impact on freshwater environments from the introduction and establishment of nonindigenous species is well documented around the globe (Sala *et al*., 2000; Shea and Chasson, 2002). Introduced species have the potential to become invasive if their presence in the ecosystem has ecological, social, or economical impacts. Further, if the introduced species also provides the means for the introduction of a non-native functional group, the addition of just one nonindigenous species could drastically alter the ecosystem (Folke *et al*., 2004). The introduction of benthivorous fish, such as the Common Carp (*Cyprinus carpio*), has been identified as one of the main causes in decreased biodiversity and water clarity in shallow lakes and ponds (Zambrano *et al*., 2001). The impact that the Common Carp has on ecological regimes in shallow lakes and ponds is higher than that in deeper lakes with lower nutrient levels. In shallow lakes and ponds, carp feed on benthic invertebrates leading to crashes in the benthos population due to overexploitation, as well as increased sediment resuspension in the water column and an increasing turbid state (Zambrano *et al*., 2001). With the introduction of a non-native functional group, not only could the ecosystem be completely altered, but environments may become more favourable or niches may open up for other non-native species (Folke *et al*., 2004). Conversely, the removal of a key species such as a top predator, due to over-exploitation or hunting, from an aquatic food-web has the potential to cause a weakening of the top-down control on a community, leading to the destabilization of an ecosystem (Britten *et al*., 2014).

1.3.3 Ecological regime shifts

The impact of various environmental stressors on the biology, chemistry, and physical properties of freshwater shallow lakes and wetland systems can result in changes in ecological status i.e. a regime shift (Scheffer *et al*., 2001; Andersen *et al*., 2008). Ecological regime shifts are abrupt changes in ecological structure and function, generally on several trophic levels, resulting in a sudden swing to an alternate ecological state (Andersen *et al*., 2008; Randsalu-Wendrup *et al*., 2014). The crossing of critical thresholds within an ecosystem will cause a regime shift and result in an alternative state, with different ecological structures and functions.

Regime shifts may be the result of either internal forcings or external forces such as climate change, invasive species, nutrient or pollution increases (Andersen *et al*., 2008), and the sensitivity of freshwater systems to these stressors will depend on various factors. Ecological change may be nonlinear in response to a stressor at a single site, and not uniform across sites (Scheffer *et al*., 2001; Andersen *et al*., 2008). Ecosystem response to crossing a threshold can either be sudden and sharp, or gradual, depending on the responder variable, with some ecosystems responding in a smooth and continuous manner to a stressor, and other systems sustaining an unchanging ecology until a critical point or threshold is met, upon which the system will respond abruptly (Walker and Meyers, 2004; Folke *et al*., 2004). Change in an environmental driver may result in the ecological shift to an alternative stable state (Scheffer *et al*., 2001). The second ecological state would be as stable as the original, but the ecological community dynamics would differ, as it is a response to different environmental parameters (Beisner *et al*., 2003). It is, therefore, critical to determine how freshwater ecosystems respond to anthropogenic and natural disturbances to the freshwater environment, and how resilient these ecosystems may be to change.

The two most common ecological regime shifts in freshwater shallow lakes are often associated with increased nutrient loadings: the regime shift from aquatic macrophyte dominated community to phytoplankton dominated community (Scheffer, 1997; Jackson, 2003, Folke *et al*., 2004), and/or a shift in the water clarity regime from a clear-water state to a turbid state (De Tezanos Pinto and O'Farrell, 2014; Rendsalu-Wendrup *et al*., 2014). Regime shifts involving switches between dominant primary producers in a lake may be caused by one or more of several sets of disturbances, beyond simply increased nutrient loadings. Changes from submerged macrophyte dominance to free-floating plant dominance may be caused by increased nutrients in the system, as well as increased water levels, increased temperatures, and decreased invertebrate predation on free-floating plants (De Tezanos Pinto and O'Farrell, 2014). Further, regime shifts from free-floating plant dominance to phytoplankton dominance may be caused by decreased nutrients, decreased water levels, increased wind and flow, decreased temperatures, and increased invertebrate predation on macrophytes. In contrast, regime shifts from phytoplankton dominance to submerged macrophyte dominance may be caused by decreased nutrients, increased water levels, decreased turbidity, decreased salinity

when concurrent with high nutrient levels, or removal of planktivorous fish due to feedbacks (De Tezanos Pinto and O'Farrell, 2014). Regime shift from free-floating plants (*Lemna* and *Pistia*) to phytoplankton (cyanobacteria) due to drought and subsequent decrease in water level, have been shown to lead to subsequent changes in the lake environment, including increasing pH, increased suspended solids, and increase in humic acids (O'Farrell *et al*., 2011). Pond mesocosm experiments have shown that increased temperatures and increased nitrogen have promoted free-floating plant growth (e.g. *Lemna*) but not excluded submerged plants (e.g. *Potamogeton*, etc) (Feuchtmayr *et al*., 2009). Clear-water regimes of shallow lakes are often perpetuated due to the presence of submerged macrophytes stabilizing sediments and reducing phosphorus cycling to phytoplankton (Scheffer, 1997).

1.3.4 Ecological resilience to abrupt environmental shifts

The resilience of an ecological system is a measure of how much disturbance or stressor is required in order to change its structure, function, feedbacks, and processes, or to shift from one ecological regime to an alternate regime (Angeler *et al*., 2013a). The magnitude of the external force and the internal resiliency of the ecosystem combine to determine regime shifts. As resilience declines, the ecosystem may become more vulnerable, with smaller and fewer external stressors required to create a regime shift (Folke *et al*., 2004). It has been observed that some ecological systems are more sensitive than others, leading to unequal shifts in similar types of environments. It is this measure of resilience that can inform as to whether a community or ecosystem would be stable enough to withstand external forces (disturbances) placed upon it.

The resilience of an ecosystem to regime shifts caused by environmental change can be reduced through the following anthropogenically-induced means: reducing biological diversity through either removing response diversity or functional diversity; impacting ecosystems with pollution or climate change; or altering a disturbance regime to which it is biologically adapted (Folke *et al*., 2004). The internal resiliency of a wetland can be related to its hydrology. Rivers and wetlands with large catchments and higher levels of connectivity are more resilient to hydrological changes (Mitsch and Gosselink, 2007). However, external disturbances which lead to a rearrangement of floodplain habitats, such as increased flood and drought events with

climate change, or altering of wet and dry cycles within a wetland, will likely decrease internal resiliency and stability of the ecosystem (Angeler *et al*., 2013a; Junk *et al*., 2013).

Over time, humans may reduce ecosystem stability in the face of disturbances and stressors, through changes in trophic structure/grazer community (top-down) or resource availability (bottom-up), which often result in trophic cascades in response to external stressors, which may lead to regime shifts. As a result, an ecosystem will suffer a loss of internal stability, and become much more vulnerable to external stressors (Diaz and Cabido, 2001; Folke *et al*., 2004; Britten *et al*., 2014). Biological diversity of an ecosystem is an important factor related to the concept of ecosystem resiliency to regime shifts, and biodiversity has been found to positively correlate with resilience (Folke *et al*., 2004; Downing *et al*., 2012; Angeler *et al*., 2013a). The resiliency of a system to regime shifts will also increase when biodiversity at larger spatial scales is increased (Folke *et al*., 2004).

In the face of environmental change, the distribution of functional groups is relevant for understanding resilience. Functional-group diversity is important for maintaining ecosystem functioning and stability, and the loss or addition (possibly in the form of an invasive species) of a functional-group can dramatically alter the ecosystem (Peterson *et al*., 1998; Folke *et al*., 2004; Angeler *et al*., 2013b; Angeler *et al*., 2013a). Furthermore, functional-response diversity of species within a single functional-group will enhance ecological resilience (Peterson *et al*., 1998; Folke *et al*., 2004; Angeler *et al*., 2013b; Angeler *et al*., 2013a). The response across different species within a single functional-group will vary depending on species tolerances and optima. Maintaining a higher number of functionally redundant species increases the ecosystem's ability to sustain its current state in the face of environmental change, and as one species is impacted by the change another species continues to perform as normal, as the responses between these species differ in the face of the same environmental stressor. It is only if these functionally redundant species have differing functional responses that they increase the ecosystem's resilience to regime shifts. If they are redundant in both functional-group and response, then they add little to the resilience of the system (Folke *et al*., 2004). Both functional-group diversity and functional-response diversity are critical ecosystem components related to ecosystem functioning, and both characteristics affect the trophic complexity of an ecosystem (Chapin *et al*., 1997; Duffy *et al*., 2007; Baskett *et al*., 2014).

Disturbances and environmental stressors that lead to rapid shifts in species community assemblages could be the mechanism behind many ecological regime shifts. Rapid shifts in community assemblages may occur if many of the existing species are unable to tolerate the geochemical, physical, or biological change brought about by the environmental stressor. This may cause a destabilization of the community and a reduction in the ecological resilience of the system, leaving it more vulnerable to external forcings (Randsalu-Wendrop *et al*., 2014). Increased ecological stability is attained when communities contain a few strong and many weak interactions (McCann *et al*., 1998). Moreover, stability and strength in top-down interactions have proven to stabilize multiple prey populations, thereby creating greater resiliency for the community dynamics as a whole (Rooney *et al*., 2006).

1.3.5 Assessing ecological response to disturbance through palaeolimnology

Long-term ecological responses to natural and anthropogenic disturbances are difficult to demonstrate using contemporary ecological studies, particularly to those disturbances which occur on longer timescales, such as eutrophication and climate change. Further, shallow lakes in remote regions lack long-term monitoring data in most respects. In the absence of long-term monitoring data palaeolimnology can be used to detect past ecological change and response to anthropogenic stressors in these environments (Smol *et al*., 2005; Davidson *et al*., 2011; McGowan *et al*., 2011; Junk *et al*., 2013). Changes in microfossil algae (diatoms) community composition are often associated with declines in submerged macrophyte abundance, observed as the loss of macrophyte-associated diatom species (Vermaire *et al*., 2013; Randsalu-Wendrop *et al*., 2014). Davidson *et al*. (2011) observed changes in plant macrofossil and cladoceran sub-fossil assemblages in sediment cores congruent with long-term shifts in primary production of a lake from benthic, submerged macrophyte dominance to phytoplankton dominance. Palaeolimnological changes associated with increasing nutrients can also be seen through the food-web from remains within sediment cores. For example, concurrent increases in the remains of both ostracod and *Daphnia* abundances in freshwater lakes from Svalbard were most likely related to increased planktonic algal productivity, and likely indicate that a nutrient enrichment threshold had been crossed (Luoto *et al*., 2014).

Further studies utilizing palaeolimnological evidence have attempted to estimate biological diversity and richness associated with changes in ecological functioning in shallow lakes.

Palaeolimnological records from eutrophic shallow lakes in the UK and Australia demonstrated that the loss of a dominant zooplanktivore fish coincided with a loss of diversity in all trophic levels, while changes in the biodiversity of diatom communities and declines in species richness of benthic cladocerans were linked to changes in macrophyte species richness and abundance (Davidson *et al*., 2013). The decline in macrophyte abundance indicated a change in ecological functioning (i.e. trophic state) to a eutrophic state, which was apparent at several trophic levels throughout the food-web (Davidson *et al*., 2013).

Changes in local land-use activities leading to increases in urbanization or industrialization can result in sources of pollution and nutrients to freshwater ecosystems. Davis *et al*. (2006) examined the sensitivity of biological communities of a freshwater lake in New Hampshire to recent changes in land use and increases in air pollution. Changes in diatom communities indicate a change in trophic state during the mid-20th century, as well as increased salinity, while increases in trace metal fluxes, both atmospheric and hydrospheric, were related to extensive shifts in the phytoplankton community. Further, Pla *et al*. (2009) examined changes in diatom and chrysophyte community assemblages from a remote Scottish loch spanning pre-industrial to contemporary time periods using lake sediment cores. Recorded changes in the benthic (diatom) community were attributed to atmospheric deposition only, possibly nitrogen enrichment, while changes in the planktonic community (chrysophytes) were determined to be a combination of atmospheric contamination and climate change.

Studies from northern, large freshwater floodplain deltas indicate ecological changes at several trophic levels in response to changes in hydrology and climate in the shallow lake ecosystems therein. Diatom community compostion in a lake from the Mackenzie River Delta, located in Arctic Canada, was found to be related to degree of river connectivity with the shallow lake, and palaeolimnological investigations revealed that temporal shifts in diatom community composition indicated fluctuations in degree of river influence (Michelutti *et al*., 2001a). The diatom community shifts were directly caused by gradients in macrophyte communities due to changing river-shallow lake connectivity. Palaeolimnological investigations carried out by Michelutti *et al*. (2001a) indicated that diatom community changes in delta lakes were sensitive to hydrological changes in the Mackenzie River, and that diatoms provide a good indication of long-term hydrological variation. Further, Wolfe *et al*. (2005) observed through

palaeolimnological analyses of the Peace-Athabasca Delta, a Ramsar-designated site in northern Canada, that changes to diatom and plant macrofossil remains in shallow lake sediment cores were indicative of natural variability in hydrology and hydrological connectivity in the delta floodplain wetland. Connectivity-related gradients of water clarity and chemistry influenced macrophyte communities, the variations in diversity and cover of which then had indirect implications for diatom communities (Wolfe *et al*., 2005).

Climate change in the High Arctic has been observed through palaeolimnological records to have significantly impacted the ecology of shallow lakes during the past 100-200 years (Quinlan *et al*., 2005; Smol *et al*., 2005; Smol and Douglas, 2007). Changes to climate in this region have greatly impacted the hydrology of shallow lake systems through changes in precipitation, evaporation rates and length of ice-free season, as well as the thermal stratification regimes of larger lakes (Douglas and Smol, 1994). Changes in diatom and cladoceran remains in lake sediment records include the appearance of genera never before seen at high abundances in both shallow and deeper Arctic lakes. Increased diatom and cladoceran taxa indicative of longer ice-free seasons in shallow lakes is likely due to the increased habitat differentiation and complexity in the littoral zone (Antoniades *et al*., 2005; Keatley *et al*., 2006). Moreover, larger lakes have recorded the appearance and increased abundance of planktonic diatom species, indicating increased strength and stability of thermal stratification regimes (Sovari *et al*., 2002; Rühland *et al*., 2003). These changes are unprecedented for the Holocene, and it is clear that ecological thresholds have been crossed, with these Arctic lakes and ponds currently entering new ecological regimes.

1.3.6 Multi-proxy approaches in palaeolimnology

Whole-community-based contemporary sampling approaches and multi-proxy studies in palaeolimnology are the most appropriate to determine temporal changes in ecological structure and functioning of a lake (Birks and Birks, 2006; Davidson *et al*., 2010). The complex biotic interactions that exist in freshwater environments make the study of change at multiple trophic levels an important part of undertanding whole-community responses to environmental stressors (Birks and Briks, 2006; Smol, 2008). An advantage to the multi-proxy approach is that the method addresses the fact that different biological groups (i.e. proxies) reflect different ecological scales, and have different environmental tolerances. Combining a variety of

ecological components into the palaeolimnological study will exploit the strengths and identify weaknesses of various biological analyses (Birks and Birks, 2006). Multi-proxy approaches can utilize contemporary ecological information and ecological indicators to address pertinent ecological questions and draw insight into past ecological processes, changes in ecological structure and functioning, and ecological responses to past disturbances (Birks and Birks, 2006). Multi-proxy palaeolimnological approaches can then be used to address potential causes of ecosystem change in the past, and assess ecosystem stability and levels of ecological resilience.

A variety of ecological questions can be addressed utilizing multi-proxy approaches in palaeolimnology, including those regarding ecological structure and functioning, and biotic responses to environmental disturbances. Multi-proxy approaches utilizing remains of diatoms, zooplankton, invertebrates, and macrophytes can reveal insights into the ecological response at multiple trophic levels to known historical increases in nutrient concentrations (e.g Taylor *et al*., 2006; Bennion *et al*. 2015; Ventela *et al*., 2016). Temporally similar shifts in functional groups (from benthic and macrophyte-associated communities to planktonic communities) are often observed across multiple trophic levels, indicating a whole-ecosystem response to increasing nutrients over time. Toxicity responses can also be better understood through the assessment of multiple trophic levels. Thienpont *et al*. (2016) assessed the long-term ecological responses in algal and zooplankton groups to lake contamination from a large gold mine in northern Canada. Synchronous changes in diatoms and cladocera were observed, with impacts noted across benthic and pelagic communities in response to extreme metal contamination (mercury, antimony, lead, and arsenic). Hydrological changes in wetland and shallow lake ecosystems may be deduced through investigations at multiple trophic levels. Changes to hydrological regime will likely result in fluctuations in water levels, which can have varying impacts on the biological community (Levi *et al*., 2016). Fluctuating water levels may directly impact macrophyte communities through changes in habitat availability, as pelagic habitats and/or littoral habitats form or disappear. Changes in depth will affect water clarity, nutrient concentrations, and sediment characteristics. Complex environmental stressors, which may incite several direct and indirect physical and biological responses, require a multi-level palaeolimnological approach to properly assess causes and response to change (Birks and

Birks, 2006). Assessment of changes in food-web interactions, and top-down and bottom-up trophic responses to environmental stressors can be carried out using multi-proxy palaeolimnological methods, and provide a long-term approach to assessing key community dynamics that are difficult to assess through contemporary data alone (Jeppesen *et al*., 2003; Vermaire *et al*., 2013). Utilizing a multi-proxy approach in shallow ecosystems which are subject to multiple stressors can be helpful in disentangling the ecological impacts and responses to individual or combined stress effects, including assessing the response of diatoms, cladoceran, and chironomids to climate change and pollution (e.g. Summers *et al*., 2017), diatoms, grain size, and geochemistry to nutrients and climate (e.g. Dong *et al*., 2011), and pigments and geochemistry to nutrient increases and hydrological regime modification (e.g. Engstrom *et al*., 2006).

1.4 Siberian freshwater ecosystems

Much of the landscape in Russia favours shallow lake and wetland development, as ~2/3 of Russia's land area is comprised of low-lying, flat lands with average heights < 600 metres (Robarts *et al*., 2013). Historically, wetland and interconnected shallow lakes in Russia were considered wastelands, and the practice of drainage for land conversion to cropland began in the late-17th century (Hartig *et al*., 1997). Much of the environmental work that has been carried out in shallow Siberian lakes to date pertains to pollen investigations of terrestrial ecosystem and climatic change (e.g. Niemeyer *et al*., 2017), geochemical and geomorphological analysis of thermokarst lakes (e.g. Fedorov *et al*., 2014; Manasypov *et al*., 2015), short-term monitoring of trace metal transport and contamination (e.g. Khazheeva and Tulokhonov, 2007) or Holocene investigations of climate change (e.g. Mackay et al. 2013; Nazarova *et al*., 2013). However, several studies have investigated ecological variability across Siberian shallow lakes, and ecological responses on shorter time scales. Several studies in northern Siberia near the Lena Delta, sought to investigate the various drivers of diatom variations across differing ecozones. Laing *et al*. (1999) found that diatom assemblages from tundra, forest-tundra, and boreal forest ecozones produced differing assemblage compositions primarily related to physicochemical characteristics, including conductivity, temperature, depth, and ion concentrations. Further, benthic taxa were dominant in shallow, northern (tundra) sites, while southern (boreal forest) sites were dominated by planktonic taxa (Laing and Smol, 2000). Laing

and Smol (2000) observed regional trends in diatom assemblages were most likely influenced by local factors, including proximity to anthropogenic disturbances; local water chemistry was primary in determining diatom assemblages, and overrode influence of climate gradients. Westover *et al*. (2006) noted that diatom diversity increased in shallow lakes at lower elevation, forested catchments, relative to higher elevation, alpine lakes. Lake depth, ionic composition, and nutrients were also primary drivers of spatial variability in chironomid assemblages across treeline shallow lakes in northern Siberia (Porinchu and Cwynar, 2000), while climate-driven changes in catchment hydrology have induced recent chironomid assemblage changes in several lakes in northern Siberia (Self *et al*., 2015). The impact of anthropogenic disturbances on ecological components of shallow Siberian lakes have been little investigated. Benthic fragilarioid diatoms dominate many unimpacted shallow lakes in Siberia (Laing *et al*., 1999; Laing and Smol, 2000; Westover *et al*., 2006; Mackay et al. 2012). Michelutti *et al*. (2001b) observed relatively little change in diatom communities in response to metal smelting in northern Siberia. These findings were dissimilar to other highly impacted smelting areas (e.g. Northern Ontario, Canada), and the authors concluded that the alkaline nature of these Siberian lakes possibly provided protection from high metal occurrences, thereby decreasing the sensitivity of these sites to metal pollution.

1.4.1 Selenga River Basin

Lake Baikal is a UNESCO World Heritage Site located in southeastern Siberia (Figure 1.1). It is the world's oldest and deepest lake, and contains approximately 20% of the global supply of surface freshwater resources (Blinnikov, 2010). These unique properties of Lake Baikal contribute to the high levels of biodiversity and endemism of species in the lake. The Selenga River is the major source of freshwater to Lake Baikal, contributing over 60% of annual water inflow (Scholz and Hutchinson, 2000). The Selenga River basin covers an area of almost 450,000 km^2 in Siberia and Mongolia and comprises over 80% of the Lake Baikal Watershed (Figure 1.2; Nadmitov *et al*., 2015). The Selenga River flows approximately 950 km from the head waters in Mongolia at the confluence of the Ider and Delger Rivers before it reaches the Selenga Delta and Lake Baikal in southeast Siberia. It receives the Orkhon River just south of the Russia-Mongolia border. The Tuul River, which flows through Ulaanbaatar, joins the Orkhon River in Mongolia. Once in Siberia, the Selenga River flows through the city Ulan-Ude, the

capital of Buryatia, and receives the Dzhida, Chikoi, Khilok, and Uda Rivers, respectively, as it flows west towards Lake Baikal. The Selenga River carries approximately 30 km^3 of water and over 3.5 million tonnes of sediment per year to Lake Baikal (Plyusnin *et al*., 2008).

The Selenga Delta is located at 52°14'N and 106°30'E in the continental subarctic of southeast Siberia (Figure 1.2). The Selenga Delta is located in a region characterized by ultracontinental climate, with dry, intensely cold winters and short, mild summers. The region is subjected to westerly and northwesterly winds all year-round (Plyusnin *et al*., 2008). The Selenga Delta is the largest inland freshwater floodplain delta in the world (Logachev, 2003; Chalov *et al*., 2014), and consists of the fan of land containing shallow lakes, ponds, and channels which drain the Selenga River into the area between the southern and central basins of Lake Baikal. The Selenga Delta is tectonic in origin and is one of the oldest, extant river deltas in the world, with the oldest portions thought to have formed over two to three million years ago, due to tectonic activity (Scholz and Hutchinson, 2000). The Selenga Delta is a designated Ramsar wetland, providing important habitat for many species endemic to Lake Baikal, including important spawning grounds for fish, and an important habitat for migratory and breeding birds (Ramsar, 2015). The Selenga Delta is flooded by two main branches, transporting water from the Selenga River to Lake Baikal. The Lobanovskaya branch floods the far northeast margin of the Selenga Delta, and carries approximately 30%-40% of the summer flow through the Selenga Delta, and 10% of the winter flow from the Selenga River and entering into Proval Bay in Lake Baikal (Sinyukovich *et al*., 2004; Khazheeva and Tulokhonov, 2007). The Levoberezhnaya branch floods the southwest side of the delta, and is the primary branch delivering water from the Selenga River to Lake Baikal, entering the lake in Cherkalov Bay, carrying approximately 50-55% of the summer flow through the Selenga Delta, and 90% of the winter flow (*ibid.*).

Permafrost continuity, a combination of mountain, forest and steppe ecozones, and agricultural practices in the Selenga River basin impact the soil characteristics within the region. Most of the soils in the basin are comprised of cryosols, as snow cover in the winter is very thin, and temperatures low, so much of the ground freezes (FAO 2001). Soils of the Selenga River basin are derived from parent materials of eluvial, deluvial, alluvial, colluvial, lacustrine, and Aeolian deposits, with textures ranging from sands to heavy loams (Tsybikdorzhiev *et al*.,

2012). Bedrock underlying the Selenga River basin in the vicinity of the Selenga Delta is Paleozoic granite, originating in the Cambrian-Early Ordovician Periods. The Gusinoozersk region is also underlain by granitic bedrock, but of the Proterozoic-Paleozoic Eras, originating between the Vendian and the Early Ordovician Periods (Heim *et al*., 2007). Further, there are areas of Cretaceous bedrock intrusion south of the Selenga Delta in the Gusinoozersk region. Quaternary sediments have been deposited on top of the bedrock, within the immediate vicinity of the Selenga Delta, Gusinoozersk, and along the path of the Selenga River (Galazi, 1993).

1.4.2 Distrubances within the Selenga River basin since the 19th century

1.4.2.1 Natural disturbance events

Figure 1.3 provides a summary of the major disturbance events in the Selenga River basin since the early-19th century. The Tsagan earthquake of 1862 was the strongest earthquake recorded in Southern Siberia (with a magnitude of 7.5) and was integral in forming the contemporary structure of the right bank of the Selenga Delta and Proval Bay of Lake Baikal (Vologina *et al*., 2010). The epicentre of the earthquake is still a point of contention, as studies produced at different times place it at different points in the area (Vologina *et al*., 2010). However, estimates place the epicentre in the northeast of Proval Bay (Golenetskii, 1996). The Tsagan earthquake resulted in substantial subsidence and flooding of the northeast corner of the Selenga Delta, with a total area of approximately 200 km^2 suffering from flooding and subsidence, and total subsidence depths of up to 9 m (Orlov, 1872). A massive flood event that occurred in the Transbaikalian region of Siberia in 1897 was caused by a catastrophic increase in precipitation in Mongolia in the summer of 1897, and resulted in the flooding of many towns and villages along the Selenga River, causing an increase in the river height by 4 metres within one day in August 1897 (Kadetova and Radziminovich, 2014). Shifts in delta morphology in the late-20th and early-21st centuries have caused a shift in discharge from the southwest to the northeast branches of the Delta (Ilyicheva, 2008; Chalov *et al*., 2016). As the proportion of river transported through each branch of the Delta may have potential implications for sediment and chemical transport, uncertainties remain as to how the changing proportions of river water flow and changes in connectivity, along with increasing anthropogenic presence and complex natural events may have influenced the shallow lakes of the Selenga Delta during the 19th, 20th, and 21st centuries.

1.4.2.2 Anthropogenic disturbance events

Earliest historical records of anthropogenic disturbances in the Selenga River basin indicate that mining began in both the Mongolian and Siberian portions of the Selenga River basin in the early-19th century (Robinson and Anisova, 2004) (Figure 1.3). Coal deposits in the region have been exploited since the 19th century, beginning with the development of the Trans-Siberian Railroad (Robinson and Anisova, 2004). The decades following the end of World War II (WWII) were characterized by rapid increases in industrial development and population growth, and the 1950s were characterized as a decade of intense economic growth and industrial expansion in the USSR, and industrial and mining growth in the Selenga River basin (Khanin, 2003; Pisarsky *et al.,* 2005). Mining activities peaked in southeast Russia during the height of Soviet power in the mid-20th century, although mining of gold, tungsten, and molybdenum began prior to the mid-19th century (Robinson and Anisova, 2004). Throughout the 20th century, mining of lithium, gold, tungsten, lead, zinc, molybdenum, and strontium has continuously occurred along tributaries of the Selenga River (Figure 1.4). In the 1940s, an open cut coal mine was established near the town of Gusinoozersk, to the south of the Selenga Delta, and tailings from the coal mine entered the Selenga River via a small tributary (Pisarsky *et al*., 2005). Population increase in the 1960s lead to the development of the Gusinoozersk State Regional Power Plant (SRPP), a coal-fired power plant on the shores of Lake Gusinoye, near Gusinoozersk. The majority of mining and mineral excavation in the Mongolian region of the Selenga River Watershed began much later than the Russian activities, and prior to 1970 the single mineral extracted from this region was coal (Robinson and Anisova, 2004). Mongolian mining operations underwent rapid development in the late-20th century, particularly with respect to gold mining operations. Long-term monitoring averages (1998-2003) of dissolved and total trace metal concentrations in surface water and flow data from tributaries along the Selenga River and within the Selenga Delta between Mongolian gold mines and Lake Baikal (approximately 600 km of river) indicate that the Tuul River is the most polluted river in Mongolia, which flows directly into the Selenga River (Thorslund *et al*., 2012). Furthermore, trace metal concentrations down the Selenga River are highest in the summer, with concentrations of lead (Pb) and iron (Fe) increasing with closer proximity to the Selenga River Delta (Thorslund *et al*., 2012).

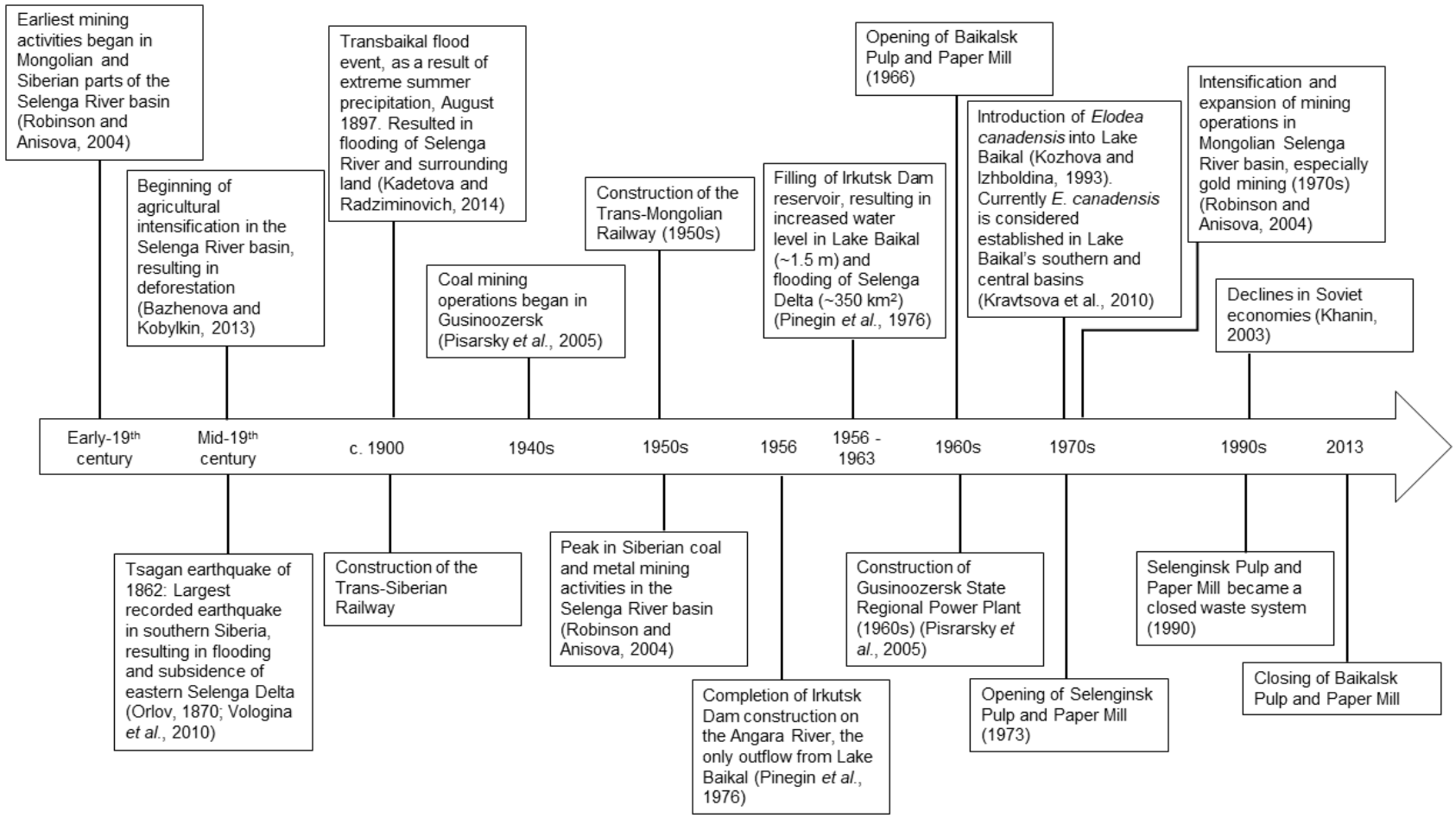

Figure 1.3. Timeline of natural and anthropogenic disturbance events recorded for the Selenga River basin since the early 19th century. Figure compiled by J.Adams.

Assessment of the contemporary geochemical impacts of mining in the Selenga River basin conclude that the Selenga River Delta may be one of the world's most impacted areas with regards to trace metal loads, but is critically under studied outside of the Russian literature (Thorslund *et al*., 2012).

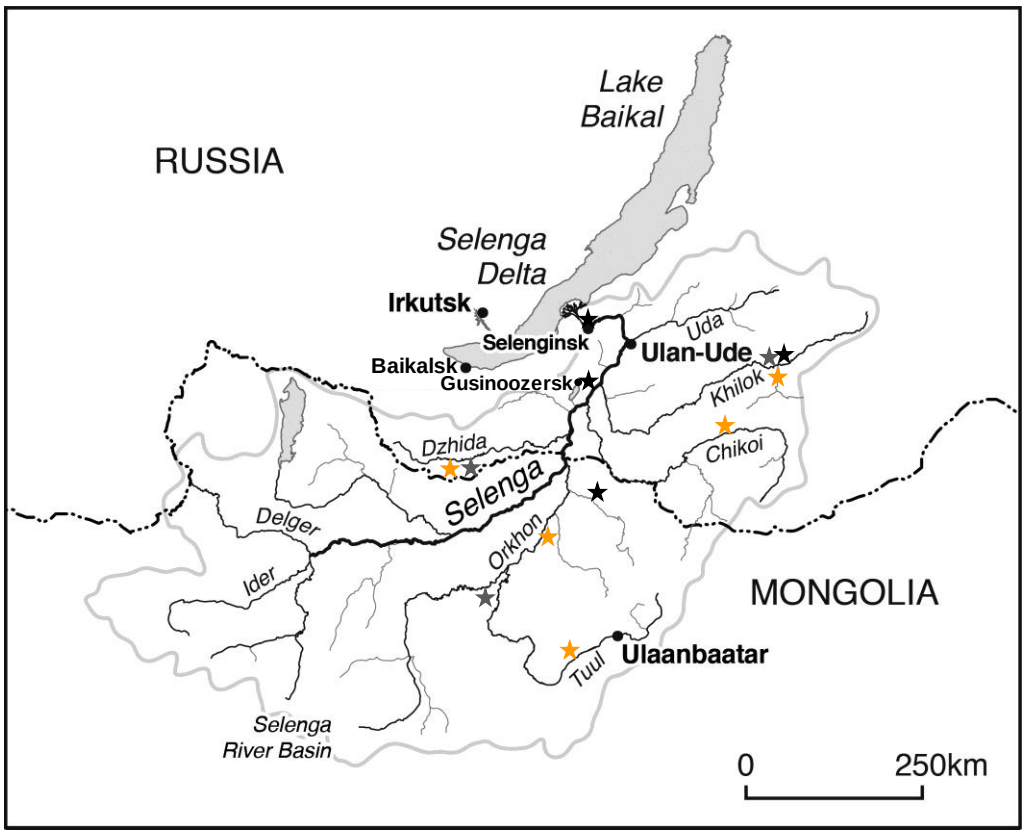

Figure 1.4. Map of the Selenga River basin, indicating sites of major mining activities. Black stars indicate coal mines, grey stars indicate general metal mines, and yellow stars indicate gold mines. Sources: Robinson and Anisova, 2004; Pisarsky *et al*., 2005.

Land-use conversion for agricultural expansion and intensification began in the Selenga River basin in the early-19th century as a response to increased populations in the region. Agricultural expansion was the primary cause of massive deforestation events and land conversion from boreal forest-steppe to croplands in the 19th century. The land conversions resulted in increases in erosion and transport of sediment directly into the Selenga River (Bazhenova and Kobylkin, 2013). Further agricultural expansion in the Selenga River basin occurred intensively post-WWII, and between the mid-1950s and mid-1970s, the total arable lands in southeast Siberia increased by almost 60% (Figure 1.5; Bazhenova and Kobylkin, 2013). Intensive increases in sheep population continued until c. 1990, which contributed to the

increase in nutrient flux to soils, and increased sediment erosion within the Selenga River basin (Figure 1.5; Bazhenova and Kobylkin, 2013).

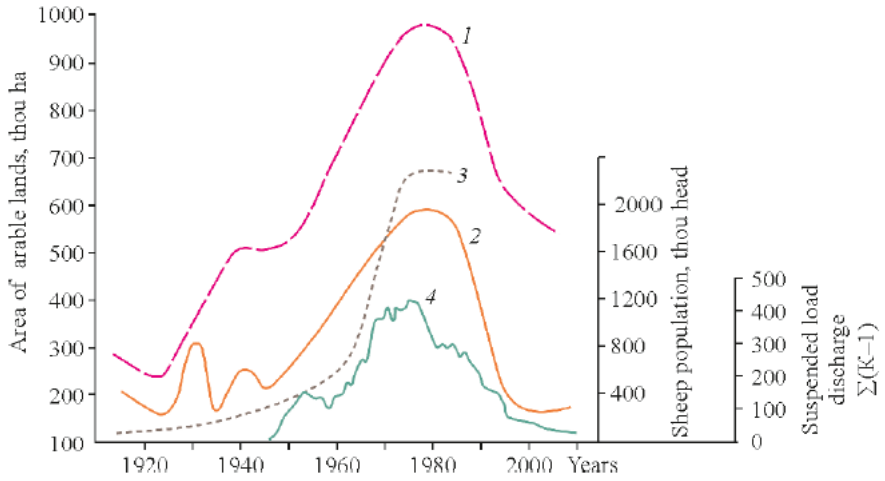

Figure 1.5. Increases in arable lands (1), livestock populations (as sheep only; 2), changes in area of eroded arable lands (3), and suspended load discharge of the Selenga River (4), through the 20th century in the Selenga River basin. (Source: Bazhenova and Kobylkin, 2013).

Population increases in larger settlements, including Irkutsk (the largest city in the region, that sits on Angara outflow current population ≈ 590,000), Ulan-Ude (current population ≈ 405,000), and Gusinoozersk (current population ≈ 24,500) (both in the Selenga basin), led to the need for increased transportation development, industry, increased utility demand, and increased wastewater and sewage production. Increased international railway developments continued into the 1950s with the construction of the Trans-Mongolian Railway (Pisarsky *et al*., 2005). Local industrial activities along the Selenga River and in the river basin are sources of organic contaminants and sources of fossil fuel combustion, including facilities along the Selenga River in Selenginsk and Ulan-Ude, and around Lake Baikal in Baikalsk. Local sources of polychlorinated biphenyls (PCBs) through the latter 20th century around the Lake Baikal region, including the pulp and paper mill in Selenginsk, upstream of the Selenga Delta, which opened in 1973 and until becoming a closed system in 1990, was an open system, leaching chlorinated by-products into the surrounding environment (Kannan *et al.,* 1998). Increasing populations in southeast Siberia have also led to changes in utility demands. The construction of the Irkutsk Hydroelectric Dam along the Angara River - the only outflow from Lake Baikal – was completed in the mid-1950s. Filling of the associated reservoir began in 1956 and within seven years the reservoir was full and Lake Baikal had risen by ~1.5 m depth (Bolgov *et al*.,

2017). Subsequently, low-lying shorelines and environments surrounding Lake Baikal were submerged and flooded. The Selenga Delta is approximately 2 m elevation above Lake Baikal, and more than 350 km^2 of the Selenga River Delta was impacted by this flooding (Pinegin *et al*., 1976).

The invasive Canadian waterweed, *Elodea canadensis*, was introduced to Lake Baikal in the 1970s and quickly spread throughout the littoral zone of the lake (Kozhova and Izhboldina, 1993). As *E. canadensis* becomes established within lakes, it alters the habitat type as it typically grows in dense patches, dominating other macrophytes. The result is that *E. canadensis* will likely crowd out native fish species, and creates a unique community of invertebrates, ultimately altering the entire ecological community and possibly altering the biology and geochemistry of the system (Kravtsova *et al*., 2010). Presently, *E. canadensis* is considered established in the southern and central basins of Lake Baikal (Kravtsova *et al*., 2010).

Southeast Siberia has experienced climate warming and increased human impacts during the 20th century, with annual mean air temperature increase of approximately 1.2°C over the past century (Shimaraev *et al*., 2002), with annual air temperature in 2016 of ~1.5°C higher than the 30-year average between 1981 and 2010 (Figure 1.6). Air temperature in the Selenga River basin in southeast Siberia warmed nearly twice as fast as the global average (a total increase of 1.6°C) for the period 1938 to 2009, with most of the warming occurring during the winter season (Törnqvist *et al*., 2014). Further, a lengthened ice-free season for Lake Baikal of approximately 16 days has been recorded over the past 137 years, primarily related to later ice onset (Magnuson *et al.,* 2000; Todd and Mackay, 2003). The climate of Siberia is predicted to continue to warm through the 21st century, with continued increases in temperatures, greater temperature increases during the winter than the summer, and increases in precipitation expected (Malsy *et al*., 2012; Törnqvist *et al*., 2014). A warmer climate in the Selenga Delta could manifest as an increase in the ice-free season with associated feedbacks and hydrological changes including modification of the current precipitation regime and increased evapotranspiration.

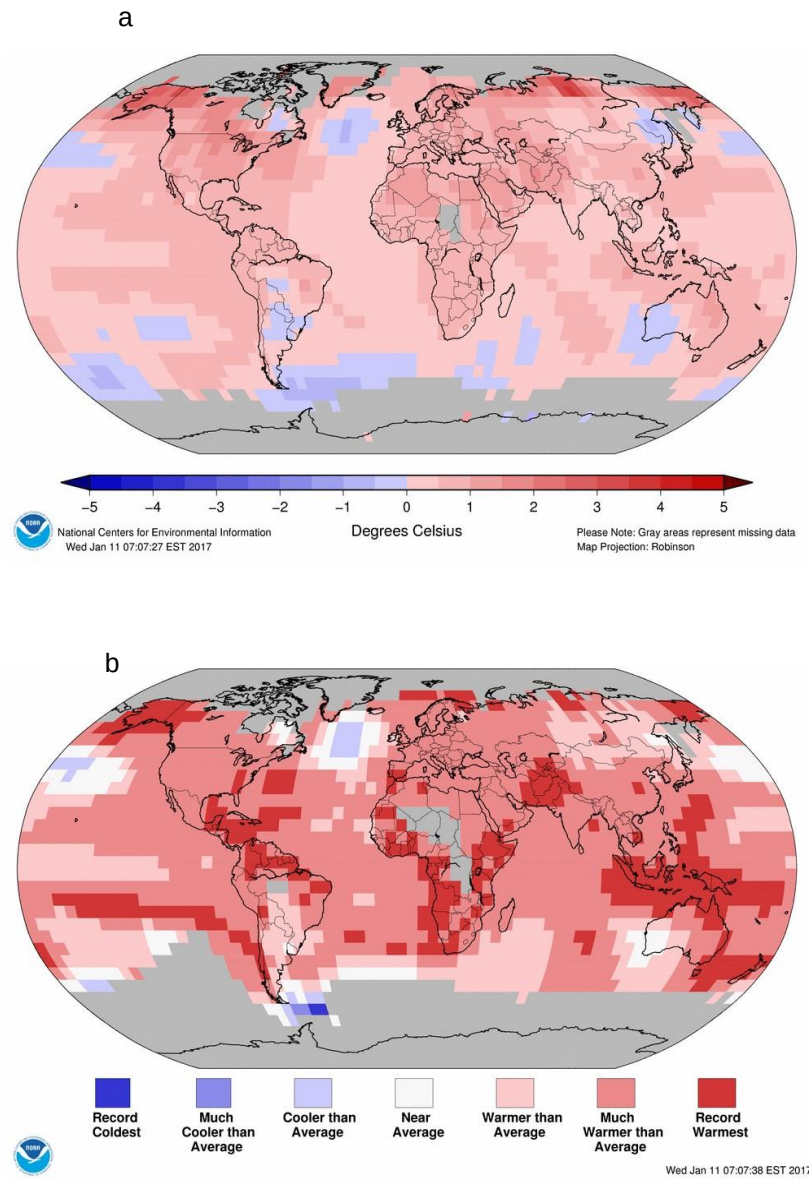

Figure 1.6. a) Global temperature departures and b) percentiles during the year 2016. Temperature averages are based on the period of 1981-2010 (Source: https://www.ncdc.noaa.gov/temp-and-precip/global-maps/)

Despite the major changes in anthropogenic disturbances in the Selenga River basin, the critical importance of the shallow lake systems of the Selenga River basin to maintaining the ecosystem health of Lake Baikal, and the likely continued effects of climate change in the region, little is known about the timing and rates of change of ecological impact of these systems, and the ecological sensitivity and response to perturbations. Shallow lake ecosystems within the Selenga River basin may differ in their sensitivity and ecological response to disturbance events, based on the relative importance of different drivers of environmental change.

1.5 Research aims and objectives

The aim of this thesis is to develop palaeolimnological records of ecological response to anthropogenic and natural disturbances to shallow lakes in southeastern Siberia, and to develop an understanding of drivers of contemporary ecological variability in shallow lakes across floodplain delta wetlands. The study focuses on shallow lakes within the Siberian portion of the Selenga River basin. The Selenga River basin has been subject to intensifying anthropogenic disturbances of varying kinds since the 19th century, yet is a critical watershed due to the Selenga River being the primary contributor of freshwater to Lake Baikal, a UNESCO World Heritage Site. The shallow lakes included in this thesis are located in two regions within the Selenga River basin: first, within the Selenga Delta itself, and second, within the more heavily industrialized Gusinoye region to the southwest of Lake Baikal.

The study has 4 primary aims:

1. To determine to what extent hydrological regime determines the ecological structure and functioning of shallow lakes within floodplain delta wetlands.
2. Determine historical levels of anthropogenic contamination to shallow lakes of the Selenga River basin.
3. Assess the impact on shallow lakes from local vs. regional vs. long-range transport of contaminants, and spatial variations in contaminant records from lakes within a floodplain delta wetland and outside of a floodplain wetland.
4. Determine potential for ecological response within shallow lakes to natural and anthropogenic disturbances across several trophic levels, including assessments of sensitivity to local vs. regional disturbances, and primary drivers of ecological change across different temporal and spatial scales.

Furthermore, the objectives of this project are:

1. Examine contemporary communities and ecological remains at various trophic levels within shallow lakes of varying connectivity to the Selenga River, including macrophytes, algae, invertebrates, and fish, to assess connectivity impacts on biotic interactions, and ecological structure and functioning across Selenga River basin lakes.
2. Examine lake sediment cores for inorganic contaminants (trace metals and other trace elements) as evidence for mining and industrial impacts, organic contaminants

(including polcyclic aromatic hydrocarbons and halogenated organic contaminants), as evidence for agricultural and industrial impacts, in three lakes within the Selenga River basin: two lakes from within the Selenga River Delta, and one lake from the more heavily industrialized Gusinoye region.

3. Examine sedimentary biological records (macrofossils, diatoms, pigments) for evidence of change to ecological structure and function as a response to natural and anthropogenic disturbances, including changes to algal biomass, and trophic structure and interactions.
4. Assess potential for ecological regime shifts using statistical approaches

1.6 Thesis structure

Chapter 2 will introduce the study sites within the Selenga River basin, as part of the contemporary study within this thesis, and outline the process undertaken in contemporary site selection. As none of the sites have been previously described, physical descriptions are provided. Contemporary field and laboratory methodologies are then described, and contemporary water chemistry of all sites presented. Analysis of water chemistry across the Selenga River basin shallow lakes is undertaken, and implications of results discussed.

Chapter 3 continues the contemporary study of Selenga River basin shallow lakes, and examines primary drivers of contemporary ecological variability in Selenga River basin lakes, primarily assessing the impact that variations in connectivity have on shallow lake ecology. Results from contemporary ecological community sampling (macrophyte, zooplankton, invertebrate, diatom, and algal pigment) are presented, and numerical analyses undertaken to address the primary aim of the chapter. Implications of results are discussed in the context of shallow lake wetland ecology.

Chapter 4 introduces the palaeolimnological study undertaken for this thesis. Palaeolimnological study sites and field methodologies are described. Methodologies and results of radioisotope dating and sediment core geochemical analyses are described. Methods used for establishing chronologies using cross-dating techniques are described in detail, and results of cross-dating

are presented. Dating uncertainties, inefficiencies, chronology formation using cross-dating methods, and palaeolimnological insights gained from geochemical analyses are discussed.

Chapter 5 presents contamination and geochemical records since the 19th century obtained from sediment cores from the three Selenga River basin palaeolimnological study lakes. Results for each of the three lakes are presented, and contamination records from Selenga River basin shallow lakes are discussed in a global context, and evidence and implications for regional and local anthropogenic contamination sources, and geochemical evidence for local change are discussed.

Chapters 6, 7, and 8 present the biological sedimentary records from SLNG04, SLNG05, and BRYT02, respectively. Changes in macrofossil, diatoms, and pigment records since the early 19th century were investigated for SLNG04 and SLNG05, while only diatoms and pigment records were investigated for BRYT02.

Chapter 9 synthesizes the contemporary and palaeolimnological findings from this thesis, addressing commonalities between records and sites, and implications for scales of change and ecological sensitivity to natural and anthropogenic disturbances. Recommendations stemming from the study are provided, and directions for future work described.

1.7 References

Andersen T., Carstensen J., Hernandez-Garcia E., & Duarte C.M. (2008) Ecological thresholds and regime shifts: approaches to identification. *Trends in Ecology and Evolution*, **24,** 49-57.

Angeler D.G., Allen C.R., Rojo C., Alvarez-Cobelas M., Rodrigo M.A., & Sanchez-Carrillo S. (2013a) Inferring the relative resilience of alternative states. *PLoS ONE*, **8,** e77338.

Angeler D.G., Allen C.R., & Johnson R.K. (2013b) Measuring the relative resilience of subarctic lakes to global change: redundancies of functions within and across temporal scales. *Journal of Applied Ecology*, **50,** 572-584.

Antoniades D., Douglas M.S.V., & Smol J.P. (2005) Quantitative estimates of recent environmental changes in the Canadian High Arctic inferred from diatoms in lake and pond sediments. *Journal of Paleolimnology*, **33,** 349-360.

Bailey S.E., & Guimond J.K. (2009) Aboveground biomass and nutrient limitation in relation to river connectivity in montane floodplain marshes. *Wetlands* **29,** 1243-1254.

Baskett M.L., Fabina N.S., & Gross K. (2014) Response diversity can increase ecological resilience to disturbance in coral reefs. *American Naturalist*, **184,** E16-E31.

Bazhenova O.I., & Kobylkin D.V. (2013) The dynamics of soil degradation processes within the Selenga Basin at the agricultural period. *Geography and Natural Resources* **34,** 221-227.

Beisner B.E., Haydon D.T., & Cuddington K. (2003) Alternative stable states in ecology. *Fronteirs in Ecology and the Enviroment* **1,** 376-382.

Bennion H., Carvalho L., Sayer C.D., Simpson G.L., & Wischnewski J. (2012) Identifying from recent sediment records the effects of nutrient and climate on diatom dynamics in Loch Leven. *Freshwater Biology* **57,** 2015-2029.

Bennion H., Davidson T.A., Sayer C.D., Simpson G.L., Rose N.L., & Sadler J.P. (2015) Harnessing the potential of the multi-indicator palaeoecological approach: an assessment of the nature and causes of ecological change in a eutrophic shallow lake. *Freshwater Biology*, doi: 10.1111/fwb.12579.

Birks H.H., & Briks H.J.B. (2006) Multi-proxy studies in palaeolimnology. *Vegetation History and Archaeobotony* **15,** 235-251.

Blinnikov M.S. (2010) A geography of Russia and its neighbors, 1st Edition. Guilford Press, United States of America.

Bolgov, M.V., Buber A.L., Korobkina E.A., Lyubushin A.A., & Filippova I.A. (2017) Lake Baikal: extreme level as a rare hydrological event. *Water Resources* **44,** 522-536.

Britten G.L., Dowd M., Minto C., Ferretti F., Boero F., & Lotze H.K. (2014) Predator decline leads to decreased stability in a coastal fish community. *Ecology Letters*, **17**, 1518-1525.

Brock B.E., Wolfe B.B., & Edwards T.W.D. (2007) Characterizing the hydrology of shallow floodplain lakes in the Slave River Delta, NWT, Canada, using water isotope tracers. *Arcitc, Antarctic, and Alpine Research* **39**, 388-401.

Brock B.E., Martin M.E., Mongeon C.L., Sokal M.A., Wesche S.D., Armitage D., Wolfe B.B., Hall R.I., & Edwards T.W.D. (2011) Flood frequency variability during the past 80 years in

the Slave River Delta, NWT, as determined from multi-proxy palaeolimnological analysis. *Canadian Water Resources Journal*, **35,** 281-300.

Chalov S.R., Jarsjo J., Kasimov N.S., Romanchenko A., Pietron J., Thorslun J., & Belazerov E. (2014) Spatio-temporal variation of suspended transport in the Selenga Basin (Mongolia and Russia). *Environmental and Earth Sciences* http://dx.doi.org/10.1007/s12665-014-3106-z.

Chalov S., Thorslund J., Kasimov N., Aybullatov D., Ilyicheva E., Karthe D., Kositsky A., Lychagin M., Nittrouer J., Pavlov M., Pietron J., Shinkareva G., Tarasov M., Garmaev E., Akhtman Y., Jarsjo J. (2016) The Selenga River delta: a geochemical barrier protecting Lake Baikal waters. *Regional Environmental Change* doi: 10.1007/s10113-016-0996-1.

Chapin F.S III., Walker B.H., Hobbs R.J., Hooper D.U., Lawton J.H., Sala O.E., & Tilman D. (1997) Biotic control over the functioning of ecosystems. *Science*, **277**, 500-504.

Cobbaert D., Wong A., & Bayley S.E. (2014) Precipitation-induced alternative regime switches in shallow lakes of the Boreal Plains (Alberta, Canada). *Ecosystems*, **17,** 535-549.

Davidson T.A., Bennion H., Jeppesen E., Clarke G.H., Sayer C.D., Morley D., Odgaard B.D., Rasmussen P., Rawcliffe R., Salgado J., Simpson G.L., & Amsinck S.L. (2010) The role of cladocerans in tracking long-term change in shallow lake trophic status. *Hydrobiologia*, **676,** 299-315.

Davidson T.A., Bennion H., Jeppesen E., Clarke G.H., Sayer C.D., Morley D., Odgaard B.D., Rasmussen P., Rawcliffe R., Salgado J., Simpson G.L., & Amsinck S.L. (2011) The role of cladocerans in tracking long-term change in shallow lake trophic status. *Hydrobiologia*, **676,** 299-315.

Davidson T.A., Reid M.A., Sayer C.D., & Chilcott S. (2013) Palaeolimnological records of shallow lake biodiversity change: exploring the merits of single versus multi-proxy approaches. *Journal of Paleolimnology*, **49,** 431-446.

Davis R.B., Anderson D.S., Dixit S.S., Appleby P.G., & Schauffler M. (2006) responses of two New Hampshire (USA) lakes to human impacts in recent centuries. *Journal of Paleolimnology*, **35,** 669-697.

De Tezanos Pinto P., & O'Farrell I. (2014) Regime shifts between free-floating plants and phytoplankton: a review. *Hydrobiologia*, **740,** 13-24.

Diaz S., & Cabido M. (2001) Vive la difference: plant functional diversity matters to ecosystem processes. *Trends in Ecology and Evolution*, **16,** 646-655.

Dong X., Bennion H., Battarbe R.W., & Sayer C.D. (2011) A multiproxy palaeolimnological study of climate and nutrient impacts on Estwaite Water, England over the past 1200 years. *The Holocene* **22**, 107-118.

Douglas M.S.V., & Smol J.P. (1994) Limnology of High Arctic ponds (Cape Herschel, Ellesmere Island, NWT). *Archiv Fur Hydrobiologie*, **131,** 401-434.

Downing A.S., van Nes E.H., Mooij W.M., & Scheffer M. (2012) The resilience and resitence of an ecosystem to a collapse of diversity. *PLoS ONE*, **7,** e46135.

Duffy JE, Cardinale BJ, France KE, McIntyre PB, Thebault E, Loreau M. 2007. The functional role of biodiversity in ecosystems: incorporating trophic complexity. Ecology Letters **10:** 522-538.

Engstrom D.R., Schottler S.P., Leavitt P.R., & Havens K.E. (2006) A reevaluation of the cultural eutrophication of Lake Okeechobee using multiproxy sediment records. *Ecological Applications* **16,** 1194-1206.

[FAO] Food and Agricultural Organization of the United Nations. (2001) Lecture Notes on the Major Soils of the World. World Soils Resources Report. Eds. Driessen P., Decker J., Rome, Italy.

Fedorov A.N., Gavriliev P.P., Konstantinov P.Y., Hiyama T., Iijima Y., & Iwahana G. (2014) Estimating the water balance of a thermokarst lake in the middle of the Lena River basin, eastern Siberia. *Ecohydrology* **7,** 188-196.

Feuchtmayr H., Moran R., Hatton K., Connor L., Heyes T., Moss B., Harvey I., & Atkinson D. (2009) Global warming and eutrophication: effects on water chemistry and autotrophic communities in experimental hypertrophic shallow lake mesocosmos. *Journal of Applied Ecology*, **46,** 713-723.

Folke C., Carpenter S., Walker B., Scheffer M., Elmqvist T., Gunderson L., & Holling C.S. (2004) Regime shifts, resilience, and biodiversity in ecosystem management. *Annual Review of Ecological and Evolutionary Systems*, **35,** 557-581.

Galazi G.I. (1993) The Baikal Atlas. Ed. Galazi G.I. Moscow, RU.

Golenetskii S.I. (1996) Macroseismic effects of the catastrophic Tsagan, Baikal earthquake of 1862. *Fizika Zemli* **11,** 3–13.

Hartig E.K., Grozev O., Rosenzweig C. (1997) Climate change, agriculture and wetlands in Eastern Europe: vulnerability, adaptation and policy. *Climatic Change* **36**, 107–121.

Heim B., Klump J., Schulze A., Schneider S., Swiercz S., Dachnowski G., Fagel N. (2007) Lithological map of the Lake Baikal catchment. *Deutsches GeoForschungsZentrum*GFZ.

Hobbs W.O., Moraska Lafrancois B., Stottlenyer R., Toczydlowski D., Engstrom D.R., Edlund M.B., Almendinger J.E., Strock K.E., VanderMeulen D., Elias J.E., & Saros J.E. (2016) Nitrogen deposition to lakes in national parks of the western Great Lakes region: Isotopic signature, watershed retention, and algal shifts. *Global Biogeochemical Cycles* **30**, 514-533.

IPCC (International Panel on Climate Change). (2007) Climate change 2007: Synthesis Report AR4. http://www.ipcc.ch/pdf/assessmentreport/ar4/syr/ar4_syr.pdf.

Jackson L.J. (2003) Macrophyte-dominated and turbid states of shallow lakes: evidence from Alberta lakes. *Ecosystems*, **6,** 213-223.

Jeppesen E., Søndergaard M., Søndergaard M., & Christoffersen K. (1998) The Structuring Role of Submerged Macrophytes in Lakes. Ecological Studies, series 131. Springer, New York, 421 pp.

Jeppesen E., Jensen J.P., Sondergaard M., Lauridsen T., & Landkildehus F. (2000) Trophic structure, species richness and biodiversity in Danish lakes: changes along a phosphorous gradient. *Freshwater Biology*, **45,** 201-218.

Jeppesen E., Jensen J.P., Jensen C., Faafeng B., Brettum P., Hessen D., Søndergaard M., Lauridsen T., & Christoffersen K. (2003). The impact of nutrient state and lake depth on top-down control in the pelagic zone of lakes: study of 466 lakes from the temperate zone to the Arctic. *Ecosystems* **6**, 313–325.

Junk W.J., An S., Finlayson C.M., Gopal B., Kvet J., Mitchell S.A., Mitsch W.J., & Robarts R.D. (2013) Current state of knowledge regarding the world's wetlands and their future under global climate change: a synthesis. *Aquatic Sciences*, **75,** 151-167.

Kadetova A.V., & Radziminovich Y.B. (2014) The catastrophic flood in Transbaikalia (Central Asia) in 1897: a case study. *Natural Hazards* **72,** 23-441.

Kannan K., Nakata H., Stafford R., Masson G.R., Tanabe S., & Giesy J.P. (1998) Bioaccumulation and toxic potential of extremely hydrophobic polychlorinated biphenyl congeners in biota collected at a superfund site contaminated with Arochlor 1268. *Environmental Science & Technology* **32**, 1214-1221.

Keatley B., Douglas M.S.V., & Smol J.P. (2006) Early-20th century environmental changes inferred using diatoms from a small pond on Melville Island, NWT, Canadian High Arctic. *Hydrobiologia*, **553,** 15-26.

Khanin G.I. (2003) The 1950s – the triumph of the Soviet economy. *Europe-Asia Studies* **55**, 1187-1212.

Khazheeva Z.I., & Tulokonov A.K. (2007) Distributions of metals in bottom deposits in the branches of Selenga River Delta. *Geochemistry International*, **45,** 185-192.

Kitaev L., Kislov A., Krenke A., Razuvaev V., Martuganov R., & Konstantinov I. (2002) The snow cover characteristics of northern Eurasia and their relationship to climatic parameters. *Boreal Environment*, **7,** 437–445.

Korhonen J.J., Wang J., & Soininen J. (2011) Productivity-diversity relationships in lake plankton communities. *PLoS ONE* **6**, e22041. doi: 10.1371/journal.pone.0022041.

Körner S. (2002) Loss of submerged macrophytes in shallow lakes in north-eastern Germany. *International Review of Hydrobiology* **87**, 377–386.

Kovalenko K.E., Brady V.J., Brown T.N., Ciborowski J.J.H., Danz N.P., Gathman J.P., Host G.E., Howe R.W., Johnson L.B., Niemi G.J., & Reavie E.D. (2014) Congruence of community thresholds in response to anthropogenic stress in Great Lakes coastal wetlands. *Freshwater Science*, **33,** 958-971.

Kozhova O.M., & Izhboldina L.A. (1993) Spread of *Elodea canadensis* in Lake Baikal. *Hydrobiologia*, **259,** 203-211.

Kravtsova L.S., Izhboldina L.A., Mekhanikova I.V., Pomazkina G.V., & Belykh O.I. (2010) Naturalization of *Elodea canadensis* Mich. in Lake Baikal. *Russian Journal of Biological Invasions*, **1,** 162-171.

Laing T.E., & Smol J.P. (2000) Factors influencing diatom distributions in circumpolar treeline lakes of northern Russia. *Journal of Phycology* **36,** 1035-1048.

Laing T.E., Pienitz R., & Smol J.P. (1999) Freshwater diatom assemblages from 23 lakeslocated near Norilsk, Siberia : A comparison with assemblages from other circumpolar treeline regions. *Diatom Research* **14,** 285-305.

Leavitt P.R., & Hodgson D.A. (2001) Sedimentary pigments. In, Smol JP, Birks HJB, Last WM (eds) Developments in paleoenvironmental research, Vol 3. Tracking environmental changes using lake sediments: terrestrial algal and siliceous indicators. Kluwer Academic Publishers, Dordrecht.

Levi E.E., Cakiroglu A.I., Bucak T., Odgaard B.V., Davidson T.A., Jeppesen E., & Beklioglu M. (2014) Similarity between contemporary vegetation and plant remains in the surface sediment in Mediterranean lakes. *Freshwater Biology*, **59,** 724-736.

Levi E.E., Bezerci G., Cakiroglu A.I., Turner S., Bennion H., Kernan M., Jeppesen E., & Beklioglu M. (2016) Multi-proxy palaeoecological responses to water level fluctuations in three shallow Turkish lakes. *Palaeogeography, Palaeoclimatology, Palaeoecology* **449,** 553-566.

Logachev N.A. (2003) History and geodynamics of the Baikal rift. *Russian Geology and Geophysics* **44**, 391–406.

Luoto T.P., Brooks S.J., & Salonen V-P. (2014) Ecological responses to climate change in a bird-impacted High Arctic pond (Nordaustlandet, Svalbard). *Journal of Paleolimnology*, **51,** 87-97.

Mackay A. W., Bezrukova E. V., Leng M. J., Meaney M., Nunes A., Piotrowska N., Self A., Shchetnikov A., Shilland E., Tarasov P., Wang L., & White, D. (2012). Aquatic ecosystem responses to Holocene climate change and biome development in boreal, central Asia. *Quaternary Science Reviews* **41**, 119-131.

Mackay A. W., Bezrukova E., Boyle J. F., Holmes J. A., Panizzo V. N., Piotrowska N., Shchetnikov A., Shilland E.M., Tarasov P., & White D. (2013). Multiproxy evidence for abrupt climate change impacts on terrestrial and freshwater ecosystems in the Ol'khon region of Lake Baikal, central Asia. *Quaternary International* **290-291**, 46-56.

Magnuson J.J., Robertson D.M., Benson B.J., Wynne R.H., Livingstone D.M., Arai T., Assel R.A., Berry R.G., Card V., Kuusisto E., Granin N.G., Prowse T.D., Stewart K.M., & Vuglinski V.S. (2000) Historical trends in lake and river ice cover in the northern hemisphere. *Science* **289**, 1743–1746.

Malsy M., Flörke M., Borchardt D. (2016) What drives the water quality changes in the Selenga Basin: climate change of socio-economic development. *Regional Environmental Change* DOI 10.1007/s10113-016-1005-4.

Manasypov R.M., Vorobyev S.N., Loiko S.V., Kritzkov I.V., Shirokova L.S., Shevchenko V.P., Kirpotin S.N., Kulizhsky S.P., Kolesnichenko L.G., Zemtzov V.A., Sinkinov V.V., & Pokrovsy O.S. (2015) Seasonal dynamics of organic carbon and metals in thermokarst lakes from the discontinous permafrost zone of western Siberia. *Biogeosciences* **12,** 3009-3028.

Mann M.E. (2002) The value of multiple proxies. *Science* **297**, 1481-1482.

Marin V.H., Tironi A., Delgado L.E., Contreras M., Novoa F., Torres-Gomez M., Garreaud R., Vila I., & Serey I. (2009) On the sudden disappearance of *Egeria densa* from a Ramsar wetland site of Southern Chile: A climatic event trigger model. *Ecological Modelling*, **220,** 1752-1763.

McCann K., Hastings A., & Huxel G.R. (1998) Weak trophic interactions and the balance of nature. *Nature*, **395,** 794-798.

McGowan S., Leavitt P.R., Hall R.I., Wolfe B.B., Edwards T.W.D., Karst-Riddoch T., & Vardy S.R (2011) Interdecadel declines in flood frequency increase primary production in lakes of a northern river delta. *Global Change Biology*, **17,** 1212-1224.

[MEA] Millennium Ecosystem Assessment. (2005) Ecosystems and Human Well-Being: Wetlands and Water Synthesis. World Resources Institute, Washington, D.C.

Michelutti N., Hay M.B., March P., Lesack L., & Smol J.P. (2001a) Diatom changes in lake sediments from the Mackenzie Delta, NWT, Canada: Paleohydrological applications. *Arctic, Antarctic, and Alpine Research*, **33,** 1-12.

Michelutti N., Laing T.E., & Smol J.P. (2001b) Diatom assessment of past environmental changes in lakes located near the Noril'sk (Siberia) smelters. *Water, Air, and Soil Pollution* **125,** 231-241.

Mitsch W.J., & Gosselink J.G. (2007) Wetlands, 4th Edition. Wiley & Sons, United States of America.

Moser K.A., Korhola A., Weckstrom J., Blom T., Pienitz R., Smol J.P., Douglas M.S.V., & Hay M.B. (2000) Paleohydrology inferred from diatoms in northern latitude regions. *Journal of Paleolimnology*, **24,** 93-107.

Nadmitov B., Hong S., Kang S.I., Chu J.M., Gomboev B., Janchivdorj L., Lee C-H., & Khim J.S. (2015) Large-scale monitoring and assessment of metal contamination in surface water of the Selenga River basin (2007-2009). *Environmental Science and Pollution Research* **22,** 2856-2867.

Naganawa H. (2012) Lake Gusinoe to Baikal via Selenga Delta: protection-destruction spiral. *Lakes, Reservoirs, and Ponds* **6,** 9-19.

Nazarova L., Lupfert H., Subetto D., Pestryakova L., & Diekmann B. (2013) Holocene climate conditions in central Yakutia (Eastern Siberia) inferred from sediment composition and fossil chironomids of Lake Temje. *Quaternary International* **290-291,** 264-274.

Nielsen D.L., & Brock M.A. (2009) Modified water regime and salinity as a consequence of climate change: prospects for wetlands in Southern Australia. *Climate Change*, **95,** 523-533.

Niemeyer B., Epp L.S., Stoof-Leichsenring K.R., Pestryakova L.A., & Herzschuh U. (2017) A comparison of sedimentary DNA and pollen from lake sediments in recording vegetation composition at the Siberian treeline. *Molecular Ecology Resources* doi: 10.1111/1755-0998.12689.

O'Dwyer B., Crockford L., Jordan P., Hislop L., & Taylor D. (2013) A palaeolimnological investigation into nutrient impact and recovery in an agricultural catchment. *Journal of Environmental Management*, **124,** 147-155.

O'Farrell I., Izaguirre I., Chaparro G., Unrein F., Sinistro R., Pizarro H., Rodriguez P.L., de Tezanos Pinto P., Lombardo R., & Tell G. (2011) Water level variation as a main driver of the alternation netween free-floating plant and a phytoplankton dominated state: a long term study in a floodplain lake. *Aquatic Sciences*, **73,** 275-287.

Orlov A.P. (1872) General remarks on earthquakes, with special reference to South Siberia and Turkestan Region. *Proceedings of the Kazan University Society of Natural Sciences*, **3.**

Peterson G.D., Allen C.R., & Holling C.S. (1998) Ecological resilience, biodiversity and scale. *Ecosystems*, **1,** 6-18.

Pinegin A.V., Rogozin A.A., Leshchikov F.N., Kulish L.Y., & Yakimov A.A. (1976) Shore dynamics of Lake Baikal at the new level regime. Nauka, Moscow.

Pisarsky B.I., Hardina A.M., & Naganawa H. (2005) Ecosystem evolution of Lake Gusinoe (Transbaikal Region, Russia). *Limnology*, **6,** 173-182.

Pla S., Monteith D., Flower R., Rose N. (2009) The recent paleolimnology of a remote Scottish loch with special reference to the relative impacts of regional warming and atmospheric contamination. *Freshwater Biology*, **54,** 505-523.

Porinchu D.F., & Cwynar L.C. (2000) The distribution of freshwater Chironomidae (Insecta: Diptera) across treeline near the lower Lena River, Northeast Siberia, Russia. *Arctic, Antarctic, and Alpine Research* **32,** 429-437.

Plyusnin A.M., Kislitsina L.B., Zhambalova D.I., Peryazeva E.G., & Udodov Y.N. (2008) Development of the chemical characteristics of ground water at the Delta of the Selenga River. *Geochemistry International*, **46,** 288-295.

Quinlan R., Douglas M.S.V., & Smol. J.P. (2005) Food web changes in arctic ecosystems related to climate warming. *Global Change Biology*, **11,** 1381-1386.

Ramsar (2015) The 4th strategic plan 2016-2024: The convention on wetlands of international importance especially as waterfowl habitat – the "Ramsar Convention". [online]

Available from: http://www.ramsar.org/about/the-ramsar-convention-and-its-mission. [Accessed: 15th June, 2017].

Randsalu-Wendrop L., Conley D.J., Carstensen J., Hansson L-A., Bronmark C., Fritz S.C., Choudhary P., Routh J., & Hammarlund D. (2014) Combining limnology and palaeolimnology to investigate recent regime shifts in a shallow, eutrophic lake. *Journal of Paleolimnology*, **51,** 437-448.

Raulings E.J., Morris K., Roache M.C., & Boon P.I. (2010) The importance of water regimes operating at small spatial scales for the diversity and structure of wetland vegetation. *Freshwater Biology*, **55,** 701-715.

Robarts R.D., Zhulidov A.V., & Pavlov D.F. (2013) The state of knowledge about wetlands and their future under aspects of global climate change: the situation in Russia. *Aquatic Sciences* **75**, 27-38.

Robinson, W.P., & Anosova G.B. (2004) Mining and mineral development management policy in the Selenga River Watershed. In: *Science for Watershed Conservation: Mulitdisciplinary Approaches for Natural Resource Management* Conference, Ulan-Ude, Russia and Ulanbaatar, Mongolia.

Rooney N., McCann K., Gellner G., & Moore J.C. (2006) Structural asymmetry and the stability of diverse food webs. *Nature*, **442,** 265-269.

Rühland K., Priesnitz A., & Smol J.P. (2003) Evidence for recent environmental changes in 50 lakes across the Canadian Arctic treeline. *Arctic, Antarctic, and Alpine Research*, **35,** 110-123.

Sala O.E., Chapin F.S., Armesto J.J., Berlow E., Bloomfield J., Dirzo R., Huber-Sanwald E., Huenneke L.F., Jackson R.B., Kinzig A., Leemans R., Lodge D.M., Mooney H.A., Oesterheld M., Poff N.L., Sykes M.T., Walker B.H., Walker M., & Wall D.H. (2000) Biodiversity – Global biodiversity scenarios for the year 2100. *Science*, **287,** 1770-1774.

Scheffer M. (1997) *The Ecology of Shallow Lakes*. London: Chapman and Hall.

Scheffer M., Carpenter S., Foley J.A., Folke C., & Walker B. (2001) Catastrophic shifts in ecosystems. *Nature*, **413,** 591-596.

Scholz C.A., & Hutchinson D.R. (2000) Stratigraphic and structural evolution of the Selenga Delta Accommodation Zone, Lake Baikal Rift, Siberia. *International Journal of Earth Science*, **89,** 212-228.

Shea K., & Chasson P. (2002) Community ecology theory as a framework for biological invasions. *Trends in Ecology and Evolution*, **17,** 170-176.

Self A.E., Jones V.J., & Brooks S.J. (2015) Late Holocene environmental change in arctic western Siberia. *The Holocene* **25,** 150-165.

Shimaraev M.N., Kuimova L.N., Sinyukovich V.N., & Tsekhanovskii V.V. (2002) Manifestation of global climatic changes in Lake Baikal during the 20th century. *Doklady Earth Sciences* **383A**, 288–291.

Smol J.P. (2008) The power of the past: using sediments to track the effects of multiple stressors on lake ecosystems. *Freshwater Biology* **55,** 43-59.

Smol J.P., & Douglas M.S.V. (2007) From controversy to consensus: making the case for recent climate change in the Arctic using lake sediments. *Frontiers in Ecology*, **5,** 466-474.

Smol J.P., Wolfe A.P., Birks H.J.B., Douglas M.S.V., Jones, V.J., Korhola A., Pientz R., Ruhland K., Sorvari S., Antoniades D., Brooks S.J., Fallu M-A., Hughes M., Keatley B.E., Laing T.E., Michelutti N., Nazarova L., Nyman M., Paterson A.M., Perren B., Quinlan R., Rautio M., Saulnier-Talbot E., Siitonen S., Solovieva N., & Weckstrom J. (2005) Climate-driven regime shifts in the biological communities of arctic lakes. *Proceedings of the National Academy of Science*, **102,** 4397-4402.

Sokal M.A., Hall R.I., & Wolfe B.B. (2008) Relationships between hydrological and limnological conditions in lakes of the Slave River Delta (NWT, Canada) and quantification of their roles in sedimentary diatom assemblages. *Journal of Paleolimnology* **39,** 533-550.

Sondergaard M, Johansson LS, Lauridsen TL, Jorgensen TB, Liboriussen L, Jeppesen E. 2010. Submerged macrophytes as indicators of the ecological quality of lakes. FWB. **55:** 893-908.

Sovari S., Korhola A., & Thompson R. (2002) Lake diatom response to recent Arctic warming in Finnish Lapland. *Global Change Biology*, **8,** 171-181.

Summers J.C., Kurek J., Ruhland K.M., Neville E.E., & Smol J.P. (2017) Assessment of multi-trophic changes in a shallow boreal lake simultaneously exposed to climate change and aerial deposition of contaminants from the Athabasca Oil Sands Region, Canada. *Science of the Total Environment* **592,** 573-583.

Taylor D., Dalton C., Leira M., Jordon P., Chen G., Leon-Vintro L., Irvine K., Bennion H., & Nolan T. (2006) Recent histories of six productive lakes in the Irish Ecoregion based on multiproxy palaeolimnological evidence. *Hydrobiologia* **571,** 237-259.

Thienpont J.R., Korosi J.B., Hargan K.E., Williams T., Eickmeyer D.C., Kimpe L.E., Palmer M.J., Smol J.P., & Blais J.M. (2016) Multitrophic level response to extreme metal contamination from gold mining in a subarctic lake. *Proceedings of the Royal Society B* **283**, 20161125. http://dx.doi.org/10.1098/rspb.2016.1125

Thorslund J., Jarsjo J., Chalov S.R., & Belozerova E.V. (2012) Gold mining impact of riverine heavy metal transport in a sparsely monitored region: the upper Lake Baikal Basin case. *Journal of Environmental Monitoring*, **14,** 2780-2792.

Todd M.C., & Mackay A.W. (2003) Large-scale climatic controls on lake Baikal ice cover. *Journal of Climate* **16**, 3186–3199.

Törnqvist R., Jarsjö J., Pietron J., Bring A., Rogberg P., Asokan S.M., & Destouni G. (2014) Evolution of the hydro-climate system in the Lake Baikal system. *Journal of Hydrology* **519,** 1953-1962.

Tsybikdorzhiev Ts.Ts., Khodoeva S.O., & Gonchikov B.-M.N. (2012) Soil cover patterns and land assessment in the Naikal region of Buryatia using the example of the Kabansk district. *Eurasian Soil Science* **45,** 348-356.

Ventela A-M., Amsinck S.L., Kauppila T., Johansson L.S., Jeppesen E., Kirkkala T., Sondergaard M., Weckstron J., & Sarvala J. (2016) Ecosystem change in the large and shallow Lake Sakylan Pyhajarvi, Finland, during the past ~400 years: implications for management. *Hydrobiologia* **778,** 273-294.

Vermaire JC, Greffard M-H, Saulnier-Talbot E, Gregory-Eaves I. 2013. Changes in submerged macrophyte abundance altered diatom and chironomid assemblages in a shallow lake. Journal of Paleolimnology **50:** 447-456.

Vologina E.G., Kalugin I.A., Osukhovskaya Y.N., Sturm M., Ignatova N.V., Radziminovich Y.B., Dar'in A.V., & Kuz'min M.I. (2010) Sedimentation in Proval Bay (Lake Baikal) after earthquake-induced subsidence of part of the Selenga River delta. *Russian Geology and Geophysics*, **51,** 1275-1284.

Walker B.H., & Meyers J.A. (2004) Thresholds in ecological and socio-ecological systems: a developing database. *Ecology and Society*, **9,** 3.

Ward J.V., Tockner K., & Schiemer F. (1999) Biodiversity of floodplain river ecosystems: ecotones and connectivity. *Regulated Rivers, Research and Management* **15**, 125-139.

Westover K.S., Fritz S.C., Blyakharchuk T.A., & Wright H.E. (2006) Diatom paleolimnological record of Holocene climate and environmental changein the Altai Mountains, Siberia. *Journal of Paleolimnology* **35,** 519-541.

Wolfe B.B., Karst-Riddoch T.L., Vardy S.R., Falcone M.D., Hall R.I., & Edwards T.W.D. (2005) Impacts of climate and river flooding on the hydro-ecology of a floodplain basin, Peace-Athabasca Delta, Canada since A.D. 1700. *Quaternary Research*, **64,** 147-162.

Zambrano L., Scheffer M., & Martinez-Ramos M. (2001) Catastrophic response of lakes to benthivorous fish introduction. *Oikos*, **94,** 344-350.

Zhou Y., Sayer C.D., Birks H.H., Hughes M., Peglar S.M. (2006) Spatial representation of aquatic vegetation by macrofossils and pollen in a small, shallow lake. *Journal of Paleolimnology* **35,** 335-350.

Chapter 2: Study Sites, Methodologies, and Contemporary Limnology of Shallow Lakes from the Selenga River basin

2.1 Introduction to the Selenga River basin

The Selenga River basin spans an area of approximately 450,000 km^2 in northern Mongolia and south-east Siberia. The Selenga River flows approximately 950 km from the confluence of the Ider and Delger Rivers in northern Mongolia, to the Selenga Delta on Lake Baikal, in south-east Siberia (See Section 1.1, Figure 1.2). Prior to entering the Selenga River Delta, the Selenga River receives water from many tributaries, and shallow and deep freshwater lakes both in northern Mongolia and southeastern Siberia (See Section 1.4.1). The upstream portions of the Selenga River basin, primarily tributaries and headwaters within Mongolia, run through mountainous and forested terrain, while further downstream, the southern Siberian portion of the Selenga River basin consists of steppe vegetation. Part of the steppe land within the Selenga River basin has been converted to pasture or crop land, and irrigation and agricultural pressures exist (Chalov *et al*., 2015). Several major population and industrial centres in Mongolia and Southern Siberia lie within the Selenga River basin, including Ulaanbaatar, the capital of Mongolia, and Ulan-Ude, capital of Buryatia.

The Selenga Delta is a floodplain wetland delta, strongly influenced by hydrological and flooding processes within the Selenga River basin and along the Selenga River (Chalov *et al*., 2015). Three annual hydrological events are the primary controls on flow and discharge within the Selenga River. First, high water periods occur during periods of ice motion and the formation of ice jams, which lead to sharp, short-term rise in water levels in winter and early spring. Second, spring high water (due to melting snow and ice) begin in April and follow a monotinic wave of high water levels. Finally, rain freshets occurring post-spring melt and throughout the summer months, but primarily during July and August (Figure 2.1; Törnqvist *et al*., 2014; Garmayev *et al*., 2016). These summer rain freshets dominate the flood regimes of the Selenga River and delta (Törnqvist *et al*., 2014; Garmayev *et al.,* 2016). The summer period of peak river discharge also transports 98% of total sediment loads through the Selenga River basin, and the length of the summer flood season and degree of flood significantly influence sediment transport through the basin (Chalov and Romanchenko, 2016).

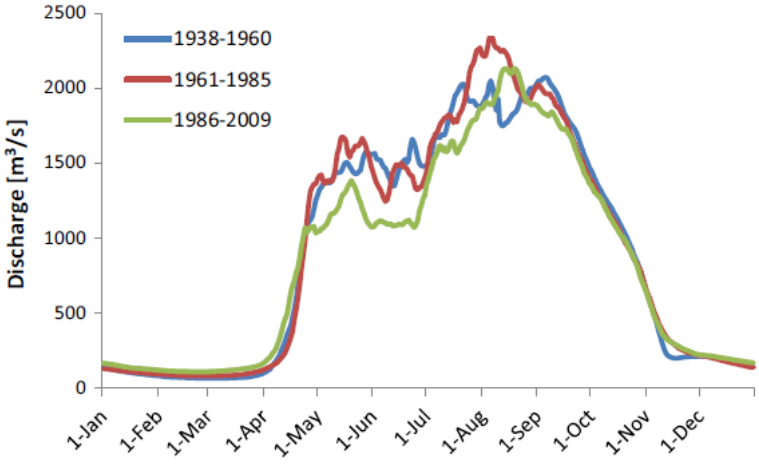

Figure 2.1. River discharge as measured between 1938 and 2009 at the closest river gauging station to the Selenga Delta, located at Mostovoy, between Selenginsk and Ulan-Ude, located ~115 km upstream of Lake Baikal along the Selenga River. Reported as mean discharge between the periods of 1938-1960, 1961-1985, and 1986-2009. (Source: Törnqvist *et al*., 2014).

The Selenga Delta consists of the fan of land containing shallow lakes, ponds, and channels which drain the Selenga River into the area between the southern and central basins of Lake Baikal. The Selenga Delta is comprised of 85% regularly flooded land (including wet meadows), 8% river branches and 8% shallow lakes (Anenkhonov and Pronin, unpublished data). The Selenga Delta is one of the most ancient river deltas in the world, with the oldest portions thought to be two to three million years old (Scholz and Hutchinson, 2000). The Selenga Delta is located in the most seismically active area of the Lake Baikal region, and many of the lakes within the Selenga River basin were formed through tectonic activity in conjunction with fluctuations in the water level of Lake Baikal (Vologina *et al*., 2010). A variety of habitat types within the Selenga Delta have been described, consisting primarily of open water/shallow aquatic habitats, and emergent herbaceous and woody wetlands. The Selenga Delta provides a critical function as part of the Lake Baikal ecosystem, providing a point of deposition, transport, or transformation for metals and contaminants flowing to Lake Baikal, as 60-70% of sediment transported from the Selenga River basin and along the Selenga River is deposited within the Selenga Delta, (Chalov *et al*., 2016). Therefore, maintaining the current structure and functioning of the Selenga Delta is crucial to protecting the ecological health of Lake Baikal.

2.1.1 Site Selection for Lake Survey

Fifteen lakes were chosen for inclusion in a contemporary study to assess possible drivers of spatial variability of limnology, biology, and pollution within shallow water bodies of the

Selenga River basin (Figures 2.2, 2.3, 2.4). The fifteen shallow lakes fall into the "shallow aquatic habitats" category, as described by Lane *et al*. (2015), and consist of submerged and floating macrophytes, surrounded by emergent, and in some cases, shrub-type vegetation. Sites located on the perimeter of the Selenga Delta are surrounded by agricultural lands, consisting primarily of livestock rearing (Figure 2.5), Location information for all lakes can be found in Table 2.1. Site photos can be found in Figure 2.6. The lakes were given unofficial names for the purposes of this scientific study, SLNG01, SLNG03 - SLNG15, and BRYT. Fourteen of the study lakes were located within the Selenga River Delta (Figure 2.2, 2.4), and one study lake, located outside of the Selenga Delta, but within the Selenga River basin (Black Lake – "BRYT"), was chosen for study due to its location in the more heavily industrialized Gusinoye region (Figure 2.3). Black Lake is one in a chain of several small, shallow freshwater lakes which formed along the previous course of the Selenga River, south of Lake Baikal (Pisarsky *et al*., 2005). Black Lake sits at the base of the Khambinsky Mountains, and receives inflows from a variety of rivers and channels to the northeast of Lake Gusinoye region. Outflow from Black Lake contributes to river flows towards Lake Gusinoye and the Selenga River (Pisarsky *et al*., 2005).

Site selection of lakes within the Selenga Delta was based on four factors, assessed in sequential order:

1. Site characteristics including minimum area and depth requirements as judged first, through aerial photos, and second, visible inspection prior to sampling;
2. Position in the Selenga Delta relative to other study lakes, to achieve a spread of sites across the two main discharge lobes of the Selenga Delta;
3. Variations in connectivity levels to the channels of the Selenga River flowing through the Selenga Delta across all study sites and into Lake Baikal;
4. Accessibility of the lake by car, row boat or motor boat.

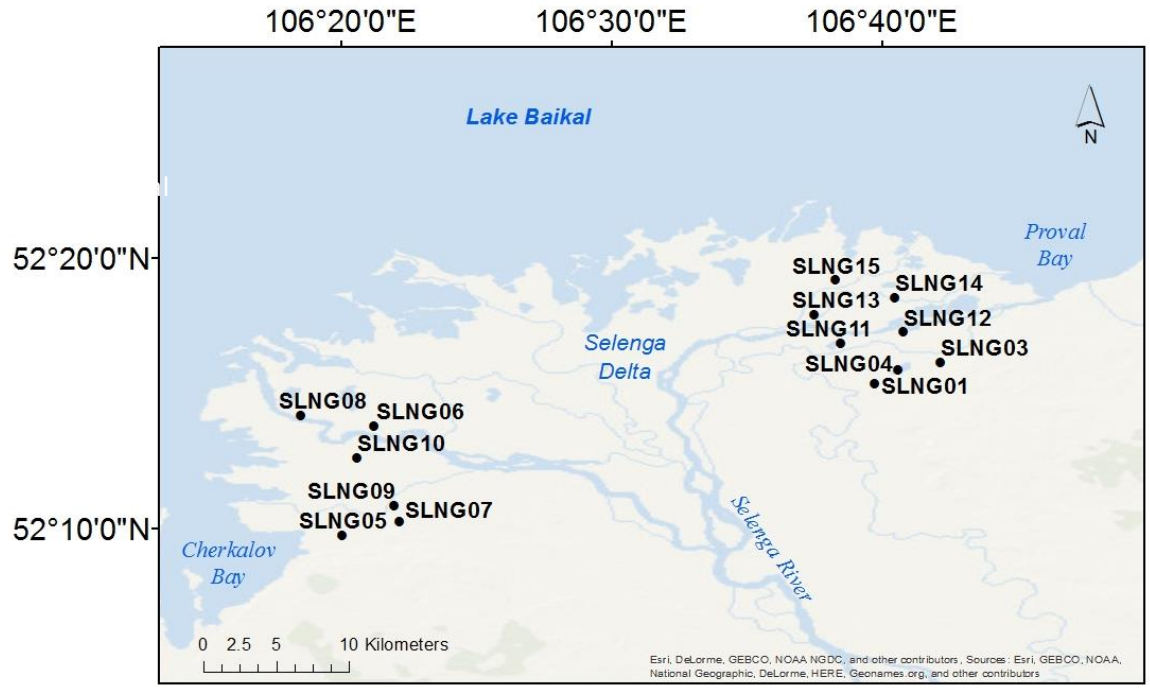

Figure 2.2. Location of all shallow lake study sites within the Selenga Delta (SLNG01, SLNG03-SLNG15)

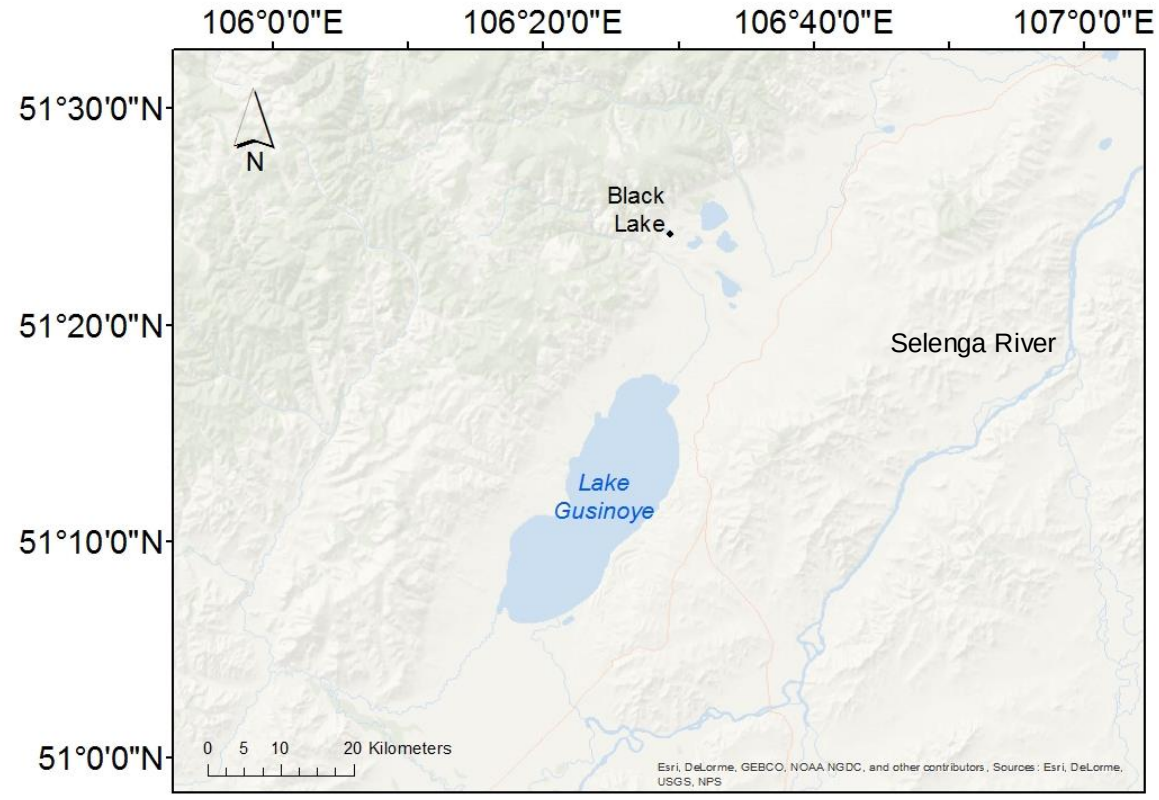

Figure 2.3. Location of Black Lake (BRYT) in the Lake Gusinoye region. See Figure 1.2 for a regional map within the Selenga River basin.

Figure 2.4a. Southwest Selenga Delta, with the six sites within this region and their situation within the delta-scape. Map source: Google Earth Pro 7.3.0, 2017 Google Inc.

Figure 2.4b. Northeast Selenga Delta, with the eight sites within this region and their situation within the delta-scape. Map source: Google Earth Pro 7.3.0, 2017 Google Inc.

Figure 2.5. Photos illustrating nearby agricultural and livestock activities on the perimeter of the Selenga Delta.

a) SLNG01

b) SLNG03

c) SLNG04

d) SLNG05

e) SLNG06

f) SLNG07

g) SLNG08

h) SLNG09

i) SLNG10

j) SLNG11

k) SLNG12

l) SLNG13

m) SLNG14

n) SLNG15

o) BRYT

Figure 2.6. Selected site photos from within the Selenga Delta and the Selenga River basin depicting differing lake types and lake environments. From row 1, left to right: a) SLNG01, b) SLNG03, c) SLNG04, d) SLNG05, e) SLNG06, f) SLNG07, g) SLNG08, h) SLNG09, i) SLNG10, j) SLNG11, k) SLNG12, l) SLNG13, m) SLNG14, n) SLNG15, o) BRYT

2.1.2 Physical Descriptions of Sites

The fifteen lakes were sampled for contemporary analyses between August 12 and September 1, 2014. All lakes included in the study were shallow, and maximum lake depth for selected sites within the Selenga Delta ranged from 55 cm to 130 cm, and maximum depth of BRYT at 2.8 m depth (Table 2.1). Mean lake depth for all sites ranged from 30 cm to 145 cm. Lake area ranged from 0.15 ha to ~85 ha. Mean lake area across sites, however, was 11.60 ha, but median lake area was 3.64 ha, as 13 of the 15 sites were smaller than 12 ha, and only two study lakes greater than 20 ha. Connectivity of sites was assessed based on on-site observations of surface water connections, aerial photos, and personal communications with local individuals. High connectivity sites are those which have a permanent connection to the Selenga River, tributaries within the Selenga Delta, or permanent inflow and outflow from other channels within the Selenga River basin. Intermittent connectivity sites are those connected to the Selenga River only during high water years, or during spring melt, while low connectivity sites are those unlikely to be connected to the Selenga River during most years. Connectivity levels for each site are shown in Table 2.1. Figure 2.7 illustrates site connectivity pathways.

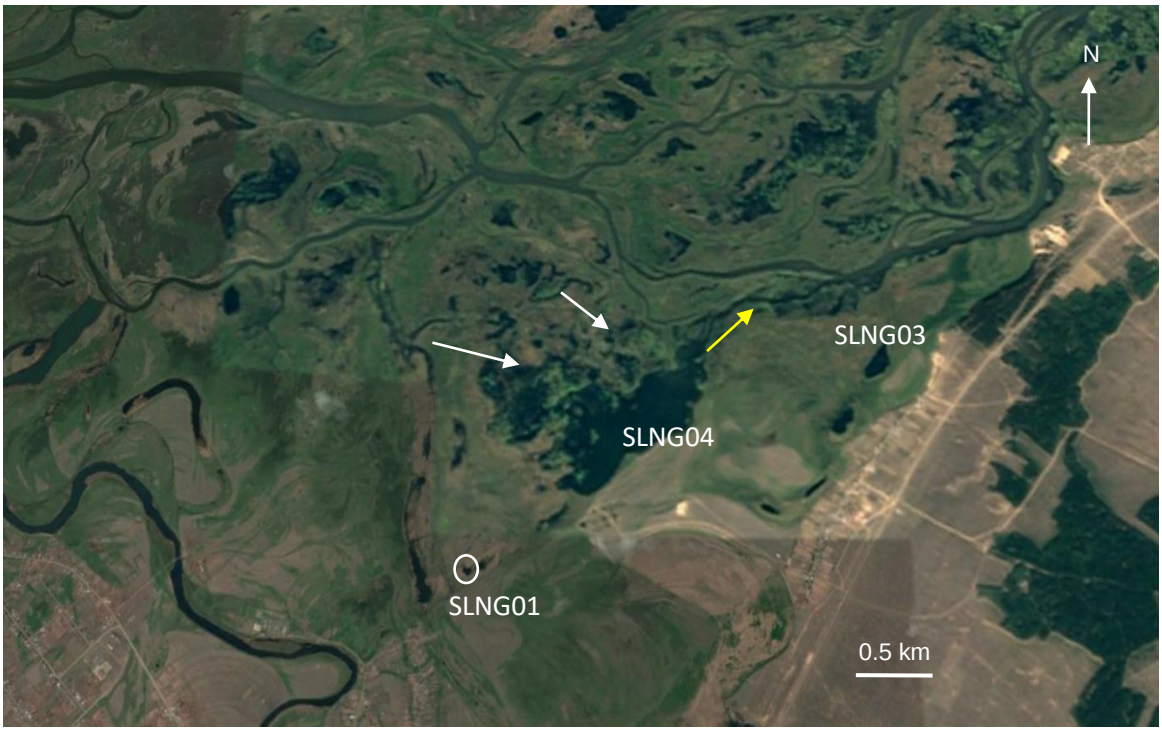

Figure 2.7a. SLNG01, SLNG03, and SLNG04 within the northeast side of the Selenga Delta. Inflows (white arrows) and outflows (yellow arrows) indicated. Note SLNG01 and SLNG03 are low connectivity systems, without inflow or outflow. Map source: Google Earth Pro 7.3.0, 2017 Google Inc.

Figure 2.7b. SLNG05, SLNG07, and SLNG09 within the southwest side of the Selenga Delta. Inflows (white arrows) and outflows (yellow arrows) indicated. Note SLNG07 and SLNG09 are low connectivity systems, without inflow or outflow. Map source: Google Earth Pro 7.3.0, 2017 Google Inc.

Figure 2.7c. SLNG06 within the southwest side of the Selenga Delta. Inflows (white arrows) and outflows (yellow arrows) indicated. Map source: Google Earth Pro 7.3.0, 2017 Google Inc.

Figure 2.7d. SLNG08 within the southwest side of the Selenga Delta. Pathways of intermittent connectivity indicated (white dashed lines). During sampling year, the areas of connectivity were intermittently flooded and marshy. Map source: Google Earth Pro 7.3.0, 2017 Google Inc.

Figure 2.7e. SLNG10 within the southwest side of the Selenga Delta. Pathways of intermittent connectivity indicated (white dashed lines). During sampling year, the areas of connectivity were intermittently flooded and marshy. Map source: Google Earth Pro 7.3.0, 2017 Google Inc.

Figure 2.7f. SLNG11 within the northeast side of the Selenga Delta. Pathways of intermittent connectivity indicated (white dashed lines). During sampling year, the areas of connectivity were intermittently flooded and marshy. Map source: Google Earth Pro 7.3.0, 2017 Google Inc.

Figure 2.7g. SLNG12 within the northeast side of the Selenga Delta. Pathways of intermittent connectivity indicated (white dashed lines). During sampling year, the areas of connectivity were intermittently flooded and marshy. Map source: Google Earth Pro 7.3.0, 2017 Google Inc.

Figure 2.7h. SLNG13 within the northeast side of the Selenga Delta. Pathways of intermittent connectivity indicated (white dashed lines). Personal communication with locals revealed that during high water years, SLNG13 is connected to the nearby branch of the Selenga. During sampling year, the area between the lake and the branch was intermittently flooded and marshy. Map source: Google Earth Pro 7.3.0, 2017 Google Inc.

Figure 2.7i. SLNG14, and SLNG15 within the northeast side of the Selenga Delta. Both SLNG14 and SLNG15 are low connectivity systems, without inflow or outflow. Map source: Google Earth Pro 7.3.0, 2017 Google Inc.

2.2 Lake Survey field methodologies

2.2.1 Physicochemical parameters

Temperature, pH, conductivity, and dissolved oxygen (DO) were measured using a HQ3od Hach multi-probe meter with Hach 1001 Intellical probes. Measurements were taken from an inflatable row boat at the deepest point in the lake, which was determined using a Platismo Echosounder. Measurements were taken at 20 cm below water surface at all sites. Secchi depth was also measured to assess light penetration in lake water columns. A 20-cm diameter quartered black and white Secchi disc attached to a 30-m measuring tape was lowered from the shaded side of the boat nearest to the deepest point. At the point at which the disc was no longer visible to the eye, the depth was recorded. The Secchi disc was then raised until it was just visible again and the mean of this and the previous depth was recorded as the final secchi depth (Preisendorfer, 1986). To account for variations in total water depth across sites, percent of total water depth was calculated for secchi depth.

2.2.2 Water chemistry

Water samples, collected from each of the 15 lakes, were analysed to determine water chemistry. The full list of water chemistry analyses and collection details can be found in Table 2.2. All sample bottles were acid washed with 2% HCl and rinsed with deionized water prior to sampling. Water was sampled from an inflatable row boat at the deepest point in the lake as determined using a Platismo Echosounder. Water was collected at 20 cm depth at all sites to avoid surface water floating particulates, submerged macrophyte and sediment contamination, and to allow a similar depth for measurements across sites regardless of total lake depth. All bottles were rinsed *in situ* with lake water three times prior to sample collection. Water chemistry sample preparation, including filtration and acid preservation, was conducted in the field, less than 24 hours following collection (Table 2.2). All water chemistry sample bottles were sealed with parafilm and electrical tape following collection or sample preparation. All samples were stored in the dark at <4°C following collection prior to analysis. See Sections 2.3.1 to 2.3.5 for details on analyses.

2.2.3 Surface sediment collection

Surface sediments were collected from the deepest point at the centre of each lake, for the analysis of contemporary sedimentary pigments, diatoms, macrofossils, geochemistry, and trace metals. Surface sediments were collected using a 1.5 m Perspex tube 6.3-cm in diameter, which was manually pushed into the bottom sediments. Total sediment depth collected was then measured, and the top 5 cm was amalgamated in a plastic bag. All surface sediment samples were stored at <4°C following collection. All water, biological, and surface sediment samples were shipped from Irkutsk, RU to London, UK immediately following the 2014 summer field season. Surface sediment data are presented and discussed in Chapter 3.

Site Name	Official Site Name	Latitude (N)	Longitude (E)	Elevation (m asl)	Area (ha)	Mean depth (cm)	Maximum depth (cm)	Connectivity level	Proximal land use/ land cover
SLNG01		52°15'23.00"	106°39'42.86"	457	0.15	36	55	Low	Agricultural
SLNG03		52°16'09.4"	106°42'10.1"	454	2.50	54	100	Low	Agricultural
SLNG04		52°15'52.5"	106°40'35.6"	455	84.94	82	130	High	Agricultural
SLNG05		52°09'46.7"	106°19'59.6"	464	7.03	75	100	High	Interior delta/marsh
SLNG06		52°13'49.0"	106°21'11.0"	461	11.09	64	120	High	Interior delta/marsh
SLNG07		52°10'16.7"	106°22'06.6"	453	0.51	53	110	Low	Agricultural
SLNG08		52°14'12.8"	106°18'27.6"	456	6.37	56	110	Intermittent	Interior delta/marsh
SLNG09		52°10'51.6"	106°21'56.8"	454	0.90	32	55	Low	Agricultural
SLNG10		52°12'38.3"	106°20'33.3"	453	9.45	50	90	Intermittent	Interior delta/marsh
SLNG11		52°16'52.8"	106°38'26.6"	451	11.34	45	90	Intermittent	Interior delta/marsh
SLNG12		52°17'17.3"	106°40'45.8"	451	3.13	53	90	Intermittent	Interior delta/marsh
SLNG13		52°17'56.1"	106°37'27.7"	457	3.60	72	120	Intermittent	Interior delta/marsh
SLNG14		52°18'32.9"	106°40'27.0"	450	3.23	44	90	Low	Interior delta/marsh
SLNG15		52°19'12.6"	106°38'16.3"	454	3.64	49	65	Low	Interior delta
BRYT	Chernoe Ozero (Black Lake)	51°24'14.2"	106°29'25.5"	453	26.61	143	280	High	Agricultural, close proximity to village

Table 2.1. Geographical location, size, depth, connectivity level, and land use type for all lakes included in the contemporary study. See Figures 2.5 and 2.6 for photos illustrating land use.

Sample	Collection and filtration	Acid preservation	Storage
Total phosphorus (TP)	Unfiltered sample		<4°C
Soluble reactive phosphorus (SRP)	Water filtered through 0.45 µm GF/F filter paper		<4°C
Mercury (Hg)	Unfiltered sample	1.25 ml suprapure HCl	<4°C
Major cations (Al^{3+}, K^{+}, Ca^{2+}, Mg^{2+}, Fe^{3+}, Sr^{2+}, Si^{4+})	Water filtered through 0.2 µm cellulose acetate filter paper	2.5 ml HNO_3 (1% total volume)	<4°C
Major anions (Cl^{-}, SO_4^{2-}, F^{-})	Water filtered through 0.2 µm cellulose acetate filter paper		<4°C
Dissolved organic carbon (DOC)	Water filtered through 0.45 µm GF/F filter paper	0.24 ml 25% H_2SO_4	<4°C
Chlorophyll *a* (Chl *a*)	Known volume of water filtered through 0.45 µm GF/F filter paper, filter paper collected for analysis, wrapped in aluminum foil		In the dark at -20°C

Table 2.2. Water chemistry parameters sampled at each site, with collection and preservation details.

2.2.4 Data collection for macrophyte communities

Macrophyte density was calculated for each site using the percent volume infested (PVI) procedure (Canfield *et al*., 1984), which provides an estimate of the density of macrophytes in the water column of a lake. Macrophyte measurements were carried out at 30 points throughout each lake along transects, bisecting the lake using an inflatable row boat. At each point, coordinates were recorded using a Etrex 30 GPS unit, water depth (D) and mean submerged plant height (M) were measured using a weighted measuring tape, and total percent submerged plant cover (C) within a 1-metre vicinity was estimated using a double-headed rake trawled along the lake bed.

$$PVI = (C \times M) / D \qquad [EQN\ 1]$$

Macrophyte species were identified, and PVI was then also calculated for individual species of submerged macrophyte. Macrophyte species observed at each site were also recorded using the abundance-based 5-1 DAFOR scale (**D**ominant, **A**bundant, **F**requent, **O**ccasional, **R**are). The DAFOR survey was conducted on a whole-site basis and included species possibly absent from the PVI survey. All submerged and emergent macrophyte species observed at the site were included in the DAFOR survey, and were ranked as either being the dominant species at the site (5), occurring in abundance (4), occurring frequently (3), often (2), or rarely (1). For confirmation of macrophyte identification, representative specimens were collected and pressed for preservation and further identification. Macrophyte data are presented and discussed in Chapter 3.

2.3 Lake survey laboratory methodologies

2.3.1 Total and Soluble Reactive Phosphorus

Prior to any phosphorus analysis, all equipment to be used was washed in a 2% HCl acid bath for a minimum of 12 hours. Total phosphorus (TP) and soluble reactive phosphorus (SRP) were analysed following the ascorbic acid method described by the American Public Health Association (1989) with a limit of detection of 10µg l^{-1}. SRP provides a measure of the biologically available phosphorus in the lake water, and the dynamics of TP and SRP are

important in shallow, nutrient-rich lakes (Bennion and Smith, 2000). Unfiltered water samples were analyzed for total phosphorus (TP) by first, undergoing microwave digestion. Ten millilitres of the water sample were mixed with 2 ml $K_2S_2O_4$ oxidizing agent and 0.2 ml 30% H_2SO_4, and digested for 15 minutes. Digested samples were then transferred to centrifuge tubes, and mixed with one drop of phenolphthalein indicator and a known volume of 4M NaOH, to achieve a faint pink colour. Samples were topped up with deionized water to 10 ml. All samples were then inoculated with 1 ml of a mixed reagent (in the ratios 5:2:2:1) of the following: 13% H_2SO_4, 1.5 g ammonium molybdate dissolved in 50 ml deionized water, 2.7 g ascorbic acid dissolved in 50 ml deionized water, and 0.34 g potassium antimonyl tartrate in 250 ml deionized water. Samples were then capped, inverted to mix, and left for approximately 2 hours to allow for a blue colour to develop. Following the two-hour reaction period, spectrophotometric analysis was carried out at an absorbance wavelength of 885 nm on a Hach CAMLAB DR/4000U spectrophotometer with a 1-cm light path. Three samples were analyzed as replicates for TP, and a set of four standards and one blank were used to create the calibration curve between 0 µg l^{-1} and 200 µg l^{-1} PO_4-P (0, 25, 50, 100 and 200 µg l^{-1}).

Soluble reactive phosphorus (SRP) followed the same methods as for TP, beginning with the inoculation with the mixed reagent of 13% H_2SO_4, 1.5 g ammonium molybdate dissolved in 50 ml deionized water, 2.7 g ascorbic acid dissolved in 50 ml deionized water, and 0.34 g potassium antimonyl tartrate in 250 ml deionized water in a 5:2:2:1 ratio. Three samples were analyzed as replicates for SRP. For SRP analysis, a set of five standards and one blank were used to create the calibration curve between 0 µg l^{-1} and 200 µg l^{-1} PO_4-P (0, 25, 50, 100, 150, and 200 µg l^{-1}). All standards for both TP and SRP analyses were created through dilutions of a phosphate stock solution of 500 µg l^{-1}, which was made up fresh from a standard phosphate solution of 50 mg KH_2PO_4 l^{-1}. Information on analytical procedures can be found in Table 2.3.

Analysis	Accuracy	Precision	Standards	Replicates	Blanks
TP	<10%	<15%	PO_4-P stock solution 500 µg l^{-1}; diluted to 25, 50, 100, and 200 µg l^{-1}	3	Deionized water
SRP	<5%	10% below 25 mg/l <5% above 25 mg/l	PO_4-P stock solution 500 µg l^{-1}; diluted to 25, 50, 100, 150, and 200 µg l^{-1}	3	Deionized water
DOC	<1%	<1%	1 x 100 ppm TOC standard	1	Deionized water
Major Cations (Ca^{2+}, Mg^{2+}, Sr^{2+}, Al^{3+}, Fe^{3+}, Si^{4+}, K^{+})	4%	<5%	Deionized water plus: Standard #1: Ca^{2+}, Mg^{2+}, Sr^{2+} Standard #2: Al^{3+}, Fe^{3+}, Si^{4+} Standard #3: K^{+}	1 for each sample	Deionized water + pure grade HNO_3
Major anions (Cl^{-}, F^{-}, SO_4^{2-})	<15%	<5%	3 standards for each anion at increasing concentrations: 18.2 MΩ pure water plus Standard #1: F^{-} Standard #2: Cl^{-} Standard #3: SO_4^{2-}	3	18.2 MΩ pure water
Hg	10% above 4 ng/l	--	1 ppb, 2 ppb, 5 ppb in 1% HCl (v:v)	--	Deionized water

Table 2.3. Information on analytical procedures used in water chemistry analysis of samples collected from SLNG and BRYT lakes.

2.3.2 Dissolved Organic Carbon

Dissolved organic carbon (DOC) water samples were analyzed at the University of Loughborough in the Department of Geography. DOC water samples were analyzed using the total organic carbon analyzer, TOC-V, which uses a combustion catalytic oxidation method, with an ASI-V autosampler (Japan Industrial Standard, 2001). Two standards and one replicate were run during the analysis for quality control. Information on sample preparations are shown in Table 2.2 and analytical procedures can be found in Table 2.3.

2.3.3 Chlorophyll-a

Chlorophyll *a* (Chl *a*) concentrations, used as a proxy for total algal biomass, were determined by analyzing pigments captured on a 0.45-µm pore size GF/F filter paper using reverse-phase high-performance liquid chromatography (HPLC). Water filteration for Chl *a* analysis was undertaken in the field. The volume of water filtered was recorded, and the filter paper was kept for analysis. The filter paper from each site was wrapped in aluminum foil and stored at -20°C at all times. All further preparation and analysis for Chl *a* occurred in the Environmental Change Laboratory at the University of Nottingham. Filter papers were kept in the dark at all times prior to and during preparation and extraction. Sample preparation and pigment extraction followed the protocol of the Environmental Change Laboratory at the University of Nottingham as follows.

First, filter papers were cut into strips and all strips from a single filter paper (sample) were placed into a single vial. To each vial, 5 ml of extraction solvent (80% HPLC-grade acetone, 15% HPLC-grade methanol, 5% nanopore deionised water) was added. Vials were then capped tightly and put in the freezer for a minimum of twelve hours to allow for the extraction of Chl *a*. Following the extracting period, the extraction solvent was decanted into an acetone-cleaned beaker. Solution was then drawn up into a 10-ml disposable syringe, and filtered through an attached 0.22 µm lock-on filter into a clean, labelled vial. Residue in the extraction vial was rinsed with HPLC-grade acetone, and the syringe-filtering procedure was repeated until the residue was no longer pigmented. Following each sample, the beaker and syringe were rinsed with analytical grade acetone. Chl *a* extraction solutions were then evaporated under nitrogen until dried. Following drying, sample vials were capped and returned to the freezer. Immediately

prior to analysis, a known volume of injection solvent was added to each dried sample extract. The dried sample extract was then dissolved completely in the injection solvent (a 70:25:5 mixture of acetone, HPLC-grade methanol, and the ion-pairing reagent – 0.75 g tetra butyl ammonium acetate, 7.7 g "Sigma®" grade ammonium acetate and 100 ml nanopore deionised water). The dissolved extract was then transferred to an autosampler vial and the volume of dissolved extract transferred was recorded.

Analysis from all 15 lakes was conducted in a single run using HPLC, along with two "green" samples, one analyzed at the beginning of the run and the other at the end of the run, utilized to check and verify retention times for specific pigments within the run. HPLC samples were analyzed using Agilent Chemstation program. Chl *a* pigment separation on the HPLC followed the Chen method utilizing acetone, methanol, acetonitrile, and ethyl acetate (Chen *et al*., 2001). Following analysis, Chl *a* was identified based on spectrum and retention time following Jeffrey *et al*. (1997). Individual Chl *a* pigment peak areas were converted to nmol l^{-1} and are reported as such.

2.3.4 Major ions

Water samples for cation analysis were analyzed in the Department of Earth Sciences, University College London, using inductively coupled plasma atomic emission spectroscopy (ICP-AES). Cations analyzed using ICP-AES included Ca^{2+}, Al^{3+}, Fe^{3+}, Mg^{2+}, Si^{4+}, Sr^{2+}, K^{+}. Control blanks (deionized water spiked with HNO_3) were run three times during analysis, at the beginning, middle and end. Three multi-standards were created at concentrations of 5 mg l^{-1}: Standard one included the cations Ca^{2+}, Mg^{2+}, and Sr^{2+}, standard two included the cations Al^{3+}, Fe^{3+}, Si^{4+}, and standard three was K^{+} only (Table 2.3). Cations were measured in intensities, and intensities of standards were calibrated as 5 mg l^{-1} to create concentration calibration regression lines for each cation using the blanks and standards. Several intensities for Ca^{2+} and Mg^{2+} were above the correlated 5 mg l^{-1}, and therefore extrapolations beyond the 0 – 5 mg l^{-1} regression lines were performed. Two replicates were run for every sample to estimate measurement error. Information on sample preparations are shown in Table 2.2 and analytical procedures can be found in Table 2.3.

Water samples for anion analysis were analyzed in the Department of Earth Sciences, University College London, using ion chromatography. Anions analyzed using ion

chromatography included F^-, Cl^-, and SO_4^{2-}. Control blanks (deionized water) were run five times during the analysis, once at the beginning, twice in the middle and twice at the end of the analysis. Three standards were included for each anion analyzed, and calibration regression lines created for each anion, the same as for each cation. Two replicates were run for three randomly selected samples (SLNG01, SLNG04, and SLNG09) to estimate measurement error. Concentrations are reported as mg l^{-1}. Measurements errors are reported in Table 2. 3. Total sum of ions (cations and anions) are expressed in milliequivelants per litre (meq l^{-1}).

2.3.5 Mercury water analysis

Water samples were chemically prepared for analysis of mercury (Hg) with the addition of 0.25 ml concentrated HCl (Romil, pure grade) and 0.25 ml 0.1N BrO_3^-/Br^- (purified), and sealed for 30 minutes, followed by the addition of 15 µl 12% $NH_2OH{\cdot}HCl$. Samples were analysed for Hg using gold trap cold vapour-atomic fluorescence spectrometry (CV-AFS) following reduction with $SnCl_2$ (US EPA, 2002). Detection limits for the method are 0.2 ng l^{-1}. Standard solutions and quality control blanks were measured in every three samples to monitor measurement stability (Table 2.3). Information on sample preparations are shown in Table 2.2 and analytical procedures can be found in Table 2.3.

2.4 Methods for statistical analysis of shallow lake water chemistry

All environmental variables measured in SLNG and BRYT lakes were assessed for normal distribution and equal variances. Several variables were found to be not normally distributed: Chl *a*, SRP, conductivity, aluminum, iron, strontium, magnesium, calcium, potassium, fluoride, and chloride. These were log transformed to normalize their distribution. Following log transformation, normal distribution was achieved for all environmental variables. Correlation matrices were then assessed between all environmental variables using Pearson Product Moment Correlations (PPMC). Tests for normal distribution and all correlation analyses were performed using SPSS 22.0 (IBM Corp., 2013). To assess the significance of connectivity variations across sites on spatial variations in limnological properties, Kruskal-Wallis and Mann-Whitney U tests were conducted on the following variables: connectivity categories tested were “high connectivity”, “intermittent connectivity”, and “low connectivity”. See Section 2.1.3 for

description of site connectivity levels. Kruskal-Wallis and Mann-Whitney-U tests were performed using SPSS 22.0 (IBM Corp., 2013).

Spatial patterns in the contemporary limnological data were explored using unconstrained ordinations (principal components analysis (PCA)), with data being centred and standardized. Within the PCA, sites were coded according to connectivity levels (high connectivity, intermittent connectivity, and low connectivity) to assess the spatial distribution and clustering of sites with similar connectivity levels. The PCA was performed using Canoco5 (ter Braak and Šmilauer, 2014).

2.5 Contemporary limnology of Selenga River basin shallow lakes - Results

2.5.1 Physicochemistry of lakes

Physico-chemical results for all SLNG and BRYT lakes are shown in Figure 2.8. All lakes are circumneutral to alkaline with respect to pH measured *in situ*. The range of pH across all study sites was 7.11 to 10.17. Conductivity ranged from 162 µS cm^{-1} to 448 µS cm^{-1}, with a mean conductivity across all sites of 231 µS cm^{-1}. The maximum conductivity of 448 µS cm^{-1} occurred at SLNG01. Minimum DO concentration was 0.81 mg l^{-1} found at SLNG09, while maximum DO concentration was found to be 9.66 mg l^{-1} at SLNG08. Secchi depth varied across sites, but was generally 100% of the water depth, indicating that light was able to penetrate to the bottom of the lake at most sites. This has implications for submerged macrophyte growth, which is an important ecosystem determinant. However, at four sites, SLNG01, SLNG06, SLNG15, and BRYT, light did not penetrate to the bottom of the lake, and barely penetrated through one-fifth of the water column at BRYT.

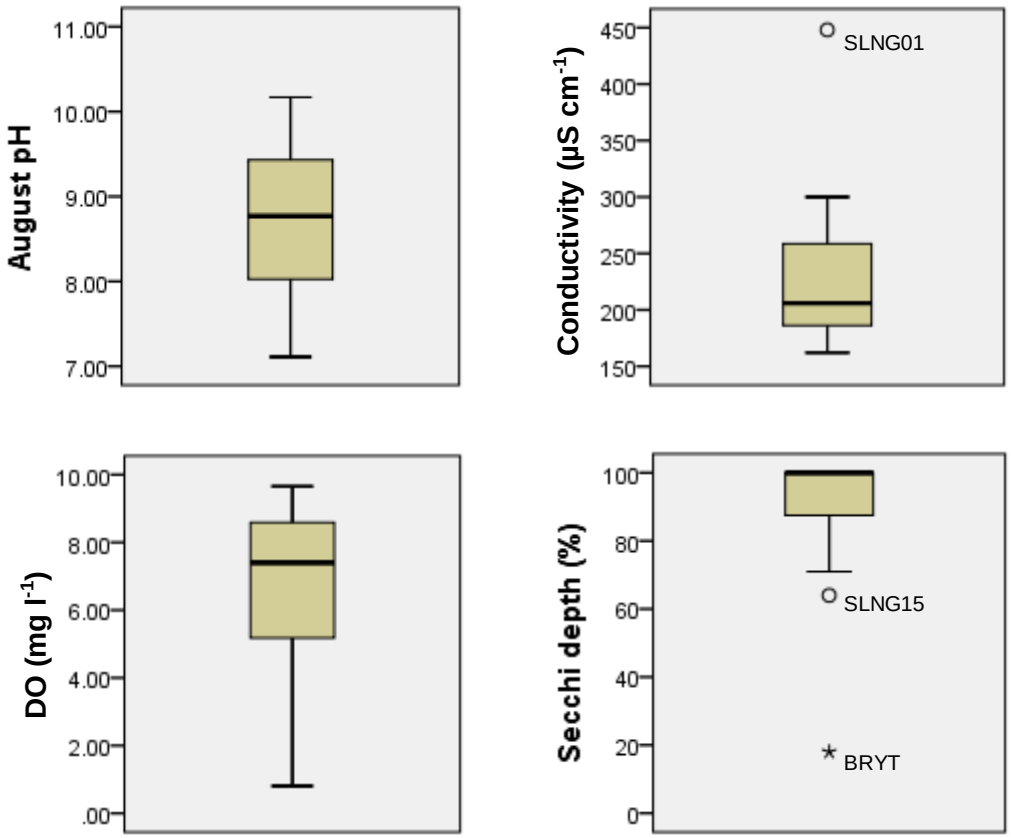

Figure 2.8. Boxplots of physicochemical properties of SLNG and BRYT study lakes. Secchi depth was recorded as proportion of water column through which light passes. i.e. 100% secchi depth was the lake bottom. Medians (bold line), 1st and 3rd quartiles, minima, maxima, and outliers (1.5 x interquartile range) are displayed. (○) indicate outliers and (*) indicate extreme outliers.

2.5.2 Nutrient water chemistry of lakes

Nutrient water chemistry results are shown in Figure 2.9. Minimum TP across study sites was 48.20 µg l^{-1} (SLNG10), and maximum TP was 342.2 µg l^{-1} (SLNG14), with mean TP across sites of 142.2 µg l^{-1}. Soluble reactive phosphorus (SRP) ranged from 7.29 µg l^{-1} (SLNG01) to 231.57 µg l^{-1} (SLNG14), with a mean SRP concentration of 48.92 µg l^{-1} across all sites. DOC was high in all lakes, with a mean DOC of 14.32 mg l^{-1}. DOC across sites ranged from a minimum of 5.71 mg l^{-1} (SLNG10) to a maximum of 28.34 mg l^{-1} (SLNG15). Mean Chl *a* concentration across all sites was 7.40 nmol l^{-1}, and Chl *a* ranged across sites from 0.74 nmol l^{-1} (SLNG13) to 30.52 nmol l^{-1} (SLNG03).

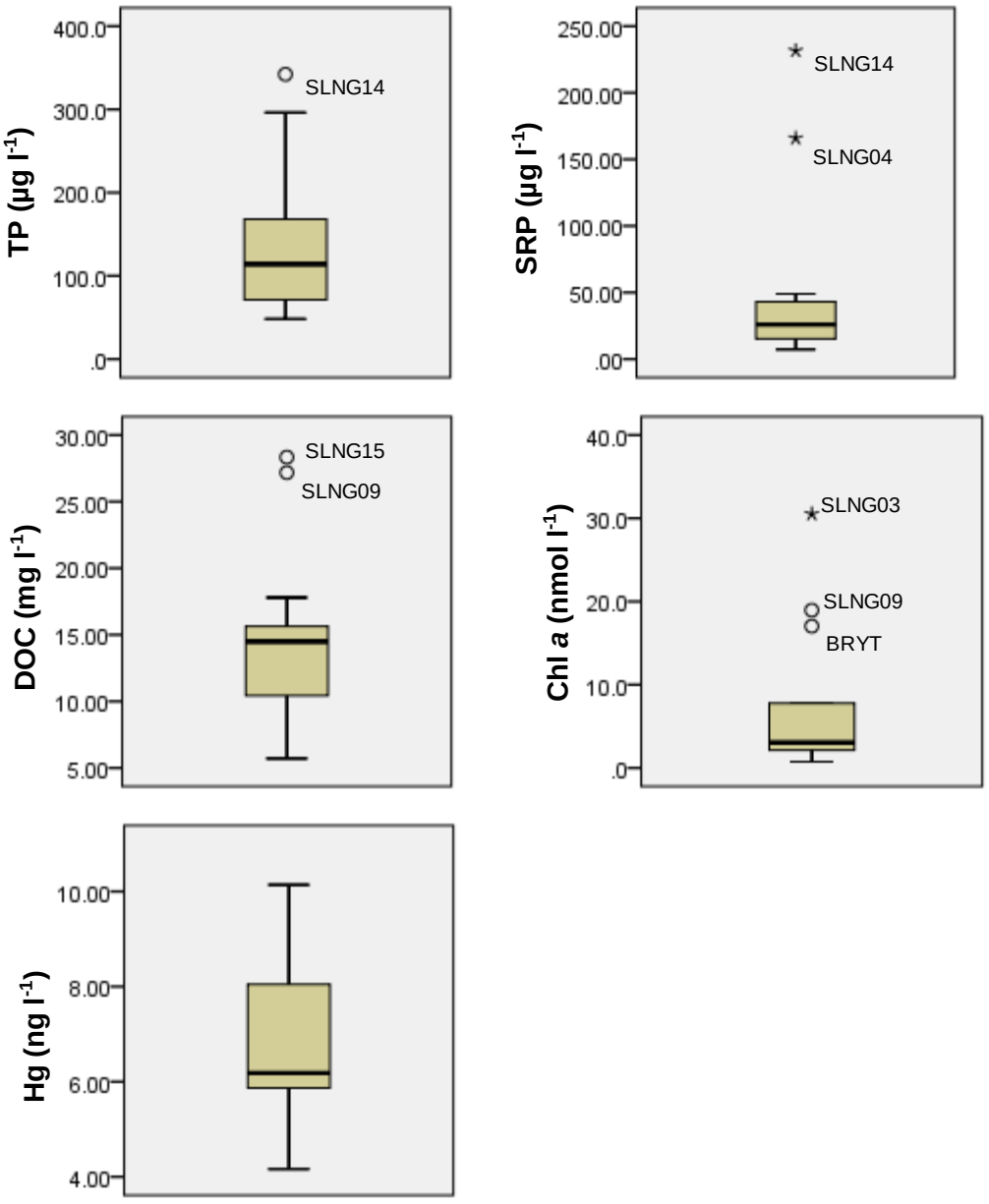

Figure 2.9. Boxplots of nutrient and mercury water chemistry of SLNG and BRYT study lakes. Medians (bold line), 1st and 3rd quartiles, minima, maxima, and outliers (1.5 x interquartile range) are displayed. (○) indicate outliers and (*) indicate extreme outliers.

2.5.3 Mercury concentrations in lakes

Mercury concentrations in lake water range from 4.16 ng l^{-1} (BRYT) to 10.14 ng l^{-1} (SLNG14), with a mean concentration across all lakes of 6.80 ng l^{-1} (Figure 2.9). Mercury concentrations are highest and more variable in lakes on the east side of the Delta, and are quite similar amongst lakes on the west side of the Delta. BRYT, the only lake outside of the Selenga Delta, has the lowest mercury concentration.

2.5.4 Major ions in lakes

All results from the major cations analysis are presented in Figure 2.10. Maximum concentrations of Ca^{2+}, Fe^{3+}, Mg^{2+}, Si^{4+}, and Sr^{2+} all occur at SLNG01, while maximum concentration of K^{+} was found at SLNG13, and maximum concentration of Al^{3+} occurred at SLNG05. Minimum concentrations of Mg^{2+} and Sr^{2+} occurred at SLNG07, while minimum concentrations of Ca^{2+} and Fe^{3+} occur at BRYT. Minimum concentration of Al^{3+} was found at SLNG13, minimum concentration of K^{+} at SLNG04, and minimum concentration of Si^{4+} at SLNG08. Mean Al^{3+} concentration across all Selenga River basin lakes was 0.029 mg l^{-1}, mean Ca^{2+} concentration across all lakes was 15.0 mg l^{-1}, mean Fe^{3+} concentration across all lakes was 1.23 mg l^{-1}, mean K^{+} concentration across all lakes was 1.53 mg l^{-1}, mean Mg^{2+} concentration across all lakes was 6.34 mg l^{-1}, mean Si^{4+} concentration across al lakes was 0.29 mg l^{-1}, and mean Sr^{2+} concentration across all lakes was 0.18 mg l^{-1}. The cation with the highest concentrations across all sites within the Selenga Delta was Ca^{2+}, followed by Mg^{2+}. However, at BRYT, Mg^{2+}occured at slightly higher concentrations than Ca^{2+}.

All results from major anion analysis are presented in Figure 2.10. Mean F^{-} concentrations across all Selenga River basin sites was 0.58 mg l^{-1}, with minimum concentration of 0.26 mg l^{-1} occurring at SLNG06, and maximum concentration of 2.23 mg l^{-1} occurring at BRYT. The high F^{-} concentration at BRYT was an outlier, and within the Selenga Delta, the maximum F^{-} concentration was 1.02 mg l^{-1} at SLNG15. Mean Cl^{-} concentration across all sites was 1.22 mg l^{-1}, and ranged from a minimum of 0.29 mg l^{-1} at SLNG04 to a maximum of 6.28 mg l^{-1} at SLNG03. Finally, SO_4^{2-} concentration across all Selenga River basin sites had a mean of 2.15 mg l^{-1}, and ranged from 0.064 mg l^{-1} at SLNG03, to a basin maximum of 6.74 mg l^{-1} at BRYT, and a Selenga Delta maximum of 6.22 mg l^{-1} at SLNG10.

When ion concentrations are converted to meq l^{-1}, relative proportions of each ion within the lake water may be assessed. Major ion concentrations in meq l^{-1} and cation and anion sums are presented in Figure 2.11. Total cations range from 0.70 meq l^{-1} (SLNG07) to 3.56 meq l^{-1} (SLNG01), and total anions range from 0.050 meq l^{-1} (SLNG09) to 0.27 meq l^{-1} (BRYT). Calcium cations dominate the ∑cation balance within the Selenga River basin at ten out of the fifteen sites, always followed by Mg^{2+}, while Mg^{2+} was the dominant cation at the remaining five sites (SLNG03, SLNG09, SLNG13, SLNG15, and BRYT), always followed by Ca^{2+} in abundance.

Study sites form four groups with respect to the order of dominating major anions. Group 1 contains SLNG03, SLNG08, SLNG13, and SLNG14, with anions on the order of $Cl^- > F^- > SO_4^{2-}$. Group 2 contains sites SLNG01, SLNG09, and SLNG15, and anions order as $F^- > Cl^- > SO_4^{2-}$. Group 3 consists of sites SLNG04, SLNG07, SLNG11, and BRYT, and anions order $SO_4^{2-} > F^- > Cl^-$, and Group 4 contains sites SLNG05, SLNG06, SLNG10, and SLNG12, with anions ordering $SO_4^{2-} > Cl^- > F^-$.

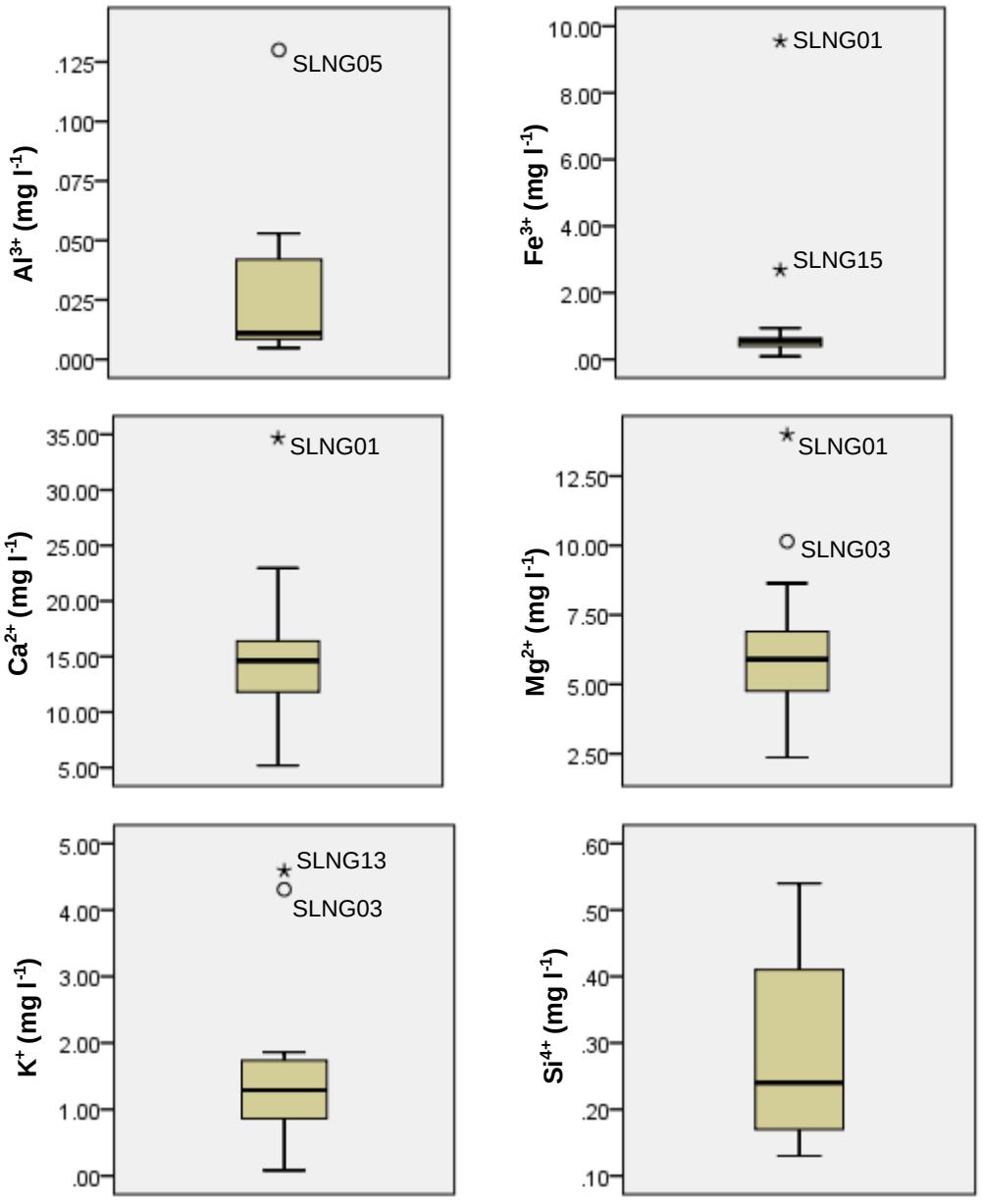

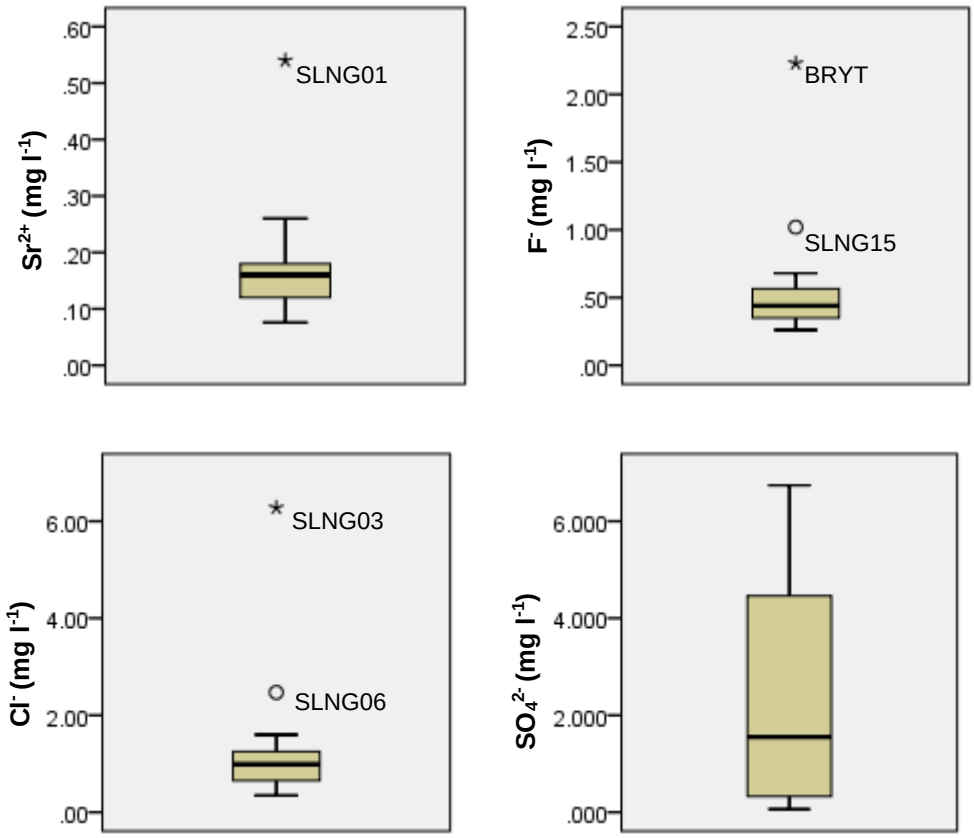

Figure 2.10. Boxplots of major cation and anion concentrations for all SLNG and BRYT lakes. All concentrations are recorded as mg l^{-1}. Medians (bold line), 1st and 3rd quartiles, minima, maxima, and outliers (1.5 x interquartile range) are displayed. (○) indicate outliers and (*) indicate extreme outliers.

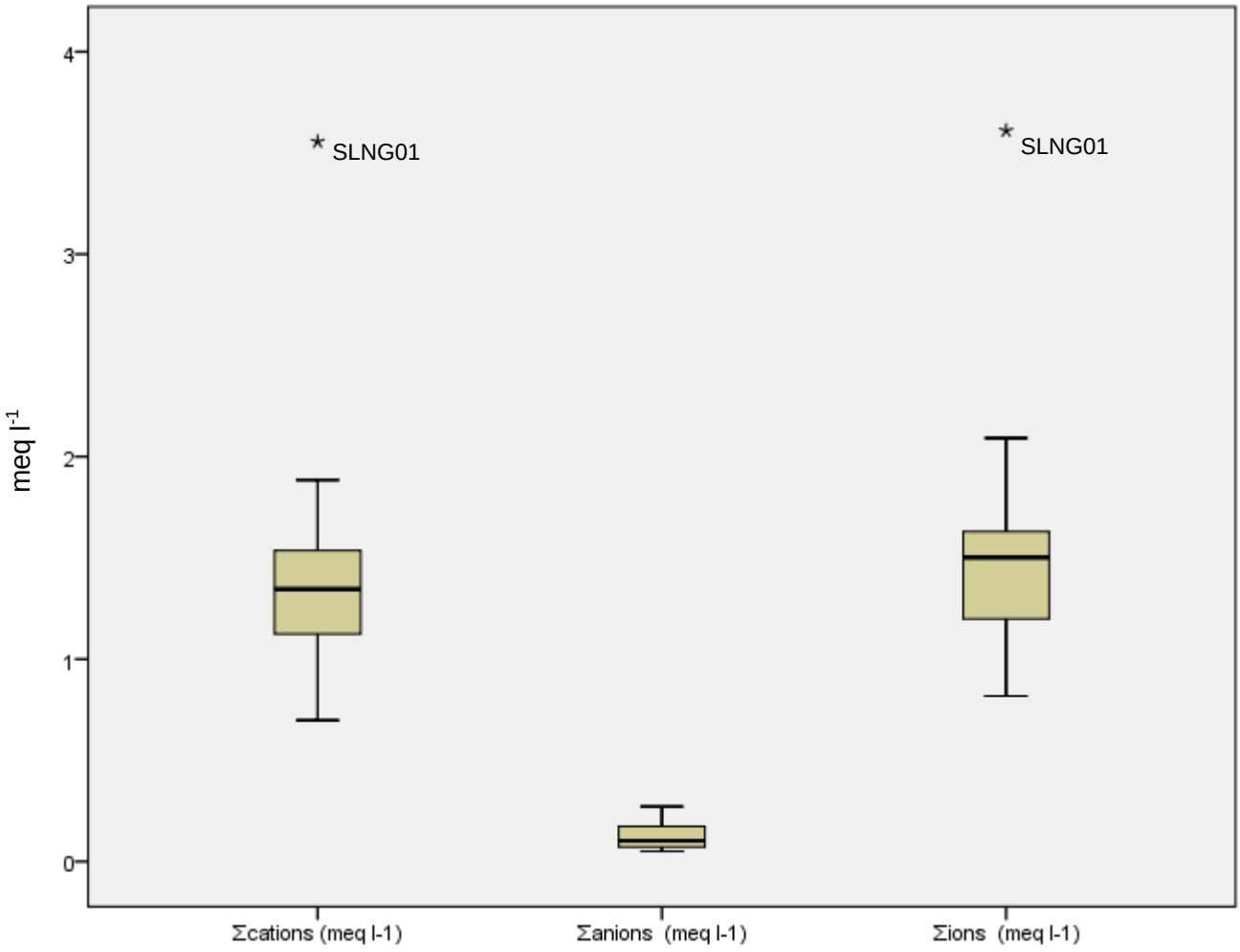

Figure 2.11. Boxplots of total cations, total anions, and total ions for all SLNG and BRYT lakes. All concentrations are recorded as meq l^{-1}. Medians (bold line), 1st and 3rd quartiles, minima, maxima, and outliers (1.5 x interquartile range) are displayed. (*) indicates extreme outliers.

2.5.5 Correlations and spatial trends in limnological variables across Selenga River basin lakes

As determined through the use of PPMC matrices, several environmental variables were found to be significantly correlated ($p<0.01$). All significant correlations are positive, with the exception of one: Fe^{3+} concentrations and lake water pH are significantly negatively correlated (-0.742). Significant positive correlations exist between Hg and SRP, magnesium and conductivity, magnesium and silicon, chloride and potassium, and strontium with conductivity, TP, calcium, magnesium, iron, and silicon. Significant ($p<0.01$) results of the Pearson Correlation matrix can be found in Table 2.8.

	TP	***SRP***	***Conductivity***	***pH***	***Ca^{2+}***	***Fe^{3+}***	***Mg^{2+}***	***K^{+}***	***Si^{4+}***	***Sr^{2+}***	***Cl^{-}***	***Hg***
TP	1											
SRP	0.489	1										
Conductivity	0.43	-0.298	1									
pH	0.099	0.570	-0.282	1								
Ca^{2+}	0.601	0.03	0.35	-0.404	1							
Fe^{3+}	0.379	-0.39	0.595	**-0.742**	0.627	1						
Mg^{2+}	0.265	-0.275	**0.844**	-0.228	0.47	0.543	1					
K^{+}	0.033	-0.131	0.307	-0.195	0.485	0.418	0.627	1				
Si^{4+}	0.352	0.019	0.502	-0.213	0.51	0.475	**0.666**	0.444	1			
Sr^{2+}	**0.645**	-0.036	**0.696**	-0.305	**0.881**	**0.668**	**0.777**	0.554	**0.729**	1		
Cl^{-}	-0.023	0.051	0.236	-0.074	0.28	0.117	0.42	**0.731**	0.184	0.328	1	
Hg	0.536	**0.648**	-0.073	0.085	0.336	0.199	0.027	0.315	0.174	0.267	0.081	1

Table 2.4. Pearson Correlation matrix values for SLNG and BRYT water chemistry variables. Bold numbers indicate significance where $p<0.01$.

Principal components analysis (PCA) was conducted on the contemporary limnological data across the 15 study sites to explore patterns in the environmental properties of the shallow lakes from the Selenga River basin. Within the initial PCA, SLNG01 presented as a positive outlier along both PCA axes 1 and 2 (Figure 2.12), strongly associated with higher concentrations of most major cations and conductivity (Figure 2.10 - 2.12), and so the PCA was re-run without this site. PCA with SLNG01 removed showed that 46.3% of variation was explained by the first two PCA axes (Table 2.5). Several major cations and anions were most strongly associated with PCA axis 1, with Cl^-, Si^{4+}, Sr^{2+}, and K^+ positively associated with PCA axis 1, and SO_4^{2-} negatively associated the axis 1 (Figure 2.13). Most low connectivity sites plotted most positively along PCA axis 1, with the exception of SLNG07, which plotted most negatively, and associated with higher concentrations of SO_4^{2-} (Figure 2.13). PCA axis 2 was most strongly associated with decreasing concentrations of F^-, and increasing DO concentrations (Figure 2.13). Most intermittent and high connectivity sites were negative along PCA axis 1, associated with lower concentrations and values of most major ions and conductivity (Figure 2.13).

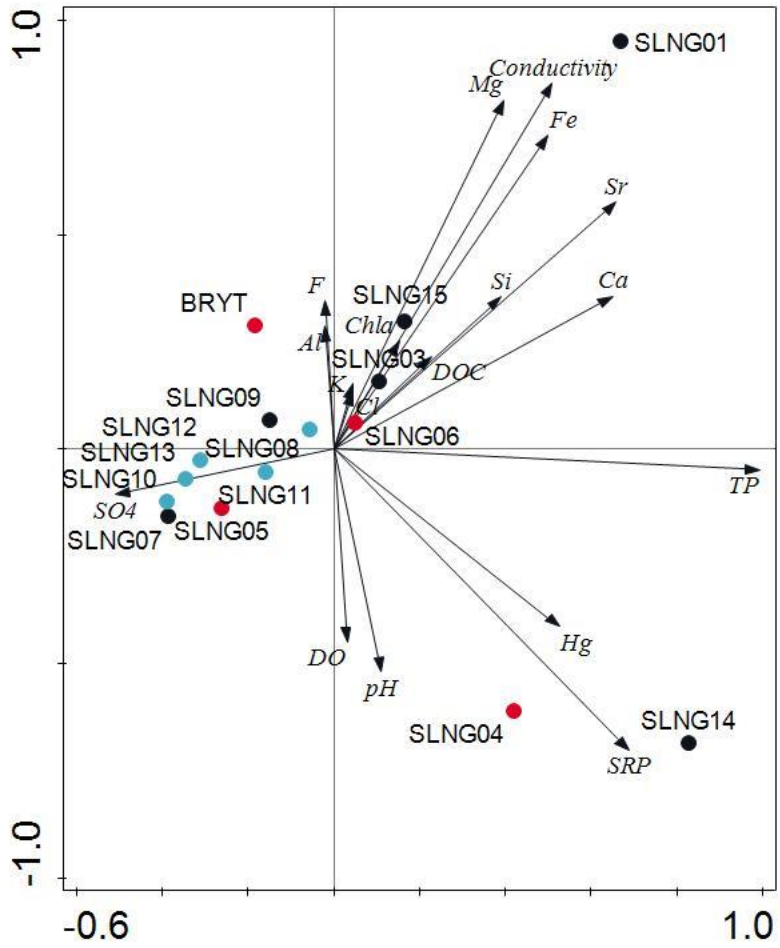

Figure 2.12. Initial PCA biplot of SLNG and BRYT sites with limnological properties (vectors). Sites are colour-coded for connectivity levels: low connectivity (black), intermittent connectivity (light blue), and high connectivity (red).

	Axis 1	***Axis 2***	***Axis 3***	***Axis 4***
Eigenvalues	0.2729	0.1897	0.1378	0.1233
Explained variation (cumulative)	27.3	46.3	60.0	72.4

Table 2.5. PCA summary table for SLNG and BRYT contemporary limnological data with SLNG01 removed. Eigenvalues and cumulative explained variation for the first four PCA axes are stated.

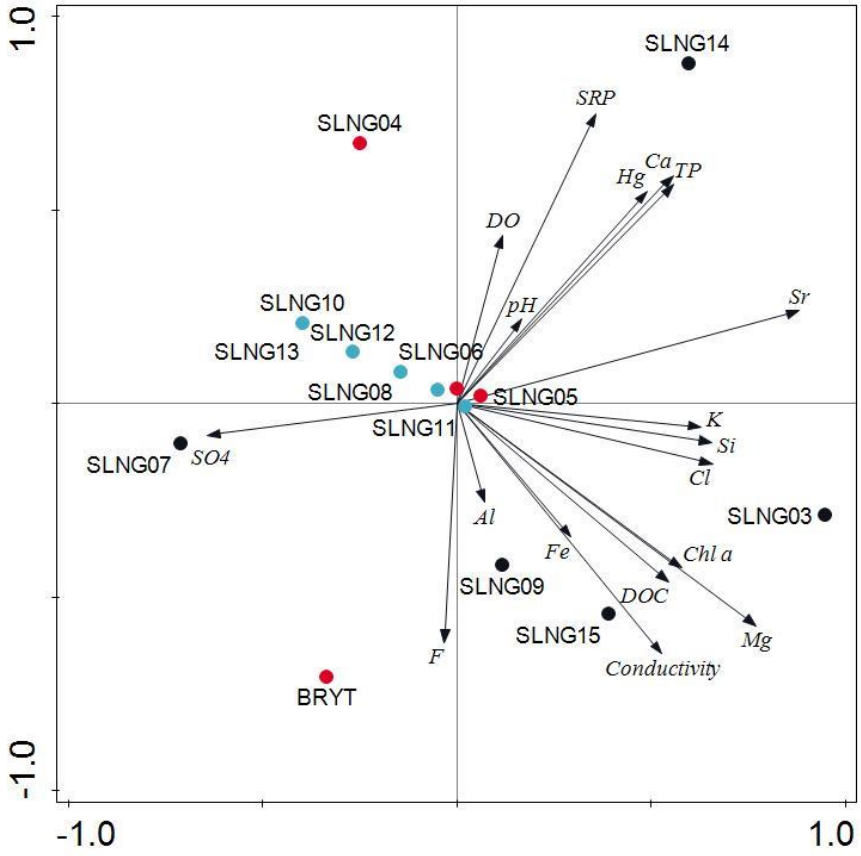

Figure 2.13. PCA biplot of SLNG and BRYT sites with limnological properties (vectors), with SLNG01 removed. Sites are colour-coded for connectivity levels: low connectivity (black), intermittent connectivity (light blue), and high connectivity (red).

Assessments to test the significance of connectivity variations on limnology of the shallow lakes indicated that of all variables tested, Fe^{3+} concentrations in surface waters was the only limnological variable to vary significantly depending on connectivity levels (Table 2.6). Mann-Whitney U tests revealed that significance was found when low connectivity sites were compared to those with intermittent and high connectivity as a single group (Table 2.6). Any significance of connectivity levels disappeared when intermittent connectivity sites were compared to either high connectivity or low connectivity sites.

Limnological variable	*Connectivity comparisons*	*MWU p-value*	*KW p-value*
Fe^{3+}	High connectivity vs. intermittent connectivity vs. low connectivity		0.022
Fe^{3+}	High/intermittent connectivity vs. low connectivity	**0.008**	
Fe^{3+}	High connectivity vs. low connectivity	0.019	
Fe^{3+}	Intermittent connectivity vs. low connectivity	0.045	
Fe^{3+}	Low/intermittent connectivity vs. high connectivity	0.040	
Dissolved oxygen	High/intermittent connectivity vs. low connectivity	0.036	
Sulphate	High/intermittent connectivity vs. low connectivity	0.018	

Table 2.6. Results from Mann-Whitney U (MWU) and Kruskal-Wallis (KW) tests, assessing the significance of variations in connectivity levels on contemporary limnological variables from the Selenga River basin shallow lakes. Only those test results with p-value <0.05 are reported. Significant test results ($p \leq 0.01$) are in **bold**.

2.6 Discussion

2.6.1 Limnological spatial variability across the Selenga River basin

Lake water pH is controlled by several factors, including bedrock geology and soil characteristics, photosynthesis, respiration, and decomposition within the lake, evapotranspiration, and content of wet and dry deposition (Wetzel, 2001). Lakes within the current study range from circumneutral to alkaline. The underlying bedrock in the Selenga River basin in the vicinity of the Selenga Delta and Black Lake is granite (See Section 1.4.1), which would likely lead to lower buffering capacities, lower weathering of material, and circumneutral to weakly acidic aquatic systems. As all lakes included in this study are shallow, with light penetration through most of the water column, and with high macrophyte abundance, the pH will tend to increase in the summer months due to the removal of CO_2 with plant photosynthesis (Talling, 1976). This is a likely reason for the high alkaline pH of lakes in a region characterized by granite bedrock. Changes in pH of this nature are most often seasonal, with fluctuations occurring throughout the year, and from year to year. Seasonal fluctuations in pH are noted in

other freshwater bodies, and attributed to annual CO_2 budgets (Ajioka, 2014). Further, increased transport of Ca^{2+} to lakes may lead to increased pH levels, which may arise from increased runoff to the lakes from basin soils, or increased weathering of silicate rocks in the basin (Wetzel, 2001).

In the PCA with all sites included, TP has a strong influence on the variability along PCA axis 1 (Figure 2.12). All study lakes within the Selenga River basin are highly productive, with six sites classified as eutrophic, and nine sites classified as hypereutrophic with concentrations greater than 100 µg TP l^{-1} (OECD, 1982). High nutrient status of all sites within the Selenga River basin is most likely a result of the agricultural activities in the region, which would lead to an increased flux of nutrients such as phosphorus and nitrogen to the Selenga River and other water bodies within the region (Carpenter *et al*., 1998). However, internal geochemical mechanisms may contribute to increasing phosphorus concentrations in lake systems, as phosphorus release from sediments into the water column have been observed with changes in pH and redox conditions at the sediment-water interface, with particularly evident increases in phosphorus release with increasing pH and reducing conditions (Koski-Vahala *et al*., 2001; Wu *et al*., 2014). Sites with lower TP concentrations are more similar to each other than sites with higher TP concentrations (TP>150 µg l^{-1}). Sites with TP above 150 µg l^{-1} include lakes SLNG01, SLNG03, and SLNG15, which appear to be strongly associated with higher ionic properties (including conductivity, cation, and anion concentrations), and SLNG04 and SLNG14, which have high pH, Hg, and DO concentrations, and very high SRP concentrations, indicating these two sites have the highest levels of biologically available phosphorus. Moreover, SRP comprises over 60% of the TP concentration at both SLNG04 and SLNG14. Conversely, SLNG01, a site which also has very high TP concentration, has the lowest SRP concentration across all study sites, comprising only 2.5% of total phosphorus. SRP:TP ratios are rather unpredictable below 500 µg l^{-1} TP (Dodds, 2003), however as mentioned above, high lake water pH can lead to increased release of phosphorus from lake sediments to the water column. High pH at SLNG04 and SLNG14 may therefore be attributed to the high proportions of SRP relative to TP, both of which have pH >9.8, while it is possible that a lower pH of 7.11 at SLNG01 (the lowest pH across the study sites) may result in relatively lower solubility of phosphorus, despite high concentrations of TP, and hence less biologically available phosphorus in the water

column. Further, Wu *et al*. (2014) found that the least amount of phosphorus was released from sediments under neutral pH.

When the outlying study site, SLNG01, is removed from the PCA, variations in major ion concentrations had a strong influence on the site variability along PCA axis 1 (Figure 2.13). Lake water cation and anion concentrations are most often controlled by bedrock and catchment soils, however variability in the major ions between study sites within close proximity is likely due to hydrological variability (related to degree of connectivity), placement within the landscape, and/or proximity to pollution sources, including agriculture and industry (Clow and Sueker, 2000; Anderson *et al*., 2001). Calcium and magnesium cations are the most common major cations at all Selenga River basin study sites. Ca^{2+} and Mg^{2+} are common cations found in surface water, while Ca^{2+} is a cation strongly linked with alkalinity in freshwater environments (Gorham *et al*., 1983). However, there is increased potential for higher Ca^{2+} and Mg^{2+} concentrations at study sites within the Selenga River basin due to agricultural runoff to lakes (Potasznik and Szymczyk, 2015). Moreover, Ca^{2+} concentrations within the study lakes are similar to, or higher than, those from the Selenga River and Lake Baikal. Major cation concentrations in Lake Baikal, Selenga River, and Selenga Delta channels are in the order: $Ca^{2+}>Mg^{2+}>K^{+}$ (Pannizo *et al*., unpublished data). Calcium ions tend to dominate in low-mineralized waters, while higher water mineralization tends to favour the dominance of Mg, as Ca tends to precipitate out at higher conductivities due to its lower solubility threshold (Gorham *et al*., 1983; Heglund and Jones, 2003). This can be seen in the Selenga River basin dataset, as with increasing conductivity the ratio of Ca:Mg (meq l^{-1}) decreases, indicating a relative increase in Mg^{2+} and decrease in Ca^{2+} in surface waters.

The shallow lakes of the Selenga River basin are surrounded by productive soils, subject to low precipitation amounts, high rates of evapotranspiration, and varying levels of connectivity (Karthe *et al*., 2014). These variables may contribute to higher conductivities and cation concentrations in some study sites due to concentrating of solutes. Significant correlations were observed in the PPMC and PCA between conductivity and cations, as is often observed (e.g. Gorham *et al*., 1983; Anderson *et al*., 2001; Heglund and Jones, 2003), as conductivity is a measurememnt of ionic strength, and is likely indicative of the importance of evaporative processes for the geochemistry of the Selenga River basin lakes. There is a significant positive

correlation between conductivity with Mg^{2+} and Sr^{2+} concentrations, and Sr^{2+} concentrations are significantly positively correlated with most measured cations. The study lake with the highest conductivity measurement is SLNG01, at 448 µS cm^{-1}. SLNG01 also contains the highest concentrations of five of the seven measured cations (Ca^{2+}, Sr^{2+}, Mg^{2+}, Si^{4+}, and Fe^{3+}). High conductivity and cation concentrations are likely due to the hydrological status of SLNG01, that being a low connectivity system, without surface water connection to the Selenga River or other body of water, it is likely dominated by strong evaporative processes, resulting in a concentrating of solutes within the lake during the summer. For these reasons, SLNG01 separates from the other study sites along PCA axes 1 and 2, and is associated most strongly with increasing cation concentrations in the PCA. Extreme values of conductivity on both ends of the spectrum correlate well with high and low values of total ions. This strengthens the conclusion that evaporative processes, as related to connectivity levels, may dictate a high degree of ionic composition variability between study sites.

Major anion Groups 1 and 2, which consist of sites dominated by either F^- or Cl^- with low concentrations of SO_4^{2-}, consist entirely of sites which are low connectivity basins or intermittently connected sites. Chloride ions within Group 1 make up 39 - 85% of the three major anions measured, and F^- within Group 2 comprises 56 - 63% of the major anions at these sites. Moreover, major anion Groups 3 and 4, dominated by SO_4^{2-}, consist primarily of sites with high connectivity or intermittent connectivity. Sulphate anions at sites within Groups 3 and 4 are present at proportions of 50 – 74%. This is in contrast to sites within Groups 1 and 2, which have lower relative concentrations of SO_4^{2-}, between 0.6 – 28%. Within Groups 1 and 2, low connectivity sites, without surface connection to the Selenga River, are at the lower end of the range, between 0.6 – 9% SO_4^{2-} while the partially connected sites are between 13 - 28 % SO_4^{2-}. Therefore, it is likely that the distinction between dominating anions is due to the connectivity of sites, with most sites with low or no connectivity with the Selenga River have higher (dominating) concentrations of F- and Cl^-, likely due to higher levels of evapotranspiration occurring at these sites (Kelly *et al*., 2012), while all sites with high levels of connectivity and some sites with partial connectivity have higher concentrations of SO_4^{2-}. The higher levels of sulphate in the open sites are likely due to riverine influence. Sulphate dominance is common in both hard waters and deeper water bodies (Anderson *et al*., 2001; Wetzel *et al*., 2001), and is

likely to result from weathering. Moreover, SO_4^{2-} is the dominant anion in Lake Baikal and Selenga River waters (Pannizo *et al*., unpublished data).

Fluoride concentrations at BRYT are higher than those found in the study sites within the Selenga Delta, and relatively high when compared to concentrations of the anion found in surface waters, which typically does not exceed 1.0 mg l^{-1} (McNeely *et al*., 1979; Wetzel, 2001). Fluoride may be high due to groundwater influences, or agricultural runoff. Further, aluminum smelters may release fluoride to the environment, and may be the reason why fluoride concentrations at BRYT are much higher than any of the SLNG lakes, due to the proximity of a coal-fire aluminum-smelter plant on the shores of the nearby Lake Gusinoye (Pisarsky, 2005).

The one exception to the trends observed in the major anion data is seen at SLNG07. While being a low connectivity site, the dominating anion at SLNG07 is SO_4^{2-} (83%), and concentrations of Cl^- are the second lowest amongst all the sites. SLNG07 is located on the southwest side if the Delta, located in close proximity to both SLNG09 and the Selenga River (but not connected to it). It is also located on the perimeter of the Delta, on primarily agricultural lands. Therefore, it is possible that the proximity of SLNG07 to agricultural activities has resulted in an increased flux of sulphates to the site due to agricultural runoff (Ehya and Marbouti, 2016).

DOC concentrations across the Selenga River basin are quite variable, with a large range, and similar concentrations have been found in a range of latitudes, including lakes from Boreal regions of North America, southern Greenland, and the sub-tropical Okavango Delta in Africa (Mladenov *et al*., 2005; Anderson and Stedmon, 2007; Haig *et al*., 2013). DOC concentrations are likely variable and high for two reasons. First, organic carbon is transported from the terrestrial landscape, which is primarily steppe and boreal forest throughout the Selenga River basin. DOC concentrations in these regions are often higher than those in regions further north of the Selenga River basin, due to the increased presence of organic matter in the terrestrial landscape, and resulting high flux of terrestrial organic matter to the lakes (Eimers *et al*., 2008). Second, DOC is highest in two sites which are low connectivity lakes, without influence from the Selenga River (SLNG09 and SLNG15). PCA indicates that DOC is highly positively correlated with increasing cation concentrations and conductivity. The strong correlation may indicate that high and variable DOC levels are related to hydrological processes in the shallow lakes of the

Selenga River basin, a trend also observed by Mladenov *et al*. (2005) in the wetlands of Okavango Delta, and by Eimers *et al*. (2008) in Southern Canada.

2.7 Conclusion

All study lakes from the Selenga River basin were highly productive systems, with eutrophic to hypereutrophic status. One lake (SLNG01) was identified as possibly being very evaporative, and when this outlier was removed, major ion concentrations were important within unconstrained ordination (PCA) in explaining variability between sites. It appears that these primary limnological differences between sites are related to connectivity differences between lakes and major anion distributions amongst lakes can be divided into groupings based on connectivity levels. However, the only variable with statistical significance between different connectivity levels of lakes was Fe^{3+}, which was significantly higher in low-connectivity lakes. Possibility for impacts stemming from agriculture on the geochemistry of study lakes, including influence on ion concentrations and pH. However it is important to acknowledge that results were based on spot samples only.

2.8 References

Ajioka T., Yamamoto M., Takemura K., Hayashida A., & Kitagawa H. (2014) Water pH and temperature in Lake Biwa from MBT'/CBT indices during the last 280,000 years. *Climate of the Past* **10,** 1843-1855.

American Public Health Association. (1989) Standard Methods for the Examination of Water and Wastewater 17th ed., Washington, D.C., United States of America.

Anderson N.J., & Stedmon C.A. (2007) The effect of evapoconcentration on dissolved organic carbon concentrations and quality in lakes of SW Greenland. *Freshwater Biology* **52,** 280-289.

Anderson N.J., Harriman R., Ryves D.B., & Patrick S.T. (2001) Dominant factors controlling variability in the ionic composition of West Greenland lakes. *Arctic, Antarctic, and Alpine Research* **33,** 418-425.

Bennion H., & Smith M.A. (2000) Variability in the water chemistry of shallow ponds in southeast England, with special reference to the seasonality of nutrients and implications for modelling trophic status. *Hydrobiologia* **436,** 145-158.

Canfield D.E., Shireman J.V., Colle D.E., Haller W.T., Watkins C.E., & Maceina M.J. (1984) Prediction of chlorophyll-a concentrations in Florida lakes: importance of aquatic macrophytes. *Canadian Journal of Fisheries and Aquatic Sciences*, **41,** 497-501.

Chalov S., & Romanchenko A.O. (2016) Linking catchments to rivers: Flood-driven sediment and contaminant loads in the Selenga River. *Water and Environment in the Selenga-Baikal Basin* Karthe D., Chalov S., Kasimov H., & Kappas M (eds.) ibidem Press, Stuttgart, pp. 83-101.

Chalov S.R., Jarsjo J., Kasimov N.S., Romanchenko A.O., Pietron J., Thorslund J., & Promakhova E.V. (2015) Spatio-temporal variation of sedimetn transport in the Selenga River basin, Mongoila and Russia. *Environmental and Earth Sciences* **73,** 663-680.

Chalov S., Thorslund J., Kasimov N., Aybullatov D., Ilyicheva E., Karthe D., Kositsky A., Lychagin M., Nittrouer J., Pavlov M., Pietron J., Shinkareva G., Tarasov M., Garmaev E., Akhtman Y., Jarsjo J. (2016) The Selenga River delta: a geochemical barrier protecting Lake Baikal waters. *Regional Environmental Change* doi: 10.1007/s10113-016-0996-1.

Chen N., Bianchi T.S., McKee B.A., & Bland J.M. (2001) Historical trends of hypoxia on the Louisiana Shelf: applications of pigments as biomarkers. *Organic Geochemistry*, **32,** 543-561.

Clow D.W., & Sueker J.K. (2000) Relations between basin characteristics and stream water chemistry in alpine/subalpine basins in Rocky Mountain National Park, Colorado. *Water Resources Research* **36,** 49-61.

Davidson T.A., Bennion H., Jeppesen E., Clarke G.H., Sayer C.D., Morley D., Odgaard B.D., Rasmussen P., Rawcliffe R., Salgado J., Simpson G.L., & Amsinck S.L. (2010) The role of cladocerans in tracking long-term change in shallow lake trophic status. *Hydrobiologia*, **676,** 299-315.

Davidson T.A., Reid M.A., Sayer C.D., & Chilcott S. (2013) Palaeolimnological records of shallow lake biodiversity change: exploring the merits of single versus multi-proxy approaches. *Journal of Paleolimnology*, **49,** 431-446.

Dodds W.K. (2003) Misuse of inorganic N and soluble reactive P concentrations to indicate nutrient status of surface waters. *Journal of North American Benthological Society* **22,** 171-181.

Ehya F., & Marbouti Z. (2016) Hydrochemistry and contamination of groundwater resources in the Behbahan plain, SW Iran. *Environment & Earth Sciences* **75,** doi: 10.1007/s12665-016-5320-3.

Eimers M.C., Watmough S.A., Buttle J.M., & Dillon P.J. (2008) Examination of the potential relationship between droughts, sulphate, and dissolved organic carbon at a wetland-draining stream. *Global Change Biology* **14,** 938-948.

Garmayev E., Borisova T., Ayurzhanayev A., & Tsydypov B. (2016) Floods in the Selenga River basin: research experience. *Water and Environment in the Selenga-Baikal Basin* Karthe D., Chalov S., Kasimov H., & Kappas M (eds.) ibidem Press, Stuttgart, pp. 223-231.

Gorham E., Dean W.E., & Sanger J.E. (1983) The chemical composition of lakes in the north-central United States. *Limnology and Oceanography* **28,** 287-301.

Haig H., Kingsbury M.V., Laird K.R., Leavitt P.R., Laing R., & Cumming BF. (2013) Assessment of drought over the past two millennia using near-shore sediment cores from a Canadian boreal lake. *Journal of Paleolimnology* **50,** 175-190.

Heglund P.J., & Jones J.R. (2003) Limnology of shallow lakes in the Yukon Flats National Wildlife Refuge, Interior Alaska. *Lake and Reservoir Management* **19,** 133-140.

IBM Corp. (2013) IBM SPSS Statistics for Windows, Version 22.0. Armonk, NY: IBM Corp.

Japan Industrial Standard Methods, 2001, K0102.

Jeffrey S.W., Mantoura R.F.C., & Wright S.W. (1997) Phytoplankton pigments in oceanography: guidelines to modern methods. UNESCO, Paris.

Jeppesen E., Jensen J.P., Sondergaard M., Lauridsen T., & Landkildehus F. (2000) Trophic structure, species richness and biodiversity in Danish lakes: changes along a phosphorous gradient. *Freshwater Biology*, **45,** 201-218.

Karthe D., Kasimov N., Chalov S., Shinkareva G., Malsy M., Menzel L., Theuring P., Hartwing M., Schweitzer C., Hofmann J., Priess J., & Lychagin M. (2014) Integrating multi-scale data for the assessment of water availability and quality in the Kharaa-Orkhon-Selenge River system. *Geography, Environment, Sustainability* **3,** 65-86.

Kelly W.R., Panno S.V., & Hackley K. (2012) The sources, distributions, and trends of chloride in the waters of Illinois. Illinois State Water Survey, Prairie Research Institute, University of Illinois at Urbana-Champagne, United States.

Koski-Vahala J., Hartikainen H., & Tallberg P. (2001) Phosphorus mobilization from various sediment pools in response to increased pH and silicate concentration. *Journal of Environmental Quality* **30,** 546-552.

Levi E.E., Cakiroglu A.I., Bucak T., Odgaard B.V., Davidson T.A., Jeppesen E., & Beklioglu M. (2014) Similarity between contemporary vegetation and plant remains in the surface sediment in Mediterranean lakes. *Freshwater Biology*, **59,** 724-736.

McClelland J.W., Stieglitz M., Pan F., Holmes R.N., & Peterson B.J. (2007) Recent changes in nitrate and dissolved organic carbon export for the upper Kuparuk River, North Slope, Alaska. *Journal of Geophysical Research* **112,** G04S60, doi: 10.1029/2006JG000371.

McNeeley R.N., Neimanis V.P., & Dwyer L. (1979) Water Quality Source Book. A Guide to Water Quality Parameters. Inland Waters Directorate, Water Quality Branch, Environment Canada.

Mladenov N., McKnight D.M., Wolski P., & Ramberg L. (2005) Effects of annual flooding on dissolved organic carbon dynamics within a pristine wetland, the Okavango Delta, Botswana. *Wetlands* **25,** 622-638.

Organisation for Economic Co-operation and Development, OECD. (1982) Eutrophication of waters: monitoring, assessment and control. Technical Report, Environmental Directorate. OECD, Paris: 154 pp.

Pisarsky B.I., Hardina A.M., & Naganawa H. (2005) Ecosystem evolution of Lake Gusinoe (Transbaikal Region, Russia). *Limnology*, **6,** 173-182.

Potasznik A., & Szymczyk S. (2015) Magnesium and calcium concentrations in the surface water and bottom deposits f a river-lake system. *Journal of Elementology* **20,** 677-692.

Preisendorfer R.W. (1986) Secchi disk science: visual optics of natural waters. *Limnology and Oceanography* **31,** 909-926.

Sondergaard M., Johansson L.S., Lauridsen T.L., Jorgensen T.B., Liboriussen L., & Jeppesen E. (2010) Submerged macrophytes as indicators of the ecological quality of lakes. *Freshwater Biology*, **55,** 893-908.

Talling S.J. (1976) The depletion of carbon dioxide from lake water by phytoplankton. *Journal of Ecology* **64,** 79-121.

Ter Braak C.J.F. & Šmilauer P. (2012): Canoco reference manual and user's guide: software for ordination, version 5.0. Microcomputer Power, Ithaca, USA, 496 pp.

Törnqvist R., Jarsjö J., Pietron J., Bring A., Rogberg P., Asokan S.M., & Destouni G. (2014) Evolution of the hydro-climate system in the Lake Baikal system. *Journal of Hydrology* **519,** 1953-1962.

United States Environmental Protection Agency (2002) Method 1631, Revision E: Mercury in water by oxidation, purge and trap, and cold vapor atomic fluorescence spectrometry. Washington, D.C, United States of America.

Vologina E.G., Kalugin I.A., Osukhovskaya Y.N., Sturm M., Ignatova N.V., Radziminovich Y.B., Dar'in A.V., & Kuz'min M.I. (2010) Sedimentation in Proval Bay (Lake Baikal) after earthquake-induced subsidence of part of the Selenga River delta. *Russian Geology and Geophysics*, **51,** 1275-1284.

Wetzel R.G. (2001) *Limnology: lake and river ecosystems, 3rd edition*. Gulf Professional Publishing.

Wu Y., Wen Y., Zhou J., & Wu Y. (2014) Phosphorus release from lake sediments: effects of pH, temperature, and dissolved oxygen. *Journal of Civil Engineering* **18**, 323-329.

Chapter 3: Examining drivers of contemporary ecological variability in Selenga River basin lakes

3.1 Shallow lake ecosystems of the Selenga River basin

The ecological properties and structure of shallow lakes can dictate important aspects of lake functioning and stability (Duffy *et al*., 2007; Bailey and Guimond, 2009; Korhonen *et al.,* 2011). Submerged macrophyte communities strongly influence shallow lake ecological structure and function, as macrophytes provide important habitat, refugia, and food supply for biota (Jeppesen *et al*., 2000; Sondergaard *et al*., 2010; Davidson *et al*., 2011; Davidson *et al*., 2013; Levi *et al.*, 2014), and are heavily involved in nutrient cycling, and sediment stability (Jeppesen *et al*., 1998). Macrophyte species richness in shallow lakes has been positively correlated with species richness at other trophic levels (Korhonen *et al*., 2011), while macrophyte species composition, biomass, and density can influence structure and concentrations of algal and invertebrate communities (Vermaire *et al*., 2013). Moreover, nutrient concentrations will often influence the primary producer structure in shallow lakes, with increasing nutrient concentrations (i.e. eutrophication) leading to destabilization in submerged macrophyte communities, including declines in species richness and lake-wide disappearance of macrophytes, and rapid and sustained shifts to phytoplankton dominated primary producer communities (Scheffer, 1998; Körner, 2002; Zhou *et al*., 2006). Variations in algal primary producer diversity and abundance within the shallow lake community are influenced by top-down and bottom-up changes in nutrient concentrations, grazing pressures, and changes in light penetration (Leavitt and Hodgson, 2001; Sokal *et al*., 2008; McGowan *et al*., 2011; Bennion *et al*., 2012). Further, resource utilization efficiency and number of limiting resources may have significant effects on the diversity and richness of phytoplankton communities within shallow lakes (Interlandi and Kilham, 2001; Korhonen *et al*., 2011). Zooplankton communities typically occupy the middle of the food-web within freshwater ecosystems, and changes in zooplankton biomass and diversity may be driven by both bottom-up and top-down influences, including predator pressure, changes in macrophyte abundance, changes in substrate availability, and changes in light conditions (Jeppesen *et al.,* 2001; Davidson *et al*., 2011; Jeppesen *et al*., 2011).

A key driver of ecological variability within shallow lakes of floodplain wetlands is degree of connectivity, which can influence biodiversity and ecosystem functioning, and influence

ecological structure within the shallow lakes of the system (Ward *et al*., 1999; Bailey and Guimond, 2009). Periods of intermittent river intrusion will bring cold, turbid waters to shallow lakes, and affect light penetration, sediment redox, nutrient cycling, and organic matter accumulation, allowing for higher levels of plant productivity, biomass, and diversity (Bailey and Guimond, 2009). Further, moderate flood pulses resulting from a variable flow regime and a range of connectivity levels within a floodplain are often responsible for high levels of productivity and biodiversity within these systems (Junk *et al.*, 1989; Opperman *et al.*, 2010; Moreno-Mateos *et al.*, 2012). It is for these reasons that flood stress has been shown to be a primary determinant of ecosystem structure and function in wetlands (Boyd, 1971; Laitenen, 1990; Robertson *et al*., 2001; Sokal *et al*., 2010). Low-levels of disturbance from river inflow may also decrease biodiversity, with low species turnover rates related to low-levels of disturbance, leading to dominance by a select few species (Hay *et al*., 2000), as well as decreased habitat heterogeneity leading to reduced biodiversity (Salo *et al.*, 1986; Opperman *et al.*, 2010). Variations in hydrological connectivity may drive strong spatial gradients in macrophyte production and diversity, with decreases associated with increased connectivity (i.e. river intrusion), often due to the influence of connectivity on nutrient dynamics (Hay *et al*., 2000; Bailey and Guimond, 2009). Ecologically, this may also manifest as a key driver of shallow lake diatom community shifts (Hay *et al*., 2000). Further, differences in connectivity levels between shallow lakes of a floodplain delta will influence the strength of evapotranspiration dominance and have resulting effects on ion and nutrient concentrations within lakes (Brock *et al.,* 2007), differences in which can lead to variations in ecological communities (Potapova and Charles, 2003). Hydrological connectivity is necessary for the restoration and conservation of floodplain systems, and higher levels of hydrological exchange between a lake/pond and river promotes greater levels of recovery within a disturbed wetland (Opperman *et al.*, 2010; Moreno-Mateos *et al.*, 2012). Variations in connectivity within the Selenga River basin and other shallow lake ecosystems may be the overarching factor influencing the key drivers of ecosystem structure and function.

The aim of this chapter is to determine to what extent connectivity determines the ecological structure and functioning of Selenga River basin shallow lakes. The hypothesis developed is that connectivity levels of shallow lakes within the Selenga River basin will have a significant

effect on the ecological structure and functioning of the shallow lake community. To address the aim, the objectives of the study will examine contemporary communities and ecological remains at various trophic levels within shallow lakes of varying connectivity to the Selenga River, including macrophytes, algae, invertebrates, and fish, to assess connectivity impacts on biotic interactions, and ecological structure and functioning across Selenga River basin lakes. The objectives are:

1) Collect and analyze contemporary data on macrophyte communities within shallow lakes of the Selenga River basin, through contemporary macrophyte surveys and macrophyte macrofossil analysis;

2) Collect and analyze data on primary producers within Selenga River basin shallow lakes, through diatom and pigment analysis;

3) Analyze data on higher trophic levels within Selenga River basin shallow lakes, though invertebrate and fish macrofossil analysis.

4) Incorporate all trophic levels of data into a whole-ecosystem analysis of spatial variability in ecology across Selenga River basin shallow lakes.

3.2 Methods

Physical site descriptions and sample collection are detailed in Sections 2.1 and 2.2.

3.2.1 Assessing ecological communities across trophic levels

3.2.1.1 Contemporary macrophyte communities

Contemporary macrophyte surveys were undertaken to determine diversity, abundance, density, and percent coverage of submerged and floating macrophytes present in Selenga river basin shallow lakes. Macrophyte density was calculated for each site using the percent volume infested (PVI) procedure (Canfield *et al*., 1984), which provides an estimate of the density of macrophytes in the water column of a lake. Macrophyte species observed at each site were also recorded using the abundance-based 5-1 DAFOR scale (**D**ominant, **A**bundant, **F**requent, **O**ccasional, **R**are). The DAFOR survey may include species possibly absent from the PVI survey, as any and all species observed at the site are included in the DAFOR survey. Methods describing the PVI and DAFOR sampling procedures are detailed in Section 2.2.4.

3.2.1.2 Surface sediment macrofossils

Assessments of macrophyte, invertebrate, and fish community structure and dynamics were conducted using surface sediment macrofossils analysis. Sediment was subsampled for analysis of aquatic macrofossils for all 15 study lakes using the displacement method and standard sieving and picking methods (Birks, 2001). Twenty cubic centimetres of wet sediment was subsampled for each of the 15 contemporary lake sites. A graduated cylinder was filled with 100 ml of water and weighed to two decimal places. Wet sediment was added to the graduated cylinder until the volume was 120 ml. The cylinder was then re-weighed to two decimal places. Sediments were then sieved through 355 and 125 µm sieves, simultaneously. The entire volume of the greater than 355 µm fraction was examined and all identifiable aquatic macrofossil remains were enumerated. Approximately one-fifth of the 125-355 µm fraction was examined and all identifiable aquatic macrofossil remains were enumerated and findings were extrapolated up to full volume. Macrofossils were identified using reference collections held in the Environmental Change Research Centre (University College London), and by using relevant taxonomic keys (Katz *et al*., 1965; Jans *et al*., 2006; Mauquoy and Van Geel, 2007; Marrotte *et al*., 2012; Birks, 2017). Plant and animal macrofossil data were standardized as the number of fossil remains per 100 cm^3 wet sediment. Macrofossil plots were constructed using C2 (Juggins, 2014).

3.2.1.3 Surface sediment diatoms

Primary producer sensitivity to changes in environmental variations were assessed through diatom analysis. Approximately 0.1g of wet surface sediment (weighed to four decimal places) was subsampled for each of the 15 contemporary lake sites for diatom analysis following standard procedures (Battarbee *et al*., 2001). Wet sediment was placed in 15 ml centrifuge tubes and approximately 10 ml of 30% hydrogen peroxide (H_2O_2) was added to each and heated to 80°C in a water bath to remove organic material. Peroxide was topped up as needed as evaporation occurred, and was allowed to react for 3-4 days, depending on level of activity. After approximately 72 to 96 hours of reaction with the H_2O_2, centrifuge tubes were removed from the hot water bath, and approximately 2 drops of 50% HCl were added to each tube to remove any carbonate material, and eliminate any remaining H_2O_2. Samples were allowed to react for approximately half an hour. Centrifuge tubes were then topped up to 15 ml with distilled

water, and centrifuged for four minutes at 1200 rpm. The resulting supernatant was then aspirated, and samples were once again topped up to 15 ml with distilled water. The washing process was repeated four more times. Two drops of 1% ammonia were added to each centrifuge tube with the final wash to help keep clays in suspension, and prevent diatoms from clumping.

For diatom slide preparation, the final cleaned diatom sample preparation was topped up to 10 ml with distilled water and mixed well. One millilitre was pipetted from the original diatom dilution (D0), into a new 15-ml centrifuge tube. To the new centrifuge tube, 1 ml of 8.0×10^4 microsphere ml^{-1} working solution was added. The new diatom sample was then topped up to 10 ml with distilled water (D1) and mixed well. Approximately 1 ml of D1 was then pipetted onto a round, 19 mm diameter cover slip. The cover slip was covered, and the diatom suspension was allowed to settle and water evaporate overnight. Once the diatom suspension was dried, slides were prepared using the resin, *Naphrax*, which has a high refractive index of 1.73 upon drying. A hot plate was heated to 130°C in a fume cupboard. The empty slide was placed on the hot plate with a drop of *Naphrax*. The dry diatom coverslip was then inverted and placed on the *Naphrax*. The *Naphrax* was allowed to heat for approximately 15 minutes to drive off the toluene. After the *Naphrax* stopped bubbling, the slide was removed from the hot plate and allowed to cool, and the resin harden, in the fume cupboard for approximately 10 minutes.

A minimum of 300 valves were counted per diatom slide. Diatom species identification was conducted following Krammer and Lange-Bertalot (2011), Diatoms of Europe Vol. 2 (Lange-Bertalot, 2001), Diatoms of Europe Vol. 3 (Krammer, 2002), and Diatoms of Europe Vol. 5 (Levkov, 2009)**.** Diatom raw counts were converted to percent relative abundance per sample. As the total number of valves counted per sample varied between sites, species richness was determined through rarefaction. The most commonly used diversity indices are dependent on sample size, and become difficult to apply in a comparison of diversity across collections of different sizes. Therefore, reporting rarefaction removes the assumption that sample size was the same across all samples (Simberloff, 1972). The minimum number of valves counted in a single sample was 316 valves (BRYT). Richness in all other samples was then assessed at 316 valves. Species rarefaction richness was conducted on the diatom raw counts using R, Vegan package (R. v.3.2.4, 2016). Hill's N2, an index of the diversity of very abundant species at a

single site, was calculated on the full diatom dataset using C2 (Juggins, 2014). Species concentrations were calculated using the microsphere method (number of valves (#)/sample), and normalized to weight of sediment of the original sample (# valves/g dry weight) (Battarbee and Kneen, 1982). A plot of surface sediment diatom assemblages was constructed for all sites using C2 (Juggins 2014), and included all species present at >5% at a minimum of 1 site.

3.2.1.4 Laboratory analysis of pigment samples

Pigments of photosynthetic organisms were analyzed from both sediment and water samples from the 15 SLNG and BRYT lakes following McGowan *et al*. (2012), to assess variations in structure of primary producer communities, and assess variations in total algal biomass across the Selenga River basin lakes. As some algal pigments are labile, and prone to post-depositional degradation, pigments were analyzed from both surface waters and surface sediments from lakes. Water collected for pigments analysis was filtered through GF/F filter paper at 0.45 µm pore size. The volume of water filtered was recorded, and the filter paper kept for analysis. No more than 5 days prior to analysis, sediment subsamples were dried in Thermo Modulyo D and Edwards Modulyo freeze-driers in the Department of Geography, UCL. Sediment samples and filter papers were stored in the dark (filter paper wrapped in aluminum foil) at -20°C at all times prior to preparation and extraction, due to the sensitivity of pigments to degradation by light and high temperatures (Reuss and Conley 2005). All pigment extraction occurred at minimal lighting to avoid degradation of pigments. All further preparation and analysis for pigments occurred in the Environmental Change Laboratory at the University of Nottingham, and sample preparation and pigment extraction followed the protocol of the Environmental Change Laboratory at the University of Nottingham.

Algal pigment biomarkers were determined using rever-phase high-performance liquid chromatography (HPLC). The analytical technique isolated and separated algal pigments based on their differing polarities. Pigment separation on the HPLC followed the Chen method utilizing acetone, methanol, acetonitrile, and ethyl acetate (Chen *et al*., 2001). During HPLC analysis, samples travel through a column at high pressure, and elute from the column based on their polarity, with pigments which are polar (more water soluble) eluting earlier than the more lipid soluble pigments (Leavitt and Hodgson, 2001; McGowan, 2013). The pigments will elute in a known certain order from the column, and pigments are identified based on their retention time

within the column (McGowan, 2013). A photodiode array (PDA) spectrophotometer then scans the pigment at multiple UV and visible wavelengths (300 - 750 nm) to produce an absorbance spectrum (McGowan, 2013).

3.2.1.5 Extraction of pigments from filter paper

A detailed description of pigment extraction from filter paper is given in Section 2.3.3 (for chlorophyll *a*).

3.2.1.6 Surface sediment pigments

Approximately 0.3 g of dried sediment for each sample was weighed into a glass vial for pigment extraction in a specially lit room to ensure low light during the extraction process. To each vial of sediment, 5 ml of extraction solvent (80% HPLC-grade acetone, 15% HPLC-grade methanol, 5% nanopore deionised water) was added. Vials were then capped tightly and put in the freezer for a minimum of twelve hours to allow pigment extraction to occur. Following the extraction period, the extraction solvent was decanted into an acetone-cleaned beaker, minimizing sediment transfer. Pigment solution was then drawn up into a 10 ml disposable syringe, and filtered through an attached 0.22 µm lock-on filter into a clean, labelled vial. Residue in the extraction vial was rinsed with HPLC-grade acetone, and the syringe-filtering procedure was repeated until the residue was no longer pigmented. Following each sample, the beaker and syringe were rinsed with analytical grade acetone. Pigment extraction solutions were then evaporated under nitrogen until dried. Following drying, sample vials were capped and returned to the freezer.

Immediately prior to analysis, a known volume of injection solvent (a 70:25:5 mixture of acetone, HPLC-grade methanol, and the ion-pairing reagent – 0.75 g tetra butyl ammonium acetate, 7.7 g “Sigma®” grade ammonium acetate and 100 ml nanopore deionised water) was added to each dried sample extract. The dried sample extract was then dissolved completely in the injection solvent. The dissolved extract was then transferred to an autosampler vial and the volume of dissolved extract transferred was recorded. Surface sediment pigment analysis from all 15 lakes was conducted in a single run on an Agilent 1200 HPLC separation system, along with two “green” samples, one analyzed at the beginning of the run and the other at the end of the run, utilized to verify retention times for specific pigments. HPLC samples were analyzed

using Agilent Chemstation program. Following analysis, pigments were identified based on spectrum and retention time using Jeffrey *et al*. (1997). Individual pigment peak areas were converted to nmol pigment/g organic carbon. Plots of surface water and surface sediment pigments were constructed for all sites using C2 (Juggins, 2014). Labile pigments (chlorophyll (Chl *c*), fucoxanthin, violaxanthin, diadinoxanthin, and peridinin) were retained for overall data interpretation, but were removed from statistical analyses of surface sediment pigments to exclude any influence of pigment degradation. Labile pigments are those which are highly prone to early post-depositional degradation, and what may appear to be increased concentrations in recent sediments of labile pigments is actually an artifact of post-depositional degradation (Leavitt, 1993; McGowan *et al.,* 2005).

3.2.1.7 Data analysis of ecological remains

Modifications and transformations made to each ecological dataset prior to statistical analysis are described in Table 3.1.

To test the significance of connectivity on variations in ecological structure and function across Selenga River basin sites, Kruskal-Wallis and Mann-Whitney U tests were conducted on the following variables: contemporary macrophyte PVI, macrofossil richness, diatom rarefacted species richness, algal pigment concentrations (Chl *a* and total carotenoids from surface water and surface sediments), LOI_{550} and LOI_{950}. Connectivity categories tested were “high connectivity”, “intermittent connectivity”, and “low connectivity”. See Section 2.1.3 for description of site connectivity levels, and how levels were determined. Kruskal-Wallis and Mann-Whitney-U tests were performed using SPSS 22.0 (IBM Corp., 2013).

Spatial patterns in ecological datasets were analysed using unconstrained ordinations. All ecological datasets were centred prior to unconstrained ordination analysis. Within the unconstrained ordinations, sites were coded according to connectivity levels (high connectivity, intermittent connectivity, and low connectivity) to assess the spatial distribution and clustering of sites with similar connectivity levels.

Proxy	*Transformation*	*Reason for transformation, if applicable*	*Modifications to dataset*	*Reason for modification*
Macrophytes	NA		NA	
Macrofossils	ln(x+1)	To reduce the influence of very common taxa	Terrestrial and marginal plant remains removed	To focus on within-lake dynamics
Diatoms	NA		Only species present >2% at any one site included	To focus on trends in common and abundant species
Water pigments	NA		NA	
Sediment pigments	NA		Labile pigments (chlorophyll *c*, fucoxanthin, violaxanthin, diadinoxanthin, and peridinin) removed	To exclude influence of post-depositional pigment degradation

Table 3.1. Data transformations and data set modifications applied to ecological data prior to statistical analysis.

To further examine potential drivers of ecological variability across sites, constrained ordination, redundancy analysis (RDA) was conducted on the ecological datasets. Explanatory variables included in the RDA were selected to assess the influence of connectivity, biotic interactions, landscape parameters, and water chemistry on the variation in biological remains across Selenga River basin shallow lakes. Significance of variables were determined through single constrained ordinations, and 499 unrestricted Monte Carlo permutations. Several variables were not normally distributed (LOI_{950}, surface area, maximum depth, mean depth, conductivity, SRP, Ca^{2+}, Mg^{2+}, Cl^{-}, and ∑anions), and so were log-transformed prior to analyses. Following transformation, all variables achieved normal distribution. Ordinations were performed using Canoco5 (ter Braak and Šmilauer, 2014). Normal distribution and equal variances of environmental variables was assessed using SPSS 22.0 (IBM Corp., 2013).

Co-correspondence analysis (CoCA) was conducted on the species data for the biological indicator records (diatoms*sediment pigments; diatoms*macrofossils; sediment pigments*macrofossils) to compare species composition variation between pairs of biological proxy records, and assess the significance ($p \leq 0.01$) of the co-occurrence of species or groups of species between proxies. CoCA assists in determining if functional groups of species/taxa or guilds tend to co-occur, further aiding in the interpretation of temporal community change (ter Braak and Schaffers, 2004). CoCA were performed using Canoco5 (ter Braak and Šmilauer, 2014).

3.2.2 Determining geochemical indicators across Selenga River basin lakes

3.2.2.1 Surface sediment trace and major elements

X-ray fluorescence (XRF) is a quick, non-destructive technique often used to determine total elemental composition of sediment. Wet sediment was subsampled from all 15 surface sediment samples, and freeze-dried in Thermo Modulyo D and Edwards Modulyo freeze-driers in preparation for analysis. Following freeze-drying, dried sediment from each sample depth was ground to a fine powder using an agate mortar and pestle. Approximately 1.0 g of dried, finely powdered sediment was weighed into a sample cuvette lined with polypropylene film. All weights were recorded to 4 decimal places. Samples were then analyzed for trace and major elements using a Spectro X-Lab 2000 energy dispersive X-ray fluorescence spectrometer (ED-XRF) with a Si(Li) semiconductor detector in the Department of Geography at University College

London (UCL). Certified standard reference materials (SRM), Buffalo River sediment (BRS; SRM 2704; Epstein *et al.*, 1989) were analyzed every 10 samples during analysis to assess the accuracy of the analytical method. Accuracy of standards was within 15%. See Table 3.2 for recovery rates from BRS reference standards run with samples. Trace and major element concentrations are then produced in units of μg g^{-1} and %, respectively. Elemental ratios were calculated for Fe/Mn to provide inferences regarding redox conditions within lakes and Ca/Ti to assess evaporative concentrations and in-lake carbonate precipitation (Davies, 2015).

Element	Recovery rate (%)
Mg	101.8
Al	99.4
Si	96.3
P	89.0
S	78.0
K	101.9
Ca	100.1
Ti	95.9
Mn	99.0
Fe	96.6
Ni	97.3
Cu	91.3
Zn	91.7
As	92.5
Br	106.3
Pb	93.3

Table 3.2. Certified reference material recovery rates for XRF trace and major element sediment analyses.

3.2.2.2 Toxicity measurements

Toxicity of selected trace elements (Cu, Ni, Pb, As, Zn) was determined for sediments according to MacDonald *et al.* (2000) using consensus-based threshold effect concentrations (TEC) and probability effect concentrations (PEC). TECs are the concentrations of individual contaminants below which toxicity-related impacts in benthic organisms would not be expected. PECs are the concentrations of individual contaminants above which toxicity-related impacts in benthic organisms would be expected. PEC-quotients of mean metals (PEC-$Q_{mean\ metals}$) were calculated, which combines the probable effect concentrations of trace elements (Ni, Cu, Pb,

As, Zn; Long *et al*., 2006). To determine PEC-$Q_{mean\ metals}$, each individual trace elements concentration within a single sample is normalized to the PEC for that particular trace element. The normalized trace element values are then summed within a single sample, and then normalized to the number of contaminants included in the analysis within a single sample. PEC-$Q_{mean\ metals}$ values above 0.5 are considered to indicate possible toxic conditions for benthic organisms (Long *et al*., 2006).

3.2.2.3 Contemporary loss-on-ignition

Wet sediment was subsampled for each site for analysis of sediment loss-on-ignition at 550°C (LOI_{550}) and 950°C (LOI_{950}). Approximately 1.5 g of wet sediment was subsampled and oven-dried at 105°C for approximately 24 hours. Following oven-drying, samples were cooled to room temperature in a desiccator, and re-weighed. The oven-dried sediment for each site was combusted for 2 hours at 550°C in a Carbolite Gero Ltd. muffle furnace (LOI_{550}). Samples were subsequently allowed to cool to room temperature in a desiccator and re-weighed. Organic matter oxidizes to CO_2 and ash at 550°C, and the weight of a sample following 2 hours at 550°C is closely correlated with organic carbon of the original sediment, and provides an estimate of organic matter content in the sediments (hydrated mineral water is also removed during the process, resulting in the organic matter content being only "an estimate" using LOI_{550}) (Dean, 1974; Bengtsson and Enell, 1986). The LOI_{550} of the sample was then expressed as a percentage of the dried sediment, and assumed to be representative of percent organic matter of the sediment. Carbonate content of each sample was estimated through further combustion of sediments in a muffle furnace at 950°C for a period of 2 hours (LOI_{950}), which evolves carbon dioxide from carbonate. Samples were then allowed to cool to room temperature in a desiccator and re-weighed. LOI_{950} of sediment shows good correlation with estimates of carbonate content of sediments assessed through other methods (Dean, 1974). All weights were recorded to 4 decimal places.

3.2.2.4 Data analysis of contemporary geochemical indicators

Pearson product-moment correlation (PPMC) calculations were conducted between selected trace and major element concentrations using SPSS 22.0 (IBM Corp., 2013) to determine associations between concentrations at study sites (Hay *et al*., 1997; Michelutti *et al*.,

2001; McGowan *et al*., 2011). For the purpose of PPMC only, non-normally distributed concentration data for trace and major elements were log-transformed to achieve normal distribution (Al, P, Si, Mn, Fe, Ca, Ni, and As). To explore spatial trends in the trace and major element and loss-on-ignition data, PCA was conducted on centred, then standardised untransformed data. Ordinations were performed using Canoco5 (ter Braak and Šmilauer, 2014). Box-and-whisker plots were constructed to display geochemical indicator trends across sites, with median, first and third quartiles, and outliers indicated. Plots were constructed using SPSS 22.0 (IBM Corp., 2013). Toxicity trends across sites were plotted using C2 (Juggins, 2014).

3.3 Results

3.3.1 Assessment of environmental drivers of ecological communities across trophic levels

3.3.1.1 Contemporary aquatic macrophyte communities of Selenga Delta lakes

The maximum number of aquatic macrophyte species present at any one site was 14 (SLNG11) and the minimum was 7 (BRYT) (Table 3.3). The total number of species present across all sites, as determined by the DAFOR survey, was 22 (Table 3.4). *Nymphaea* sp1 was present at only one site, SLNG07, however *Nuphar* sp. was present in 10 study lakes. Charophytes were present in four of the study lakes (BRYT, SLNG04, SLNG11, SLNG13), however the species present in BRYT appeared to be a different species of charophyte than that found in the Selenga Delta lakes. The only species to occur in all 15 lakes was *Ceratophyllum demersum*, however *Potamogeton* spp. were common and species of this genus were found at all sites. The invasive macrophyte *Elodea canadensis* was present in four lakes, SLNG04, SLNG13, SLNG14, and BRYT. *E. canadensis* was present in high abundances in all cases of occurrence, dominating (DAFOR = 5) the macrophyte assemblages in two out of the four lakes (SLNG04 and SLNG13), and present at greater than 10% PVI at the same sites (Table 3.5). Across most sites, *Ceratophyllum demersum* and *Myriophyllum sibericum* dominated macrophyte communities, and were often present at greater than 10% PVI. The exception to this was at BRYT, where a combination of *Potamogeton* spp. dominated. Total lake PVI varied considerabley between sites, with a maximum PVI of 77% and a minimum PVI of 22% calculated across all sites, with a mean PVI of 44.5% (Table 3.3).

Approximately 72% of variation in macrophytes was captured by the first two PCA axes (Table 3.6). Sites were fairly spread out within the PCA ordination space, with respect to macrophyte communities. However, 3 out of 4 high connectivity sites plotted negatively along axis 1, while 4 out of 6 low connectivity sites plotted positively along axis 1, and most sites with intermittent connectivity plotted around the origin of both axes (Figure 3.1a). Most *Potamogeton* spp. were strongly associated with PCA axis 2, with the exception of *Potamogeton* sp.3, and *P. crispus*, both of which only occurred at a single site (Figure 3.1b). *Ceratophyllum demersum* (CDEM) was most positively and strongly associated with PCA axis 1 (Figure 3.1b).

Site	*SLNG 01*	*SLNG 03*	*SLNG 04*	*SLNG 05*	*SLNG 06*	*SLNG 07*	*SLNG 08*	*SLNG 09*	*SLNG 10*	*SLNG 11*	*SLNG 12*	*SLNG 13*	*SLNG 14*	*SLNG 15*	*BRYT*
PVI (%)	48	22	47	27	49	64	42	53	42	33	37	41	48	77	38
Species no.	10	10	11	11	8	12	10	11	12	14	12	13	10	10	7
Dominant species	CDEM	CDEM	ECAN	MSIB	CDEM	CDEM	MSIB	CDEM	CDEM	CDEM	CDEM	ECAN	CDEM	CDEM	PPUS/ PBER

Table 3.3 Mean PVI measurements for all study lakes (%), total number of species found in each lake as determined using the DAFOR survey, and dominant species in each lake as determined through the DAFOR survey. Macrophyte codes can be found in Appendix 5.

Species	SLNG 01	SLNG 03	SLNG 04	SLNG 05	SLNG 06	SLNG 07	SLNG 08	SLNG 09	SLNG 10	SLNG 11	SLNG 12	SLNG 13	SLNG 14	SLNG 15	BRYT
Ceratophyllum demersum	5	5	4	3	5	5	4	5	5	5	5	4	5	5	3
Myriophyllum spicatum															3
M. sibericum	4	4	4	5	4	4	5	4	4	3	4	4	4	4	
Elodea canadensis			5									5	4		3
Callitriche hermaphrodidica										2		1			
Potamogeton pectinatus	4	2	2	2		1		2	3	2	2	2		2	3
P. crispus								1							
P. perfoliatus	1	4	3	2	3	1	2	2	3	3	4	4	3	3	
P. compressus	2	2	3	3	3	2	2	3	3	4	3	3	3	2	1
P. pusillus/ berchtoldii	3	3		1		3	2	2	2	1	2		2		4
Unknown hybrid Potamogeton Sp.3				4											
Chara Sp.1			1							1		1			
Chara Sp.2															3

Lemna trisulca	1	3	3	2	2	3	3	3	3	3	3	4	4	3
L. minor		2		2	2	3	3	3	3	1	2	3	1	1
Utricularia vulgaris	2	2	2			4		3	2	2	2	2		2
Nuphar Sp.1			2		2	3	2		3	1	2	2	1	1
Sagitariolatus Sp.1	3	3	2		2	2	2		3	1	2	2	1	1
Spirodela polyrhiza	1			2				2	2		2			
Nymphaea Sp.1						1								
Hippuris vulgaris										1				
Ranunculus Sp.1				2			1							

Table 3.4. Species abundances expressed using the DAFOR survey system for all sites: dominant (5), abundant (4), frequent (3), occasional (2), rare (1)

Species	SLNG 01	SLNG 03	SLNG 04	SLNG 05	SLNG 06	SLNG 07	SLNG 08	SLNG 09	SLNG 10	SLNG 11	SLNG 12	SLNG 13	SLNG 14	SLNG 15	BRYT
Ceratophyllum demersum	22	8	4	3	32	24	17	22	19	11	12	9	15	35	2
Myriophyllum spicatum															4
M. sibericum	5	2	7	7	6	20	16	14	11	8	12	7	13	26	
Elodea canadensis			22									11	7		7
Callitriche hermaphroditica										0.5		0.4			
Potamogeton pectinatus	16	1	3	1				1	2	2	3	3		3	7
P. crispus								0.1							
P. perfoliatus	0.2	5	4	2	2	0.1	3	0.6	2	2	6	1	3	3	0.3
P. compressus	1	0.5	6	2	3	2	1	1	2	5	1	3	1	5	0.6
P. pusillus/ berchtoldii	3	1		0.3		8	3	2	1	0.4	0.8		3		12
Unknown hybrid Potamogeton Sp.3				10											
Chara Sp.1			0.5							0.1		0.4			
Chara Sp.2															4

Lemna trisulca	0.1	2	0.3	4	2	3	5	4	1	2	5	7	4
L. minor		0.1		2	1	0.5	4	0.1			0.1		
Utricularia vulgaris	2	0.7	0.3		4		2	0.9	0.7	1			0.1
Nuphar Sp.1				0.2	2							0.1	0.5
Sagitariolatus Sp.1					0.1			0.2					
Hippuris vulgaris									0.1				
Spirodela polyrhiza							1						

Table 3.5. Mean macrophytes species PVI at each site as determined using the PVI survey. All values are expressed as %.

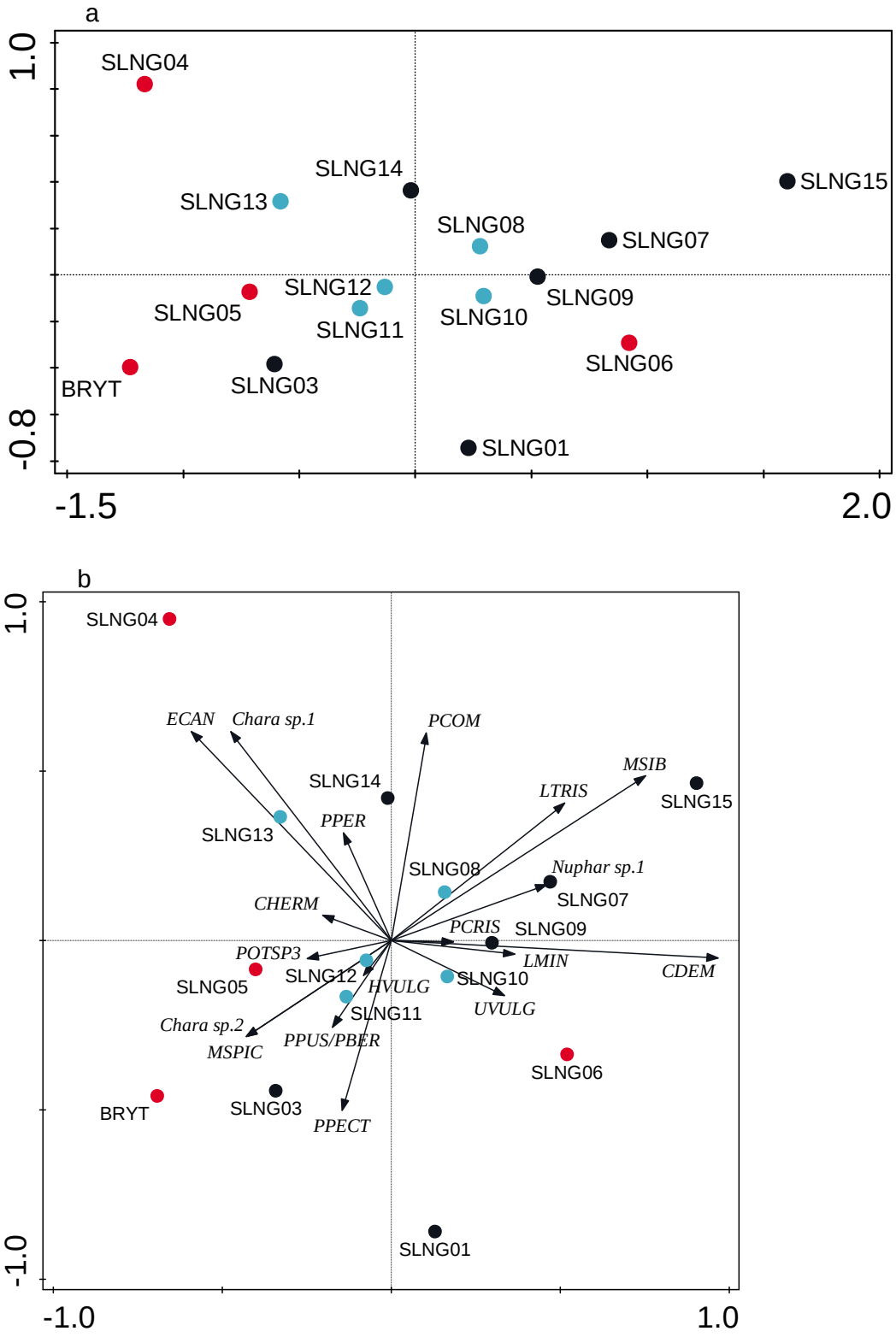

Figure 3.1. a) PCA plot of SLNG and BRYT site PVI records; b) PCA biplot of SLNG and BRYT sites and species recorded during PVI surveys. Sites are colour-coded for connectivity levels: low connectivity (black), intermittent connectivity (light blue), and high connectivity (red). Macrophyte codes can be found in Appendix 5.

	Axis 1	*Axis 2*	*Axis 3*	*Axis 4*
Eigenvalues	0.5851	0.1392	0.1161	0.0636
Explained variation (cumulative)	58.5	72.4	84.0	90.4

Table 3.6. PCA summary table for SLNG and BRYT macrophyte PVI, with eigenvalues and cumulative explained variation for the first four PCA axes.

3.3.1.2 Contemporary surface sediment macrofossils

Macrofossil counts found in the surface sediment are shown in Figure 3.2. Plant macrofossil remains included seeds and fruits, leaf-spines, leaf tips, leaf fragments (including water lilies leaf cell trichosclereids), and charophyte oospores. The trichosclereids of *Nymphea* sp. and *Nuphar* sp. were found, but are identical, and were therefore grouped as the Nymphaeaceae trichosclereids. Charophyte oospores were found in several sites, but are difficult to identify to species due to a high morphological variability. Therefore, all oospores were combined to represent all charophytes. Calcified and uncalcified oospores were counted separately. Invertebrate macrofossils found included bryozoan statoblasts (counted as valves), cladoceran ephippia, chydorid carapaces and postabdomen, molluscs, and fragments of benthic invertebrates. Molluscs were not identified beyond genus. Benthic invertebrate fragments were typically identified to order or family, with the exception of Trichoptera fronto-clypei, which were identified to genus. Fish scales and vertebrae of both percid and cyprinid fish were also recovered and enumerated.

Exploratory detrended correspondence analysis (DCA) carried out on the ln(x+1)-transformed macrofossil dataset indicated a first axis gradient length of 1.9 SD and showing the appropriateness of linear ordination techniques. Nearly 40% variation in macrofossils is captured by the first two PCA axes (Table 3.7). SLNG03 and SLNG13 cluster closely in the upper-left of the plot, while BRYT separates out from the SLNG sites slightly, towards the right of the plot (Figure 3.3a). A grouping of sites SLNG04, SLNG05, SLNG06, and SLNG11 forms in the lower-right side of the plot, with positive axis 1 but negative axis 2 values. Most other sites plot negatively along axis 1, and spread out along axis 2 (Figure 3.3a). Macrofossil richness was higher at sites which plotted more negatively along PCA axis 1 (Figures 3.2b, and 3.3b). Sites which plotted more negatively along axis 1 were intermittent or low connectivity sites. These sites were recorded as having *E. fluviatile* fragments, and higher numbers of *Potamogeton* spp.

remains. High connectivity sites plotted most positively on axis 1, and were characterized by lower abundances of *Myriophyllum* spp. and *Ceratophyllum demersum* remains, as well as lower numbers of fish remains, chydorid chitinous remains, and some bryozoans. However, *Plumatella* sp. remains were higher at higher connectivity sites (Figure 3.2c). *Potamogeton* spp. seeds, and gastropods are positively correlated with axis 2, and sites SLNG03 and SLNG13. *D. pulex* was more common at sites with higher *Potamogeton* spp. abundance, while *Simocephalus* sp. strongly associated with sites containing higher abundance of bryophytes, *Myriophyllum* spp., and *Ceratophyllum demersum*, benthic invertebrates, and chydorids (Figure 3.3b).

	Axis 1	***Axis 2***	***Axis 3***	***Axis 4***
Eigenvalues	0.2111	0.1650	0.1279	0.1004
Explained variation (cumulative)	21.1	37.6	50.4	60.4

Table 3.7. PCA summary table for SLNG and BRYT surface sediment macrofossils, with eigenvalues and cumulative explained variation for the first four PCA axes.

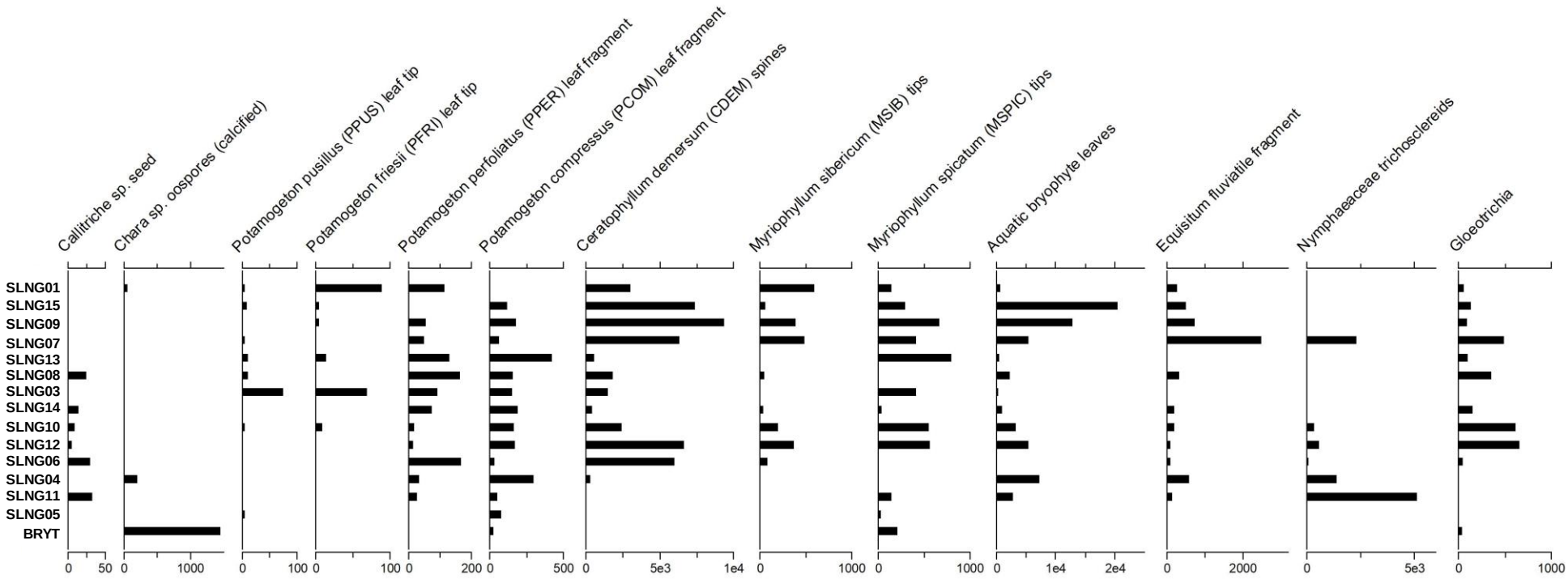

Figure 3.2a. Aquatic macrophyte remains from SLNG and BRYT surface sediments. Sites are ordered according to PCA axis 1 scores top to bottom, from most negative to most positive. Units are no. of individuals 100 cm^{-3} wet sediment.

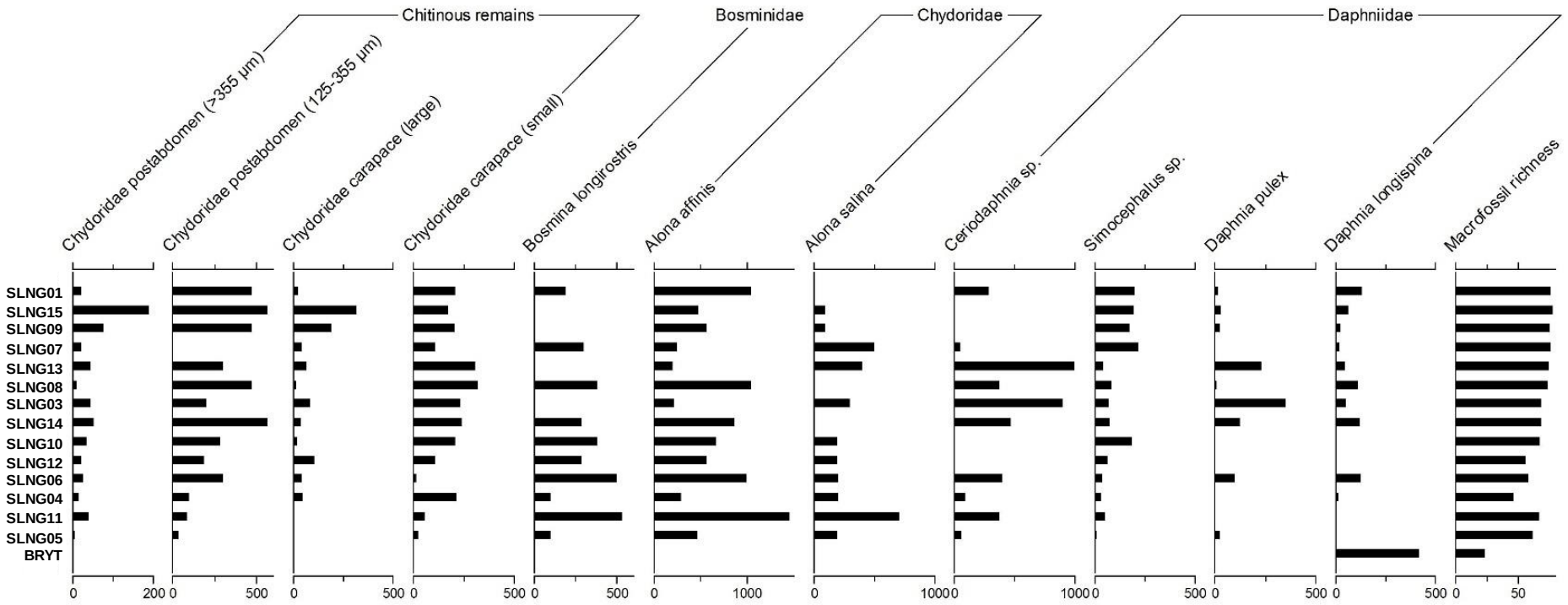

Figure 3.2b. Zooplankton remains enumerated from SLNG and BRYT surface sediments. Total macrofossil richness per sample is displayed. Sites are ordered according to PCA axis 1 scores top to bottom, from most negative to most positive. Units for all remains are no. of individuals 100 cm^{-3} wet sediment. Units for macrofossil richness is no. remain types.

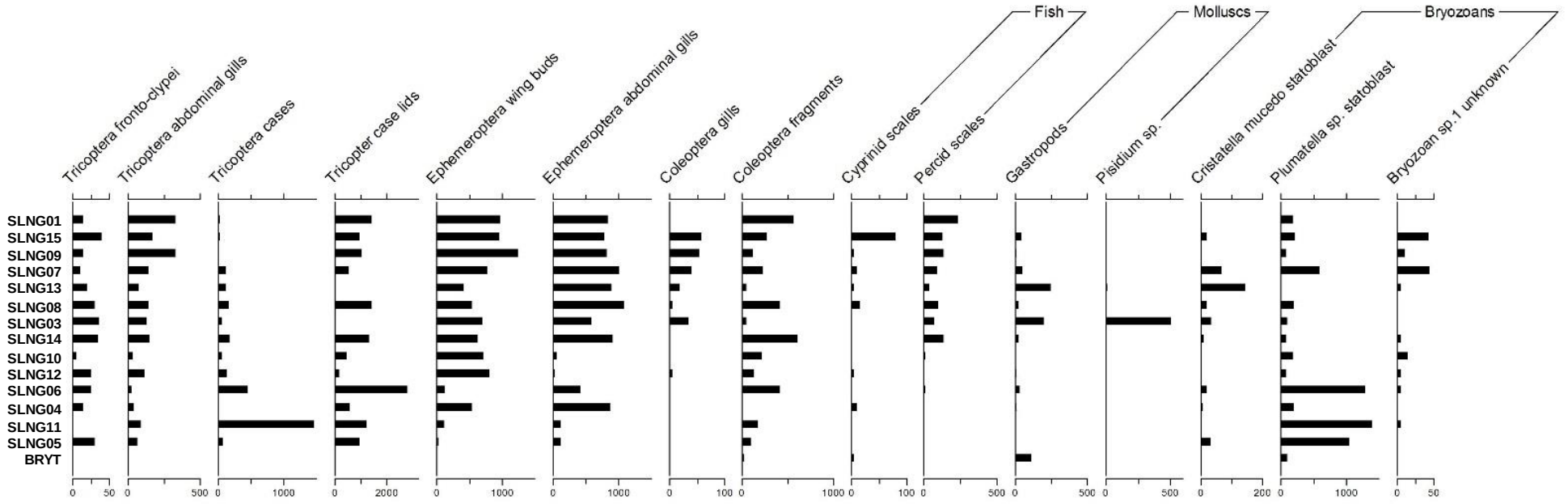

Figure 3.2c. Benthic invertebrate, fish, mollusc, and bryozoan remains enumerated from SLNG and BRYT surface sediments. Sites are ordered according to PCA axis 1 scores top to bottom, from most negative to most positive. Units are no. of individuals 100 cm^{-3} wet sediment.

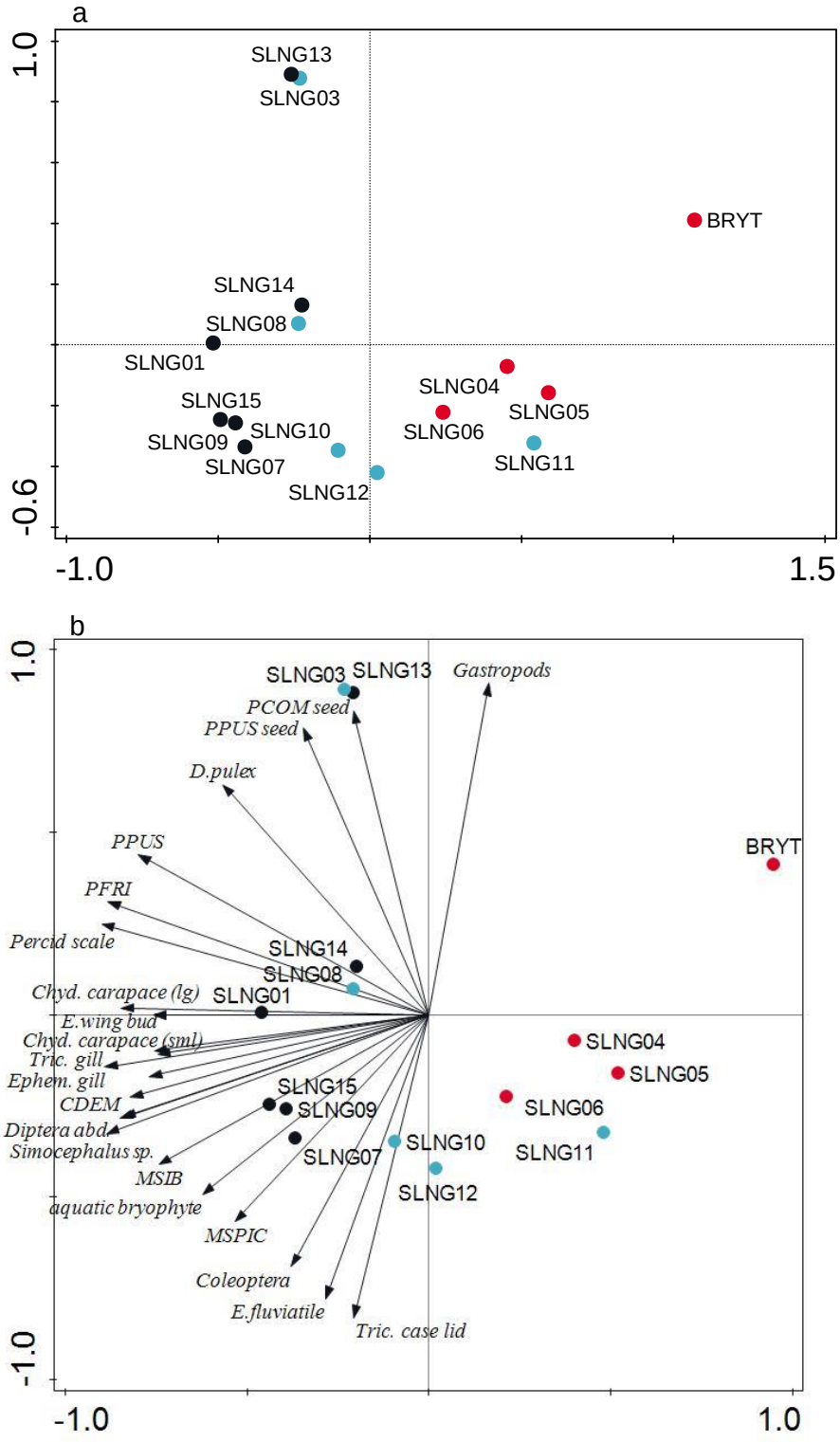

Figure 3.3. a) PCA plot of SLNG and BRYT site macrofossil records; b) PCA biplot of SLNG and BRYT macrofossil remains, with top 25 species by fit plotted. Sites are colour-coded for connectivity levels: low connectivity (black), intermittent connectivity (light blue), and high connectivity (red). Macrofossil codes can be found in Appendix 5.

Across all sites, connectivity, surface area, maximum depth, and sulphate concentrations were significant in explaining spatial variability of remains (Table 3.8). See Section 2.5 for details of physico-chemical characteristics and water chemistry across sites. The RDA with the four explanatory variables is highly significant (p = 0.002), explaining approximately 33% of total variability in aquatic macrofossil remains (Table 3.9). Lake surface area and connectivity are strongly positively associated with axis 1, but strongly negatively associated with many species remains (Figure 3.4a and b). Maximum lake depth was also negatively correlated with many macrophyte and zooplankton remains, particularly *Myriophyllum* spp., *Ceratophyllum demersum*, *Simocephalus* sp., and chydorid cladocera. Sulphate concentrations were strongly negatively correlated primarily with *Potamogeton* spp., percid scale remains, and *Daphnia* spp. (Figure 3.4b).

Variable Fraction	***% variation explained***	***p-value***	***F-value***
Connectivity	9.6	0.002	2.5
Maximum depth	9.4	0.002	2.4
Surface area	7.8	0.002	2.2
Sulphate	6.7	0.004	2.0

Table 3.8. SLNG and BRYT macrofossil significance level for all explanatory variables determined to be significant (p≤0.01) through RDA single constrained ordination with 499 Monte Carlo permutations.

	Axis 1	***Axis 2***	***Axis 3***	***Axis 4***
Eigenvalues	0.1772	0.1313	0.0709	0.0436
Explained variation (cumulative)	17.7	30.8	37.9	42.3

Table 3.9. RDA summary table for SLNG and BRYT surface sediment macrofossils, with eigenvalues and cumulative explained variation for the first four RDA axes.

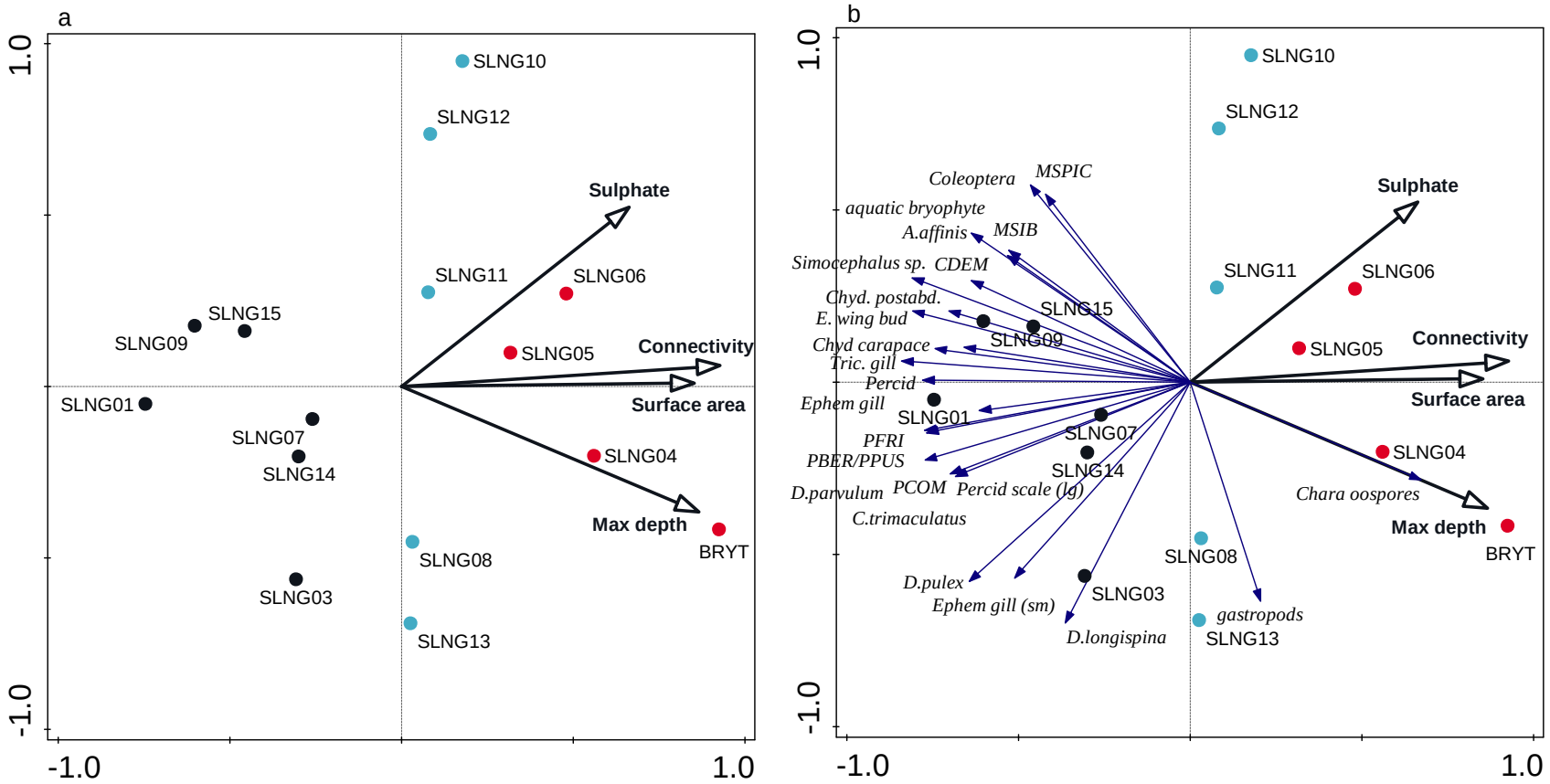

Figure 3.4. a) RDA biplot of sites with four signficant environmental variables; b) RDA biplot of four significant environmental variables plotted with identified macrofossil remains, top 25 species by fit. Sites are colour-coded for connectivity levels: low connectivity (black), intermittent connectivity (light blue), and high connectivity (red). Macrophyte codes can be found in Appendix 5.

3.3.1.3 Contemporary surface sediment diatoms

A total of 228 species taxa from 40 genera were identified within the surface sediments from Selenga River basin lakes. Seventy-nine of the 228 species are present at only one site, and three species (*Amphora copulata*, *Navicula radiosa*, and *Cocconeis placentula* v. *euglypta*) are present at all 15 sites. These three species range in relative abundance from a low of 0.3-0.6% to a high of 16-25%. Taxa present at ≥ 5% at a single site are presented in Figure 3.5, and are primarily benthic or epiphytic, with two planktonic species, *Fragilaria berolinensis* and *Stephanodiscus parvus* (Figure 3.5). Diatom concentrations ranged from 1.11 x 10^5 valves/g dry weight (BRYT) to 4.78 x 10^6 valves/g dry weight (SLNG13). Species richness after rarefaction, ranged from 30.7 species (SLNG03) to 80.9 species (SLNG06), with a mean rarefacted species richness across the 15 sites of 57.1 species. Hill's N2 measure of the diversity of very abundant species ranged from 5.76 at SLNG03 to 33.01 at SLNG05. Hill's N1 ranged from 10.79 at SLNG03 to 51.7 at SLNG05 (Figure 3.5).

Exploratory DCA indicated a gradient length of 2.6 SD, indicating the appropriateness of linear ordination techniques. PCA on a reduced dataset (species present at >2% at any one site) containing 44 species indicated SLNG03 as an outlier from the other sites (Figure 3.6). PCA was re-run on the reduced dataset with SLNG03 removed. Almost 60% of variation was captured by the first two ordination axes (Table 3.10). High connectivity lakes were positive along both PCA axis 1 and 2, while sites with lower connectivity plotted negatively along either axis 1 or 2 or both (Figure 3.7a). Higher abundances of epiphytic and large benthic species were negatively associated with axes 1 and 2, and characteristic of lower connectivity sites. Smaller benthic, small fragilarioid, and planktonic species were positively associated with axes 1 and 2, and characteristic higher connectivity sites (Figure 3.7b).

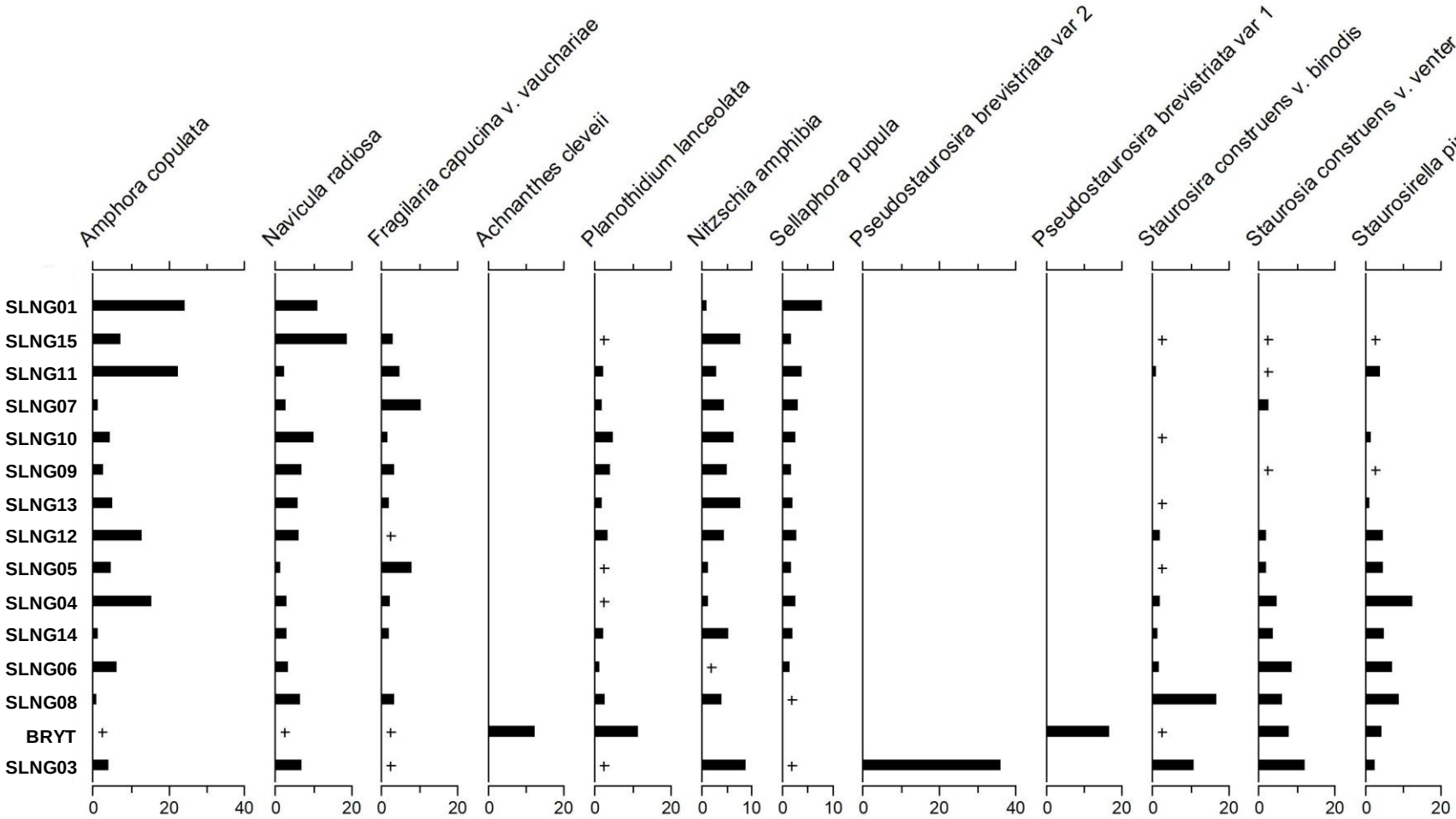

Figure 3.5a. Benthic diatoms present at >5%, in any one sample (% relative abundance), diatom concentration (no. valves g^{-1} dry sediment), rarefacted species richness, Hill's N2 and Hill's N1 measures of diversity. (+) indicates presence of species in sample at <1% relative abundance. Sites are ordered according to PCA axis 1 scores top to bottom, from most negative to most positive.

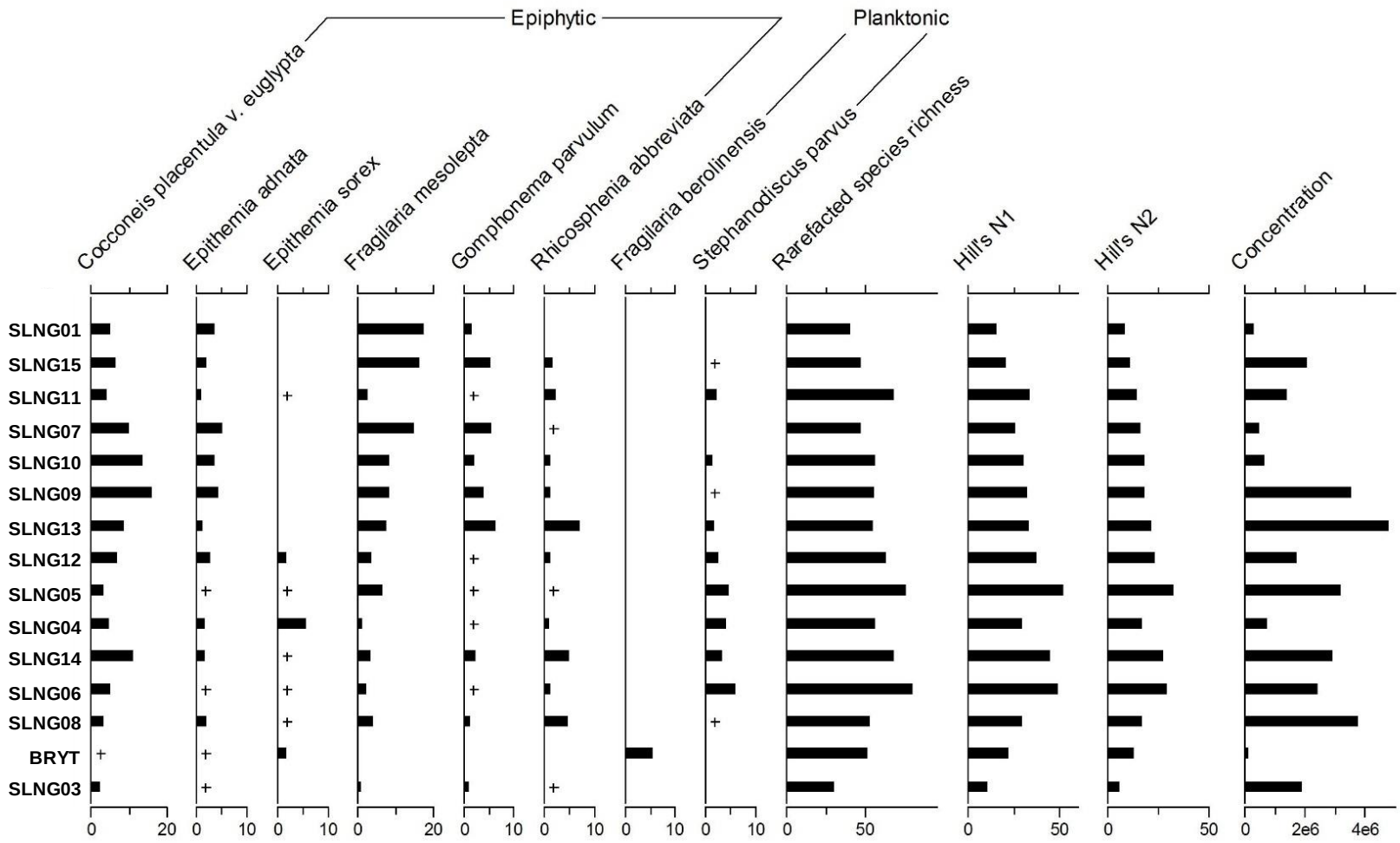

Figure 3.5b. Epiphytic and planktonic diatoms present at >5%, in any one sample (% relative abundance), rarefacted species richness, Hill's N1 and Hill's N2 measures of diversity, and diatom concentration (no. valves g^{-1} dry sediment). (+) indicates presence of species in sample at <1% relative abundance. Sites are ordered according to PCA axis 1 scores top to bottom, from most negative to most positive.

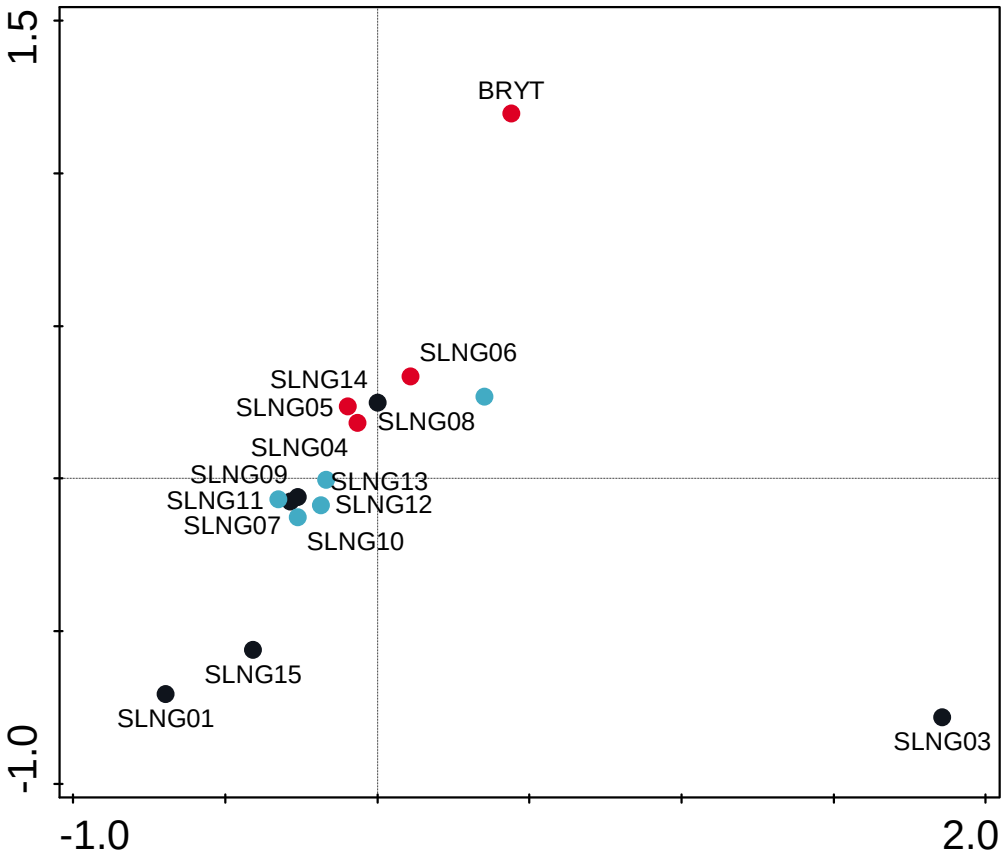

Figure 3.6. Initial PCA plot of surface sediment diatom assemblages across all Selenga River basin sites, showing SLNG03 as an outlier. Sites are colour-coded for connectivity levels: low connectivity (black), intermittent connectivity (light blue), and high connectivity (red).

	Axis 1	***Axis 2***	***Axis 3***	***Axis 4***
Eigenvalues	0.3366	0.2554	0.1449	0.0893
Explained variation (cumulative)	33.7	59.2	73.7	82.6

Table 3.10. PCA summary table for SLNG and BRYT surface sediment diatoms, with eigenvalues and cumulative expalined variation for the first four PCA axes. SLNG03 removed as an outlier.

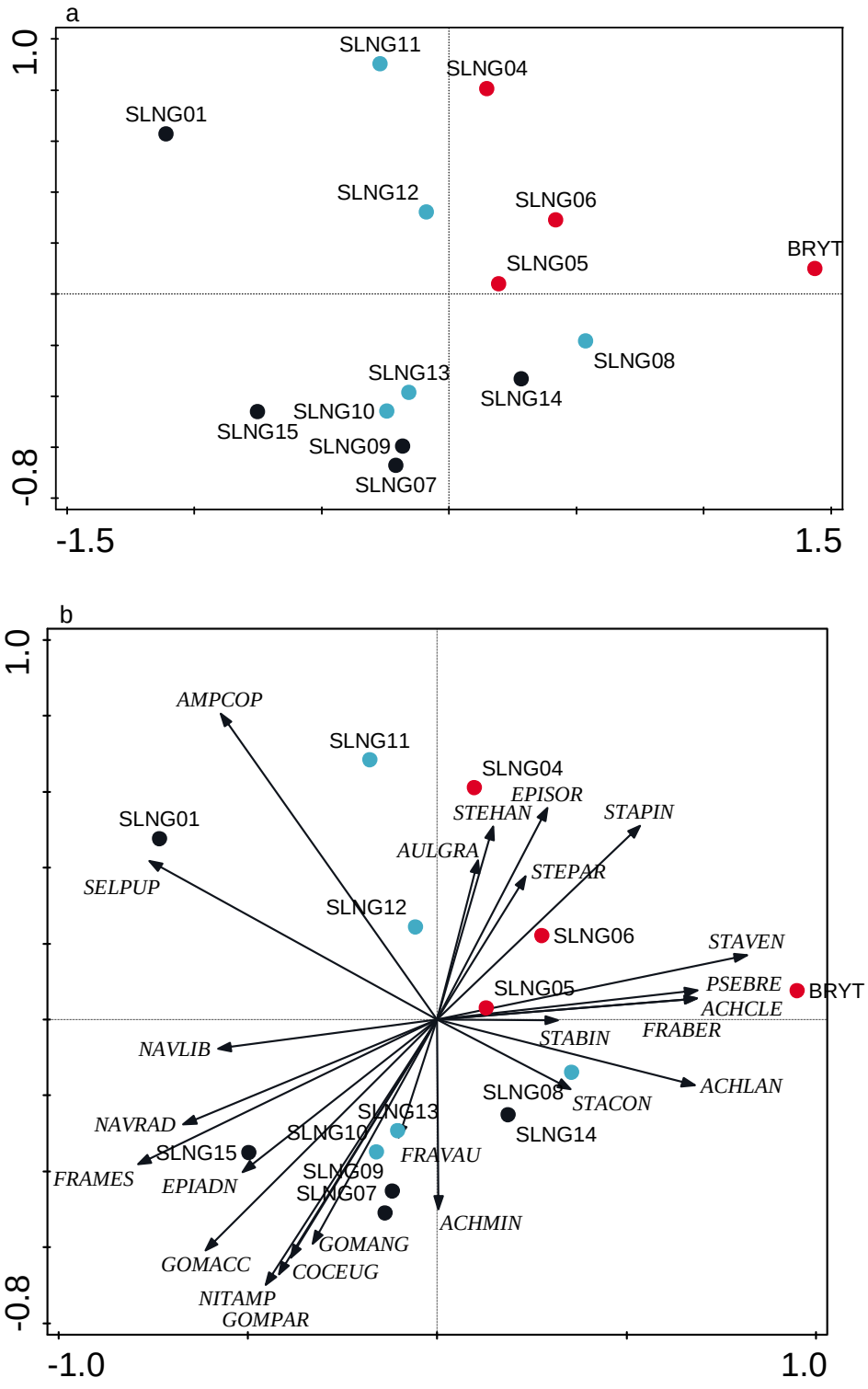

Figure 3.7. a) PCA plot of all sites Selenga River basin shallow lake surface sediment diatom assemblages; b) PCA biplot of sites with outlying sites removed, and 44 diatom species >2% at any one site. Top 25 species only shown in diagram. Sites are colour-coded for connectivity levels: low connectivity (black), intermittent connectivity (light blue), and high connectivity (red). Diatom codes can be found in Appendix 6.

Across all sites, macrofossil richness, macrofossil PCA axis 1 scores, connectivity, maximum depth, and pH were significant ($p \leq 0.01$) in explaining variability in the surface sediment diatom community variability (Table 3.11). The RDA with the five explanatory variables is highly significant ($p = 0.002$), explaining over 40% of total variability in surface sediment diatoms (Table 3.12). Highly connected lakes plot to the right of the ordination diagram, more positively associated with increasing depth and pH. Intermittent or low connectivity sites plot further to the left within the ordination diagram, more positively associated with increasing macrofossil richness (Figure 3.8a). Macrofossil richness and connectivity are negatively associated within the diatom RDA, while connectivity and macrofossil PCA axis 1 scores were closely positively associated (Figure 3.8). Macrofossil richness is positively associated with many of the common epiphytic and large benthic diatoms (Figure 3.8b). Maximum depth, connectivity, and macrofossil PCA axis 1 scores were positively associated with many of the common planktonic, small benthic, and small fragilarioid species.

Variable	*% variation explained*	*p-value*	*F-value*
Maximum depth	9.9	0.002	4.2
Macrofossil richness	9.8	0.002	4.2
Macrofossil PCA axis 1 scores	9.2	0.002	3.9
Connectivity	6.8	0.004	3.0
pH	6.0	0.004	2.8

Table 3.11. SLNG and BRYT diatom significance level for all explanatory variables determined to be significant ($p \leq 0.01$) through RDA single constrained ordination with 499 Monte Carlo permutations.

	Axis 1	*Axis 2*	*Axis 3*	*Axis 4*
Eigenvalues	0.2864	0.1465	0.0876	0.0242
Explained variation (cumulative)	28.6	43.3	53.0	54.5

Table 3.12. RDA summary table for SLNG and BRYT surface sediment diatoms, with eigenvalues and cumulative explained variation for the first four RDA axes.

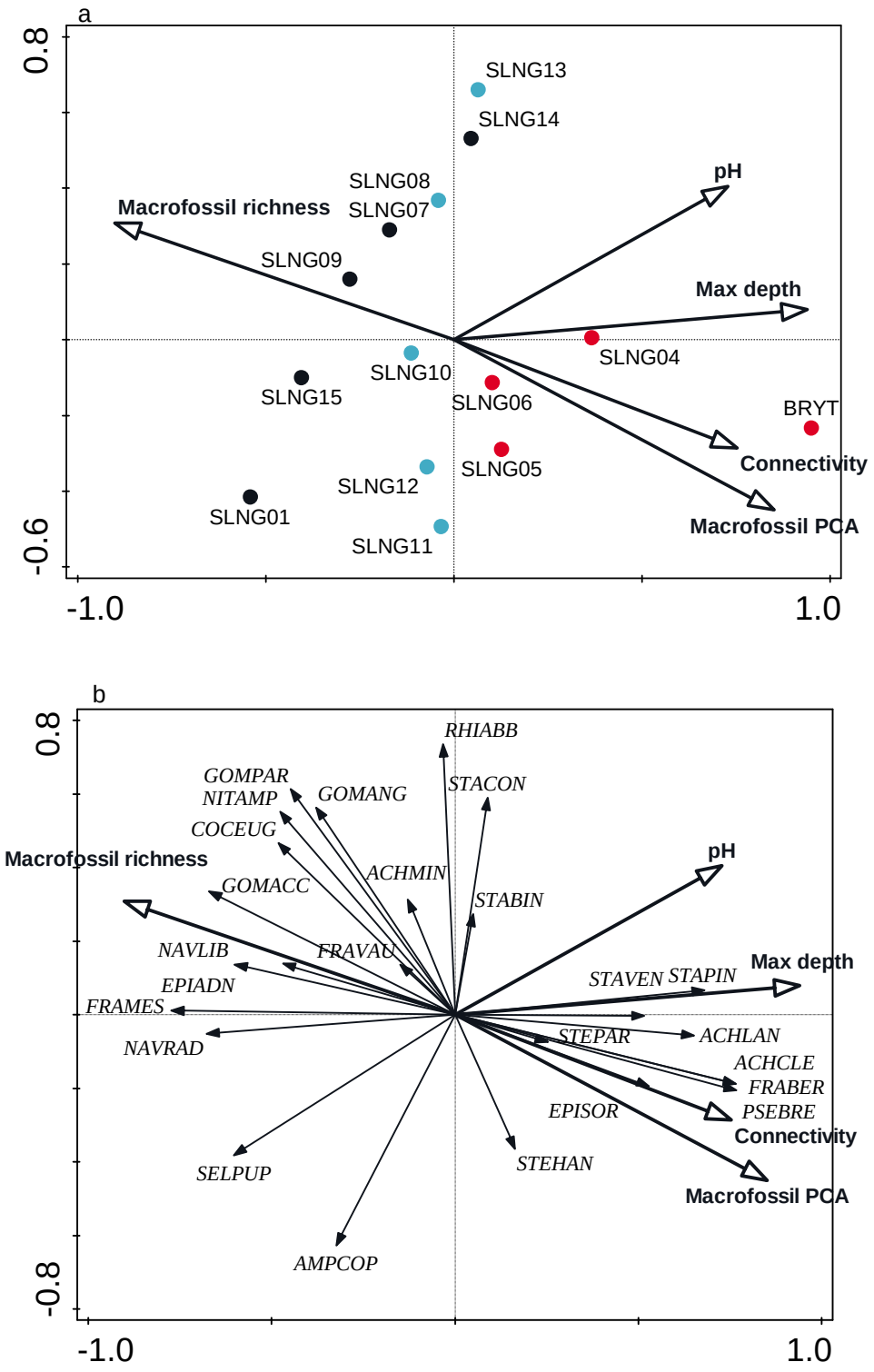

Figure 3.8. a) RDA biplot of sites with five signficant environmental variables; b) RDA biplot of four significant environmental variables plotted with diatom species diatom species, top 25 species by fit. Sites are colour-coded for connectivity levels: low connectivity (black), intermittent connectivity (light blue), and high connectivity (red). Diatom codes can be found in Appendix 6.

3.3.1.4 Surface water pigment assemblages

Pigment concentrations found in surface waters of the 15 lakes are shown in Figure 3.9. Pigments representing total algae (Chl *a*, Chl *a* degradation products, and β-carotene), chlorophytes (Chl *b*, Chl *b* degradation product pheophytin *b*, lutein, violaxanthin, and neoxanthin), total cyanobacteria (zeaxanthin), colonial cyanobacteria (myxoxanthophyll and canthaxanthin), siliceous algae (fucoxanthin), diatoms (diatoxanthin), cryptophytes (alloxanthin and violaxanthin), chromophytes (Chl *c*), prasinophytes (neoxanthin and violaxanthin), and higher plants (violaxanthin) were detected. Total algal biomass (pigments for Chl *a*, Chl *a* degradation products, and β-carotene) was highest at SLNG03 and SLNG09, and lowest at SLNG08, SLNG10 and SLNG13. Chlorophytes (Chl *b*, Chl *b* degradation products, and lutein) are highest at SLNG09, and lowest at SLNG13. Total and colonial cyanobacteria (zeaxanthin and canthaxanthin) are highest in SLNG03 and BRYT, respectively, and absent from the surface waters of SLNG01, SLNG06, SLNG05, SLNG07, SLNG13, SLNG15, SLNG10, and SLNG12 (Figure 3.9).

Exploratory DCA indicated a gradient length of 2.1 SD, and the appropriateness of linear ordination techniques. Initial PCA of all sites indicated SLNG01 as an outlier with respect to surface water pigments (Figure 3.10), and so SLNG01 was removed from related subsequent analyses. PCA with SLNG01 removed showed that 82% of variation was explained by the first two PCA axes (Table 3.13). Most sites clustered in the lower left of the PCA: SLNG04, SLNG05, SLNG06, SLNG08, SLNG10, SLNG11, SLNG12, SLNG13, and SLNG14. This clustering was mainly comprised of intermittent or high connectivity sites (Figure 3.11a). Most low connectivity sites, SLNG03, SLNG07, SLNG09, and SLNG15, plot positively along axis 2 (Figure 3.11a). Indicators of total algal biomass (Chl *a* and β-carotene) along with most chlorophylls and carotenoids were positively associated with PCA axis 1, and so axis 1 is primarily a gradient of total algal biomass. Indicators of siliceous algae and diatoms (diadinoxanthin and diatoxanthin), as well as total algae (Chl *a* degradation products) and chlorophytes (pheophytin *b*) were associated with PCA axis 2 (Figure 3.11b). The clustering of most sites along the negative portion of PCA axis 1 indicated that these intermittent to high connectivity sites had lower algal biomass, with lower concentrations of pigments from total algae and various algal groups, while low connectivity sites SLNG03 and SLNG09 were more

positive along axis 1, with higher algal biomass and higher concentrations of pigments from total algae and most algal groups.

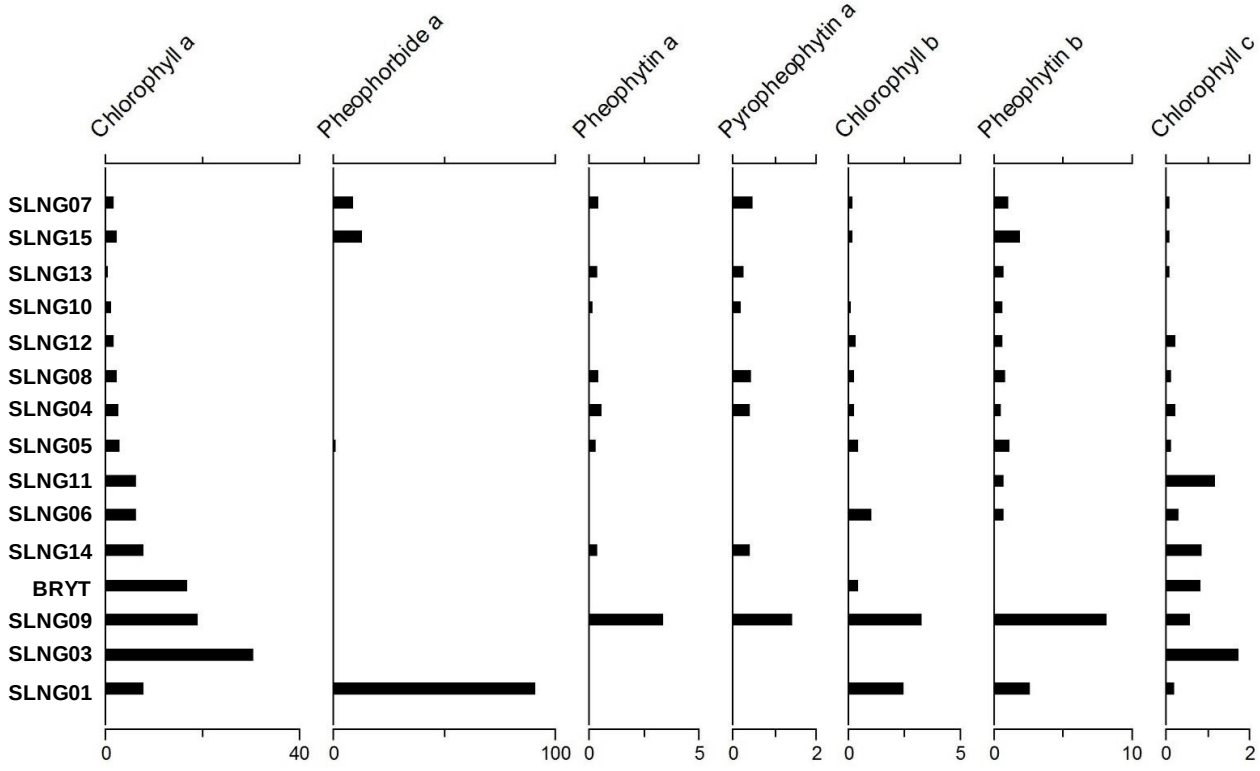

Figure 3.9a. Concentrations (nmol l^{-1}) of chlorophyll pigments and chlorophyll degradations products identified from Selenga River basin surface waters. Sites are ordered according to PCA axis 1 scores top to bottom, from most negative to most positive.

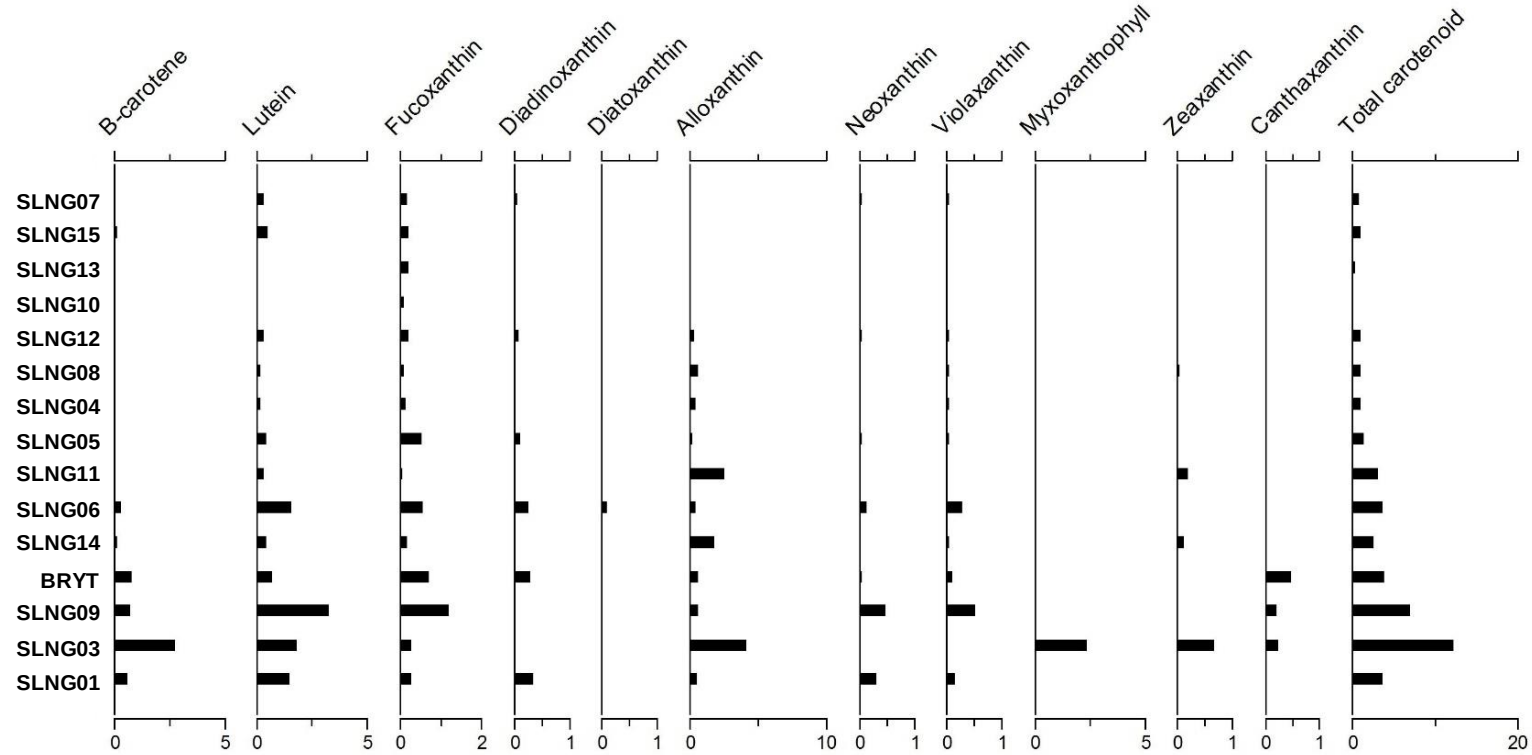

Figure 3.9b. Concentrations (nmol l^{-1}) of carotenoid pigments identified from Selenga River basin surface waters. Sites are ordered according to PCA axis 1 scores top to bottom, from most negative to most positive.

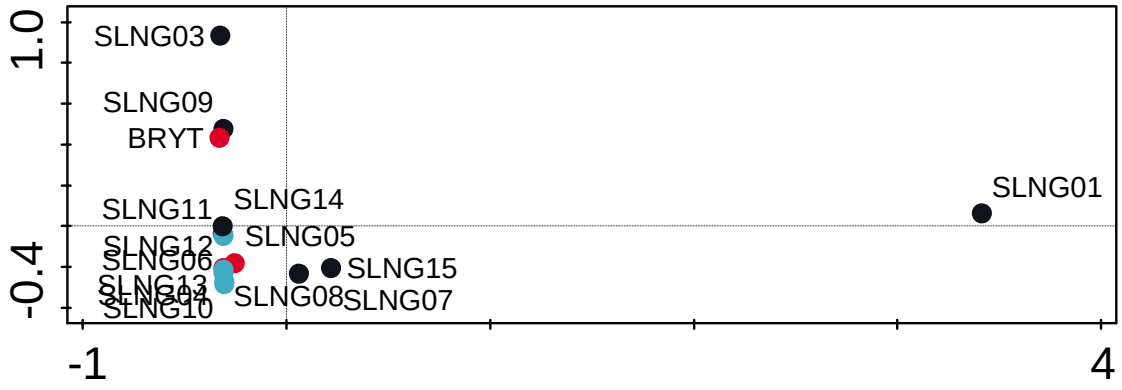

Figure 3.10. Initial surface water pigment PCA site plot, indicating SLNG01 as an outlier. Sites are colour-coded for connectivity levels: low connectivity (black), intermittent connectivity (light blue), and high connectivity (red).

	Axis 1	***Axis 2***	***Axis 3***	***Axis 4***
Eigenvalues	0.6970	0.1315	0.1219	0.0455
Explained variation (cumulative)	69.7	82.8	95.0	99.6

Table 3.13. PCA summary table for SLNG and BRYT surface water pigments, with eigenvalues and cumulative expalined variation for the first four PCA axes.

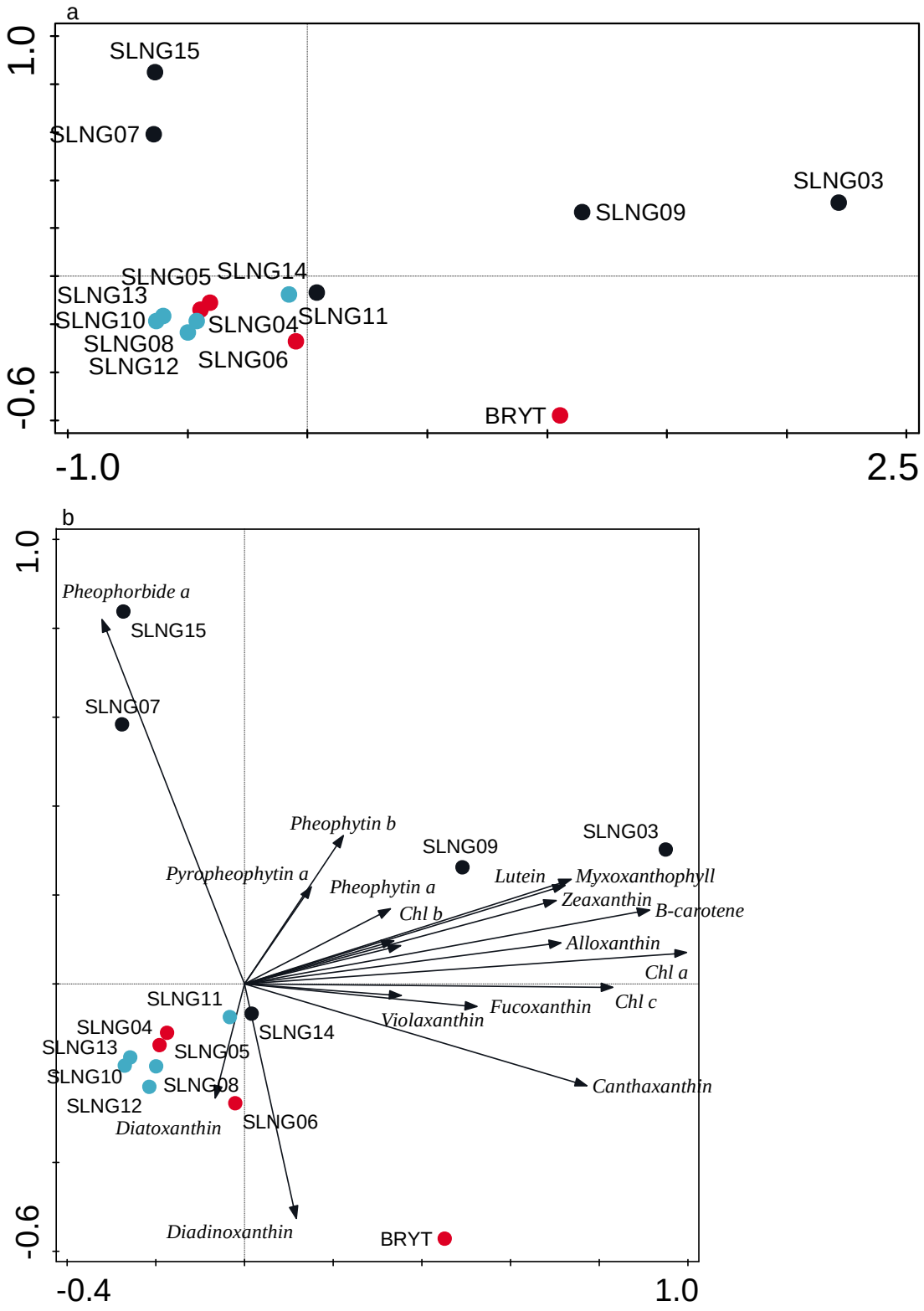

Figure 3.11. a) PCA plot of all sites for surface water pigments; b) PCA biplot of surface water pigments (vectors) and all SLNG and BRYT sites (dots). Sites are colour-coded for connectivity levels: low connectivity (black), intermittent connectivity (light blue), and high connectivity (red).

3.3.1.5 Surface sediment pigment assemblages

Pigment concentrations found in surface sediments are shown in Figure 3.12. Pigments representing total algae (Chl *a*, Chl *a* degradation products, and β-carotene), chlorophytes (Chl *b*, Chl *b* degradation product, and lutein), total cyanobacteria (echinenone and zeaxanthin), colonial cyanobacteria (canthaxanthin), siliceous algae (fucoxanthin), diatoms (diatoxanthin), dinoflagellates (peridinin), cryptophytes (alloxanthin), and chromophytes (Chl *c*) were identified in the surface sediments from SLNG and BRYT lakes.

Exploratory DCA indicated a gradient length of 1.0 SD, indicating the appropriateness of linear ordination techniques. Nearly all variation, 96%, in surface sediment pigment concentrations across study sites was explained between the first two PCA axes (Table 3.14). Total algal biomass (Chl *a* degradation product pheophorbide *a*) is most negatively associated with PCA axis 1, and total algal production (β-carotene) and most carotenoids are positively associated with PCA axis 2 (Figure 3.13b). Sites with higher concentrations of total algae (Chl *a*), total carotenoids (variety of algal groups) and chlorophytes (Chl *b*, pheophytin *b*, and lutein) were more positive along PCA Axis 2 and negative along PCA axis 1. Pheophorbide *a* was not detected in the surface sediments of SLNG03 and SLNG06, which are the most positive sites located along PCA axis 1.

	Axis 1	***Axis 2***	***Axis 3***	***Axis 4***
Eigenvalues	0.7281	0.2294	0.0262	0.0114
Explained variation (cumulative)	72.8	95.8	98.4	99.5

Table 3.14. PCA summary table for SLNG and BRYT surface sediment pigments, with eigenvalues and cumulative expalined variation for the first four PCA axes.

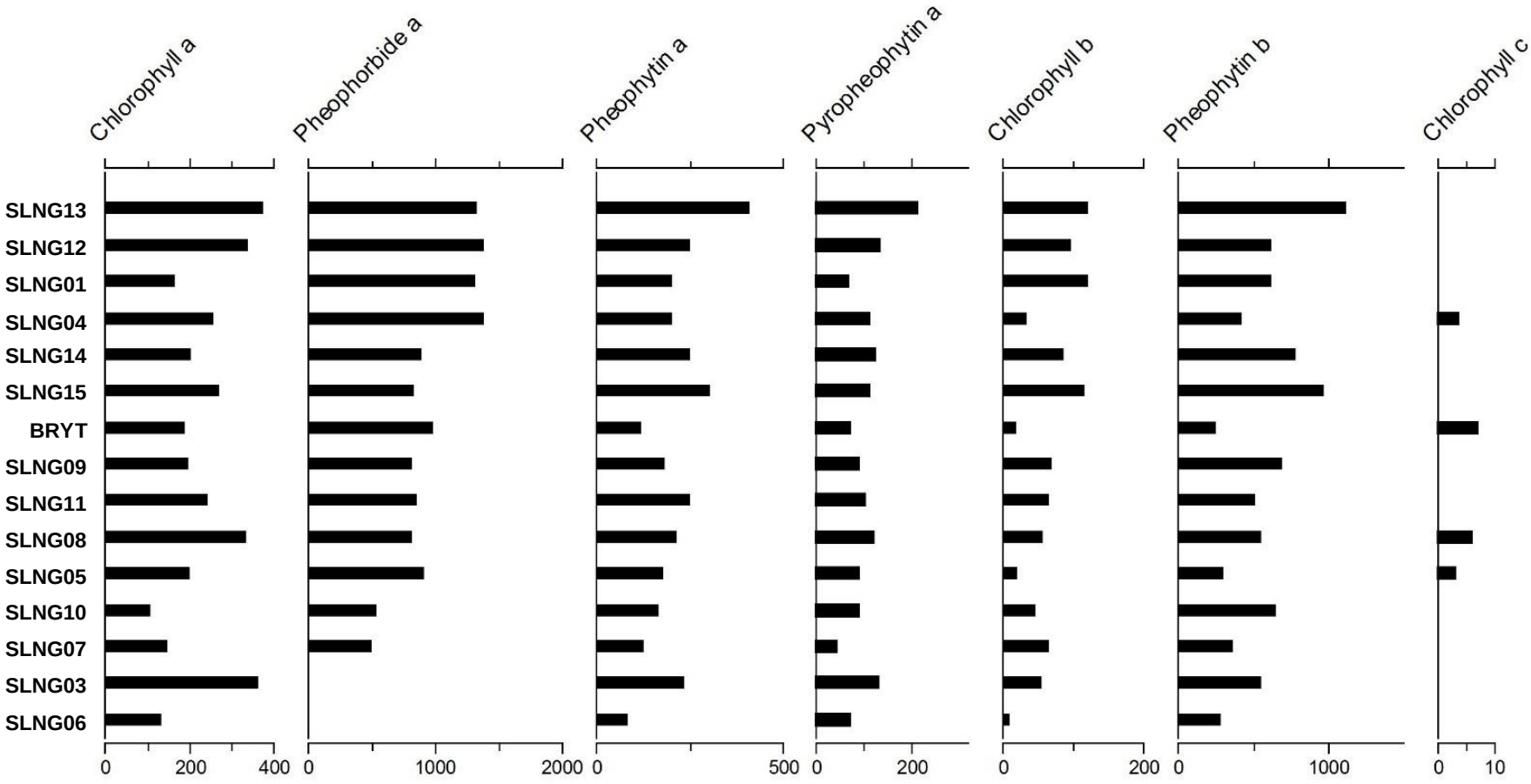

Figure 3.12a. Concentrations (nmol g^{-1} organic matter) of chlorophyll pigments and chlorophyll degradation products identified from Selenga River basin surface sediments. Sites are ordered according to PCA axis 1 scores top to bottom, from most negative to most positive.

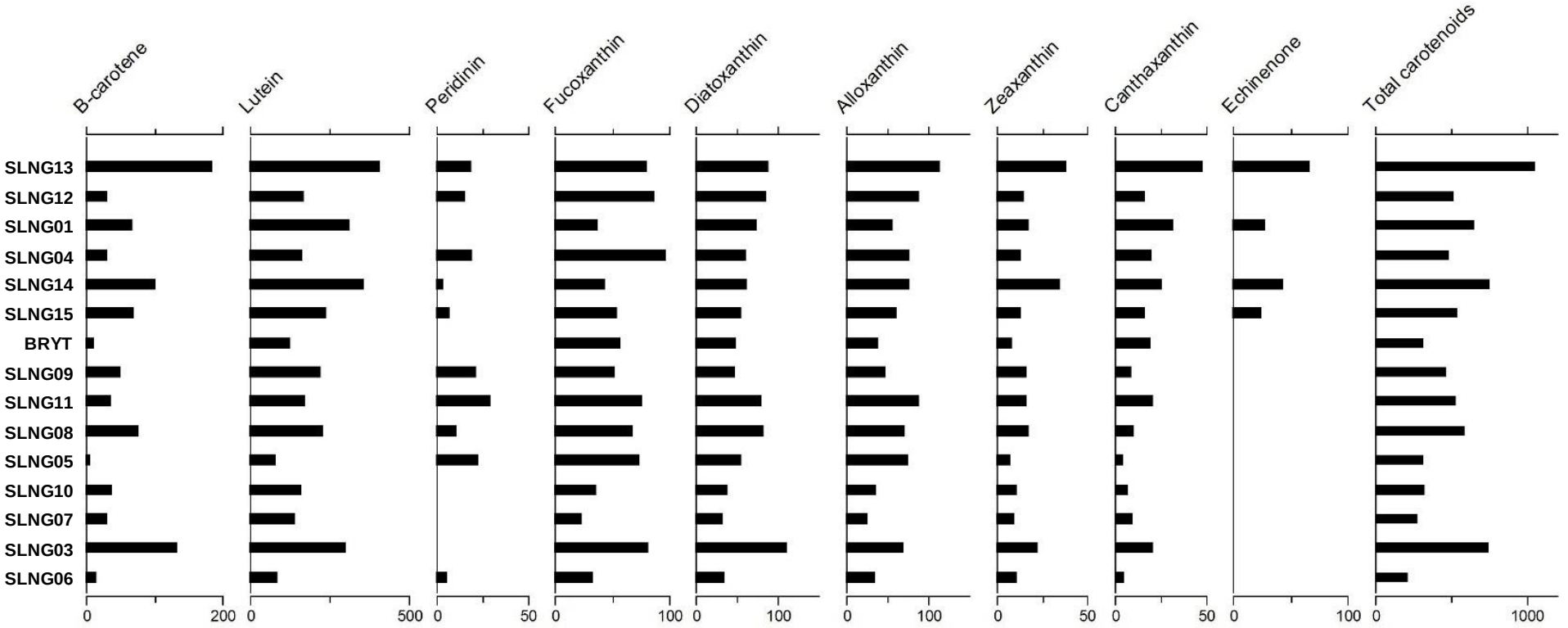

Figure 3.12b. Concentrations (nmol g^{-1} organic matter) of carotenoid pigments identified from Selenga River basin surface sediments. Sites are ordered according to PCA axis 1 scores top to bottom, from most negative to most positive.

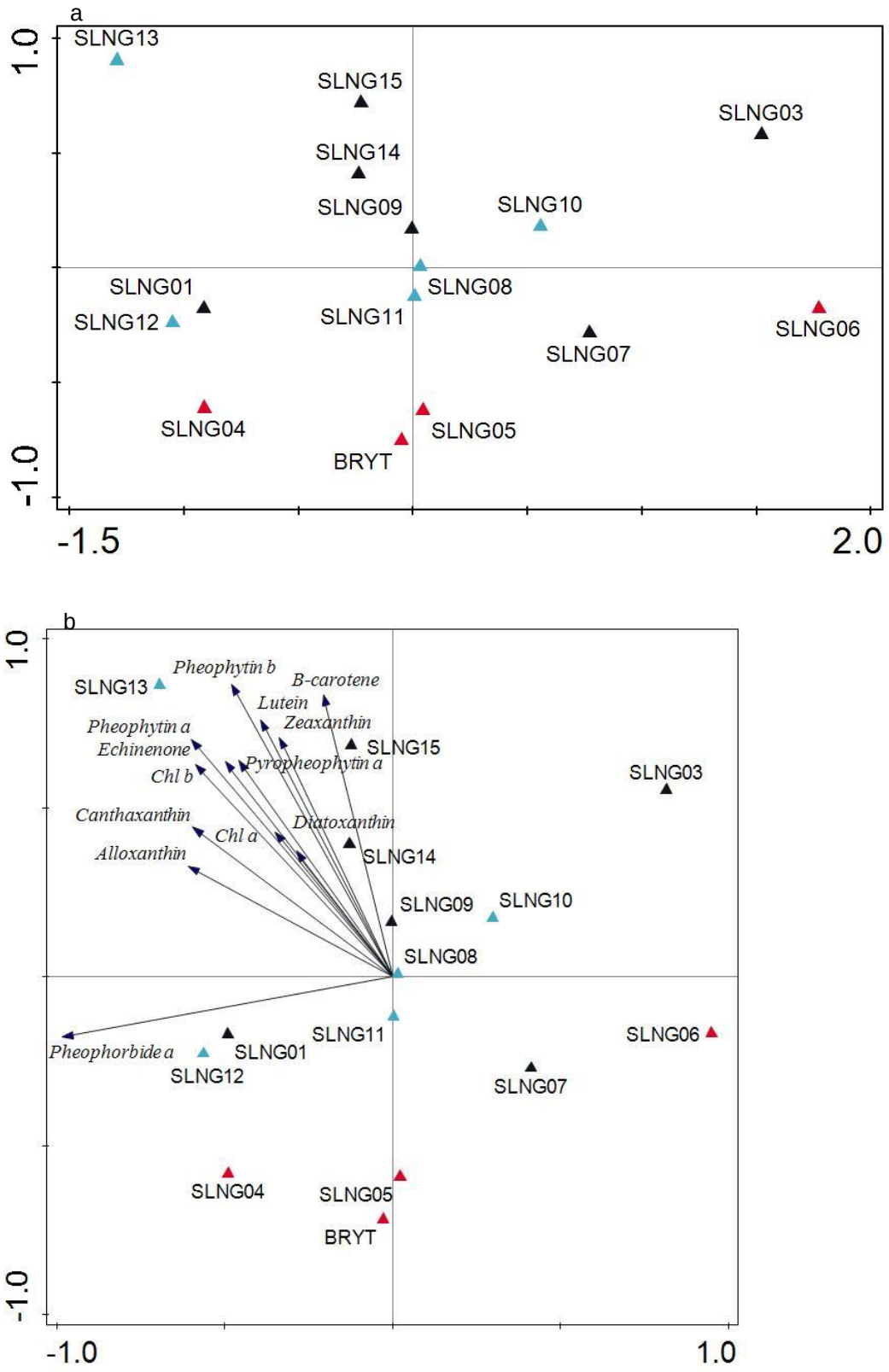

Figure 3.13. a) Surface sediment pigment PCA plot of all sites; b) PCA biplot of all sites and surface sediment pigments. Sites are colour-coded for connectivity levels: low connectivity (black), intermittent connectivity (light blue), and high connectivity (red).

Differences existed between surface water pigment assemblages, and surface sediment pigment assemblages (Figure 3.14). Water samples cluster on the negative side of PCA axis 1, while sediment samples are spread on the positive side of axis 1, and throughout PCA axis 2. Concentrations of pigments found in both the surface waters and sediments were higher in sediments. Several pigments were only found in the surface waters, including myxoxanthophyll, pyropheophorbide a, and neoxanthin (Figure 3.14b).

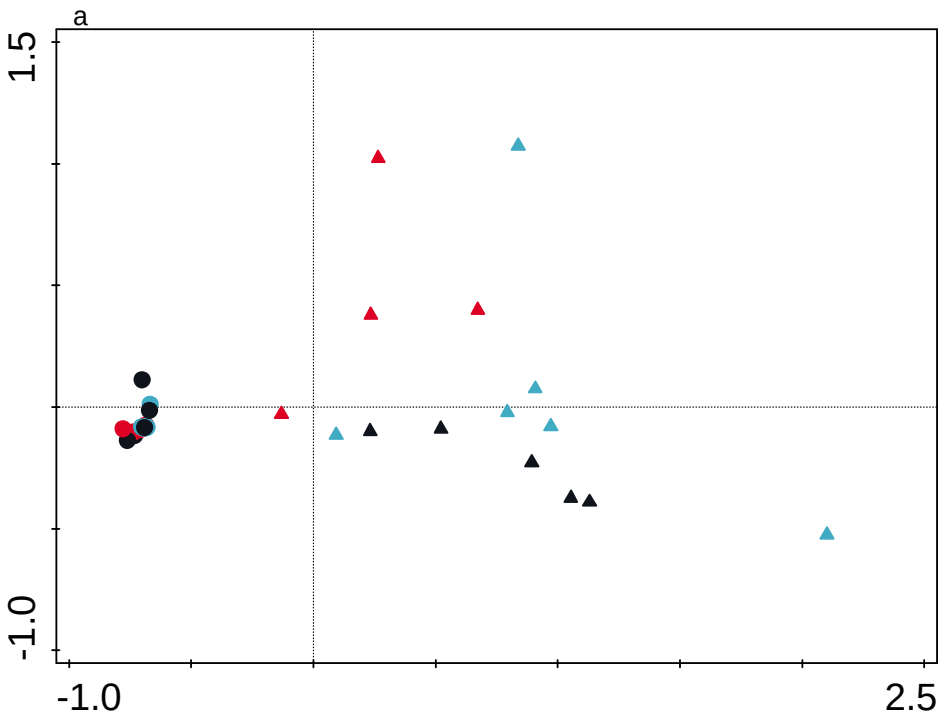

Figure 3.14a. Comparing pigment concentrations across sites between sediment and water samples. Triangles are sediment samples, circles are water samples. Sites are colour-coded for connectivity levels: low connectivity (black), intermittent connectivity (light blue), and high connectivity (red).

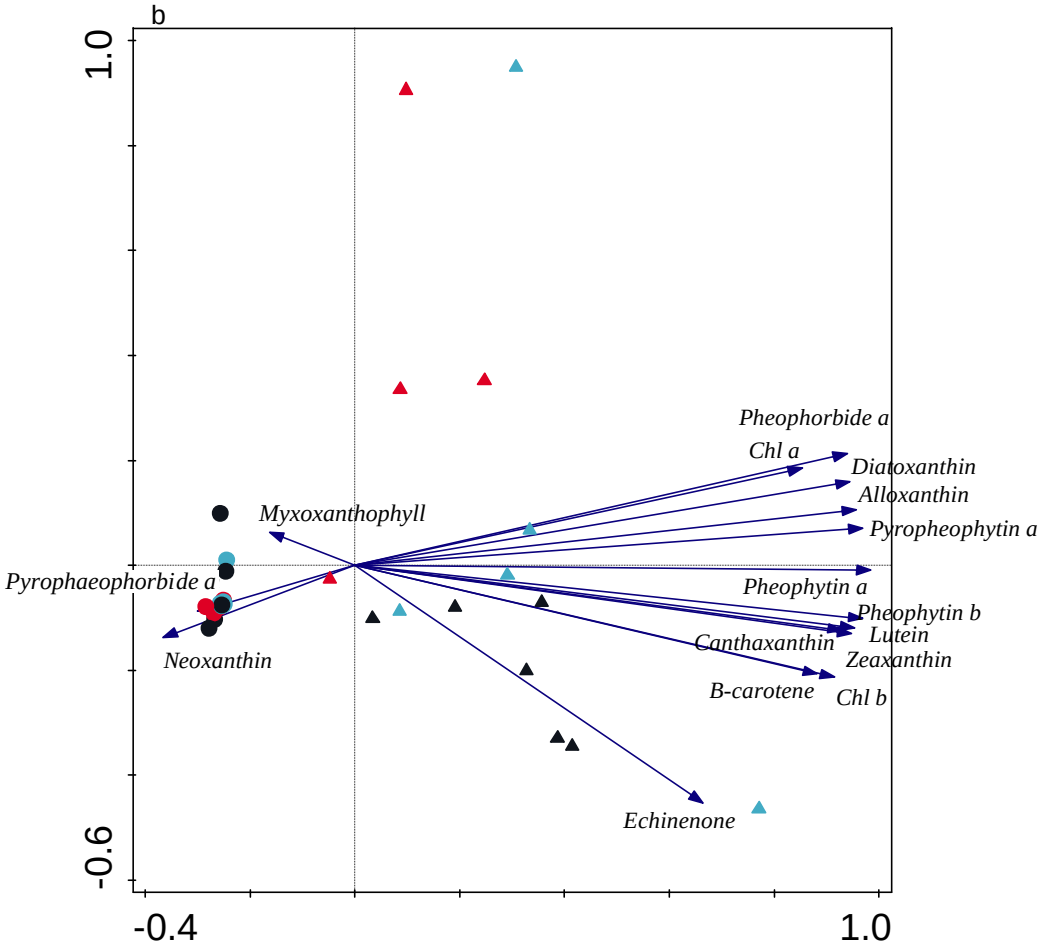

Figure 3.14b. Comparing pigment concentrations across sites between sediment and water samples, with pigments as vectors. Triangles are sediment samples, circles are water samples. Sites are colour-coded for connectivity levels: low connectivity (black), intermittent connectivity (light blue), and high connectivity (red).

3.3.2 Assessing significance of connectivity level across ecological parameters

Assessments to test the significance of connectivity variations on ecological communities indicated that of all response variables tested, macrofossil richness was the only ecological variable to vary significantly depending on connectivity levels (Table 3.15). Kruskal-Wallis test indicated that significant differences existed between the three connectivity categories of high connectivity, intermittent connectivity, and low connectivity (Table 3.15). Further investigations, using Mann-Whitney U tests, revealed that significance was found between high connectivity sites and low connectivity sites (Table 3.15). Any significance of connectivity levels disappeared when intermittent connectivity sites were compared to either high connectivity or low connectivity sites.

Ecological variable	*Connectivity comparisons*	*MWU p-value*	*KW p-value*
Macrofossil richness	High connectivity vs. intermittent connectivity vs. low connectivity		**0.009**
Macrofossil richness	High connectivity vs. low connectivity	**0.01**	
Macrofossil richness	High connectivity vs. intermittent connectivity	0.05	
Macrofossil richness	Intermittent connectivity vs. low connectivity	0.044	
Diatom species richness (rarefaction)	Low connectivity vs. intermittent/high connectivity	0.045	
Total carotenoids concentration (sediment)	High connectivity vs. intermittent/low connectivity	0.026	

Table 3.15. Results from Mann-Whitney U (MWU) and Kruskal-Wallis (KW) tests, assessing the significance of variations in connectivity levels on ecological variables from the Selenga River basin shallow lakes. Only those test results with p-value <0.05 are reported. Significant test results ($p \leq 0.01$) are in **bold**.

3.3.3 Comparing similarities in spatial variability across biological indicators

CoCA between diatoms and macrofossils was the only significant CoCA produced amongst the SLNG and BRYT datasets. The first two axes of the CoCA very strongly capture the extent of cross-correlation between the two communities (Table 3.16), and the relation between the two communities is highly significant (Table 3.16). *Bosmina longispina* co-occurs with several planktonic diatoms in the upper left-side of the plots, including *Cyclostephanos dubius*, and *Stephanodiscus* spp. (Figure 3.15). *Potamogeton friesii* (PFRI) co-occurs with several epiphytic diatoms in the lower left-side of the plots, including several *Gomphonema* spp., and *Nitzschia amphibia*. *Myriophyllum spicatum* co-occurs with *Staurosira construens* v. *venter*, and *Planothidium lanceolata*, on the right-side of the plots, while *Myriophyllum sibericum* tends to co-occur with several of the more common epiphytic diatom species, including *Epithemia adnata*, *Cocconeis placentula* v. *euglypta*, and *Fragilaria mesolepta*, in the lower left-central area of the plot.

Proxies	Axis 1	Axis 2	Axis 3	Axis 4	p-value
Diatom*Macrofossil	+0.9 874	+0.8 878	+0.8 725	+0.9 241	0.006

Table 3.16. Cross correlations between axes determined through co-correspondence analysis of the SLNG and BRYT diatom and macrofossil records. High positive values indicate strong correlation between the first CoCA axes. Tests for significance across axes for Diatom*Macrofossil analysis in CoCA. Significance p ≤ 0.01.

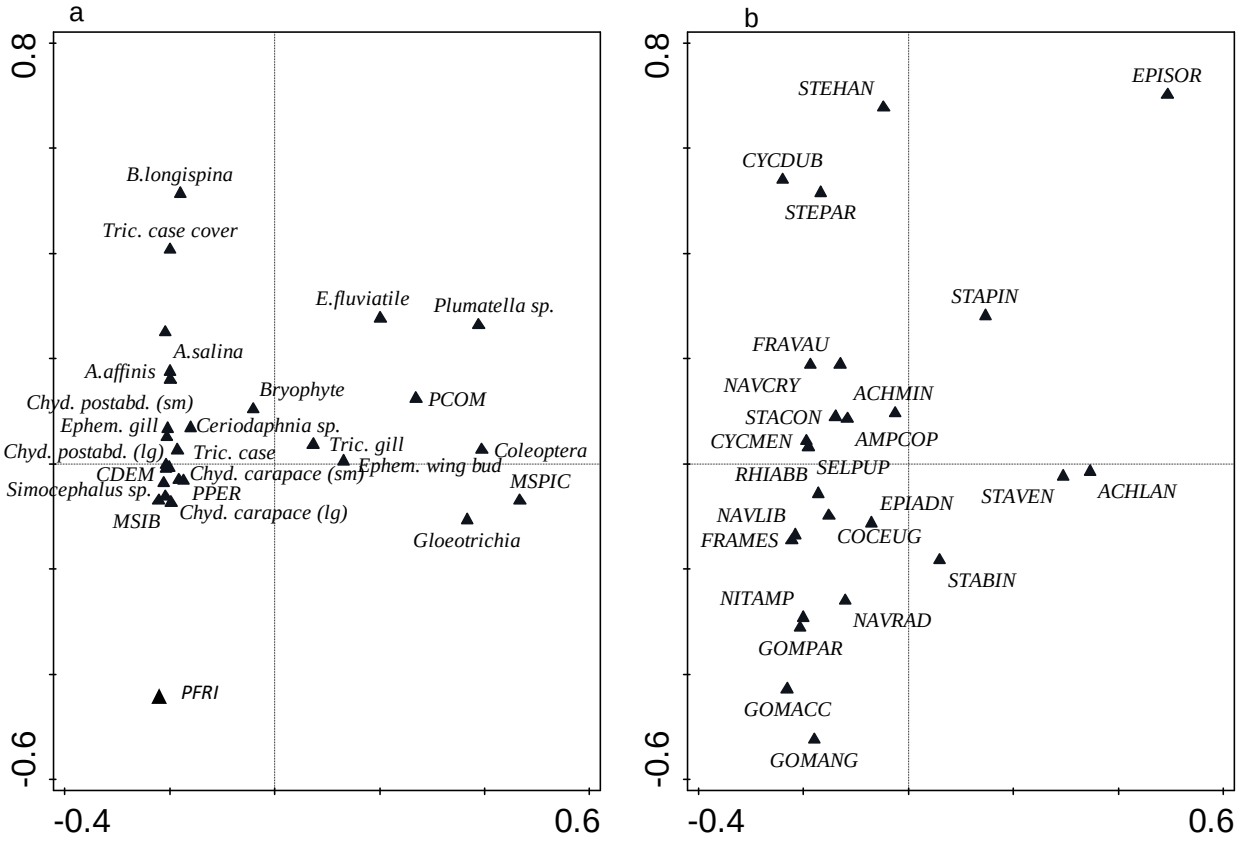

Figure 3.15. Macrofossil (a) and diatom (b) CoCA community biplots. Species falling in the same area across plots tend to co-occur in the proxy records. Top 25 species by fit plotted for each proxy.

3.3.4 Determining geochemical gradients across Selenga River basin lakes

3.3.4.1 Contemporary surface sediment trace and major elements

Trace and major element concentrations, and element ratios are shown in Figure 3.16. SLNG03 had exceptionally high Ca content, but very low values of many other lithogenic elements, including Ti, Al, and K. The very high Ca and low Ti content in the surface sediments of SLNG03 led to a very high Ca/Ti ratio for the lake, of 274.5, when the mean Ca/Ti ratio across all lakes was 27.65. As determined through PPMC analyses, many of the trace and major elements are found to be significantly correlated (p≤0.01) (Table 3.17). Significant positive

correlations existed between trace metals, including Ni and Cu, Ni and Zn, Ni and Pb, Pb and Zn, Cu and Zn and Cu and Pb. Phosphorus, Ca, and As have a significant negative correlation with Ti. Moreover, As is negatively correlated with many of the measured elements, with the exceptions of Ca, Mn, Fe, Ca/Ti, and P, the latter of which is a significant positive correlation. Cu is the only trace element not significantly correlated with Ti. Last, Ca is significantly negatively correlated with Fe/Mn ratio.

Total variation explained by the first two PCA axes was 83% (Table 3.18). SLNG01, SLNG03, SLNG04, and SLNG07 are most positive along PCA axis 1, and most sites form a cluster in the negative side of PCA axis 1, while BRYT, SLNG15, and SLNG09 cluster around the origin of PCA axes 1 and 2. SLNG10 separates from the group along PCA axis 2 (Figure 3.17). As, P, Mn, and Ca are positively associated with PCA axis 1. S and Br are positively associated with PCA axis 2, while Fe, negatively. Most other trace and major elements are negatively correlated with PCA axis 1 (Figure 3.17).

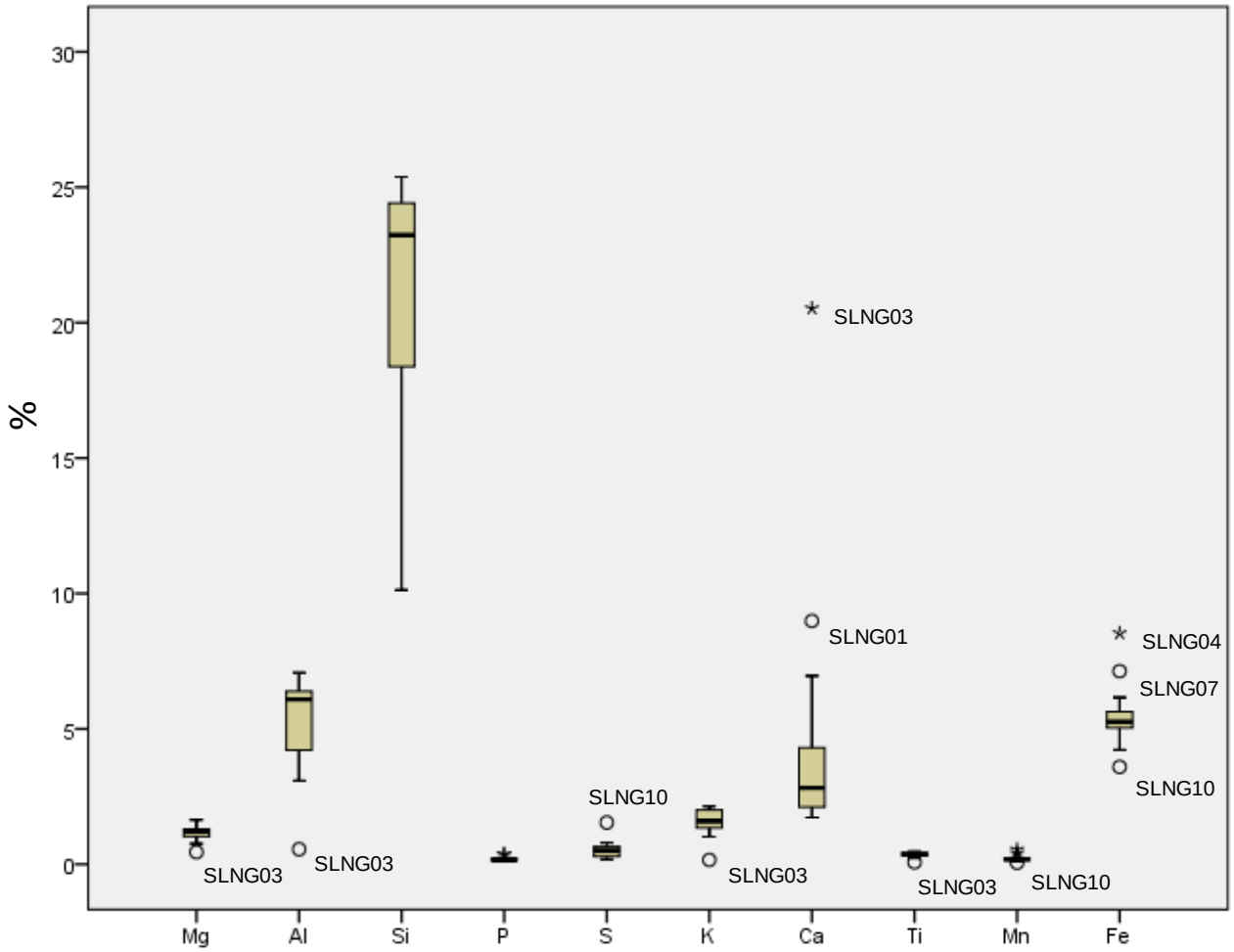

Figure 3.16a. Major lithogenic element percentage boxplots from Selenga River basin shallow lake surface sediments. Medians (bold line), 1st and 3rd quartiles, minima, maxima, and outliers (1.5 x interquartile range) are displayed. (○) indicate outliers and (*) indicate extreme outliers.

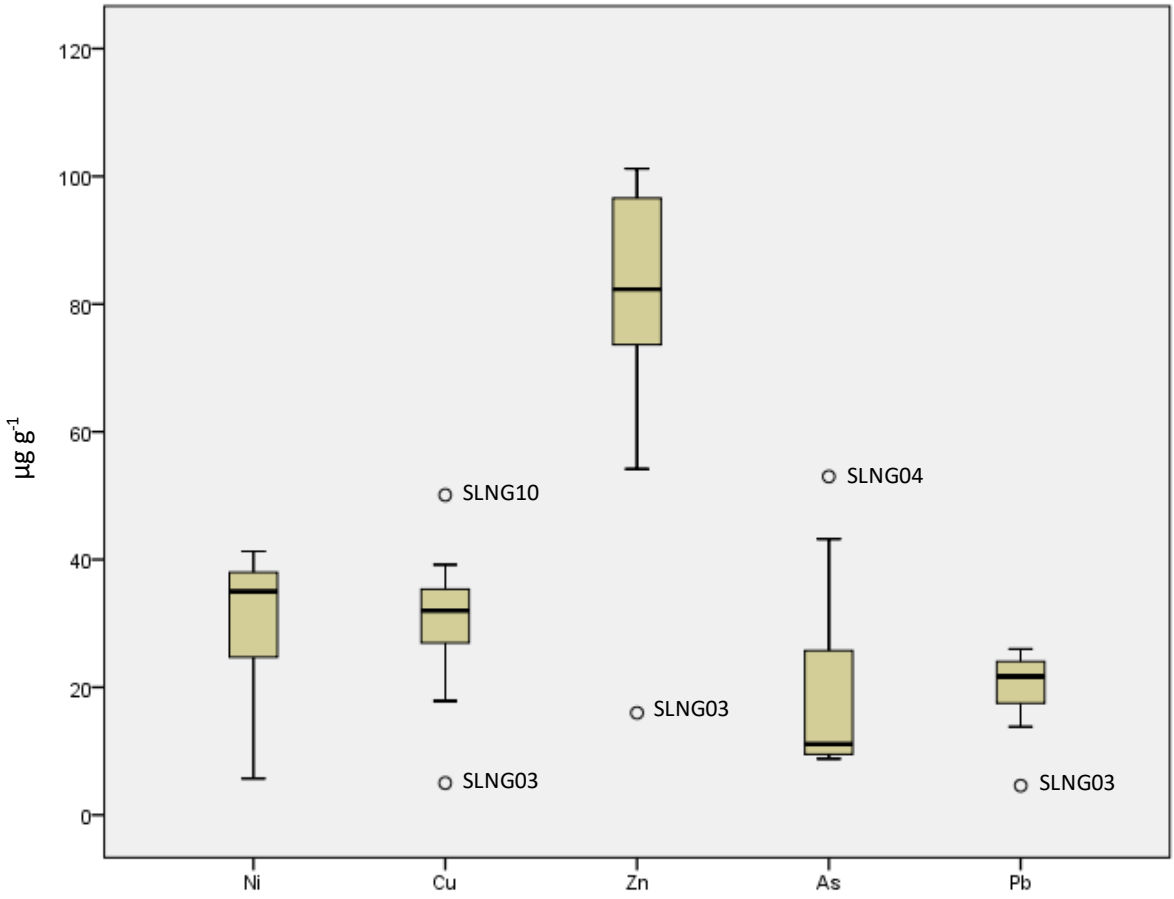

Figure 3.16b Trace element concentration boxplots from Selenga River basin shallow lake surface sediments. Medians (bold line), 1st and 3rd quartiles, minima, maxima, and outliers (1.5 x interquartile range) are displayed.

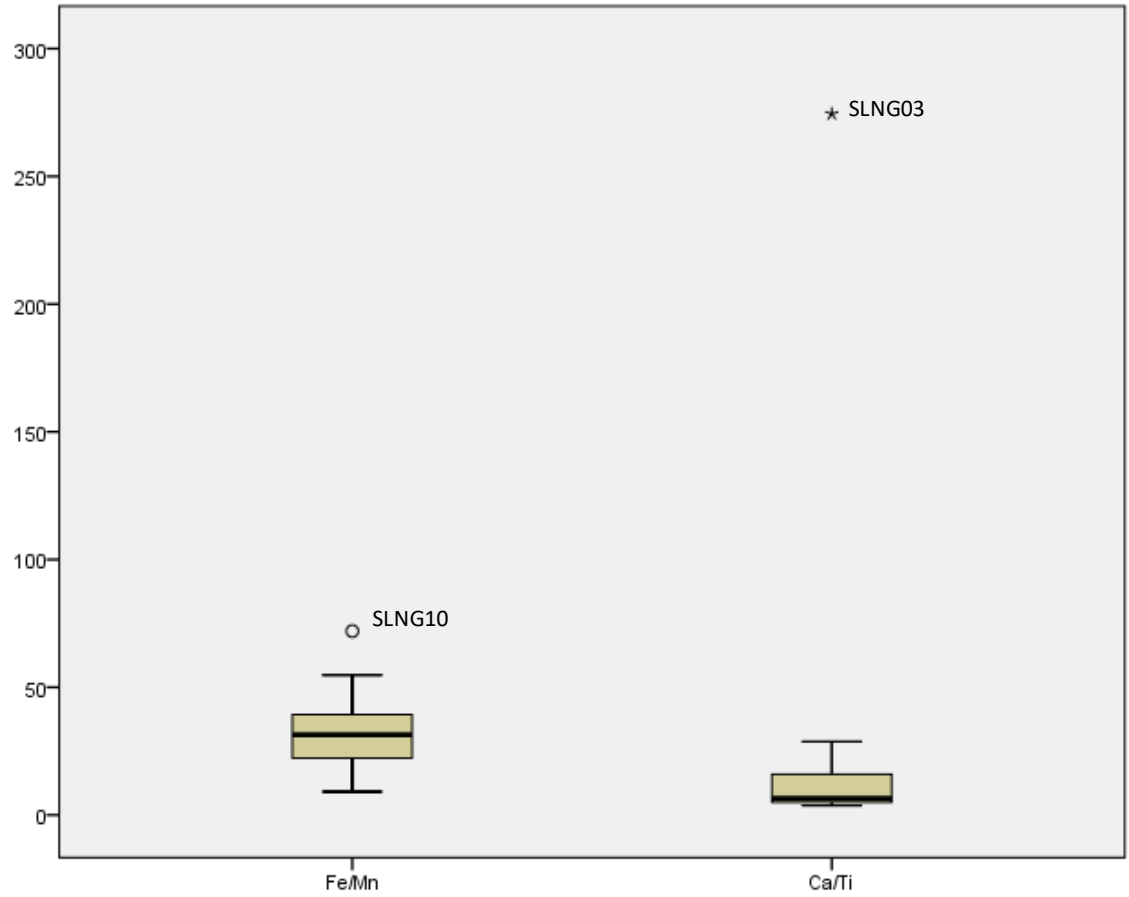

Figure 3.16c Trace element ratio boxplots from Selenga River basin shallow lake surface sediments. Medians (bold line), 1st and 3rd quartiles, minima, maxima, and outliers (1.5 x interquartile range) are displayed. (○) indicate outliers and (*) indicate extreme outliers.

	Mg	***Al***	***Si***	***P***	***K***	***Ca***	***Ti***	***Mn***	***Fe***	***Ni***	***Cu***	***Zn***	***As***	***Pb***
Mg	1													
Al	**0.914**	1												
Si	**0.784**	**0.871**	1											
P	-0.530	**-0.751**	**-0.666**	1										
K	**0.908**	**0.956**	**0.949**	**-0.667**	1									
Ca	**-0.642**	**-0.719**	**-0.918**	0.472	**-0.842**	1								
Ti	**0.928**	**0.984**	**0.903**	**-0.682**	**0.978**	**-0.786**	1							
Mn	-0.359	-0.535	**-0.746**	0.593	-0.602	**0.827**	-0.570	1						
Fe	0.012	-0.218	-0.167	**0.676**	-0.070	-0.068	-0.099	0.261	1					
Ni	**0.770**	**0.805**	**0.947**	-0.605	**0.930**	**-0.854**	**0.844**	-0.624	-0.069	1				
Cu	0.426	0.521	**0.803**	-0.528	**0.678**	**-0.850**	0.573	**-0.797**	-0.065	**0.826**	1			
Zn	**0.859**	**0.959**	**0.943**	**-0.737**	**0.974**	**-0.851**	**0.971**	**-0.671**	-0.159	**0.888**	**0.718**	1		
As	**-0.657**	**-0.804**	**-0.726**	**0.772**	**-0.724**	0.494	**-0.745**	0.446	.620	-0.616	**-**0.313	**-0.739**	1	
Pb	**0.731**	**0.874**	**0.931**	**-0.771**	**0.913**	**-0.884**	**0.887**	**-0.779**	-0.211	**0.872**	**0.818**	**0.966**	**-0.70**	1

Table 3.17. Pearson Correlation matrix values for SLNG and BRYT trace and major elements. Bold numbers indicate significance where p<0.01.

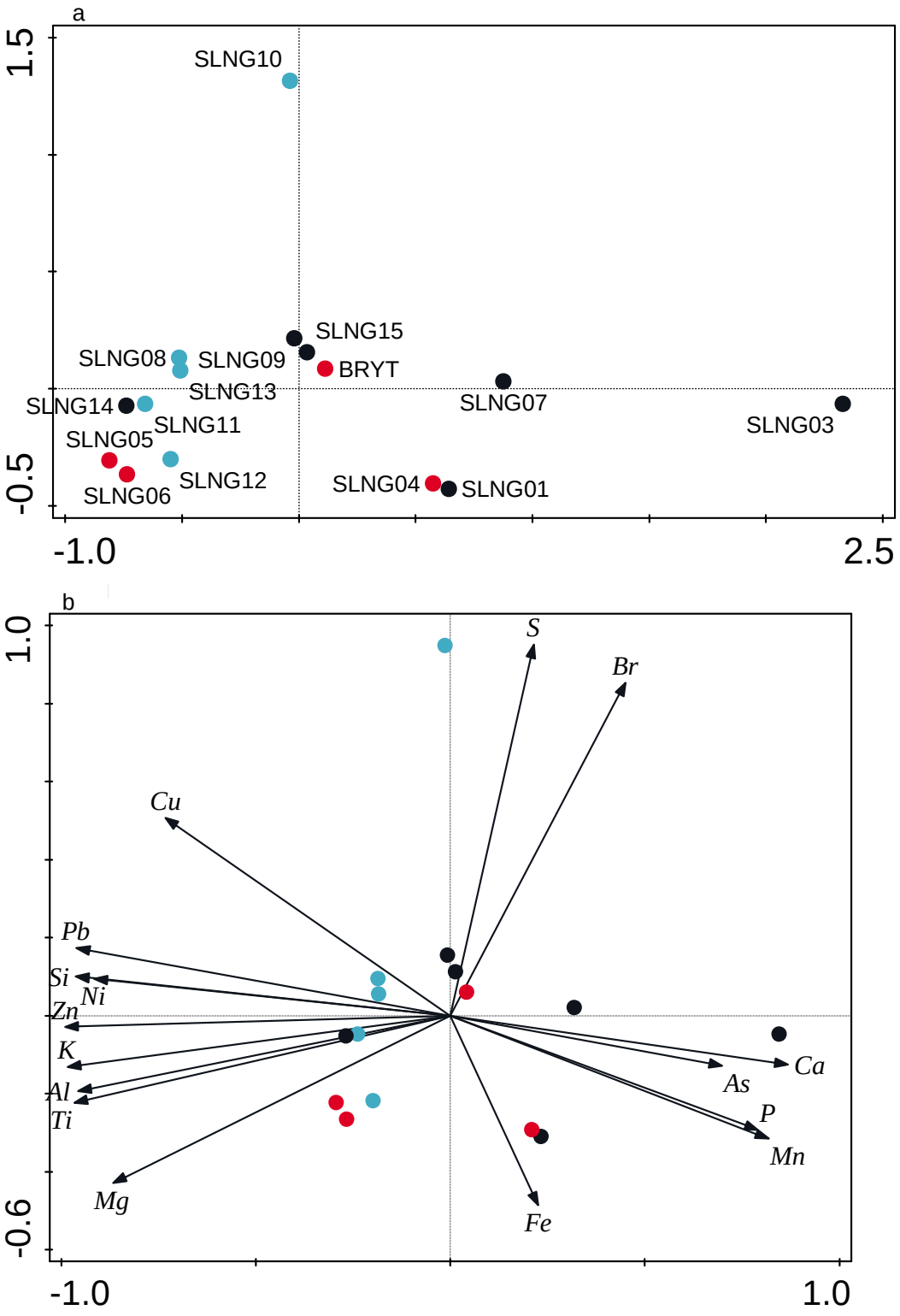

Figure 3.17. a) PCA site plot of trace element and lithogenic elements from SLNG and BRYT surface sediments; b) PCA biplot for trace metals and elements (vectors) from the 15 shallow lakes (dots). Sites are colour-coded for connectivity levels: low connectivity (black), intermittent connectivity (light blue), and high connectivity (red).

	Axis 1	*Axis 2*	*Axis 3*	*Axis 4*
Eigenvalues	0.6633	0.1678	0.1114	0.0264
Explained variation (cumulative)	66.3	83.1	94.2	96.9

Table 3.18. PCA eigenvalues for SLNG and BRYT surface sediment trace metals and major lithogenic elements, with eigenvalues and cumulative expalined variation for the first four PCA axes.

3.3.4.2 Toxicity

Consensus-based threshold effect concentration (TEC) of nickel as determined by MacDonald et al. (2000) is 22.7 µg g^{-1} and is exceeded in surface sediments at most study sites, including SLNG01, SLNG04, SLNG05, SLNG06, and SLNG08-SLNG15 (Figure 3.18). Consensus-based TEC of copper is 31.6 µg g^{-1} and was exceeded in sediment from lakes SLNG05, SLNG08-SLNG11, SLNG13, SLNG14, and SLNG15. Consensus-based TEC of arsenic is 9.79 µg g^{-1}, and was exceeded in lake sediments from SLNG01, SLNG03, SLNG04, SLNG07-SLNG11, SLNG13, and SLNG15 (Figure 3.18). Consensus-based probable effect concentration (PEC) was only exceeded for a single trace element, arsenic. The PEC of arsenic is 33.0 µg g^{-1}, and was exceeded in the sediments of three study lakes: SLNG01 (35.4 µg g^{-1}), SLNG04 (53 µg g^{-1}), and SLNG07 (43.2 µg g^{-1}) (Figure 3.18). The consensus-based probable effect concentration quotient of all trace metals combined (PEC-$Q_{mean\ metals}$) ranged from 0.228 at BRYT and 0.229 at SLNG03 to 0.460 at SLNG04, and mean PEC-$Q_{mean\ metals}$ across all study lakes is 0.332 (Figure 3.19).

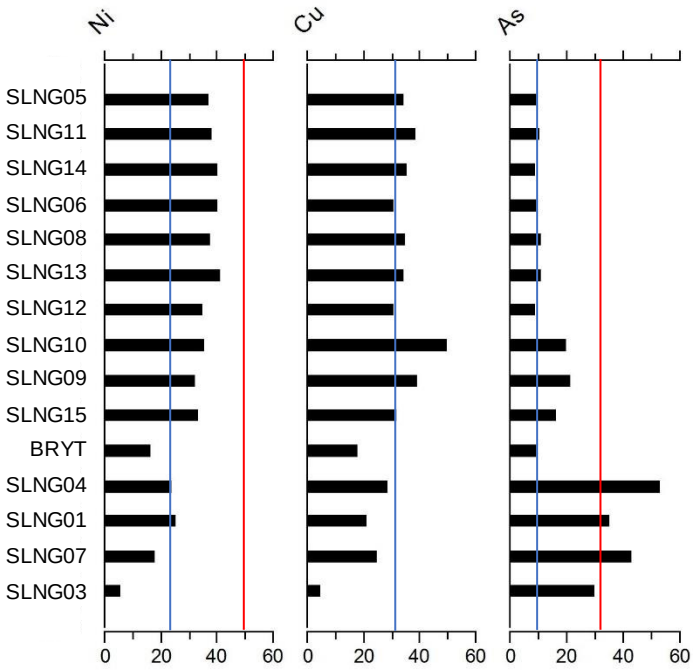

Figure 3.18. Toxicity thresholds of Selenga River basin surface sediments. Concentrations are in µg g^{-1}. Blue vertical lines indicate the threshold effect concentration (TEC), below which toxic effects on aquatic organisms are unlikely to occur, and red lines indicate probable effect concentration (PEC), concentrations above which toxic effects to aquatic organisms are likely to occur. Sites are ordered according to PCA axis 1 scores.

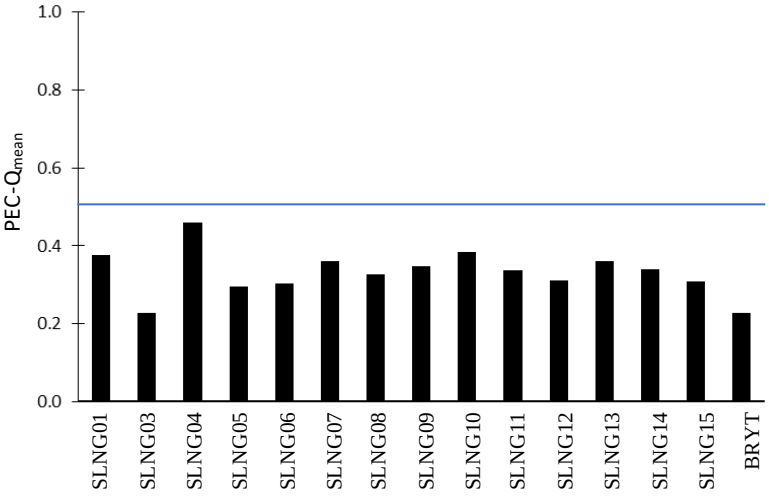

Figure 3.19. PEC-$Q_{mean\ metals}$ toxicity calculated for Selenga River basin surface sediments. Horizontal line indicates 0.5, a level below which toxicity effects are unlikely to be seen in aquatic benthic organisms.

3.3.4.3 Sediment geochemistry

Sediment geochemical properties across Selenga River basin lakes are shown in Figure 3.20. The average LOI_{550} across all lakes was 18.1%, with the range in LOI_{550} between 7.9% (SLNG06) and 33.8% (SLNG10). The average LOI_{950} was 4.6%, and ranged from a minimum of c. 2.0% at SLNG06 to a maximum of 21.6% at SLNG03. Positive association was shown between LOI_{550} and PCA axis 2, and elements S and Br, while positive association was found between LOI_{950} with PCA axis 1, and trace and major elements P, Ca, Mn, As, and Fe (Figure 3.21).

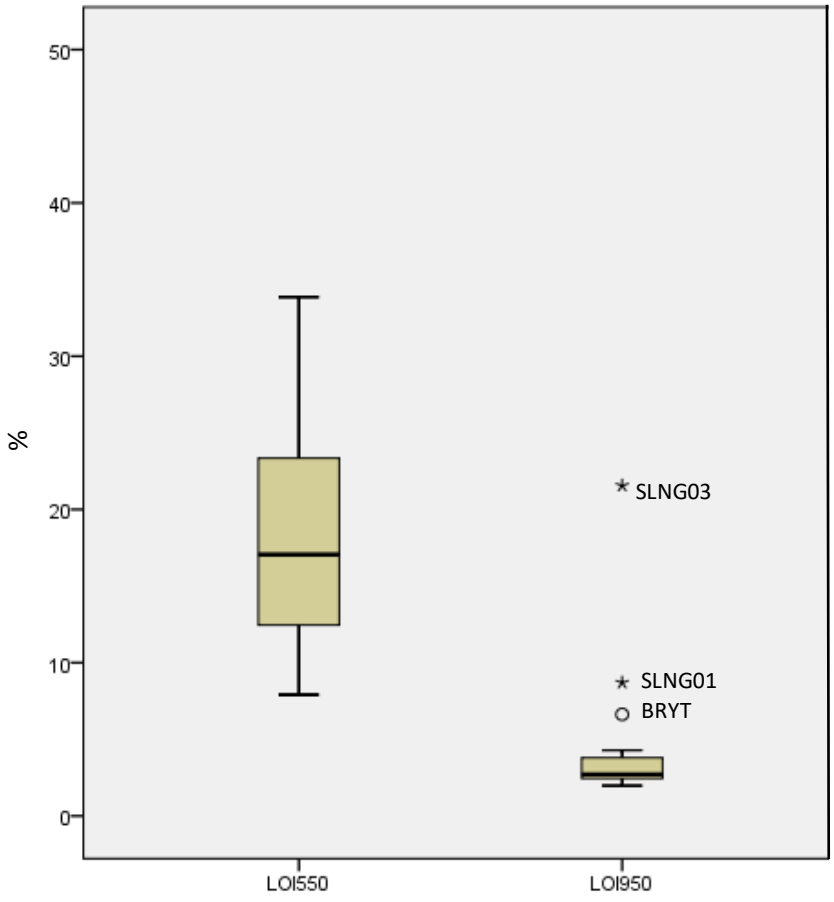

Figure 3.20. LOI_{550}, and LOI_{950} of surface sediments from the 15 SLNG and BRYT shallow lakes. Medians (bold line), 1st and 3rd quartiles, minima, maxima, and outliers (1.5 x interquartile range) are displayed. (○) indicate outliers and (*) indicate extreme outliers.

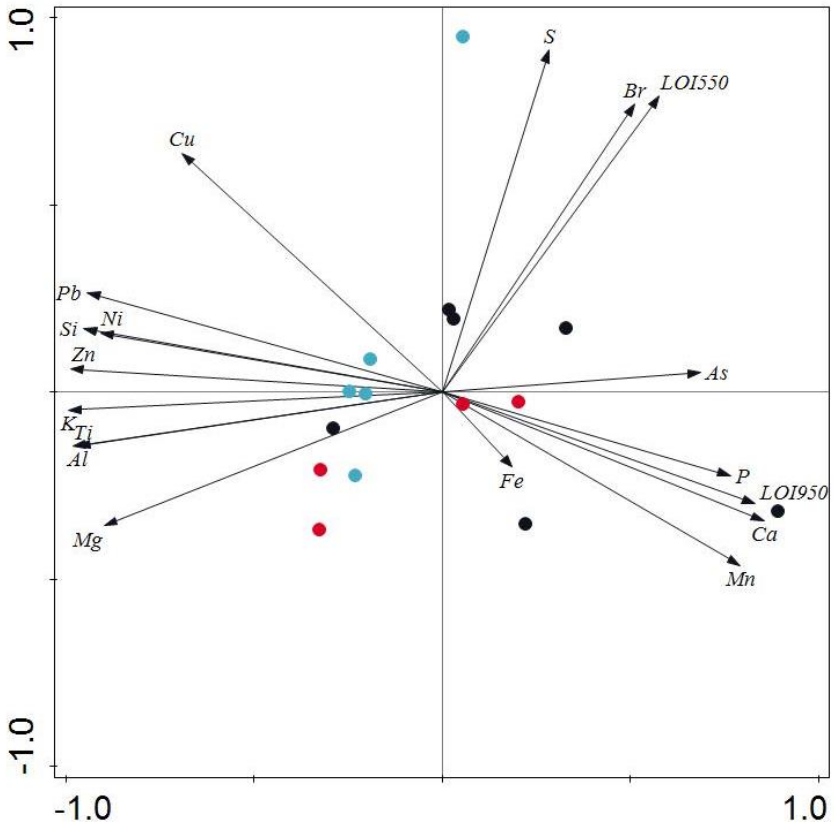

Figure 3.21. PCA biplot indicating variability in all geochemical indicators including major trace metals and lithogenic elements, and loss-on-ignition (vectors) across the 15 lakes (dots). Sites are colour-coded for connectivity levels: low connectivity (black), intermittent connectivity (light blue), and high connectivity (red).

3.4 Discussion

3.4.1 Drivers of ecological variability of Selenga River basin shallow lakes

Degree of connectivity has historically been considered a key factor for floodplain wetlands in determining structure and function (Hay *et al.*, 2000; Brock *et al*., 2007; Mitsch and Gosselink, 2007). Certainly, connectivity appears to significantly influence aspects of the ecological structure across shallow lakes of the Selenga River basin, particularly macrofossil richness between high connectivity and low connectivity sites (Table 3.15), spatial variation in macrofossil assemblages (Figure 3.4), and diatom assemblages (Figure 3.8). Macrofossil richness was significantly greater in sites with no connectivity to the Selenga River or other tributaries. Higher counts of most types of macrofossil remains, including macrophytes, zooplankton, and benthic invertebrates, were found at sites with lower connectivity, while high connectivity sites were found to contain fewer remains overall (Figure 3.3). Several key diatom assemblage characteristics across the lakes correlated well with degree of connectivity.

Planktonic (primarily *Stephanodiscus* spp.) and small benthic fragilarioid species are present at much higher abundances in intermittent or high connectivity sites, and also correlated highly with increasing lake surface area (Figure 3.7). Low connectivity sites are dominated by epiphytic taxa or large naviculoids, and *Gomphonema* spp., *Fragilaria mesolepta*, and *Navicula radiosa* are present at higher abundances at low connectivity lakes, while *Nitzschia amphibia* is much more common in these lakes than in high connectivity lakes. Further, *Navicula trophicatrix* and *Fragilaria parasitica* agg. are absent from small, low connectivity lakes, with increasing abundance of the species in large and highly connected lakes. Further, as also observed by Hay *et al*. (2000), *Diatoma* spp. and *Diploneis* spp. are present only in high connectivity or intermittent connectivity lakes. Sokal *et al*. (2008) noted similar assemblage characteristics of high connectivity and intermittent connectivity lakes with higher-connectivity to Slave River in northern Canada, with greater diversity of diatom guilds, as epiphytic, benthic diatoms, and planktonic diatoms, including *Stephanodiscus* spp. and *Cyclostephanos* spp. were very abundant, while evaporative-dominated, low connectivity lakes, were primarily dominated by epiphytic diatoms. Table 3.19 lists the common species from diatom assemblages of Selenga River basin lakes, and describes autecology of each.

Species	**Guild**	**Autecology**	**Authority**	**References**
Planothidium lanceolata	Benthic	Eutrophic, neutral to alkaline waters.	(Brébisson) Lange-Bertalot 1999	Van Dam *et al*., 1994
Nitzschia amphibia	Benthic	Neutral to alkaline waters, including subaerial habitats, eutrophic.	Grunow 1862	Van Dam *et al*., 1994
Stephanodiscus parvus	Planktonic	Occurs exclusively in alkaline pH. Meso-eutrophic, high total phosphorus concentration.	Stoermer & Håkansson 1984	Stoermer, 1978; Stoermer *et al*., 1978; Van Dam *et al*., 1994; Reavie and Kireta, 2015.
Staurosirella pinnata	Benthic	Prefers shallow, littoral habitats. Mesoeutrophic to eutrophic or oligotrophic to eutrophic. Requires highly oxygenated waters.	(Ehrenberg) Williams and Round 1987	Van Dam *et al*., 1994
Staurosira construens v. venter	Benthic	Shallow, littoral habitats. Mesoeutrophic to eutrophic or oligotrophic to eutrophic. Highly oxygenated waters.	(Ehrenberg) Hamilton 1992	Bradbury 1971; Metcalfe et al. 1997; Patrick and Reimer, 1966; Van Dam *et al*.,1994

Staurosira construens v. binodis	Benthic	Prefers shallow, littoral habitats. Mesoeutrophic to eutrophic or oligotrophic to eutrophic. Littoral assemblage. Requires highly oxygenated waters.	(Ehrenberg) Hamilton 1992	Bradbury, 1971; Haberzettl *et al*., 2005; Metcalfe *et al*., 1997; Patrick and Reimer, 1966; Van Dam *et al*., 1994.
Fragilaria berolinensis	Planktonic	Mainly occurring in alkaline waters, hypereutrophic.	(Lemmermann) Lange-Bertalot 1993	Van Dam and Mertens, 1993; Van Dam *et al*., 1994
Pseudostaurosira brevistriata	Benthic	Mainly occurring in alkaline waters, nearly continuous 100% oxygen saturation required, low tolerance for pollution, wide range of trophic state tolerances.	(Grunow) Williams and Round 1987	Van Dam *et al*., 1994
Amphora copulata	Benthic	Mainly occurring in alkaline waters, eutrophic.	(Kütz.) Schoeman and R.E.M.Archibald 1986	Van Dam *et al*., 1994
Navicula radiosa	Benthic	Meso-eutrophic.	Kützing 1844	Van Dam *et al*., 1994
Fragilaria capucina v. vaucheriae	Benthic	Mainly occurring in alkaline and eutrophic waters, can occur on moist/wet places.	(Kützing) Petersen 1938	Van Dam *et al*., 1994
Cocconeis placentula v. euglypta	Epiphytic	Mainly occurring in alkaline waters, eutrophic.	Ehrenberg 1838	Van Dam *et al*., 1994
Epithemia adnata	Epiphytic	Exclusively occurring in alkaline pH waters, meso-eutrophic.	(Kützing) Brébisson 1838	Van Dam *et al*., 1994
Gomphonema parvulum	Epiphytic	Best development in nutrient rich waters and circumneutral pH. Can occur on moist/wet places. Tolerant to polluted waters.	(Kützing) Kützing 1849	Patrick and Reimer, 1966; Round, 1990; Van Dam *et al*., 1994
Fragilaria mesolepta	Epiphytic	Alkaline, freshwater, tolerant of higher ionic concentration.	Rabenhorst 1861	Van Dam *et al*., 1994
Rhoicosphenia abbreviata	Epiphytic	Very common epiphyte of filamentous algae, non-motile, eutrophic, freshwater, alkaline, pollution tolerant, freshwater with high ionic content.	(Agardh) Lange-Bertalot 1980	Van Dam *et al*., 1994
Sellaphora pupula	Benthic	Circumneutral to alkaline waters, meso-eutrophic.	(Kützing) Mereschkovsky 1902	Wetzel *et al*., 2015 Van Dam *et al.,* 1994

Table 3.19. Ecologies of dominant species of diatoms found across the Selenga River basin shallow lakes.

Intermittent and low connectivity sites tend to have higher algal biomass, with higher concentrations of most pigments in water samples, and chlorophytes (Chl *b* and lutein) and measures for total algae (β-carotene), and higher cyanobacteria (echinenone) concentrations in both water and sediment pigment samples. High connectivity sites differed from other sites based primarily on the low concentrations of most pigments in sediments (Figure 3.9, Figure 3.11, Figure 3.12, Figure 3.13). Conversely, rarefacted diatom species richness and Hill's N2 indicated decreasing diversity and richness with decreasing connectivity to the Selenga River, and several low connectivity lakes, SLNG03, SLNG01, SLNG07 and SLNG15, had the lowest Hill's N2 and species richness. Moreover, all sites which contain any one species at greater than 20% relative abundance, are intermittent or low connectivity sites, including SLNG01, SLNG03, SLNG11, and SLNG15, while other low or intermittent connectivity sites contain at least one species at greater than 15% relative abundance (SLNG07, SLNG08, and SLNG09). Lake comparisons conducted in Yellowstone National Park, U.S.A by Interlandi and Kilham (2001), indicated a significant negative relationship between species diversity and system productivity. A similar negative relationship is seen amongst Selenga River basin lakes, as pigment Chl *a* is higher in lakes with lower diatom Hill's N2 and diatom rarefacted species richness. Low connectivity lakes and ponds have minimal levels of disturbance from river intrusions, and often become dominated over time by a select few species, and have low species turnover rates, resulting in overall lower species richness and diversity in low connectivity sites (Hay *et al*., 2000).

Connectivity-related disturbance at individual sites may contribute to the relationships observed in Selenga River basin lakes between connectivity with primary producer biomass, richness and diversity. Bailey and Guimond (2009) observed that plant productivity in small lakes in Jasper National Park, Canada, was related to degree of flooding and related nutrient dynamics, and that flood disturbance, or degree of river connectivity, was a greater driver in determining plant production, than resource availability. As lakes with higher levels of river connectivity are subject to persistent intrusions of cold, turbid waters, the negative impacts of which on plant productivity outweigh the concurrent increase in nutrients brought to lakes by river water, flood stress and disturbance is often an important determinant of ecological productivity and structure within floodplain wetlands (Robertson *et al*., 2001; Sokal *et al*., 2010).

Hay *et al.* (2000) observed that diatom assemblages from floodplain lakes within the Mackenzie River Delta, Northwest Territories, Canada, varied along a macrophyte gradient related to level of connectivity to the Mackenzie River. A similar significant ecological relationship is observed between macrofossils and diatom assemblages across Selenga River basin lakes. Increases in the abundance of particular diatom taxa correlated positively with increasing macrofossil richness, primarily epiphytes and large benthic naviculoids, and many of the diatom taxa which are characteristic of low connectivity sites, are also those taxa observed to increase in abundance with increasing macrofossil richness (Figure 3.15). It appears that increased macrofossil richness, which is significantly related to connectivity levels, is significant in determining abundances of certain diatom taxa within Selenga River basin lakes.

Biodiversity within a food-web can influence the functioning and resilience of a system, and increases in diversity of either predators or prey will have varying effects on top-down or bottom-up processes, including biomass and resource utilization (Duffy *et al*., 2007). In this study, low and intermittent connectivity lakes are characteristized by higher benthic invertebrate abundance, higher fish abundance, and higher macrophyte abundance. Increased fish predation can reduce interspecific competition, and therefore promote co-existence between different zooplankton species (Hessen *et al*., 2006). Further cyprinid fish are omnivorous, often found in shallow, eutrophic lakes, and have been found to feed on zooplankton (which feed on microalgae), and also on macrophytes themselves, and so can act as an important link between the various trophic levels within shallow, nutrient-rich lakes (Kanaya *et al*., 2009). Higher abundances and volume of submerged macrophytes, common in the intermittent and low connectivity lakes in the Selenga River basin, may facilitate increases in large-bodied Daphniidae, including *Daphnia magna, Simocephalus* sp., and *Daphnia pulex*, as a high abundance of submerged macrophytes provide refugia for zooplankton and invertebrates, resulting in higher abundances regardless of overall fish abundance and predation (Jeppesen *et al*., 1997; Jeppesen *et al*., 2011). As evidence for fish presence was found across all Selenga River basin lakes, lower submerged macrophyte abundance and density would likely result in declines in pelagic zooplankton abundance, due to related increases in fish predation on the larger-bodied daphnids, and concurrent increases in pelagic, small-bodied bosminids, which often increase in abundance when fish predation on the larger daphnids increases (Mills *et al*.,

1987; Jeppesen *et al*., 2001; Jeppesen *et al.,* 2011). Therefore, the influence of varying levels of connectivity are likely to be seen across trophic levels, and influence biotic interactions within these shallow lake ecosystems.

A strong negative spatial relationship was observed between surface area and macrophyte macrofossil richness, with richness higher at sites with lower surface area, while depth was determined to have significant influence over spatial variation in both diatom assemblages and macrofossil remains (Figure 3.4, and Figure 3.8). Lake surface area has a complex relationship with biodiversity, species richness, and ecological structure. In lakes with larger surface areas, submerged macrophyte abundance and diversity can be impacted by light penetration and colonization depth, and hence may be linked to nutrient status and turbidity, as well as wave exposure and percent habitable area (Middelboe and Markager, 1997; Vestergaard and Sand-Jensen, 2000). Smaller lakes tend to be shallower, and a greater proportion of the lake bottom will be covered by macrophytes, increasing the overall density (Van Geest *et al*., 2005), while larger lakes with greater depths will have less of the lake bottom inhabited (Duarte *et al*., 1986; Vestergaard and Sand-Jensen, 2000). Therefore, the relationship between colonization depth, substrate availability, light penetration, and disturbance, contribute to the role that surface area and depth play in determining macrophyte and diatom spatial variability in Selenga River basin lakes.

The impact of low connectivity on nutrient-rich, perimeter shallow lakes may be a reason for the current situation of SLNG03. This particular lake, located on the north-east margin of the Selenga Delta, continually presents as an outlier across most of the sediment geochemical properties (Figure 3.16) and biological profiles of the Selenga River basin lakes. The lake currently has high evaporative properties, with high conductivity and cation concentrations, with magnesium as the dominant cation, and very high Ca/Ti ratio (Figure 3.16). PVI is lowest in SLNG03, at 22% (Table 3.3), and total phosphorus is high (See 2.5.2). Moreover, algal biomass is high, with high concentrations of β-carotene, Chl *a*, and total carotenoid pigments in both water and sediment pigment samples from SLNG03 (Figure 3.9 and Figure 3.12). Further, diatom species richness is very low, and the diatom assemblage at SLNG03 is dominated *P. brevistriata*, a species not found in any of the other site within the Selenga Delta (Figure 3.6). Observation indicated carbonate precipitation evident in the lake, as well as high levels of

submerged plant decomposition as observed through macrophyte sampling. Carbonate content of the sediment (from LOI_{950}) is highest amongst all lakes (Figure 3.20), while Fe/Mn ratio is lowest amongst all lakes, indicating higher reducing conditions, possibly as a result of high organic matter accumulation and plant decomposition (Randsalu-Wendrop *et al*., 2014). There is a potential link between carbonate precipitation and reducing conditions at SLNG03, with a pH of 8.9, resulting in in-lake release of phosphorus from sediments into water column, leading to further nutrient enrichment (Koski-Vahala *et al*., 2001; Wu *et al*., 2014). Taking all physical, chemical, and biological indicators together, it is possible that SLNG03 is undergoing a shift from a macrophyte-rich lake, as all of the other study sites are, to one characterized by high algal biomass and low macrophyte abundance, likely as a response to high nutrient levels, and the feedback mechanisms associated with elevated phosphorus in shallow lakes (Randsalu-Wendrup *et al.*, 2014). This may serve as a warning signal for other lakes within the region, as most lakes within this study have yet to display ecological instability related to the eutrophic to hypereutrophic conditions observed. Further, it may display the implications of combined low-levels of connectivity with direct anthropogenic impacts (agricultural practices).

3.4.2 Influence of geochemical and pollution variability on ecology across the Selenga River basin

Apart from the primary role that connectivity appears to play in driving ecological variability across the Selenga River basin, the hydrological differences between sites, as well as proximity to anthropogenic disturbance (e.g. agricultural practices), appears to contribute as drivers of variability in sediment trace metal and elemental differences between lakes. Primarily, sites which are well connected to the Selenga River, or partially connected, and located within the interior of the delta or away from direct anthropogenic impacts, have higher concentrations of most trace metals (nickel, zinc, and copper) and lithogenic elements (titanium, aluminum, potassium, silicon). Sites located on the margins of the Delta with higher proximity to agricultural lands (SLNG01, SLNG03, SLNG04, and SLNG07), while having varying levels of connectivity, are all associated with elevated As, Fe, Mn, Ca, and P levels.

Arsenic levels within three of the marginal Selenga Delta lakes currently exceed the sediment probable effect concentration (PEC), making arsenic the primary contaminant of concern in the Selenga Delta (MacDonald *et al*., 2000). Possible sources of As to these lakes

include metal-refining, mining by-products, metal smelting, fossil fuel combustion, agricultural sources including pesticides, livestock feed, and herbicides, untreated sewage, or groundwater input (Smedley and Kinniburgh, 2002; Ren *et al*., 2010; Revenga *et al*., 2012; Wang *et al*., 2015). See Figure 1.4 of major mining activities within the Selenga River basin. Arsenic is also a redox-sensitive element, and the distribution, mobilization, and speciation of As is typically influenced by the chemistry of the lake, and/or organic matter content (Mason *et al*., 2000; Smedley and Kinniburgh, 2002; Dovick *et al*., 2016). In the Selenga River basin, surface sediment arsenic concentrations are not significantly correlated with Fe/Mn, although the low correlation is negative (Table 3.17). Arsenic concentrations are negatively correlated with many elemental concentrations, but is significantly positively correlated with phosphorus. As arsenic is highest in marginal Delta sites with varying degrees of connectivity to the Selenga River, and low correlation with Fe/Mn ratios and redox conditions, it is likely that the elevated As levels are related to increased proximity to agricultural practices and human settlements.

High As concentrations may have a detrimental effect on the aquatic organisms within lakes. Arsenic has been found to bioaccumulate across trophic levels, however does not biomagnify through the food-web, and in some cases has been noted to biodilute with increasing trophic level (Wagemann *et al*., 1978; Mason *et al*., 2000; Dovick *et al*., 2016). Primary producers and primary consumers have been found to contain the highest As concentrations within As-contaminated lakes, while certain benthic invertebrates, including Ephemeroptera, may be absent from As-contaminated lakes (Wagemann *et al*., 1978, Revenga *et al*., 2012; Dovick *et al*., 2016). Therefore, it is likely that elevated As concentrations in lakes pose a greatest risk to phytoplankton and herbivorous invertebrates. Accumulation of As may be promoted through adsorption to exoskeleton of invertebrates, or within detoxifying organs of biota (Mason *et al*., 2000). Toxicity of As to phytoplankton, zooplankton, other invertebrates, and fish have been observed and measured in previous studies, however, specific values at which arsenic inhibits biomass, growth or development of biota at different trophic levels varies, and is dependent upon water chemistry and speciation of As (Tisler and Zagorc-Koncan, 2002; Mason *et al*., 2000; Caumette *et al*., 2011). Further, as As is the only measured element to currently exceed the PEC at any study site, sediments should be considered as low toxicity risk, as exceedance of the PEC by a single element may not necessarily indicate toxic conditions (Long

and MacDonald, 1998). The observed levels of As contamination in several Selenga River basin lakes may prove to be an early sign of modern increases in As contamination across the Selenga River basin, and monitoring to address any increases in contamination in the future, and related ecological consequences, should be undertaken.

3.5 Conclusions

The primary aim of the chapter was to determine to what extent connectivity determines the ecological structure and function of Selenga River basin shallow lakes, through the examination of contemporary ecological communities within lakes of varying connectivity, with the hypothesis that connectivity levels of shallow lakes within the Selenga River basin will have a significant effect on the ecological structure and functioning of the shallow lake community. It was determined that variations in ecological properties across Selenga River basin shallow lakes are primarily explained through connectivity levels, biotic interactions, and landscape parameters. These environmental variables drive variations in diversity, richness, and trophic structure of the shallow lakes. Connectivity was determined to be related to variations in primary producer biomass and diversity across the shallow lakes. Spatial variations in macrofossil richness were related to extremes in connectivity across sites with a significant relationship observed when comparing macrofossil richness between low connectivity and high connectivity lakes. Further, spatial variability in diatom communities and macrofossil remains were significantly explained by the level of connectivity of the site. Primarily, connectivity dictated diversity of diatom guilds present, with a higher diversity of guilds in high connectivity sites with the presence of planktonic species in lakes connected to the Selenga River. A significant relationship was observed between macrofossils and diatom communities across sites, with increased macrofossil richness associated with increased abundances of epiphytic species and large naviculoids. Increased algal biomass occurred primarily at sites with low connectivity, with higher concentrations of most pigments present at these sites. It is also possible that decreased macrophyte biomass at high connectivity sites is related to increased connectivity with the Selenga River, and the negative implications of the increased intrusions of cold, sediment-rich river water. Variations in connectivity appear to be a significiant factor in driving ecological variations within shallow lakes of the Selenga River basin, both directly through disturbance and influx of nutrients and sediment, and indirectly, through trophic interactions.

3.6 References

Battarbee R.W., & Kneen M.J. (1982) The use of electronically counted microspheres in absolute diatom analysis. *Limnology and Oceanography* **27,** 184-188.

Battarbee R.W. Jones V., Flower R., Cameron N., Bennion H., Carvalho L., & Juggins S. (2001) Diatoms. In Terrestrial, algal and siliceous indicators. Eds. J. Smol, H.J.B. Birks, and M. Last, Kluwer Academic Publishers,The Netherlands. pp. 155–202.

Bailey S.E., & Guimond J.K. (2009) Above ground biomass and nutrient limitation in relation to river connectivity in montane floodplain marshes. *Wetlands* **29,** 1243-1254.

Bengtsson L., & Enell M. (1986) Chemical analysis. In, Handbook of Holocene Palaeoecology and Palaeohydrology, The Blackburn Press, U.S.A.

Bennion H., Carvalho L., Sayer C.D., Simpson G.L., & Wischnewski J. (2012) Identifying from recent sediment records the effects of nutrient and climate on diatom dynamics in Loch Leven. *Freshwater Biology* **57,** 2015-2029.

Birks H.H. (2001) Plant macrofossils. In: Tracking Environmental Change Using Lake Sediments. Volume 3: Terrestrial, Algal, and Siliceous Indicators. Eds. J.P. Smol, H.J.B. Birks & W.M. Last, Kluwer Academic Publishers, Dordrecht, the Netherlands. pp. 49–74.

Birks H.H. (2017) Plant Macrofossil Introduction, Reference Module in Earth Systems and Environmental Sciences, Elsevier. doi: 10.1016/B978-0-12-409548-9.10499-3.

Boyd C.E. (1971) Further studies on productivity, nutrient, and pigment relationships in Typha latifolia populations. *Bulletin of the Torrey Botanical Club* **98,** 144–150.

Bradbury J.P. (1971) Paleolimnology of lake Texoco Mexico: Evidence from diatoms. *Limnology and Oceanography* **16,** 180-200.

Brock B.E., Wolfe B.B., & Edwards T.W.D. (2007) Characterizing the hydrology of shallow floodplain lakes in the Slave River Delta, NWT, Canada, using water isotope tracers. *Arcitc, Antarctic, and Alpine Research*, **39,** 388-401.

Canfield D.E., Shireman J.V., Colle D.E., Haller W.T., Watkins C.E., & Maceina M.J. (1984) Prediction of chlorophyll-a concentrations in Florida lakes: importance of aquatic macrophytes. *Canadian Journal of Fisheries and Aquatic Sciences*, **41,** 497-501.

Caumette G., Koch I., House K., & Reimer K.J. (2014) Arsenic cycling in freshwater phytoplankton and zooplankton cultures. *Environmental Cheistry* **11,** 496-505.

Chen N., Bianchi T.S., McKee B.A., & Bland J.M. (2001) Historical trends of hypoxia on the Louisiana Shelf: applications of pigments as biomarkers. *Organic Geochemistry* **32**, 543-561.

Davidson T.A., Bennion H., Jeppesen E., Clarke G.H., Sayer C.D., Morley D., Odgaard B.D., Rasmussen P., Rawcliffe R., Salgado J., Simpson G.L., & Amsinck S.L. (2011) The role of cladocerans in tracking long-term change in shallow lake trophic status. *Hydrobiologia* **676**, 299-315.

Davidson T.A., Reid M.A., Sayer C.D., & Chilcott S. (2013) Palaeolimnological records of shallow lake biodiversity change: exploring the merits of single versus multi-proxy approaches. *Journal of Paleolimnology* **49**, 431-446.

Davies S. J. (2015) Micro-XRF core scanning in palaeolimnology: recent developments. In: Developments in Paleoenvironmental Research. Volume 17: Micro-XRF Studies of Sediment

Cores: Applications of a Non-Destructive Tool for Environmental Sciences. Eds. I.W. Croudace, & R.G. Rothwell, Springer, the Netherlands. pp. 189-226.

Dean W.E. Jr. (1974) Determination of carbonate and organic matter in calcareous sediments and sedimentary rocks by loss on ignition: Comparison with other methods. *Journal of Sedimentary Petrolology* **44**, 242‑248.

Dovick M.A., Kulp T.R., Arkle R.S., & Pillio D.S. (2016) Bioaccumulation trends of arsenic and antimony in a freshwater ecosystem affected by mine drainage. Environmental Chemistry 13, 149-159.

Duarte C.M., Kalff J., & Peters R.H. (1986) Patterns in biomass and cover of aquatic macrophytes in lakes. *Canadian Journal of Fisheries and Aquatic Sciences* **43**, 1900–1908.

Duffy J.E., Cardinale B.J., France K.E., McIntyre P.B., Thebault E., & Loreau M. (2007) The functional role of biodiversity in ecosystems: incorporating trophic complexity. *Ecology Letters* **10**, 522-538.

Epstein M.S., Diamondstone B.I., & Gills T.E. (1989) A new river sediment standard reference material. *Talanta* **36**, 141-150.

Haberzettl T., Fey M., Lucke A., Maidana N., Mayr C., Ohlendorf C., Schabitz F., Schelser G.H., Wille M. and Zolitschka B. (2005) Climatically driven lake level changes during the last two millennia as reflected in sediments of Laguna Potrok Aike, southern Patagonia (Santa Cruz, Argentina). *Journal of Paleolimnology 33*, 283-302.

Hay M.B., Smol J.P., Pipke K.J., & Lesak L.F.W. (1997) A diatom-based paleohydrological model for the Mackenzie Delta, Northwest Territories, Canada. *Arctic and Alpine Research*, **29,** 430-444.

Hay M.B., Michelutti N., & Smol J.P. (2000) Ecological patterns of diatom assemblages from Mackenzie Delta lakes, Northwest Territories, Canada. *Canadian Journal of Botany* **78**, 19-33.

Heiri O., Lotter A.F., & Lemcke G. (2001) Loss on ignition as a method for estimating organic and carbonate content in sediments: reproducibility and comparability of results. *Journal of Paleolimnology*, **25**, 101-110.

Hessen D.O., Faafeng B.A., Smith V.H., Bakkestuen V., & Walseng B. (2006) Extrinsic and intrinsic controls of zooplankton diversity in lakes. *Ecology* **87**, 433–443.

IBM Corp. (2013) IBM SPSS Statistics for Windows, Version 22.0. Armonk, NY: IBM Corp.

Interlandi S.J., & Kilham S.S. (2001) Limiting resources and the regulation of diversity in phytoplankton communities. Ecology **82,** 1270-1282.

Jans J.E.A., Bekker R.M., & Cappers R.T.J. (2006) Digital seed atlas of the Netherlands, Barkhuis, The Netherlands. pp. 502.

Jeffrey S.W., Mantoura R.F.C., & Wright S.W. (1997) Phytoplankton pigments in oceanography: guidelines to modern methods. UNESCO, Paris.

Jeppesen E., Jensen J.P., Sondergaard M., Lauridsen T., Pedersen L.J., & Jensen L. (1997) Top-down control in freshwater lakes: the role of nutrient state, submerged macrophytes, and water depth. *Hydrobiologia* **342/343**, 151-164.

Jeppesen E., Søndergaard M., Søndergaard M., & Christoffersen K. (1998) The Structuring Role of Submerged Macrophytes in Lakes. Ecological Studies, series 131. Springer, New York, 421 pp.

Jeppesen E., Jensen J.P., Sondergaard M., Lauridsen T., & Landkildehus F. (2000) Trophic structure, species richness and biodiversity in Danish lakes: changes along a phosphorous gradient. *Freshwater Biology* **45**, 201-218.

Jeppesen E., Leavitt P., De Meester L., & Jensen J.P. (2001) Functional ecology and paleolimnology: using cladoceran remains to reconstruct anthropogenic impact. *Trends in Ecology and Evolution* **16,** 191-198.

Jeppesen E., Noges P., Davidson T.A., Haberman J., Noges T., Blank K., Lauridsen T.L., Sondergaard M., Sayer C., Laugaste R., Johansson L.S., Bjerring R., Amsinck S.L. (2011) Zooplankton as indicators in lakes: a scientific-based plea for including zooplankton in the ecological quality assessment of lakes according to the European Water Framework Directive (WFD). *Hydrobiologia* **676,** 279-297.

Juggins S. 2014. C2 data analysis, Version 1.7.6. University of Newcastle, United Kingdom.

Junk W.J., Bayley P.B., & Sparks R.E. (1989) The flood pulse concept in river floodplain systems. In: Proceedings of the International Large River Symposium (LARS). Ed: D.P. Dodge, *Canadian Special Publication of Fisheries and Aquatic Sciences* **106**, 110-127.

Kanaya G., Yadrenkina E.N., Zuykova E.I., Kikuchi E., Doi H., Shikano S., Mizota C., & Yurlova N.I. (2009) Contribution of organic matter sources to cyprinid fishes in the Chany Lake-Kargat River estuary, western Siberia. *Marine and Freshwater Research* **60,** 510-518.

Katz, N. Ja., S. V. Katz, and M. G. Kipiani. 1965. Atlas and keys of fruits and seeds occurring in the Quaternary deposits of the U.S.S.R. Academy of Sciences of the U.S.S.R., Commission for Investigations of the Quaternary Period, Nauka, Moscow, 367 pp. (Partial English translation by J. C. Ritchie).

Korhonen J.J., Wang J., & Soininen J. (2011) Productivity-diversity relationships in lake plankton communities. *PLoS ONE* **6**, e22041. doi: 10.1371/journal.pone.0022041.

Körner S. (2002) Loss of submerged macrophytes in shallow lakes in north-eastern Germany. *International Review of Hydrobiology* **87**, 377–386.

Koski-Vahala J., Hartikainen H., & Tallberg P. (2001) Phosphorus mobilization from various sediment pools in response to increased pH and silicate concentration. *Journal of Environmental Quality* **30,** 546-552.

Krammer, Kurt. (2002) Diatoms of the European Inland Waters and Comparable Habitats. Volume 3: Cymbella. Edited by Horst Lange - Bertalot., 194 photographic plates. 584 p

Krammer K., & Lange-Bertalot H. (2004) Bacillariophyceae. In: Susswasser von Mitteleuropa Band 2/1-4. Eds. H. Ettl, J. Gerloff, H. Heynig, and D. Mollenhauer. Gustav Fischer Verlag, Stuttgart.

Laitenen, J. (1990) Periodic moisture fluctuation as a factor affecting mire vegetation. *Aquilo Series Botanica* **28,** 45–55.

Lange-Bertalot, Horst. (2001) Diatoms of the European Inland Waters and Comparable Habitats. Volume 2: Navicula sensu stricto, 10 Genera Separated from Navicula sensu stricto, Frustulia. Edited by Horst Lange-Bertalot, 140 photographic plates. 526 p.

Leavitt P.R. (1993) A review of factors that regulate carotenoid, and chlorophyll deposition, and fossil pigment abundance. *Journal of Paleolimnology* **9**, 109–127.

Leavitt P.R., & Hodgson D.A. (2001) Sedimentary pigments. In : Developments in paleoenvironmental research, Vol 3. Tracking environmental changes using lake sediments: terrestrial algal and siliceous indicators. (Eds) Smol JP, Birks HJB, Last WM, Kluwer Academic Publishers, Dordrecht, The Netherlands. pp. 295-325.

Levi E.E., Cakiroglu A.I., Bucak T., Odgaard B.V., Davidson T.A., Jeppesen E., & Beklioglu M. (2014) Similarity between contemporary vegetation and plant remains in the surface sediment in Mediterranean lakes. *Freshwater Biology* **59**, 724-736.

Levkov Z. (2009) Diatoms of the European Inland Waters and Comparable Habitats. Volume 5: Amphora sensu lato. Edited by H. Lange – Bertalot, 287 photographic. plates. 916 p.

Long E.R., & MacDonald D.D. (1998) Recommended uses of empirically derived, sediment quality guidelines for marine and estuarine ecosystems. *Human and Ecological Risk Assessment: An International Journal* **4,** 1019-1039.

Long E.R., Ingersoll C.G., & MacDonald D.D. (2006) Calculation and uses of mean sediment quality guideline quotients: a critical review. *Environmental Science and Technology* **40,** 1726-1736.

MacDonald D.D., Ingersoll C.G., & Berger T.A. (2000) Development and evaluation of consensus-based sediment quality guidelines for freshwater ecosystems. *Archives of Environmental Contamination and Toxicology* **39**, 20-31.

Marrotte R.R., Chmura G.L., & Stone P.A. (2012) The utility of Nymphaeaceae sclerids on palaeoenvironmental research. *Review of Palaeobotany and Palynology* **169,** 29-37.

Mason R.P., Laporte J.-M., & Andres S. (2000) Factors controlling the bioaccumulation of mercury, methylmercury, arsenic, selenium, and cadmium by freshwater invertebrates and fish. *Archives of Environmental Contamination and Toxicology* **38,** 283-297.

Mauquoy D., & Van Geel B. (2007) Plant macrofossil methods and studies: Mire and peat macros In: Encyclopedia of Quaternary Science, Elsevier. 2315-2336.

McGowan S. (2013) Pigment Studies. In: Elias S.A. (ed.) The Encyclopedia of Quaternary Science, vol. 3, pp. 326-338. Amsterdam: Elsevier.

McGowan S., Leavitt P.R., Hall R.I., Anderson N.J., Jeppesen E., & Odgaard B.V. (2005) Controls on algal abundance and community composition during ecosystem state change. *Ecology* **86**, 2200-2211.

McGowan S., Leavitt P.R., Hall R.I., Wolfe B.B., Edwards T.W.D., Karst-Riddoch T., & Vardy S.R. (2011) Interdecadal declines in flood frequency increase primary production in lakes of a northern river delta. *Global Change Biology* **17,** 1212–1224.

McGowan S., Barker P., Haworth E.Y., Leavitt P.R., Maberly S.C., & Pates J. (2012) Humans and climate as drivers of algal community change in Windermere since 1850. *Freshwater Biology* **57**, 260-277.

Metcalfe S.E., Bimpson A., Courtice A.J., O'Hara S.L. and Taylor D.M. (1997) Climate change at the monsoon/Westerly boundary in northern Mexico. *Journal of Paleolimnology* **17**, 155-171.

Michelutti N., May M.B., Marsh P., Lesack L., & Smol J.P. (2001) Diatom changes in lake sediments from the Mackenzie Delta, N.W.T., Canada: Paleohydrological applications. *Arctic, Antarctic, and Alpine Research* **33,** 1-12.

Middelboe A.L., & Markager S. (1997) Depth limits and minimum light requirements of freshwater macrophytes. *Freshwater Biology* **37,** 553–568.

Mills E.L., Green D.M., & Schiavone A.J. (1987) Use of zooplankton size to assess the community structure of fish populations in freshwater lakes. *North American Journal of Fisheries Management* **3,** 369-378.

Mitsch W.J., & Gosselink J.G. (2007) Wetlands, 4th Edition. Wiley & Sons, United States of America.

Moreno-Mateos D., Power M.E., Comin F.A., & Yockteng R. (2012) Structural and functional loss in restored wetland systems. *PLoS Biology* **10**, e1001247 doi:10.1371/journal.pbio.1001247.

Opperman J.J., Luster R., McKenney B.A., Roberts M., Meadows A.W. (2010) Ecologically functional floodplains: connectivity, flow regime, and scale. *Journal of American Water Resources Association* **46**, 211-226.

Patrick R., & Reimer C.W. (1966) The diatoms of the United States. The Academy of Natural Sciences, Philadelphia.

Potapova M., & Charles D.F. (2003) Distribution of benthic diatoms in U.S. rivers in relation to conductivity and ionic composition. *Freshwater Biology* **48**, 1311-1328.

R. v.3.2.4 R. 2016. The R Foundation, R Development Team. Vienna.

Reavie E.D., & Kireta A.R. (2015) Centric, Araphid and Eunotioid Diatoms of the Coastal Laurentian Great Lakes. *Bibliotheca Diatomologica* **62,** 1-184.

Ren J.L., Zhang J., Li D.D., Cheng Y., & Liu S.M. (2010) Behaviour of dissolved inorganic arsenic in the Yellow Sea and East China Sea. *Deep-Sea Research II* **57**, 1035-1046.

Randsalu-Wendrop L., Conley D.J., Carstensen J., Hansson L-A., Bronmark C., Fritz S.C., Choudhary P., Routh J., & Hammarlund D. (2014) Combining limnology and palaeolimnology to investigate recent regime shifts in a shallow, eutrophic lake. *Journal of Paleolimnology* **51**, 437-448.

Reuss N., & Conley D.J. (2005) Effects of sediment storage conditions on pigment analyses. *Limnology and Oceanology: Methods* **3,** 477-487.

Revenga J.E., Campbell L.M., Arribere M.A., & Guevera S.R. (2012) Arsenic, cobalt, and chromium food web biodilution in a Patagonia mountain lake. *Ecotoxicology and Environmental Safety* **81,** 1-10.

Robertson A.I., Bacon P., & Heagney G. (2001) The responses of floodplain primary production to flood frequency and timing. *Journal of Applied Ecology* **38,** 126-136.

Round F.E. (1990) Diatom communities, their response to changes in acidity. *Philosophical Transactions of the Royal Society: Series B, Biological Sciences* **327,** 243-249.

Salo J., Kalliola R., Hakkinen I., Makinen Y., Niemela P., Puhakka M., & Coley P.D. (1986) River dynamics and the diversity of Amazon lowland forest. *Nature* **322**, 254-258.

Scheffer M. (1998) Ecology of Shallow Lakes. Chapman and Hall, London, 357 pp.

Simberloff D. (1972) Properties of the rarefaction diversity measurement. *The American Naturalist* **106,** 414-418.

Smedley P.L., & Kinniburgh D.G. (2002) A review of the source, behaviour, and distribution of arsenic in natural waters. *Applied Geochemistry* **17,** 517-568.

Sokal M. A., Hall R.I., & Wolfe B.B. (2008) Relationships between hydrological and limnological conditions in lakes of the Slave River Delta (NWT, Canada) and quantification of their roles on sedimentary diatom assemblages. Journal of Paleolimnology 39, 533-550.

Sokal M.A., Hall R.I., Wolfe B.B. (2010) The role of flooding on inter-annual and seasonal variability of lake water chemistry, phytoplankton diatom communities, and macrophyte biomass in the Slave River Delta (Northwest Territories, Canada). *Ecohydrology* **3,** 41-54.

Sondergaard M., Johansson L.S., Lauridsen T.L., Jorgensen T.B., Liboriussen L., & Jeppesen E. (2010) Submerged macrophytes as indicators of the ecological quality of lakes. Freshwater Biology 55, 893-908.

Stoermer E.F. (1978). Phytoplankton as indicators of water quality in the Laurentian Great Lakes. *Transactions of the American Microscopical Society* **97,** 2-16.

Stoermer E.F., Ladewski B.G., & Schelske C.L. (1978) Population response of Lake Michigan phytoplankton to nitrogen and phosphorus enrichment. *Hydrobiolgia* **57,** 249-265.

Ter Braak C.J.F., & Schaffers A.P. (2004) Co-correspondence analysis: a new ordination method to relate two community compositions. *Ecology* **85**, 834–846.

Ter Braak C.J.F. & Šmilauer P. (2012) Canoco reference manual and user's guide: software for ordination, version 5.0. Microcomputer Power, Ithaca, USA, 496 pp.

Tisler T., & Zagorc-Koncan J. (2002) Acute and chronic toxicity of arsenic to some aquatic organisms. Bulletin of Environmental Contamination *and Toxicology* **69,** 421-429.

Van Dam H., & Mertens A. (1993) Diatoms on herbarium macrophytes as indicators for water quality. *Hydrobiologia* **269/270,** 437-445.

Van Dam H., Mertens A., & Sinkeldam J. (1994) A coded checklist and ecological indicator values of freshwater diatoms from the Netherlands. *Netherlands Journal of Aquatic Ecology* **28,** 117-133.

Van Geest G.J., Wolters H., Roozen F.C.J.M., Coops H., Roijakers R.M.M., Buijse A.D., & Scheffer M. (2005) Water-level fluctuations affect macrophyte richness in floodplain lakes. *Hydrobiologia* **539,** 239-238.

Vermaire J.C., Greffard M-H., Saulnier-Talbot E., & Gregory-Eaves I. (2013) Changes in submerged macrophyte abundance altered diatom and chironomid assemblages in a shallow lake. *Journal of Paleolimnology* **50,** 447-456.

Vestergaard O., & Sand-Jensen K. (2000) Aquatic macrophyte richness in Danish lakes in relation to alkalinity, transparency and lake area. *Canadian Journal of Fisheries and Aquatic Sciences* **57,** 2022-2031.

Wagemann R., Snow N.B., Rosenberg D.M., & Lutz A. (1978) Arsenic in sediments, water and aquatic biota from lakes in the vicinity of Yellowknife, Northwest Territories, Canada. *Archives of Environmental Contamination and Toxicology* **7,** 169-191.

Wang H., Wang J., Yu W., & Shen Z. (2015) Spatial variation, environmental risk, and biological hazard assessment of heavy metals in surface sediments of the Yangtze River estuary. *Marine Pollution Bulletin* **93,** 250-258.

Ward J.V., Tockner K., & Schiemer F. (1999) Biodiversity of floodplain river ecosystems: ecotones and connectivity. *Regulated Rivers, Research and Management* **15**, 125-139.

Wetzel C.E., Ector L., Van de Vijver B., Compère P., & Mann D.G. (2015) Morphology, typification and critical analysis of some ecologically important small naviculoid species (Bacillariophyta) *Fottea, Olomouc* **15,** 203–234. 10.5507/fot.2015.020.

Wu Y., Wen Y., Zhou J., & Wu Y. (2014) Phosphorus release from lake sediments: effects of pH, temperature, and dissolved oxygen. *Journal of Civil Engineering* **18**, 323-329.

Zhao Y., Sayer C.D., Birks H.H., Hughes M., & Peglar S.M. (2006) Spatial representation of aquatic vegetation by submerged aquatic macrofossils and pollen in a small and shallow lake. *Journal of Paleolimnology* **35,** 335-350.

Chapter 4: Palaeolimnological Analyses of Select Selenga River Basin Shallow Lakes: Chronologies and Physical Description of Sediment Cores

4.1 Introduction

4.1.1 Introduction to palaeolimnological study sites

Three lakes from the contemporary spatial survey of Selenga River basin lakes (See Chapter 3) were selected for palaeolimnological analysis: SLNG04, SLNG05, and BRYT (Figure 4.1). These three lakes were analyzed to determine recent increases in anthropogenic contaminants (persistent organic pollutants and trace metals) and by-products of anthropogenic processes (spheroidal carbonaceous particles). Further, long-term variability and changes in the ecology of these lakes were used to inform on the impact of anthropogenic stressors on biodiversity, food-web dynamics, and ecological stability.

Figure 4.1a. Locations of SLNG04 and SLNG05, the two shallow lakes chosen for palaeolimnological studies from within the Selenga Delta, Lake Baikal.

Figure 4.1b. Location of Black Lake (BRYT), one of the shallow lakes chosen for palaeolimnological studies, within the Gusinoye region of the Selenga River basin.

Within the Selenga Delta, SLNG04 and SLNG05 were primarily chosen based on their location within the Delta; different proportions of the Selenga River flow through the northeast and southwest channels of the Delta (Fig 4.1a, 4.1b). A secondary consideration was based on their connectivity to the Selenga River and other channels within the Delta, and both SLNG04 and SLNG05 are connected to the Selenga River through tributaries within the Selenga Delta. The factors of location and connectivity for the study lakes were intended to allow for the assessment that the degree of Selenga River contribution could have on potential anthropogenic impacts. Similar levels of connectivity but differing levels of contribution from the Selenga River could indicate if those lakes on the northeast side of the Delta are more impacted due to heavier influence of the Selenga River. Black Lake (BRYT) was chosen for analysis as a lake outside of the Selenga Delta and within close proximity to industrial influences, to provide contrast to lakes within the Selenga Delta, and to allow for the investigation into how similar lakes in the Selenga River basin are impacted by anthropogenic pressures irrespective of direct influence of the Selenga River.

4.2 Field methodologies

4.2.1 Sediment core extraction

Sediment cores were extracted from all lakes with an *Uwitec* piston corer (UWITEC Ltd., Austria) fitted with a 6.3 cm internal diameter perspex tube. Sediment cores were extracted from SLNG04 and BRYT02 in March 2014 and from SLNG05 in August 2014 (Figure 4.2; Table 4.1). Three sediment cores were extracted from each site and labelled as A, B, or C (Table 4.1). All cores were collected within a 5 m^2 area. Sediment cores extracted in March 2014 were taken while lakes were ice-covered, through an auger-drilled hole in the ice (Figure 4.3a). The corer was lowered through the hole and into the water to retrieve the sediment core. A new hole was drilled into the ice for each new sediment core (Figure 4.3b). Cores extracted in August 2014 were taken from a small inflatable row boat. Sediment cores ranged from 60.0 cm to 86.5 cm length (Figure 4.4; Table 4.1). All sediment cores were collected from the deepest point in the lake, as determined through previous surveys. Sediment cores were extracted from the same spot as all water chemistry measurements (See Chapter 2).

a

b

c

Figure 4.2. Site photos at time of core extraction. Clockwise from top left: a) SLNG04, b) SLNG05, and c) BRYT.

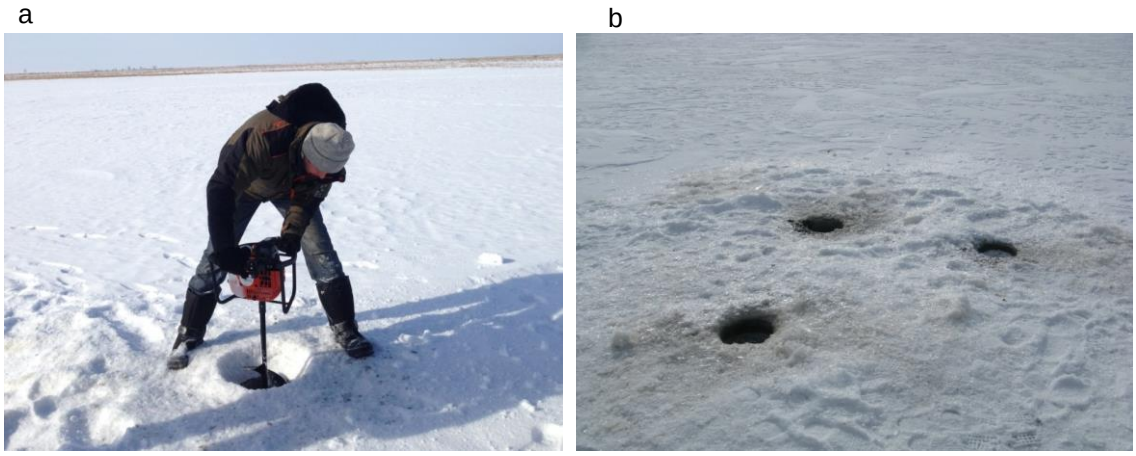

Figure 4.3. a) Drilling a hole through the ice of SLNG04 in March 2014 for the purposes of sediment core extraction; b) Holes drilled into the ice for multiple sediment core extraction.

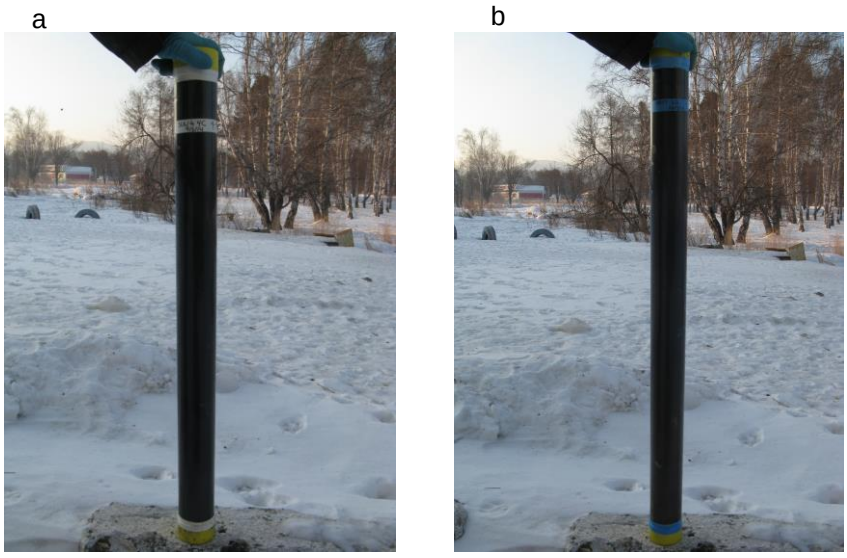

Figure 4.4. Unextruded sediment core from a) SLNG04, and b) BRYT**.**

Site	Coring location	Date of extraction	Water depth at core site (cm)	Number of cores extracted	Core lengths (cm)
SLNG04	52°15'52.5" N, 106°40'35.6" E	March 9, 2014	130	3	A: 76.5 B: 71.5 C: 73.5
SLNG05	52°09'46.7" N, 106°19'59.6" E	August 11, 2014	100	3	A: 60.0 B: 63.5 C: 63.5
BRYT	51°24'14.2" N, 106°29'25.5" E	March 10, 2014	280	3	A: 85.5 B: 80.5 C: 86.5

Table 4.1. Sediment core extraction location and date, lake depth at coring site, and sediment core lengths.

4.2.2 Sediment core extruding

Sediment core B and C from each site were extruded vertically in the field at 0.5 cm intervals, into labelled plastic bags and sealed. Sediment core C was intended for the majority of the planned analyses (Table 4.2). Sediment core B was collected in a hexane-cleaned perspex tube to eliminate the presence of organic contaminants. Sediment from this core was extruded using hexane-cleaned equipment and was extruded into hexane-cleaned aluminum foil before being placed in a plastic bag and sealed. This sediment core was intended for the analysis of persistent organic pollutants (POPs). Sediment core A was not extruded.

All extruded cores (B and C) were shipped from Irkutsk, RU to London, UK immediately following the 2014 winter and summer field seasons. Unextruded sediment core A for each lake remained in Irkutsk, RU for further analyses and archiving purposes. Sediment from core B was stored at -20°C prior to analysis.

Analysis	A	B	C
Radioisotope dating			X
Dry weights	X	X	X
Loss-on-ignition (550°C and 950°C)	X	X	X
Magnetic susceptibility	X		
Lithology	X		
Trace and major elements			X
Persistent organic pollutants		X	
SCPs			X
Macrofossils			X
Diatoms			X
Pigments			X

Table 4.2. Palaeolimnological analyses allocated to each sediment core collected at each lake site.

4.3 Physical descriptions and geochemistry of Selenga River basin sediment cores

4.3.1 Introduction to physical and geochemical indicators

Physical descriptions and geochemical properties of sediment composition within a sediment core from an aquatic system has the possibility to indicate large changes to the ecosystem that have occurred in the past, such as changes in hydrology, sedimentation rates, productivity, and water chemistry, among others. For example, wet density and water content of lake sediments may vary depending on the degree of compaction, and may indicate fluctuations in sediment composition, possibly related to changes in sediment source (Bengtsson and Enell, 1986). Loss-on-ignition (LOI) is a quick method for approximating the organic matter (LOI_{550}) and carbonate content (LOI_{950}) of sediments (Bengtsson and Enell, 1986). LOI analyses in palaeoenvironmental research are often interpreted as reflecting variations in organic matter content within the lake or watershed (Peros and Gajewski, 2008).

Magnetic susceptibility refers to the degree to which a material can be magnetized when it is exposed to a weak magnetic field. The magnetic susceptibility is proportional to the quantity and shape of magnetic minerals in the sediment, such as magnetite and other iron-containing minerals (Sandgren and Snowball, 2001). The highest values of magnetic susceptibility in lake sediments often correspond to periods of increased or altered mineral erosion and therefore can be an indication of variations in the amount or sources of allochthonous inorganic material being washed into the lake (Thompson *et al*., 1975). Magnetic susceptibility values may also indicate atmospheric pollution (Guo et al., 2015). Further, very minimal or negative values of magnetic susceptibility may indicate an extreme reduction of allochthonous inorganic mineral deposition into the lake, and possibly low sedimentation rates, resulting in an absence of mineral material in the sediments (Marshall *et al*., 2002; Oldfield, 2013). The presence of organic-rich lake sediments, possibly leading to reducing conditions at the sediment-water interface, may also result in very low or negative magnetic susceptibility values, possibly due to the dissolution of mineral materials (Snowball, 1993; Chen *et al*., 2013).

4.3.2 Methods

4.3.2.1 Sediment description

A visual inspection was carried out following the extraction of all cores. During the extrusion and subsampling processes, major changes in sediment properties, such as colour, moisture and texture, were noted, as well as the presence of macrofossils. Sediment cores SLNG04-A, SLNG05-A, and BRYT02-A were photographed and studied for changes in lithology and biology down-core at the Institute of the Earth's Crust, Irkutsk, Russia by Dr. Lena Vologina.

4.3.2.2 Densities and Loss-on-Ignition

Sediment cores SLNG04-C, SLNG05-C, and BRYT02-C were each subsampled at 1.0-cm intervals for analysis of wet density (g/cm^3), dry weights (%), loss-on-ignition at 550°C (LOI_{550}; %), and loss-on-ignition at 950°C (LOI_{950}; %). Wet sediment density was calculated by measuring the mass of a known volume (2 cm^3) of wet sediment. Percent dry weights, LOI_{550} and LOI_{950} were analyzed as for contemporary sediments (refer to methods described in Section 3.2.3.3).

4.3.2.3 Magnetic susceptibility

Sediment cores SLNG04-A, SLNG05-A, and BRYT02-A were analyzed for magnetic susceptibility at the Institute of the Earth's Crust, Siberian Branch - Russian Academy of Sciences, Irkutsk, Russia by Dr. Lena Vologina. Magnetic susceptibility was analyzed at 1.0-cm increments using a Bartington meter with an MS2E1 sensor.

4.3.3 Results

4.3.3.1 SLNG04 sediment description

Four main sections were identified in the SLNG04-A sediment core (Figure 4.5). The first section occurred from the base of the core to 57 cm, during which time sediments primarily consisted of coarse clay containing both sand and silt fractions, and were devoid of biological remains. The second section occurred between 57 cm and 40 cm, and while sediments were similar in texture and grain size, biological remains were observed. Between 40 cm and 27 cm, molluscs (including ostracods, snails, and mussels) appear in the sediment core, and the sediment becomes siltier. The final section was characterized by declining mollusc remains

towards the surface, and a decreasing amount of sand in the sediments, with sediment mostly silty clays.

4.3.3.2 SLNG04 densities and LOIs

Wet density decreased from 2.02 g/cm^3 at the base of the core to 1.16 g/cm^3 at the surface (Figure 4.6). The decline was mostly steady apart from between 53 and 49 cm, when wet density declined more rapidly from 1.92 g/cm^3 to 1.38 g/cm^3 followed by a slight increase between 39 and 37 cm, from 1.29 g/cm^3 to 1.61 g/cm^3. Percent dry weight experienced a very similar trend throughout the core, with a mostly steady decline from 79% at the base to 20% at the surface (Figure 4.6). As with wet density, a departure from the steady decline occurred between 53 and 48 cm, when dry weight declined more rapidly from 72% to 41%, and an increase from 36% to 50% occurred between 41 and 37 cm.

Organic matter (LOI_{550}) underwent several fluctuations throughout the sediment core (Figure 4.6). Very low levels of organic matter were found at the bottom of the core, remaining consistently low at 3-4% between the base of the core and 53 cm. Organic matter increased beginning at 54 cm, reaching the record maximum organic matter content at 41 cm. Organic content declined following, and remained between 13% and 16% until 27 cm, followed by an increase to around 23% by 22 cm, with relatively constant values to the surface. Carbonate content was low in the earliest part of the sediment core, remaining at 1% until 51 cm (Figure 4.6). Carbonate content increased beginning at 50 cm, and reached a record maximum of 16% by 32 cm. Carbonate content then declined to 3% by 22 cm, followed by small fluctuations and low values to the surface.

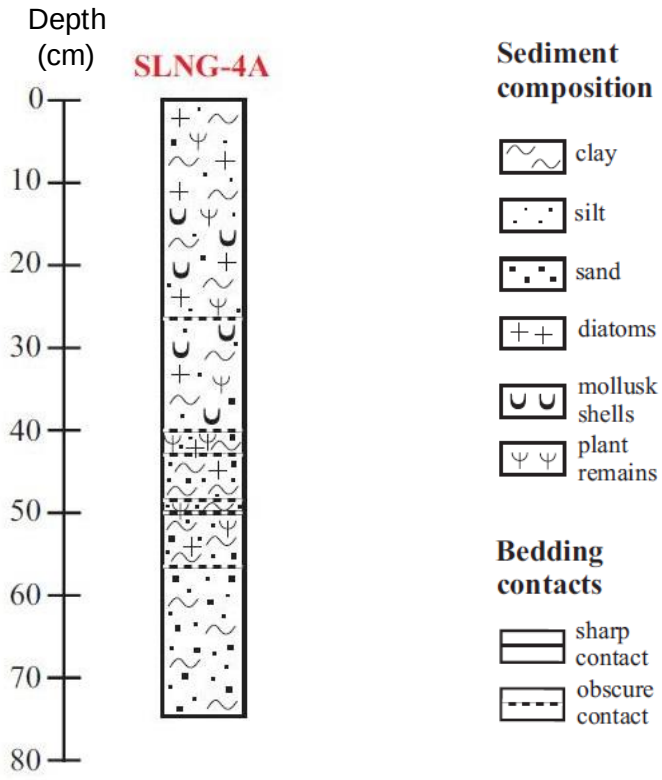

Figure 4.5. Sediment profile for core SLNG04-A.

4.3.3.3 SLNG04 magnetic susceptibility

From the base of the core to the surface, there was a general decreasing trend in MS (Figure 4.6). Finer scale fluctuations between the base of the core and ~40 cm occurred, and high values of 132 SI units, 121 SI units, and 129 SI units occurred at 69 cm, 64 cm, and 46 cm, respectively (Figure 4.6).

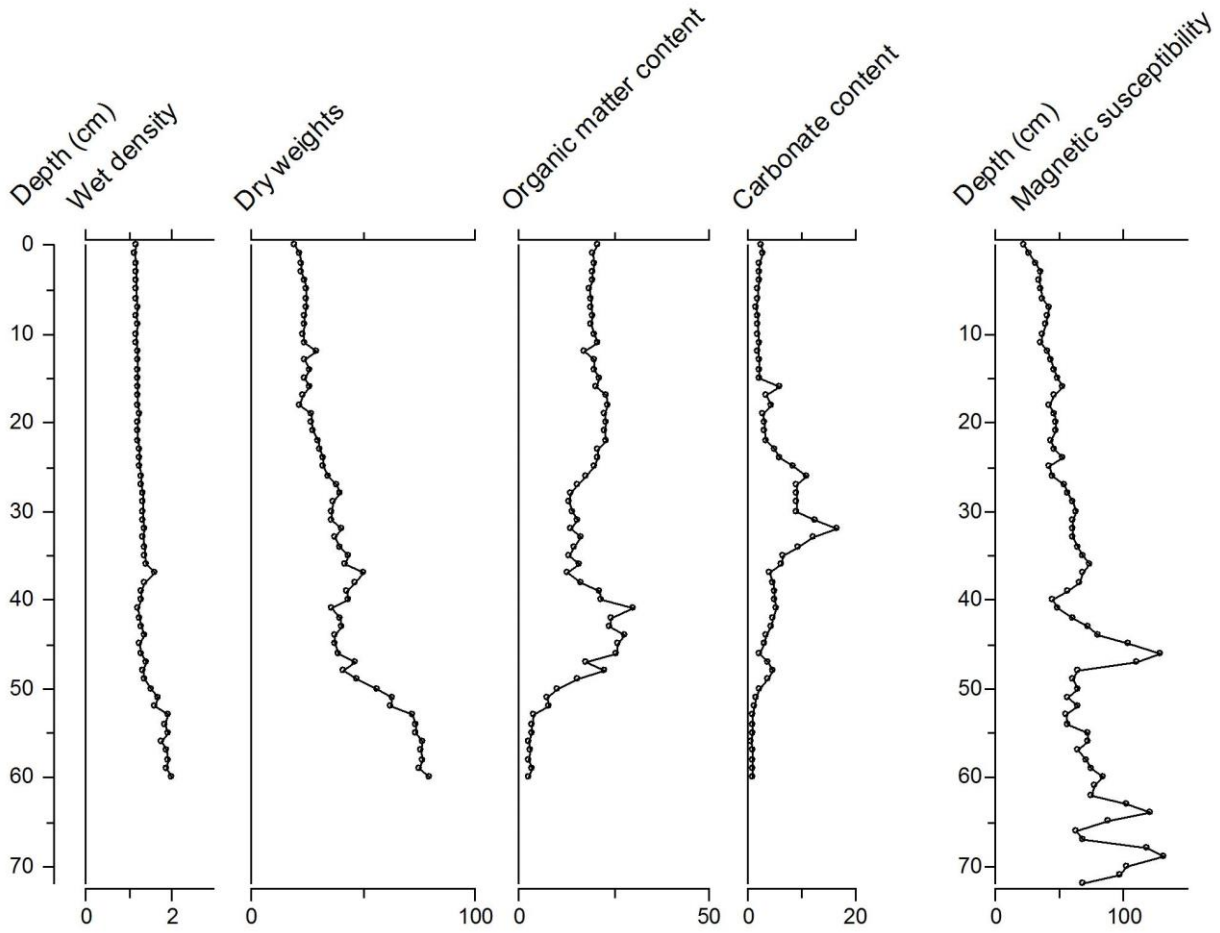

Figure 4.6. Lithostratigraphic profiles from SLNG04: wet density (g cm^{-3}), dry weights (%), organic matter content (%), carbonate content (%), and magnetic susceptibility (SI units). Note the separate depth axis for magnetic susceptibility.

4.3.3.4 SLNG05 sediment description

Four sections were identified within the sediment core SLNG05-A (Figure 4.7). The lowermost sediment section occurred between the base of the core and 48 cm, and contained sediments primarily composed of silty clays with minor sand intrusions. Sediments then became less sandy between 48 cm and 39 cm, and mollusc remains (ostracods, snails, and mussels) appear for the first time. Between 39 cm and 20 cm, sediments consisted of silty clays. The uppermost sediments consisted of mostly silty clay sediments with minor sand intrusions, and mollusc remains declined (Figure 4.7).

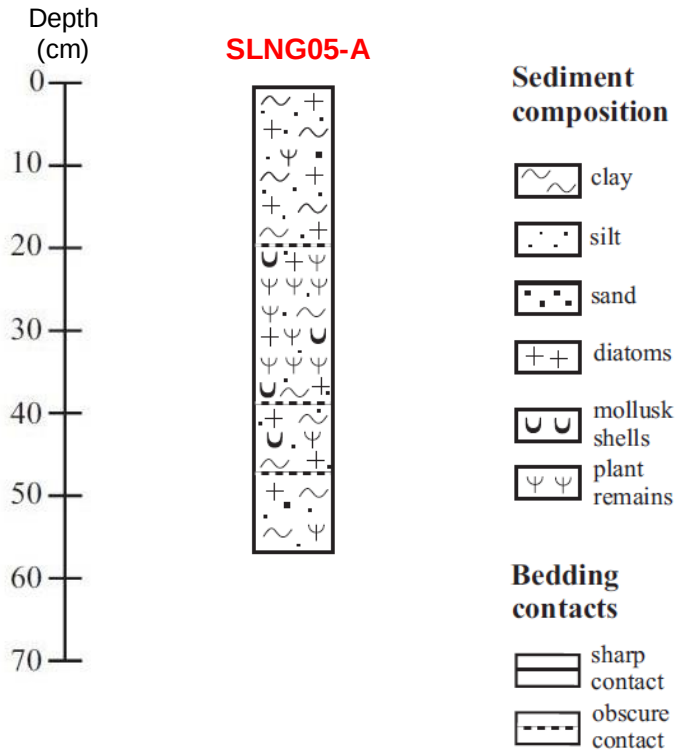

Figure 4.7. Sediment profile for core SLNG05-A.

4.3.3.5 SLNG05 densities and LOIs

Wet density was fairly constant between 1.5 g/cm^3 and 1.6 g/cm^3 between the base of the core and 48 cm (Figure 4.8). A steady and consistent decline followed, reaching 1.1 g/cm^3 by 22 cm. The decline was followed by a rapid increase in wet density to 1.6 g/cm^3 by 18 cm. Wet density then declined towards the surface. Percent dry weight followed a very similar trend throughout the sediment core, generally decreasing from 65% at the base of the core to 22% by 24 cm (Figure 4.8). A similarly rapid increase in dry weight also occurred, increasing to 62% by 18 cm (Figure 4.8).

Organic content measured 8% at the base of the core, and steadily increased to 39% by 24 cm (Figure 4.8). A rapid decrease in organic content followed, decreasing to 7% by 19 cm. Organic content increased to 11% by the surface. Carbonate content remained low at ~ 2% between the base of the sediment core and 48 cm, followed by a generally steady increase to the record maximum of 12% by 29 cm (Figure 4.8). A decline to 3% by 23 cm followed, and carbonate content remained steady to the surface.

4.3.3.6 SLNG05 magnetic susceptibility

Magnetic susceptibility (MS) was relatively steady between the base of the sediment core and 52 cm (Figure 4.8). A decline in MS values occurred between 51 cm and 21 cm, reaching negative MS values at the end of this period. A rapid increase in MS values to 65 SI units by 18 cm was observed, after which time values remained relatively high, reaching record maximum value of 74 SI units at 12 cm. Values decreased from 69 SI units at 9 cm to a sediment record low of -22 SI units at the surface (Figure 4.8).

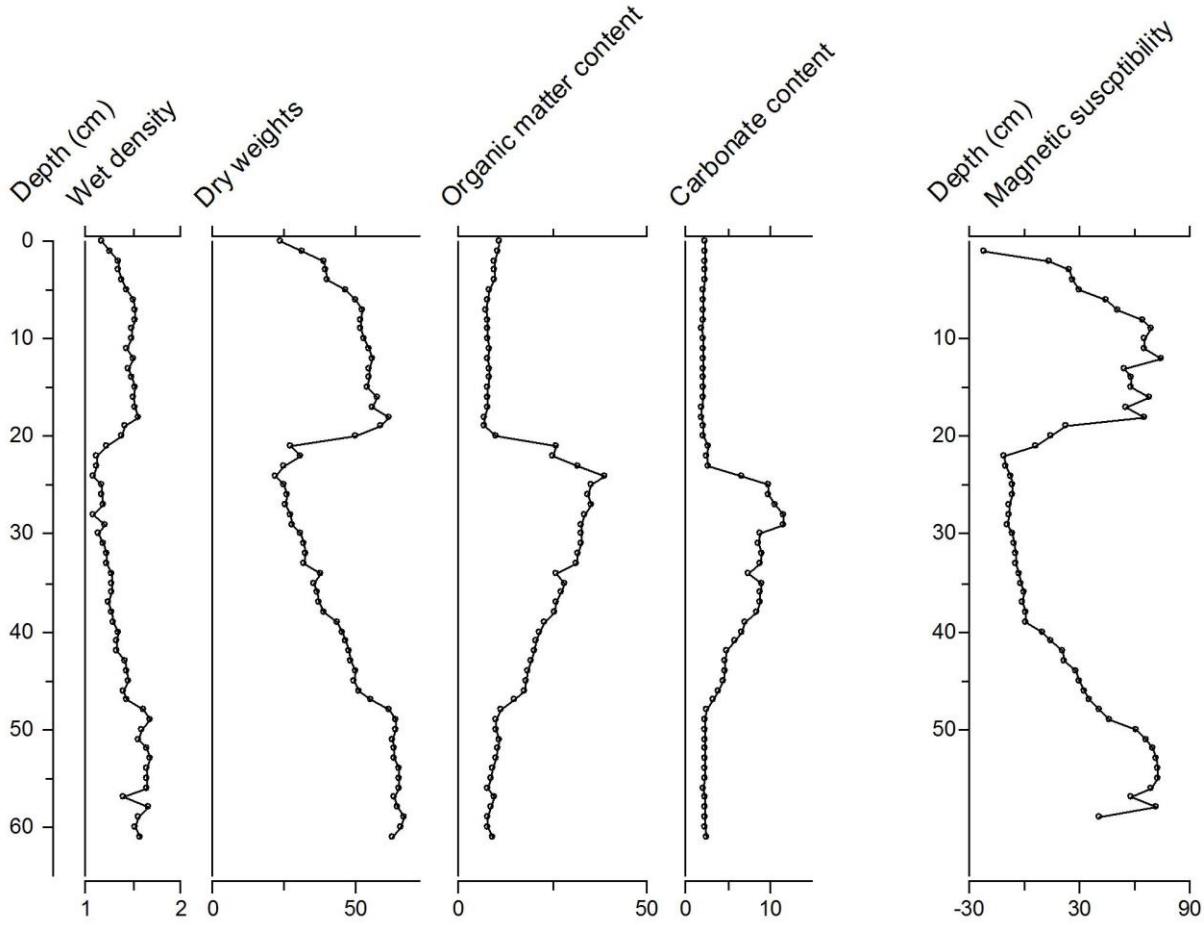

Figure 4.8. Lithostratigraphic profiles from SLNG05: wet density (g cm^{-3}), dry weights (%), organic matter content (%), carbonate content (%), and magnetic susceptibility (SI units). Note the separate depth axis for magnetic susceptibility.

4.3.3.7 BRYT02 sediment description

Two primary sections were identified within the sediment core BRYT02-C (Figure 4.9). The lowermost section spanned from the base of the core until 45 cm, was composed of mainly silty clays, with some sand intrusions. These early sediments also contained mollusc remains (snails and mussels). A transitionary section of the sediment core existed from 45 cm until 38 cm, and is characterized primarily by the disappearance of mollusc remains, with sediments composed

of silty clays, with declining sand fractions. The uppermost sediments were composed of silty clays with increasing sand intrusions (Figure 4.9).

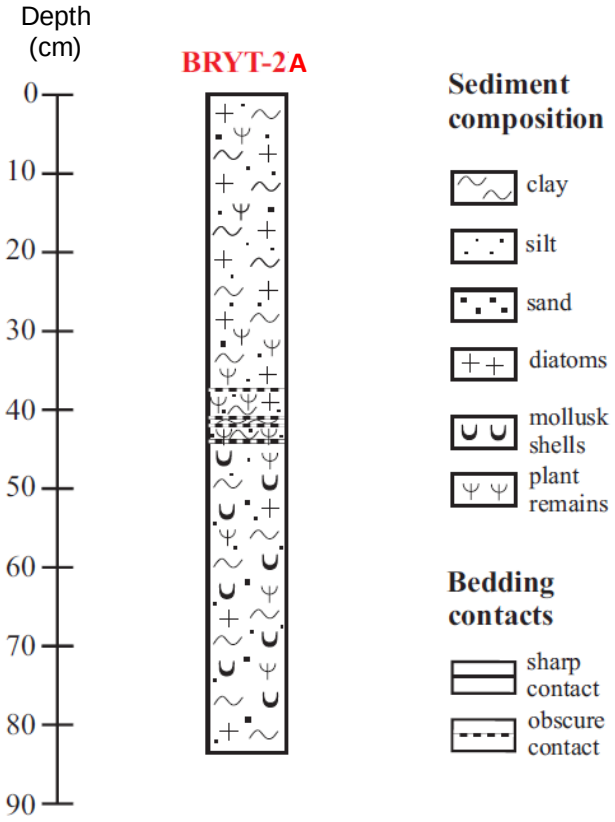

Figure 4.9. Sediment profile for core BRYT02-A.

4.3.3.8 BRYT02 densities and LOIs

Wet density was constant throughout the sediment record from BRYT02, remaining approximately 1.2 g/cm^3 throughout, with a range of 1.1 g/cm^3 to 1.3 g/cm^3 (Figure 4.10). Percent dry weights displayed a similar general trend throughout the sediment core, however slight fluctuations were more apparent (Figure 4.10). Fluctuations in dry weights occurred primarily between 45 cm and 38 cm, increasing to 30% at 43 cm, then declining to 16% by 38 cm. Dry weights then increased to 22% by 37 cm and remained steady to the surface. Fluctuations in organic matter content occurred from the base of the core until ~30 cm, with fluctuations between 16% and 41% organic content during this period (Figure 4.10). Organic matter content above 29 cm was relatively steady (Figure 4.10). Carbonate content fluctuated between 6% and 21% between the base of the core and 39 cm (Figure 4.10). Carbonate content remained below 10% from 38 cm to the surface.

4.3.3.9 BRYT02 magnetic susceptibility

Magnetic susceptibility (MS) values for sediment core BRYT02-A are low throughout the record (Figure 4.10). From the base of the core until 25 cm, MS values decreased from 21 SI units to 8 SI units, with low fluctuations throughout this section of the core. MS values increased rapidly to 22 SI units by 22 cm. MS values decreased steadily from 22 SI units to 10 SI units between 10 cm and the surface (Figure 4.10).

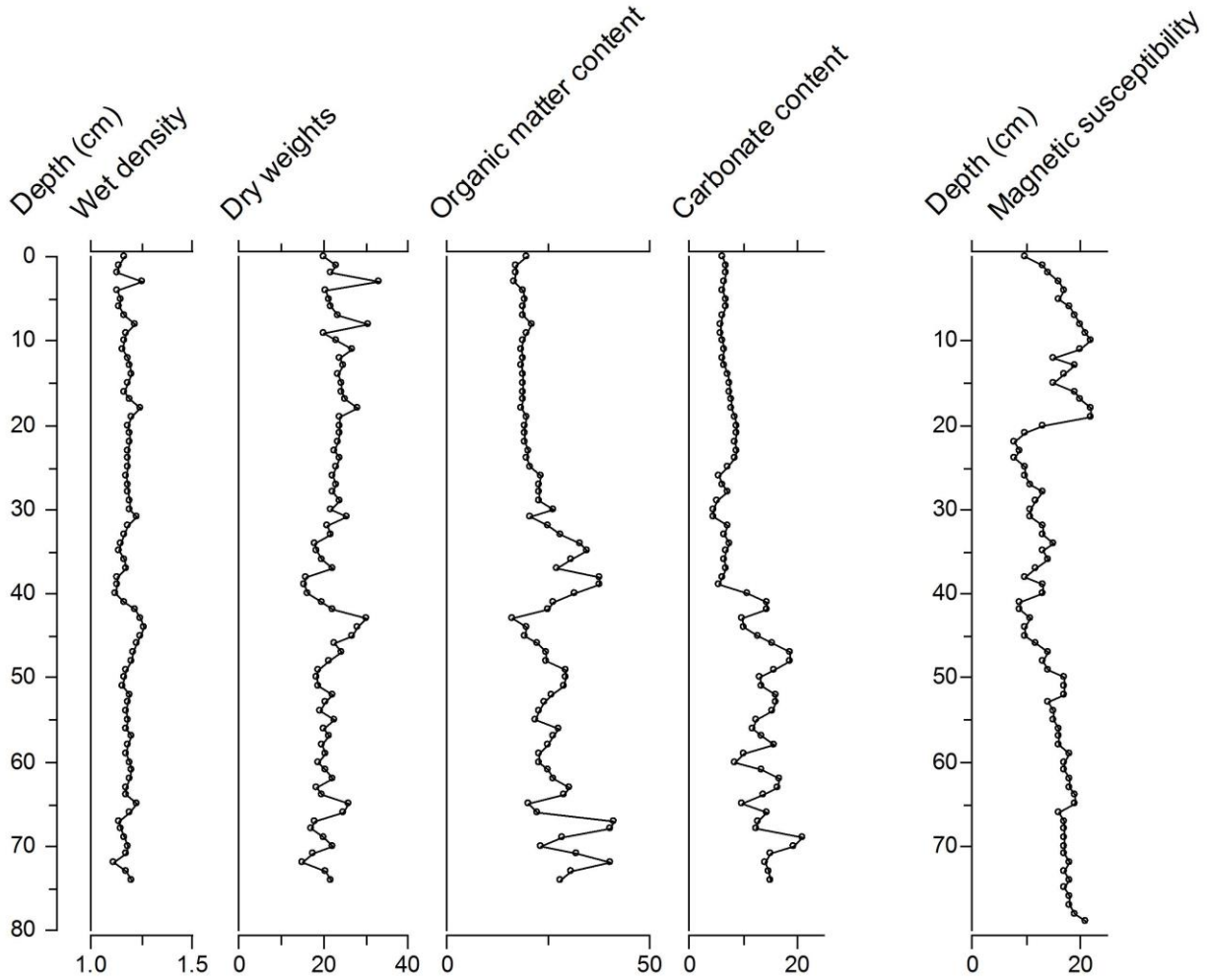

Figure 4.10. Lithostratigraphic profiles from BRYT02: wet density (g cm^{-3}), dry weights (%), organic matter content (%), carbonate content (%), and magnetic susceptibility (SI units). Note the separate depth axis for magnetic susceptibility.

4.4 Establishing chronologies for Selenga River basin lakes using radioisotope dating

4.4.1 Introduction to Radioisotope Dating Techniques

The radioisotope ^{210}Pb is produced both in the atmosphere (considered "unsupported"), where it is removed by both wet and dry deposition, and in the solid earth (considered "supported"), through the radioactive decay process of ^{238}U > ^{226}Ra > ^{222}Rn > ^{210}Pb > ^{210}Bi > ^{210}Po (Faure and Mensing, 2005). Radioisotope ^{210}Pb is commonly used to date recent sediments of up to approximately 150 years, or less than 7 half-lives (each of 22.3 years), which is often the period of interest for recent environmental issues of concern (Binford *et al*., 1993; Michelutti *et al*., 2008). Total ^{210}Pb and ^{226}Ra ("supported" ^{210}Pb) are measured within sediments (Bq/kg), and unsupported ^{210}Pb activity is calculated by subtracting supported from the total activity.

Several assumptions are made when constructing ^{210}Pb-derived age models on lake sediment cores. An understanding of the assumptions, and the related uncertainties in ^{210}Pb dating is required to properly interpret and construct age models. The amount of ^{210}Pb which enters an aquatic system and is eventually incorporated into the sediments is dependent on several factors, which are likely contributors to any apparent discrepancies in ^{210}Pb dating and chronologies constructed using standard age models. The initial supply of ^{210}Pb to the aquatic system from the environment is dependent on a number of factors, including variations in atmospheric depositional flux, which can depend largely on precipitation amounts. Moreover, annual ^{210}Pb flux is likely to be dictated by precipitation amounts in areas dominated by continental air masses and characterized by low annual levels of precipitation (Wolfe *et al*., 2004; Baskaran *et al*., 2014). This can result in variable supplies of the radionuclide to the system. Furthermore, in cold regions, the supply of ^{210}Pb to aquatic systems may be low, and depend strongly on the length of the ice-free season as longer periods of ice cover will prevent atmospheric deposition of ^{210}Pb, as is often cited for low levels of total ^{210}Pb activity in Arctic and subarctic aquatic systems (Wolfe *et al.,* 2004).

Independent dating techniques, such as ^{137}Cs and ^{241}Am, will inform and strengthen the reliability of ^{210}Pb-derived age models. The most common way to corroborate radioisotope ^{210}Pb radiometric dating is with ^{137}Cs and ^{241}Am. ^{137}Cs and ^{241}Am are artificially-produced radionuclides. Both ^{137}Cs and ^{241}Am appear in lake sediments due to atmospheric fallout from

nuclear weapons testing, while ^{137}Cs also occurs as a result of nuclear reactor incidents. These artificial radionuclides have been frequently used in the dating of recent sediments. The activities of these radionuclides are known to begin to increase globally in 1954 and peak in 1963, as a result of nuclear weapons testing. Additionally, a lower concentration peak can be observed across much of Europe as a result of the 1986 Chernobyl nuclear reactor catastrophe (Appleby, 2001).

4.4.2 Methods for radioisotope dating of sediment cores

Radiometric dating techniques (^{210}Pb, ^{137}Cs, ^{241}Am) were used to date sediment cores SLNG04-C, SLNG05-C and BRYT02-C. Wet sediment was subsampled from sediment cores SLNG04-C, SLNG05-C, and BRYT02-C at 3.0-cm intervals and freeze-dried. Dried sediment samples were analysed for ^{210}Pb, ^{226}Ra, ^{137}Cs and ^{241}Am by direct gamma assay in the Environmental Radiometric Facility at UCL, using ORTEC HPGe GWL series well-type coaxial low background intrinsic germanium detectors. ^{210}Pb was determined via its gamma emissions at 46.5keV, and ^{226}Ra by the 295keV and 352keV gamma rays emitted by its daughter isotope ^{214}Pb following 3 weeks storage in sealed containers to allow radioactive equilibration. ^{210}Pb chronologies for all three sediment cores were constructed using the constant rate of supply (CRS) dating model (Appleby and Oldfield, 1978; Appleby, 2001). Approximate dates were extrapolated beyond the dating provided by ^{210}Pb CRS model, using an average of the pre-1980 sedimentation rates from the dated portion of the sediment cores from SLNG05 and BRYT, and the pre-1990 sedimentation rates from SLNG04, to achieve an approximate background sedimentation rate for older sediments. Averaged pre-1980 and pre-1990 sedimentation rates were used in each of the sediment cores due to low, constant rates prior to these dates.

Artificial radionuclides ^{137}Cs and ^{241}Am were measured by their emissions at 662keV and 59.5keV (Appleby *et al*., 1986). The absolute efficiencies of the detector were determined using calibrated sources and sediment samples of known activity. Corrections were made for the effect of self absorption of low energy gamma rays within the sample (Appleby *et al*., 1992).

4.4.3 Results

4.4.3.1 Chronology of SLNG04-C

Total ^{210}Pb activity reached equilibrium with supported ^{210}Pb at a depth of 30.75 cm (Figure 4.11a). The unsupported ^{210}Pb activity profile for the sediment core can be divided into three sections: from the surface of the sediment core to 12.5 - 13.0 cm, unsupported ^{210}Pb activities declined exponentially with depth, while between 15.5 – 16.0 cm to 24.5 – 25.0 cm there was another stage of exponential decline in unsupported ^{210}Pb activities, with a dip at 23.5 - 24.0 cm, and finally below 24.5 – 25.0 cm there was a rapid decline in unsupported ^{210}Pb activities until 30.75 cm (Figure 4.11b). A well resolved peak in ^{137}Cs activity occurred at 23.5 – 24.0 cm, with a peak in ^{241}Am at the same depth confirming the ^{137}Cs peak as derived from the 1963 maximum fallout from nuclear weapons testing (Figure 4.11c).

The constant rate of supply (CRS) model was used to construct the age-model for recent sediments from SLNG04-C. Although ^{210}Pb dates calculated using the CRS model placed 1963 at about 20 cm, this depth is shallower than the depth dated by ^{137}Cs and ^{241}Am, which places 1963 at 23.75 cm (Figure 4.11c). CRS chronologies and sedimentation rates for SLNG04-C were therefore corrected using 23.75 cm as formed in 1963, as indicated by the ^{137}Cs and ^{241}Am records. The corrected model suggests that sedimentation rates between the 1940s and 1980s were relatively constant with a spike in the 1960s (Figure 4.12). Sedimentation rates of the last twenty years were constant, but at an increased level.

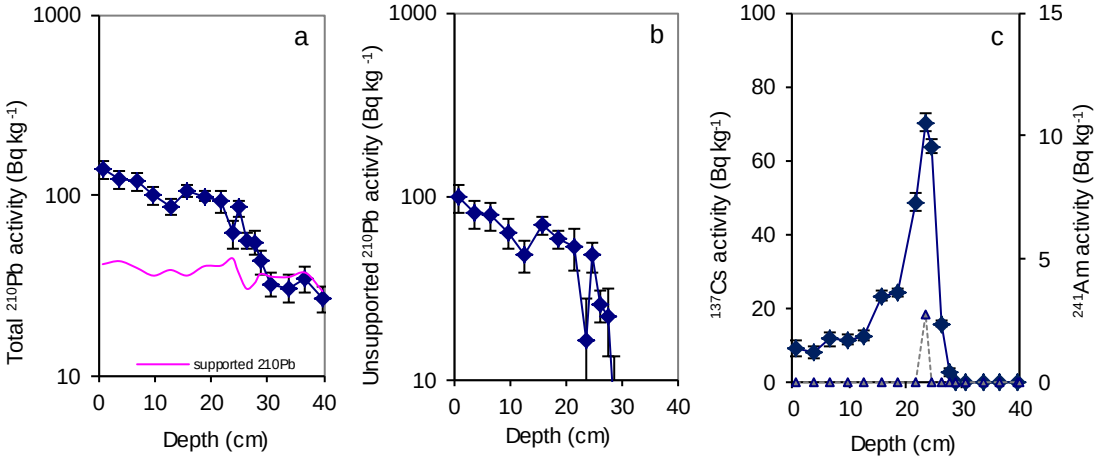

Figure 4.11. Radionuclide concentration profiles for sediment core SLNG04-C: (a) total ^{210}Pb and supported ^{210}Pb activity, (b) unsupported ^{210}Pb activity, (c) ^{137}Cs and ^{241}Am activity

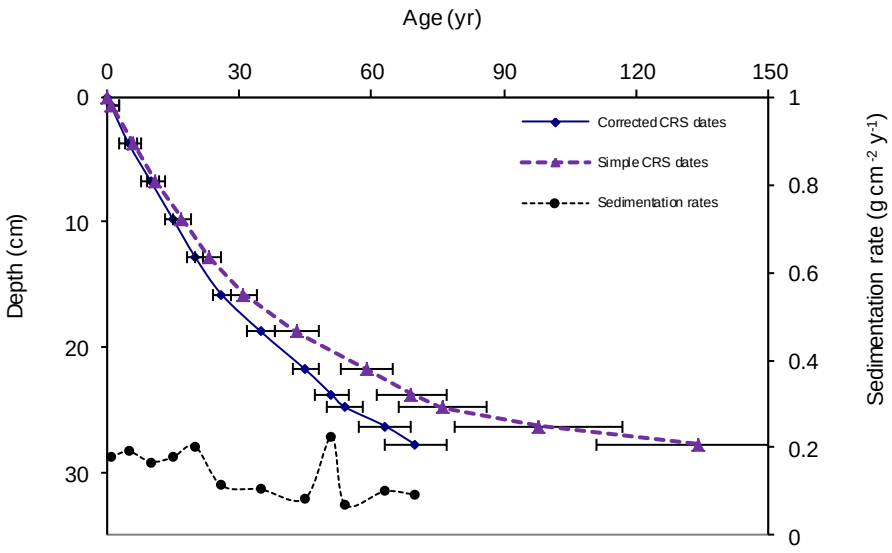

Figure 4.12. Radiometric ^{210}Pb CRS-derived age model and corrected CRS-derived age model (both with error margins) and sedimentation rate for core SLNG04-C.

4.4.3.2 Chronology of SLNG05-C

Total ^{210}Pb activity reached equilibrium with supported ^{210}Pb at a depth of 27 cm (Figure 4.13a). Unsupported ^{210}Pb activities vary unusually in the core, and are separated into 3 sections: within the top 16 cm activities declined irregularly with depth, followed by increasing unsupported ^{210}Pb activities with depth between 16 and 22 cm, and finally, a rapid decline in ^{210}Pb activities to 27 cm (Figure 4.13b). The unsupported ^{210}Pb profile suggests rapid sedimentation rates between 27 and 22 cm, followed by a change in phase of sedimentation processes, with reduced sedimentation rates between 22 cm and 16 cm depth. Sedimentation rates started to increase at 15.5 cm, followed by fluctuations in sedimentation rates in recent years. A well resolved peak in ^{137}Cs activity occurred at 24.75 cm, likely derived from the 1963 maximum fallout from nuclear weapons testing (Figure 4.13c). Am-241 was not detected in sediments from SLNG05-C. The CRS dating model using ^{210}Pb placed 1963 at about 17 cm. The CRS ^{210}Pb depth for 1963 is shallower than the depth dated by ^{137}Cs, which places 1963 at 24.75 cm. Due to low unsupported ^{210}Pb activities with relatively high counting errors, the SLNG05-C sediment core is dated up to 1968 ± 4 (21.75 cm) by ^{210}Pb technique, and extrapolated to 1963 using the ^{137}Cs-derived date (Figure 4.14).

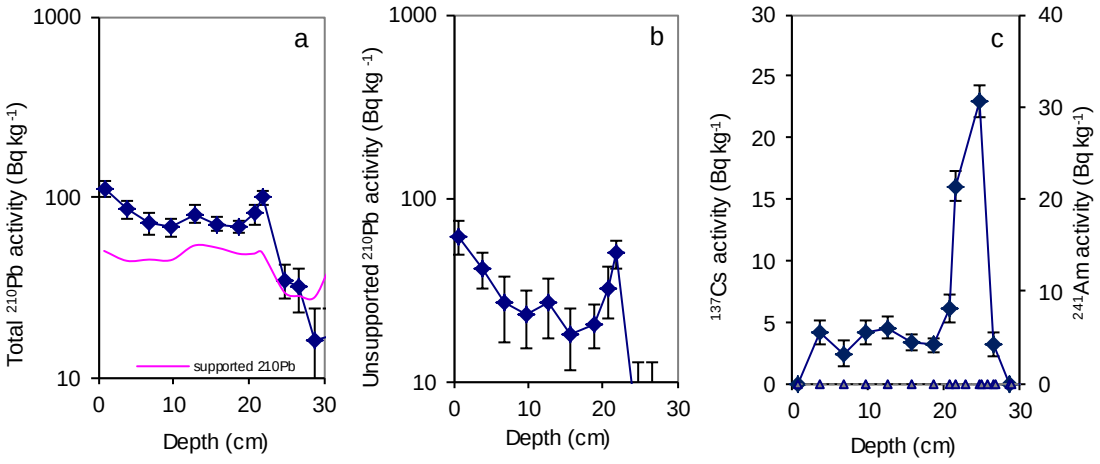

Figure 4.13. Radionuclide concentration profiles for sediment core SLNG05-C: (a) total ^{210}Pb and supported ^{210}Pb activity, (b) unsupported ^{210}Pb activity, (c) ^{137}Cs and ^{241}Am activity

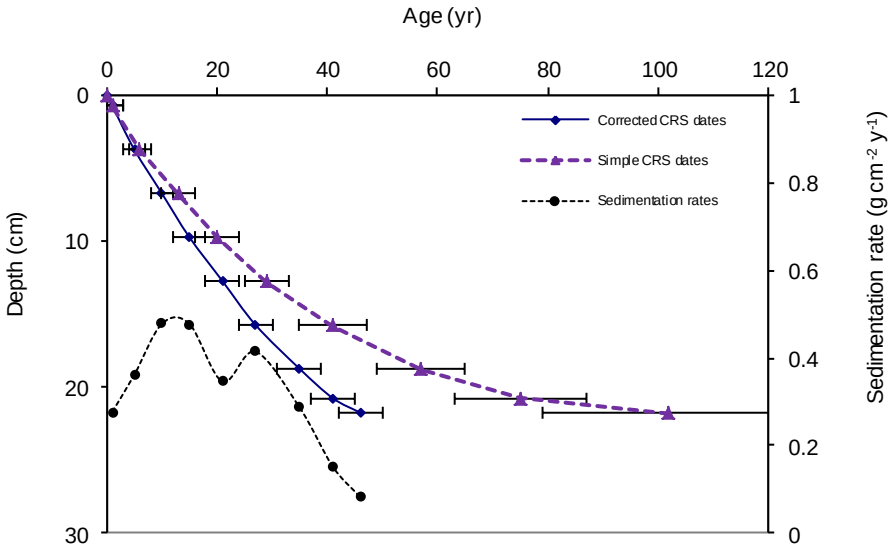

Figure 4.14. Radiometric ^{210}Pb CRS-derived age model and corrected CRS-derived age model (both with error margins) and sedimentation rate for core SLNG5-C.

4.4.3.3 Chronology of BRYT02-C

Total ^{210}Pb activity reached equilibrium with supported ^{210}Pb activity at a depth of 40 cm (Figure 4.15a). Unsupported ^{210}Pb activity declined mostly exponentially with depth, with some departures (Figure 4.15b). The trend in unsupported ^{210}Pb activity decline suggests a relatively uniform sediment accumulation rate throughout the recent sediments. A well resolved peak in ^{137}Cs activity occurred at 32.25 cm, and detection of ^{241}Am at 33.75 cm suggests that the ^{137}Cs peak was derived from 1963 maximum fallout of nuclear weapons testing (Figure 4.15c).

Departures of unsupported ^{210}Pb activities from completely exponential decline preclude the use of the CIC dating model. Use of the CRS dating model places 1963 at 22.5 cm based on unsupported ^{210}Pb activity, while the ^{137}Cs and ^{241}Am records place 1963 at 32.25 cm. Therefore, final CRS chronologies and sedimentation rates for BRYT02-C were corrected using 32.25 cm as formed in 1963. Sedimentation rates were relatively uniform since the 1950s with a mean of 0.18 g cm^{-2} yr^{-1}, and briefly increased in the 1960s and 1980s, with sustained increases since the mid-1980s (Figure 4.16).

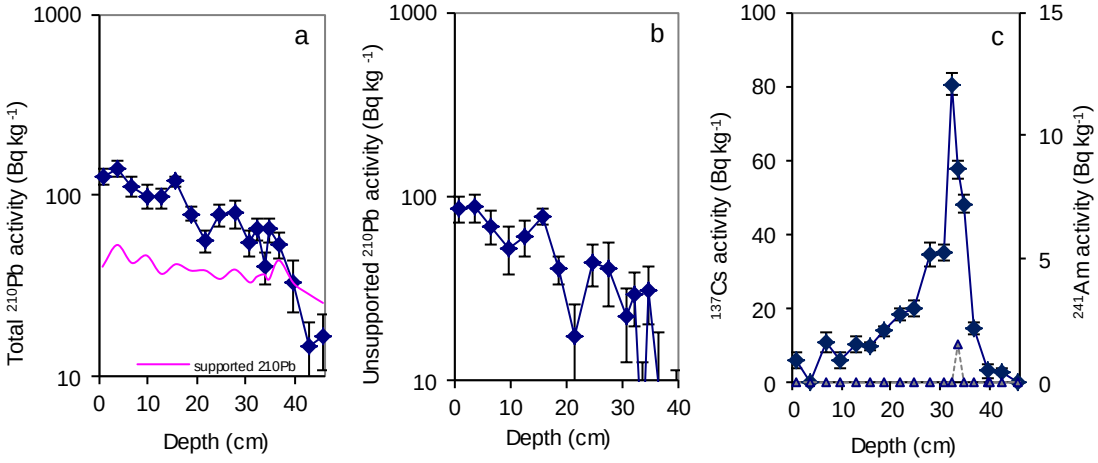

Figure 4.15. Radionuclide concentration profiles for sediment core BRYT02-C: (a) total ^{210}Pb and supported ^{210}Pb activity, (b) unsupported ^{210}Pb activity, (c) ^{137}Cs and ^{241}Am activity

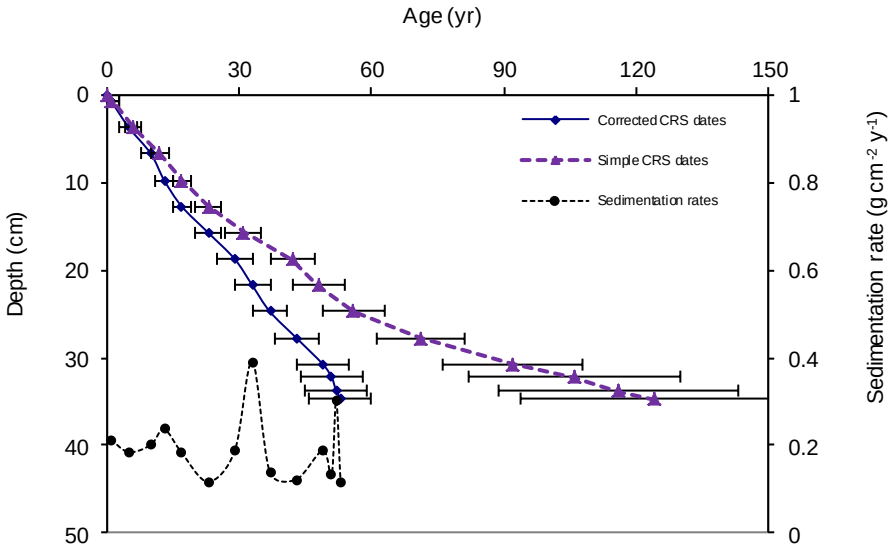

Figure 4.16. Radiometric ^{210}Pb CRS-derived age model and corrected CRS-derived age model (both with error margins) and sedimentation rate for core BRYT02-C.

4.5 Establishing chronologies for sediment cores using cross-dating techniques

4.5.1 Methods for cross-dating of sediment cores

Correlations between the sediment cores from each site was required in order to apply the ^{210}Pb resolved dates to the undated cores. Cross-dating of sediments from sediment cores not dated using radiometric ^{210}Pb-dating techniques were performed using loss-on-ignition cross-correlations with sediment cores on which radioisotopic dating was performed. Palaeolimnological studies which involve a number of proxies which require minimum volumes of sediment for analyses, often must utilize multiple sediment cores collected from a single site. Comparing contaminant and biological proxy records between multiple sediment cores within a single site, as well as comparing records of chronologies from sediment cores between sites, requires certainty and reliability in the constructed chronology. Loss-on-ignition is one of the commonly used tools for cross-correlating chronologies between sediment cores (Birks and Birks, 2006). Correlations between cores was done by identifying distinct features (tie-points) in the loss-on-ignition profiles from each of the dated and undated cores. The ^{210}Pb-derived dates were then applied to these tie-points in the undated profiles, and interpolation of dates between correlated dates was applied. A minimum of three tie-points were confirmed between cores to construct the cross-dated age-models for cores not dated radiometrically.

4.5.2 Results of the cross-dating of sediment cores

Cross-dating of sediments from sediment cores not dated using radiometric ^{210}Pb-dating techniques, were performed using loss-on-ignition cross-correlations with sediment cores on which radioisotopic dating was performed. The high level of reproducibility of LOI_{550} and LOI_{950} between sediment cores within a single site from the study lakes in the Selenga River basin, provided a good degree of reliability with the cross-correlation of ^{210}Pb-derived dating from a single core at each site.

4.5.2.1 Cross-dating between SLNG04-C and SLNG04-B

SLNG04-B was the sediment core collected for persistant organic pollutant analysis. The LOI_{550} profiles between sediment cores SLNG04-C and SLNG04-B were nearly identical, which, given uncertainties in ^{210}Pb-derived dates, eliminated the need for specific tie-points between

profiles (Figure 4.17). An age-depth model was created for sediment core SLNG04-B based on the correlation with the ^{210}Pb-dated CRS model established for SLNG04-C (Figure 4.18).

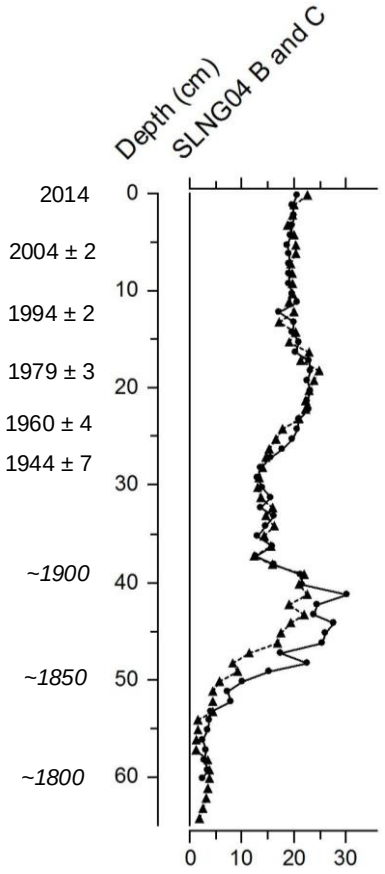

Figure 4.17. Correlations in % organic matter (LOI_{550}) between radioisotopically dated sediment core SLNG04-C (solid line with closed circles) and POPs sediment core, SLNG04-B (dashed line with closed triangles).

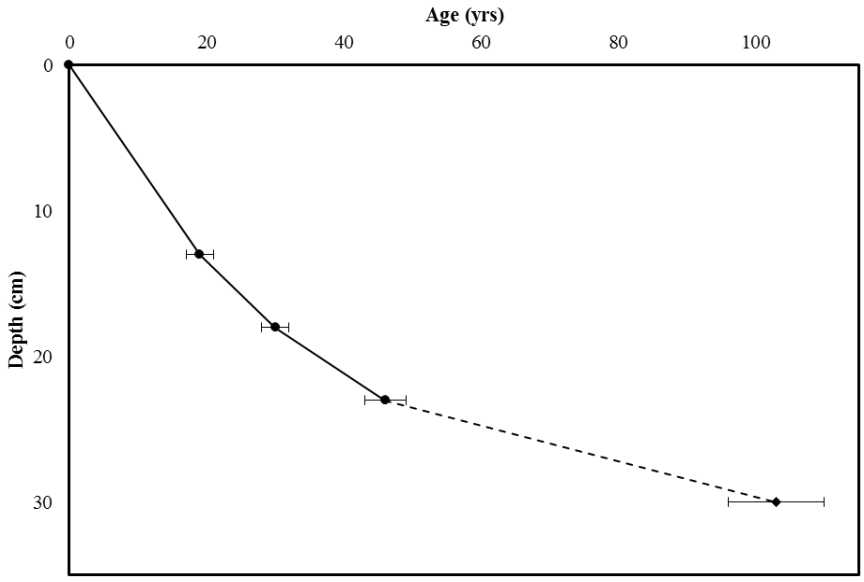

Figure 4.18. Age-depth model for core SLNG04-B. One extrapolated date indicated by diamond symbol, and interpolation with adjacent date indicated with dashed line. Errors (yrs) are given for each point.

4.5.2.2 Cross-dating between SLNG04-C and SLNG04-A

The profiles of LOI_{550} and LOI_{950} matched well between sediment cores SLNG04-C and SLNG04-A, indicating good potential for cross-correlation. Three tie-points were determined through the ^{210}Pb-dated portion of sediment core SLNG04-C, with sediment core SLNG04-A, based on % organic matter and LOI_{950} (% carbonate) (Figure 4.19). A further two tie-points based on % carbonate were determined below the ^{210}Pb-dated portion. Tie-point one of cross-dating occurs at 16 cm depth in SLNG04-C, and corresponds to 20 cm depth in SLNG04-A based on % carbonate, indicating a date of ~1985. Tie-point two occurs at 22 cm depth in SLNG04-C, and corresponds to 25 cm in SLNG04-A based on % organic matter, indicating a date of ~1970. Tie-point three was determined at 26 cm depth in SLNG04-C, and corresponds to sample depth 27 cm in SLNG04-A based on % carbonate, indicating a ~1950. Cross-dating tie-points four and five occur below the ^{210}Pb CRS modelled portion of sediment core SLNG04-C. Tie-point four was determined at 32 cm in the dated sediment core SLNG04-C, and corresponds to sample depth of 38 cm in SLNG04-A based on % carbonate, and indicates an extrapolated date of 1907. Cross-dating tie-point five occurs at 53 cm depth in SLNG04-C, and corresponds to sample depth of 62 cm in SLNG04-A, as determined using % organic matter, and indicates an extrapolated date of 1838. An age-depth model was created for sediment core SLNG04-A based on the cross-correlation with the ^{210}Pb-dated CRS model established for SLNG04-C (Figure 4.20).

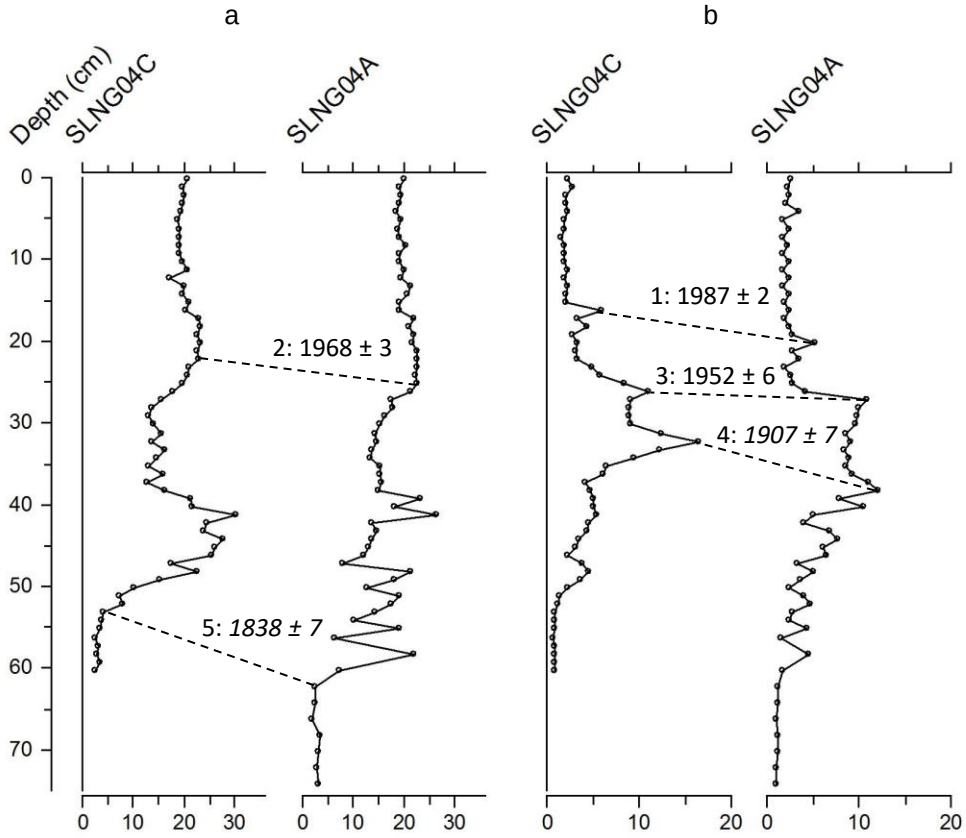

Figure 4.19. Correlations in a) % organic matter (from LOI_{550}) and b) % carbonate (LOI_{950}) between radioisotopically dated sediment core SLNG04-C and lithology sediment core, SLNG04-A. Tie-points between the sediment cores are indicated by dashed lines. Radioisotopically-derived dates (yrs AD) and confidence limits corresponding to tie-points are indicated. Italicized dates are extrapolated beyond ^{210}Pb radioisotope dating.

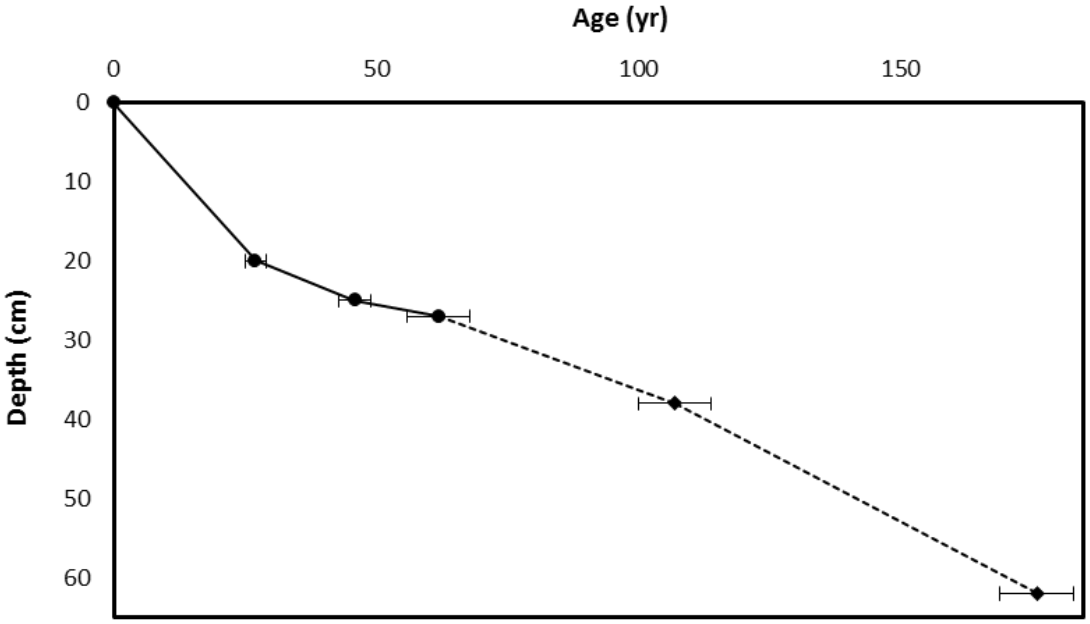

Figure 4.20. Age-depth model constructed for SLNG04-A using cross-dating methods.

4.5.2.3 Cross-dating between SLNG05-C and SLNG05-A

The profiles of LOI_{550} and LOI_{950} matched well between sediment cores SLNG05-C and SLNG05-A, indicating good potential for cross-correlation. Two tie-points were determined through the dated portion of sediment cores SLNG05-C and SLNG05-A, based on a combination of % organic matter and % carbonate (Figure 4.21). Tie-point one occurs at 19 cm in the ^{210}Pb-dated core SLNG05-C and 17 cm depth in SLNG05-A, correlated through % organic matter and indicating a date in the late-1970s. Tie-point two occurs at 23 cm in the ^{210}Pb-dated sediment core SLNG05-C and 25 cm in SLNG05-A, correlated using % carbonate, and indicates a date of ~1965 AD. Two tie-points occur below the ^{210}Pb-dated portion of the sediment cores. A third tie-point occurs just below the dated portion of sediment core SLNG05-C, using % carbonate, at a depth of 29 cm, correlating with 31 cm depth in SLNG05-A, and is extrapolated as the early 1930s, while a fourth tie-point, using % organic matter, occurs at a depth of 48 cm in both sediment cores SLNG05-C and SLNG05-A, and is extrapolated as the late-19th century. An age-depth model was created for sediment core SLNG05-A based on the cross-correlation with the Pb-dated CRS model established for SLNG05-C (Figure 4.22).

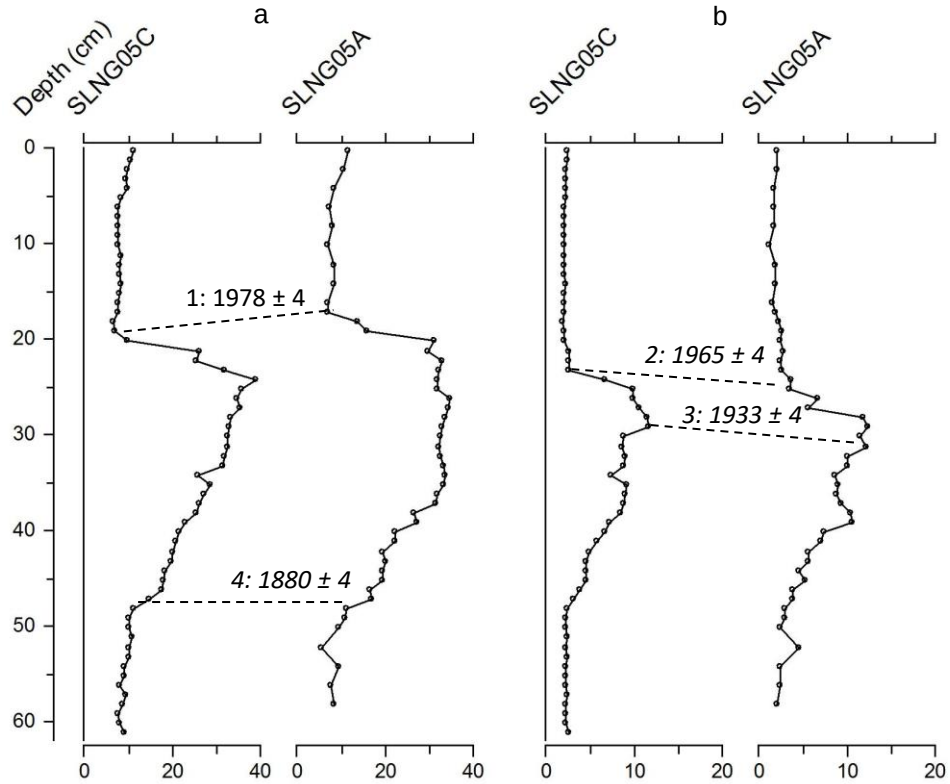

Figure 4.21. Correlations in a) % organic matter (LOI_{550}) and b) % carbonate (LOI_{950}) between radioisotopically dated sediment core SLNG05-C and lithology sediment core, SLNG05-A. Tie-points between the sediment cores are indicated by dashed lines. Radioisotopically-derived dates (yrs AD) and confidence limits corresponding to tie-points are indicated. Italicized dates are extrapolated beyond ^{210}Pb radioisotope dating.

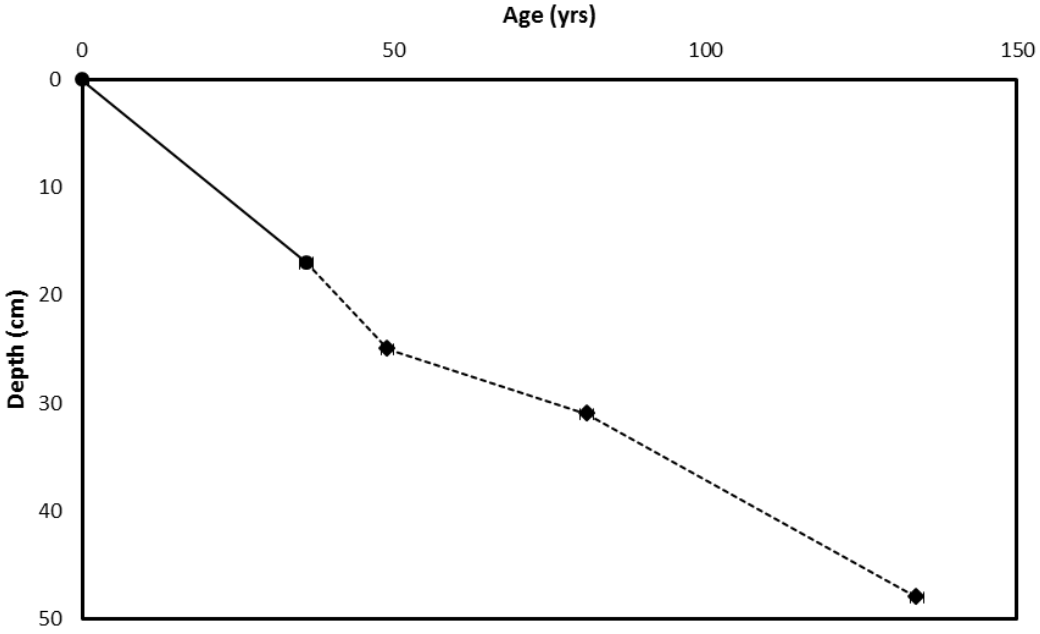

Figure 4.22. Age-depth profile for core SLNG05-A using cross-dating methods.

4.5.2.4 Cross-dating between BRYT02-C and BRYT02-B

The profiles of LOI_{550} and LOI_{950} matched well between sediment cores BRYT02-C and BRYT02-B, indicating good potential for cross-correlation. Three tie-points were determined through the dated portion of BRYT02-C with sediment core BRYT02-B, based on a combination of % organic matter and % carbonate (Figure 4.23). Tie-point one occurs at 26 cm depth in BRYT02-C, and correlates with 17 cm depth in BRYT02-B using both % organic matter and % carbonate, indicating a date of ~1975. Tie-point two was determined at 31 cm in the dated sediment core BRYT02-C, correlating with a depth of 22 cm in BRYT02-B, through % carbonate, and indicating a date of ~1965. Tie-point three occurs at 35 cm depth in BRYT02-C, correlating with a depth of 27 cm in BRYT02-B using % organic matter, and indicating a date of ~1960. Tie-point three correlates with the oldest date determined through 210Pb radiometric dating of BRYT02-C. An age-depth model was created for sediment core BRYT02-B based on the cross-correlation with the ^{210}Pb-dated CRS model established for BRYT02-C (Figure 4.24).

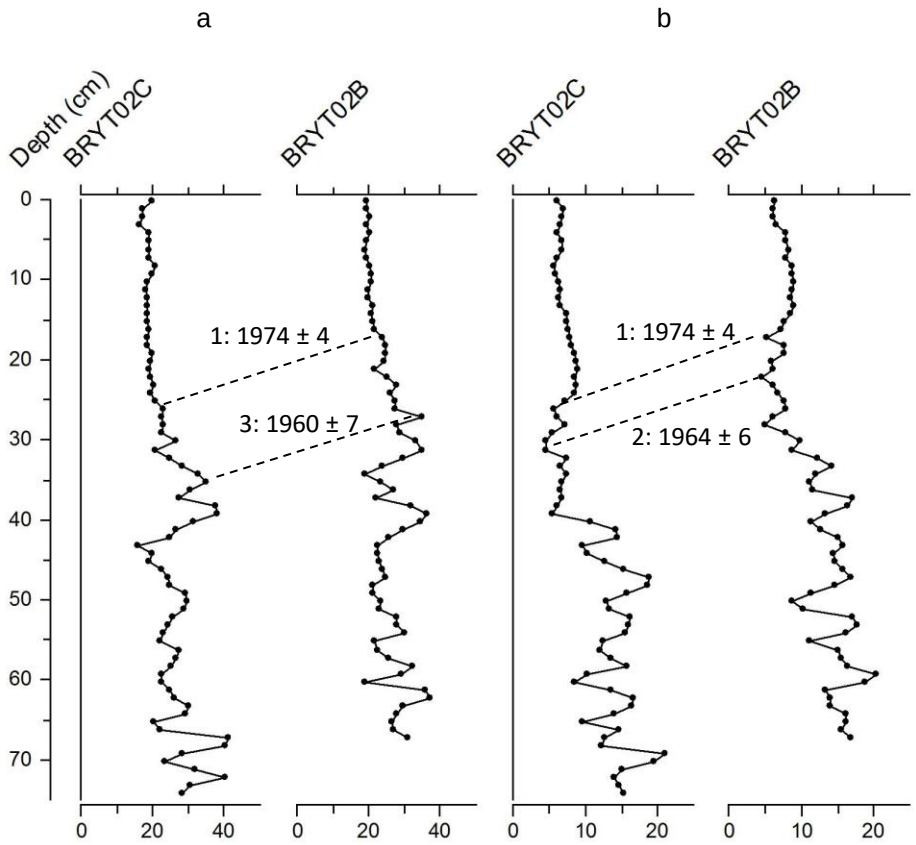

Figure 4.23. Correlations in a) % organic matter (LOI_{550}) and b) % carbonate (LOI_{950}) between radioisotopically dated sediment core BRYT02-C and POPs sediment core, BRYT02-B. Tie-points between the sediment cores are indicated by dashed lines. Radioisotopically-derived dates (yrs AD) and confidence limits corresponding to tie-points are indicated. Italicized dates are extrapolated beyond ^{210}Pb radioisotope dating.

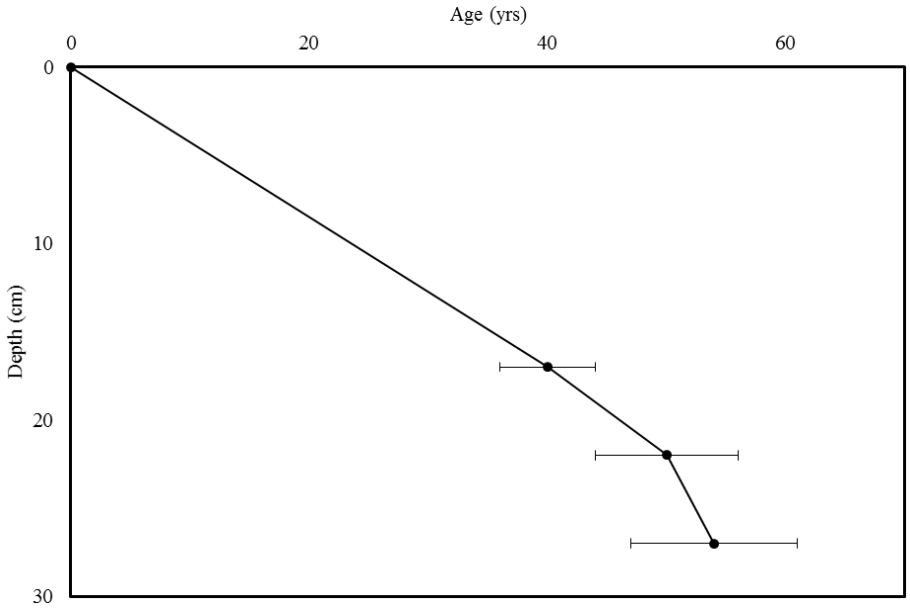

Figure 4.24. Age-depth model for core BRYT02-B using cross-dating methods.

4.5.2.5 Cross-dating between BRYT02-C and BRYT02-A

BRYT02-A was the sediment core collected for magnetic susceptibility and lithology analyses, and archiving purposes. The profiles of LOI_{550} and LOI_{950} matched well between sediment cores BRYT02-C and BRYT02-A, indicating good potential for cross-correlation. Two tie-points between BRYT02-A and the ^{210}Pb-dated sediment core, BRYT02-C were determined through the CRS model dated portion based on a combination of % organic matter and % carbonate (Figure 4.25). Tie-point one occurs at 26 cm in the dated sediment core BRYT02-C, which correlates with 30 cm depth in BRYT02-A, using both % organic matter and % carbonate, and indicates a date of ~1975. Tie-point two occurs at 35 cm in dated core BRYT02-C, and correlates with 39 cm in BRYT02-A using % organic matter, and indicates a date of ~1960. Cross-correlated tie-point two between BRYT02-C and BRYT02-A occurs at the oldest date determined through ^{210}Pb radiometric dating of BRYT02-C. Two further tie-points are noted between the two cores. The third cross-correlated tie-point occurs at 39 cm in BRYT02-C and 43 cm BRYT02-A as determined using both % organic matter and % carbonate, and indicates an extrapolated age of ~1950. The fourth tie-point between core BRYT02-C and BRYT02-A occurs at 43 cm in BRYT02-C and 47cm in BRYT02-A, determined using % organic matter, with an extrapolated date of ~1945. An age-depth model was created for sediment core BRYT02-A based on the cross-correlation with the Pb-dated CRS model established for BRYT02-C (Figure 4.26).

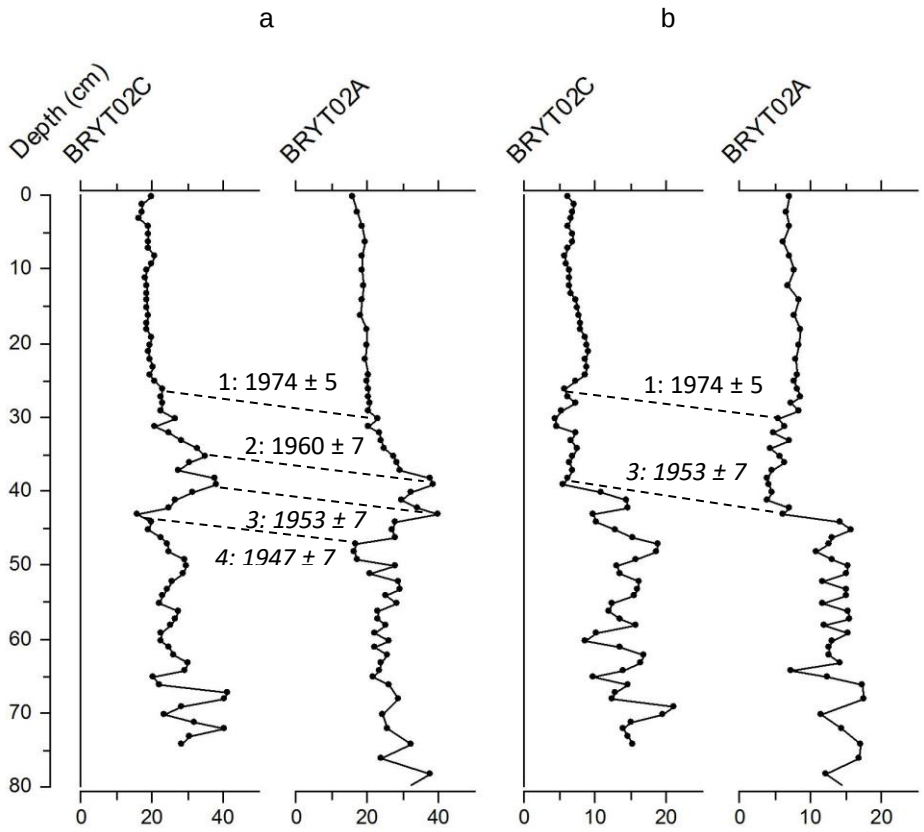

Figure 4.25. Correlations in a) % organic matter (LOI_{550}) and b) % carbonate (LOI_{950}) between radioisotopically dated sediment core BRYT02-C and lithology sediment core, BRYT02-A. Tie-points between the sediment cores are indicated by dashed lines. Radioisotopically-derived dates (yrs AD) and confidence limits corresponding to tie-points are indicated. Italicized dates are extrapolated beyond ^{210}Pb radioisotope dating.

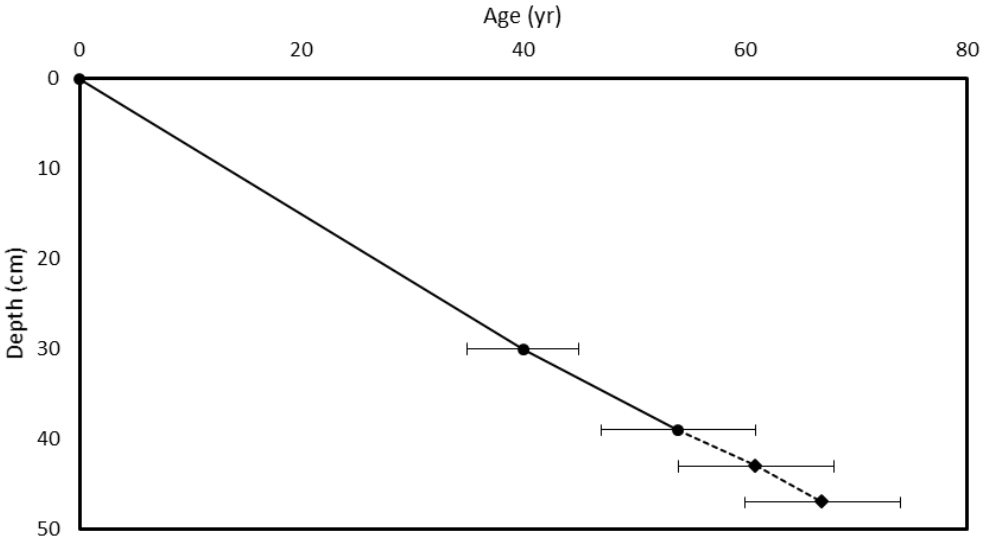

Figure 4.26. Age-depth model for core BRYT02-A using cross-dating methods.

4.6 Discussion

4.6.1 Chronology formation and cross-dating of sediment cores

Chronologies established from the radiometric dating for sediment cores SLNG04-C, SLNG05-C, and BRYT02-C were relatively short, with oldest dates derived being 1944 (±7), 1968 (±4), and 1961 (±7), for SLNG04, SLNG05, and BRYT02, respectively. However, the SLNG05 record can be extended slightly using ^{137}Cs, placing the oldest age of 1963 at 24.5-25.0 cm depth. These time periods are much shorter than the possible ~150-year record that may be produced from the use of ^{210}Pb dating. Radiometric dating is strongly affected by processes dictating the supply of radioisotopes to the sediment (Appleby, 2008), and hence, such processes may impact the ability to accurately ^{210}Pb-date a sediment core. The transport of ^{210}Pb to aquatic systems may be influenced by high levels of disturbance within a river basin, and shallow lakes and floodplain systems are susceptible to disturbances which would impact the establishment of lengthy chronology, leading to complex records (e.g. Larsen and MacDonald, 1993; Gilbert and Lamoureux, 2004; Dong *et al*., 2012; Dong *et al*., 2016). The influence of land use changes, hydrological regime shifts, and changes in erosional input on ^{210}Pb flux is greater in smaller systems, where disturbances in the basin and/or changes in sedimentation accumulation rates are likely to have greater and more direct impact on the radionuclide supply to the system (Baskaran *et al*., 2014; Dong *et al.,* 2016). Further, variations in organic matter delivery to the lake may influence the delivery of the radionuclide, and increased organic matter transport from the watershed due to increased erosion or changes in land use may result in increased in-wash of the radionuclide from the catchment to the lake (Baskaran *et al*., 2014; Dong *et al*., 2016).

It is likely that the difficulties experienced with ^{210}Pb-dating of the sediment cores collected from the Selenga River basin are due to sediment disturbances during the mid-20th century. Comparisons of the ^{210}Pb dating efficiencies with records of loss-on-ignition, water content, and magnetic susceptibility profiles within the SLNG05 and SLNG04 sediment cores indicate great change in these records coinciding approximately with the oldest calculated ^{210}Pb dates (Figures 4.12 and 4.14), likely indicating a disturbance event, prior to which lower accumulation rates of the radionuclide were experienced. The ^{210}Pb dating of sediment core SLNG04-C is hindered by low unsupported ^{210}Pb activity prior to 28 cm depth (Figure 4.11). Fluctuating

activity and irregular decline in unsupported ^{210}Pb activity between 21 and 28 cm depth suggests environmental disturbance prior to the mid-1960s. In the SLNG05 sediment core, unsupported ^{210}Pb activity declines rapidly between 21.75 and 24.75 cm depth (Figure 4.13), possibly indicating a change in the sedimentation environment at this time (Dong *et al*., 2016). The rapid decline in unsupported ^{210}Pb activity at this time coincides with an increase in sedimentation rates in the early to mid-1960s.

4.6.2 Insights from geochemical indicators

Magnetic susceptibility (MS) can also be used as a tool for detecting changes in pollution/trace metal loading to a lake (e.g. Guo *et al*., 2015). However declining MS values through the 20th/21st centuries at SLNG04, high correlation between MS profile and dry weights and LOI_{550} profiles at SLNG05, and low overall MS values at Black Lake, make it unlikely that these profiles are related to anthropogenic pollution. Negative MS values were recorded only at SLNG05 between the early to mid-20th century (Figure 4.8). Negative MS values may arise in the absence of magnetic minerals, when organic matter, carbonates, and/or diatom silica dominate the sediments (Oldfield, 2013). High levels of organic matter (high LOI_{550}, Figure 4.8) accumulation in SLNG05 occurred between the late-19th century and mid-20th century, possibly indicating high levels of within-lake productivity. High levels of organic matter in the sediment likely led to increased rates and high occurrences of decomposition, and decreased oxygen concentrations in the water, leading to reducing conditions at the sediment-water interface (Oldfield, 2013). The divergence and increase in MS values observed beginning in the mid-20th century may indicate a change in source to the lake, representing increased connectivity with the Selenga River, and signalling an in-wash of sediments linked to a flood occurrence (Figure 4.8) (Gell *et al*., 2007; Guo *et al*., 2015).

Increases in MS values may also be tied to increases in sedimentation rates in shallow lakes, with sustained elevated MS values co-occurring with increased loading of magnetic mineral materials (Macreadie *et al*., 2012). The increase in MS values observed at Black Lake occurred in the mid-1980s, at approximately the same time as the increase in sedimentation rates in the BRYT02 sediment core (Figure 4.10, Figure 4.16). The connection between sedimentation rates and magnetic susceptibility values may also be the reason for rapidly

increased MS values observed in the SLNG05 record in the mid-20th century, and may also be tied to the difficulty in radioisotope dating prior to this increase in MS values.

High levels of fluctuating MS values early in the SLNG04 record (Figure 4.6) are not seen in either the SLNG05 or BRYT02 record. These events in the MS record throughout the 19th century at SLNG04 likely indicate high levels of sediment influx/erosion or a range of sources providing material to the site (Eriksson and Sandgren, 1999; Gell *et al*., 2007). Gell *et* al. (2007) observed similar early MS trends for the River Murray floodplain system of Australia, when the wetland was receiving waters and sediments originating from a range of sources. The combined MS, LOI_{550} and LOI_{950} records for SLNG04 during the early- to mid-19th century may indicate a time during lake development, progressing from a marginal semi-aquatic or terrestrial site to a lake basin (Figure 4.6). The increase in LOI_{550} and LOI_{950} in the mid-19th century (Figure 4.6) coincides with a large magnitude earthquake just off-shore of the Selenga Delta in 1862. The Tsagan earthquake of 1862 was the strongest ever recorded in East Siberia (with a magnitude of 7.5) and was integral in forming the contemporary structure of the right bank of the Selenga Delta and Proval Bay of Lake Baikal (Vologina *et al*., 2010). The earthquake resulted in substantial subsidence and flooding of a large area of the northeast corner of the Delta, with a total area of approximately 200 km^2 suffering from flooding and subsidence, and total subsidence depths of up to 9 m (Orlov, 1872). It is possible that the earthquake is responsible for the formation of SLNG04.

Increases in LOI_{950} are recorded in sediment records from both Selenga Delta lakes (SLNG04 and SLNG05) in the mid-20th century (Figure 4.6 and Figure 4.8). Records of increasing carbonate content coincided at both lakes with calcite precipitation in the sediment. Increased agricultural activity and anthropogenic disturbances within the Selenga River basin in the early-20th century, may have resulted in increased nutrient flux to the Selenga Delta. Increased nutrient levels in shallow lakes at this time likely stimulated plant production, leading to increased photosynthetic removal of CO_2 from the water column, and resulting in increased carbonate content and increasing alkalinity (Talling, 1976). Moreover, increased agricultural activity in the region would have led to increased transport of calcium to lakes in the early 20th century (Potasznik and Szymczyk, 2015).

4.7 Conclusions

Selenga River basin lakes were likely subject to landscape-scale disturbance in the mid-20th century, as confirmed through loss-on-ignition and magnetic susceptibility profiles at each of the three sites. Given the well-defined ^{137}Cs peak all three sediment cores, and ^{241}Am peak in SLNG04 and BRYT02, Pb-derived age models can be reliably constructed for the Selenga River basin sediment cores from the mid-20th century only. The highly reproducible LOI_{550} and LOI_{950} profiles for multiple cores collected from each study lake, allows for confident cross-dating to be undertaken between cores.

4.8 References

Appleby P.G. (2001) Chronostratigraphic techniques in recent sediments. In, Tracking Environmental Change Using Lake Sediments. Vol. 1: Basin Analysis, Coring, and Chronological Techniques. Kluwer Academic Publishers, The Netherlands.

Appleby P.G. (2008) Three decades of dating recent sediments by fallout radionuclides: a review. *The Holocene*, **18**, 83-93.

Appleby P.G., & Oldfield F. (1978) The calculation of ^{210}Pb dates assuming a constant rate of supply of unsupported ^{210}Pb to the sediment. *Catena*, **5,** 1-8.

Appleby P.G., Nolan P.J., Gifford D.W., Godfrey M.J., Oldfield F., Anderson N.J., & Battarbee R.W. (1986) ^{210}Pb dating by low background gamma counting. *Hydrobiologia*, **141,** 21-27.

Appleby P.G., Richardson N., & Nolan P.J. (1992) Self-absorption corrections for well-type germanium detectors. *Nuclear Inststruments & Methods B*, 71: 228-233.

Bengtsson L., & Enell M. (1986) Chemical analysis. In, Handbook of Holocene Palaeoecology and Palaeohydrology, The Blackburn Press, U.S.A.

Baskaran M., Nix J., Kuyper C., & Karunakara N. (2014) Problems with the dating of sediment core using excess ^{210}Pb in a freshwater system impacted by large scale watershed changes. *Journal of Environmental Radioactivity*, **138,** 355-363.

Binford M.W., Kahl J.S., & Norton S.A. (1993) Interpretation of ^{210}Pb profiles and verification of the CRS dating model in PIRLA project lake sediment cores. *Journal of Paleolimnology*, **9**, 275-296.

Birks H.H., & Briks H.J.B. (2006) Multi-proxy studies in palaeolimnology. *Vegetation History and Archaeobotony* **15,** 235-251

Chen F., Liu J., Xu Q., Li Y., Chen J., Wei H., Liu Q., Wang Z., Cao X., & Zhang S. (2013) Environmental magnetic studies of sediment cores from Gonghai Lake: implications for monsoon evolution in North China during the late Glacial and Holocene. *Journal of Paleolimnology*, **49,** 447-464.

Dong X., Sayer C.D., Bennion H., Maberly S.C., Yang H., & Battarbee R.W. (2016) Identifying sediment discontinuities and solving dating puzzles using monitoring and palaeolimnological records. *Frontiers in Earth Science*, DOI 10.1007/s11707-016-0578-z.

Eriksson M. G. & Sandgren P. (1999) Mineral magnetic analyses of sediment cores recording recent soil erosion history in central Tanzania. *Palaeogeography. Palaeoclimatology. Palaeoecology*. **152,** 365–383.

Faure G., & Mensing T.M. (2005) Isotopes: Principles and Applications, 3rd Edition. John Wiley and Sons, Inc., United States of America.

Gell P., Tibby J., Little F., Baldwin D., & Hancock G. (2007) The impact of regulation and salinization on floodplain lakes: the lower River Murray, Australia. *Hydrobiologia* **591,** 135-146.

Guo W., Huo S., & Ding W. (2015) Historical record of human impact in a lake in northern China: Magnetic susceptibility, nutrients, heavy metals, and OCPs. *Ecological Indicators* **57,** 74-81.

Heiri O., Lotter A.F., & Lemcke G. (2001) Loss on ignition as a method for estimating organic and carbonate content in sediments: reproducibility and comparability of results. *Journal of Paleolimnology*, **25,** 101-110.

Macreadie P.I., Allen K., Kelaher B.P., Ralph P.J., & Skilbeck C.G. (2012) Paleoreconstruction of estuarine sediments reveal human-induced weakening of coastal carbon sinks. *Global Change Biology* **18,** 891-901.

Marshall J.D., Jones R.T., Crowley S.F., Oldfield F., Nash S., & Bedford A. (2002) A high resolution Late-Glacial isotopic record from Hawes Water, Northwest England climatic oscillations: calibration and comparison of palaeotemperature proxies. *Palaeogeography, Palaeoclimatology, and Palaeoecology*, **18**, 25-40.

Michelutti N., Blais J.M., Liu H., Keatley B.E., Douglas M.S.V., Mallory M.L., & Smol J.P. (2008) A test of the possible influence of seabird activity on the 210Pb flux in High Arctic ponds at Cape Vera, Devon Island, Nunavut: implications for radiochronology. *Journal of Paleolimnology*, **40,** 783-791.

Oldfield F. (2013) Mud and magnetism: records of late Pleistocene and Holocene environmental change recorded by magnetic measurements. *Journal of Paleolimnology*, **49,** 465-480.

Peros M.C., & Gajewski K. (2008) Holocene climate and vegetation change on Victoria Island, western Canadian Arctic. *Quaternary Science Reviews*, **27,** 235-249.

Pisarsky B.I., Hardina A.M., & Naganawa H. (2005) Ecosystem evolution of Lake Gusinoe (Transbaikal Region, Russia). *Limnology*, **6,** 173-182.

Potasznik A., & Szymczyk S. (2015) Magnesium and calcium concentrations in the surface water and bottom deposits f a river-lake system. *Journal of Elementology* **20,** 677-692.

Sandgren P., & Snowball I. (2001) Application of mineral magnetic techniques to paleolimnology. In, Tracking Environmental Change Using Lake Sediments Volume 2: Physical and Geochemical Methods, Kluwer Academic Publishers, The Netherlands.

Snowball I.F. (1993) Geochemical control of magnetite dissolution in sub-arctic lake sediments and the implications for environmental magnetism. *Journal of Quaternary Science*, **8**, 339-346.

Talling S.J. (1976) The depletion of carbon dioxide from lake water by phytoplankton. *Journal of Ecology* **64,** 79-121.

Thompson R., Battarbee R.W., O'Sullivan P.E., & Oldfield F. (1975) Magnetic susceptibility of lake sediments. *Limnology and Oceanography*, **20,** 687-698.

Wolfe A.P., Miller G.H., Olsen C.A., Forman S.L., Doran P.T., & Holmgren S.U. 2004: Geochronology of high latitude lake sediments. In R. Pienitz, M.S.V. Douglas, J.P. Smol (eds.), *Long-term environmental change in Arctic and Antarctic lakes*. Springer, The Netherlands, pp. 19-52.

Chapter 5: Contaminant and geochemical sedimentary records of environmental change in the Selenga River Basin

5.1 Introduction to contaminants in the Selenga River basin

Historical and contemporary inorganic and organic contamination of aquatic ecosystems is a global concern, with population growth and economic development since the 19th century resulting in increasing industrialization and extent of anthropogenic activities, all of which have the potential to cause ecological damage. Further, anthropogenic development and rapid industrialization in the second half of the 20th century, occurred in many countries around the world (Steffen *et al.*, 2015). Persistent organic pollutants (POPs), including polycyclic aromatic hydrocarbons (PAHs) and halogenated organochlorines (HOCs), are characterized by their toxicity, persistence in the environment, and tendency to bioaccumulate and biomagnify in the food web due to an affinity for organic mtter. Due to these tendencies, POPs tend to accumulate in the environment and in ecological communities (Wania and Mackay, 1996; Kanzari *et al*., 2014; Lorgeoux *et al.,* 2016). HOCs are anthropogenically produced, and their production and use includes pesticides and in industrial applications. PAHs have both natural and anthropogenic sources, and are produced from the incomplete combustion of fossil fuels, volcanic eruptions, and biomass burning. Sources of inorganic contaminants (e.g. trace metals) to aquatic ecosystems can be both natural and anthropogenic, and the transport of such contaminants can be influenced by natural processes as well as anthropogenic disturbances (Boyle, 2001). Influx of inorganic contaminants to aquatic ecosystems can lead to potentially toxic conditions (MacDonald *et al*., 2000). Inorganic and organic contaminants can be transported atmospherically or through fluvial processes, and may be locally sourced, or undergo long-range atmospheric transport prior to arrival at a destination (Wania, 2003).

The Selenga River flows approximately 950 km from the head waters in Mongolia before it reaches the Selenga Delta and Lake Baikal in southeast Siberia. The Selenga River basin contains many anthropogenic sources of pollutants, with the potential to deliver contaminants downstream to the Selenga Delta and Lake Baikal. The Selenga River basin is very rich in minerals, and has been heavily impacted by mining activities in both Mongolia and Siberia since the early-19th century (Robinson and Anisova, 2004). Mining of gold (Au), tungsten (W), and molybdenum (Mo) began prior to 1850 in southeast Siberia, and coal deposits in the region

have been exploited since the 19th century, beginning with the development of the Trans-Siberian Railroad (Robinson and Anisova, 2004). Mining activities in the Selenga River basin peaked during the mid-20th century, with expanded mining operations for coal, lithium (Li), Au, W, lead (Pb), zinc (Zn), Mo, and strontium (Sr) along tributaries of the Selenga River. Long-term monitoring averages (1998-2003) of dissolved and total trace metal concentrations in tributaries along the Selenga River indicate that the Tuul River (which flows directly into the Selenga River) is the most polluted river in Mongolia (Figure 5.1) (Thorslund *et al*., 2012). Mining activities since the 19th century in Mongolia and Siberia have led to the increased concentrations of trace metals in surface water, increased turbidity, decreased fish diversity and bird populations around mines (Robinson and Anisova, 2004; Thorslund *et al*., 2012).

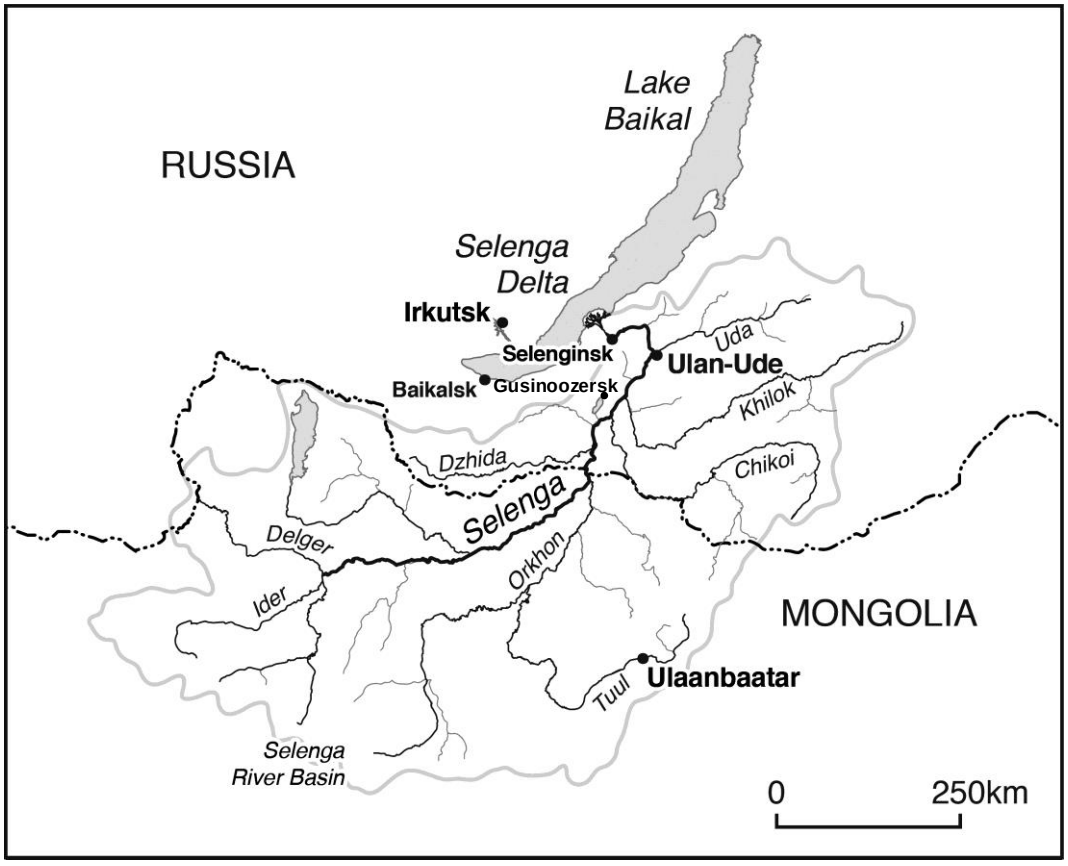

Figure 5.1. Map of the Selenga River basin (grey line delineated) and major rivers flowing into the Selenga River in Mongolia and Siberia. Major cities within the Selenga River basin are labelled. Dashed line denotes boundary between Mongolia and Russia.

Increasing industrialization and development in the Selenga River basin post-World War II (WWII) has contributed to increased mining and potential for increased inorganic contaminant release and transport to riverine systems. Population increases in settlements, including Irkutsk

(the largest city in the region, that sits on Angara outlow), Ulan-Ude, and Gusinoozersk (both in the Selenga basin) (Figure 5.1), led to the need for increased transportation development, and increased international railroad development continued into the 1950s (Pisarsky *et al*., 2005). Increases in population in the 1950s in the Gusinoye region of the Selenga River basin led to the construction of the Gusinoozersk State Regional Power Plant (SRPP) in the 1960s, a coal power plant on the shores of Lake Gusinoye which began operations in 1976 (Pisarsky *et al.,* 2005). The need for brown-coal as fuel for the power plant resulted in increased coal mining operations in the area and workings from the open-pit coal mine encroached within 200m of the lake (Pisarsky *et al*., 2005). Developments in the mid-20th century near Gusinoozersk led to tailings from the coal mine entering the Selenga River via the only outflow from Lake Gusinoye, a small tributary of the Selenga River (Pisarsky *et al*., 2005).

Agricultural and industrial expansion and intensification in the Selenga River basin post-WWII are potential sources of organic contaminants. Agricultural application of organic contaminants, such as dichlorodiphenyltrichloroethane (DDT), were used as a pest control in Russia until the early-1990s (Iwata *et al.,* 1995). High concentrations of DDT in both surface water and air samples in the 1990s indicated usage of DDT in the Selenga River basin up until that point, and both atmospheric and riverine sources as modes of contaminant delivery through the Selenga River basin and to Lake Baikal (Iwata *et al.,* 1995). Industrialization of many towns and cities through the 19th and 20th centuries in southeast Siberia included the construction of factories in the towns of Irkutsk and Ulan-Ude, and pulp and paper mills in Selenginsk and Baikalsk (Figure 5.1). Industrial towns in the Selenga River basin (e.g. Selenginsk) recorded high atmospheric levels of organic contaminants of a potentially industrial source, including polychlorinated biphenyls (PCBs) and polycyclic aromatic hydrocarbons (PAHs), in the 1980s (Mamontov *et al*., 2000; Imaeda *et al.,* 2009; Ok *et al.,* 2013). High surface water concentrations of PCBs, coupled with very low air concentrations, indicated primary delivery of contaminants to Lake Baikal through rivers and tributaries (Iwata *et al.,* 1995). Further, the dominance of high-weight PCB congeners, and regionally high surface water PCB concentrations in the Selenga Delta and southern Lake Baikal indicate likely sources of PCBs within the river basin, from local industrial centres, rather than long-range transport (Iwata *et al.,* 1995). Production of PCBs and usage of most organic contaminants (e.g. DDT) halted in southern Siberia (and all of Russia)

between 1990 and 1993 (AMAP, 2000), however no facilities exist for the removal of PCB stockpiles in Russia, therefore the potential exists for increased mobilization of deposited contaminants in the future (Tsydenova *et al*., 2004; Ma *et al.,* 2011).

Local and regional contamination has historically been considered the greatest threat to the Lake Baikal ecosystem. The higher rates and earlier onset of industrialization in the southern Lake Baikal region compared with the northern Lake Baikal region have been implicated in most of the more heavily contaminated sediment records from the South Basin of Lake Baikal in previous studies. For example, higher concentrations (1-2 orders of magnitude) of PCBs have consistently been observed in the southern Baikal basin relative to the northern basin (Kucklick *et al.,* 1996; Mamontov *et al.,* 2001). Fly-ash particles produced only through high temperature fossil-fuel combustion, spheroidal carbonaceous particles (SCPs), have indicated earlier onset and higher rates of contamination in the southern Lake Baikal basin than the north, and Rose *et al*. (1998) attributed mid-20th century increases in SCP concentration profiles in the southern basin of Lake Baikal to increasing industrialization in the Irkutsk region beginning in the 1940s. Further, sites closest to Irkutsk had the highest concentrations of SCPs, while sites in the central basin, those furthest removed from industry, had the lowest concentrations. Moreover, Rose *et al*. (1998) found the highest concentrations of SCPs in the northern basin at the northern most site, an indication that much of the atmospheric deposition to the northern basin of Lake Baikal was from industry to the north of the lake.

Analysis of lake sediments for inorganic and organic contaminant concentrations provide data on geochemical properties of the sediments, and may impart valuable information regarding timing, sources, and impacts to the lake ecosystem stemming from development in the river basin and changing sources of contamination (Boyle *et al*., 2004). Sediment records from Selenga River basin lakes can provide a record of contamination of Selenga River basin sources, and the potential such sources have for impacting the Selenga River and downstream ecosystems, including the Selenga Delta and Lake Baikal. Therefore, the primary aim of this chapter is to assess the history of anthropogenic contamination at shallow lakes within the Selenga River basin. Assessment of the impact from local vs. regional vs. long-range transport of contaminants will be discussed, along with spatial variations in contaminant records from two

regions of the Selenga River basin. Moreover, potential for continued contamination into the 21st century will be assessed. The aims will be addressed through the following objectives:

1) Three sediment cores will be analyzed from lakes within the Selenga River basin, two from the Selenga River Delta and one from the more heavily industrialized Gusinoye region;

2) Sediment cores will be analyzed for inorganic contaminants (trace metals and other trace elements) as evidence for mining and industrial impacts, and organic contaminants (including PAHs and halogenated organic contaminants), as evidence for agricultural and industrial impacts;

3) Pollutant profiles derived from radiometrically-dated lake sediment cores will then be compared with records of development and industrialization in the Selenga River basin and southeast Siberia since the 19th century.

5.2 Methods

Details of coring method, sediment core extruding, and sediment core partitioning for analyses are described in Section 4.2. Details of sediment core dating are given in Section 4.4.

5.2.1 Trace metals and major elements

Sediment was analyzed for trace and major element concentrations from sediment cores SLNG04-C, SLNG05-C, and BRYT02-C (See 4.2.2). Wet sediment was subsampled for analysis at 1.0-cm intervals, freeze-dried in Thermo Modulyo D and Edwards Modulyo freeze-driers and prepared for X-ray fluorescence (XRF) analysis following methods described in Section 3.2.2. Samples were analyzed for trace and major elements using a Spectro X-Lab 2000 energy dispersive X-ray fluorescence spectrometer (ED-XRF) with a Si(Li) semiconductor detector in the Department of Geography at University College London (UCL). See Section 3.2.2.1 for analytical methods, sample accuracy, and recovery rates for BRS SRM (Epstein *et al*., 1989). Trace and major element results are then produced in units of μg g^{-1} and %, respectively. Elemental ratios were calculated for Fe/Mn and Ca/Ti to provide inferences regarding redox conditions within lakes and evaporative concentrations and in-lake carbonate precipitation, respectively (Davies, 2015).

Radiometric dating (Section 4.3.2) was used to determine sediment accumulation rates (SAR) (g cm^{-2} yr^{-1}) which were then used to convert trace element and metal concentrations to

fluxes (µg cm^{-2} yr^{-1}). Concentrations of trace and major elements can be further utilized to determine pollution histories of lakes through the calculation of enrichment factors (Boës *et al.,* 2011). Enrichment factors were calculated by normalizing the concentration of an element or metal (M) to the conservative lithogenic element Ti, within the sample, to the background ratio within the core. An enrichment factor of 1 throughout the record is equivalent to background concentrations, values above 1 indicate enrichment, while enrichment factors greater than 3 indicate definite anthropogenic contamination of the metal (Boës *et al.,* 2011). Enrichment factors (EFs) for SLNG04-C, SLNG05-C, and BRYT02-C were calculated, using the following equation from Weiss *et al.* (1999):

$$EFs = (M_{sample}/Ti_{sample}) / (M_{background}/Ti_{background}) \quad [EQN1]$$

Background was taken as the oldest sample of the sediment core, as this was assumed to be the most minimally impacted. To explore temporal trends in the trace and major element data, unconstrained ordinations (Principal components analysis (PCA)) were conducted on the centred and standardized concentration datasets using Canoco5 (ter Braak and Šmilauer, 2014). All stratigraphical plots were constructed using C2 (Juggins, 2014).

5.2.2 Mercury sediment analysis

Sediment was analyzed for mercury content from one sediment core: SLNG04-C at a minimum temporal resolution of approximately 15 years. Approximately 0.2 g of freeze-dried, finely powdered sediment was weighed into Teflon tubes. All weights were recorded to 4 decimal places. Dried samples were digested with 8 ml of aqua regia (2 ml concentrated HNO_3 and 6 ml concentrated HCl), and heated to 100°C on a hotplate for 2 hours. Following digestion, samples were diluted to 50 ml with deionized water, capped and mixed. Digested solutions were then analyzed for mercury using cold vapour-atomic fluorescence spectrometry (CV-AFS), following reduction with $SnCl_2$. Standard reference stream sediment (GBW07305; certified mercury (Hg) value of 100 ± 10.0 ng g^{-1}, SLNG04 measured standard mean value was 103 ng g^{-1}; reference standard deviation = 3.2 ng g^{-1}; N = 3) and a sample blank (deionized water) were digested with every 30 samples, and measured in every 10 samples, to assess the accuracy of the analytical method. Mercury fluxes and EFs were calculated as for other metals (See EQN 1).

5.2.3 Persistent organic pollutants (POPs)

Sediment was analyzed for persistent organic pollutants (POPs) from sediment cores SLNG04-B, and BRYT02-B (See 4.2.2). Sediment samples were stored at -20°C, in hexane-cleaned foil packets prior to analysis. Analysis of POPs was undertaken at the Marine Studies Centre at the Federal University of Paraná, Brazil. Nineteen major polycyclic aromatic hydrocarbons (PAHs) were analysed, including eight low molecular weight (LMW) PAHs (naphthalene, biphenyl, anthracene, anaphthylene, acenaphthene, fluorene, dibenzothiophene, and phenanthrene), and 11 high molecular weight (HMW) PAHs (fluoranthene, pyrene, benzo(a)anthracene, chrysene, benzo(b)fluoranthene, benzo(j+k)fluoranthene, benzo(e)pyrene, benzo(a)pyrene, indeno [1,2,3-c,d]pyrene, dibenzo(a,h)anthracene, and benzo(g,h,i)perylene), as well as six alkyl PAHs (C_1 and C_2- methylnaphthalenes, C_2- and C_3-naphthalenes, and C_1- and C_2-phenanthrenes), and two biogenic/diagenetic PAHs (perylene and retene). Total PAH concentration included all LMW, HMW and alkyl PAHs. All LMW and HMW PAHs are considered amongst the 16 US EPA priority PAHs, with the exception of biphenyl, dibenzothiophene, and benzo(e)pyrene.

Samples were also analysed for halogenated organic contaminants (HOCs). A total of 50 PCB congeners were investigated, as well as several types of organochlorinated pesticides, including DDT (o,p'- DDT, p,p'-DDT) and its toxic and persistent degradation products (o,p'-DDE, p,p'-DDE, o,p'- DDD, p,p'- DDD), several congeners of hexachlorocyclohexanes (HCHs) (α-HCH, β-HCH, γ-HCH, δ-HCH), two congeners of chlordane (α-chlordane and γ-chlordane), and four PBDEs (PBDE 28, 47, 99, and 100). Aldrin, and dieldrin were also detected in sediment samples. Total concentrations for major HOC types were calculated, and are reported as the summative concentrations of 1) 50 PCB congeners (∑PCBs), 2) DDT plus degradation products (∑DDT), 3) HCH congeners (∑HCH), 4) chlordane congeners (∑chlordane), 5) four PBDEs (∑PBDEs), and 6) Dieldrin.

5.2.3.1 Sample extraction and instrumental analysis

The analytical procedure for organic contaminants analysis is based on United Nations Environmental Programme (UNEP, 1992) with minor modifications (Bícego *et al.,* 2006). Freeze-dried sediments (10.000 g to 15.000 g) were individually extracted in a Soxhlet apparatus for 8 hours with 80 ml of a 50% mixture of *n*-hexane in dichloromethane (DCM) (1:1,

v/v). A surrogate standards mixture of five deuterated PAHs (naphthalene-d_8, acenaphthene-d_{10}, phenanthrene-d_{10}, chrysene-d_{12}, and perylene-d_{12}) and two polychlorinated biphenyls (PCB-103 and PCB-198) was added in each blank or sample extraction flask to evaluate the analytical method and to quantify the organic contaminants. The resulting extract was concentrated to 4 ml in a rotary vacuum evaporator and divided into two portions of 2 ml. The extracts were purified and fractionated by liquid chromatography on a 30 cm x 1 cm i.d. glass column. The first portion was cleaned using 3.2 g of 5% deactivated alumina column. HOC elution was performed with 20 ml of a DCM/n-hexane (3:7, v/v) mixture and the eluate concentrated to 0.5 ml under a gentle gas stream of purified nitrogen. TCMX (tetrachloro-m-xylene) was added as internal standard prior to the gas chromatograph analysis. The second portion was fractioned and cleaned with 5% deactivated alumina (1.8 g) and silica (3.2 g). The hydrocarbons were removed by eluting 10 ml of *n*-hexane through the column, followed by the addition of 15 ml of a 30% mixture of DCM in *n*-hexane. The second fraction, containing the PAHs, was concentrated to 0.5 ml in a rotary vacuum evaporator. An internal standard (benzo[b]fluoranthrene-d_{12}) was added prior to the gas chromatograph analysis.

The identification and quantification of the organic contaminants were performed by analyzing 2 μl of the final extracts in a gas chromatograph (Agilent 7890A GC) coupled to a mass spectrometer (Agilent 5975C inert MSD with Triple-Axis Detector). A capillary column of fused silica coated with 5% diphenyl-dimethyl siloxane (30 m length, 0.25 mm internal diameter and 0.25 μm thick film) was used. Helium was used as the carrier gas. For PAHs, the oven temperature was programmed to heat from 40° C to 60° C at 20° C min^{-1}, then to 250°C at 5°C min^{-1}, and finally to 300°C at 6°C min^{-1} where it remained constant for 20 min. For the HOCs, heating was from 75° C to 150° C at 15° C min^{-1}, then to 260°C at 2°C min^{-1}, and finally to 300°C at 20°C min^{-1} where it remained constant for 10 min. The injector was conditioned at 280°C, the interface with the detector at 300°C and the ion source at 230°C.

The data were acquired in the SIM (Selected Ion Monitoring) mode. The HOCs were identified by matching the retention times and the mass/charge of ion fragments with those obtained from a mixture of external standards (Z-014G-FL – PAHs, C-WNN and C-WCFS – PCBs, AE-00010 – Pesticides, and Individual BDEs, all of them from AccuStandard, New Haven, CT, USA). The calibration curve for PAH quantification ranged from 0.10 to 2.00 ng μl^{-1}.

For the quantification of HOCs, calibration curves were prepared at different concentrations: 1, 5, 10, 20, 80, 100, 150, and 200 pg μ^{-1}. The individual organic compounds concentrations were based on the integration of the main fragment peak area for each compound using the HP Chemstation program.

5.2.3.2 Analytical control

The quality assurance procedures included analyses of procedural blanks, matrix spikes, surrogate standards recoveries and use of certified reference material (IAEA-408; IAEA-417) from the Marine Environment Laboratory of the International Atomic Energy Agency (IAEA, Vienna, Austria) (Wade and Cantillo, 1994). See Table 5.1 for all recovery rates, precision and detection limits (LD). Procedural blanks were performed for each extraction series of 10 samples. In general, the organic contaminants concentrations in the blanks were sufficiently low (< three times the detection limit). The LD was calculated based on the lowest sensitive concentration multiplied by the final extracted volume, and divided by the weight of sediment before extraction.

	Surrogate recovery rates (deuterated compounds)	**Mean standard recoveries (spiked sediment)**	**Certified reference material recoveries**	**Accuracy**	**Detection limits**
PAHs	49-89%	84% ± 8.6%	85-110%	<10%	<0.3 ng g^{-1}
PCBs	52-117%	84% ± 19%	90-110%	NA	NA
HOCs	----	91% ± 14%	75-105%	<10%	<0.01 ng g^{-1}

Table 5.1. Recovery rates, accuracy between replicates, and detection limits (LD) for PAH, PCB, and HOC compounds.

5.2.3.3 Data analysis

Ratios were calculated between several of the PAH compounds with the intent of assessing shifts in potential PAH sources, and are explained in Table 5.2. (Martins *et al.,* 2011). Fluxes of PAHs and HOCs were calculated using the sediment accumulation rate (SAR) of the radiometrically dated core. PAH and HOC concentrations were normalized to organic matter (OM) as determined through loss-on-ignition at 550°C (LOI_{550}), to understand if and how changes in organic matter influence changes in POPs concentrations:

$$Normalized\ POP_{sample} = (POP_{sample}/LOI550_{sample}) \qquad [EQN2]$$

All stratigraphical plots were constructed using C2 (Juggins, 2014).

Ratio	PAHs	Interpretation	Threshold ratio values
Ant/178	Anthracene / Phenanthrene + Anthracene	Petroleum vs. combustion source	Petroleum < 0.1; Combustion > 0.1
Fl/Fl+Py	Fluoranthrene / Fluoranthrene + Pyrene	Petroleum combustion vs. biomass burning and coal combustion	Petroleum combustion < 0.5; Biomass and coal combustion > 0.5
Bza+228	Benzo(a)anthracene / Benzo(a)anthracene + crysene	Pure petroleum sources vs. combustion	Petroleum < 0.2; Mixed sources > 0.2 < 0.35; Combustion > 0.35
Ip/Ip+Bghi	Indeno(1,2,3-c,d)pyrene / Indeno(1,2,3-c,d)pyrene + benzo(g,h,i)pyrilene	Pure petroleum vs. petroleum combustion vs. coal combustion and biomass burning	Petroleum < 0.4; > 0.4 < 0.5 Petroleum combustion; > 0.5 Coal combustion
C0-P/C0-C1-P	Phenanthrene / Phenanthrene + C1-Phenanthrene	Biomass burning and coal combustion	Biomass and coal combustion > 0.5

Table 5.2. PAH ratios explained, including threshold ratio values and interpretations for ratio values indicated.

5.2.4 Spheroidal carbonaceous particles

Sediment was analyzed for spheroidal carbonaceous particle (SCP) concentrations in sediment cores SLNG04-C, SLNG05-C, and BRYT02-C (See 4.2.2). Approximately 0.15 g of freeze-dried sediment from each 3.0 cm interval sub-sample was weighed into a 12-ml polypropylene tube. Approximately 0.15 g of standard reference sediment was also weighed into a 12-ml polypropylene tube and analyzed concurrently to the samples (Rose, 2008). All weights were recorded to 4 decimal places. Samples then underwent a sequential attack of mineral acids to breakdown organic matter, carbonates, and silica components: concentrated HNO_3 (1.5 ml; overnight); concentrated HNO_3 (1.5 ml; 2 hours at 80°C), concentrated HF (3 ml; 3 hours at 80°C), 50% HCl (3 ml; 2 hours at 80°C). Following each acid stage, samples were topped up with distilled water and centrifuged at 1800 rpm for 5 minutes, after which the supernatant was pipetted off. Following the completion of all acid stages, the centrifuge and washing process was undertaken three times. Mean recovery rate for this method is 95.2%, with detection limits of 80-100 SCPs g^{-1} dry mass (Rose, 1994). Concurrently to the above processing of samples and standard, a sample blank was processed using only acids and distilled water.

A sub-sample of the resulting SCP residue was then transferred to a coverslip and allowed to evaporate. The dried coverslips were then mounted onto microscope slides using *Naphrax*. The SCP concentration is reported in units of number of particles per gram dry mass of sediment (gDM^{-1}). Two reference standards and two sample blanks were analyzed alongside the 63 SCP samples. All blanks resulted in 0 SCPs, and standard reference samples resulted in 6,294-6,499 ± 10% SCPs g^{-1} dry mass, within a single standard deviation of the mean concentration for the standard reference material, as determined by Rose (2008). SCP fluxes were calculated using sedimentation accumulation rates from each respective sediment core. All stratigraphical plots were constructed using C2 (Juggins, 2014).

5.2.5 Toxicity

Toxicity of selected trace elements (Cu, Ni, Pb, As, Zn) and POPs (∑PAHs, ∑PCBs, ∑DDT, ∑chlordanes, dieldrin) was determined for sediments according to MacDonald *et al.* (2000), using consensus-based threshold effect concentrations (TEC) and probability effect

concentrations (PEC). TECs are the concentrations of individual trace metals and POPs below which toxicity-related impacts in benthic organisms would not be expected. PECs are the concentrations of individual trace metals above which toxicity-related impacts in benthic organisms would be expected.

5.3 Results

5.3.1 SLNG04

5.3.1.1 Trace and major elements

Trace and major element concentrations from SLNG04 sediment core are shown in Figure 5.2. Most major element and trace metal concentrations and ratios were fairly steady through the early part of the record, until the mid-19th century. Ca concentrations and Ca/Ti ratios increased post-1920, reaching maximum values for the record between c. 1920 and c. 1960. Concurrent declines in Ni, Cu, Zn, Pb, and Mn concentrations, and increases in concentrations of As, P and Fe occurred between c.1920 and c. 1960. Minimum Fe/Mn ratios occurred c. 1920, followed by increasing ratios until c. 1990. Concentrations of trace metals Hg, Ni, Cu, Zn, and Pb increased gradually from the mid-20th century until 1990, and remained relatively constant to the surface (Figure 5.2).

Enrichment factor profiles for the selected trace metals are presented in Figure 5.3. Enrichment factors for Ni, Cu, Pb, Zn, Hg, and As remained above one through most of the temporal record, indicating enrichment above background levels since the early-19th century, with greater enrichment beginning in the mid- to late-19th century. Enrichment factors for all trace elements were above 1 at the surface. EFs for As, Hg, and Cu are above 2 during the record, indicting anthropogenic enrichment of these elements. By the early- to mid-20th century, As was enriched ~25x background levels, while Cu and Hg experienced sustained enrichment relative to background concentrations to present.

Flux profiles for selected trace element and metals are presented in Figure 5.4. Fluxes of most metals and elements followed a similar temporal trend as SAR, with the most prominent features being a singular peak in the early-1960s, and a sustained increase at c. 1990 (See 4.3.2.1). Exception was As, which did not exhibit an increase in flux when SAR increased in c. 1990. This would indicate, therefore, that total inputs of metals to the lake are controlled by sedimentation rate changes since the mid-1940s in SLNG04.

PCA indicated a total of 78.6% of total variation in trace metal and element data was explained across the first two PCA axes, with PCA axis 1 explaining almost 60% variation (Table 5.3). In the ordination, depths formed distinct groupings, with older samples plotting most negatively along PCA axis 1, depths from the middle of the record plotting across the origin of axis 1 and positively along axis 2, and recent depths plotting across the origin of axis 1 and negatively along axis 2 (Figure 5.5).

	Axis 1	***Axis 2***	***Axis 3***	***Axis 4***
Eigenvalues	0.5906	0.1955	0.0689	0.0602
Explained variation (cumulative)	59.1	78.6	85.5	91.5

Table 5.3. PCA eigenvalues for SLNG04 sediment core trace metals and lithogenic elements, with eigenvalues and cumulative explained variation for the first four PCA axes.

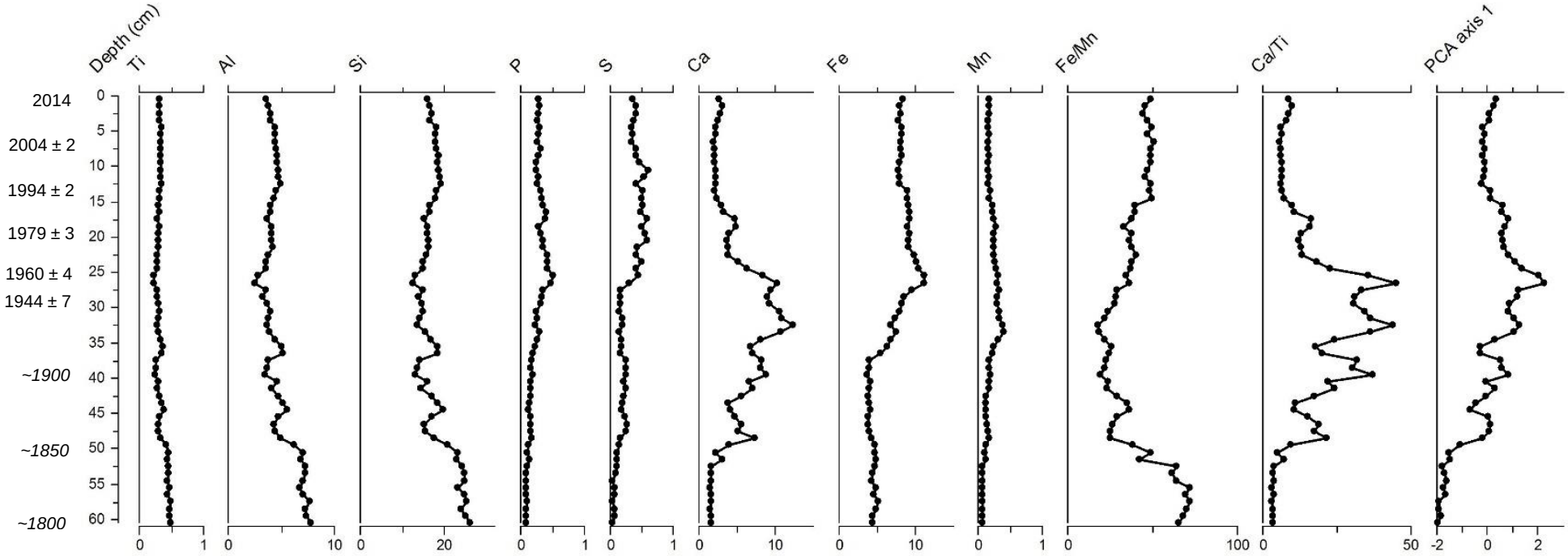

Figure 5.2a. Major lithogenic element contributions for SLNG04. Units of measurements from Ti to Mn are %. PCA axis 1 scores plotted. Radioisotope-derived dates and confidence limits are highlighted on the y-axis. Italicized dates are extrapolated beyond ^{210}Pb radioisotope dating.

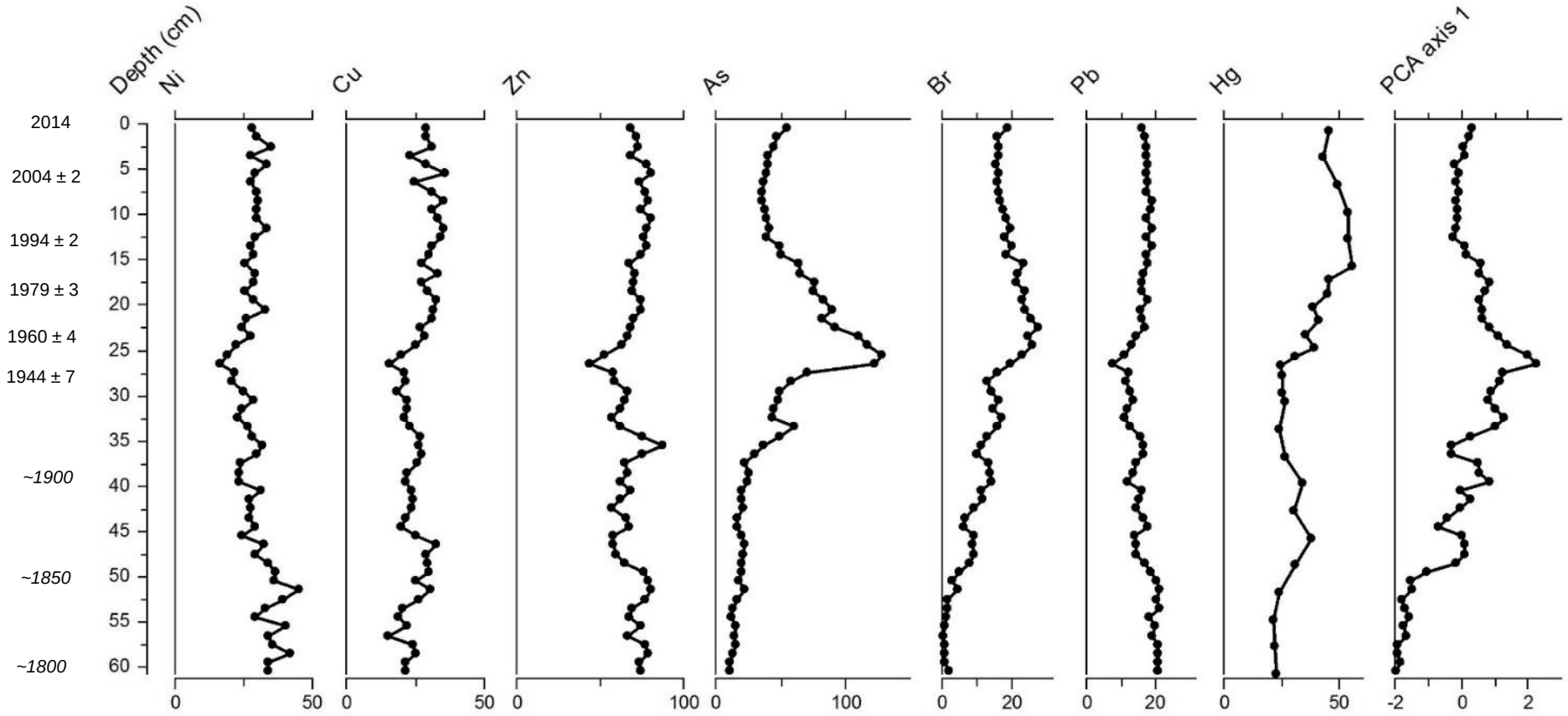

Figure 5.2b. Trace metal and element concentrations for SLNG04. Units of measurements from Ni to Pb are µg g^{-1}, and ng g^{-1} for Hg. PCA axis 1 scores plotted. Radioisotope-derived dates and confidence limits are highlighted on the y-axis. Italicized dates are extrapolated beyond ^{210}Pb radioisotope dating.

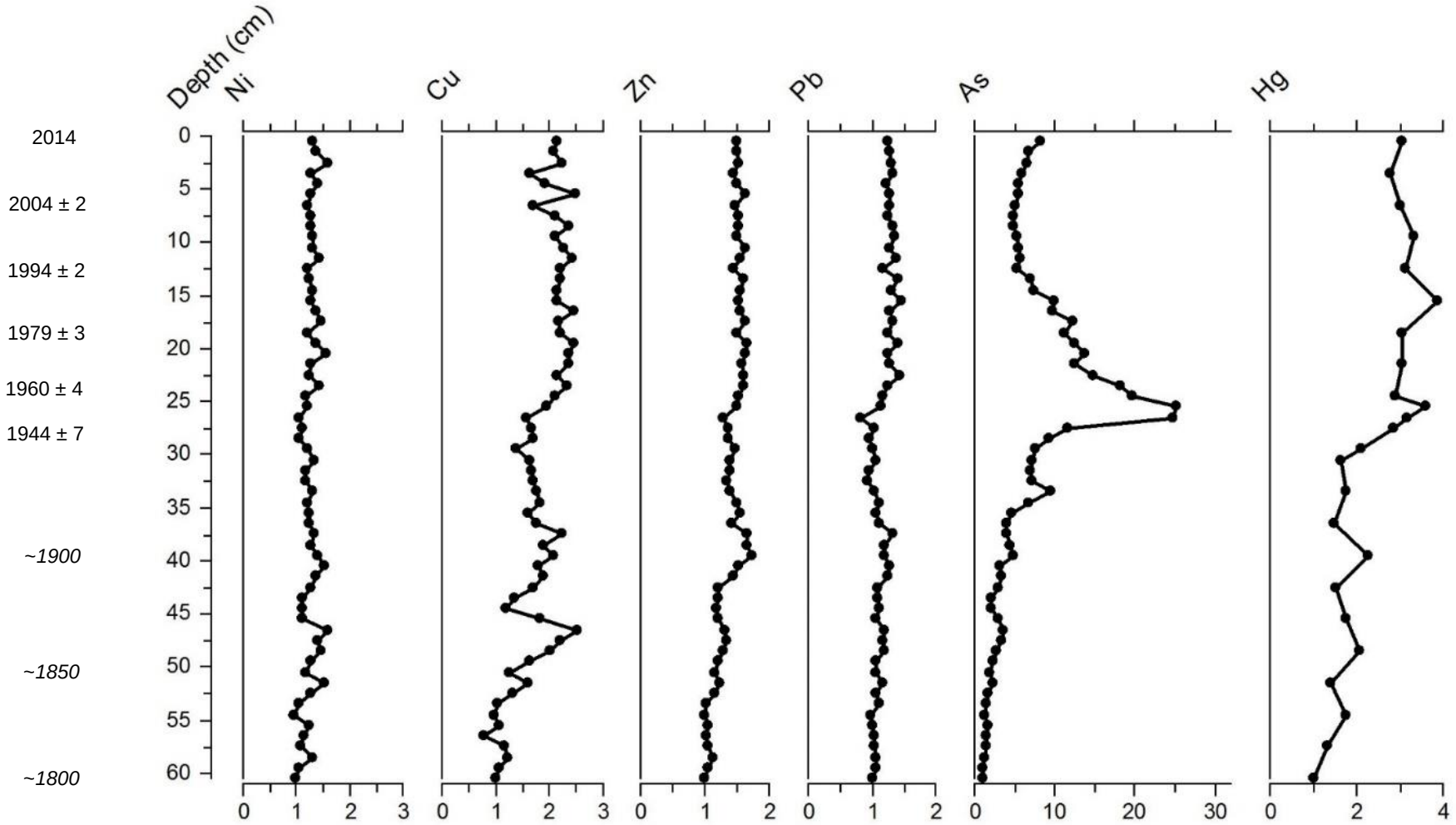

Figure 5.3. Enrichment factors for trace elements and metals for SLNG04. Radioisotope-derived dates and confidence limits are highlighted on the y-axis. Italicized dates are extrapolated beyond ^{210}Pb radioisotope dating.

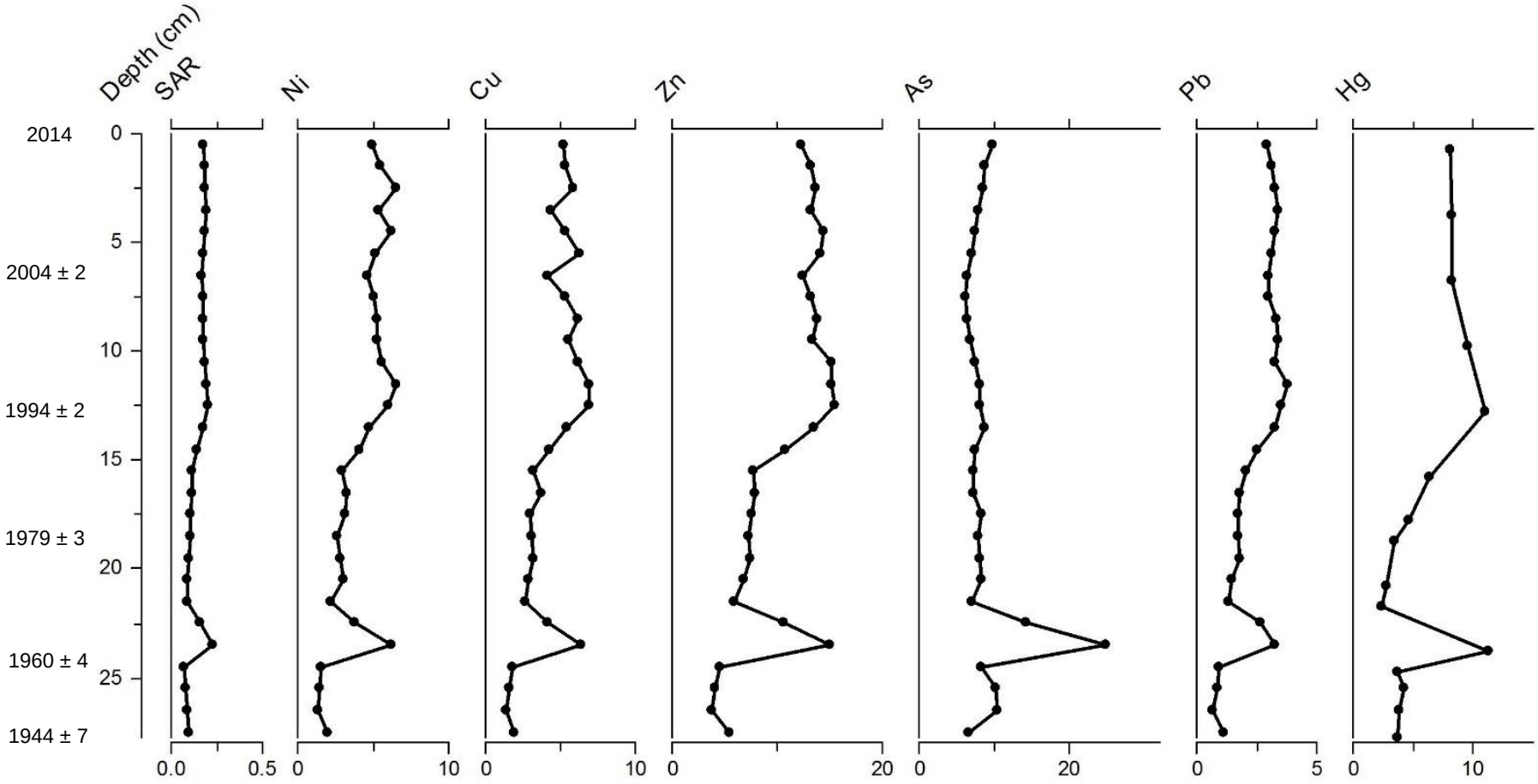

Figure 5.4. Sediment accumulation rate (SAR) and fluxes of trace metals and elements for SLNG04. Unit for SAR is g cm^{-2} yr^{-1}. Unit for elemental fluxes from Ni to Pb is µg cm^{-2} yr^{-1}. Unit for mercury flux is ng cm^{-2} yr^{-1}. Radioisotope-derived dates and confidence limits are highlighted on the y-axis. Italicized dates are extrapolated beyond ^{210}Pb radioisotope dating.

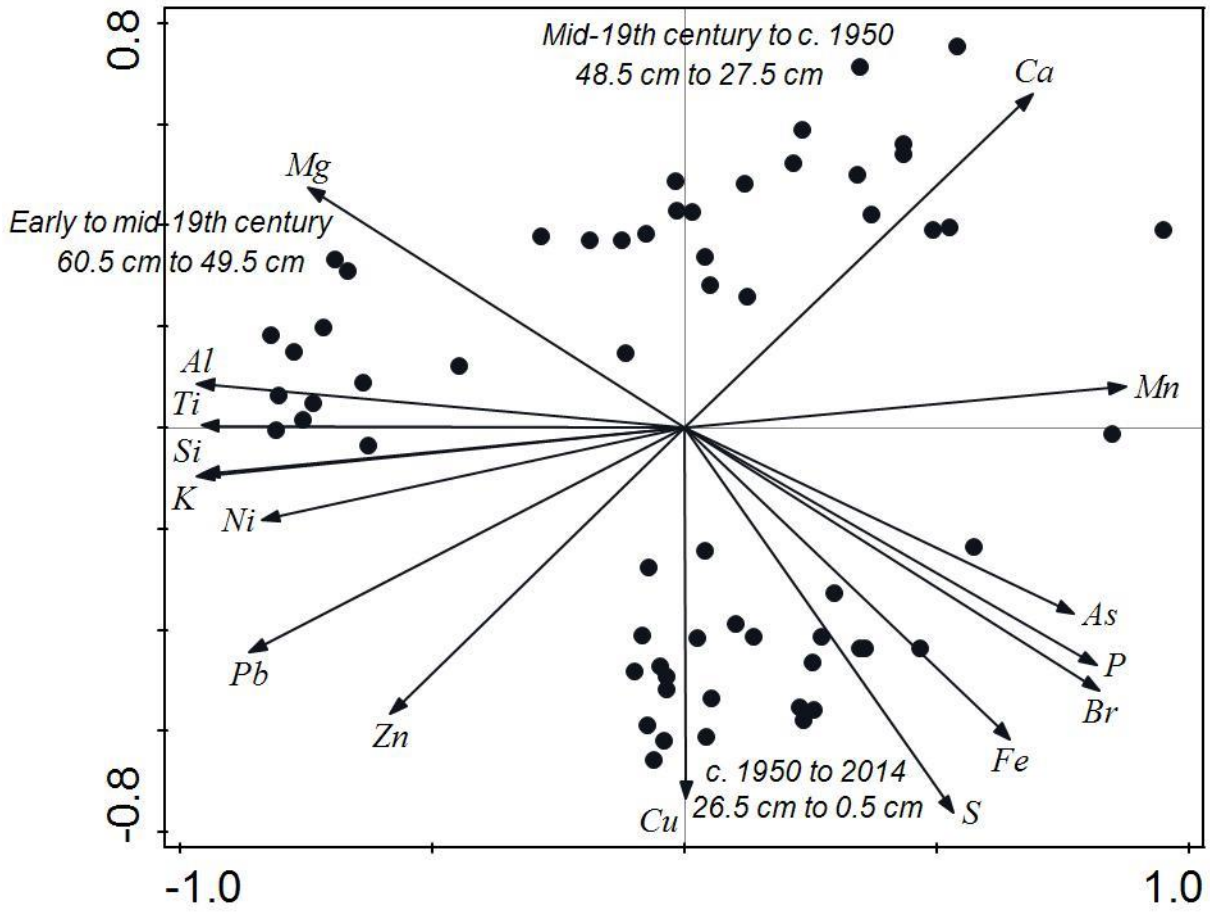

Figure 5.5. PCA biplot of trace elements and metals (vectors) with sample depths from the SLNG04 record. Groupings of depths, and corresponding ranges of years, are indicated.

5.3.1.2 Toxicity

Consensus-based threshold effect concentration (TEC) of nickel as determined by MacDonald et al. (2000) is 22.7 µg g^{-1} and is exceeded throughout most of the record from SLNG04, with the exception of between ~1945 and ~1965, while consensus-based TEC of copper is 31.6 µg g^{-1} and was exceeded periodically between the mid-1970s and ~2005 at SLNG04 (Figure 5.6). Consensus-based TEC of arsenic is 9.79 µg g^{-1}, and was exceeded in SLNG04 from the base of the sediment core until the late-19th century, at which time arsenic concentrations increased, to exceed the PEC of 33 µg g^{-1} between the late-19th century and 2014 (Figure 5.6). All other metals and organic pollutant concentrations fall below the TEC throughout the SLNG04 record.

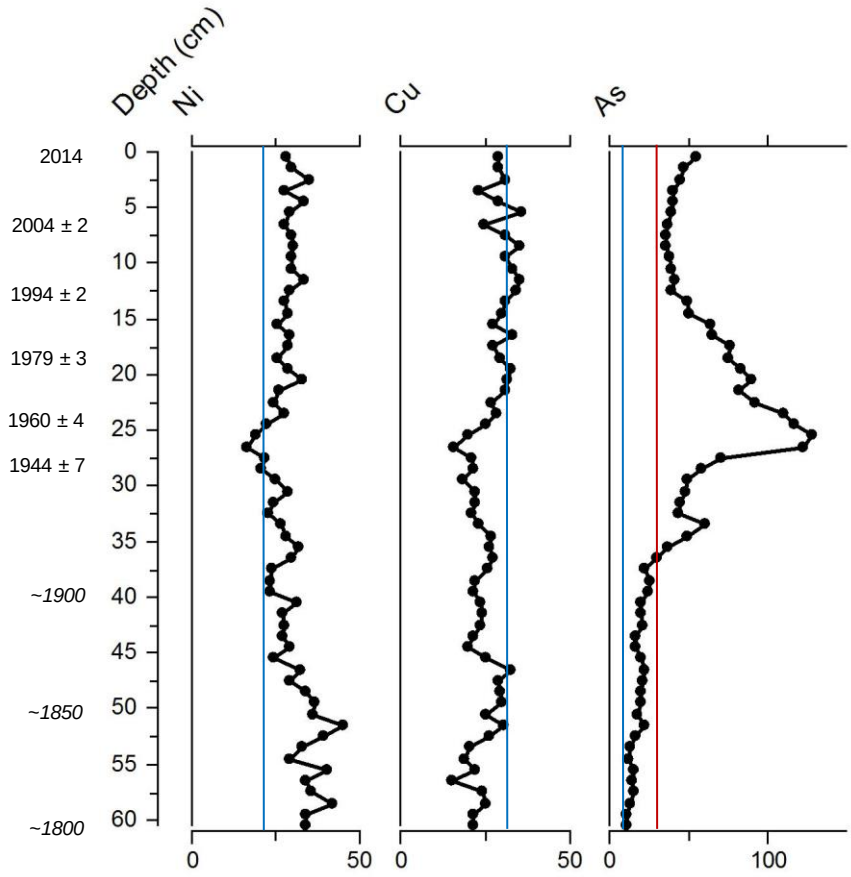

Figure 5.6. Toxicity graph of Ni, Cu, and As concentrations from the SLNG04 record. Concentrations are in units of µg g^{-1}. The vertical blue line indicates the threshold effect concentration, and the vertical red line indicates the probable effect concentration for that element.

5.3.1.3 PAHs

Concentrations of polycyclic aromatic hydrocarbons (PAHs) from SLNG04 are shown in Figure 5.7. Total concentrations of PAHs (∑PAH) are lowest at the base of the core at 1.78 ng g^{-1}, and peak just below the surface of the sediment core, at 188.3 ng g^{-1} (~2010 AD). The first observed increase in ∑PAHs was small, and occurred c. 1930, briefly reaching 67 ng g^{-1}. Following the brief increase in ∑PAHs, concentrations declined by 1935 AD to pre-1930 levels. The most pronounced shift in PAH concentrations occurred c. 1960, at which time ∑PAHs, ∑HMW PAHs, and ∑alkyl PAHs concentrations began to increase. Concentrations continued to increase through the mid- to late-20th century. ∑PAHs reached concentrations of approximately 100 ng g^{-1} by the mid-1970s, and continued to increase until the mid-1990s (Figure 5.7). Increases in ∑HMW PAH and ∑alkyl PAH concentrations occurred concurrently between the late-1950s and 1980s, peaking in the mid-1980s (Figure 5.7). The recent PAH record is

dominated by the LMW PAHs naphthalene and phenanthrene, which became more dominant as perylene declined in the late-1970s. The increased ∑PAH concentrations have been sustained through to the latter part of the 20th century.

LOI_{550}-normalized PAH concentration profiles from SLNG04 are shown in Figure 5.8. OM-normalization resulted in a sharp increase in most profiles in the early-19th century, when LOI_{550} was very low. Otherwise, normalizing PAH concentrations to organic matter (LOI_{550}) did not change the greater part of the concentration profiles for any compound, or groups of compounds. Flux profiles for the selected PAH compounds and sums from SLNG04 are presented in Figure 5.9. Selected PAH compounds and sums display increased fluxes corresponding with the increase in sediment accumulation rate (SAR) in the early-1960s (See 4.3.2.1). The flux of the ∑Alkyl PAHs displays a similar trend through time as SAR, while other PAH compounds and sums are dissimilar to SAR, with distinct increasing fluxes until the early-1990s, followed by declining fluxes to the surface, with the exception of increased flux of total PAHs and LMW PAHs c. 2010.

Biomass burning and coal combustion is determined through ratios Fl/Fl+Py for the entire record, in the 1960s by IP/IP+Bghi, and C0-P/C0-C1-P throughout the entire record (Figure 5.10). Petroleum combustion is also indicated through IP/IP+Bghi through most of the record, pre-1960s and post-1960s. BzA/228 is only calculated since the early-20th century, and indicates combustion as the dominant PAH source. Ant/178 is only measured from c. 1970 to the surface due to an absence of anthracene from the record prior to this time, and indicates a source of uncombusted petroleum products.

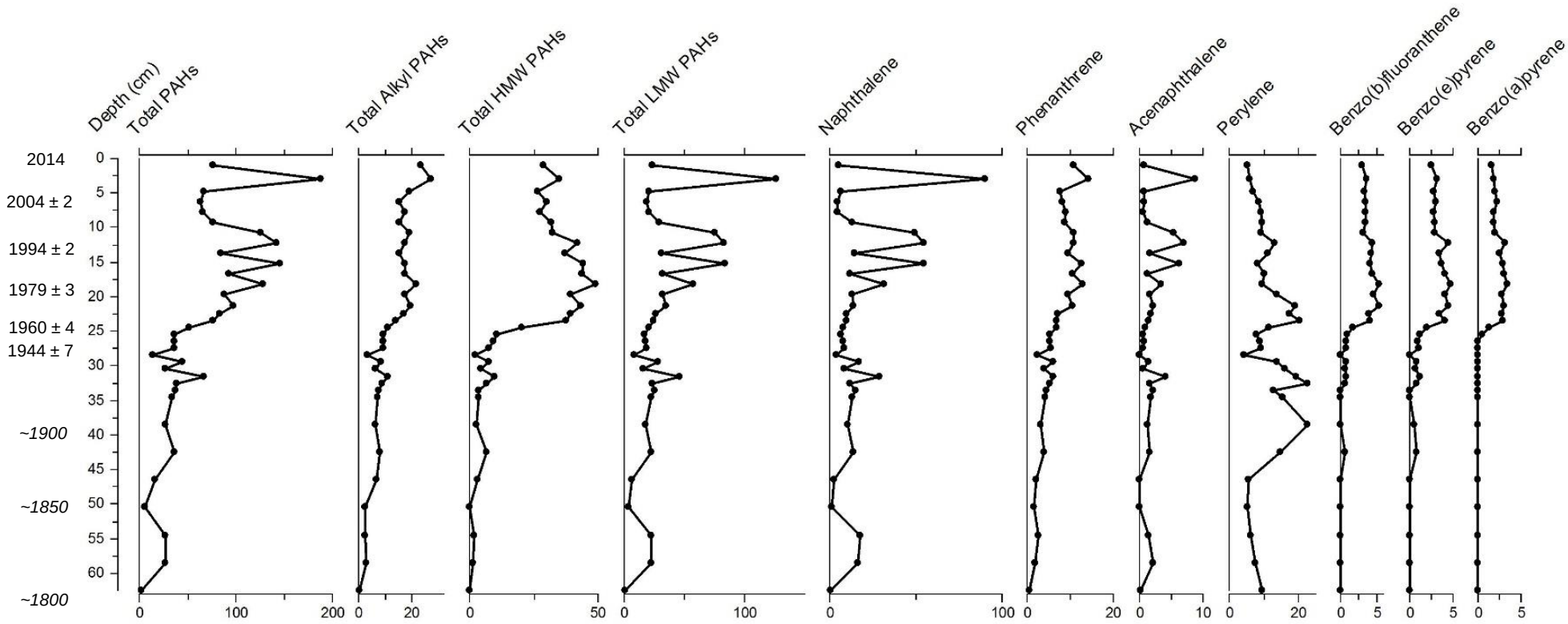

Figure 5.7. PAH concentrations and sums of PAH groups for SLNG04. Units of measurements are ng g^{-1}. Radioisotope-derived dates and confidence limits are highlighted on the y-axis. Italicized dates are extrapolated beyond ^{210}Pb radioisotope dating.

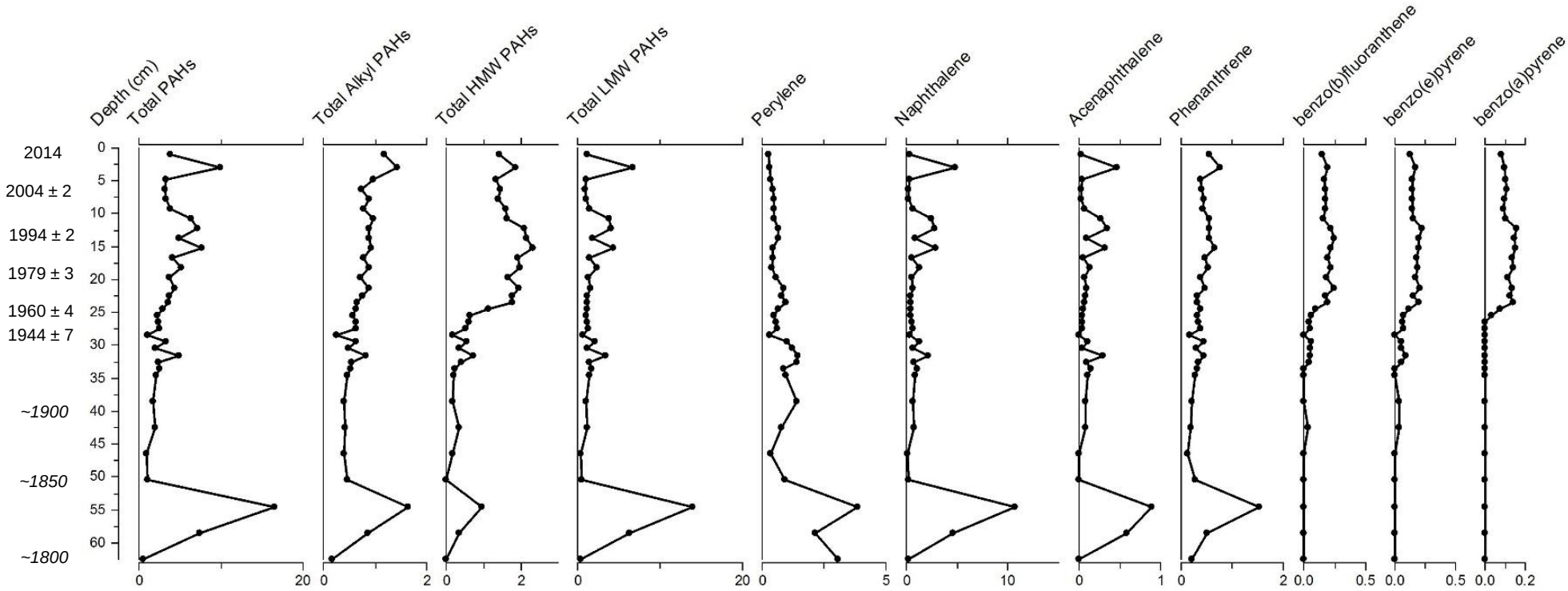

Figure 5.8. LOI_{550}-normalized PAH concentrations from the SLNG04 record. Units of measurements are ng g^{-1}. Radioisotope-derived dates and confidence limits are highlighted on the y-axis. Italicized dates are extrapolated beyond ^{210}Pb radioisotope dating.

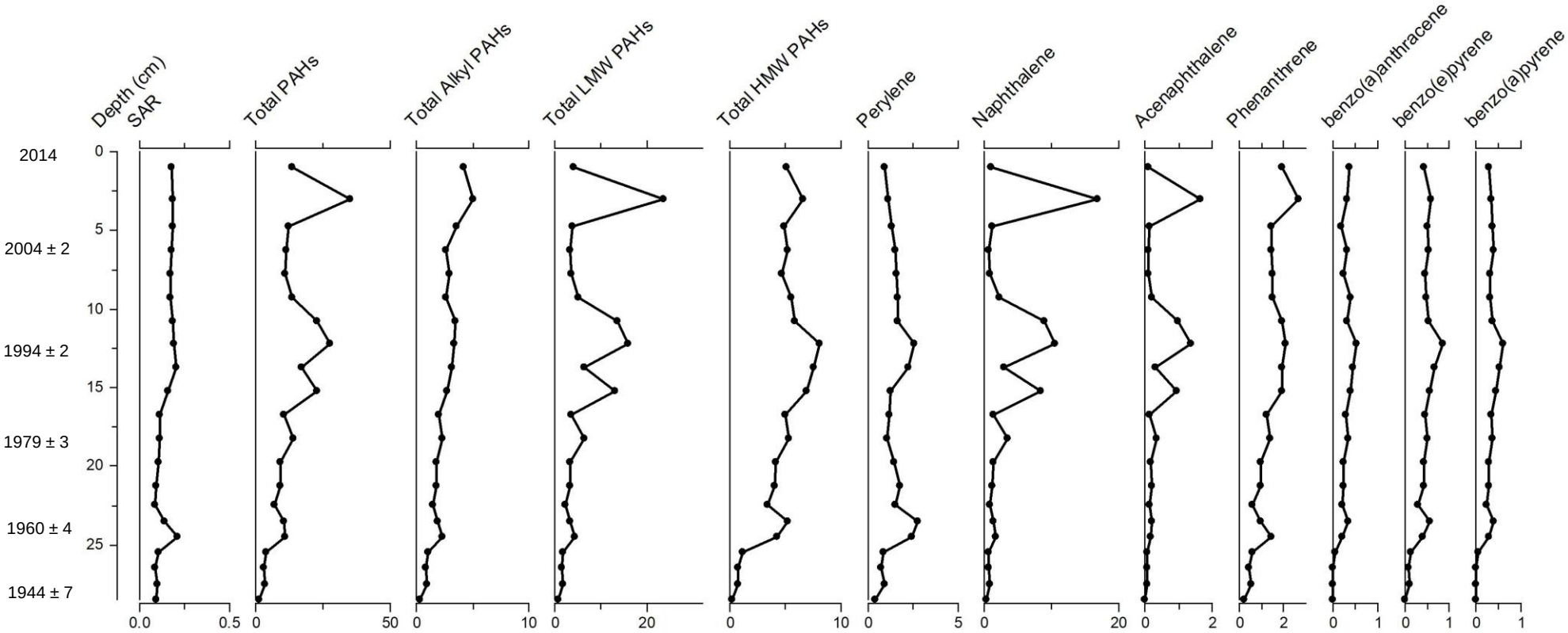

Figure 5.9. Sediment accumulation rate (SAR) and fluxes of PAHs for the SLNG04 record. Unit for SAR is g cm^{-2} yr^{-1}. Unit for PAH fluxes is ng cm^{-2} yr^{-1}. Radioisotope-derived dates and and confidence limits are highlighted on the y-axis. Italicized dates are extrapolated beyond ^{210}Pb radioisotope dating.

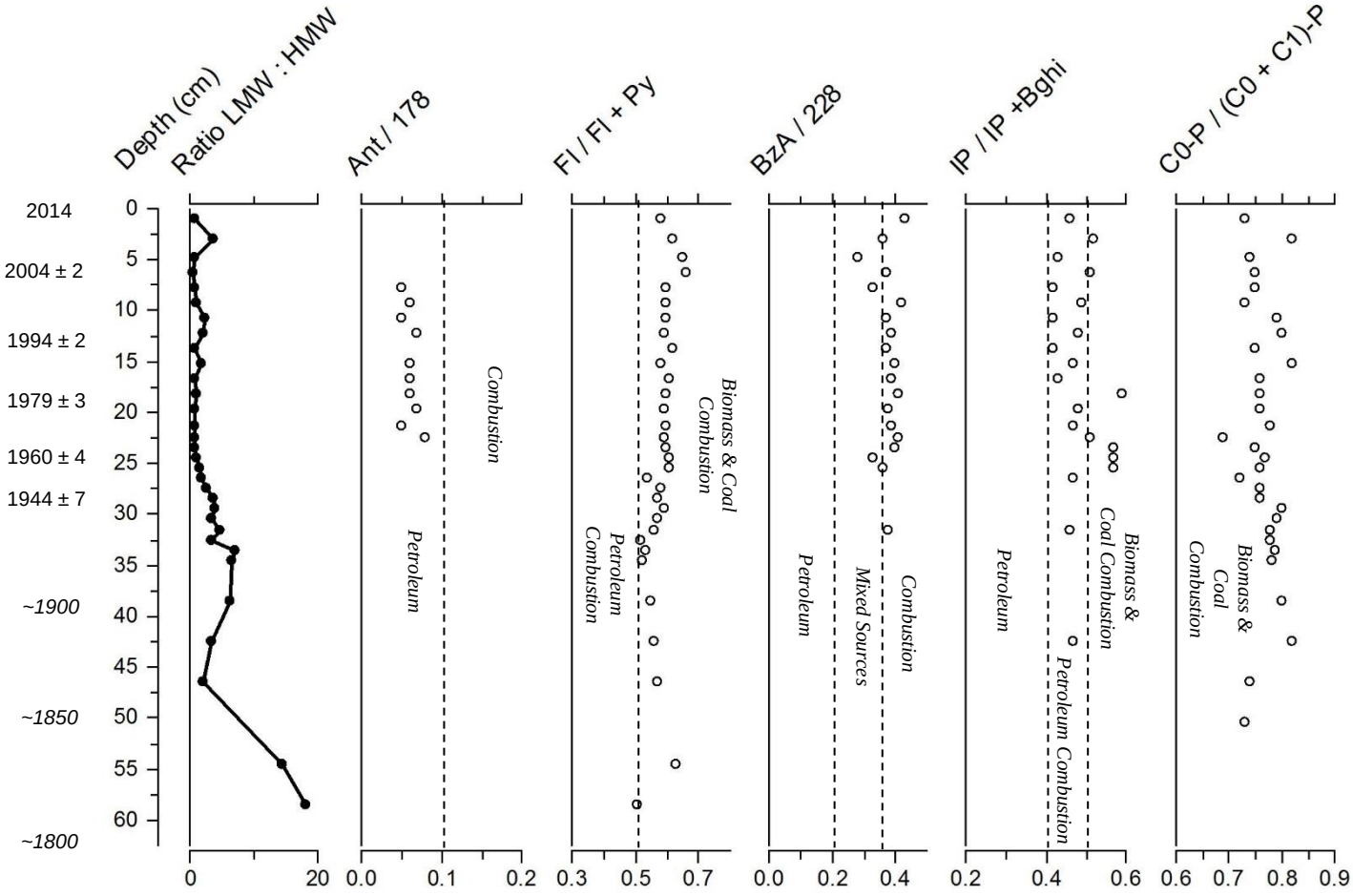

Figure 5.10. PAH ratios for SLNG04. Radioisotope-derived dates and and confidence limits are highlighted on the y-axis. Italicized dates are extrapolated beyond ^{210}Pb radioisotope dating.

5.3.1.4 Halogenated organic contaminants

Concentrations of HOCs from SLNG04 are shown in Figure 5.11. Initial increases in HOC concentrations occurred c. 1920, with all HOCs showing minor, yet detectable, increases in concentrations around this time, with the exception of ∑chlordanes. ∑PCBs, ∑HCHs, and ∑DDTs begin to notably increase in the mid-1950s, ~1960, and mid-1960s, respectively, with the greatest increases in concentrations for all HOCs occurring c. 1960 (Figure 5.11). Following the rapid increase in ∑PCBs through the 1950s and 1960s to a maximum concentration of 2.88 ng g^{-1} by the mid-1960s, ∑PCBs slowly decline to the surface, concentrations of 0.74 ng g^{-1} by 2014. The decline is particularly evident since the mid-1970s. Following the rapid increase in ∑HCHs c. 1960s, ∑HCHs remain elevated above background levels through the remainder of the 20th century, increasing in the early-21st century to the maximum concentration for the record of 3.43 ng g^{-1} c. 2007. ∑PBDEs had two major peaks in the record occurring in the mid-1960s (maximum of 0.17 ng g^{-1}) and mid-1970s, which are concurrent with the increases in ∑chlordane concentrations above detection limits in the mid-1960s (maximum of 0.02 ng g^{-1}), and the mid-1970s. ∑DDT concentrations continued to increase into the early-1970s, peaking at 0.72 ng g^{-1}, after which concentrations show a fluctuating, but general decline to the surface (Figure 5.11). Surface concentrations of ∑DDT are the lowest for the record since the late-1940s. Concentrations of dieldrin peaked c. 1960, and fluctuated around 1.0 ng g^{-1} until the surface.

LOI_{550}-normalized HOC concentration profiles from SLNG04 are shown in Figure 5.12. OM-normalization of HOC compounds did not result in a change to the concentration profiles for any compound or groups of compounds. All concentration profiles retained their rapid increase in the mid-20th century, and gradual decline through the latter part of the 20th century. Flux profiles for the total sums of major HOC compounds from SLNG04 are presented in Figure 5.13. All HOC fluxes exhibited an increase in the early-1960s, corresponding with the increase in SAR at the time (See 4.3.2.1). Fluxes of these HOCs remained steady until the 1990s, at which point most fluxes increased, even if only briefly. Flux of ∑PCBs remained similar to SAR, increasing and remaining steady to the surface. Fluxes and ∑DDTs declined to the surface after the brief increase ~1990. Fluxes of dieldrin underwent fluctuations in the 1990s, but otherwise remained constant through the latter half of the 20th and early-21st centuries. Fluxes of ∑HCHs remained

constant until the 21st century, after which time fluxes increased until ~2010, before declining to the surface.

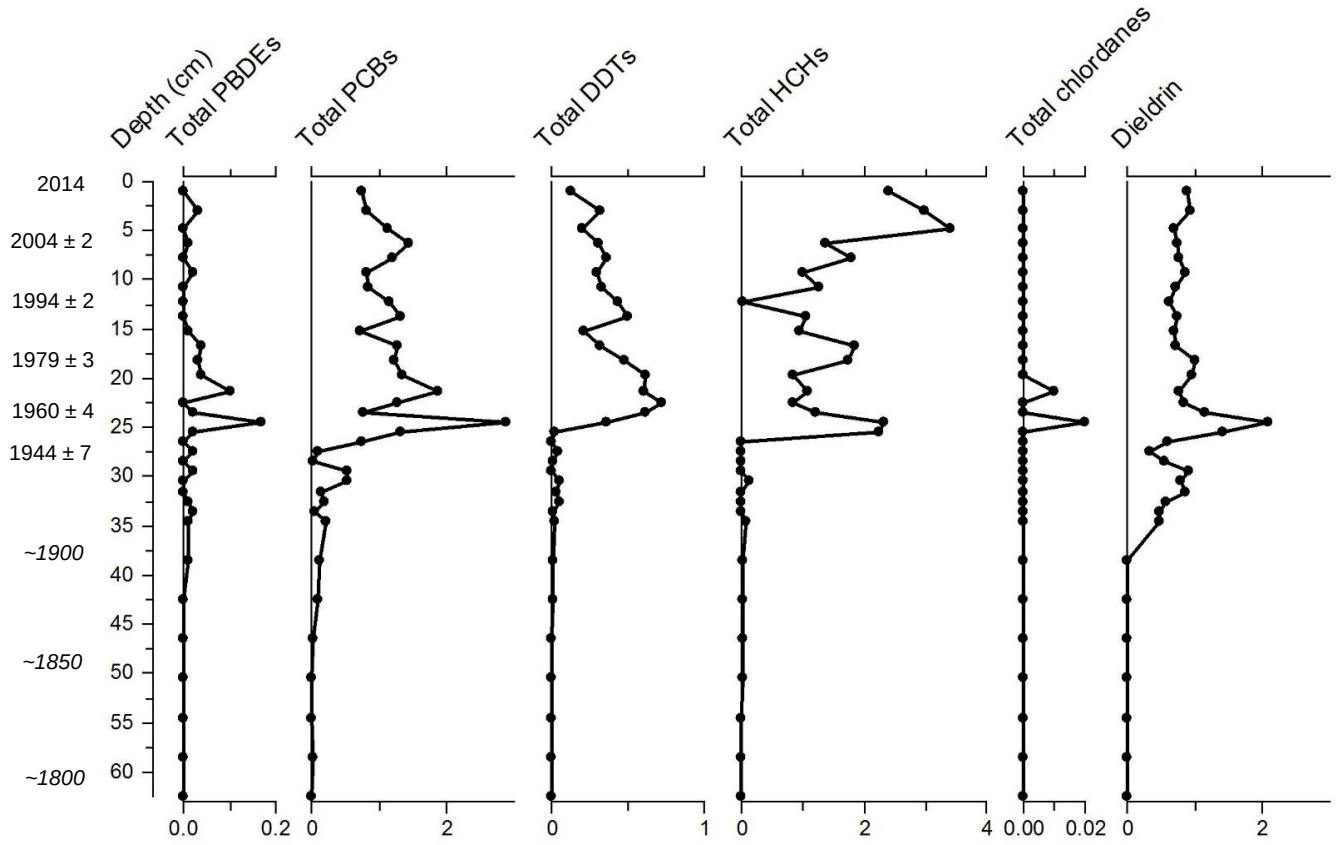

Figure 5.11. HOC concentrations from the SLNG04 record. Units of measurements are ng g^{-1}. Radioisotope-derived dates and and confidence limits are highlighted on the y-axis. Italicized dates are extrapolated beyond ^{210}Pb radioisotope dating.

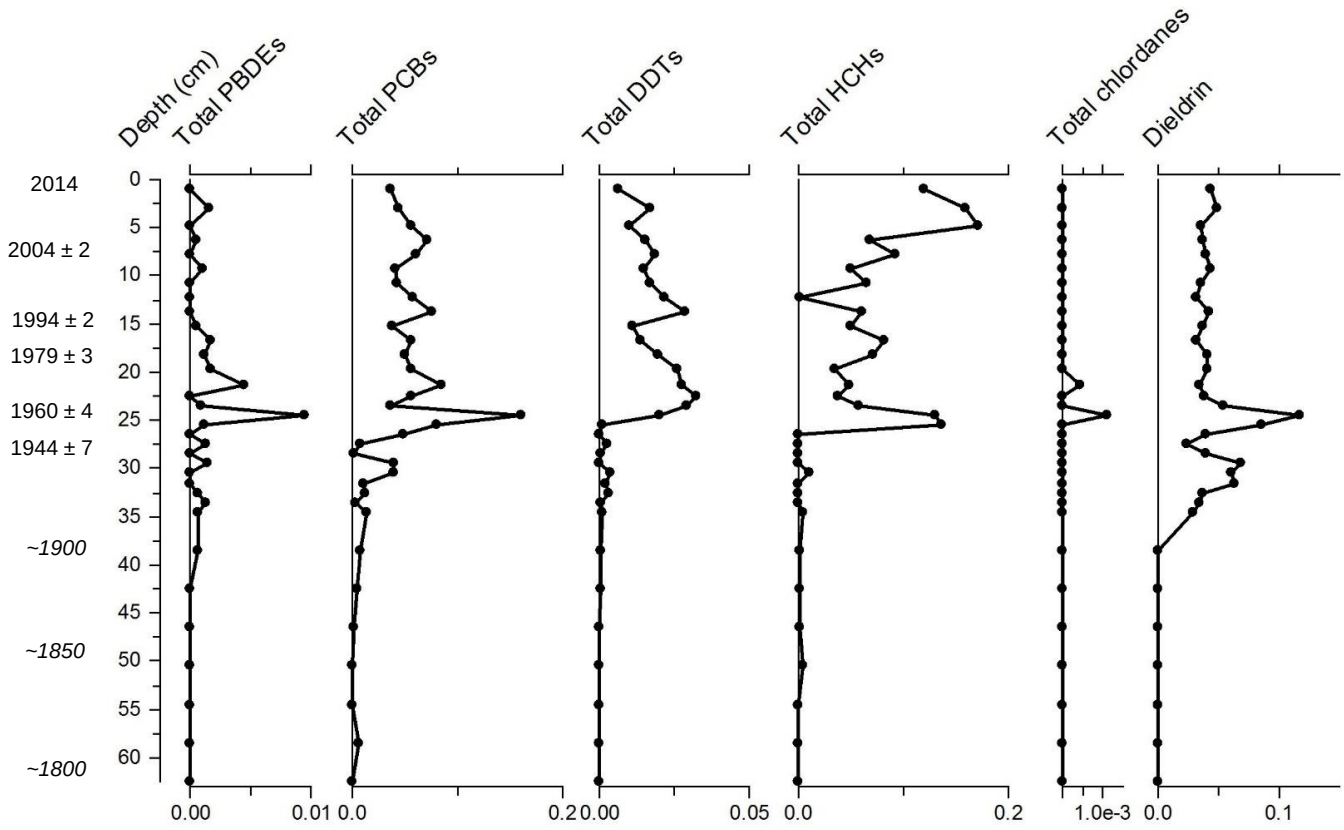

Figure 5.12. LOI_{550}-normalized HOC concentrations from the SLNG04 record. Units of measurements are ng g-1. Radioisotope-derived dates and confidence limits are highlighted on the y-axis. Italicized dates are extrapolated beyond ^{210}Pb radioisotope dating.

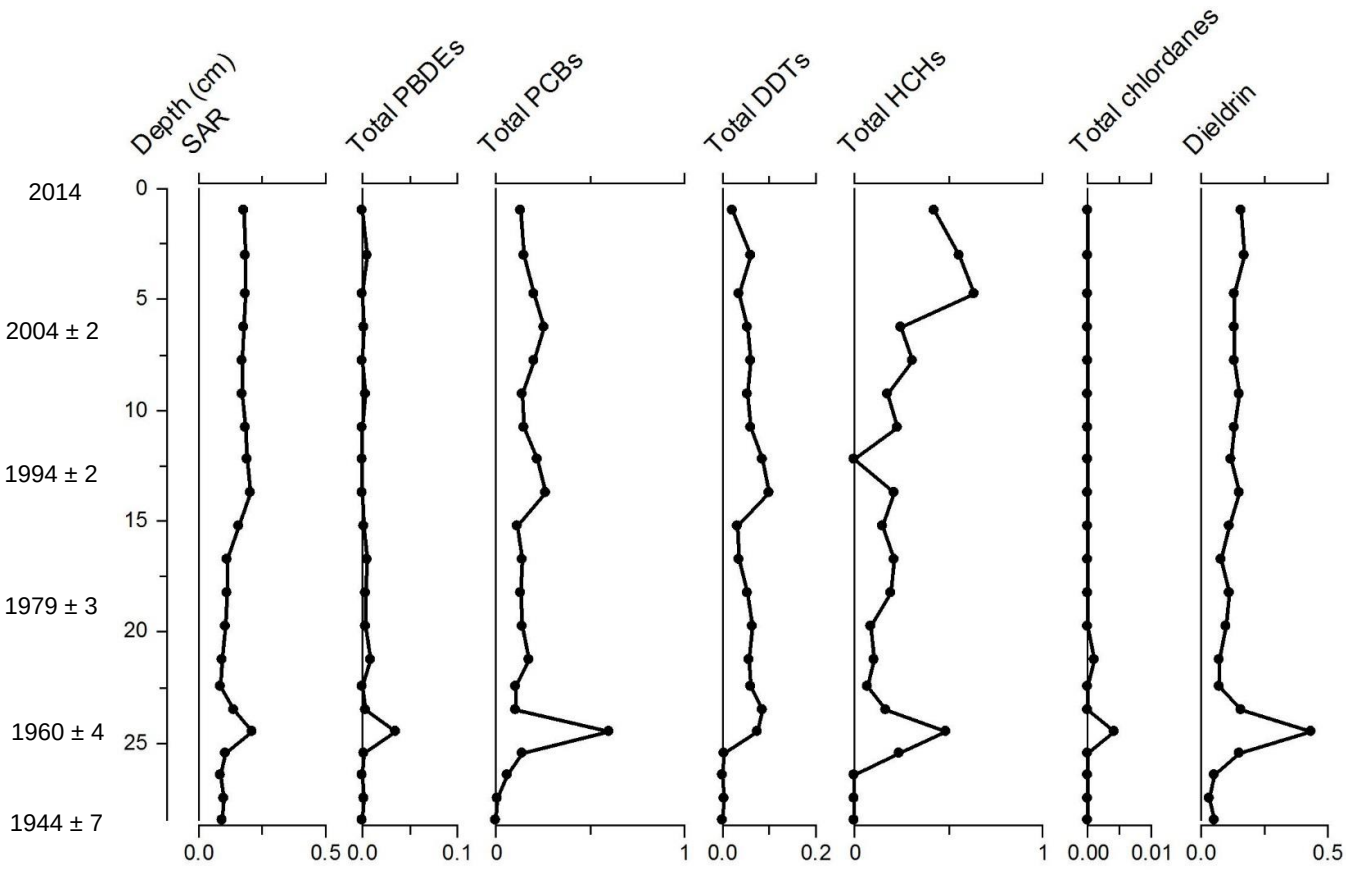

Figure 5.13. Sediment accumulation rate (SAR) and fluxes of HOCs for the SLNG04 record. Unit for SAR is g cm^{-2} yr^{-1}. Unit for HOC fluxes is ng cm^{-2} yr^{-1}. Radioisotope-derived dates and confidence limits are highlighted on the y-axis. Italicized dates are extrapolated beyond ^{210}Pb radioisotope dating.

5.3.1.5 Spheroidal carbonaceous particles

SCP concentration and accumulation rate profiles from SLNG04 sediment core are shown in Figure 5.14. SCPs were first detected in the mid-19th century, and concentrations remained low, below 1000 SCPs g^{-1} dry mass, c. 1960. SCP concentrations increased post-1960 and remained elevated until c. 2000. Since c. 2000, SCP concentrations declined to the surface. SCP fluxes since c. 1945 have followed sedimentation accumulation rates, with low SCP fluxes early in the record, followed by increased fluxes since c. 1990. Both SCP fluxes and concentrations declined since c. 2000.

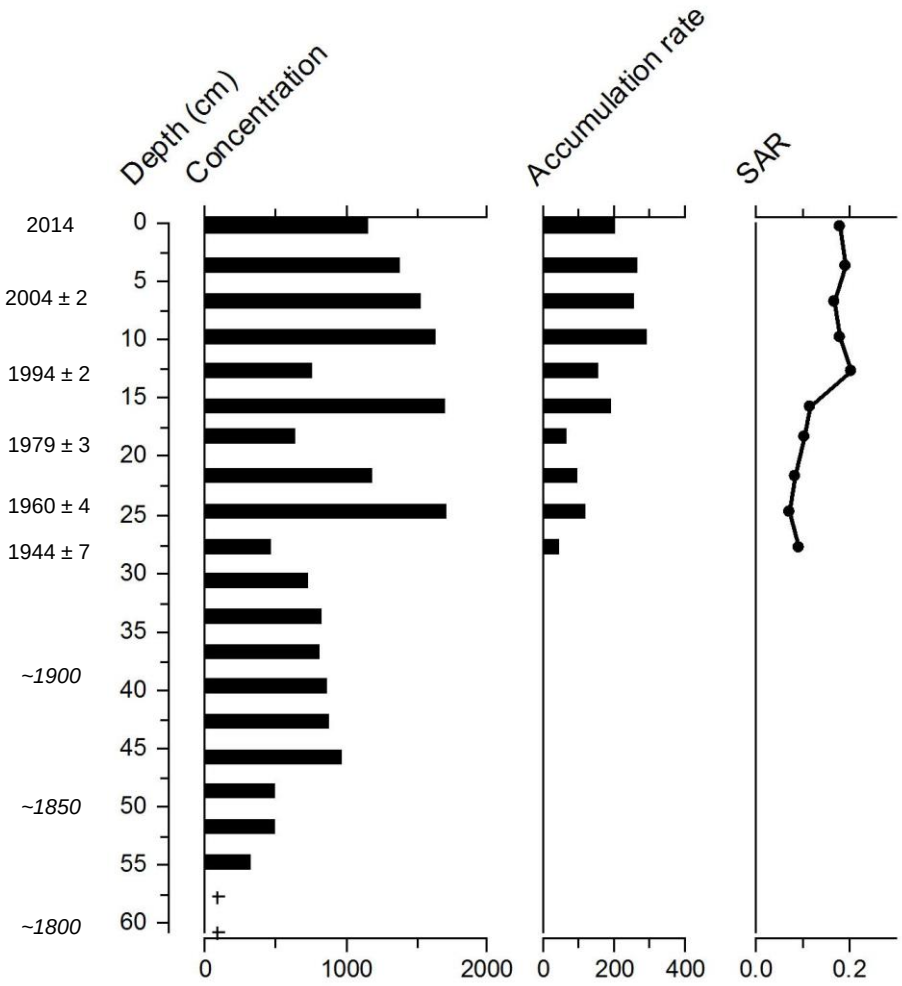

Figure 5.14. Concentrations and accumulation rates of SCPs from the SLNG04 record. Units for concentrations are no. SCPs g^{-1} dry mass, unit for accumulation rate is no. SCP cm^{-2} yr^{-1}. Sediment accumulation rate (SAR) is also plotted. Unit for SAR is g cm^{-2} yr^{-1}. (+) indicates a sample was counted with zero SCPs found. Radioisotope-derived dates and confidence limits are highlighted on the y-axis. Italicized dates are extrapolated beyond ^{210}Pb radioisotope dating.

5.3.1.6 Summary of contaminant history at SLNG04

The earliest signs of anthropogenic contamination at SLNG04 occurred with the appearance of SCPs in the sediment record in the mid-19th century (Figure 5.14), along with initial increases in Hg above background concentrations beginning in the mid-19th century indicating a likely increase in coal combustion. Twentieth century increases in contamination at SLNG04 continued in the 1950s and early 1960s, with the start of increasing PAH and HOC concentrations, and an approximate doubling of SCP concentrations post-1960. PAH ratios post-1960 indicate a mixture of combustion sources (Figure 5.10). Increasing P concentration beginning c. 1930 may be linked with increasing agricultural practices in the catchment (Figure 5.2a and 5.5), while continued increases in enrichment factors of Cu, Hg, and As in the 1950s

and early-1960s indicate anthropogenic contamination through the mid-20th century (Figure 5.3). Extensive anthropogenic contamination of SLNG04 continued until the late-20th and early-21st centuries, first as most HOC concentrations began to decline in the mid-1970s, and continued with declining PAH concentrations in the 1990s, and SCP concentrations beginning c. 2000. However, EFs remain elevated to the surface for both Cu and Hg. Always enriched, As began to increase in concentration in the late-19th century, and remained above its probable-effect concentration since the early 20th century.

5.3.2 SLNG05

5.3.2.1 Trace and major elements

Major lithogenic element and trace metal concentrations from SLNG05 sediment core are shown in Figure 5.15. Concentrations of most major elements and trace metals within the SLNG05 record displayed similar temporal trends. Concentrations of As, Br, Mn, Fe, P, S, Ca, and Ca/Ti were low until the late-19th century, and steadily increased to maximum values in the early-1960s. Rapid declines in the early-1960s were followed by minimum concentrations for the record in the mid-1970s. Conversely, concentrations of Ni, Cu, Zn, Pb, Al, Ti, K, Mg, Si, and Fe/Mn were relatively high until the late-19th century, gradually declined to minimum values in the early-1960s, and by the mid-1970s returned to concentrations similar to those of the 19th century. Trace and major element concentrations showed little change since the 1970s, with values similar to those of the early to mid-19th century.

Enrichment factor profiles from SLNG05 are presented in Figure 5.16. Enrichment factors for most trace metals and lithogenic elements from SLNG05 remain around 1, or fall below 1, through the entire record, indicating little to no enrichment. As, Mn, Fe, S, Ca, Br, and P experience enrichment factors greater than five in the late-1950s and early-1960s. However, the enrichment factors for these trace metals and lithogenic elements remain around one both prior to c.1870, and post-1960s.

Flux profiles for selected trace element and metals from SLNG05 are presented in Figure 5.17. Many of the selected trace metal and element flux profiles display similar temporal trends to SAR at SLNG05 since the 1960s (See 4.3.2.2). Exceptions include the fluxes for As and Br, which deviated from SAR in the late-20th and early-21st centuries. Arsenic flux gradually

increased between the late-1960s and present, while the Br flux remained relatively constant throughout the temporal record.

PCA indicated a total of 95% of total variation in trace metal and element data was explained across the first two PCA axes, with PCA axis 1 explaining 90.8% (Table 5.4). In the ordination, depths formed distinct groupings, with older and recent sample depths plotting negatively along PCA axis 1, while depths from the middle of the record plotted positively along PCA axis 1 (Figure 5.18).

	Axis 1	***Axis 2***	***Axis 3***	***Axis 4***
Eigenvalues	0.9080	0.0419	0.0218	0.0098
Explained variation (cumulative)	90.8	95.0	97.2	98.2

Table 5.4. PCA eigenvalues for SLNG05 sediment core trace metals and lithogenic elements, with eigenvalues and cumulative explained variation for the first four PCA axes.

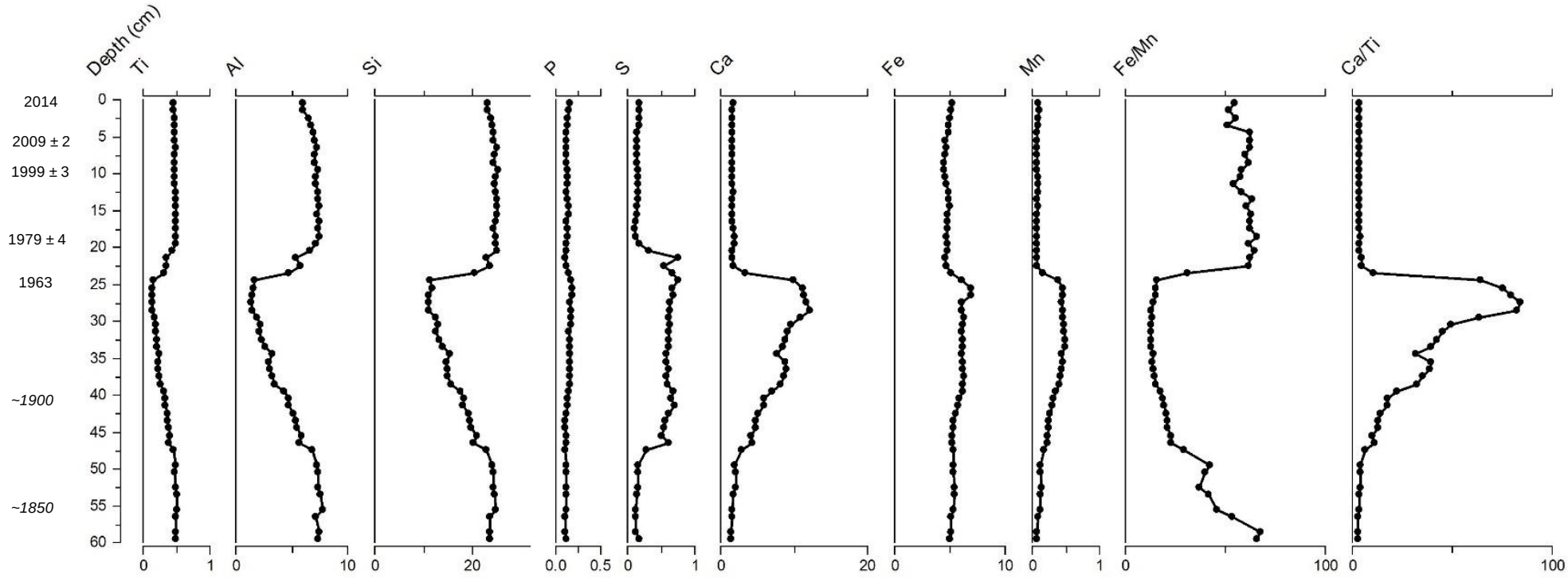

Figure 5.15a. Major lithogenic element contributions for SLNG05. Units of measurements from Ti to Mn are %. Radioisotope-derived dates and confidence limits are highlighted on the y-axis. Italicized dates are extrapolated beyond ^{210}Pb radioisotope dating.

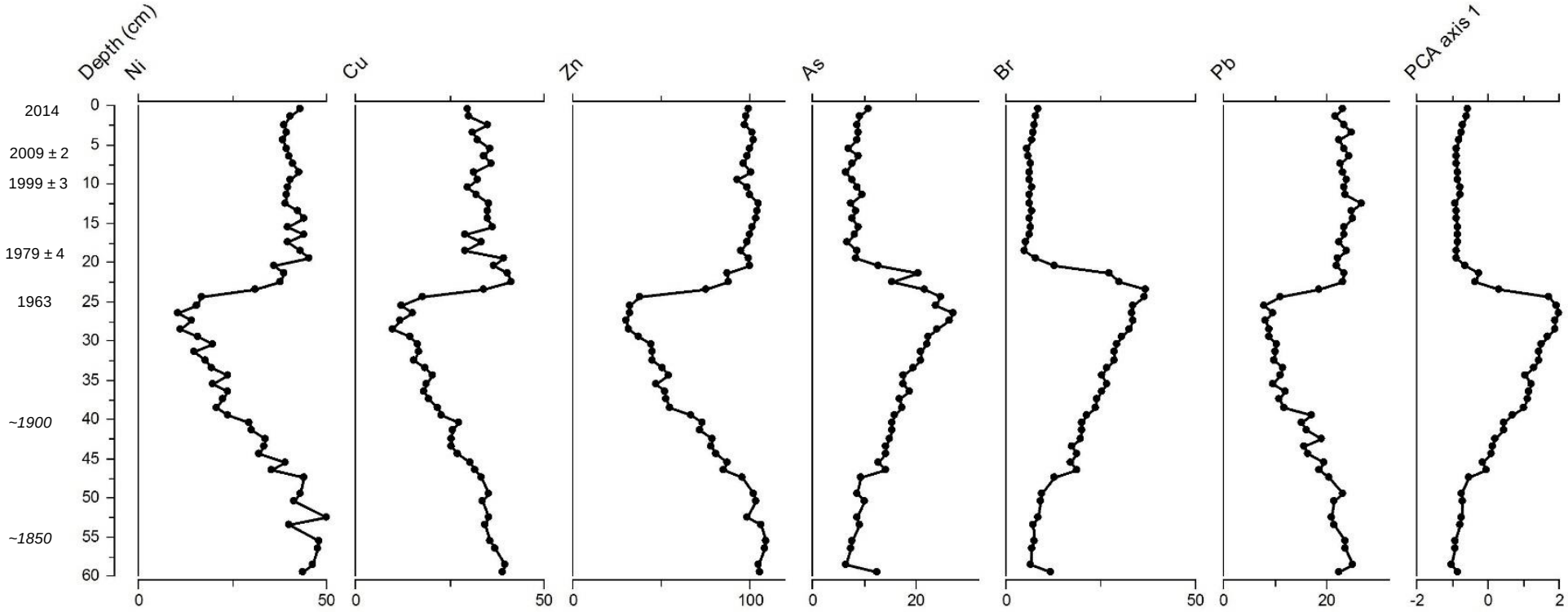

Figure 5.15b. Trace metal and element concentrations for SLNG05. Units of measurements are µg g^{-1}. PCA axis 1 scores plotted. Radioisotope-derived dates and confidence limits are highlighted on the y-axis. Italicized dates are extrapolated beyond ^{210}Pb radioisotope dating.

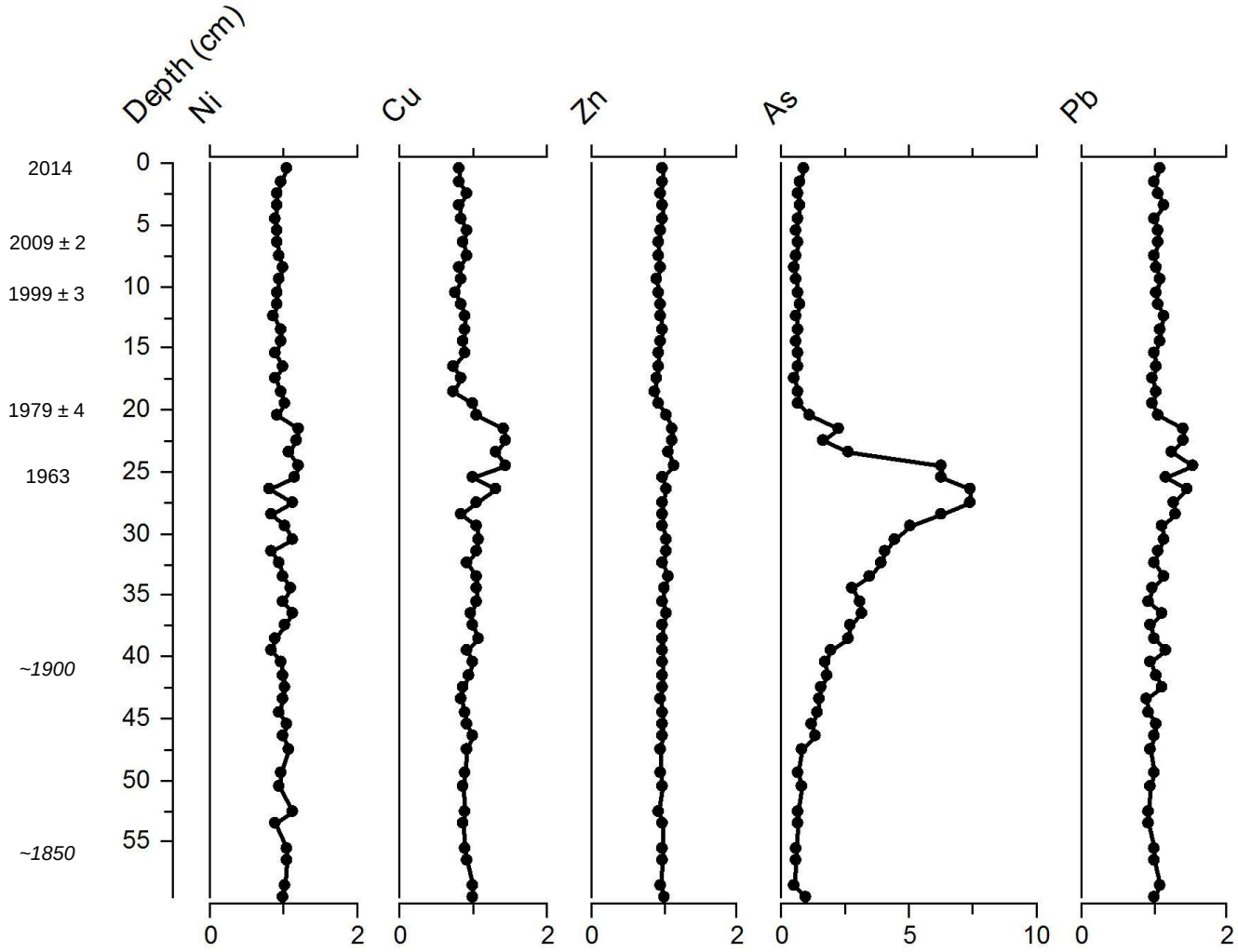

Figure 5.16. Enrichment factors for trace elements and metals for SLNG05. Units of measurements are µg cm^{-2} yr^{-1}. Radioisotope-derived dates and confidence limits are highlighted on the y-axis. Italicized dates are extrapolated beyond ^{210}Pb radioisotope dating.

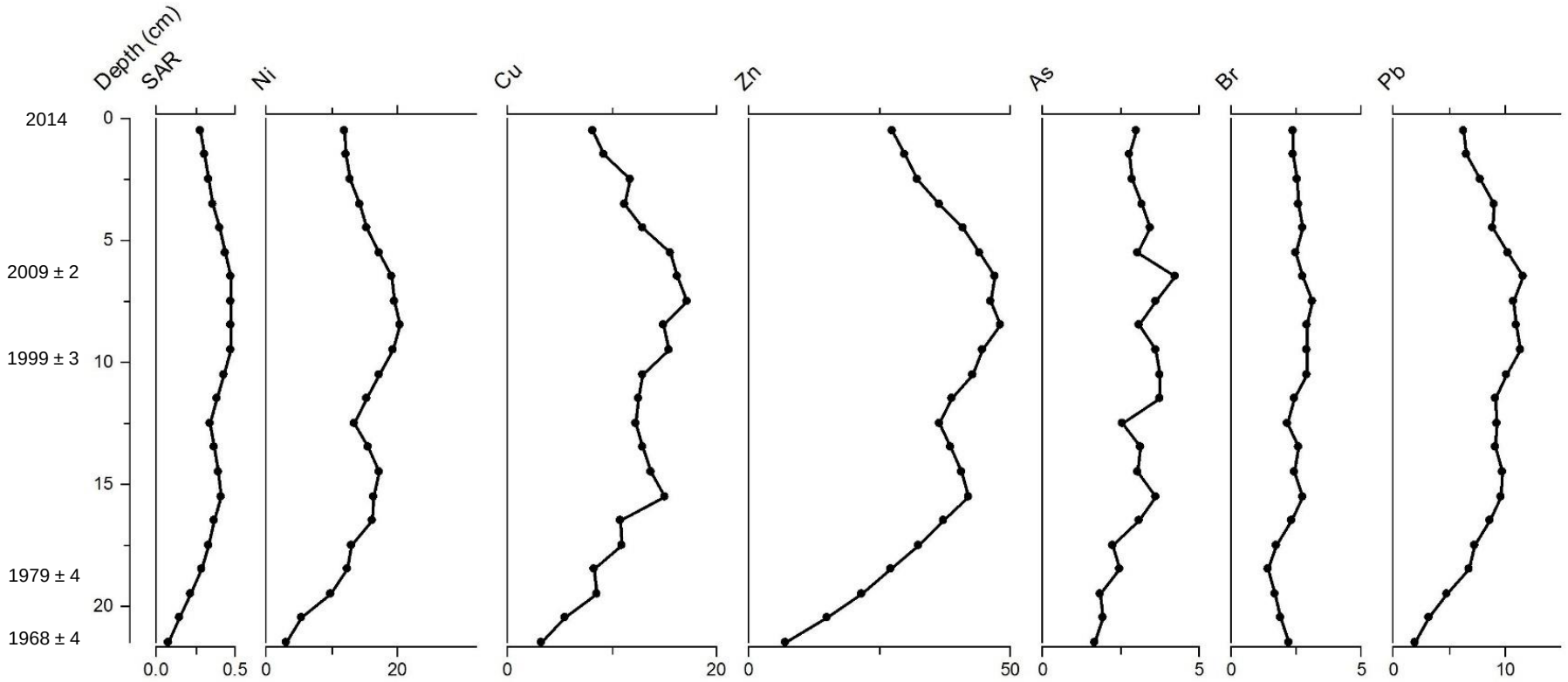

Figure 5.17. Sediment accumulation rate (SAR) and fluxes of trace metals and elements from the SLNG05 record. Unit for SAR is g cm^{-2} yr^{-1}. Unit for elemental fluxes is µg cm^{-2} yr^{-1}. Radioisotope-derived dates and confidence limits are highlighted on the y-axis. Italicized dates are extrapolated beyond ^{210}Pb radioisotope dating.

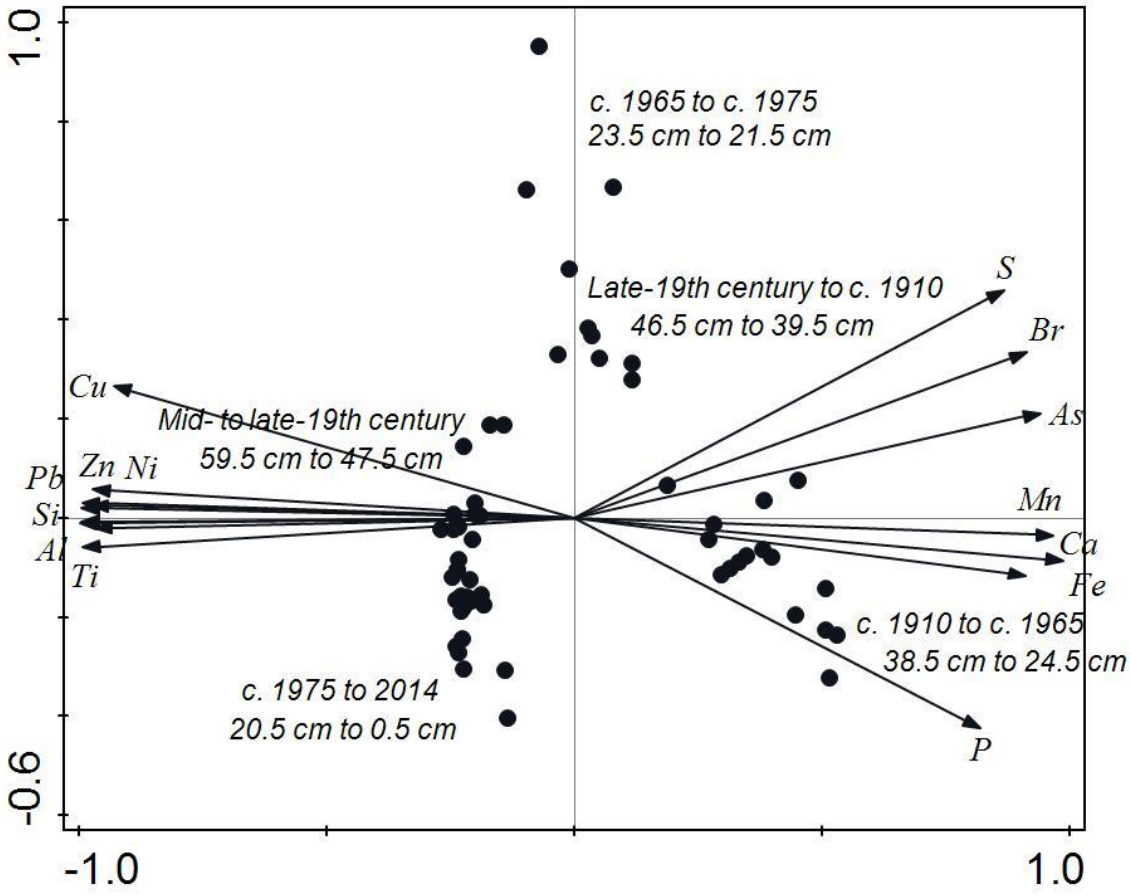

Figure 5.18. PCA biplot of trace elements and metals (vectors) with sample depths from the SLNG05 record. Groupings of depths, and corresponding ranges of years, are indicated.

5.3.2.2 Spheroidal carbonaceous particles

SCP concentration and accumulation rate profiles from SLNG05 sediment core are detailed in Figure 5.19. SCPs are first detected in the SLNG05 sediment core in the late-19th century. Concentrations remain below 500 SCPs g^{-1} dry mass until the mid-1940s. By the mid-1940s, concentrations increase to ~1000 SCPs g^{-1} dry mass, continuing to increase until the late-1980s. Concentrations declined in the late-1980s and were low until ~2010, after which time a peak in concentration in observed at the surface. Increases in SCP flux are observed concurrently with increase in SAR between the late-1960s and late-1980s. The decline in SCP concentrations in the late-1980s is mirrored in the SCP flux, but occurred concurrently with increased SAR. The increase in SCP concentration and flux increased since ~2005 was concurrent with a decline in SAR.

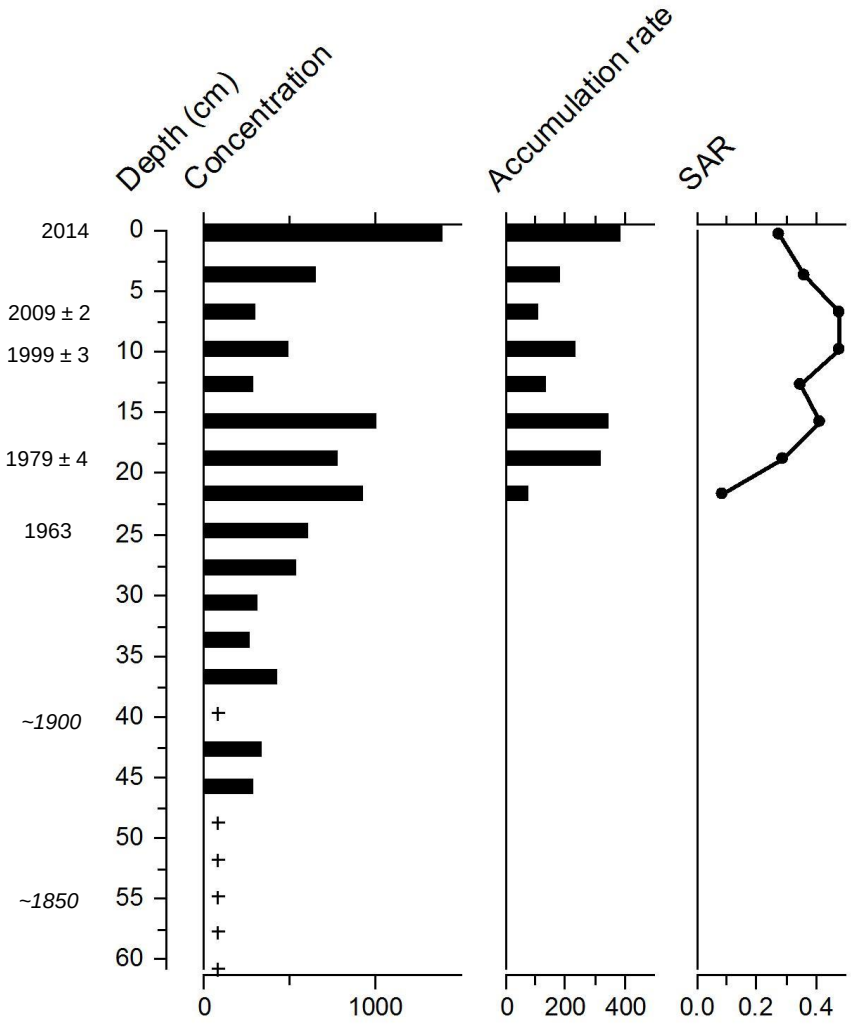

Figure 5.19. Concentrations and accumulations rates of SCPs from the SLNG05 record. Units for concentrations are no. SCPs g^{-1} dry mass, unit for accumulation rate is no. SCP cm^{-2} yr^{-1}. Sediment accumulation rate (SAR) is also plotted. Unit for SAR is g cm^{-2} yr^{-1}. (+) indicates a sample was counted with zero SCPs found. Radioisotope-derived dates and confidence limits are highlighted on the y-axis. Italicized dates are extrapolated beyond ^{210}Pb radioisotope dating.

5.3.2.3 Summary of contaminant history at SLNG05

Earliest signs of anthropogenic contamination at SLNG05 occurred with the first detection of SCPs at low concentrations in the late-19th century (Figure 5.19). An approximate doubling of SCPs concentrations occurred in the mid-1940s, signalling the increase in local/regional anthropogenic development and industrialization. The anthropogenic signal remains elevated until c. 1990, at which time SCP concentrations decline, independent of sedimentation rates, likely indicating a decline in coal-production or increased efficiency of particle emission-capture in the region in the 1990s. Trace element concentrations remained low throughout the SLNG05 record, although EF for As began to increase above background concentrations in the late-19th century (Figure 5.16). Arsenic EF increased to above 2 early in the 20th century, and peaked at

~7 c. 1950. Enrichment of As declined in the latter half of the 20th century, and reached background concentrations c. 1970.

5.3.3 BRYT02 (Black Lake)

5.3.3.1 Trace and major elements

Major lithogenic element and trace metal concentrations from BRYT02 sediment core are shown in Figure 5.20. From the late-19th century until c. 1950, Ca, Br, and Mn concentrations and Ca/Ti ratios were high, while all other trace element concentrations and Fe/Mn ratios were low. Post-1950, Ca, Br, Mn concentrations and Ca/Ti ratios declined and remained low for the remainder of the record, while most other trace element concentrations and Fe/Mn ratios increased and remained high until the surface. Enrichment factor profiles from BRYT02 are presented in Figure 5.21. Enrichment factors for most trace and major elements fluctuated around 1 throughout the record, indicating no increase in contamination of the metals and elements at Black Lake, and possibly indicating that the base of the sediment core was not unimpacted. The greatest period of enrichment for some elements was c. 1900, with EFs for Mn and Mg briefly exceeding 2, and Ca EFs nearly reaching 4 c. 1900. However, enrichment factors for most trace elements rarely exceeded 1 in the early record. Flux profiles for trace metals and elements since the early-1960s are shown in Figure 5.22. Most element fluxes since the early-1960s followed the trend of SAR at Black Lake (See 4.3.2.3), and all exhibited increases in flux in the early-1960s and early-1980s.

PCA indicated a total of 85.7% total variation in trace metal and element data explained across the first two PCA axes, with PCA axis 1 explaining 77.0% (Table 5.5). In the ordination, samples formed groupings following the previously described temporal trends in concentrations, with older samples plotting positively along axis 1, and recent samples plotting negatively along axis 1, while the most recent samples also plotted negatively along PCA axis 2 (Figure 5.23). Older samples were associated with higher concentrations of Ca, Mn, and Br. Recent samples were more strongly associated with higher concentrations of most trace metals and elements (Figure 5.23).

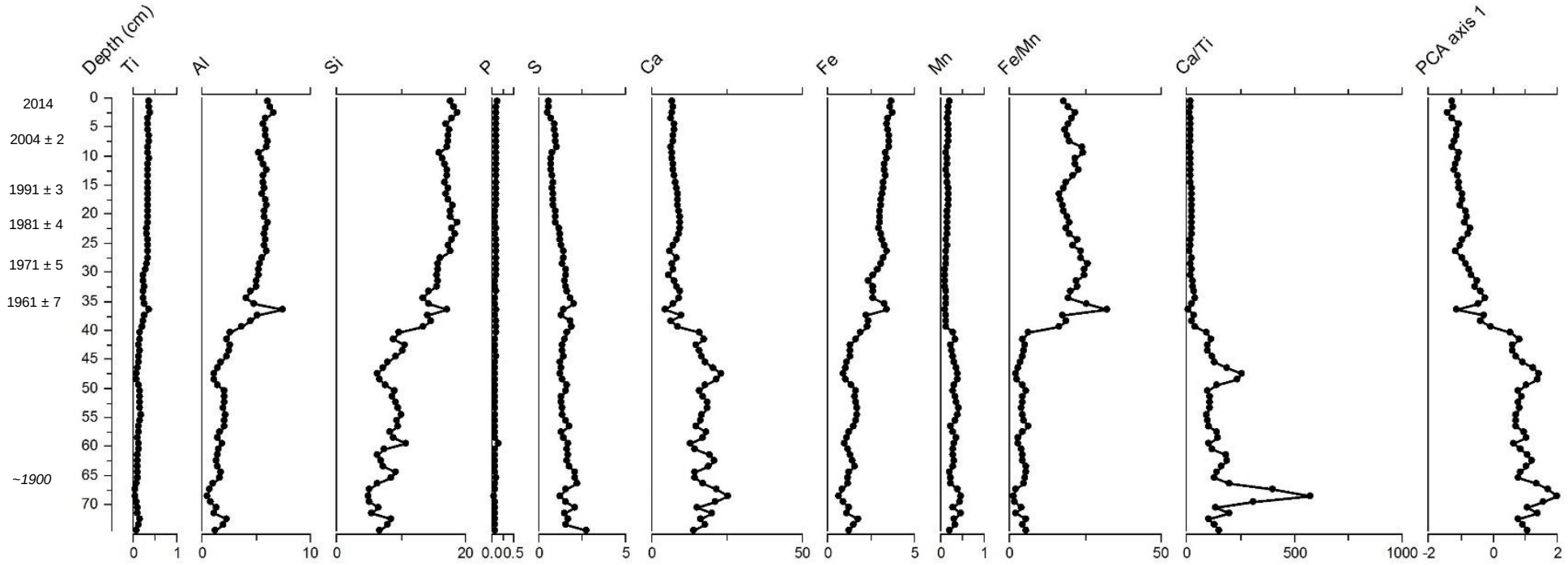

Figure 5.20a. Major lithogenic element contributions from Black Lake. Units of measurements from Ti to Mn are %. PCA axis 1 scores are plotted. Radioisotope-derived dates and confidence limits are highlighted on the y-axis. Italicized dates are extrapolated beyond ^{210}Pb radioisotope dating.

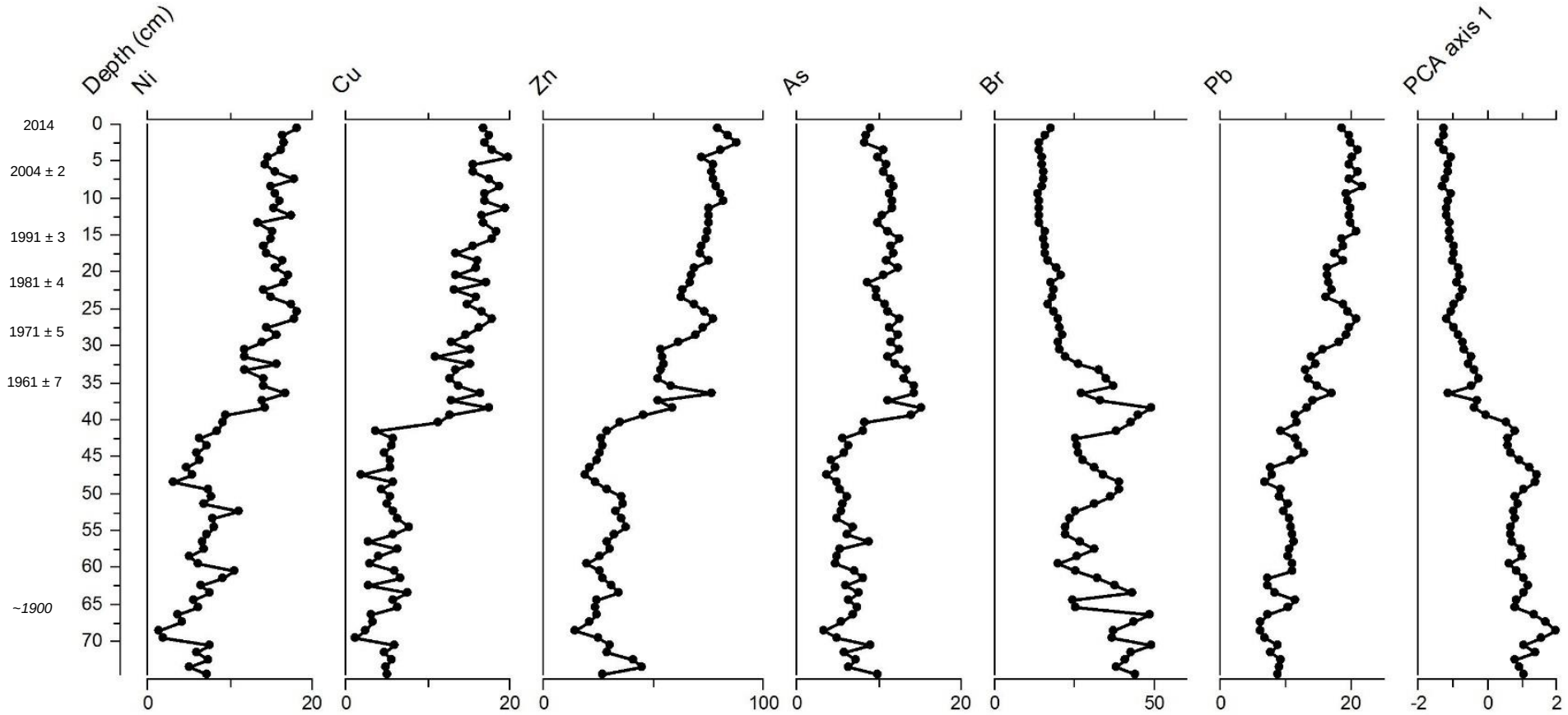

Figure 5.20b. Trace metal and element concentrations from Black Lake. Units of measurements are µg g^{-1}. PCA axis 1 scores are plotted. Radioisotope-derived dates and confidence limits are highlighted on the y-axis. Italicized dates are extrapolated beyond ^{210}Pb radioisotope dating.

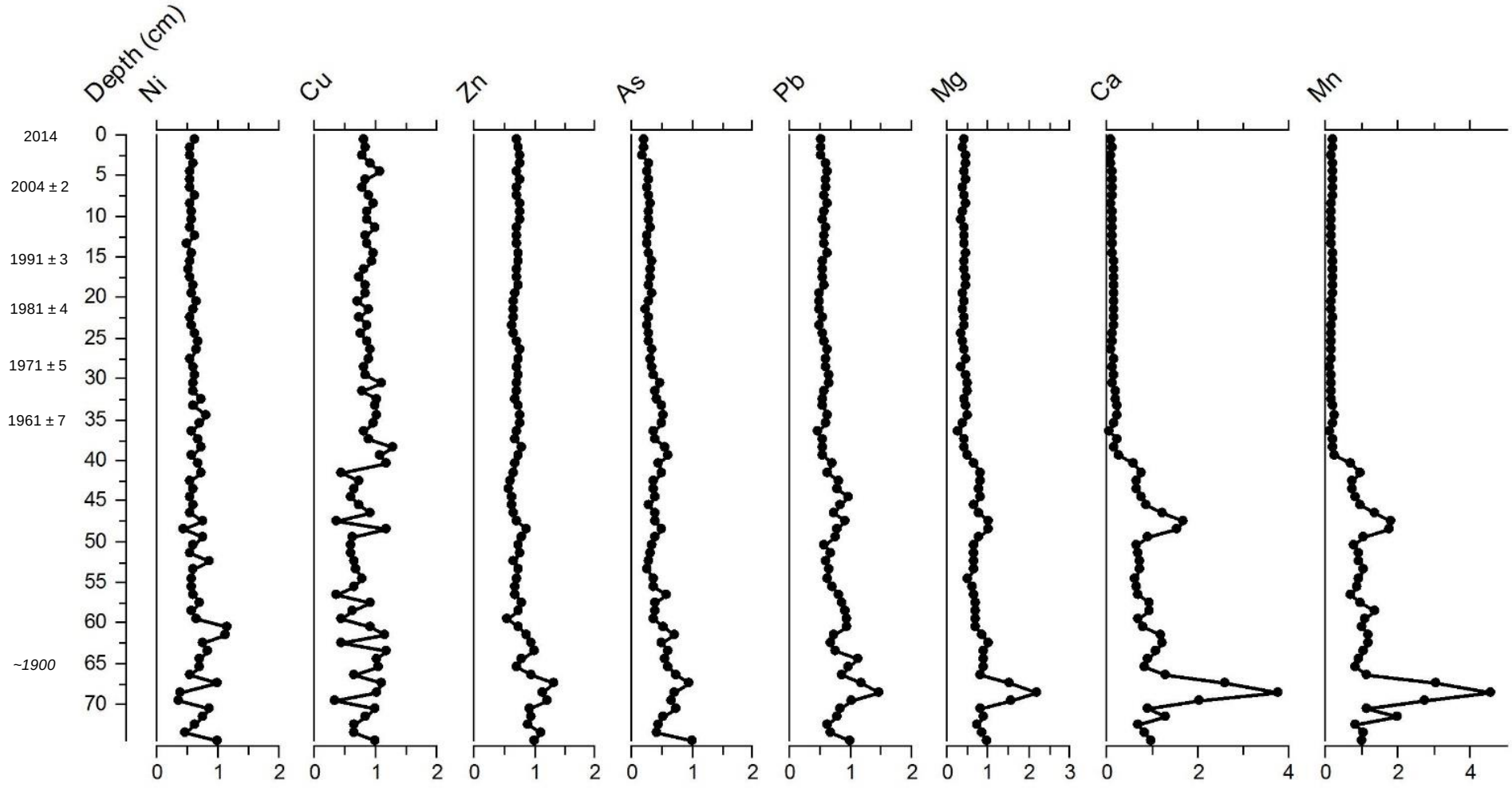

Figure 5.21. Enrichment factors for major and trace elements from Black Lake. Radioisotope-derived dates and confidence limits are highlighted on the y-axis. Italicized dates are extrapolated beyond ^{210}Pb radioisotope dating.

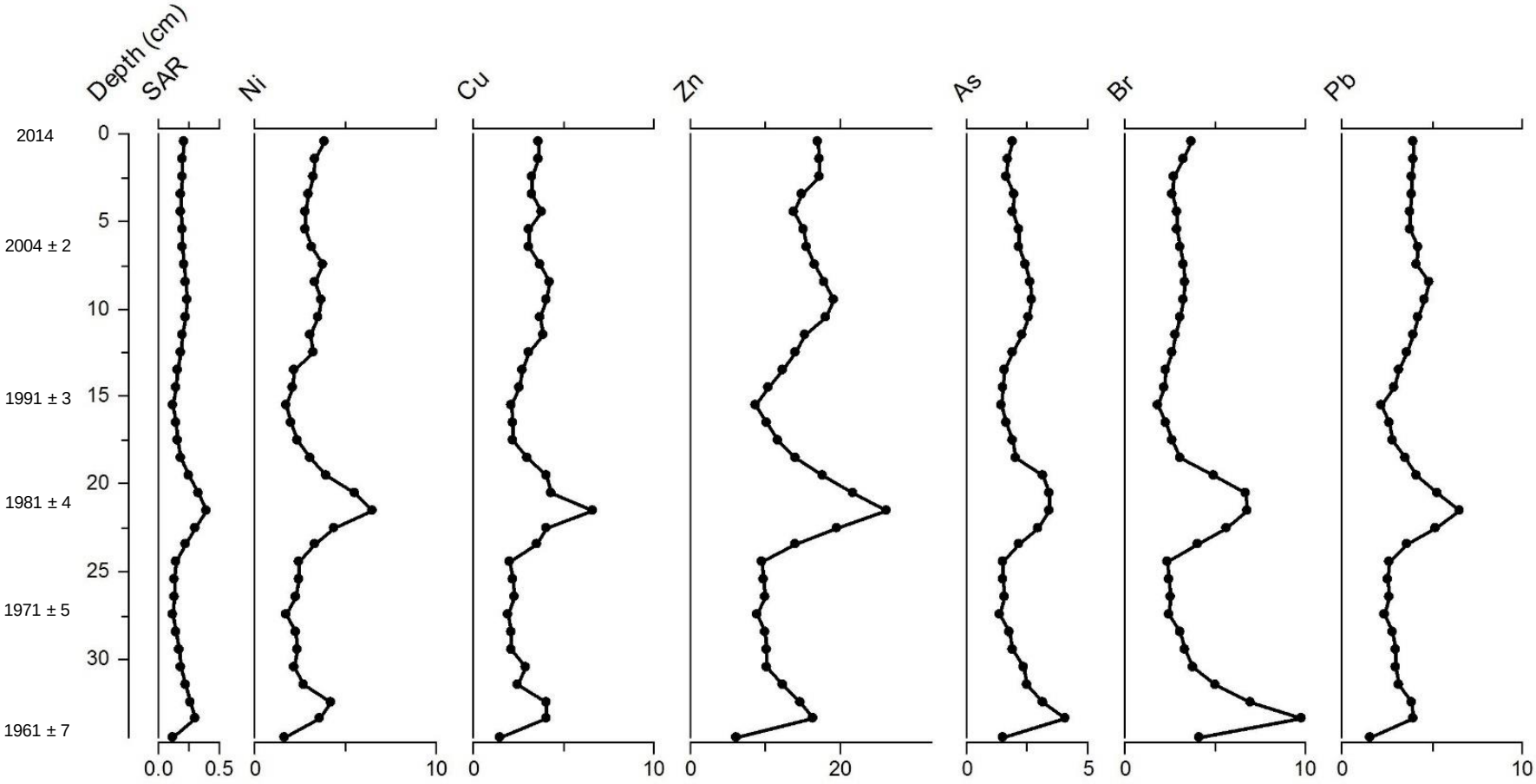

Figure 5.22. Sediment accumulation rate (SAR) and fluxes of trace metals and elements from Black Lake. Unit for SAR is g cm^{-2} yr^{-1}. Unit for elemental fluxes is µg cm^{-2} yr^{-1}. Radioisotope-derived dates and confidence limits are highlighted on the y-axis. Italicized dates are extrapolated beyond ^{210}Pb radioisotope dating.

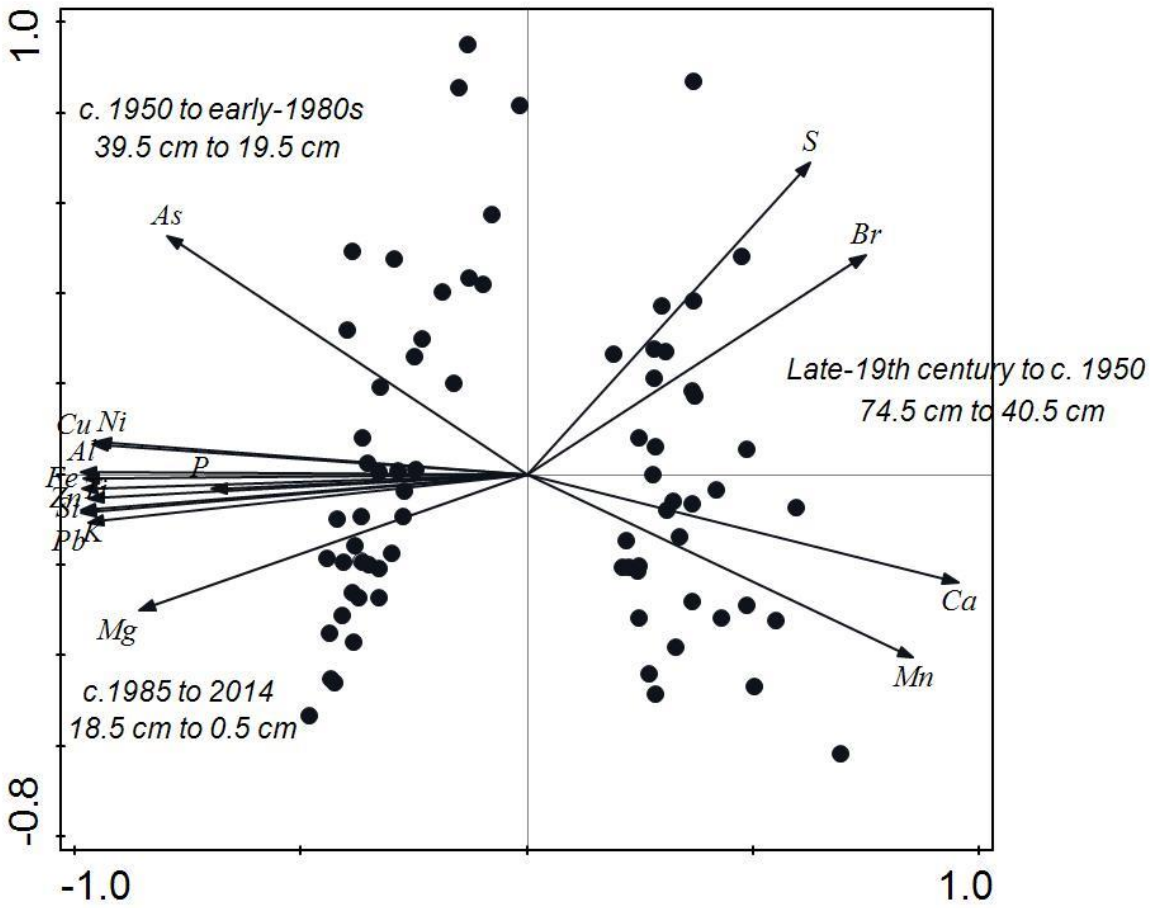

Figure 5.23. PCA biplot of trace elements and metals (vectors) with sample depths from Black Lake. Groupings of depths, and corresponding ranges of years, are indicated.

	Axis 1	***Axis 2***	***Axis 3***	***Axis 4***
Eigenvalues	0.7687	0.0884	0.0533	0.0357
Explained variation (cumulative)	76.9	85.7	91.0	94.6

Table 5.5. PCA eigenvalues for trace metals and lithogenic elements from Black Lake, with eigenvalues and cumulative explained variation for the first four PCA axes.

5.3.3.2 Toxicity

Arsenic is the only trace element exceeding the threshold effect concentration at any point at Black Lake (Figure 5.24). Arsenic concentrations are low, falling below the TEC prior to the late-1940s, after which time concentrations exceeded the TEC almost continuously until ~2010.

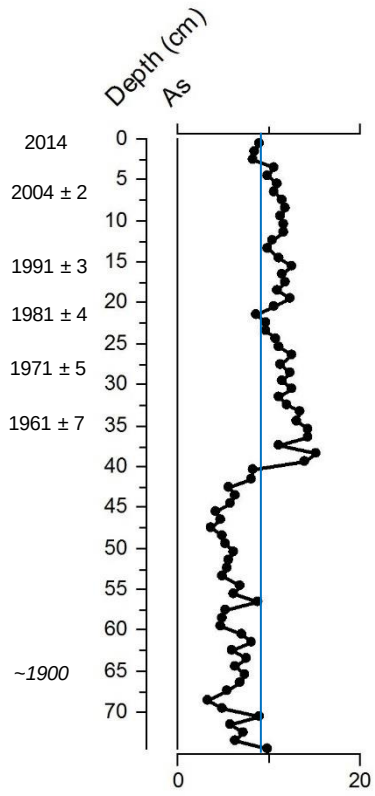

Figure 5.24. Toxicity of arsenic concentrations from Black Lake. As concentration is in units of µg g^{-1}. The vertical blue line indicates the threshold effect concentration for As, at 9.79 µg g^{-1}. Radioisotope-derived dates and related uncertainties are posted. Italicized dates are extrapolated beyond ^{210}Pb radioisotope dating.

5.3.3.3 Black Lake PAHs

Concentrations of PAHs from the BRYT02 record are detailed in Figure 5.25. Individual PAH concentrations were low in the first half of the record, and began to increase in the mid-1940s. The early PAH record was dominated by perylene, a naturally occurring PAH, which peaked near the base of the core at 114 ng g^{-1}, and exhibited a steady decline towards the surface. Post-1945, the PAH record was dominated by the LMW PAHs naphthalene and phenanthrene, which increased in relative abundance in the 1960s. While ∑PAH concentrations exhibited a slow general decline from the base of the sediment record to the surface, concentrations of the 16 USEPA PAHs declined only until the early-1940s, followed by increasing concentrations beginning in the mid-1940s, reaching 138 ng g^{-1} by c. 1975. Concurrently, ∑HMW PAHs increased in concentration between c. 1945 and the early-1970s, with a decline in the LMW:HMW PAH ratio (Figure 5.28). ∑HMW PAHs peaked in the early-1970s. Total LMW PAH concentrations exhibited a decline from the late-19th century until the mid-1960s, with a

subsequent increase in ∑LMW PAH concentrations occurring due to the increase in naphthalene in the 1960s.

LOI_{550}-normalized PAH concentration profiles from the BRYT02 record are shown in Figure 5.26. OM-normalization appeared to smooth many of the fluctuations in concentrations that occurred in the PAH profiles in the early record. Therefore, much of the fluctuation in PAH concentration pre-1950 was likely due to the fluctuations in organic matter. Normalization to organic matter also made the increase in total PAHs c. 1950 more defined.

Flux profiles for selected PAH compounds and sums from the BRYT02 record are presented in Figure 5.27. Selected PAH compounds and sums displayed increased fluxes corresponding with the increase in sedimentation accumulation rate (SAR) c. 1980 (See 4.3.2.3). However, ∑LMW PAH fluxes began to increase in the late-1960s, prior to the increase in SAR, while perylene exhibited a decline in flux prior to the c.1980 increase in SAR. Post-1980, ∑HMW PAH flux followed a very similar trend as SAR, however most other PAH concentrations undergo fluctuations to the surface, which do not follow trends in SAR, as declines in most PAH fluxes are observed when SAR increases c. 2000.

Bza+228 indicated mixed sources of coal and petroleum combustion throughout the record, while a general decline in the Ant/178 ratio indicated a shift away from coal combustion in the early record, to the direct introduction of petroleum products in the early to mid-1960s, and IP/IP+Bghi indicated purely petroleum combustion (liquid fossil fuels, such as vehicle or crude oil) throughout the record. Fl/Fl+Py and C0-P/C0-C1-P indicated biomass + coal combustion throughout the record, but an increase in the C0-P/C0-C1-P ratio beginning in the mid-1930s indicated a shift away from biomass burning towards coal combustion (Figure 5.28).

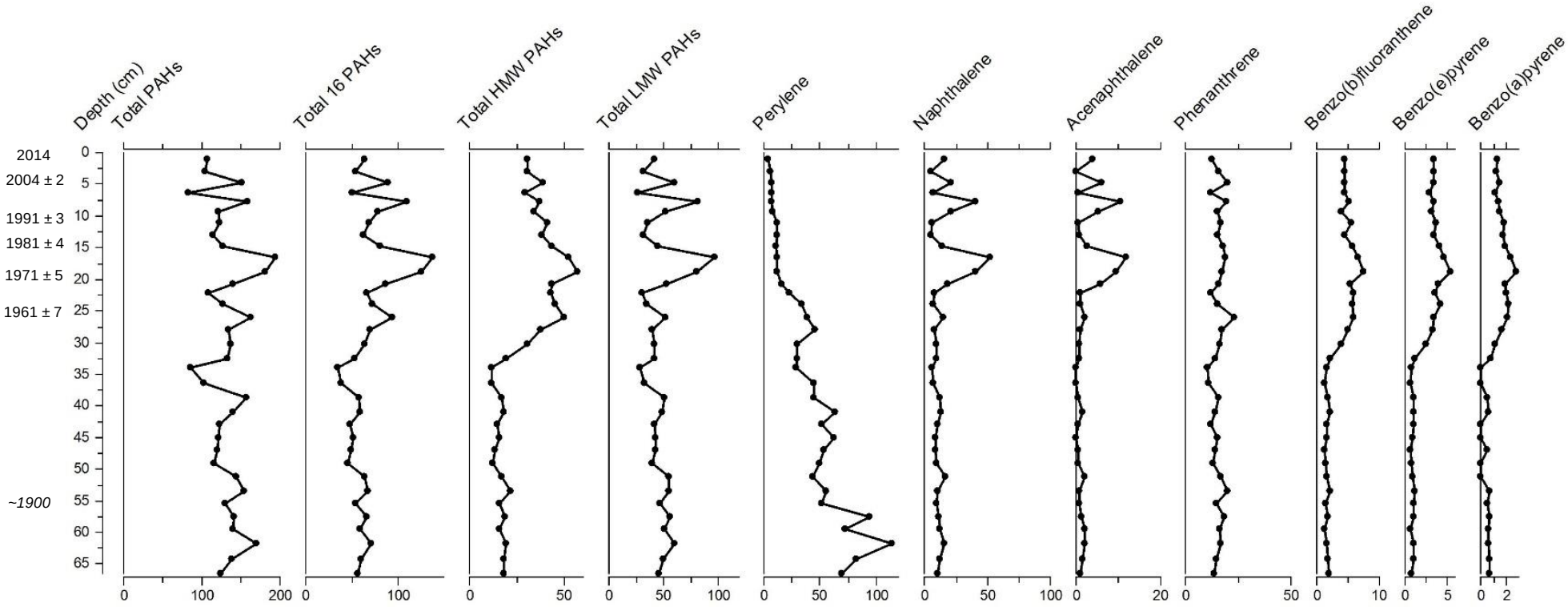

Figure 5.25. PAH concentrations and sums of PAH groups for Black Lake. Units of measurements are ng g^{-1}. Radioisotope-derived dates and confidence limits are highlighted on the y-axis. Italicized dates are extrapolated beyond ^{210}Pb radioisotope dating.

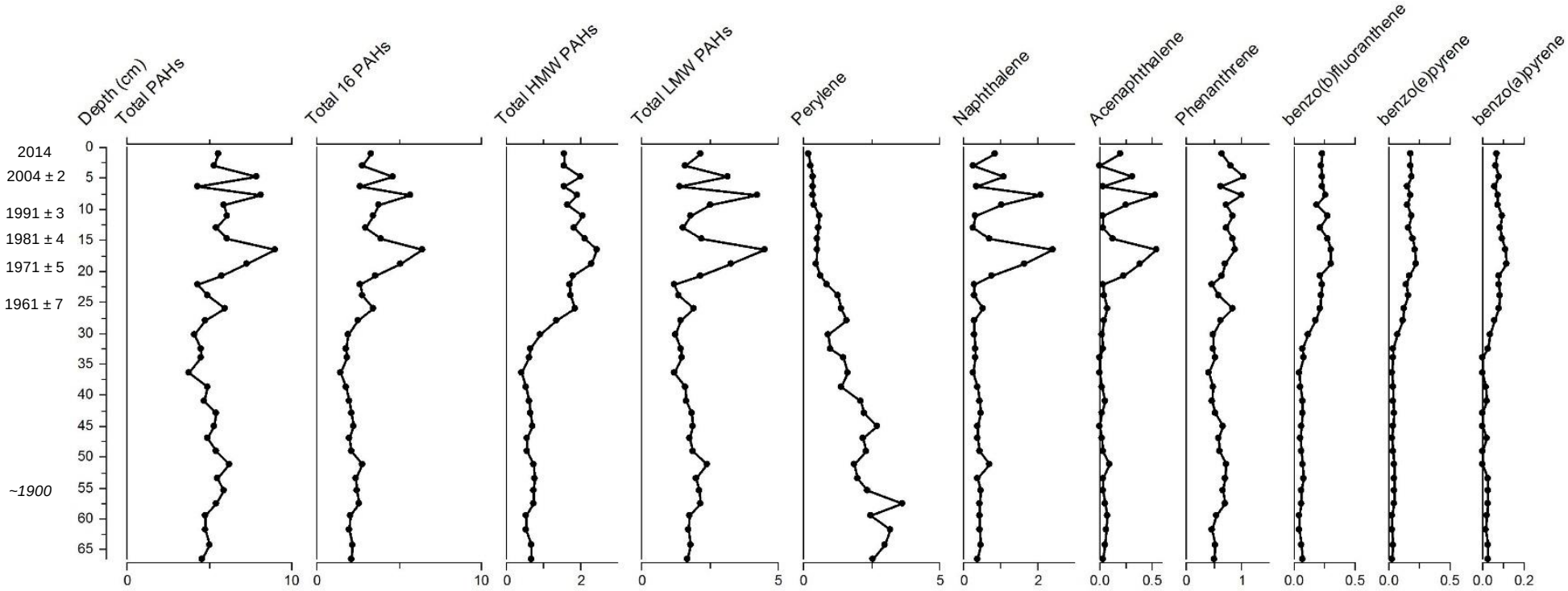

Figure 5.26. LOI_{550}-normalized PAH concentrations from Black Lake. Units of measurements are ng g^{-1}. Radioisotope-derived dates and confidence limits are highlighted on the y-axis. Italicized dates are extrapolated beyond ^{210}Pb radioisotope dating.

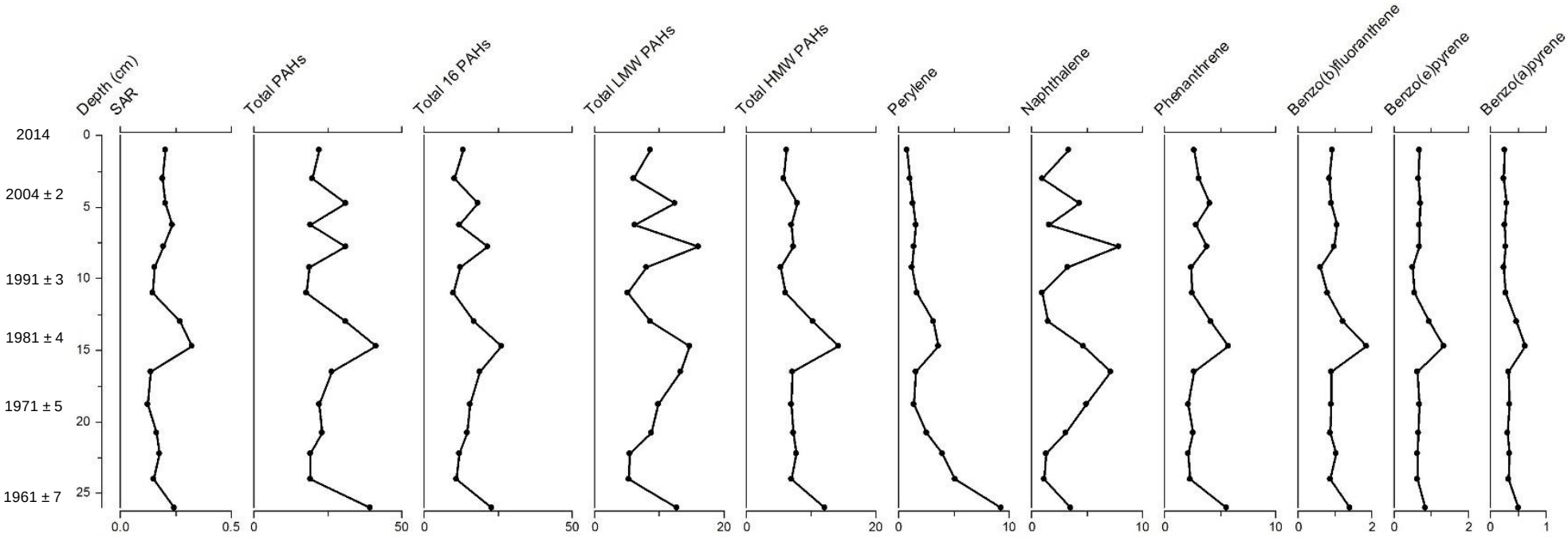

Figure 5.27. Sediment accumulation rate (SAR) and fluxes of PAHs from Black Lake. Unit for SAR is g cm^{-2} yr^{-1}. Unit for PAH fluxes is ng cm^{-2} yr^{-1}. Radioisotope-derived dates and confidence limits are highlighted on the y-axis. Italicized dates are extrapolated beyond ^{210}Pb radioisotope dating.

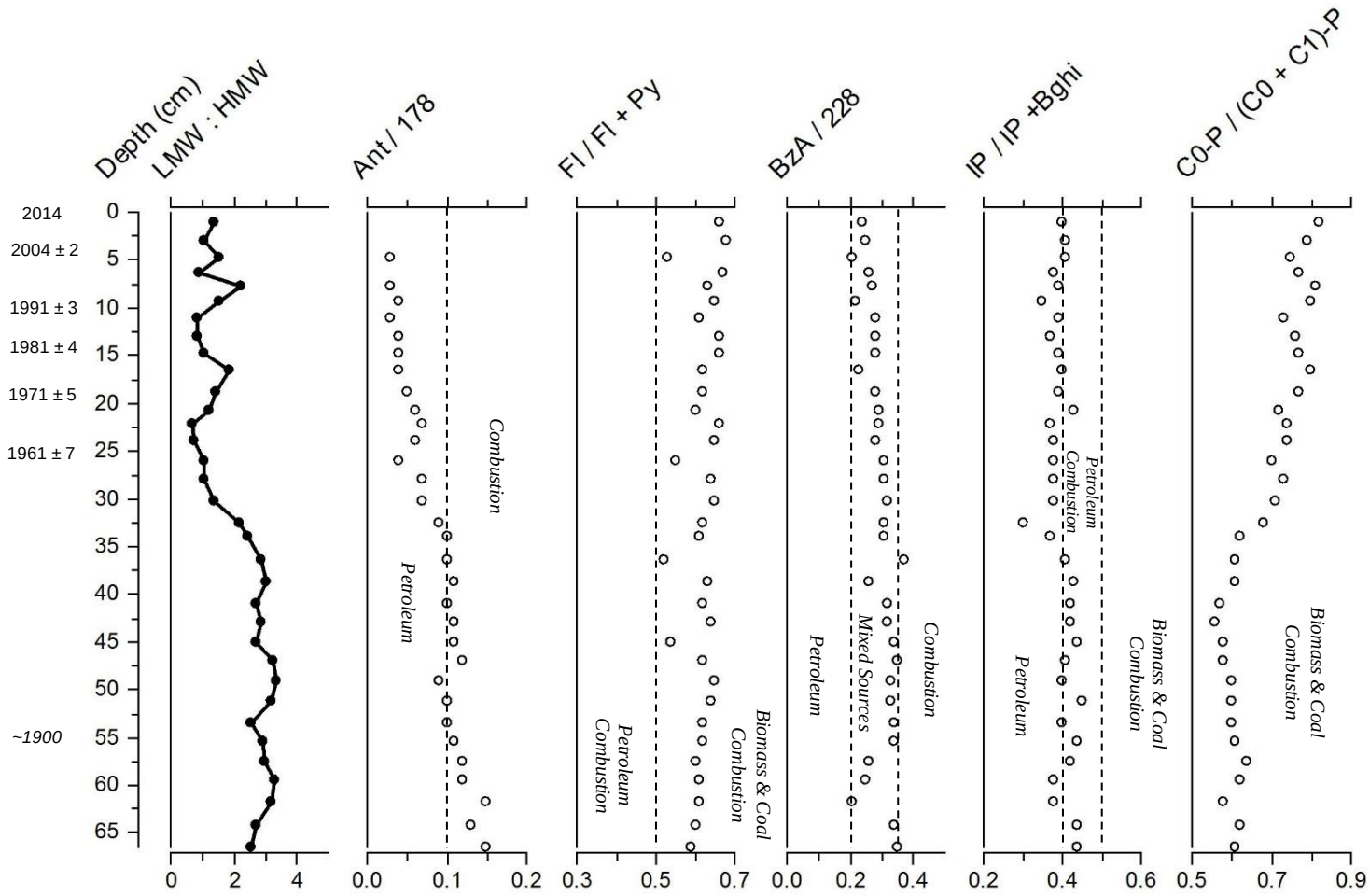

Figure 5.28. PAH ratios from Black Lake. Radioisotope-derived dates and confidence limits are highlighted on the y-axis. Italicized dates are extrapolated beyond ^{210}Pb radioisotope dating.

5.3.3.4 Halogenated organic contaminants

Concentrations of HOCs from the BRYT02 record are detailed in Figure 5.29. Prior to the mid-1920s, HOC concentrations were low for all compounds. Concentrations of most HOC compounds began to increase c.1920. Total PCB concentrations fluctuated from the base of the core to the surface between 0.06 ng g^{-1} and 1.35 ng g^{-1}, with increasing concentrations c. 1920, and generally higher concentrations beginning in the mid-1940s, with continued increases until the late-1950s (Figure 5.29). Concentrations continued to be relatively high until the mid-1970s, after which time ∑PCB concentrations declined to the surface. ∑DDT concentrations fluctuated near the limits of detection from the base of the core until c. 1920. The major period of increasing ∑DDT concentrations was from c. 1950 to the mid-1960s (Figure 5.29). Declines in ∑DDT concentrations occurred between the mid-1960s and early-1980s. Dieldrin concentrations rapidly increased c. 1920, and remained elevated until c. 1960, after which time dieldrin concentrations were low or <LD to the surface. ∑PBDEs increase in concentrations c. 1950 and continue to increase until the early-1960s, with signs of continued presence until the mid-1970s. HCHs only appear in the sediment record between the mid-1930s and late-1940s (Figure 5.29). After this point, concentrations of ∑HCHs remain <LD to the surface. ∑chlordane concentrations are <LD until the mid-1950s, after which time concentrations remain elevated until the mid-1970s, followed by declines to the surface (Figure 5.29).

LOI_{550}-normalized HOC concentration profiles from the BRYT02 record are shown in Figure 5.30. OM-normalization of HOC compounds did not result in a change to the concentration profiles for any compound or groups of compounds. All concentration profiles retained their increase in the mid-20th century, and decline through the latter part of the 20th century. Flux profiles for the total sums of major HOC compounds from the BRYT02 record are presented in Figure 5.31. Fluxes of HOCs from Black Lake did not appear to follow SAR trends. Flux of ∑DDTs declines from the 1960s to the surface, with slight fluctuations, while ∑chlordane and ∑PBDE fluxes are low with slight fluctuations in the latter 20th and early-21st centuries. ∑PCB fluxes increase from the early-1960s until the early-1980s, after which point, fluxes decline and are steady to the surface, with the exception of an increase in the uppermost sample.

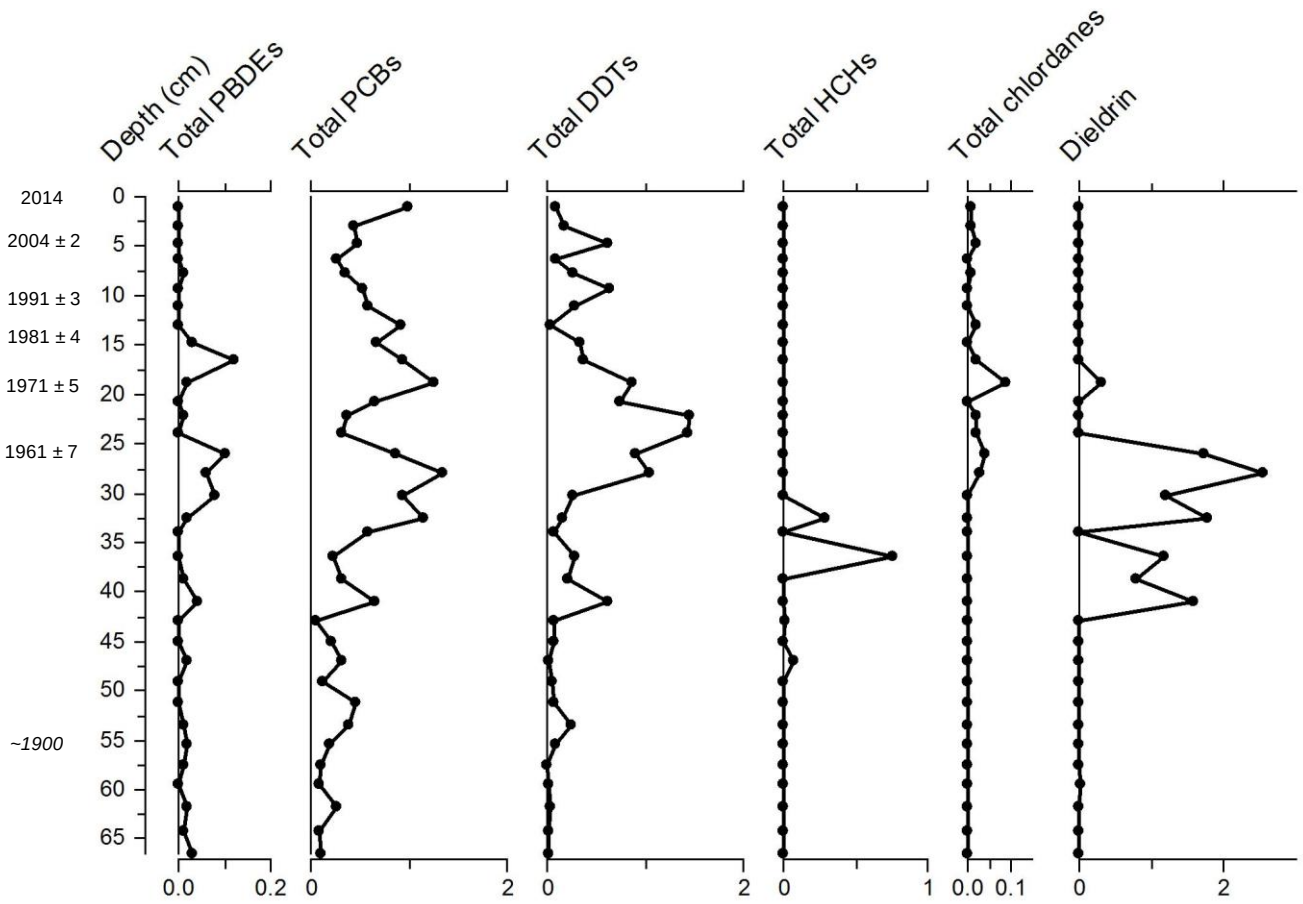

Figure 5.29. HOC concentrations from Black Lake. Units of measurements are ng g^{-1}. Radioisotope-derived dates and confidence limits are highlighted on the y-axis. Italicized dates are extrapolated beyond ^{210}Pb radioisotope dating.

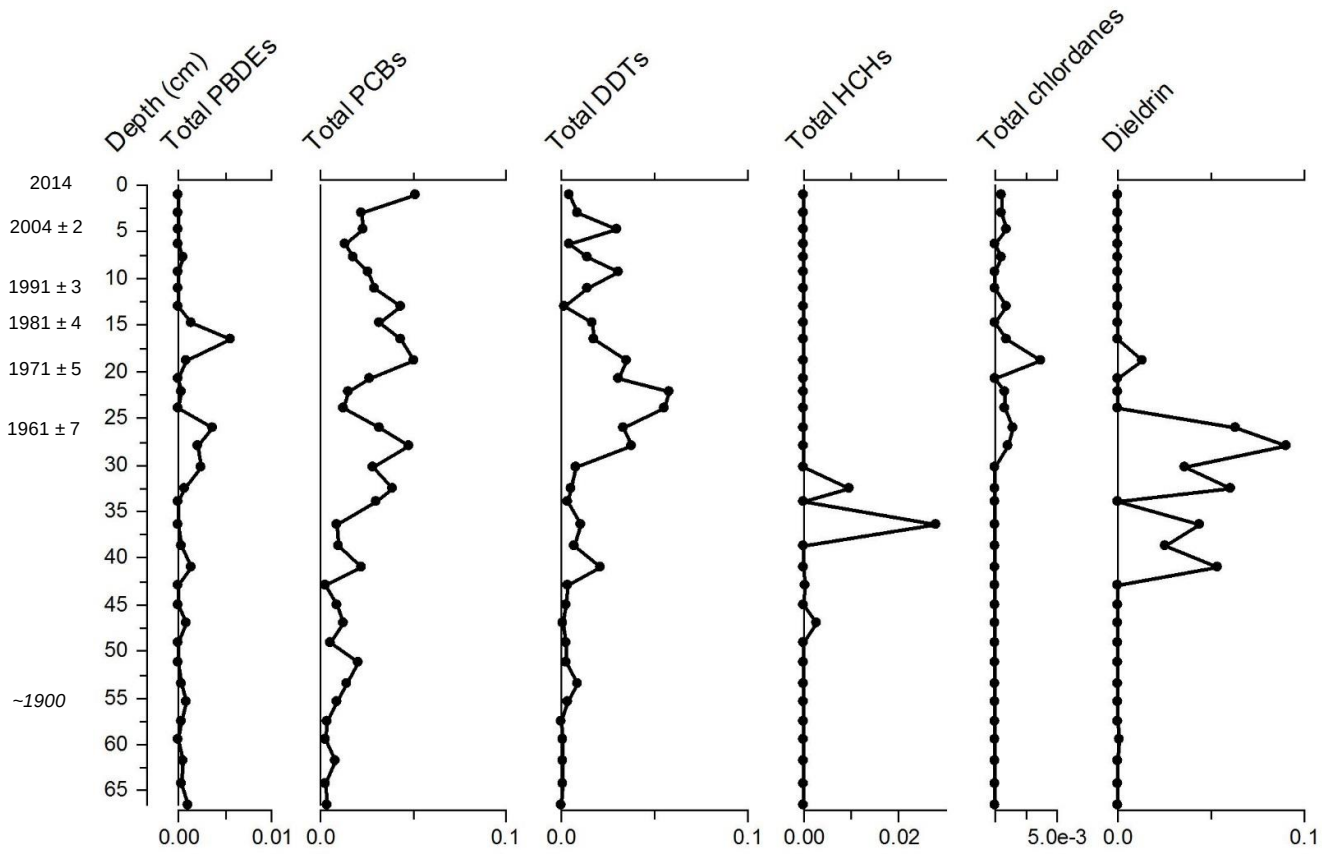

Figure 5.30. LOI_{550}-normalized HOC concentrations from Black Lake. Units of measurements are ng g^{-1}. Radioisotope-derived dates and confidence limits are highlighted on the y-axis. Italicized dates are extrapolated beyond ^{210}Pb radioisotope dating.

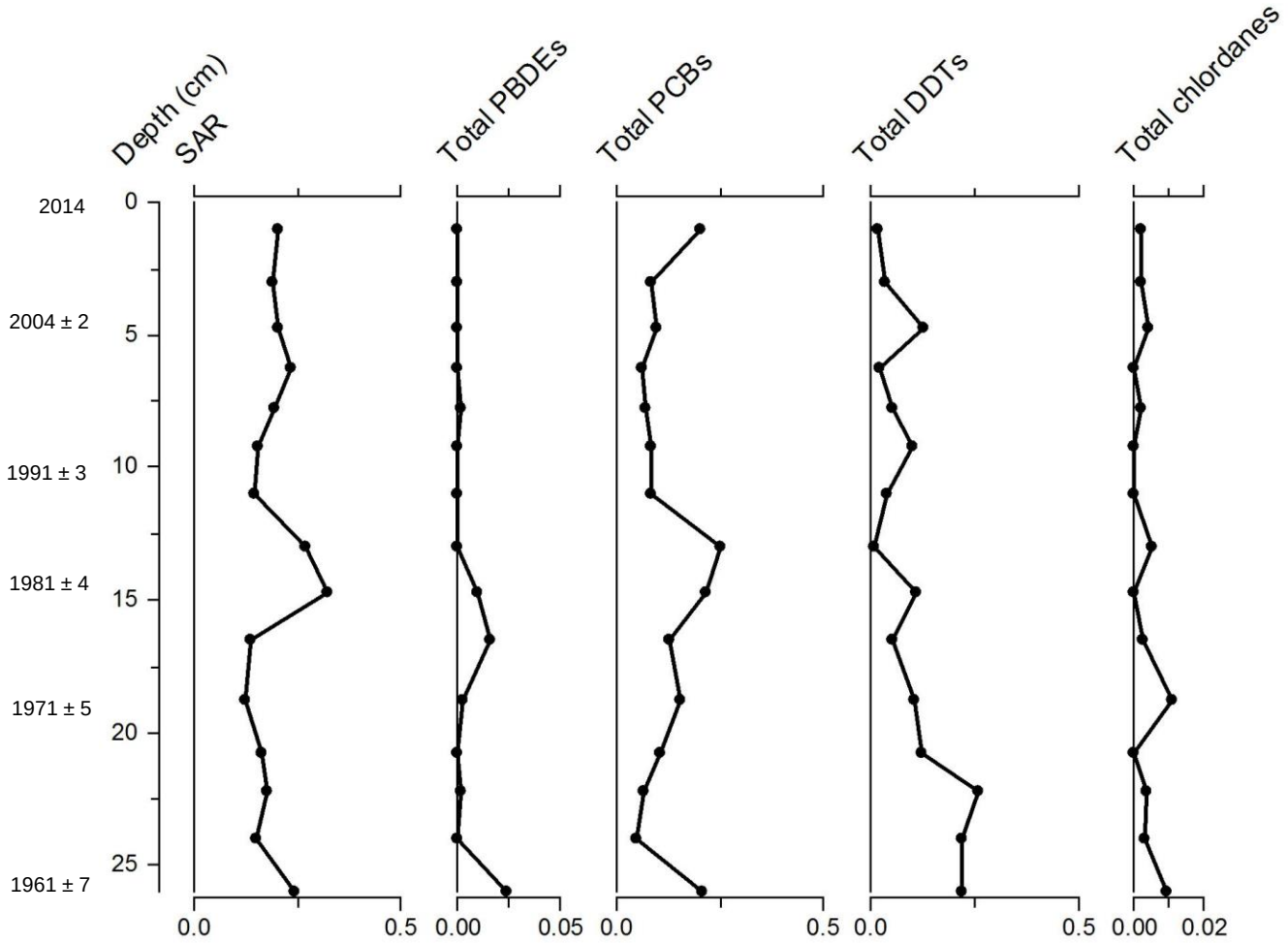

Figure 5.31. Sediment accumulation rate (SAR) and fluxes of HOCs from Black Lake. Unit for SAR is g cm^{-2} yr^{-1}. Unit for HOC fluxes is ng cm^{-2} yr^{-1}. Radioisotope-derived dates and confidence limits are highlighted on the y-axis. Italicized dates are extrapolated beyond ^{210}Pb radioisotope dating.

5.3.3.5 Spheroidal carbonaceous particles

SCP concentration and accumulation rate profiles from the BRYT02 sediment core are detailed in Figure 5.32. SCPs are first detected at Black Lake c. 1930. Concentrations were below 1000 SCPs g^{-1} dry mass until c. 2000, when concentrations increased above 1000 SCPs g^{-1} dry mass in the early-2000s and remained elevated until the surface. Elevated SCP concentrations and flux since ~2005 at Black Lake may be linked to increases in SAR since ~2000.

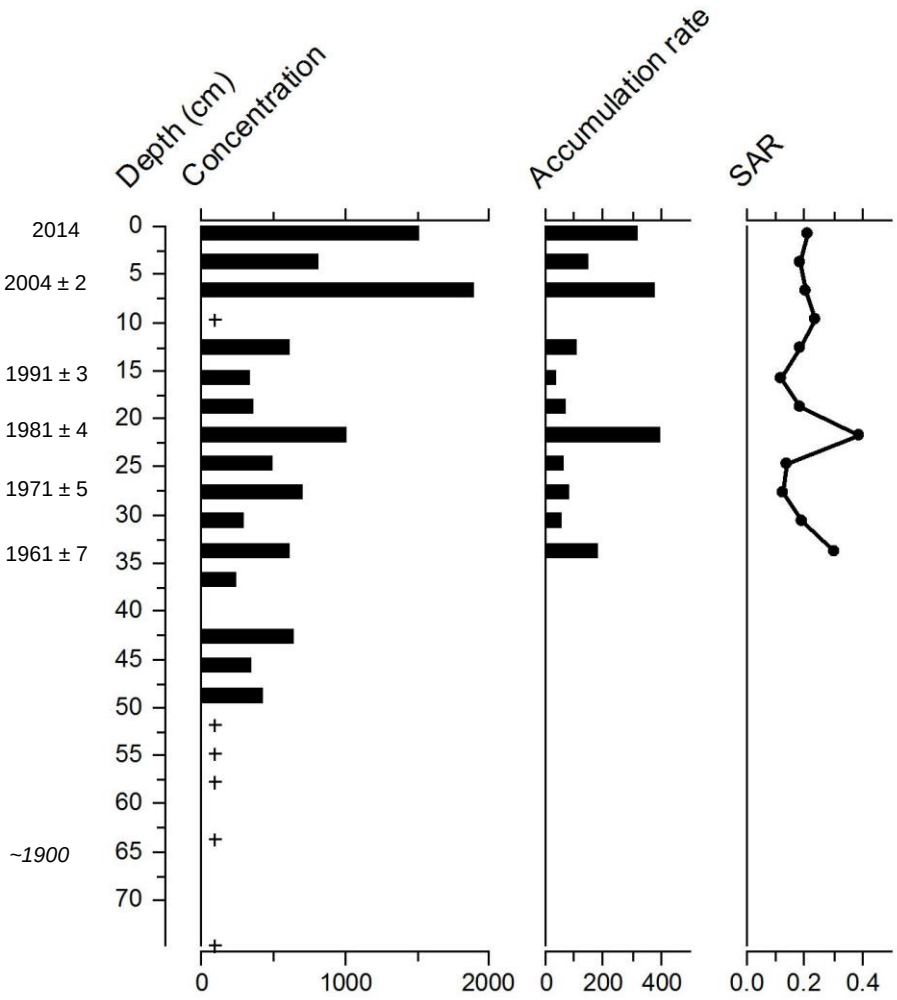

Figure 5.32. Concentrations and accumulations rates of SCPs from Black Lake. Units for concentrations are no. SCPs g^{-1} dry mass, unit for accumulation rate is no. SCP cm^{-2} yr^{-1}. Sediment accumulation rate (SAR) is also plotted. Unit for SAR is g cm^{-2} yr^{-1}. (+) indicates a sample was counted with zero SCPs found. Radioisotope-derived dates and related uncertainties are posted. Italicized dates are extrapolated beyond ^{210}Pb radioisotope dating.

5.3.3.6 Summary of contaminant history at Black Lake

SCPs were first detected at Black Lake c. 1930 (Figure 5.32), approximately the same time as the first detection of HOCs in the lake sediment record (Figure 5.29), likely indicating this to be a time of increasing anthropogenic contamination in the Gusinoye region. PAH concentration began to increase in the mid-1940s, while the period of major contamination for both PAHs and HOCs spanned the 1950s to 1970s (Figure 5.25, Figure 5.29). Despite increases in other anthropogenic contaminants, trace metal and elemental enrichment factors remain around background levels for most of the record. Declining concentrations of PAHs and HOCs occurred in the late-1970s and into the 1980s, however many PAHs remain elevated above background concentrations into the 21st century.

5.4 Discussion

5.4.1 Contamination of Selenga River basin lakes in a global context

Concentrations of anthropogenic contaminants, SCPs, PAHs and HOCs recorded in lake sediments of the Selenga River basin, southeast Siberia throughout the past ~150 years, are 1-3 orders of magnitude lower than many highly-contaminated sites, such as those in close proximity or downwind of industrial or urban sources, including urban freshwater river systems (Kanzari *et al.,* 2014), Scandinavian lakes (Korhola *et al.*, 1999), and lakes in European alpine regions (van Drooge *et al.,* 2011). Total PAH and total PCB concentrations found in this study were also lower than those observed in a recent contemporary study of surface sediments from Lake Baikal (Ok *et al.*, 2013). However, PAH and HOC contaminant concentrations observed are 1-2 orders of magnitude higher than 20th century concentrations from some very remote systems, including freshwater lakes in the Canadian Arctic (0.20 ng/g ∑DDT, 0.33 ng/g ∑HCHs) (Stern *et al.,* 2005). SCPs concentrations during the peak period, between ~1950 and ~2000, were similar in scale to those concentrations reported from surface sediments in the 1990s of other northern hemisphere remote lakes, including from the Shetland Islands (250-1500 g^{-1} dry mass) (Rose and Juggins, 1994), Scandinavia (100-2000 g^{-1} dry mass) (Wik and Renberg, 1991), and Svalbard (500-1000 g^{-1} dry mass) (Rose, 2004). Similarly, PAH and HOC concentrations found in this study are similar to remote areas, including freshwater systems of the Northern Tibetan Plateau (11-279 ng/g $\sum_{15}$PAHs) and the North American Rocky Mountains (31-280 ng/g $\sum_{16}$PAHs) (Usenko *et al.,* 2007; Wang *et al.,* 2010), as well as other freshwater deltas, including the Mekong River Delta, Vietnam (<LD – 6.6 ng/g ∑DDT, <LD – 1.3 ng/g ∑HCH) (Minh *et al*., 2007). Therefore, the contaminant records from the shallow lakes of the Selenga River basin indicate low to moderate levels of contamination during the 20th and 21st centuries, with definite signals of increasing anthropogenic contamination from POPs and SCPs.

5.4.2 Regional signals of anthropogenic contamination across the Selenga River basin since the 19th century

The earliest signs of potential anthropogenic contamination of the ecosystems of the Selenga River basin are from low concentrations of SCPs found at SLNG04 and SLNG05 in the mid- to late-19th century. However, low concentrations of SCPs at this time mean that local and

regional activities cannot be separated out from long-range sources (Rose *et al.*, 2003). These signals of anthropogenic contaminants do not occur simultaneously across the Selenga River basin, as SCPs are not detected at Black Lake until the 20th century (c. 1930). However, SCP concentrations are very low especially during the early years of detection, and it may be that SCPs at Black Lake prior to c. 1930 fall below the limits of detection (Rose, 1994). Temporal SCP records from the Baikal region have indicated limited contamination in the 19th century, with rare findings of SCPs in sediments from the mid-19th century (Rose *et al*., 1998). While Rose *et al*. (1998) reported one record from the southern basin of Lake Baikal in which the SCP profile extended back to c. 1850, other evidence resulted in their postulation that long-range transport of the SCPs to Lake Baikal was unlikely. Yet regional/local industrial activities which used high temperature combustion did not commence in the area until the 20th century. Therefore the mid-19th century occurrence of SCPs was most likely the result of either early long-range transport, as the start of the SCP records from SLNG04 and SLNG05 do not pre-date the start of SCP profiles from Europe (1850s – 1860s), or contamination from more recent sediments.

Time period	*Mid-19th century*	*Late-19th century*	*Early-20th century (c. 1920/1930)*	*Mid-20th century (c. 1950/1960)*	*Late-20th century (c.1980/1990)*	*Early-21st century (c. 2000/2010)*
SLNG04	Start of SCP record Hg EF >1	As EF >3	Start of HOC record (PCBs and Dieldrin) Total PAH increase	Hg increase EF >3 Cu increase EF >2 Peak As EF ~30 SCP concentration increase HMW PAH and HOC increase	As decline, EF>3 HMW PAH decrease Total PAH decrease HOC decrease	SCP decrease As EF > 3 Cu EF > 2 Hg EF ~ 3
SLNG05		Start of SCP record As EF >1	As EF >3	Peak As EF >5 SCP concentration increase	As EF decrease (EF <1) SCP concentration decrease	SCP concentration increase
Black Lake			Start of SCP record Start of HOC record	Total PAH and HOC increases HMW PAH increase	Most PAHs decrease HOC decrease	SCP concentration increase
Main drivers	Long-range transport	Long-range transport	Regional development Agricultural intensification Economic development	Local and regional development Industrial expansion Pulp and Paper Mill construction Construction of Gusinoozersk State Regional Power Plant Agriculture	Decline in local and regional soviet economies Improvement of factories (e.g. Selenginsk Pulp and Paper Mill became a closed system)	Continued local and regional sources Gusinoozersk State Regional Power Plant Mining operations

Table 5.6. Summary table of contamination records obtained from sediment cores from the Selenga River basin, including main drivers and spatial scales.

Regional signals of contamination from organic pollutants start in the 1920s and 1930s, primarily in the form of increases in PAH concentrations above background levels and detectable concentrations of ∑PBDEs, ∑PCBs and ∑HCHs at SLNG04, and detectable concentrations of most HOCs at Black Lake. The increase in organic contaminant concentrations at both sites in the 1920s and 1930s may indicate the earliest use of pesticides and industrial applications in the Selenga River basin. The increase in PAH concentrations at SLNG04 in the 1930s occurred from increases in both LMW and HMW PAHs, possibly indicating a local source, but doesn't preclude the possibility of an increase in atmospherically transported pollutants to the region, which was the likely cause of mid-19th century detection of SCPs in SLNG04 and SLNG05. SCPs were first detected at Black Lake c. 1930, approximately the same time as the first detection of HOCs in the Black Lake sediment record, likely indicating this to be the timing of increased anthropogenic contamination in the Gusinoye region. The initial increase in SCP concentration from Lake Baikal sediment records also occurred in the 1920s/1930s, particularly in the south and central basins (Rose *et al*., 1998), while the SCP record from Lake Kholodnoye, in the southern Baikal region, increased c. 1940 (Flower *et al*., 1997). These SCP and POPs records indicate a likely regional source for contamination in the southern Baikal region, beginning in the 1920s/1930s. This first increase in contaminants is concurrent with the onset of the 5-year plans for economic growth in the USSR, which would stretch from 1928 through to 1991 (Dienes, 1987; Khanin, 2003). The 1930s and 1940s in the USSR saw the beginning of infrastructure development for the expansion of industries and transportation in Siberia, and led to great industrial growth beginning in the 1930s relative to previous decades (Orlov, 1970).

Beginning in the late-1940s, Selenga River basin lakes began to experience extensive and continuous anthropogenic contamination. In the mid-1940s, rapid increases in most PAHs and HOCs occurred at Black Lake, likely signaling the increase in local industrialization (Figure 5.25, Figure 5.29; Pisarsky *et al*., 2005). This initial increase in POPs concentrations at Black Lake occurred concurrently with increasing SCP concentrations at SLNG05 (Figure 5.32). Increasing POPs concentrations occurred slightly later at SLNG04, with rapid increases in POPs concentrations occurring in the 1950s and 1960s in this lake (Figure 5.7), concurrently with increases in HOC concentrations at Black Lake. Increases in Hg, Cu, and SCP concentrations

at SLNG04 began to increase at similar times, beginning in the 1950s, likely indicating increases in coal combustion. The concurrent increases in trace metals, POPs and SCPs across Selenga River basin lakes during the 1940s/1950s/1960s, suggests that the decades immediately following WWII were a time of rapid development in this region of southern Siberia, the timing of which coincides nationally with the Russian economy's recovery to pre-war levels during the fourth to sixth five-year plans (Orlov, 1970), and the global trends in post-war anthropogenic development and rapid industrialization in the second half of the 20th century, termed "the Great Acceleration" (Steffen *et al*., 2015). Sedimentary SCP profiles from Lake Baikal also indicated the start of rapid increase in SCP concentrations in the 1950s/1960s across most of the lake, and likely reflected local to regional increases in industrialization across southeast Siberia (Rose *et al*., 1998). Further, the start of the rapid increase in SCP concentrations in sedimentary records is a global indicator of rapid industrialization c. 1950 (Rose, 2015).

PAH concentration increases recorded at both sites in the 1950s and 1960s is largely due to an increase in ∑HMW PAHs likely indicating the increase in local sources of combustion. This, coincident with the increase in SCPs at all sites during these decades, likely indicates increasing local sources of combustion in southern Siberia. The decades closely following the end of WWII were characterized by great increases in industrial development and population growth in southeastern Siberia, and the 1950s have been characterized as a decade of intense economic growth and industrial expansion in the USSR (Khanin, 2003). Much of the industrial and mining expansions began in the Selenga River basin in the 1940s (Pisarsky *et al.,* 2005), it is likely that the increased organic contaminant and trace metal concentrations detected in the sediment record at this time at Black Lake reflects the industrial and population growth experienced in the region in the 1940s. Opencut coal mining began in the Gusinoye region in the 1940s, quickly followed by military installations, the construction of the Trans-Mongolian Railroad, and the construction of the Gusioozersk State Regional Power Plant by the 1960s (Pisarsky *et al*., 2005). Sources of combustion related to local industrial activities along the Selenga River and in the river basin, included facilities along the Selenga River in Selenginsk and Ulan-Ude, and around Lake Baikal in Baikalsk. Local sources of PCBs through the latter 20th century around the Lake Baikal region, including the pulp and paper mill in Selenginsk,

upstream of the Selenga Delta, which opened in 1973 and until becoming a closed system in 1990, was an open system, leaching chlorinated by-products into the surrounding environment (Kannan *et al.,* 1998).

Subsurface peaks and then declines to the surface are observed for most HOCs, PAHs, SCPs, and trace metals across sedimentary records. Most POPs concentrations peak at both SLNG04 and Black Lake in the 1970s/1980s, and undergo declines in concentrations starting in the mid- to late-1970s and early-1980s, with some HOCs returning to near background levels in the late-20th century. Noted declines in contaminant concentrations of some HOCs into the 21st century are likely due to the discontinued production of HOCs in the Baikal region in the late-20th century, including the halted production of PCBs in Russia between 1990 and 1993, but also potentially related to the decline in agricultural activities and reduction in arable lands in the Selenga River basin beginning c.1990 (Bazhenova and Kobylkin, 2013). Reduction may also be attributed to the global restrictions on the production of POPs, and use following the 1998 Aarhus Protocol on POPs, and the 2001 Stockholm Convention (AMAP, 2000; UNEP, 2001; Tsydenova *et al.,* 2004). Further, the decline in concentrations of organic contaminants coincided with increased destabilization in the economy of the USSR in the mid-1980s, and recorded declines in economic and industrial growth (Khanin, 2003), preceding the collapse of the Soviet Union in 1991. Sampson *et al.* (2002) found that ∑PCB concentrations of the 1990s from sediments and fish tissue along the Selenga River between Selenginsk and the middle of the Selenga Delta were not significantly different from each other, with decreasing concentrations from Selenginsk to the entrance to the Selenga Delta, after which ∑PCBs increased and were relatively elevated into the Delta. Sampson *et al.* (2002) postulated that the lack of clear geographic pattern and relatively low concentrations between Selenginsk and the Selenga Delta may indicate lack of a local PCB source by the late-1990s. While findings from SLNG04 and Black Lake confirm declining PCB concentrations between the early-1970s and the late-1990s, recent concentrations of ∑PCBs and other HOCs remained above pre-1930s concentrations throughout most of the recent record at both sites. Continued elevated contaminant concentrations into the 21st century may indicate either continued production in the region, continued long-range transport to the region, or possible leaching of legacy

contaminants into aquatic systems due to their persistence in the environment and lack of proper disposal and removal of contaminant stockpiles (Tsydenova *et al.,* 2004).

SCP concentrations begin to decline at SLNG05 in the 1990s, while both SCPs and Hg concentrations decline in the early years of the 21st century at SLNG04. Declining concentrations of ∑HMW PAHs, SCPs, and Hg by the end of the 20th century may be attributed to the declining Soviet economy, and resulting declines in local fossil fuel combustion sources. Rose *et al*. (1998) also observed SCP concentration peaks c. 1990, and subsequent declines, to the surface, likely related to reductions in fossil fuel consumption in southeast Siberia. However, evidence for continued combustion is recorded into the 21st century, with increased SCP concentrations at Black Lake in the 21st century, peak ∑PAH concentrations at SLNG04 occurring as recently as 2010, and SLNG04 HMW PAHs, and Black Lake PAH and HMW PAH concentrations well above "background" levels to the surface at both sites (Figures 5.7, Figure 5.25). Concentrations remaining above pre-industrial levels may be caused by shifts in primary energy sources in the region, including shifts away from primarily coal to oil, which produces both PAHs and SCPs, and/or natural gas, which will produce PAHs (e.g. Simcik *et al*., 1996). Moreover, Cu, As, and Hg concentrations remained enriched above background levels at SLNG04 into the 21st century. A local source for elevated contaminant levels at Black Lake, and regional to SLNG04, is the continued use of the Gusinoozersk State Regional Power Plant (SRPP), a coal-fired power plant, located near to Black Lake. The plant is in continued use today, and has been running at full-capacity since 1992, utilizing brown-coal from the Guzinoozersk coal mine (A. Shchetnikov, pers. comm.). The records from the shallow lakes of the Selenga River basin, while not displaying high levels of contamination through the 19th to 21st centuries, have recorded distinct regional industrialization trends through southeastern Siberia since the early-20th century, and continue to illustrate the impact potential of anthropogenic industrial activities on aquatic ecosystems.

5.4.3 Geochemical indicators of change at individual Selenga River basin lakes

5.4.3.1 SLNG04

Trace metal and element concentrations and variations in the SLNG04 sediment record may convey more than a history of anthropogenic contamination at the lake, as such variables may be strongly influenced by changes in hydrology due to related changes in allochthonous and

autochthonous inputs to the lake. Hydrological variability is a dominant factor influencing structure and function of wetland systems (Mitsch and Gosselink, 2007), and has likely played an important role in the state of SLNG04 through the 19th and 20th centuries. The first major transition in trace metals and elements occurred in the mid-19th century, with relatively stable concentrations and ratios in the early-19th century giving way to increases or decreases in some element concentrations and ratios by the mid-19th century, including Ca, Ti, Al, Si, and Fe/Mn and Ca/Ti ratios. The timing of the change in concentration and ratio records at SLNG04 coincides with a major earthquake off-shore of the Selenga Delta in Lake Baikal in 1862, which resulted in flooding, and structural changes to the Delta (Vologina *et al.,* 2010). As SLNG04 is in close proximity to the affected region of the Delta, it is possible the earthquake resulted in structural changes to the lake itself, creating a larger or more connected body of water. Further, this is a time of highly fluctuating magnetic susceptibility, likely indicating high levels of sediment influx/erosion or a range of sources providing material to the site (Eriksson and Sandgren, 1999; Gell *et al.,* 2007) (See Section 4.3.3, Figure 4.6).

Trace metal and element concentrations reflect a dynamic, changing lake environment through most of the late-19th to mid-20th centuries. Increasing concentrations of some metals and elements in the early-20th century (c. 1900) including Zn, P, Mn, Fe, and As, likely signals early anthropogenic development in the river basin, and changes in hydrology (Wang *et al.,* 2015). A catastrophic flood event in the late-19th century in Transbaikalia (Kadetova and Radziminovich 2014), possibly captured by the SLNG04 magnetic susceptibility profile as a sharp peak (See Section 4.3.3, Figure 4.6), may have resulted in the remobilization of redox-sensitive elements within the sediment, due to a reduction of the redox potential of the sediments at this time (Yang *et al.*, 2016). Further, flood events may have resulted in increased permanency of the connection between SLNG04 and the Selenga River, leading to increased element and metal influxes and concentrations.

Increased Ca concentrations between the mid-19th century and c. 1960 (Figure 5.2) is accompanied by increased LOI_{950} (See Section 4.3.3, Figure 4.6), and the appearance of calcite precipitate in the sediment. Increased connectivity to the Selenga River, and increased agricultural activity and anthropogenic disturbances within the Selenga River basin in the early-20th century, may have resulted in increased nutrient flux to SLNG04. Increased nutrient levels

at SLNG04 at this time likely stimulated plant production, leading to increased photosynthetic removal of CO_2 from the water column, and resulting in increased carbonate content and increasing pH and alkalinity (Talling, 1976). Increased transport of calcium to SLNG04 in the early-20th century due to increased agricultural activity in the region may further have contributed to elevated pH and alkalinity (Potasznik and Szymczyk, 2015). Increased pH coinciding with reducing conditions may lead to increased phosphorus release from sediments (Koski-Vahala *et al.,* 2001; Sondergaard *et al.,* 2003; Wu *et al*., 2014). Increased autochthonous phosphorus production would add to the already increasing eutrophic conditions at SLNG04, further stimulating plant productivity, and increasing alkalinity. Increased plant abundance during the early- to mid-20th century may have led to slight reducing conditions at SLNG04, as minimum Fe/Mn ratios coincide with maximum Mn levels and increasing Fe levels c. 1920. Concurrently, increases in P and As are observed, peaking c. 1950, which occurs at a similar timing as As increases in SLNG05, suggesting a similar disturbance or event at the two Selenga Delta sites.

5.4.3.2 SLNG05

The trace metal and lithogenic element record likely depicts hydrological variability of the lake, rather than contamination from anthropogenic sources. The earliest and most recent zones of trace metal and element concentrations and ratios depict relatively stable lake environments at SLNG05 prior to c. 1880 and post-early-1960, however, the concentration profiles between c. 1880 and the early-1960s indicate a progressively changing system. Gradual increases are observed during this ~80-year period in Ca/Ti ratios, As, Fe, Mn, Br, and P concentrations, in combination with declining and low Fe/Mn ratios and declining concentrations of most other elements and metals. These changes in the trace metal and element record occur concurrently with similar increases in LOI_{550} and LOI_{950}, and similar declines in magnetic susceptibility at SLNG05 (See Section 4.3.3, Figure 4.8). It is likely that the increasing organic matter (LOI_{550}) led to increased rates and occurrences of decomposition, and decreased oxygen concentrations in the water. High levels of organic matter can induce or enhance reducing conditions at the sediment-water interface (Oldfield, 2013), which are evidenced at this time in SLNG05 through low Fe/Mn ratios (Figure 5.15). The low oxygen concentrations and increased reducing conditions likely resulted in dissolution diagenesis of

many of the lithogenic elements upon burial in the early- to mid-20th century, which has been shown to coincide with high within-lake productivity (Boyle *et al.,* 2004; Oldfield, 2013). The increased organic matter in SLNG05 likely resulted from a shallowing of the lake due to disconnection from the Selenga River c. 1880. Increasing Ca/Ti ratios between c. 1880 and the early-1960s may be evidence of decreasing size and depth of the lake or more rapid in-filling (Figure 5.15), which indicate increased evaporative conditions in the lake and increased autochthonic calcite production (Davies, 2015). Reducing conditions in the late-19th century to mid-20th century at SLNG05 may have also led to increased mobilization of As. Positive correlations between As with SO_4^{2-} and Fe may indicate sulphide- or iron-oxyhydroxide-induced remobilization of As from sediments (Yang *et al*., 2016). The increase in As at SLNG05 occurred simultaneously to increased As concentrations at SLNG04, suggesting an event or disturbance that was experienced throughout the Selenga Delta in the late-19th to mid-20th century, including changes in water levels resulting in chemical changes to the lakes.

5.4.3.3 Black Lake

The record of trace metals and element concentrations and ratios from Black Lake may indicate that the series of industrialization events in the Gusinoye region in the 1940s and 1950s resulted in a change in source to the lake in the late-1940s. Prior to the late-1940s, Black Lake had low Fe/Mn ratios (Figure 5.20), high evaporative properties characterized by autochthonic calcite production and mollusc communities (See Section 4.3.3, Figure 4.9). Most major and trace element concentrations were low, with the exceptions of Ca, Br, and Mn. Rapidly in the late-1940s and early 1950s, conditions at Black Lake changed, with increased Fe/Mn ratios, lower evaporative properties and a disappearance of molluscs, and increases in most trace metals and elements, with the exception of Ca, Br, and Mn, which declined in concentrations. Further, concentrations remained steady following the increase or decrease. The change in trace element concentrations occurred at a similar time as the increase in PAH concentrations at Black Lake. Fe and Mn concentrations in the Black Lake sediment record have opposing temporal trends, with peaks in the Fe/Mn ratio coinciding with peaks in iron concentrations, indicating that the change in the ratio is likely explained by changes in supply from the river basin (Boyle, 2001). Further, it is unlikely that the low Fe/Mn ratios are indicative of a reducing environment, as As and other redox-sensitive elements concentration profiles, while similar to

Fe, are also temporally similar to other trace metals (Boyle, 2001). Ti is positively correlated with most trace metals and elements, while Ca, Br, and Mn are positively correlated with LOI_{550}. Moreover, Ti and LOI_{550} are negatively correlated, indicating differing controls for mineral and organic matter supply (Boyle *et al.,* 2004), and potentially indicating a higher influx of mineral sources post-1950, coinciding with increased development and industrialization near Lake Gusinoye and in close proximity to Black Lake in the 1950s (Pisarsky *et al.*, 2005).

5.5 Conclusions

Selenga River basin lakes record regional and long-range atmospheric contamination since the 19th century. Analysis of trace element, SCP, and POPs sediment records from three lakes within the Selenga River basin in southeast Siberia, indicate varying levels of anthropogenic and natural disturbances. The earliest detection of contamination occurred in the mid to late-19th century with increases in SCP concentrations, likely as a result of long-range atmospheric transport of contaminants to the region. The major period of increasing contamination in the Selenga River basin began in the mid-20th century, in the decades immediately following World War II, coinciding with much of the Northern Hemisphere post-war development, the Great Acceleration, and the Russian economic growth plans of the 20th century. There is minimal variability between lakes with respect to the onset of contamination in the 20th century, and all lake sediment records show increasing contamination in the mid-20th century, continuing into the late-20th and early 21st centuries. Declines in contaminant concentrations in the late-20th and early-21st centuries are likely due to declining industrialization in Russia following destabilization of the former U.S.S.R. However, contamination into the 21st century is observed, indicating the continued existence of contamination sources. Temporal changes in trace element and metal concentrations at individual lakes are likely related to local influences, primarily hydrological changes and local anthropogenic disturbances. High concentrations of trace elements are most likely related to naturally high levels in the watershed, chemically-enhanced concentrations due to changing redox conditions, or allochthonous inputs from local human disturbances, including nearby agricultural practices and development. Sediment records from the Selenga River basin lakes indicate the impact that changes in lake chemistry, owing, for example, to changes in nutrient status and redox conditions, may have upon the trace metal and element records within

shallow lakes, and indicates the importance of considering within-lake changes when interpreting such sediment records.

5.6 References

AMAP Report. (2000) PCB in Russia Federation: Inventory and proposals for priority remedial actions. Arctic Monitoring and Assessment Program, Oslo, Norway.

Bícego M.C., Taniguchi S., Yogui G.T., Montone R.C., da Silva D.A.M., Lourenço R.A., Martins C.C., Sasaki S.T., Pellizari V.H., & Weber R.R. (2006) Assessment of contamination by polychlorinated biphenyls and aliphatic and aromatic hydrocarbons in sediments of the Santos and São Vicente Estuary System, São Paulo, Brazil. *Marine Pollution Bulletin* **52**, 1784–1832.

Boës X., Rydberg J., Martinez-Cortizas A., Bindler R., & Renberg L. (2011) Evaluation of conservative lithogenic elements (Ti, Zr, Al, and Rb) to study anthropogenic element enrichments in lake sediments. *Journal of Paleolimnology* **46**, 75-87.

Boyle J.F. (2001) Inorganic geochemical methods in Palaeolimnology. In: Tracking Environmental Change Using Lake Sediments. Volume 2: Physical and Geochemical Methods. Eds. W.M. Last, & J.P. Smol, Kluwer Academic Publishers, Dordrecht, the Netherlands. pp. 83-141.

Boyle J.F., Rose N.L., Appleby P.G., & Birks H.J.B. (2004) Recent environmental change and human impact on Svalbard: the lake sediment geochemical record. *Journal of Paleolimnology*, **31**, 515-530.

Davies S. J. (2015) Micro-XRF core scanning in palaeolimnology: recent developments. In: Developments in Paleoenvironmental Research. Volume 17: Micro-XRF Studies of Sediment Cores: Applications of a Non-Destructive Tool for Environmental Sciences. Eds. I.W. Croudace, & R.G. Rothwell, Springer, the Netherlands. pp. 189-226.

Dienes L. (1987) The soviet oil industry in the twelfth five-year plan. *Soviet Geography* **28**, 617-655.

Epstein M.S., Diamondstone B.I., & Gills T.E. (1989) A new river sediment standard reference material. *Talanta* **36**, 141-150.

Eriksson M. G. & Sandgren P. (1999) Mineral magnetic analyses of sediment cores recording recent soil erosion history in central Tanzania. *Palaeogeography. Palaeoclimatology. Palaeoecology*. **152,** 365–383.

Flower R.J., Politov S.V., Rippey B., Rose N.L., Appleby P.G., & Stevenson A.C. (1997) Sedimentary records of the extent and impact of atmospheric contamination of a remote Siberian highland lake. *The Holocene* **7,** 161-173.

Gell P., Tibby J., Little F., Baldwin D., & Hancock G. (2007) The impact of regulation and salinization on floodplain lakes: the lower River Murray, Australia. *Hydrobiologia* **591,** 135-146.

Imaeda D., Kunisue T., Ochi Y., Iwata H., Tsydenova O., Takahashi S., Amano M., Petrov E.A., Batoev V.B., & Tanabe S. (2009) Accumulation features and temporal trends of PCDDs, PCDFs, and PCBs in Baikal seals (Pusa siberica). *Environmental Pollution* **157**, 737-747.

Iwata H., Tanabe S., Ueda K., & Tatsukawa R. (1995) Persistent organochlorine residuesin air, water, sediments, and soils from the Lake Baikal region, Russia. *Environmental Science & Technology* **29,** 792-801.

Juggins S. (2014) C2 data analysis, Version 1.7.6. University of Newcastle, United Kingdom.

Kadetova A.V., & Radziminovich Y.B. (2014) The catastrophic flood in Transbaikalia (Central Asia) in 1897: a case study. *Natural Hazards* **72,** 23-441.

Kannan K., Nakata H., Stafford R., Masson G.R., Tanabe S., & Giesy J.P. (1998) Bioaccumulation and toxic potential of extremely hydrophobic polychlorinated biphenyl congeners in biota collected at a superfund site contaminated with Arochlor 1268. *Environmental Science & Technology* **32**, 1214-1221.

Kanzari F., Syakti A.D., Asia L., Malleret L., Piram A., Mille G., & Doumenq P. (2014) Distributions and sources of persistent organic pollutants (aliphatic hydrocarbons, PAHs, PCBs, and pesticides) in surface sediments of an industrialized urban river (Huveaune), France. *Science of the Total Environment* **478**, 141-151.

Khanin G.I. (2003) The 1950s – the triumph of the Soviet economy. *Europe-Asia Studies* **55**, 1187-1212.

Korhola A., Weckstrom J., & Nyman M. (1999) Predicting long-term acidification trends in small subarctic lakes using diatoms. *Journal of Applied Ecology* **36**, 1021-1034.

Koski-Vahala J., Hartikainen H., & Tallberg P. (2001) Phosphorus mobilization from various sediment pools in response to increased pH and silicate concentration. *Journal of Environmental Quality* **30**, 546-552.

Kucklick J.R., Harvey H.R., Ostrom P.H., Ostrom N.E., & Baker J.E. (1996) Organochlorine dynamics in the pelagic food web of Lake Baikal. *Environmental Toxicology and Chemistry* **15**, 1388 – 1400.

Lorgeoux C., Moilleron R., Gasperi J., Ayrault S., Bonté P., Lefèvre I., & Tassin B. (2016) Temporal trends of persistent organic pollutants in dated sediment cores: Chemical fingerprinting of the anthropogenic impacts in the Seine River basin, Paris. *Science of the Total Environment* **541,** 1355-1363.

Ma J., Hung H., Tian C., & Kallenborn R. (2011) Revolatilization of persistent organic pollutants in the Arctic induced by climate change. *Nature Climate Change* **1**, 255-260.

MacDonald D.D., Ingersoll C.G., & Berger T.A. (2000) Development and evaluation of consensus-based sediment quality guidelines for freshwater ecosystems. *Archives of Environmental Contamination and Toxicology* **39**, 20-31.

Mamontov A.A., Mamontova E.A., & Tarasova E.N. (2000) Tracing the sources of PCDD/Fs and PCBs to Lake Baikal. *Environmental Science & Technology* **34**, 741-747.

Martins CC., Bícego M.C., Mahiques M.M., Figueira R.C.L., Tessler M.G., & Montone R.C. (2011) Polycyclic aromatic hydrocarbons (PAHs) in a large South American industrial coastal area (Santos Estuary, Southeastern Brazil): Sources, and depositional history. *Marine Pollution Bulletin* **63**, 452-458.

Minh N.H., Minh T.B., Kajiwara N., Kunisue T., Iwata H., Viet P.H., Tu N.P.C., Tuyen B.C., & Tanabe S. (2007) Pollution sources and occurrences of selected persistent organic pollutants (POPs) in sediments of the Mekong River delta, south Vietnam. *Chemosphere* **67**, 1794-1801.

Mitsch W.J., & Gosselink J.G. (2007) Wetlands, 4th Edition. Wiley & Sons, United States of America.

Ok G., Shirapova G., Matafonova G., Batoev V., & Lee S.H. (2013) Characteristics of PAHs, PCDD/Fs, PCBs, and PBDEs in the sediment of Lake Baikal. *Polycyclic Aromatic Compounds* **33**, 173-192.

Oldfield F. (2013) Mud and magnetism: records of late Pleistocene and Holocene environmental change recorded by magnetic measurements. *Journal of Paleolimnology* **49,** 465-480.

Orlov B.P. (1970) Tendencies of economic development in Siberia and Promotion of the region's role in the national economy. *Soviet Geography* **11**, 1-13.

Pisarsky B.I., Hardina A.M., & Naganawa H. (2005) Ecosystem evolution of Lake Gusinoe (Transbaikal Region, Russia). *Limnology*, **6**, 173-182.

Potasznik A., & Szymczyk S. (2015) Magnesium and calcium concentrations in the surface water and bottom deposits f a river-lake system. *Journal of Elementology* **20,** 677-692.

Robinson W.P., & Anosova G.B. (2004) Mining and mineral development management policy in the Selenga River Watershed. In: Science for Watershed Conservation: Mulitdisciplinary Approaches for Natural Resource Management Conference, Ulan-Ude, Russia and Ulanbaatar, Mongolia.

Rose N.L. (1994) A note on further refinements to a procedure for the extraction of carbonaceous fly-ash particles from sediments. *Journal of Paleolimnology* **11**, 201-204.

Rose N.L. (1995) Carbonaceous particle record in lake sediments from the Arctic and other remote areas of the Northern Hemisphere. *Science of the Total Environment* **160/161,** 487-496.

Rose N.L. (2008) Quality control in the analysis of lake sediments for spheroidal carbonaceous particles *Limnology and Oceanography: Methods* **6**, 172–179.

Rose N.L. (2015) Spheroidal carbonaceous fly ash particles provide a globally synchronous stratigraphic marker for the Anthropocene. *Environmental Science and Technology* **49,** 4155-4162.

Rose N.L., & Juggins S. (1994) A spatial relationship between carbonaceous particles in lake sediments and sulphur deposition. *Atmospheric Environment* **28**, 177-183.

Rose N.L., Rose C.L., Boyle J.F, & Appleby P.G. (2004) Lake sediment evidence for local and remote sources of atmospherically deposited pollutants on Svalbard. *Journal of Paleolimnology* **31**, 499 – 513.

Rose N.L., Appleby P.G., Boyle J.F., Mackay A.W., & Flower R.J. (1998) The spatial and temporal distribution of fossil-fuel derived pollutants in the sediment record of Lake Baikal, eastern Siberia. *Journal of Paleolimnology* **20**, 151-162.

Rose N.L., Flower R.J., & Appleby P.G. (2003) Spheroidal carbonaceous particles (SCPs) as indicators of atmospherically deposited pollutants in North African wetlands of conservation importance. *Atmospheric Environment* **37**, 1655‑1663.

Sampson J.R., Tarasova E.A., Mamontova E.M., Mamontov A.A., Chandra S., Kalmychkov G.V., & Toupitsyn I.I. (2002). Polychlorinated biphenyls and mercury in sediments and aquatic biota, nearshore juvenile fish communities and aquatic food web structure in the Lower Selenga River, Russia. 10,000 Years Institute, 84 pp.

Simcik M.F., Eisenreich S.J., Golden K.A., Liu S.P., Lipiatou E., Swackhamer D.L., & Long D.T. (1996) Atmospheric loading of polycyclic aromatic hydrocarbons to Lake Michigan as recorded in the sediments. *Environmental Science & Technology* **30**, 3039-3046.

Sondergaard M., Johansson L.S., Lauridsen T.L., Jorgensen T.B., Liboriussen L., & Jeppesen E. (2010) Submerged macrophytes as indicators of the ecological quality of lakes. *Freshwater Biology* **55**, 893-908.

Steffen W., Broadgate W., Deutsch L., Gaffney O., & Ludwig C. (2015) The trajectory of the Anthropocene: The Great Acceleration. *The Anthropocene Review* **2,** 81-98.

Stern G.A., Braekevelt E., Helm P.A., Bidleman T.F., Outridge P.M., Lockhart W.L., McNeeley R., Rosenberg B., Ikonomou M.G., Hamilton P., Tomy G.T., & Wilkinson P. (2005) Modern and historical fluxes of halogenated organic contaminants to a lake in the Canadian arctic, as determined from annually laminated sediment cores. *Science of the Total Environment* **342**, 223-243.

Talling S.J. (1976) The depletion of carbon dioxide from lake water by phytoplankton. *Journal of Ecology* **64,** 79-121.

Ter Braak C.J.F. & Šmilauer P. (2012): Canoco reference manual and user's guide: software for ordination, version 5.0. Microcomputer Power, Ithaca, USA, 496 pp.

Thorslund J., Jarsjo J., Chalov S.R., & Belozerova E.V. (2012) Gold mining impact of riverine heavy metal transport in a sparsely monitored region: the upper Lake Baikal Basin case. *Journal of Environmental Monitoring* **14,** 2780-2792.

Tsydenova O., Binh Minh T., Kajiwara N., Batoev V., & Tanabe S. (2004) Recent contamination by persistent organochlorines in Baikal seal (Phoca sibirica) from Lake Baikal, Russia. *Marine Pollution Bulletin* **48**, 749-758.

UNEP (United Nations Environment Programme). (1992) Determinations of Petroleum Hydrocarbons in Sediments. Reference Methods for Marine Pollution Studies, 75 pp.

UNEP (United Nations Environment Programme). (2001) Stockholm Convention on POPs , Text and Annexes, Interim Secretariat for the Stockholm Convention on Persistent Organic Pollutants, UNEP Chemicals, Geneva, Switzerland.

Usenko S., Landers D.H., Appleby P.G., & Simonich S.L. (2007) Current and historical deposition of PBDEs, pesticides, PCBs, and PAHs to rocky mountain national park. *Environmental Science & Technology* **41**, 7235-7241.

van Drooge B.L., Lopez J., Fernandez P., Grimalt J.O., & Stuchlik E. (2011). Polycyclic aromatic hydrocarbons in lake sediments from the High Tatras. *Environmental Pollution* **159**, 1234-1240.

Vologina E.G., Kalugin I.A., Osukhovskaya Y.N., Sturm M., Ignatova N.V., Radziminovich Y.B., Dar'in A.V., & Kuz'min M.I. (2010) Sedimentation in Proval Bay (Lake Baikal) after earthquake-induced subsidence of part of the Selenga River delta. *Russian Geology and Geophysics*, **51,** 1275-1284.

Wade T.L., & Cantillo A.Y. (1994) Use of standards and reference materials in the measurement of chlorinated hydrocarbon residues. Chemistry Workbook. NOAA Technical Memorandum NOS ORCA, vol. 77, p. 59.

Wang X.P., Yang H.D., Gong P., Zhao X., Wu G.J., Turner S., & Yao T.D. (2010) One century sedimentary records of polycyclic aromatic hydrocarbons, mercury and trace elements in the Qinghai Lake, Tibetan Plateau. *Environmental Pollution* **158**, 3065-3070.

Wang H., Wang J., Yu W., & Shen Z. (2015) Spatial variation, environmental risk, and biological hazard assessment of heavy metals in surface sediments of the Yangtze River estuary. *Marine Pollution Bulletin* **93,** 250-258

Wania F. (2003) Assessing the potential of persistent organic chemicals for long-range transport and accumulation in polar regions. *Environmental Science and Technology* **37**, 1344-1351.

Wania F., & Mackay D. (1996) A global distribution model for persistent organic chemical. Science of the Total Environment 160/161, 211-232.

Weiss D., Shotyk W., Appleby P.G., Kramers J.D., & Cheburkin A.K. (1999) Atmospheric Pb deposition since the industrial revolution recorded by five Swiss peat profiles: enrichment factors, fluxes, isotopic composition, and sources. *Environmental Science and Technology* **33**, 1340-1352.

Wik M., & Renberg I. (1991) Recent atmospheric deposition in Sweden of carbonaceous particles from fossil-fuel combustion surveyed using lake sediments. *Ambio* **20**, 289–292.

Wu Y., Wen Y., Zhou J., & Wu Y. (2014) Phosphorus release from lake sediments: effects of pH, temperature, and dissolved oxygen. *Journal of Civil Engineering* **18**, 323-329.

Yang H.J., Lee C.J., Chiang Y.J., Jean J.S., Shau Y.H., Takazawa E., & Jiang W.T. (2016) Distribution and hosts of arsenic in a sediment core from the Chianan Plane in SW Taiwan: Implications on arsenic primary source and release mechanisms. *Science of the Total Environment* **569,** 212-222.

Chapter 6: Sedimentary record of biological change in SLNG04

6.1 Introduction to SLNG04 and the north-east side of Selenga Delta

Local and regional events have the potential to impact ecological structure and functioning of shallow lake ecosystems. Many northern delta and shallow lake ecosystems have been impacted by direct or indirect modifications of flow regimes and flood disturbances, anthropogenic pollution, and introduction of invasive species (Dynesius and Nilsson, 1994, Wolfe et al., 2005; Brock et al., 2011). Water depth is a significant variable influencing diatom and macrophyte distributions in shallow wetland lakes, which may be related to changes in hydrological regimes (Moser *et al.,* 2000; Michelutti *et al*., 2001). Moreover, climate-induced changes in the hydrological regime of freshwater delta wetlands are often attributed to changes in precipitation levels, which can result in complete shifts in the ecological structure of the shallow lakes within the delta wetland due to the strong influence of hydrology on these systems (Marin *et al*., 2009; Cobbaert *et al*., 2014). Inputs of nutrients into the system derived from agricultural runoff, sewage, or industrial waste are the principle causes of eutrophication in freshwater ecosystems, but can also be released from soils during increased periods of sedimentation and erosion (O'Dwyer *et al*., 2013). Such contaminant loadings often impact both ecological structure and function of systems, and cause shifts in primary producer groups in shallow lake environments (Jackson, 2003; Rendsalu-Wendrup *et al*., 2014).

Study site SLNG04 sits within the Selenga Delta, and is a perimeter lake on the northeast side of the Delta. SLNG04 is an expansive, shallow lake, with surface flow connections to both the Selenga River and Lake Baikal, connected to the Lobanovskaya branch of the Selenga Delta (Figure 6.1, Figure 6.2). The northeast perimeter of the Selenga Delta is heavily utilized for agricultural lands, which increased in intensity beginning in the 19th century (Bazhenova and Kohylkin, 2013). As a perimeter lake with high connectivity to the Selenga River currently, SLNG04 has high potential for influence from agricultural practices, runoff from terrestrial environments, and transport of pollutants or invasive species from the river. SLNG04 was likely formed by a combination of multiple natural events in the 19th and 20th centuries. The Tsagan earthquake is 1862 heavily impacted the northeast side of the Selenga Delta, as it was centred just offshore in what is now Proval Bay, resulting in significant morphological changes to the Delta (Vologina *et al*., 2010). Flood events which impacted the whole Selenga Delta occurred c.

1900 as a result of increased rainfall patterns (Kadetova and Radziminovich, 2014), and c. 1960 following the construction of the Irkutsk Dam on the Angara River (Pinegin *et al*., 1976). Agriculture in the Selenga River basin, intensification of related deforestation beginning in the 19th century, and 20th century increases in industrial activities in the Selenga River basin, may have resulted in increased erosion and transport of sediment and contaminants directly into the Selenga River (Bazhenova and Kohylkin, 2013; See Section 1.4.2, Figure 1.3, for detail on the timeline of events within the Selenga River basin).

Figure 6.1. Map of the Selenga Delta with SLNG04 location indicated.

The multitude of physical and chemical changes that have occurred through the 19th and 20th centuries in the Selenga River basin have potential to influence the ecology of SLNG04. However, the ecological response of any shallow lake ecosystem within the Selenga Delta remains unknown. Therefore, the aim of this and following chapters is to investigate how natural and anthropogenic disturbances, beginning in the 19th century, have influenced the structure and functioning of the shallow lake ecosystems in the Selenga River basin, and determine if regional Selenga River basin disturbances, and/or local disturbances within the Selenga Delta have had greater impact, and whether these disturbances have resulted in changes in primary producer biomass, trophic interactions, and ecosystem biodiversity. For this chapter, the aim is

to investigate these impacts in the northeast Selenga Delta, from SLNG04. Specific objectives include:

1) Changes in ecological structure since the early-19th century will be assessed by analyzing algal communities, including diatoms, macrophyte, and invertebrate communities from a sediment core extracted from SLNG04;
2) Changes in ecological functioning of SLNG04 since the early-19th century will be assessed using sedimentary pigment, diatom, and macrofossil records enumerated from a sediment core extracted from SLNG04;
3) Reconstructed ecological shifts derived from sediment cores will be assessed and compared with historical records of local (Selenga River Delta) and regional (Selenga River basin) events during the 19th and 20th centuries.

a b

Figure 6.2. a) SLNG04, view from open water, facing southeast; b) SLNG04 view from shore, facing northwest.

6.2 Methods for analysis of biological proxies from SLNG04

Details of coring method, sediment core extruding, and sediment core partitioning for analyses are described in Section 4.2.

6.2.1 Sedimentary macrofossils

Subsamples at 3.0-cm intervals from sediment core SLNG04-C were analysed for macrofossils using the displacement method, and standard sieving and picking methods (Birks, 2001). All methods for macrofossil laboratory processing, microscopy, enumeration, and identification followed procedures outlined in Section 3.2.1.2. Plant and animal macrofossil data were standardized as the number of fossil remains per 100 cm^3 wet sediment. To facilitate comparisons between sites, and to assess abundance of macrofossil remains within a single

core taking into account influences of varying sedimentation, fluxes of macrofossils were calculated by first determining the total number of remains per g dry sediment. Fluxes were then calculated using sedimentation accumulation rates of sediment core SLNG04-C since c. 1945 AD (See Section 4.4.3.1 for details of radioisotope dating of sediment core SLNG04-C).

6.2.2 Sedimentary aquatic macrofossil data analysis

Macrofossil data were transformed by taking the natural ln (x+1) of each count prior to statistical analysis to de-emphasize the influence of very common taxa. Terrestrial macrofossil remains were removed from statistical analysis to focus on within-lake dynamics. To explore spatial trends in the data, detrended correspondence analysis (DCA) was conducted on the transformed and centred aquatic macrofossil dataset. DCA was detrended by segments, and rare species were downweighted to reduce the impact of rare taxa. DCA was performed using Canoco5 (ter Braak and Šmilauer, 2014). Constrained cluster analysis was performed on the transformed aquatic macrofossils to determine major groupings of depths. Broken stick analysis was performed to determine the number of significant zones within the sedimentary aquatic macrofossil profile for SLNG04-C. Breakpoint analysis was undertaken on the SLNG04 macrofossil DCA axis 1 scores, to determine points of significant change through time. Breakpoint analysis was performed in R, using the segmented package, and cluster analysis and broken stick analysis were performed in R, using the rioja package (R. v.3.2.4, 2016). All stratigraphical plots were constructed using C2 (Juggins, 2014).

6.2.3 Sedimentary diatoms

Diatom analysis was followed according to standard procedures (Battarbee *et al.,* 2001). All diatom laboratory processing and slide preparation methods followed those detailed in Section 3.2.1.3. Enumeration, identification, and numerical analysis followed procedures outlined in Section 3.2.1.3, unless otherwise stated below. Samples were enumerated at 1-cm intervals between 0 cm and 18 cm depth, 2-cm intervals between 20 and 32 cm, 1-cm intervals between 32 and 38 cm depth, and 5-cm intervals between 40 and 60 cm depth. Diatom concentration varied greatly between samples in SLNG04-C, and a minimum of 300 valves were counted per diatom slide when possible: a minimum of 300 valves were enumerated between 0 cm and 20 cm depth and 33 cm and 38 cm depth, while a minimum of 100 valves were enumerated for

depths 22 cm, 24 cm, 40 cm, 45 cm, and 50 cm. Samples 26 cm to 32 cm, and 55 cm and 60 cm (the base of the sediment core) were sparse of diatom valves, and the entire slide was counted. Diatom raw counts were converted to percent relative abundance per sample for those samples with greater than 100 valves enumerated. Only those samples for which a minimum of 300 valves were enumerated were included in species rarefaction analysis. Species rarefaction for SLNG04 was set to 300 valves, which was the total number of valves enumerated at 8 cm, 14 cm, 20 cm, and 38 cm depths. Richness in all other samples was then assessed at 300 valves. Diatom accumulation rates were calculated using sedimentation accumulation rates of sediment core SLNG04-C since c. 1945 AD (See Section 4.4.3.1 for details of radioisotope dating of sediment core SLNG04-C).

6.2.4 Sedimentary diatom assemblage data analysis

To explore temporal trends in the data, unconstrained ordinations were conducted on the centred relative abundance diatom dataset. Only those samples for which a minimum of 100 valves were enumerated were included in the ordinations. Further, ordinations were performed on a condensed dataset which included only those species present at >2% relative abundance, in order to reduce the influence of very rare species. The reduced SLNG04 diatom dataset included 70 species. Exploratory DCA indicated a gradient length of 2.2 SD, indicating the appropriateness of linear ordination techniques. DCA and PCA were performed using Canoco5 (ter Braak and Šmilauer, 2014). Stratigraphical plots of diatom community assemblage relative abundances were constructed, and included all species present at >5% at any one depth (22 species). Cluster analysis was performed to determine major groupings of depths. Broken stick analysis was performed to determine the number of significant zones within the sedimentary diatom profile for SLNG04-C. Cluster analysis and broken stick analysis were performed in R, using the rioja package (R. v.3.2.4, 2016). Stratigraphical plots were constructed using C2 (Juggins, 2014).

6.2.5 Sedimentary pigments

Pigments of photosynthetic organisms were analyzed from sediment samples from SLNG04-C following McGowan *et al.* (2012), and laboratory methods were followed as described in Section 3.2.1.4. Sediment was subsampled for pigment analysis at 1.0-cm intervals

from SLNG04-C as described in Section 3.2.1.6. Pigment fluxes were calculated using sedimentation accumulation rates of SLNG04-C since c. 1945 AD (See Section 4.4.3.1 for details of radioisotope dating of SLNG04-C).

6.2.6 Sedimentary pigment data analysis

To explore temporal trends in the data, unconstrained ordinations were conducted on the centred SLNG04-C sedimentary pigment dataset. Labile pigments (chlorophyll (Chl) *c* and fucoxanthin) were removed from statistical analysis of sedimentary pigments, to exclude major influence of pigment degradation, as described in Sections 3.2.1.4 and 3.2.1.6. Only those samples for which pigments were detected (48 cm to the surface) were included in analyses. Exploratory DCA indicated a gradient length of 1.7 SD, indicating the appropriateness of linear ordination techniques. PCA was then performed on the sedimentary pigment dataset. Unconstrained ordinations were performed using Canoco5 (ter Braak and Šmilauer, 2014). Constrained cluster analysis was performed on SLNG04-C pigments to determine zones of ecological dissimilarity in palaeolimnological data. Broken stick analysis was performed to determine the number of significant zones within the sedimentary pigment profile for SLNG04. Breakpoint analysis was undertaken on the SLNG04 pigment PCA axis 1 scores, to determine points of significant change through time. Breakpoint analysis was performed in R, using the segmented package, and cluster analysis and broken stick analysis were performed in R, using the rioja package (R. v.3.2.4, 2016). All stratigraphical plots were constructed using C2 (Juggins, 2014).

6.2.7 Data analysis of all biological proxies

Co-correspondence analysis (CoCA) was conducted on the species data for the biological indicator records (diatoms*sediment pigments; diatoms*macrofossils; sediment pigments*macrofossils) to compare species composition variation between pairs of biological proxy records, and assess the significance ($p \leq 0.01$) of the co-occurrence of species or groups of species between proxies. CoCA assists in determining if functional groups of species/taxa or guilds tend to co-occur, further aiding in the interpretation of temporal community change (ter Braak and Schaffers, 2004). CoCA were performed using Canoco5 (ter Braak and Šmilauer, 2014).

6.3 Results

6.3.1 SLNG04 sedimentary macrofossil record

Macrofossil counts found in the SLNG04 sedimentary record can be found in Figure 6.3a-c. Plant macrofossil remains included seeds and fruits, leaf-spines, leaf tips, leaf fragments (including water lilies leaf cell trichosclereids), and charophyte oospores. The trichosclereids of *Nymphea* sp. and *Nuphar* sp. are identical and therefore grouped as the Nymphaeaceae. Oospores are difficult to identify to species due to a high amount of morphological variability. Therefore, all oospores were combined to represent all charophytes. Calcified and uncalcified oospores were counted separately. Invertebrate macrofossils included bryozoan statoblasts (counted as valves), cladoceran ephippial remains, chydorid carapaces and postabdomen, molluscs, and fragments of benthic invertebrates. Molluscs were not identified beyond genus. Benthic invertebrate fragments were typically identified to order or family, with the exception of Tricoptera fronto-clypei, which were identified to genus. Fish scales and vertebrae were also recovered and enumerated.

DCA aquatic macrofossil dataset from SLNG04 calculated a gradient length of 3.6 SD along the first DCA axis (Table 6.1). Total variation explained along the first two DCA axes was 37.2%, with axis 1 explaining 28.9% and axis 2 explaining 8.2%. DCA indicates two main groupings of macrofossil samples from the SLNG04 sedimentary record: pre-1900 and post-1900 (Figure 6.4). Increased abundance of most macrofossil remains are indicated by the clustering of most species with the post-1900 samples along DCA axis 1 (Figure 6.4). Broken stick analysis indicated two primary zones within the SLNG04 aquatic macrofossil record (Figure 6.5). Cluster analysis confirms that the two primary zones within the aquatic macrofossil record are from 1) the early-19th century to c. 1900 (61 cm to 39 cm), and 2) c. 1900 to 2014 (36 cm to 0 cm) (Figure 6.6). Breakpoint analysis indicated one significant ($p \leq 0.01$) point of change in the macrofossil DCA axis 1 scores through Macrofossil Zone 2, c. 1965 (Figure 6.7).

	Axis 1	*Axis 2*	*Axis 3*	*Axis 4*
Eigenvalues	0.4227	0.1199	0.0664	0.0433
Explained variation (cumulative)	28.9	37.2	41.7	44.7
Gradient length	3.57	2.43	1.96	1.33

Table 6.1. DCA summary table of the SLNG04 aquatic macrofossil ln(x+1) transformed record. Eigenvalues and explained variation of the first four DCA axes indicated, as well as gradient lengths of the first four DCA axes.

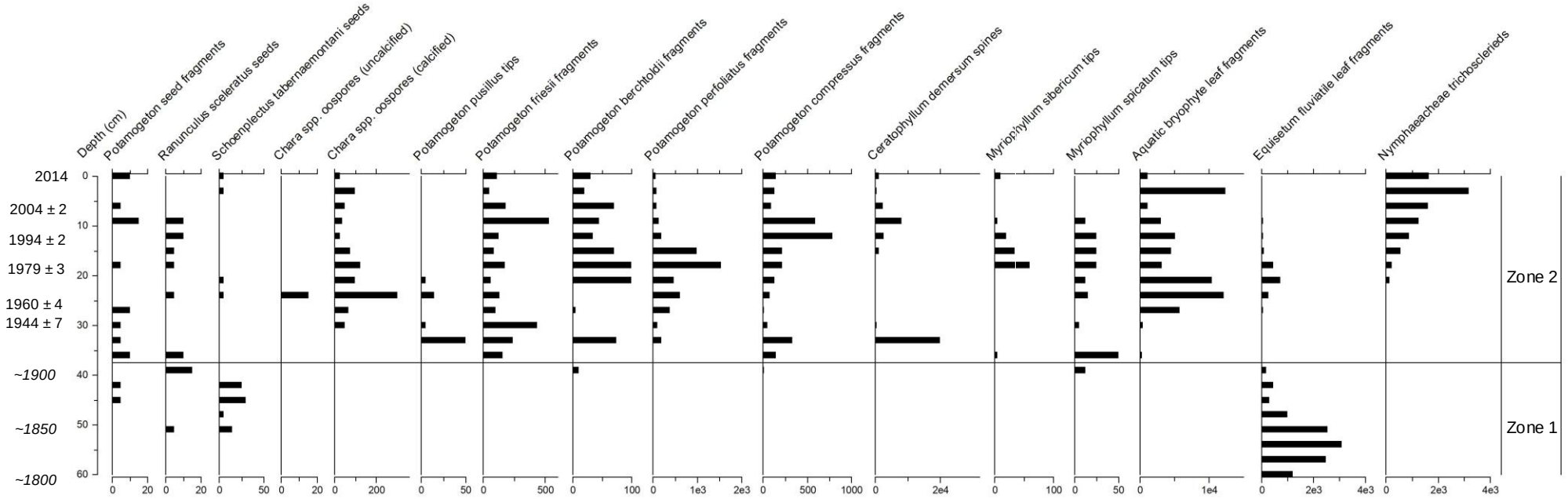

Figure 6.3a. Aquatic macrophyte remains from the SLNG04 record. Macrofossil Zones 1 and 2 are indicated. Units for all remains are in no. counts 100 cm^{-3} wet sediment. Radioisotope-derived dates and confidence limits are highlighted on the y-axis. Italicized dates are extrapolated beyond ^{210}Pb radioisotope dating.

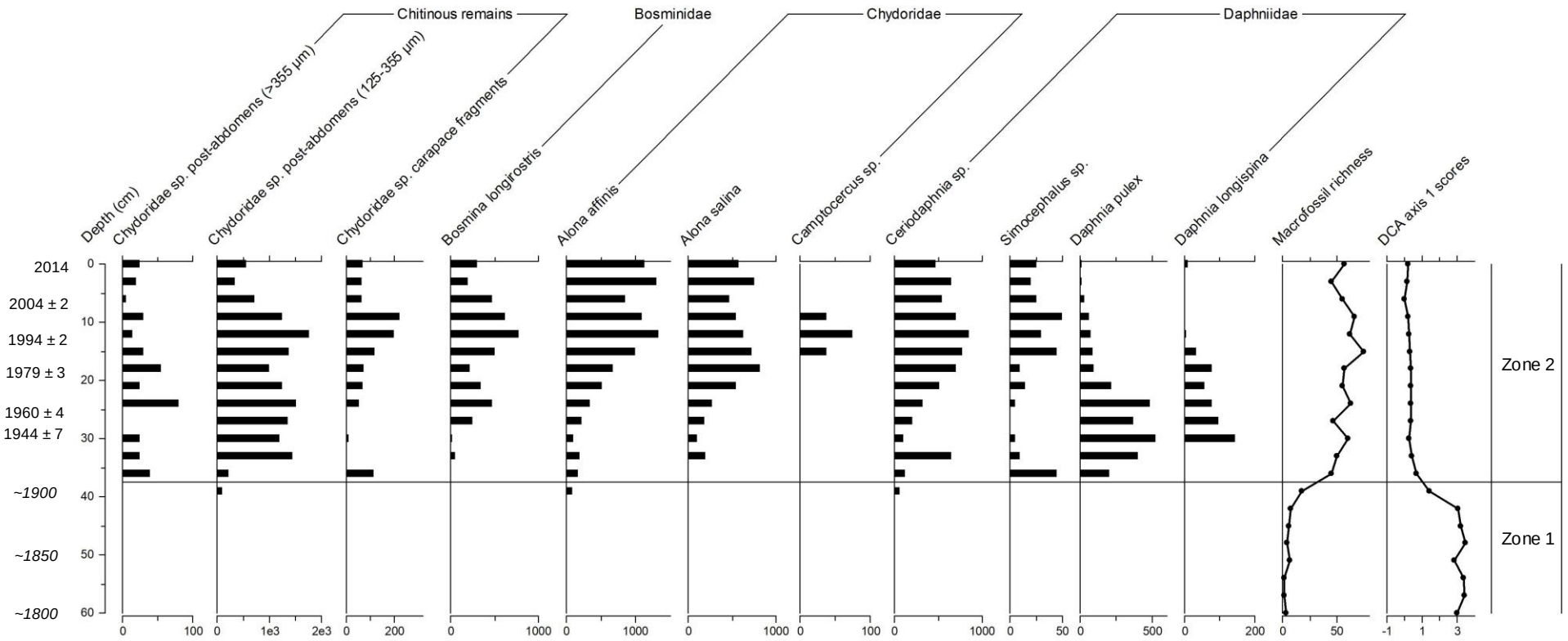

Figure 6.3b. Zooplankton chitinous and ephippial remains enumerated from the SLNG04 macrofossil record. Total macrofossil richness per sample and DCA axis 1 scores are displayed. Macrofossil Zones 1 and 2 are indicated. Units for all remains are in no. counts 100 cm^{-3} wet sediment. Radioisotope-derived dates and confidence limits are highlighted on the y-axis. Italicized dates are extrapolated beyond ^{210}Pb radioisotope dating.

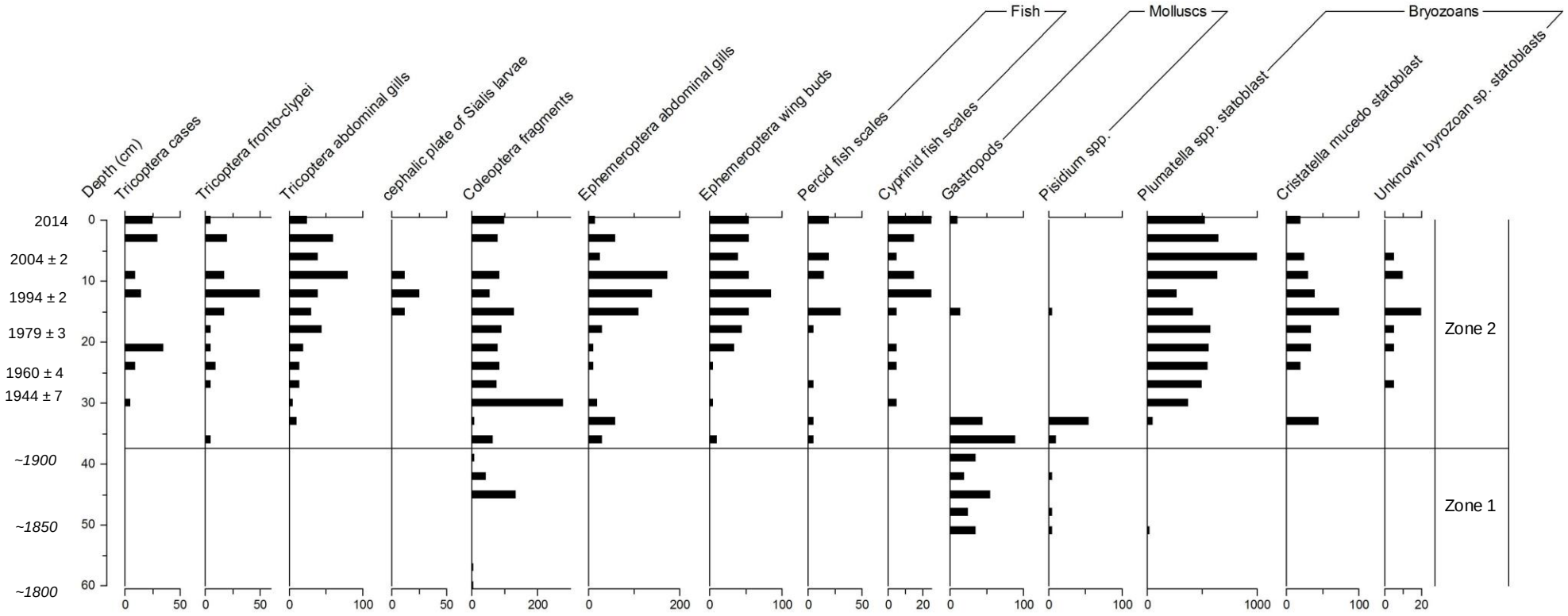

Figure 6.3c. Benthic invertebrate, fish, mollusc, and bryozoan remains enumerated from the SLNG04 macrofossil record. Macrofossil Zones 1 and 2 are indicated. Units for all remains are in no. counts 100 cm^{-3} wet sediment. Radioisotope-derived dates and confidence limits are highlighted on the y-axis Italicized dates are extrapolated beyond ^{210}Pb radioisotope dating.

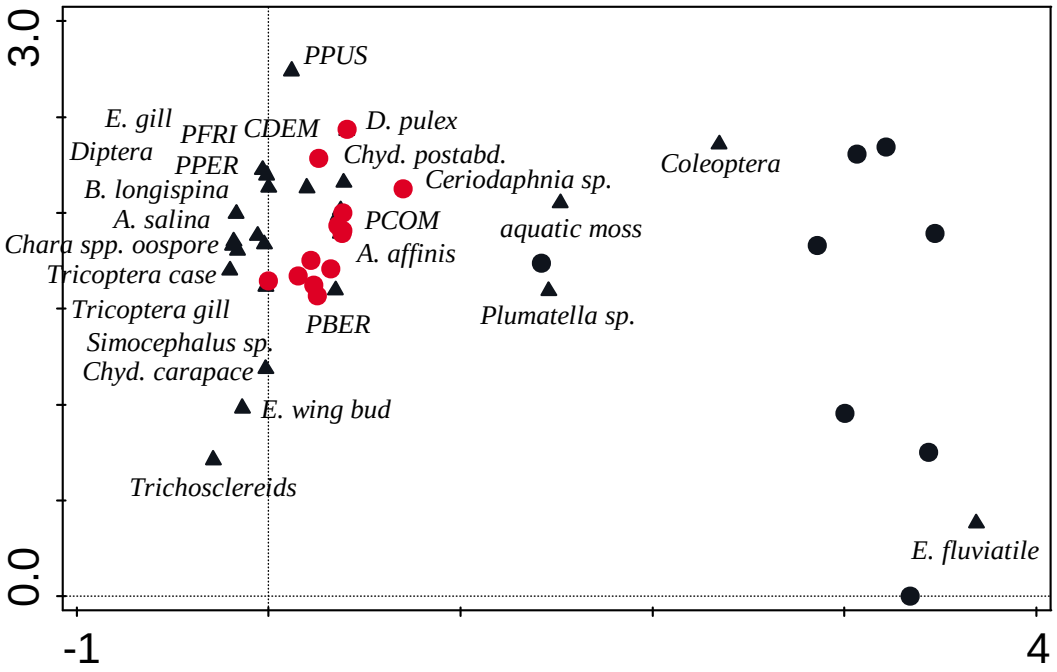

Figure 6.4. DCA biplot of aquatic macrofossil remains (▲) and samples (●) from SLNG04. Top 25 remains are plotted according to best species fit. Sample depths are colour-coded according to zone: Macrofossil Zone 1 (early-19th century to c. 1900) (black), Macrofossil Zone 2 (c. 1900 to 2014) (red). Macrofossil codes can be found in Appendix 5.

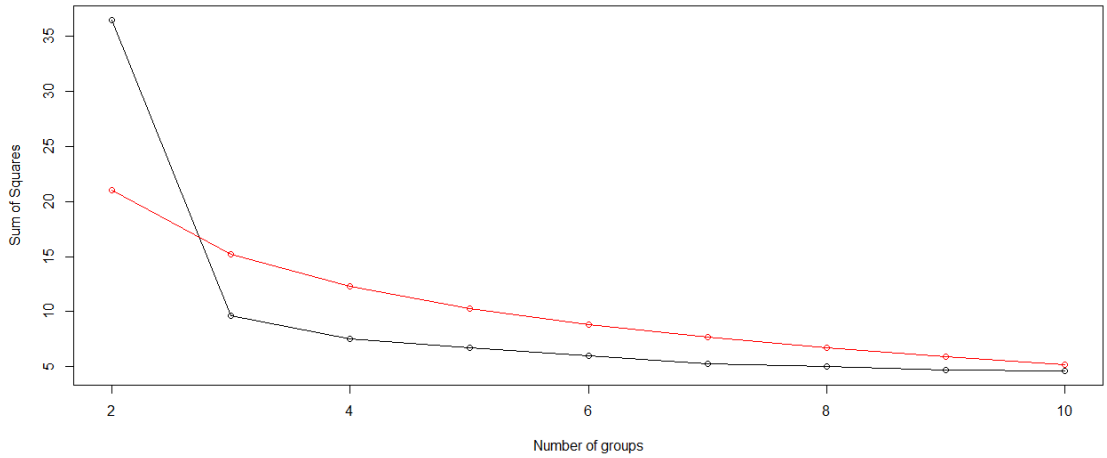

Figure 6.5. Broken stick of the SLNG04 ln(x+1)-transformed aquatic macrofossil record. Two significant groupings of samples are indicated.

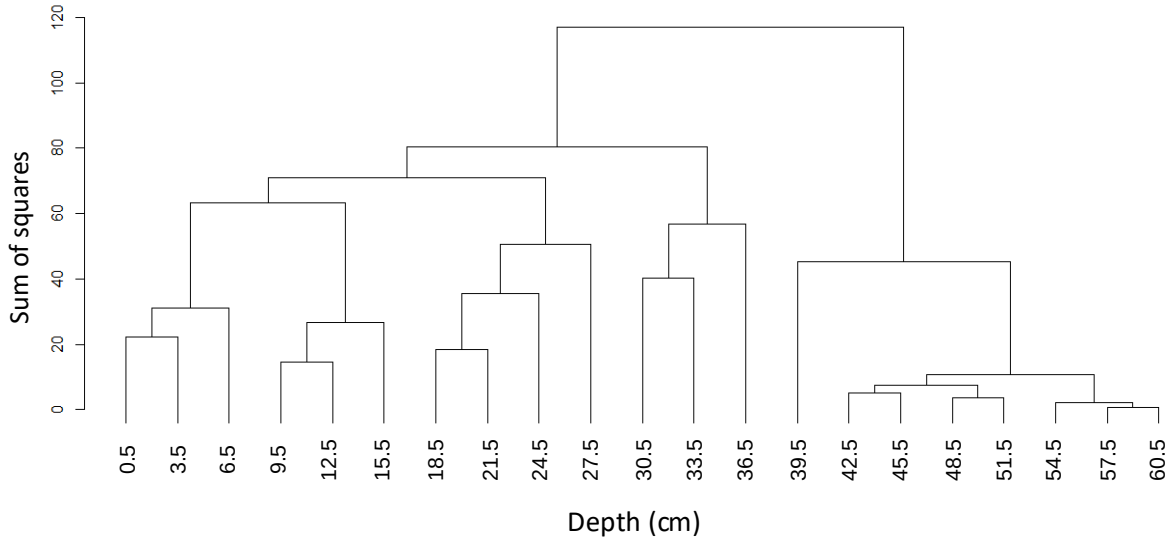

Figure 6.6. Cluster analysis of SLNG04 ln(x+1)-transformed aquatic macrofossil samples. Sample depths are indicated (cm). Two significant groupings occur, as determined through broken stick analysis.

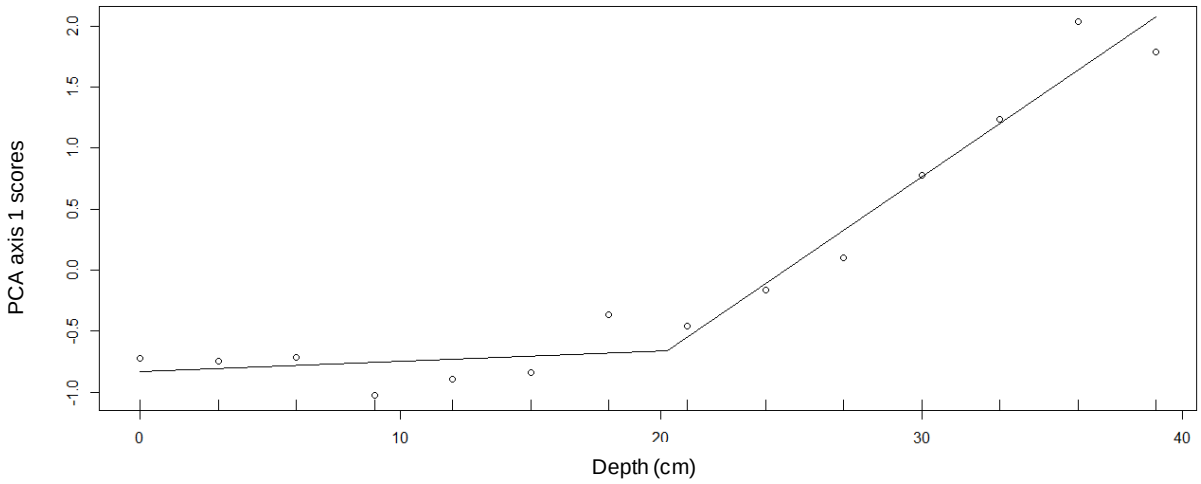

Figure 6.7. Breakpoint analysis of the SLNG04 macrofossil DCA axis 1 scores for Macrofossil Zone 2. One significant ($p \leq 0.01$) point of change was identified c. 1965.

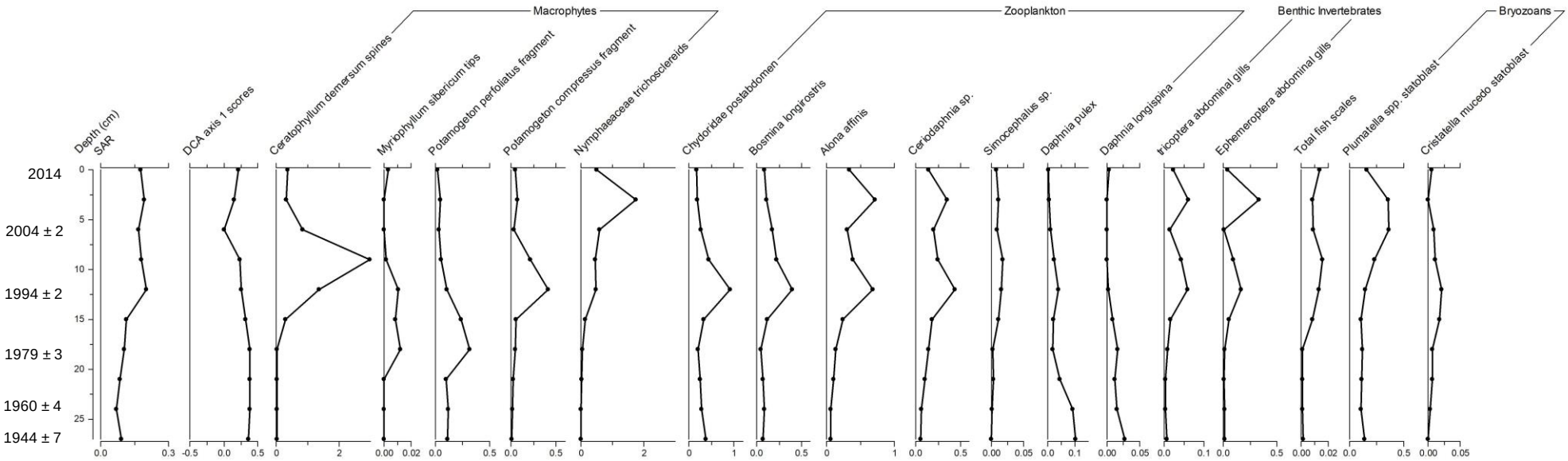

Figure 6.8. Macrofossil fluxes (no. counts cm^{-2} yr^{-1}) of select remains from SLNG04 sediment core. Sediment accumulation rate (SAR; g cm^{-2} yr^{-1}) and PCA axis 1 scores since c. 1945 are included.

Macrofossil Zone 1: Early 19th century to c. 1900 (60 cm to 39 cm)

The early part of Macrofossil Zone 1 lacked submerged aquatic macrofossils, and rather, macrofossil remains consisted primarily of marginal wetland species *Equisetum fluviatile* (Figure 6.3a-c). The appearance of mollusc remains, as well as seeds of aquatic macrophytes *Ranunculus sceleratus* and *Schoenoplectus tabernaimontanii*, and the small bryozoan, *Plumatella* sp., in the mid-19th century, indicated the diversification of the aquatic ecosystem around this time. The appearance of aquatic remains in the record at this time coincided with the decline of *E. fluviatile* remains. Towards the end of Macrofossil Zone 1, seed fragments of *Potamogeton* sp. and *Schoenoplectus lacustris*, as well as Coleoptera larval remains appeared in the record, which coincided with the further decline of *E. fluviatile* remains. DCA indicated that the sample from 39 cm depth (c. 1900) was likely a transitionary sample between Macrofossil Zone 1 and Macrofossil Zone 2, however it is more similar to other samples from Macrofossil Zone 1. Around 1900 AD, *Potamogeton* leaf fragments appeared in the macrofossil record, as did chydorid remains, including post-abdomen remains and ephippial remains of *Alonis* spp., indicating increasing ecological complexity of the system

Macrofossil Zone 2: c. 1900 to 2014 (36 cm to 0 cm)

Changes to the SLNG04 aquatic macrofossil record during Macrofossil Zone 2 indicated increasing complexity to the SLNG04 aquatic ecosystem through the 20th and 21st centuries. A proliferation of the submerged macrophyte community occurred at the beginning of Macrofossil Zone 2 (Figure 6.3a), with increases in leaf fragment remains of *Potamogeton* spp. and *Ceratophyllum demersum* spines. *Chara* sp. oospores appeared in the record in the early-1930s, and increased in abundance until c. 1980, after which time *Chara* sp. oospores decreased in abundance. Remains of *Equisetum fluviatile* also re-appeared briefly in the macrofossil record between c. 1960 and the late-1980s. The return of *E. fluviatile* in the record coincided with high abundances of aquatic mosses between c. 1950 and c. 1970. Increases in *Potamogeton* spp. and *Myriophyllum* spp. occur in the 1970s and 1980s. Trichosclereids also increase in abundance since c. 1970. Sedimentation rates remained relatively stable since the early-1990s, however there was a decline in flux of all aquatic macrophyte remains since c. 2000 (Figure 6.8). All *Potamogeton* spp. showed decreased abundances since c. 2005,

coinciding with the decline in *Ceratophyllum demersum* since c. 2000 (Figure 6.3a). Breakpoint analysis indicated significant point of change in DCA axis 1 scores coinciding with the increase in *Potamogeton* spp., *Myriophyllum* spp., and Trichosclereids in Macrofossil Zone 2 (Figure 6.7).

Development of the zooplankton community early in Macrofossil Zone 2 was indicated by increased abundances of chydorid post abdominal remains and low abundances of ephippial remains of the Chydoridae, *Alona* spp., and the appearance and increased numbers of *Daphnia pulex* ephippial remains (Figure 6.3b). *Daphnia pulex* ephippial remains quickly increased in numbers in the macrofossil record, and remained high starting in the early-20th century until c. 1970, coinciding with the significant shift indicated by breakpoint analysis (Figure 6.6). All other cladocera ephippial remains, including Chydoridae *Alona* spp., and Daphniidae *Simocephalus* sp, and *Ceriodaphnia* sp., display low abundances in the early to mid-20th century. Beginning at c. 1980, flux and abundance of *Daphnia pulex* and *Daphnia longispina* ephippial remains decline, while increases are observed in the flux and abundance of ephippial remains of Daphniidae *Simocephalus* sp., and the small pelagic *Ceripdaphnia* sp., and small, benthic Chydoridae *Alona* spp. in the 1980s (Figure 6.8).

Early in Macrofossil Zone 2, remains of benthic invertebrates increased in abundance and diversified, with Ephemeroptera, Trichoptera, and Coleoptera remains present at low abundances at this time (Figure 6.3c). Mollusc remains quickly declined in abundance and disappear from the record early in Macrofossil Zone 2. Peaks in numbers of Chydoridae and small Daphniidae ephippial remains between c. 1980 and c. 1995 coincided with increases and peaks in benthic invertebrate Ephemeroptera remains and Trichoptera gills, and increases in the remains of both percid and cyprinid fish scales. Trichoptera fronto-clypei from a variety of species were found throughout Macrofossil Zone 2, however numbers were low and sporadic for each species and are not shown in the invertebrate stratigraphy, Figure 6.2c. Cephalic plate of *Sialis* sp. larvae were found in small numbers between c. 1990 and 2000. Further, increased flux and abundance of the bryozoan, *Plumatella* sp. since the early 1990s coincided with the decline of the bryozoan, *Cristatella mucedo* (Figures 6.3c and 6.8).

6.3.2 SLNG04 sedimentary diatom record

Taxa present at ≥ 5% at a single depth, and zones of change within the diatom record for SLNG04 are presented in the stratigraphy in Figures 6.9a-b. A total of 223 species from 38

genera were identified within SLNG04 diatom assemblages. Throughout the entire record, diatom concentrations ranged from approximately 450 valves g^{-1} dry weight (c. 1920) to 1.12 x 10^6 valves g^{-1} dry weight (c. 1910) (Figure 6.9). Rarefacted species richness of sample depths with greater than 300 valves enumerated ranged from 47.4 (c. 1920) to 77.8 (c. 1995), and sample N2 ranged from 7.09 (c. 1980) to 28.46 (c. 1910) (Figure 6.9). PCA of the SLNG04 diatom record explained 54.6% of total variation along the first two axes (Table 6.2). In the ordination, older samples plotted positively along PCA axis 1, while samples since c. 1920 (33 cm) plotted more negatively along PCA axis 1, and spread throughout PCA axis 2 (Figure 6.10). Also, the sample clusters appear to be strongly associated with differing species assemblages (Figure 6.10). Broken stick analysis of sample depths with greater than 100 valves enumerated indicated two significant groupings of samples (Figure 6.11). Groupings of diatom samples from the SLNG04 record within cluster analysis (Figure 6.12), PCA, and broken stick analysis align with major changes in diatom concentration through the record, and hence diatom zones were constructed based on points of major concentration changes through the record: 1) Early-19th century to mid-19th century (60 cm to 51 cm), 2a) Mid-19th century to c. 1900 (50 cm to 40 cm), 2b) c. 1900 to c. 1920 (38 cm to 33 cm), 3) c. 1920 to c. 1960 (32 cm to 26 cm, and 4) c. 1960 to 2014 (24 cm to 0 cm). While diatom concentration increased from 40 cm to 38 cm, Diatom Zones 2a and 2b were differentiated only as sub-zones as they were determined not to be significantly different through broken stick analysis (Figure 6.11).

	Axis 1	***Axis 2***	***Axis 3***	***Axis 4***
Eigenvalues	0.4022	0.1440	0.1309	0.0757
Explained variation (cumulative)	40.2	54.6	67.7	75.3

Table 6.2. PCA summary table of the SLNG04 diatom relative abundance record. Eigenvalues and explained variation of the first four PCA axes indicated.

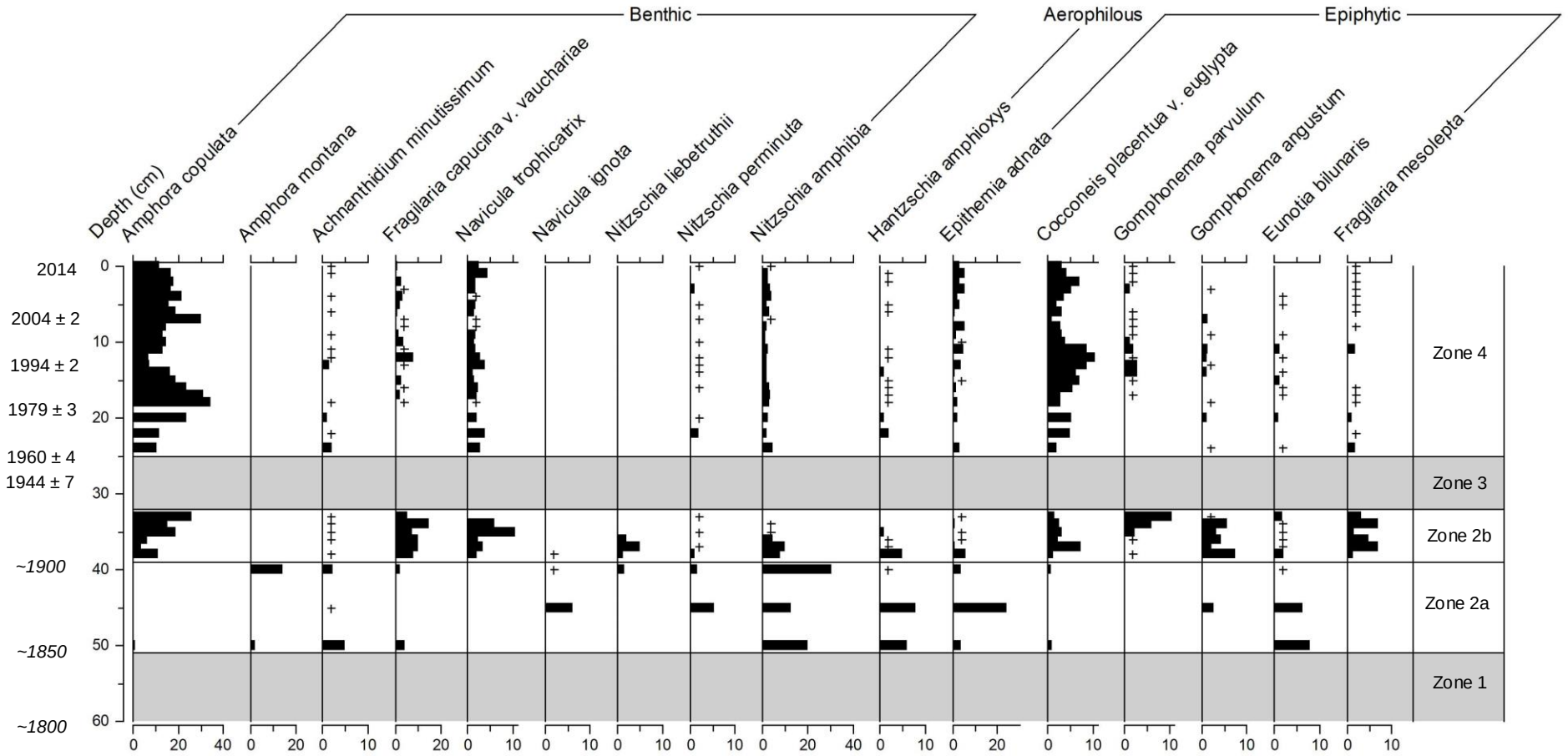

Figure 6.9a. SLNG04 relative abundances (%) of benthic, aerophilous, and epiphytic diatoms >5%, (+) indicates present in sample at <1% relative abundance. Diatom Zones 1 to 4 are indicated, based on diatom concentration. Grey bands indicate time of very low diatom concentrations. Radioisotope-derived dates and confidence limits are highlighted on the y-axis. Italicized dates are extrapolated beyond ^{210}Pb radioisotope dating.

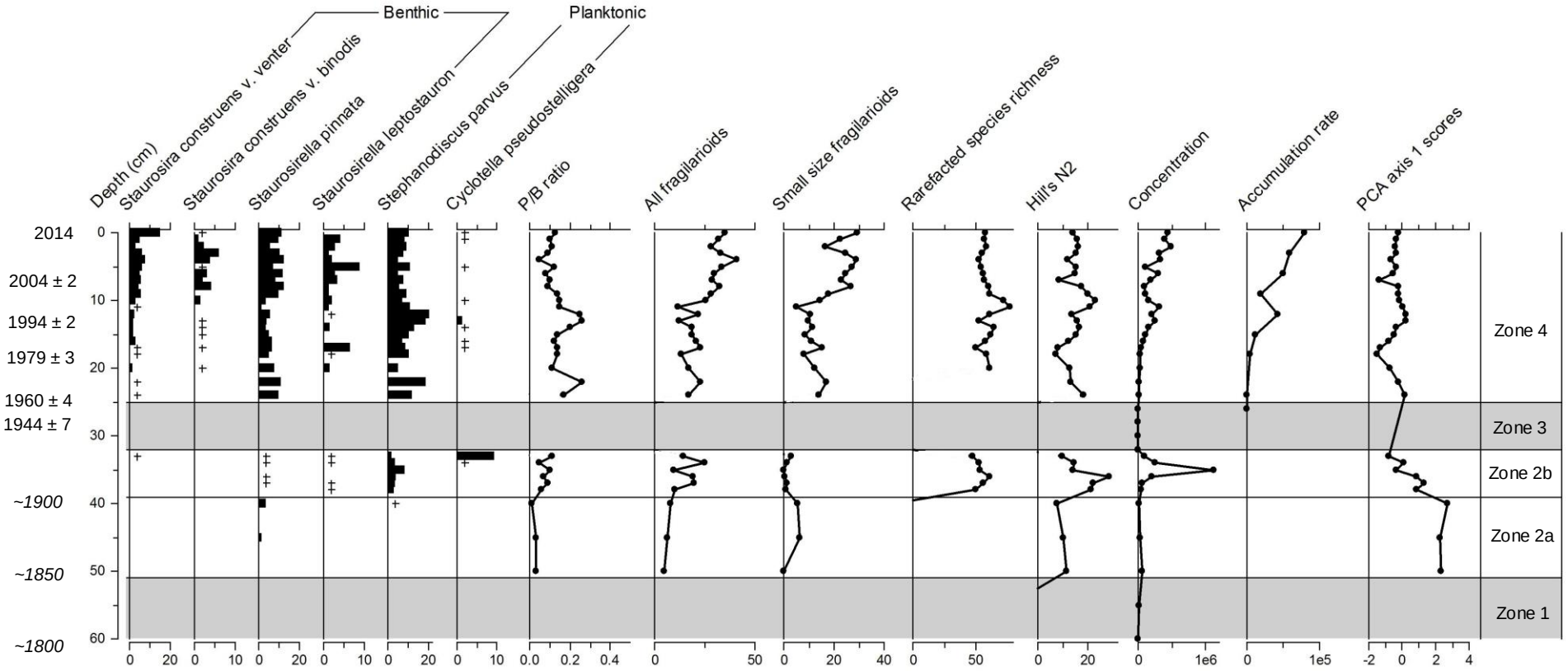

Figure 6.9b. SLNG04 relative abundances (%) of small, periphytic fragilarioids of the *Staurosira-Staurosirella-Pseudostaurosira* (SSP) complex, and planktonic diatoms present at >5%, (+) indicates present in sample at <1% relative abundance. Planktonic/Benthic (P/B) ratio, total sum all fragilarioids (%), total sum small fragilarioids of the SSP complex (%), diatom rarefacted species richness (no. species), Hill's N2 (no. species) measure of diversity, concentrations (no. valves g^{-1} dry weight), diatom accumulation rates (no. valves cm^{-2} yr^{-1}), and PCA axis 1 scores are plotted. Diatom Zones 1 to 4 are indicated, based on diatom concentration. Grey bands indicate time of very low diatom concentrations. Radioisotope-derived dates and confidence limits are highlighted on the y-axis. Italicized dates are extrapolated beyond ^{210}Pb radioisotope dating.

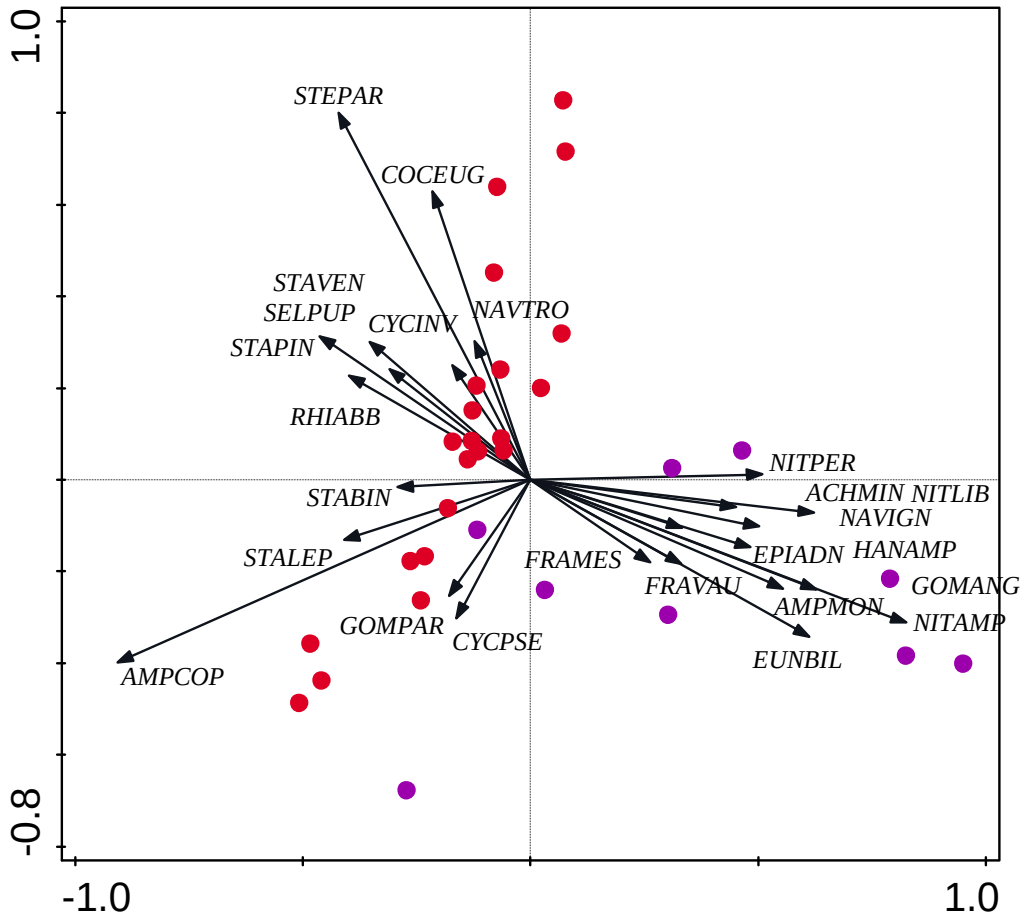

Figure 6.10. PCA biplot of diatom species and samples from SLNG04, for which >100 valves were enumerated. Top 25 species are plotted according to relative abundance. Sample depths are colour-coded according to zone: Diatom Zone 1 (Early-19th century to mid-19th century) (not included in analysis), Diatom Zone 2 (Mid-19th century to c. 1920) (purple), Diatom Zone 3 (c. 1920 to c. 1960) (not included in analysis), and Diatom Zone 4 (c. 1960 to 2014) (red). Diatoms species codes can be found in Appendix 6.

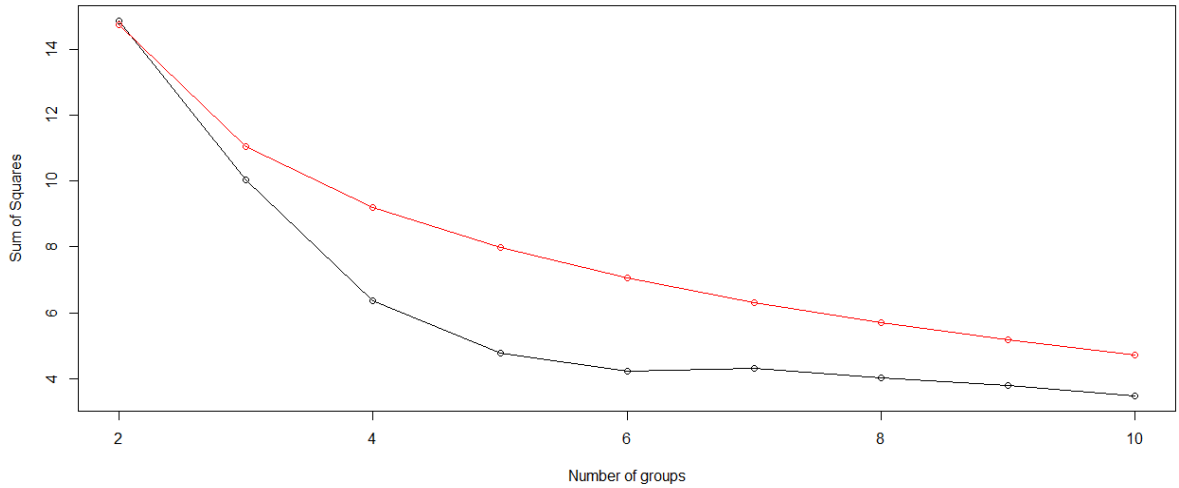

Figure 6.11. Broken stick model of SLNG04 diatom record. Two significant groups detected between samples with >100 valves enumerated.

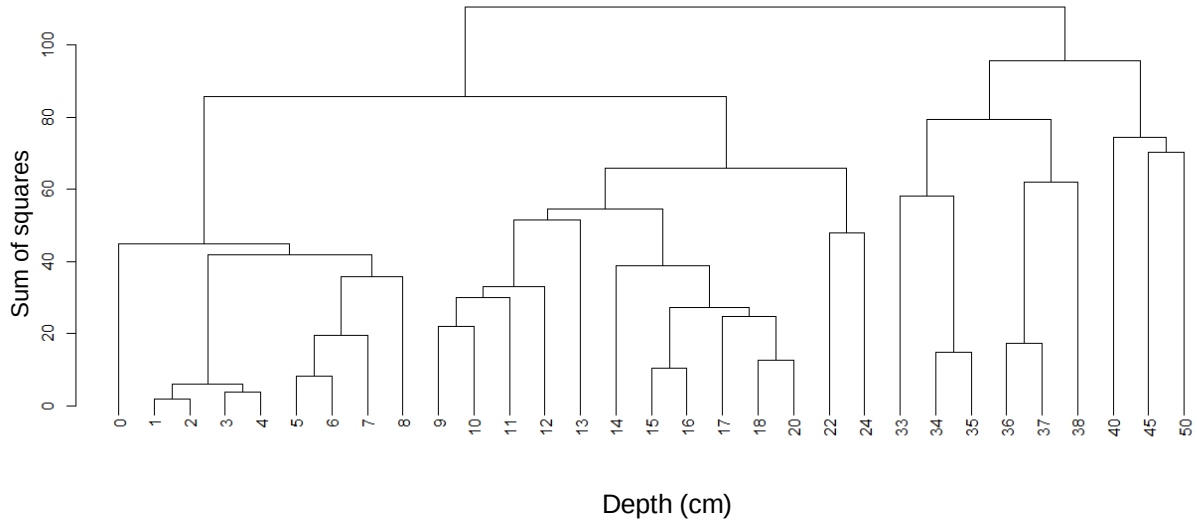

Figure 6.12. Cluster analysis of SLNG04 diatom samples with >100 valves enumerated. Sample depths are indicated. Two significant groupings of depths as determined through broken stick analysis.

Diatom Zone 1: Early-19th century to mid-19th century (60 cm to 51 cm)

Diatom Zone 1 is characterized primarily by very low diatom concentrations (Figure 6.9b). However, those valves that are enumerated appear intact and for the most part, undissolved. The absence of dissolved central areas and girdle bands in these samples indicated that low concentrations are more a factor of low numbers of diatoms, or dilution of diatoms due to high sedimentation rates (this is below the dated section of the core), rather than high levels of dissolution. Four valves were enumerated at 60 cm (early-19th century) depth: *Epithemia adnata, Eunotia bilunaris, Pseudostaurosira brevistriata,* and *Gomphonema angustatum*. Eleven valves were enumerated at 55 cm depth, from species including: *Cocconeis placentula v. euglypta*, *Epithemia adnata, Eunotia bilunaris, Gomphonema truncatum*, *Hantzschia amphioxys*, and *Nitzschia amphibia*. Most of these species have been documented as typically ephiphytic species, living on emergent or submerged aquatic vegetation. Further, *N. amphibia* and *H. amphioxys* have been recorded in moist, subaerial, often times moss-rich habitats as aerophilous species (Table 6.6; Reichardt, 1985; Van Dam *et al*., 1994).

Diatom Zone 2a: Mid-19th century to late-19th century (50 cm to 40 cm)

Diatom Zone 2a is characterized primarily by an increase in diatom concentration (Figure 6.9b). Diatom concentration increased by approximately one order of magnitude in the early- to mid-19th century. Dominant and common species in this zone were similar to those from Diatom Zone 1, including dominant *N. amphibia*, along with *E. bilunaris*, *E. adnata*, *G. angustatum*, and *H. amphioxys.* However, diversification of species with high abundances in this zone include *Amphora montana*, *Nitzschia perminuta*, *Epithemia zebra*, *Achanthidium minutissimum*, and *Navicula ignota* (Figures 6.9a and b).

Diatom Zone 2b: c. 1900 to c. 1920 AD (38 cm to 33 cm)

Diatom Zone 2b was characterized by a further increase in concentration of diatoms, and a minimum of 300 valves per sample were enumerated within this zone. Diatom concentrations increased in Zone 2b by 1-2 orders of magnitude relative to the previous zone, with the diatom concentration maximum of 1.12 x 10^6 valves g^{-1} for the record occurring in the early-20th century (Figure 6.9b). Rarefacted diatom species richness increased from 50 species to 62 species early in Diatom Zone 2b, then decreased to 47 species by the end of the zone (Figure 6.9). A similar trend in Hill's N2 was observed, increasing from 21 species to 28 species early in Diatom Zone 2b, and declining to 10 species by the end of the zone (Figure 6.9b). Hill's N2 indicated that by the end of Diatom Zone 2b, the assemblage contained mostly rare species and only a few very abundant species. The large benthic species, *Amphora copulata,* appeared and rose to dominance in Diatom Zone 2b, while *N. amphibia* declined in abundance through the zone and disappeared from the record by the end of Diatom Zone 2b. Epiphytic species *Fragilaria mesolepta*, *Cocconies placentula v. euglytpa*, and *Gomphonema* spp. either appeared or increased in abundance in this zone, along with the large benthic *Navicula trophicatrix*, and planktonic species *Stephanodiscus parvus* and *Cyclotella pseudostelligera* (Figures 6.9a and b).

Diatom Zone 3: c. 1920 to c. 1950 AD (32 cm to 26 cm)

Diatom concentrations abruptly declined at the start of Diatom Zone 3, with fewer than 100 valves counted per sample throughout Diatom Zone 3, and as low as 2 valves enumerated at the start of the zone. Some degree of pitting of those few diatoms present in these samples indicated the possibility of increased dissolution during this time. Diatom concentration

decreased by two orders of magnitude at the transition from Diatom Zone 2 to Diatom Zone 3, to a minimum concentration of approximately 450 valves g^{-1} dry weight (Figure 6.9b). Concentrations increased slightly to ~1000 to 2000 valves g^{-1} dry weight for the remainder of Diatom Zone 3. Diatom community composition displayed no major change in the early stages of this zone, with the previously common species *E. bilunaris*, *E. adnata, N. amphibia, H. amphioxys,* and *A. copulata* present from c. 1920 until c. 1940. By c. 1950, the diatom assemblage is composed of primarily planktonic, large benthic, and small fragilarioid species, including *S. parvus*, *Cyclotella meneghiniana, Staurosirella pinnata, Navicula clementis,* and *Navicula rheinhardtii* (Figure 6.9a and b).

Diatom Zone 4: c. 1960 to 2014 AD (24 cm to 0 cm)

Diatom concentrations increased at the start of Diatom Zone 4, and were up to three orders of magnitude higher in Diatom Zone 4 than in Diatom Zone 3 (Figure 6.9b). Diatom concentrations remained below pre-1920 levels until c. 1990. Through most of Diatom Zone 4 rarefacted species richness was equivalent to that from Diatom Zone 2b, and ranged from 50 species to 65 species. An increase in richness was observed for a short period of time in the late-1990s, with increases to 78 species. Similarly, Hill's N2 peaked in the late-1990s at 23 species (Figure 6.9b). The large benthic species *Amphora copulata* returned as the dominant species in Diatom Zone 4. Small benthic fragilarioid species increased in abundance during Diatom Zone 4, including *Staurosira construens v. venter*, *Staurosirella pinnata,* and *Staurosirella leptostauron*, and high abundances of the planktonic, meso-eutrophic *Stephanodiscus parvus* continued in Diatom Zone 4 (Figures 6.9a and b).

6.3.3 SLNG04 sedimentary pigment record

Pigment concentrations found in the SLNG04-C (hereafter referred to as SLNG04) sedimentary record are detailed in Figure 6.13. Pigments representing total algae (chlorophyll *a* (Chl *a*), Chl *a* degradation products, and β-carotene), chlorophytes (Chl *b*, pheophyin *b* (Chl *b* degradation product), and lutein), chromophytes (Chl *c*), total cyanobacteria (zeaxanthin), colonial cyanobacteria (canthaxanthin), siliceous algae (fucoxanthin), diatoms (diatoxanthin), and cryptophytes (alloxanthin), were identified in the record obtained from SLNG04. Pigments were absent from the SLNG04 record below 48 cm depth, and only Chl *a* and pheophytin *b*

were detected between 48 cm and 39 cm. Initial broken stick analysis indicated two main groupings within the pigment record from SLNG04 (Figure 6.14), and cluster analysis confirmed these grouping to be between 1) 60 cm and 37 cm, and 2) 36 cm to 0 cm depth (Figure 6.15). As Pigment Zone 1 consisted primarily of samples in which pigments were absent, analyses were rerun on Pigment Zone 2. PCA of 36 cm to the surface indicated that nearly all variation in pigment concentrations was explained by the first two PCA axes, which explained 96.7% of total pigment variability (Table 6.3). In the ordination, all pigments plotted strongly and positively along PCA axis 1, with pheophytin *a* and indicators of chlorophytes (lutein and Chl *b*) most strongly associated with PCA axis 1 (Figure 6.16). Broken stick analysis indicated that Pigment Zone 2 was divided into four significant groupings (Figure 6.17). Cluster analysis confirmed that these groupings were: 1) Early-20th century (36 cm to 35 cm), 2) c. 1920 to late-1940s (34 cm to 27 cm), 3) early-1950s to c. 2000 (26 cm to 8 cm), and 4) c. 2000 to 2014 (7 cm to 0 cm) (Figure 6.18). Breakpoint analysis of the SLNG04 pigment PCA axis 1 scores identified one significant ($p \leq 0.01$) shift in the pigment assemblage in the late-1940s (Figure 6.19).

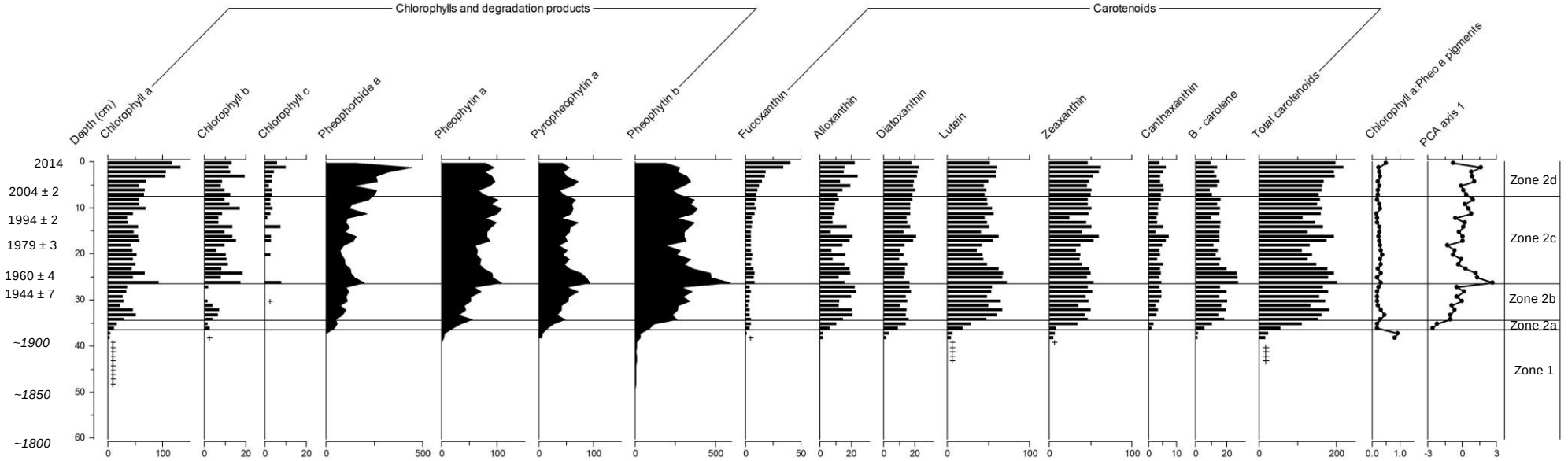

Figure 6.13. Pigment concentrations of chlorophylls, degradation products, and carotenoids for SLNG05, with indications of zones. Concentration units are in nmol g^{-1} organic matter. (+) indicates concentrations of <1 nmol/g organic matter dry weight. Pigment Zones 1 and 2 are indicated. Measure of preservation, ratio of Chl *a* : Chlorophyll *a* degradation products (Pheo *a* pigments), indicated as well as PCA axis 1 scores for Pigment Zone 2 only. Radioisotope-derived dates and confidence limits are highlighted on the y-axis. Italicized dates are extrapolated beyond ^{210}Pb radioisotope dating.

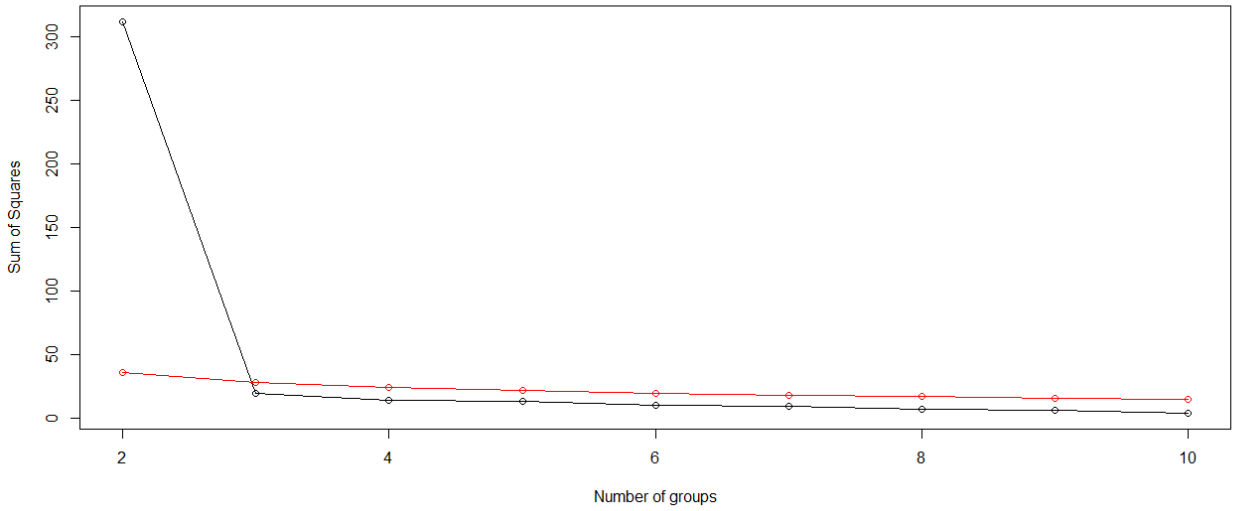

Figure 6.14. Broken stick of the full SLNG04 pigment record. Two significant groupings of samples are indicated.

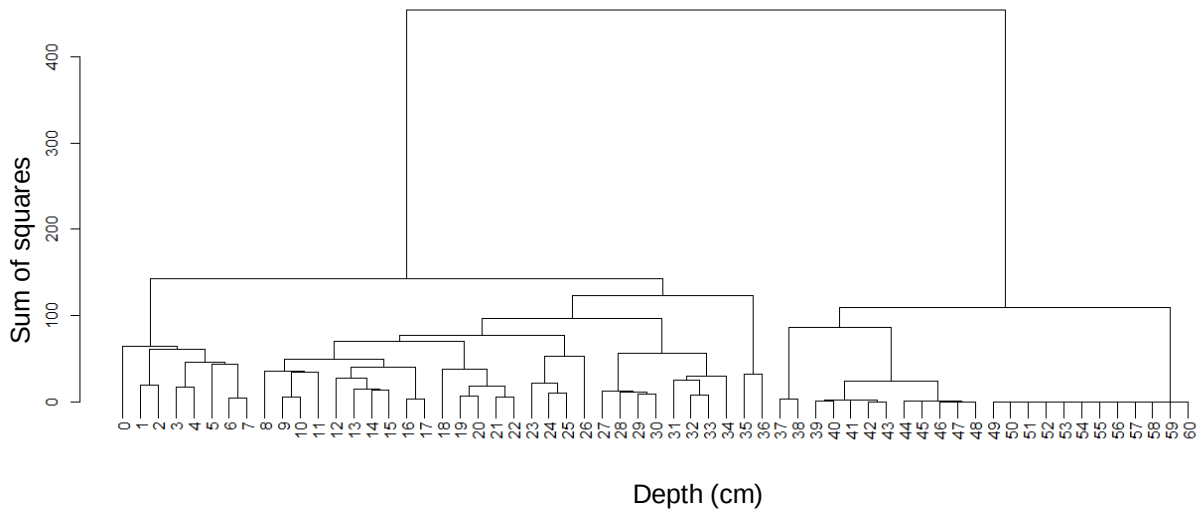

Figure 6.15. Cluster analysis of the full SLNG04 pigment record. Sample depths are indicated (cm). Two significant groupings occur, as determined through broken stick analysis.

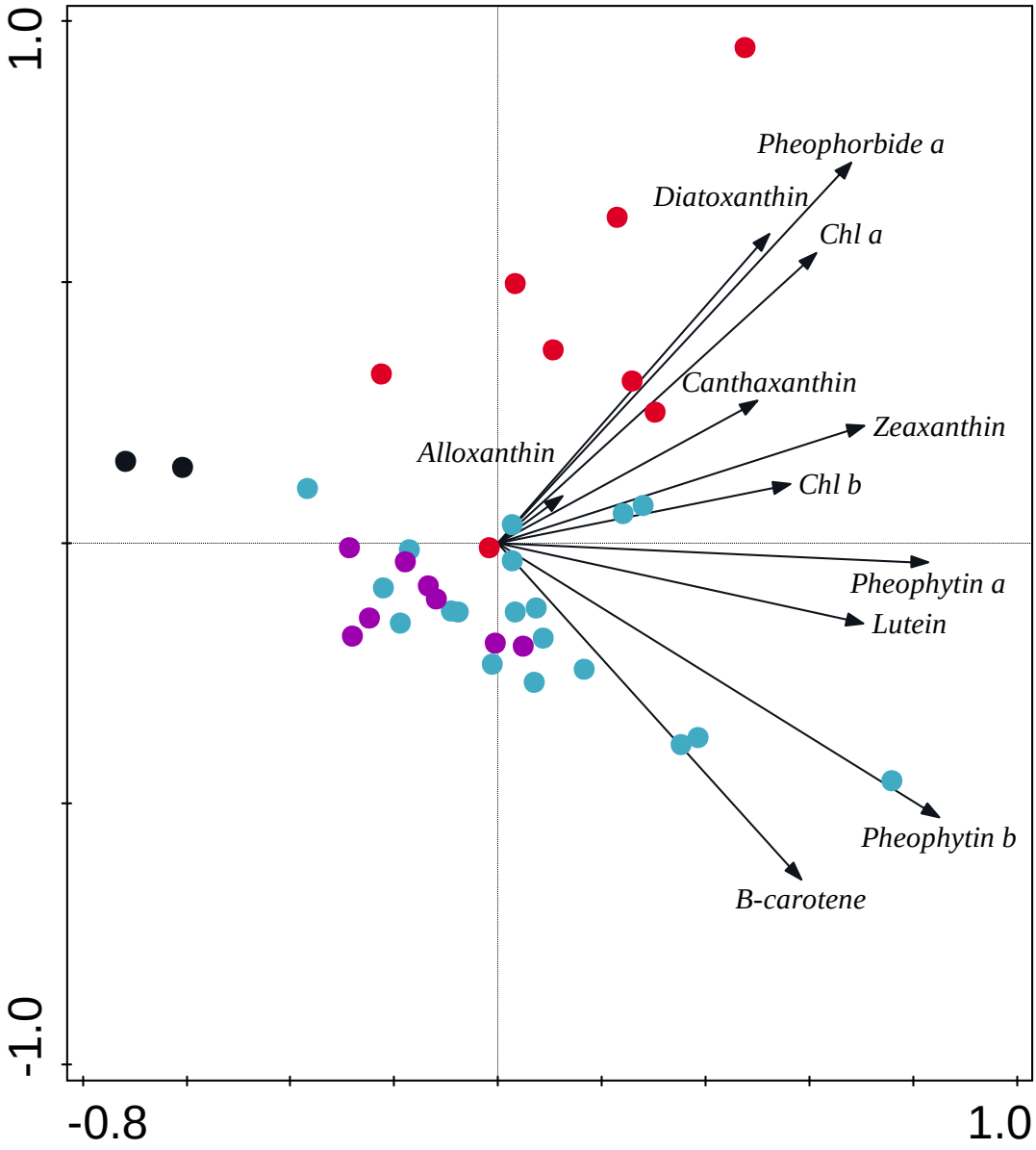

Figure 6.16. PCA biplot of pigments and sample depths for Pigment Zone 2 from SLNG04. Sample depths are colour-coded according to zone: Pigment Zone 2a (Early-20th century) (black), Pigment Zone 2b (c. 1920 to late-1940s) (purple), Pigment Zone 2c (c. 1950 to c. 2000) (light blue), Pigment Zone 2d (c. 2000 to 2014) (red).

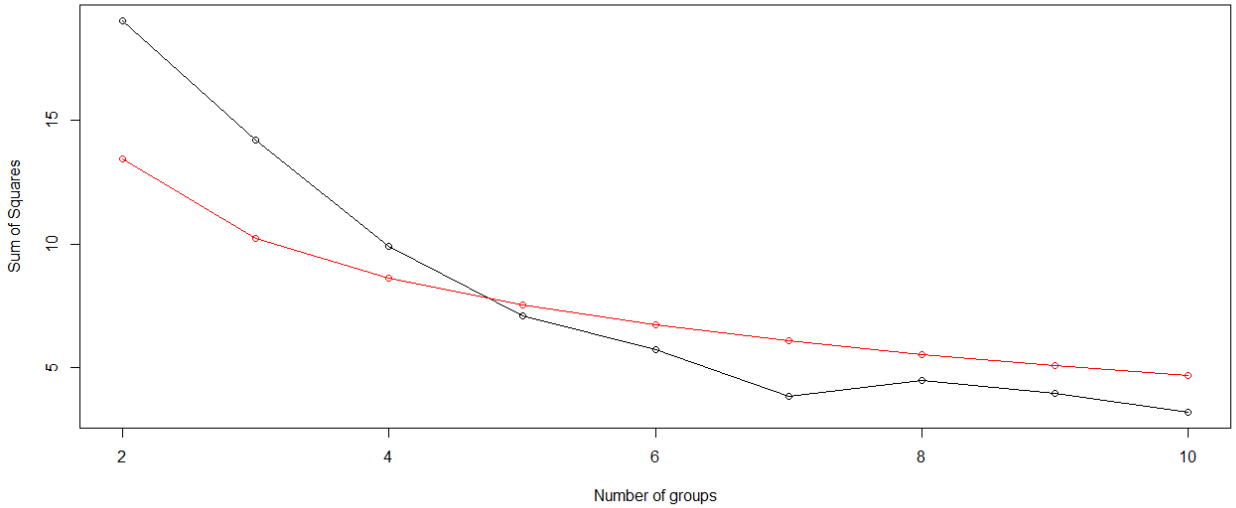

Figure 6.17. Broken stick of the SLNG04 pigment record from Pigment Zone 2. Four significant groupings of samples are indicated between 36 cm and 0 cm depth.

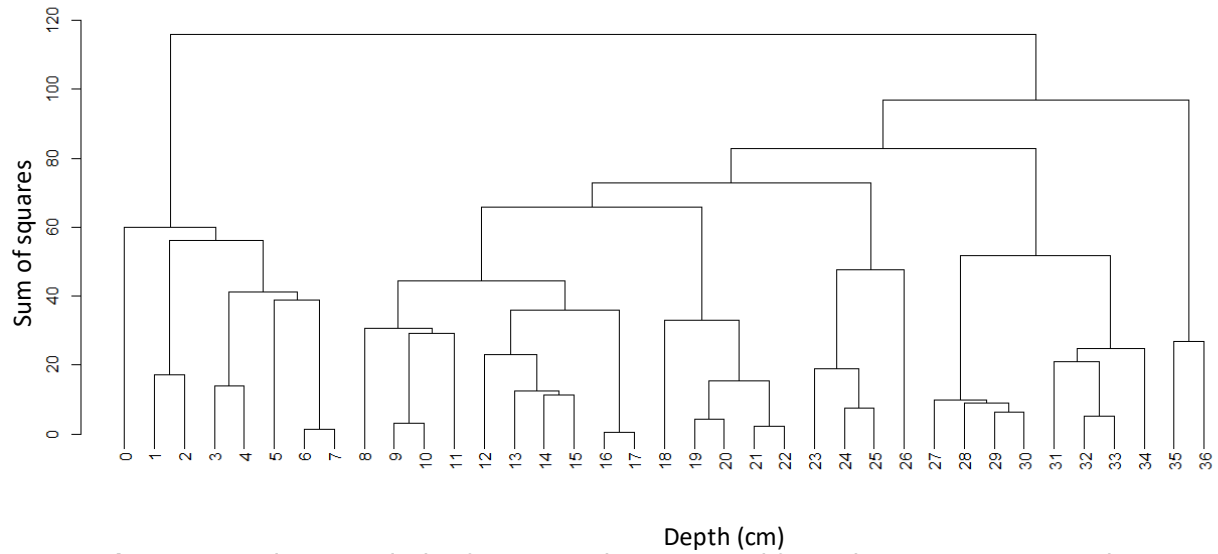

Figure 6.18. Cluster analysis of SLNG04 pigment record from Pigment Zone 2. Sample depths are indicated. Four significant groupings occur, as determined through broken stick analysis.

	Axis 1	***Axis 2***	***Axis 3***	***Axis 4***
Eigenvalues	0.5942	0.3727	0.0165	0.0104
Explained variation (cumulative)	59.4	96.7	98.4	99.4

Table 6.3. PCA summary table for SLNG04 Pigment Zone 2 only. Eigenvalues and explained variation of the first four PCA axes indicated.

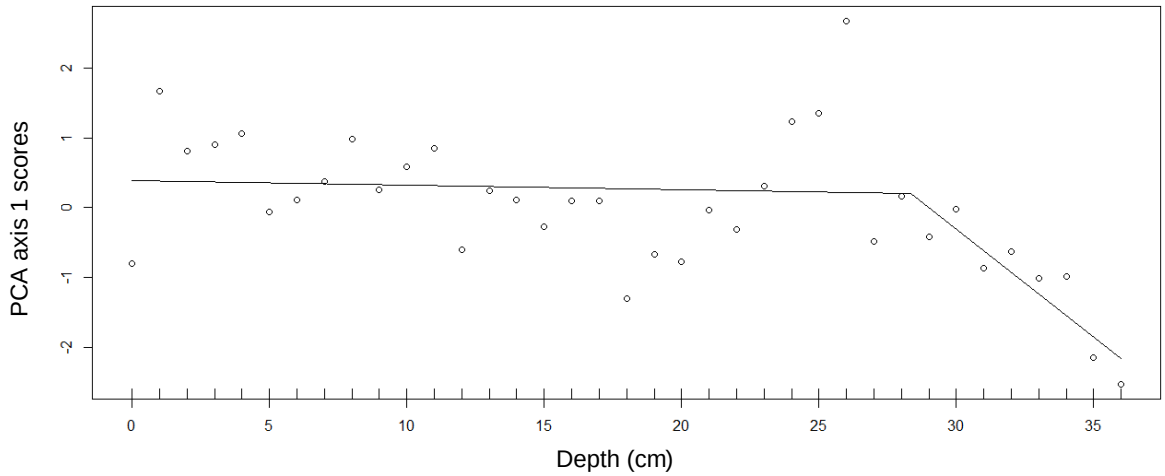

Figure 6.19. Breakpoint analysis of the SLNG04 pigment PCA axis 1 scores. One significant ($p \leq 0.01$) point of change was identified in the late-1940s.

Pigment Zone 1: Early-19th century to late-19th century (60 cm to 37 cm)

No pigments were detected early in Zone 1 (Figure 6.13). Chl *a* and pheophytin *b* were both detected in very low concentrations beginning in the mid-19th century, indicating a slight increase in overall algal biomass at this time (Figure 6.13). However, Chl *a* remained below 1 nmol g^{-1} organic matter throughout most of the 19th century. Lutein (chlorophytes) appeared in the record at very low concentrations towards the late-19th century. To further the diversification of the pigment record in the late-19th century, zeaxanthin (total cyanobacteria) appeared at the end of the zone (39 cm) at very low concentrations.

A transitionary period in pigment concentrations existed c. 1900, at the end of Zone 1. Around 1900 AD, algal diversification is observed at SLNG04, as Chl *b*, alloxanthin, β-carotene, fucoxanthin, diatoxanthin and Chl *a* degradation products, appear in the record (Figure 6.13). Further, Chl *a*, lutein, and zeaxanthin increase in concentration during this time. However, concentrations of all pigments remain quite low through to the end of Zone 1.

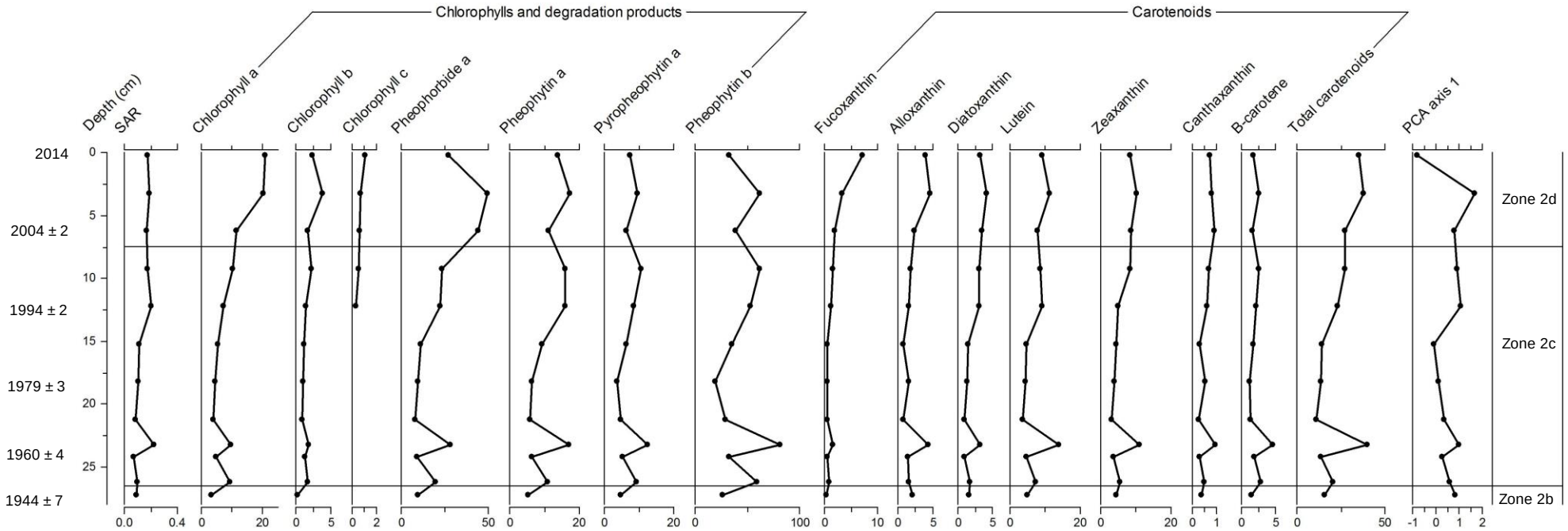

Figure 6.20. Fluxes of chlorophylls, degradation products, and carotenoids for SLNG04 from Pigment Zones 2. Units of fluxes are in nmol cm^{-2} yr^{-1}. Sedimentation accumulation rate (SAR; g cm^{-2} yr^{-1}) and PCA axis 1 scores since c. 1945 are shown. Radioisotope-derived dates and related uncertainties are posted.

Pigment Zone 2a: Early- 20th century (36 cm to 35 cm)

At the start of Zone 2, all indicators for algae increased in concentration, including chlorophytes (lutein, Chl *b*), cryptophytes (alloxanthin), siliceous algae (fucoxanthin and diatoxanthin), and total and colonial cyanobacteria (zeaxanthin and canthaxanthin) (Figure 6.13).

Pigment Zone 2b: c. 1920 to late-1940s (34 cm to 27 cm)

Total concentration of carotenoids and chlorophylls increased at the transition from Pigment Zone 2a and 2b, and through Pigment Zone 2b. At the onset of Pigment Zone 2b, several pigment concentrations became steady until the end of Pigment Zone 2b, including those for total cyanobacteria (zeaxanthin), siliceous algae (fucoxanthin and diatoxanthin), and total algae (β-carotene). Chl *b* disappeared briefly in the middle of Pigment Zone 2b, between c. 1930 and 1940, coinciding with a decline in lutein and pheophytin *b*, indicating a brief decline in the abundance of chlorophytes at SLNG04. Further, β-carotene and total carotenoid concentrations exhibited slight declines at this time (Figure 6.13).

Pigment Zone 2c: c. 1950 to c. 2000 (26 cm to 8 cm)

At the beginning of Pigment Zone 2c, a significant shift was observed in the PCA axis scores, through breakpoint analysis (Figure 6.19). Pigments most associated with Pigment Zone 2c in the PCA are β-carotene and pheophytin *b* (Figure 6.16). Chl *c* appeared at low concentrations early in Pigment Zone 2c. Several pigment biomarkers peaked in concentration during the first couple of decades of Pigment Zone 2c, including pigment for total algal production (β-carotene and pyropheophytin *a*) and chlorophytes (lutein and pheophytin *b*). Many other pigment biomarkers exhibited increases at this time including those for total algal biomass (Chl *a*), chlorophytes (Chl *b*), cryptophytes (alloxanthin), and total cyanobacteria (zeaxanthin). Following the increases in concentrations, most pigments declined slightly by c. 1970 (Figure 6.13). Concentrations of pigments for cyanobacteria (both total and colonial) increased briefly in the 1980s, and pigment for colonial cyanobacteria (canthaxanthin) reaches maximum concentrations at this time.

Increased flux of all pigments, driven by increased SAR, c. 1950, corresponded with increased concentrations of most pigments (Figures 6.13, 6.20). SAR and pigment fluxes

declined by c. 1960, while concentrations increased or remained elevated. A brief increase in SAR c. 1965 resulted in increased flux of all pigments, and increased concentrations of some pigments, including lutein and β-carotene (Figures 6.13, 6.20).

Pigment Zone 2d: c. 2000 to 2014 (7 cm to 0 cm)

Pigments most associated with this zone in PCA are Chl *a,* diatoxanthin, and pheophorbide *a* (Figure 6.16). Total carotenoid and Chl *a* concentrations increased in Pigment Zone 2d, with increases in individual pigment concentrations for siliceous algae (fucoxanthin and diatoxanthin), cyanobacteria (zeaxanthin), and to a lesser degree, chlorophytes (alloxanthin) (Figure 6.13).

6.3.4 Community-level change: Comparisons of temporal variation between proxies

6.3.4.1 Pigment and diatom sedimentary records

The first two axes of the co-correspondence analysis (CoCA) very strongly captured the extent of cross-correlation between the two communities (Table 6.4), and the relation between the two communities was highly significant (Table 6.5). Pheophytin *b* (chlorophytes) and Chl *a* (total algae), which were present earlier in the record than other pigments (Pigment Zone 1), co-occurred with the diatom assemblages most common in the early record (Diatoms Zones 1 and 2a), including *Nitzschia amphibia*, *Epithemia adnata*, and *Hantzschia amphioxys* (Figure 6.21a and b). This is likely because those were the only pigments detected during diatom Zone 2a. Most pigments and diatom species clustered on the right side of the ordination graph, and coincided with the large benthic (e.g. *Amphora copulata)*, planktonic (e.g. *Stephanodiscus parvus)*, and epiphytic (e.g. *Cocconeis placentula v. euglypta)* species of Diatom Zone 4 (Figure 6.21a and b). Further, those pigments which fell to the lower right of the ordination, canthaxanthin (colonial cyanobacteria), Chl *b* (chlorophytes), and pheophorbide *a*, were more likely to occur at higher concentrations with the small benthic fragilarioids, common in Diatom Zone 4 (Figure 6.21a and b).

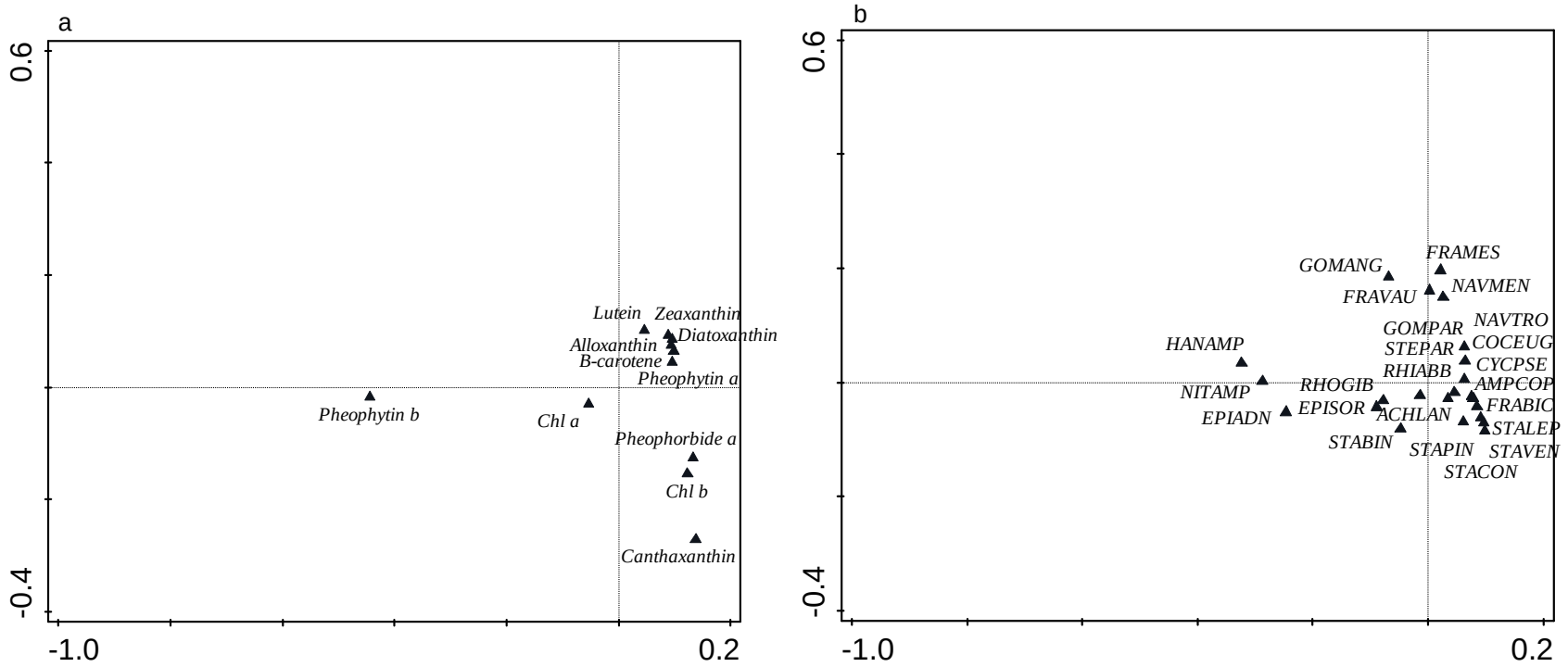

Figure 6.21. a) Pigment, and b) diatom CoCA community biplots. Species falling in the same area across plots tend to co-occur in the proxy records. Diatom species codes can be found in Appendix 6.

Proxies	Axis 1	Axis 2	Axis 3	Axis 4
Diatom*Pigment	+0.9645	+0.8502	+0.7552	+0.8122
Diatom*Macrofossil	+0.9759	+0.9545	+0.9521	+0.9011

Table 6.4. Cross correlations between axes determined through co-correspondence analysis. High positive values indicate strong correlation between the first CoCA axes.

Proxies	Test on all axes (p-value)	Test on first axis (p-value)
Diatom*Pigment	0.002	0.002
Diatom*Macrofossil	0.002	0.002

Table 6.5. Tests for significance across axes for each analysis in CoCA. Significance $p \leq 0.01$.

6.3.4.2 Macrofossils and diatoms

The first two axes of the CoCA very strongly captured the extent of cross-correlation between the two communities (Table 6.4), and the relation between the two communities is highly significant (Table 6.5). Diatom species more common in Diatom Zone 2a, including *Nitzschia amphibia*, *Epithemia adnata*, *Eunotia bilunaris*, and *Hantzschia amphioxys*, fell on the left of the ordination, and co-occurred with macrofossil remains more common in Macrofossil Zone 1, including gastropods and *Equisetum fluviatile* remains (Figure 6.22a and b). Epiphytic and benthic diatom species common in Diatom Zone 2b plotted in the upper right side of the ordination area, and co-occurred with remains common early in Macrofossil Zone 2, including *D. pulex* ephippial remains, *Ceratophyllum demersum*, and *Potamogeton* spp. Lastly, the small fragilarioid, planktonic, and benthic diatoms common in Diatom Zone 4 plotted in the lower right of the ordination, and co-occurred with macrofossil remains more abundant in the recent record, including various benthic invertebrates, and trichoschlereids (Figure 6.22a and b). Overall there was very good agreement between changes in community composition between diatoms and macrofossils, with distinct assemblages representing the earlier, mid- and more recent parts of the record.

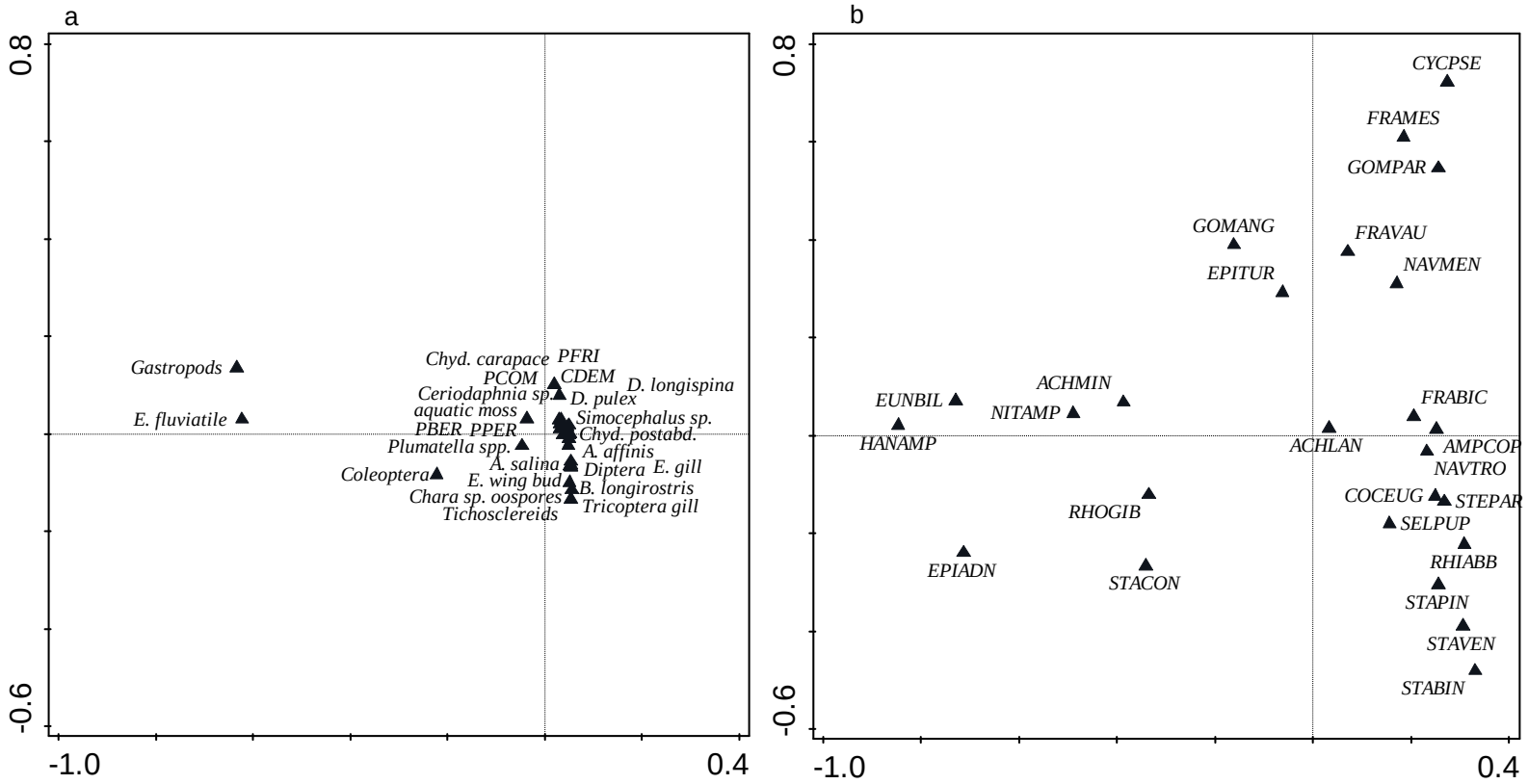

Figure 6.22. a) Macrofossil, and b) diatom CoCA community biplots. Species falling in the same area across plots tend to co-occur in the proxy records. Macrofossil codes can be found in Apendix 4. Diatoms species codes can be found in Appendix 6.

6.4 Discussion

6.4.1 Initial lake development in the 19th century

The bottom 10 cm of the SLNG04 sediment record (60 to 50 cm) are characterized by an absence of submerged aquatic macrophytes and aquatic animal remains, an absence of preserved algal pigments, and very low diatom concentrations and diatom diversity, with primarily epiphytic and aerophilic diatoms present. The combined biological records likely indicate a period of time prior to or during lake development, and indicate a semi-terrestrial or marshy ecosystem (Figure 6.23), with high exposure to light and air present at SLNG04 prior to the mid-19th century (Reuss *et al*., 2005; Luoto *et al*., 2017). The sparse biological communities and presence of marginal macrophytes at SLNG04 at this time coincide with very low LOI_{550}, LOI_{950}, and low water content of sediments. Further, this is a time of highly fluctuating magnetic susceptibility, likely indicating high levels of sediment influx/erosion or a range of sources providing material to the site (Eriksson and Sandgren, 1999; Gell *et al*., 2007) (See 4.3.3). The appearance of mollusc remains beginning in the mid-19th century indicates transition to more permanent body of water or increasingly wet conditions (White *et al*., 2008). The appearance of molluscs in the SLNG04 core coincides with slight increase in diatom concentrations, and increases in water content and LOI_{550}, likely indicating the transition to the permanent inundation period of SLNG04 (Gell *et al*., 2007). However, the diatom community consists mainly of epiphytic and small benthic diatoms at this point, including some taxa common to aerophilic environments (*Epithemia adnata*, *Nitzschia amphibia*, *Eunotia bilunaris*, *Hantzschia amphioxys*), indicating a small, shallow water body, high-closure system with mostly littoral and epiphytic habitats (Table 6.6) (Hay *et al*., 2000; Summers *et al*., 2017). The appearance of pigments in the mid-19th century, and increasing diatom concentrations during this time coincides with a large magnitude earthquake just off-shore of the Selenga Delta in 1862. The Tsagan earthquake of 1862 was the strongest ever recorded in East Siberia (with a magnitude of 7.5) and was integral in forming the contemporary structure of the right bank of the Selenga Delta and Proval Bay of Lake Baikal (Vologina *et al*., 2010). The earthquake resulted in substantial subsidence and flooding of a large area of the northeast corner of the Delta, with a total area of approximately 200 km^2 suffering from flooding and subsidence, and total subsidence depths of up to 9 m (Orlov, 1872). It is possible that the earthquake is responsible

for the more permanent development of SLNG04. Further, *Achnanthidium minutissimum*, a species tolerant of disturbance and a known early colonizer, becomes common around this time (Stevenson and Bahls, 1999; Nakanishi *et al*., 2004; Ponader and Potapova, 2007), and water content of sediments remains relatively high to the surface (See 4.3.3).

Species	Guild	Autecology	Authority	References
Amphora copulata	Benthic	Mainly occurring in alkaline waters, eutrophic, never or rarely occurring outside of water bodies.	(Kütz.) Schoeman and R.E.M.Archibald 1986	Van Dam *et al*., 1994
Achnanthidium minutissimum	Benthic	Pioneer species, phosphorus specialist. Requires nearly continuous 100% oxygen saturation in water, pH circumneutral. Opportunistic species with wide tolerance of trophic state.	(Kütz.) Czarn. 1994	Cholnoky, 1968; Kuhn *et al*., 1981; Van Dam *et al.,* 1994; Reavie and Smol, 1998; Brown *et al*., 2008; Watchorn *et al*., 2008
Fragilaria capucina v. vaucheriae	Benthic	Mainly occurring in alkaline waters, eutrophic, can occur on moist/wet places.	(Kützing) Petersen 1938	Van Dam *et al*., 1994
Nitzschia amphibia	Benthic	Neutral to alkaline waters, including subaerial habitats, eutrophic environments	Grunow 1862	Reichardt, 1985; Van Dam *et al*., 1994
Hantzschia amphioxys	Aerophilic/ benthic/ epiphytic	Circumneutral, pollution tolerant, tolerant to drying.	Grunow 1877	Reichardt, 1985; Van Dam *et al*., 1994
Cocconeis placentula v. euglypta	Epiphytic	Mainly occurring in alkaline waters, eutrophic; C. placentula's preferred habitat is *Ceratophyllum demersum*	Ehrenberg 1838	Van Dam *et al*., 1994
Epithemia adnata	Epiphytic	Exclusively occurring in alkaline pH waters, meso-eutrophic.	(Kützing) Brébisson 1838	Van Dam *et al*., 1994
Gomphonema parvulum	Epiphytic	Best development in nutrient rich waters and circumneutral pH. Can occur on moist/wet places. Tolerant to polluted waters.	(Kützing) Kützing 1849	Patrick and Reimer, 1966; Round, 1990; Van Dam *et al*., 1994
Fragilaria mesolepta	Epiphytic	Alkaline, freshwater, tolerant of higher ionic content.	Rabenhorst 1861	Van Dam *et al*., 1994
Staurosirella pinnata	Benthic	Prefers shallow, littoral habitats. Mesoeutrophic to eutrophic or oligotrophic to eutrophic. Requires highly oxygenated waters (nearly 100% saturation).	(Ehrenberg) Williams and Round 1987	Van Dam *et al*., 1994
Staurosirella leptostauron	Benthic	Mainly occurring at pH >7. Requires highly oxygenated waters, pollution intolerant. Meso-eutrophic.	(Ehrenberg) Hustedt 1931	Van Dam *et al*., 1994

Staurosira construens v. binodis	Benthic	Prefers shallow, littoral habitats. Mesoeutrophic to eutrophic or oligotrophic to eutrophic. Littoral assemblage. Requires highly oxygenated waters.	(Ehrenberg) Hamilton 1992	Patrick and Reimer, 1966; Bradbury, 1971; Van Dam *et al*., 1994; Metcalfe *et al*., 1997; Haberzettl *et al*., 2005
Staurosira construens v. venter	Benthic	Prefers shallow, littoral habitats. Mesoeutrophic to eutrophic or oligotrophic to eutrophic. Requires highly oxygenated waters (nearly 100% saturation).	(Ehrenberg) Hamilton 1992	Patrick and Reimer, 1966; Bradbury, 1971; Van Dam *et al*., 1994; Metcalfe *et al*., 1997; Haberzettl *et al*., 2005
Stephanodiscus parvus	Planktonic	Occurs exclusively in alkaline pH. Meso-eutrophic, high total phosphorus and moderate chloride concentration	Stoermer & Håkansson 1984	Stoermer, 1978; Stoermer *et al*. 1978; Stoermer and Håkansson, 1984; Van Dam *et al*., 1994; Reavie and Kireta, 2015

Table 6.6. Summary of main ecological characteristics of dominant diatom species from SLNG04 sediment core.

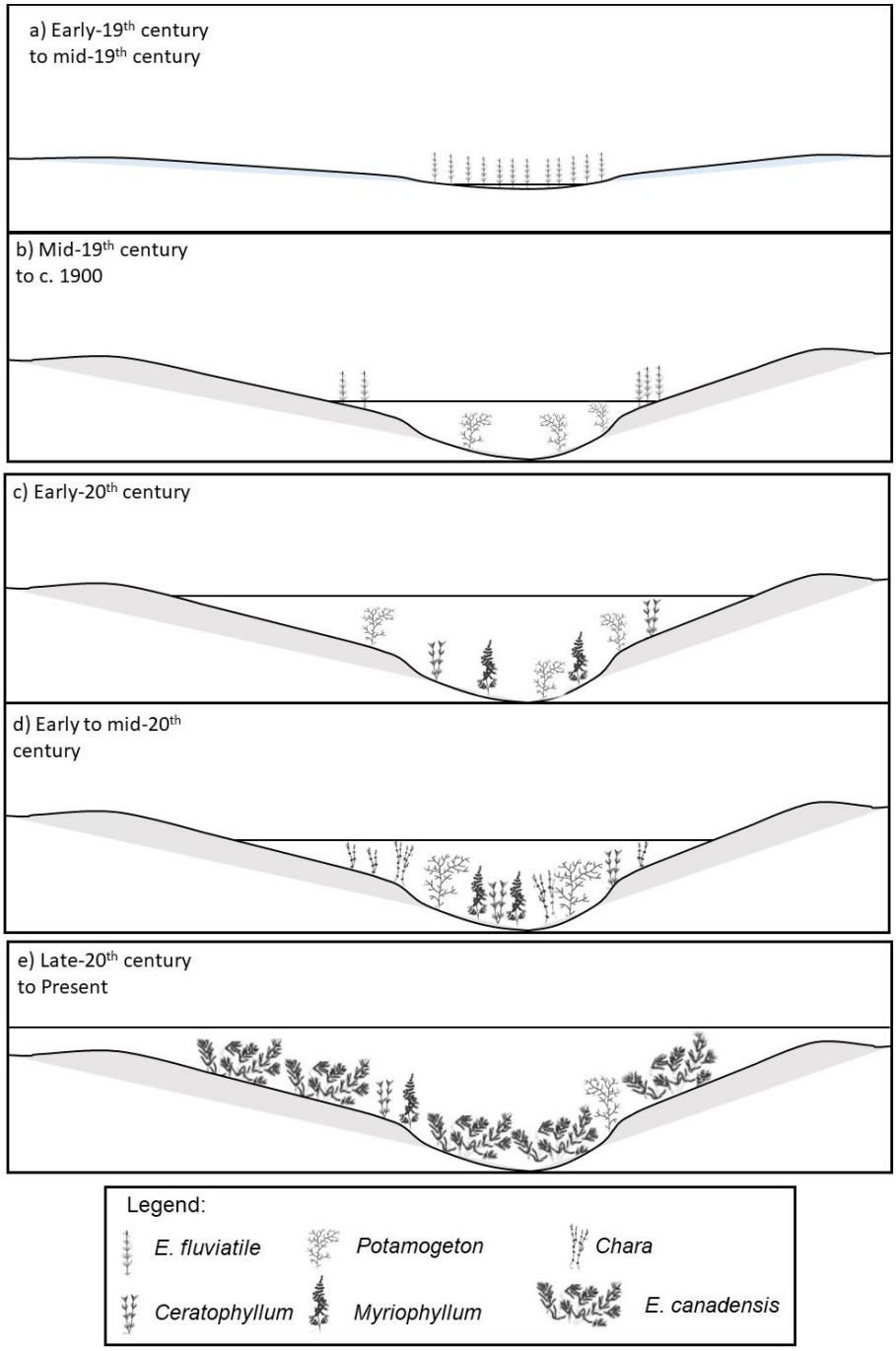

Figure 6.23. Progression of SLNG04 ecosystem from the early-19th century to present (2014), from a) primarily marginal/marsh macrophyte community in the early- to mid-19th century, b) increased inundation and open water zone as a result of the 1862 Tsagan earthquake which resulted in the appearance of submerged macrophyte *Potamogeton* spp., c) increasing depth of SLNG04 in the very early 20th century resulting in greater diversification of submerged macrophytes with *Myriophyllum-Ceratophyllum-Potamogeton* community, d) decreased depth/connectivity and increasing nutrient in the early to mid-20th century led to greater submerged macrophyte abundance, e) increased connectivity of SLNG04 beginning in the 1960s, and invasion of *Elodea canadensis*, resulting in decline in macrophyte diversity.

6.4.2 Mid-twentieth century alkalinity changes

In the early-20th century, there is a major change in the diatom community that is not recorded as significantly in either the macrofossil or pigment records. The change from Diatom Zone 2 to Diatom Zone 3 is due to a decline in diatom concentration of approximately two to three orders of magnitude over the course of only a few years around 1920. The very low diatom concentrations between c. 1920 and c. 1960 coincided with increases in ostracod density (Figure 6.12; Kuznetsova, 2015), increases in *Chara* sp. oospore and *Plumatella* sp. statoblast remains, continued high abundances of *Daphnia longispina* and *D. pulex* ephippial remains, low abundances of benthic invertebrate and Chydoridae remains, low abundance of fish remains, and increases in aquatic moss remains. Decline in diatom concentrations also coincided with sediment content increases in Ca (%), P (%), and LOI_{950}, and low Fe/Mn ratios (See 4.4.3 and 5.3.1). Many of the geochemical changes began in the early-20th century and subsided by the late-1950s.

The decline in diatom concentration at this time is most likely related to increases in pH and alkalinity, resulting in increased dissolution of diatom silica frustules (Ryves *et al*., 2002; Ryves *et al*., 2006). While obvious signs of diatom dissolution are not always present in the samples from Diatom Zone 3 (e.g. high abundance of girdle bands, pitting on valves, only heavily silicified central areas or species remaining), Ryves *et al*. (2013) indicated that dissolution of diatoms may not always be evident, and that dissolution may only be inferred by diatom concentration data (Ryves *et al*., 2002; Florian *et al*., 2015). Further, changes in water chemistry and surface sediment chemistry may result in increased diatom dissolution in freshwater systems, including increased lake water pH, conductivity, and alkalinity, as well as reduced sedimentation rates (Ryves *et al*., 2001; Ryves *et al*., 2002; Ryves *et al*., 2013; Paull *et al*., 2017). Moreover, diatom dissolution may occur over time after burial in carbonate-rich sediment (Outridge *et al*., 2017).

In the early-20th century, increasing agricultural activity and anthropogenic disturbances in the river basin, and increased connection to the Selenga River during recent decades, likely resulted in increasing nutrient flux to SLNG04 resulting in increased primary producer abundance and biomass, and is evidenced by increased pigment concentrations beginning c. 1900, and diatom concentrations in the early-20th century (Figure 6.9 and Figure 6.13). Elevated

nutrient levels in SLNG04 in the early-20th century likely led to increased plant production at this time, resulting in increased photosynthetic removal of CO_2 from the water column, and increased carbonate content and calcite precipitation, and increasing pH and alkalinity, during high productivity months (Talling, 1976). Further, increased plant productivity may have resulted in declining silica levels in the lake (e.g. Hay *et al*., 2000), leading to further diatom dissolution. Increasing alkalinity in SLNG04 beginning c. 1920 is signalled in the sediment record with concurrent increases in LOI_{950}, sediment calcium (%), and the appearance of calcite precipitate forming on macrophyte remains. Increased transport of calcium to SLNG04 in the early-20th century due to increased agricultural activity in the region may also have contributed to elevated pH and alkalinity (Potasznik and Szymczyk, 2015). It is likely that during the early- to mid-20th century, SLNG04 underwent slight reducing conditions due to increased plant abundance, as extended periods of ice-cover in the winter would lead to increased macrophyte decomposition, producing reducing conditions (Anema *et al*., 1990; Hay *et al*., 2000). Increased pH coinciding with reducing conditions may lead to increased phosphorus release from sediments (Koski-Vahala *et al*., 2001; Sondergaard *et al*., 2003; Wu *et al*., 2014). Increased within-lake phosphorus production would add to the already increasing eutrophic conditions at SLNG04, further stimulating plant productivity, and increasing alkalinity, and resulting in increased dissolution of diatoms. Early increases in total phosphorus occur c. 1920 in the sediment record and coincide with maximum Mn levels and minimum Fe/Mn ratios (See Section 5.3.1, Figure 5.2). Further, increasing P in the sediment record coincides with increasing Fe, which peaked at the end of Diatom Zone 3. Shallow depths at this time potentially led to increased turbulence, increased mixing, and increased wave-action, and facilitated increased fragmentation and breakage of diatom frustules, and leading to enhanced dissolution (Flower and Nicholson, 1987; Ryves *et al*., 2006). Maximum lake productivity levels are reached in the late-1950s as observed through pigment concentrations, coinciding with maximum sedimentary P peaks (See Section 5.3.1, Figure 5.2).

6.4.3 Anthropogenic disturbance in the late-20th and early-21st centuries

Diatoms return in greater concentrations to SLNG04 c. 1960, with concentrations increasing by one order of magnitude by the early-1960s, and 2-3 orders of magnitude by c. 1970. The diatom community also undergoes changes in abundance of many of the most common

species, and increased diversity of guilds upon return to the record, relative to the pre-1920 assemblages. Diversity of diatom community is similar between Diatom Zone 2b and Diatom Zone 4, with species richness ranging from 47 species to 62 species in Diatom Zone 2b, and 50 species to 65 species in Diatom Zone 4, with the exception of a brief increase to 77 species in the 1990s. Diatom species assemblages from SLNG04 in the late-20th and early-21st centuries indicate greater connectivity with the Selenga River than pre-1920 assemblages. Increasing abundance and dominance of small benthic fragilariods and planktonic *Stephanodiscus* spp. beginning c. 1970 are probable indicators of increased river inoculation, and connection to the Selenga River (Hay *et al*., 2000; Sokal *et al*., 2008; Brock *et al*., 2011); Genkal and Popovskaya (2008) observed high abundances of *Stephanodiscus* spp. and *Cyclotella* spp. in plankton samples from the Selenga River. Also, analysis of contemporary SLNG diatom communities in Section 3.3.1.3 indicate that *Staurosirella pinnata* and *S. parvus* are strongly associated with increasing surface area in contemporary sites. Increased connectivity, and surface area/depth of SLNG04 may contribute to slightly decreased alkalinity and increased preservation of diatoms beginning in the early-1960s.

The increase in diatom concentrations in the 1960s coincided with the point of significant change in the macrofossil breakpoint analysis (Figure 6.6). Macrophyte assemblages have been observed to have strong ties to levels of connectivity within shallow lakes and wetland ecosystems (Hay *et al*., 2000; Sokal *et al*., 2010). Moreover, changes in submerged macrophyte assemblages often incite changes in other biological communities, as they provide vital services of refugia, food, and habitat in shallow lake ecoystems (Jeppesen *et al*., 2000; Levi *et al.*, 2014). A signficiant relationship was observed in Section 3.3.1 between macrofossil remains and diatom assemblage variability across contemporary Selenga River basin lakes (Figure 3.8), a relationship that has been observed in other floodplain wetland systems (e.g. Hay *et al*., 2000; Sokal *et al*., 2010). It was observed in Section 3.3.2 that macrofossil richness was significantly linked with connectivity levels in the Selenga River basin. Water depth is a significant variable influencing diatom and macrophyte distributions in shallow wetland lakes, which may be related to changes in hydrological regimes (Moser et al., 2000; Michelutti et al., 2001). Moreover, small fluctuations in water levels in shallow lake systems may have a large influence on dilution/evapoconcentration and light penetration (Cobbaert et al., 2014). Brock et al. (2011)

observed that following the construction of the Peace River hydroelectric dam, flood regimes were altered downstream along the Slave River, resulting in increased flood frequency and higher water levels in shallow lakes in the Slave River Delta, altering the macrophyte and diatom communities. Indeed, connectivity changes at SLNG04 in the mid-20th century resulted in significant ecological community shifts, observed at multiple trophic levels.

The return of diatoms in the early-1960s, macrophyte and zooplankton assemblage changes, and signs of greater levels of connectivity at SLNG04 post-1960 may be related to extensive flooding that occurred around Lake Baikal at this time, due to the completion, in 1956, of the Irkutsk Dam on the Angara River, Lake Baikal's only outflow. Filling of the associated reservoir began in 1956 and within seven years the reservoir was full and Lake Baikal had risen by ~1.5 m depth (Bolgov *et al*., 2017). Subsequently, low-lying shorelines and environments surrounding Lake Baikal were submerged and flooded, and over 350 km^2 of the Selenga River Delta was flooded at the time (Pinegin *et al.*, 1976). Due to the proximity of SLNG04 to Lake Baikal, it is likely that a flood of this magnitude would impact the lake, possibly increasing its surface area, depth, and connectivity. The sharp and temporary increase in sedimentation rate in the early-1960s (1963 ± 4 yrs), may correspond with the timing of the flood (See Section 4.3.3, Figure 4.6), although there is no corresponding event recorded in the magnetic susceptibility profile, which would signal an in-wash of sediments linked to a flood occurrence.

In the early-1990s, there is a doubling of sedimentation rate which has been sustained and is fairly constant to the present day, and may indicate establishment of current connectivity status with the Selenga River. This increased connection may have also facilitated the transport of the invasive species *Elodea canadensis,* an aquatic submerged macrophyte, to SLNG04. The invasive waterweed was introduced to and became established in Lake Baikal in the 1970s (Kozhova and Izhboldina, 1993), and the spread of *E. canadensis* into the branches of the Selenga Delta likely occurred due to both natural spread and anthropogenic transportation (Kravtsova *et al*., 2009). *E. canadensis* does not preserve in sediment cores and it is therefore difficult to directly track its introduction and establishment without historical records. However, indirect effects of *E. canadensis* introduction and establishment may be captured by the palaeo-record. Most submerged macrophyte remains underwent a decline in both flux and abundance in the 1990s, including declines in *Potamogeton* spp. and *Myriophyllum* spp. at SLNG04.

Elsewhere, Mjelde *et al*. (2012) noted impacts on the submerged macrophyte community of a Norwegian shallow lake following *E. canadensis* invasion, which included displacement of *Potamogeton* spp., and extirpation of *Callitriche* sp. and *Najas* sp. As current percent volume infested (PVI) of SLNG04 is nearly 50% (Section 3.3.1, Table 3.3), indicating high abundance of submerged macrophytes (Sayer *et al*., 2010b), with *E. canadensis* being the dominant submerged macrophyte (Section 3.3.1, Table 3.4), it is likely that the recent decline in abundance and flux of many aquatic macrophytes in the SLNG04 record was driven by the establishment of *E. canadensis* by the late 1990s. It is known to have outcompeted many *Potamogeton* sp. and *Myriophyllum* sp. in Lake Baikal since the 1970s (Kravtsova *et al*., 2009). *E. canadensis* prefers habitats with highly calcified bottom sediments, and so the high calcium levels and calcite precipitate in sediment of SLNG04 until the early-1990s may have aided the establishment of this invasive species. However, once established, the invasive waterweed actively takes up available calcium from within the lake during the first few years of invasion, causing calcium levels in the lake to decline (Kravtsova *et al*., 2009), and the establishment of *E. canadensis* in SLNG04 may coincide with the decline in LOI_{950} in the early-1990s. Therefore, the introduction of *E. canadensis* may have contributed a decline in lake alkalinity in the early-1990s, and to the recovery of the diatom community, as diatom concentrations reach pre-1920s concentrations in the early-1990s and remain high to the surface.

Shifts in trophic structure are apparent in the late-20th century. The shift in Cladocera community structure recorded in the 1980s away from large-bodied pelagic *Daphnia pulex* and *D. longispina*, and subsequent rise in small pelagic *Bosmina longirostris*, plant-associated *Ceriodaphnia* sp., and benthic *Simocephalus* sp., *Alona affinis,* and *Alona salina,* is likely related to increased fish predation beginning in the 1980s (Mills *et al*., 1987; Jeppesen *et al*., 2011). A second possible explanation for the shift in zooplankton community is a shift in habitat type. Contemporary Selenga River basin macrofossil analysis indicated strong association between *Daphnia* spp. and increased abundance of *Potamogeton* spp., and strong association between Chydoridae cladocera with *Ceratophyllum demersum* and *Myriophyllum* spp. (See Section 3.3.1.2). The decline in many submerged macrophyte plant remains in the late-20th century at SLNG04, including *Potamogeton* spp. and *Myriophyllum* spp., co-occurred with a change in zooplankton and benthic invertebrate communities. The change in habitat structure

that followed the establishment of *Elodea canadensis* in the 1990s may have contributed to shifts in trophic structure, as dense *E. canadensis* stands may lead to increasing biomass of invertebrates, including zooplankton and insect larvae, as the dense vegetation provides protection from fish predation (Kravtsova *et al*., 2009).

6.5 Conclusion

The expansive, shallow lake that currently is SLNG04 has undergone several significant shifts in state, structure, and functioning since the early-19th century. Palaeolimnological records from SLNG04 reveal the early development of the lake as a shallow, likely marshy habitat in the 19th century, possibly related to a nearby earthquake in 1862 caused flooding and subsidence of much of the land surrounding SLNG04. A further catastrophic flood event in southern Siberia in 1897 (a result of unusually high summer precipitation), coinciding with the end of a three-decade-long dry period in 1905, likely resulted in the expansion of SLNG04 very early in the 20th century, and the development of a deeper open water zone, now hospitable to diverse communities of submerged macrophytes, algae, and zooplankton. Increased agricultural disturbances in the Selenga River basin likely led to early eutrophication in SLNG04 in the early-20th century, resulting in enhanced macrophyte growth. The high nutrient and macrophyte levels in SLNG04 resulted in increased alkalinity and pH, and lead to substantial dissolution of the diatom communities between c. 1920 and c. 1960, while other algae and zooplankton communities were not significantly affected. Major flooding of the Selenga Delta in the early-1960s as a result of construction of the Irkutsk Dam on the Angara River, and resulting increased connectivity of SLNG04 with the Selenga River in the mid- to late-20th century, resulted in signficiant shifts in ecological structure of SLNG04, including recovery of the diatom community and shifts in zooplankton and macrophyte communities, and likely promoted the establishment of the invasive Canadian waterweed *Elodea canadensis* and increased fish predation in SLNG04, both of which likely incited shifts in trophic interactions and structure of zooplankton and submerged macrophyte communities. SLNG04 remains eutrophic at present day, with high abundance of submerged macrophytes, the majority of which are the invasive *E. canadensis*. It can therefore be concluded that local natural disturbances, regional natural variability in climate, and anthropogenic stressors have incited ecological responses within the shallow, Selenga Delta lake during the last two centuries. These findings have implications for

how variations in connectivity and anthropogenic disturbances may impact the biological nature of shallow lakes within highly connected deltaic systems.

6.6 References

Battarbee R.W. Jones V., Flower R., Cameron N., Bennion H., Carvalho L., & Juggins S. (2001) Diatoms. In Terrestrial, algal and siliceous indicators. Eds. J. Smol, H.J.B. Birks, and M. Last, Kluwer Academic Publishers,The Netherlands. pp. 155–202.

Bazhenova O.I., & Kobylkin D.V. (2013) The dynamics of soil degradation processes within the Selenga Basin at the agricultural period. *Geography and Natural Resources* **34,** 221-227.

Birks H.H. (2001) Plant macrofossils. In: Tracking Environmental Change Using Lake Sediments. Volume 3: Terrestrial, Algal, and Siliceous Indicators. Eds. J.P. Smol, H.J.B. Birks & W.M. Last, Kluwer Academic Publishers, Dordrecht, the Netherlands. pp. 49–74.

Bolgov, M.V., Buber A.L., Korobkina E.A., Lyubushin A.A., & Filippova I.A. (2017) Lake Baikal: extreme level as a rare hydrological event. *Water Resources* **44,** 522-536.

Bradbury J.P. (1971) Paleolimnology of lake Texoco Mexico: Evidence from diatoms. *Limnology and Oceanography* **16,** 180-200.

Brock B.E., Martin M.E., Mongeon C.L., Sokal M.A., Wesche S.D., Armitage D., Wolfe B.B., Hall R.I., & Edwards T.W.D. (2011) Flood frequency variability during the past 80 years in the Slave River Delta, NWT, as determined from multi-proxy palaeolimnological analysis. Canadian Water Resources Journal, 35, 281-300.

Brown L., May J. & Hunsaker C. (2008) Species composition and habitat associations of benthic algal assemblages in headwater streams of the Sierra Nevada, California. *Western North American Naturalist* **68**, 194-209.

Cholonky B.J. (1968) Die Okologie der Diatomeen in Binnengewasser. J. Cramer, Lehre, 699 pp.

Eriksson M. G. & Sandgren P. (1999) Mineral magnetic analyses of sediment cores recording recent soil erosion history in central Tanzania. *Palaeogeography. Palaeoclimatology. Palaeoecology*. **152,** 365–383.

Florian C., Miller G., Fogel M., Wolfe A., Vinebrooke R., & Geirsdottir A. (2015) Algal pigments in Arctic lake sediments record biogeochemical changes due to Holocene climate variability and anthropogenic global change. *Journal of Paleolimnology* **54,** 53–69.

Flower R.J., & Nicholson A.J. (1987) Relationships between bathymetry, water quality, and diatoms in some Hebridean lochs. *Freshwater biology* **18,** 71-85.

Gell P., Tibby J., Little F., Baldwin D., & Hancock G. (2007) The impact of regulation and salinization on floodplain lakes: the lower River Murray, Australia. *Hydrobiologia* **591,** 135-146.

Genkal S.I., & Popovskaya G.I. (2008) Centric datom algae of the Selenga River and its delta branches. *Inland Water Biology* **1,** 120-128.

Gorham E., Dean W.E., & Sanger J.E. (1983) The chemical composition of lakes in the north-central United States. *Limnology and Oceanography* **28,** 287-301.

Guo W., Huo S., & Ding W. (2015) Historical record of human impact in a lake in northern China: Magnetic susceptibility, nutrients, heavy metals, and OCPs. *Ecological Indicators* **57,** 74-81.

Haberzettl T., Fey M., Lucke A., Maidana N., Mayr C., Ohlendorf C., Schabitz F., Schelser G.H., Wille M. and Zolitschka B. (2005) Climatically driven lake level changes during the last two millennia as reflected in sediments of Laguna Potrok Aike, southern Patagonia (Santa Cruz, Argentina). *Journal of Paleolimnology 33*, 283-302.

Hay M.B., Michelutti N., & Smol J.P. (2000) Ecological patterns of diatom assemblages from Mackenzie Delta lakes, Northwest Territories, Canada. Canadian Journal of Botany 78, 19-33.

Heglund P.J., & Jones J.R. (2003) Limnology of shallow lakes in the Yukon Flats National Wildlife Refuge, Interior Alaska. Lake and Reservoir Management 19, 133-140.

Jeppesen E., Jensen J.P., Sondergaard M., Lauridsen T., & Landkildehus F. (2000) Trophic structure, species richness and biodiversity in Danish lakes: changes along a phosphorous gradient. *Freshwater Biology*, **45,** 201-218.

Jeppesen E., Noges P., Davidson T.A., Haberman J., Noges T., Blank K., Lauridsen T.L., Sondergaard M., Sayer C., Laugaste R., Johansson L.S., Bjerring R., Amsinck S.L. (2011) Zooplankton as indicators in lakes: a scientific-based plea for including zooplankton in the ecological quality assessment of lakes according to the European Water Framework Directive (WFD). *Hydrobiologia* **676,** 279-297.

Juggins S. 2014. C2 data analysis, Version 1.7.6. University of Newcastle, United Kingdom.

Kadetova A.V., & Radziminovich Y.B. (2014) The catastrophic flood in Transbaikalia (Central Asia) in 1897: a case study. *Natural Hazards* **72,** 23-441.

Khazheeva Z.I., & Tulokhonov A.K. (2007) Distribution of metals in bottom deposits in the branches of Selenga River Delta. *Geochemistry International* **45,** 185-192.

Koski-Vahala J., Hartikainen H., & Tallberg P. (2001) Phosphorus mobilization from various sediment pools in response to increased pH and silicate concentration. Journal of Environmental Quality 30, 546-552.

Kozhova O.M., & Izhboldina L.A. (1993) Spread of Elodea canadensis in Lake Baikal. Hydrobiologia, 259, 203-211.

Kravtsova L.S., Izhboldina L.A., Mekhanikova I.V., Pomazkina G.V., & Belykh O.I. (2009) Naturalization of Elodea canadensis Mich. in Lake Baikal. Russian Journal of Biological Invasions, 1, 162-171.

Kuznetsova D. (2015) Temporal and spatial variations in ostrcod communities in the Selenga Delta, Lake Baikal. Unpublished MSc thesis, Department of Geography, University College London.

Kuhn D.L., Plafkin J.L., Cairns J. & Lowe R.L. (1981) Quantitative characterisation of aquatic environments using diatom life-form strategies. *Transactions of the American Microscopial Society* **100**, 165-182.

Levi E.E., Cakiroglu A.I., Bucak T., Odgaard B.V., Davidson T.A., Jeppesen E., & Beklioglu M. (2014) Similarity between contemporary vegetation and plant remains in the surface sediment in Mediterranean lakes. *Freshwater Biology*, **59,** 724-736.

Luoto T.P., Kuhry P., Holzkamper S., Solovieva N., & Self A.E. (2017) A 2000-year record of lake ontogeny and climate variability from the north-eastern Russian Arctic. *The Holocene* **27,** 339-348.

McGowan S., Barker P., Haworth E.Y., Leavitt P.R., Maberly S.C., & Pates J. (2012) Humans and climate as drivers of algal community change in Windermere since 1850. Freshwater Biology 57, 260-277.

Metcalfe S.E., Bimpson A., Courtice A.J., O'Hara S.L. and Taylor D.M. (1997) Climate change at the monsoon/Westerly boundary in northern Mexico. *Journal of Paleolimnology* **17**, 155-171.

Mills E.L., Green D.M., & Schiavone A.J. (1987) Use of zooplankton size to assess the community structure of fish populations in freshwater lakes. *North American Journal of Fisheries Management* **3,** 369-378.

Mjelde M., Lombardo P., Berge D., & Johansen S.W. (2012) Mass invasion of non-native *Elodea canadensis* Michx. In a large, clear-water, species-rich Norwegian lake – impact on macrophyte biodiversity. *International Journal of Limnology* **48,** 225-240.

Nakanishi, Y., Sumita, M., Yumita, K., Yamada, T., & Honjo, T. (2004). Heavy-metal pollution and its state in algae in Kakehashi river and Godani river at the foot of Ogoya mine, Ishikawa Prefecture. Analytical Sciences, 20, 73–78.

Orlov A.P. (1872) General remarks on earthquakes, with special reference to South Siberia and Turkestan Region. *Proceedings of the Kazan University Society of Natural Sciences*, **3,** 1-10.

Outridge P.M., Sanei H., Courtney Mustaphi C., & Gajewski K. (2017) Holocene climate change influences on trace metal and organic matter geochemistry in a varved Arctic lake sediment over 7,000 years. *Applied Geochemistry* **78,** 35–48.

Patrick R., & Reimer C.W. (1966) The diatoms of the United States. The Academy of Natural Sciences, Philadelphia.

Pinegin A.V., Rogozin A.A., Leshchikov F.N., Kulish L.Y., & Yakimov A.A. (1976) Shore dynamics of Lake Baikal at the new level regime. Nauka, Moscow.

Ponader K.C., & Potapova M.G. (2007) Diatoms from the genus *Achnanthidium* in flowing waters of the Appalacian Mountains (North America): Ecology, distribution, and taxonomic notes. *Limnologica* **37,** 227-241.

Potasznik A., & Szymczyk S. (2015) Magnesium and calcium concentrations in the surface water and bottom deposits f a river-lake system. *Journal of Elementology* **20,** 677-692.

R. v.3.2.4 R. 2016. The R Foundation, R Development Team. Vienna.

Reavie E.D. & Smol J.P. (1998) Epilithic diatoms of the St. Lawrence river and their relationships to water quality. *Canadian Journal of Botany* **76**, 251-257.

Reavie E.D., & Kireta A.R. (2015) Centric, Araphid and Eunotioid Diatoms of the Coastal Laurentian Great Lakes. *Bibliotheca Diatomologica* **62,** 1-184.

Reichardt E. (1985) Diatomeen an feuchten Felsen des Sudlichen Frankenjuras. *Berichte Bayerische Botanische Gesellschaft* **56,** 167-187.

Reuss N., Conley D.J., & Bianchi T.S. (2005) Preservation conditions and the use of sediment pigments as a tool for recent ecological reconstructions in four Northern Europe estuaries. *Marine Chemistry* **95,** 283-302.

Round F.E. (1990) Diatom communities, their response to changes in acidity. *Philosophical Transactions of the Royal Society: Series B, Biological Sciences* **327,** 243-249.

Ryves D., Juggins S., Fritz S., & Battarbee R.W. (2001) Experimental diatom dissolution and the quantification of microfossil preservation in sediments. *Palaeogeography. Palaeoclimatology. Palaeoecology*. **172,** 99–113.

Ryves D., McGowan S., & Anderson N.J. (2002) Development and evaluation of a diatom-conductivity model from lakes in West Greenland. *Freshwater Biology* **47,** 995–1014.

Ryves D., Battarbee R., Juggins S., Fritz S., & Anderson N.J. (2006) Physical and chemical predictors of diatom dissolution in freshwater and saline lake sediments in North America and West Greenland. *Limnology and Oceanography* **51,** 1355–1368.

Ryves D., Anderson N.J., Flower R., & Rippey B. (2013) Diatom taphonomy and silica cycling in two freshwater lakes and their implications for inferring past lake productivity. *Journal of Paleolimnology* **49,** 411–430.

Sayer C., Davidson T.A., Jones J.I., & Langdon P.G. (2010a) Combining contemporary ecology and paleolimnology to understand shallow lake ecosystem change. *Freshwater Biology* **55,** 487-499.

Sayer C., Davidson T.A., &b Jones J.I. (2010b) Seasonal dynamics of macrophytes and phytoplankton in shallow lakes: a eutrophication-driven pathway from plants to plankton. Freshwater Biology 55, 500-513.

Sokal M. A., Hall R.I., & Wolfe B.B. (2008). Relationships between hydrological and limnological conditions in lakes of the Slave River Delta (NWT, Canada) and quantification of their roles on sedimentary diatom assemblages. Journal of Paleolimnology 39, 533 ‐ 550.

Sokal M.A., Hall R.I., Wolfe B.B. (2010) The role of flooding on inter-annual and seasonal variability of lake water chemistry, phytoplankton diatom communities, and macrophyte biomass in the Slave River Delta (Northwest Territories, Canada). *Ecohydrology* **3,** 41-54.

Sondergaard M., Johansson L.S., Lauridsen T.L., Jorgensen T.B., Liboriussen L., & Jeppesen E. (2010) Submerged macrophytes as indicators of the ecological quality of lakes. Freshwater Biology, 55, 893-908.

Stevenson R.J., & Bahls L.L. (1999). Periphyton protocols. In: Rapid bioassessment protocols for use in wadeable streams and rivers: Periphyton, benthic macroinvertebrates, and fish. EPA 841-B-99-002 (2nd ed., pp. 6.1–6.22). Eds. M.T. Barbour, J.Gerritsen, & B.D. Snyder. Washington: United States Environmental Protection Agency.

Stoermer E.F. (1978). Phytoplankton as indicators of water quality in the Laurentian Great Lakes. *Transactions of the American Microscopical Society* **97,** 2-16.

Stoermer E.F., & Håkansson H. (1984) Stephanodiscus parvus: Validation of an enigmatic and widely misconstrued taxon. *Nova Hedwigia* **39,** 497-511.

Stoermer E.F., Ladewski B.G., & Schelske C.L. (1978) Population response of Lake Michigan phytoplankton to nitrogen and phosphorus enrichment. *Hydrobiolgia* **57,** 249-265.

Summers J.C., Kurek J., Ruhland K.M., Neville E.E., & Smol J.P. (2017) Assessment of multi-trophic changes in a shallow boreal lake simultaneously exposed to climate change and aerial deposition of contaminants from the Athabasca Oil Sands Region, Canada. *Science of the Total Environment* **592,** 573-583.

Talling S.J. (1976) The depletion of carbon dioxide from lake water by phytoplankton. *Journal of Ecology* **64,** 79-121.

Ter Braak C.J.F. & Šmilauer P. (2012): Canoco reference manual and user's guide: software for ordination, version 5.0. Microcomputer Power, Ithaca, USA, 496 pp.

Van Dam H., Mertens A., & Sinkeldam J. (1994) A coded checklist and ecological indicator values of freshwater diatoms from the Netherlands. *Netherlands Journal of Aquatic Ecology* **28,** 117-133.

Vologina E.G., Kalugin I.A., Osukhovskaya Y.N., Sturm M., Ignatova N.V., Radziminovich Y.B., Dar'in A.V., & Kuz'min M.I. (2010) Sedimentation in Proval Bay (Lake Baikal) after earthquake-induced subsidence of part of the Selenga River delta. *Russian Geology and Geophysics*, **51,** 1275-1284.

Watchorn M., Hamilton P., Anderson T., Roe H. and Patterson R.(2008) Diatoms and pollen as indicators of water quality and land-use change: a case study from the Oak Ridges Moraine, Southern Ontario, Canada. *Journal of Paleolimnology* **39**, 491-509.

White D., Preece R.C., Shchetnikov A.A., Parfitt S.A., & Dlussky K.G. (2008) A Holocene molluscan succession from floodplain sediments of the upper Lena River (Lake Baikal Region), Siberia. *Quaternary Science Reviews* **27,** 962-987.

Wu Y., Wen Y., Zhou J., & Wu Y. (2014) Phosphorus release from lake sediments: effects of pH, temperature, and dissolved oxygen. *Journal of Civil Engineering* **18**, 323-329.

Chapter 7: Sedimentary record of biological change in SLNG05

7.1 Introduction to SLNG05 and the southwest side of Selenga Delta

Since the mid-19th century, the Selenga Delta has undergone dramatic changes in morphology, hydrology, and chemistry. Primary events include one of the largest earthquakes recorded in eastern Siberia, the 1862 Tsagan earthquake which resulted in significant morphological changes to the northeast Selenga Delta (Vologina *et al*., 2010), the construction of the Irkutsk Dam on the Angara River and subsequent flooding of Lake Baikal and the Selenga Delta between 1956 and the mid-1960s (Pinegin *et al*., 1976), and 20th century increases in industrial activities in the Selenga River basin (See Section 1.4.2, Figure 1.3, for detail on the timeline of events within the Selenga River basin). The impact of such changes on the chemical and physical properties of these systems, can result in changes in ecological status of floodplain delta wetland lakes i.e. a regime shift (Scheffer *et al*., 2001; Andersen *et al*., 2008). Ecological regime shifts are abrupt changes in ecological structure and function, generally on several trophic levels, resulting in a sudden swing to an alternative ecological state (Andersen *et al*., 2008; Randsalu-Wendrup *et al*., 2014). The crossing of critical thresholds within an ecosystem will cause a regime shift and result in an alternative state from the original, with different ecological structures and functions. Regime shifts may be the result of internal forcings, or external forces such as climate change, invasive species, nutrient or pollution increases (Andersen *et al*., 2008).

Figure 7.1. Location of SLNG05 within the Selenga Delta, with connection to the Selenga River through the Levobereznaya branch of the Selenga Delta.

Study site SLNG05 sits within the Selenga Delta, on the southwest side of the Delta. SLNG05 is a shallow lake with surface flow connections to the Selenga River, and is connected to the Levoberezhnaya branch of the delta, which is the primary branch delivering water from the Selenga River to Lake Baikal, entering the lake in Cherkalov Bay (Khazheeva and Tulokhonov, 2007) (Figures 7.1 and 7.2). The lake is near the margin of the Delta, however is removed from direct anthropogenic disturbances, such as agricultural practices. As a lake with high connectivity to the Selenga River currently, SLNG05 has high potential for influence from runoff and transport of pollutants, and terrestrial and aquatic stressors from the Selenga River. However, the ecological response of the shallow lake ecosystems within this region of the Delta remains uncertain. Therefore, the aim of this chapter is to investigate how natural and anthropogenic disturbances, beginning in the 19th century, have influenced the structure and functioning of the shallow lake ecosystems of the southwest Selenga Delta, and determine if regional Selenga River basin disturbances, and/or local disturbances within the Selenga Delta have had greater impact, and whether these disturbances have resulted in changes in primary producer biomass, trophic interactions, and ecosystem biodiversity. Specific objectives have been chosen to address the aims of the chapter:

1) Changes in ecological structure since the early-19th century will be assessed by analyzing algal communities, including diatoms, macrophyte, and invertebrate communities from a sediment core extracted from SLNG05;
2) Changes in ecological functioning of SLNG05 since the early-19th century will be assessed using sedimentary pigment, diatom, and macrofossil records enumerated from a sediment core extracted from SLNG05;
3) Potential for regime shifts will be evaluated through the use of statistical analyses (e.g. breakpoint analysis)

a b

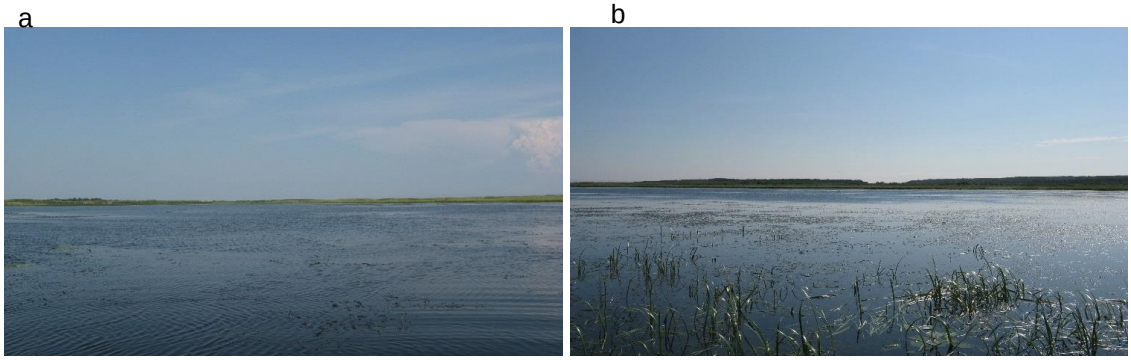

Figure 7.2. a) SLNG05 view from open water, facing north; b) SLNG05 view from shore, facing southeast.

7.2 Methods

Details of coring method, sediment core extruding, and sediment core partitioning for analyses are described in Section 4.2.

7.2.1 Sedimentary macrofossils

Subsamples at 3.0-cm intervals from sediment core SLNG05-C were analysed for macrofossils using the displacement method, and standard sieving and picking methods (Birks, 2001). All methods for macrofossil laboratory processing, microscopy, enumeration, and identification followed procedures outlined in Section 3.2.1.2. Plant and animal macrofossil data were standardized as the number of fossil remains per 100 cm^3 wet sediment. To facilitate comparisons between sites, and to assess abundance of macrofossil remains within a single core taking into account influences of varying sedimentation, fluxes of macrofossils were calculated by first determining the total number of remains per g dry sediment. Fluxes were then

calculated using sedimentation accumulation rates of SLNG05-C since c. 1965 AD (See Section 4.4.3.2 for details of radioisotope dating of SLNG05-C).

7.2.2 Sedimentary aquatic macrofossil data analysis

For detailed account of macrofossil data analytical procedures, see Section 6.2.2.

7.2.3 Sedimentary diatoms

Subsamples at 2.0-cm intervals from sediment core SLNG05 were analysed for diatom analysis according to standard procedures (Battarbee *et al.,* 2001). All diatom laboratory processing and slide preparation methods, enumeration, identification, and numerical analysis followed procedures outlined in Section 3.2.1.3. Species rarefaction for SLNG05 was set to 301 valves, which was the total number of valves enumerated at 12 cm depth, and the minimum number of valves counted in a single sample. Richness in all other samples was then assessed at 301 valves. Diatom accumulation rates were calculated using sedimentation accumulation rates of sediment core SLNG05 since 1965 AD (See Section 4.4.3.2 for details of radioisotope dating of sediment core SLNG05-C).

7.2.4 Sedimentary diatom assemblage data analysis

For detailed account of diatom data analytical procedures, see Section 6.2.4. SLNG05 PCA was performed on a condensed dataset which included only those species present at >2% relative abundance, which included 59 species. Stratigraphical plots of diatom community assemblage relative abundances were constructed, and included all species present at >5% at any one depth (22 species). In addition, breakpoint analysis was performed on the diatom PCA axis 1 scores, as described in Section 6.2.2 for macrofossil analyses.

7.2.5 Sedimentary pigments

Pigments of photosynthetic organisms were analyzed from sediment samples from SLNG05-C following McGowan *et al.* (2012), and laboratory methods were followed as described in Section 3.2.1.4. Sediment was subsampled for pigment analysis at 1.0-cm intervals from SLNG05-C as described in Section 3.2.1.6. Pigment fluxes were calculated using sedimentation accumulation rates of SLNG05-C since c. 1965 AD (See Section 4.4.3.2 for details of radioisotope dating of SLNG05-C).

7.2.6 Sedimentary pigment data analysis

For detailed account of pigment data analytical procedures, see Section 6.2.6.

7.2.7 Data analysis of all biological proxies

Co-correspondence analysis (CoCA) was conducted on pairs of biological indicator records (diatoms*pigments; diatoms*macrofossils; pigments*macrofossils) as described in Section 6.2.7. Exploratory detrended correspondence analysis (DCA) indicated short gradient lengths (< 3.0 SD) for all sedimentary biological records, indicating the appropriateness of linear ordination techniques. Principal components analysis (PCA) was performed on all biological records using Canoco5 (ter Braak and Šmilauer, 2014). Breakpoint analysis was performed in R, using the segmented package, and cluster analysis and broken stick analysis were performed in R, using the rioja package (R. v.3.2.4, 2016). All stratigraphical plots were constructed using C2 (Juggins, 2014).

7.3 Results

7.3.1 SLNG05 sedimentary macrofossil record

Aquatic macrofossil counts found in the SLNG05-C (hereafter referred to as SLNG05) sedimentary record are shown in Figure 7.3a-c. Refer to Section 6.3.1 for details of identification and enumeration grouping strategies. Plant macrofossil remains included seeds and fruits, leaf-spines, leaf tips, leaf fragments (including water lilies leaf cell trichosclereids), and charophyte oospores. Invertebrate macrofossils included bryozoan statoblasts (counted as valves), cladoceran ephippia, chydorid carapaces and postabdomen, molluscs, and fragments of benthic invertebrates. Fish scales and vertebrae were also recovered and enumerated. Total variation explained along the first two PCA axes was 55.0%, with PCA axis 1 explaining 41.5% and axis 2 explaining 13.4% (Table 7.1). PCA indicated two main groupings of macrofossil samples from the SLNG05 sedimentary record: pre-1970 and post-1970 (Figure 7.4). Higher abundances of most macrofossil remains pre-1970 are indicated by the negative association of most species with PCA axis 1 (Figure 7.4). However, some benthic invertebrate remains, including Coleoptera abdominal gills and Ephemeroptera wing buds, as well as fragments of *Potamogeton* sp. 3, an unidentified hybrid species of *Potamogeton*, are positively associated with PCA axis 1, and more recent depths. Broken stick analysis indicated two (marginally) significant zones within the

SLNG05 aquatic macrofossil record (Figure 7.5). Cluster analysis confirms that the two primary zones within the aquatic macrofossil record are from 1) the early-19th century to c. 1970 (61 cm to 21 cm), and 2) c. 1980 to 2014 (18 cm to 0 cm) (Figure 7.6). Breakpoint analysis indicated two significant ($p \leq 0.01$) points of change in the macrofossil PCA axis 1 scores, first c. 1940, and second c. 1980 (Figure 7.7).

	Axis 1	***Axis 2***	***Axis 3***	***Axis 4***
Eigenvalues	0.4150	0.1345	0.0936	0.0648
Explained variation (cumulative)	41.5	55.0	64.3	70.8

Table 7.1. PCA summary table of the SLNG05 aquatic macrofossil record. Eigenvalues and explained variation of the first four PCA axes indicated.

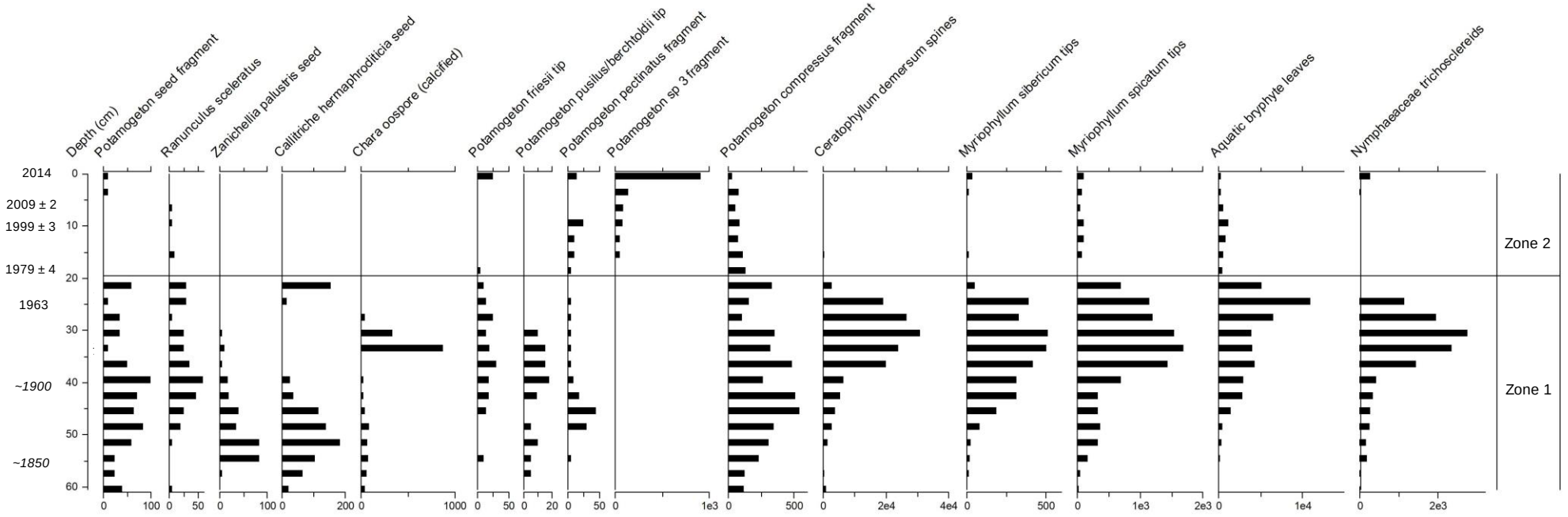

Figure 7.3a Aquatic macrophyte remains from the SLNG05 record. Zones 1 and 2 are indicated. Units for all remains are in no. counts 100 cm^{-3} wet sediment. Radioisotope-derived dates and confidence limits are highlighted on the y-axis. Italicized dates are extrapolated beyond ^{210}Pb radioisotope dating.

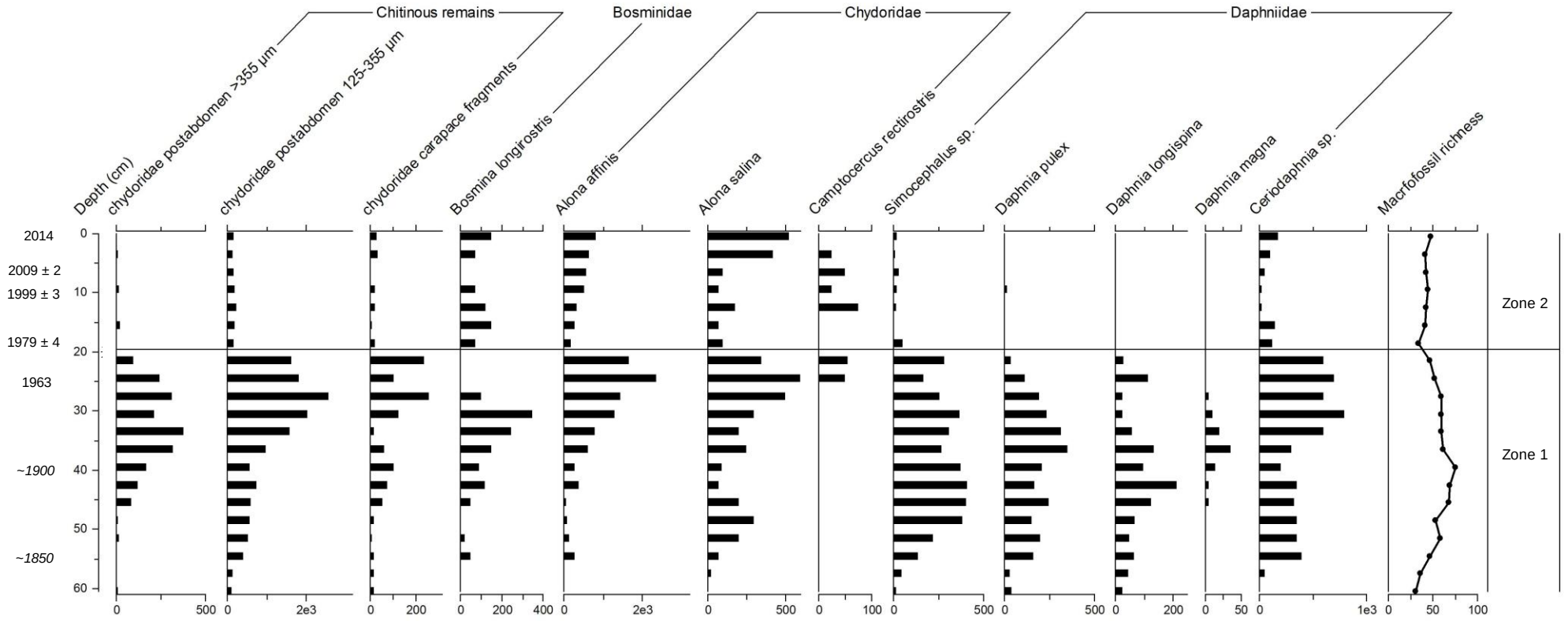

Figure 7.3b. Zooplankton chitinous and ephippial remains enumerated from the SLNG05 macrofossil record. Units for all remains are in no. counts 100 cm^{-3} wet sediment. Total macrofossil richness per sample is displayed. Zones 1 and 2 are indicated. Radioisotope-derived dates and related uncertainties are posted. Italicized dates are extrapolated beyond ^{210}Pb radioisotope dating.

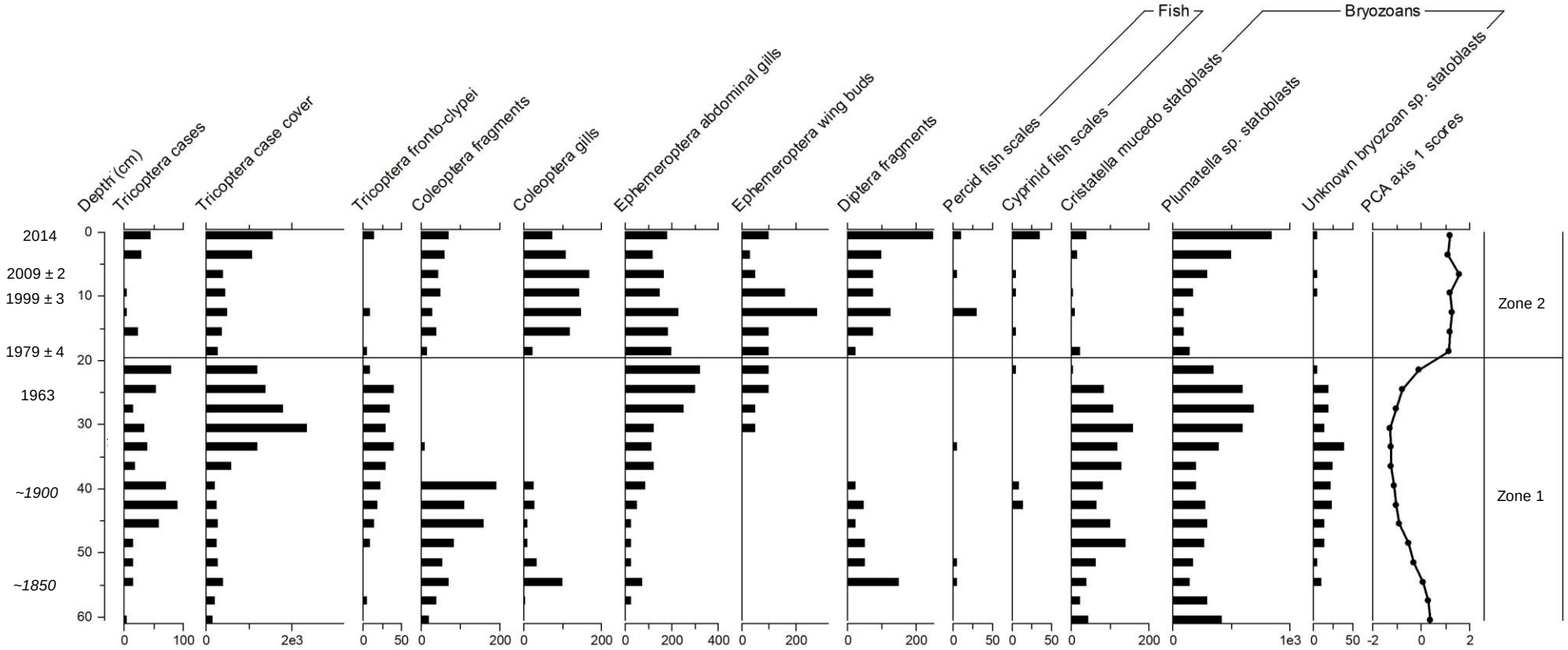

Figure 7.3c. Benthic invertebrate, fish, and bryozoan remains enumerated from the SLNG05 macrofossil record. Macrofossil Zones 1 and 2 are indicated. Units for all remains are in no. counts 100 cm^{-3} wet sediment. Radioisotope-derived dates and confidence limits are highlighted on the y-axis. Italicized dates are extrapolated beyond ^{210}Pb radioisotope dating.

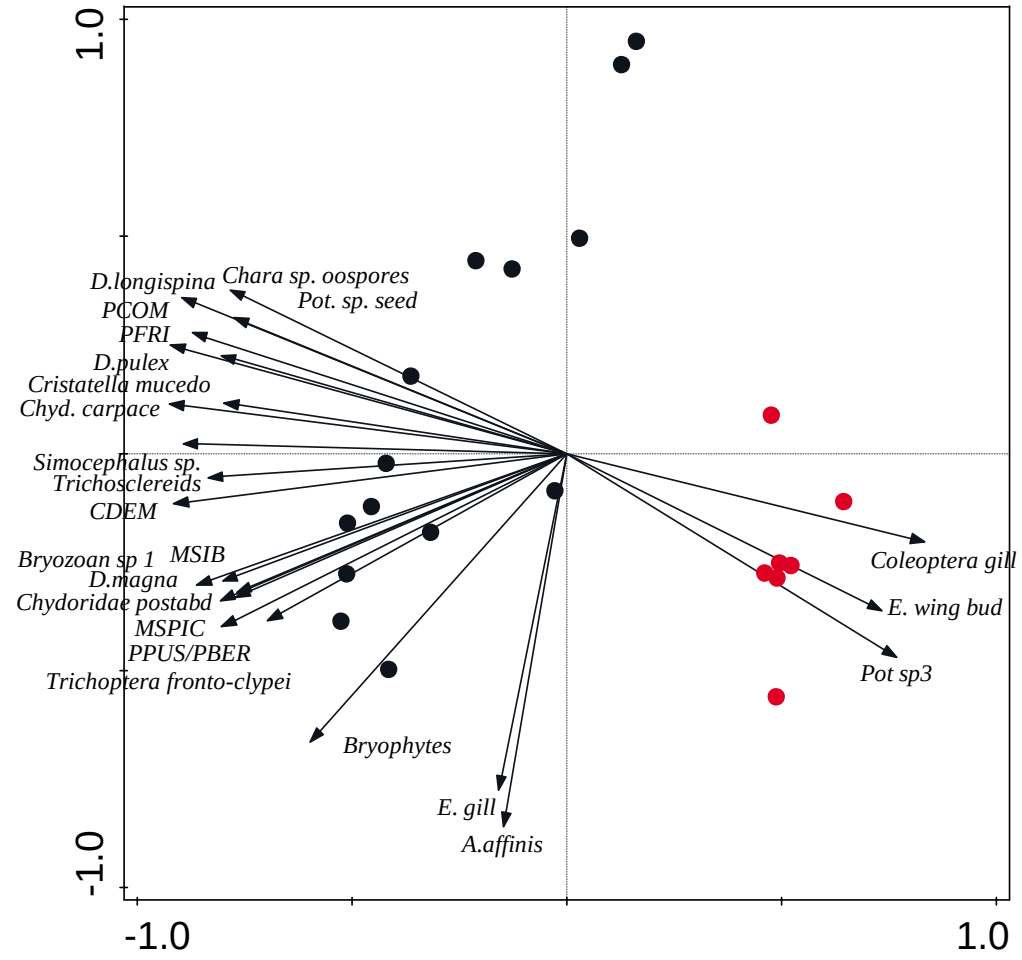

Figure 7.4. PCA biplot of aquatic macrofossil remains and samples from SLNG05. Top 25 remains are plotted according to best species fit. Sample depths are colour-coded according to zone: Macrofossil Zone 1 (early-19th century to c. 1970) (black), Macrofossil Zone 2 (c. 1970 to 2014) (red). Macrofossil codes can be found in Appendix 5.

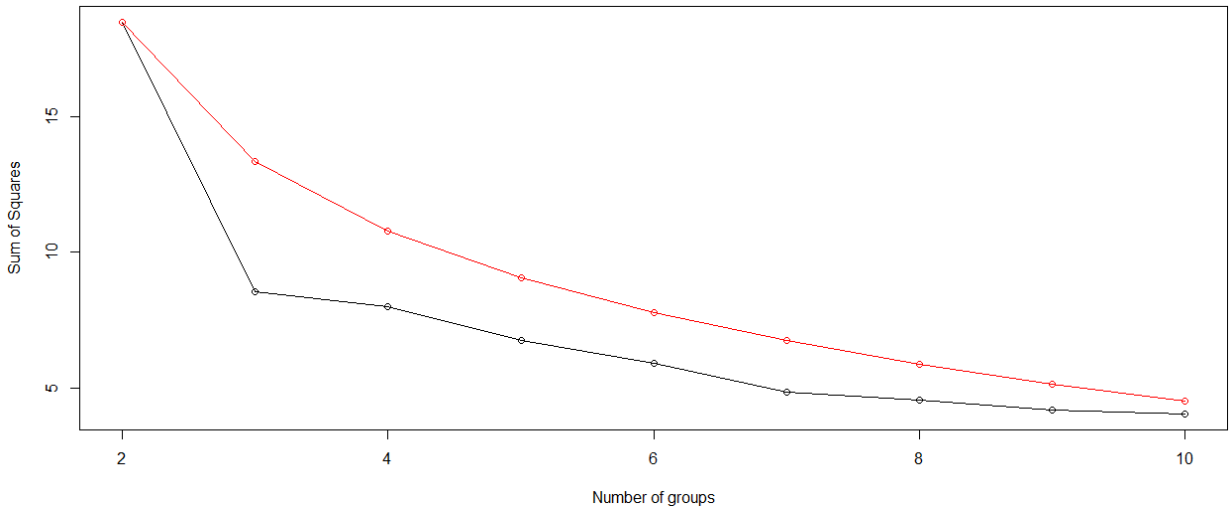

Figure 7.5. Broken stick of the SLNG05 ln(x+1)-transformed aquatic macrofossil record. Two significant groupings of samples are indicated.

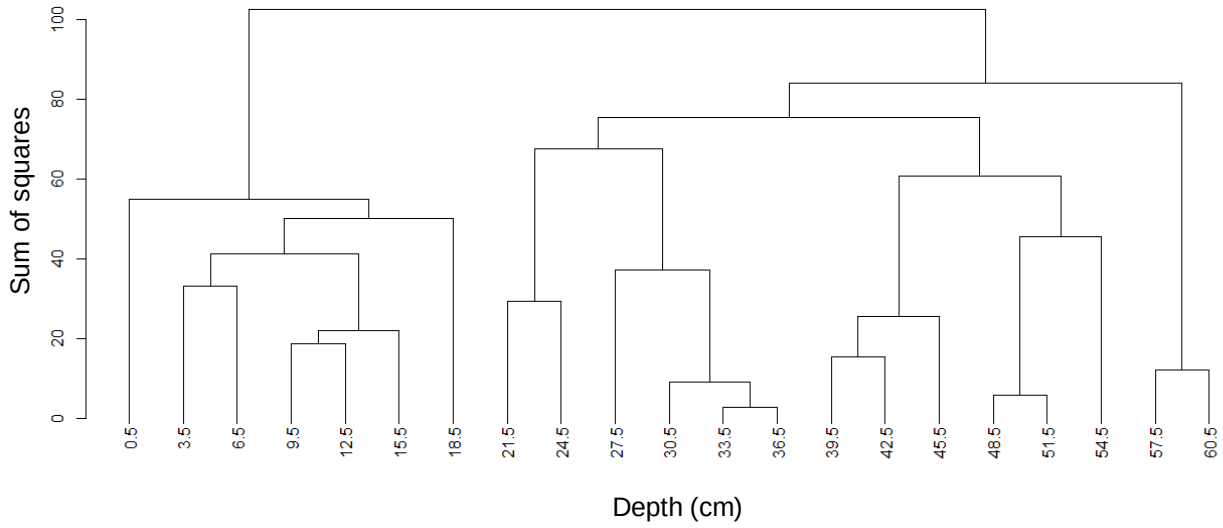

Figure 7.6. Cluster analysis of SLNG05 ln(x+1)-transformed aquatic macrofossil samples. Sample depths are indicated (cm). Two significant groupings occur, as determined through broken stick analysis.

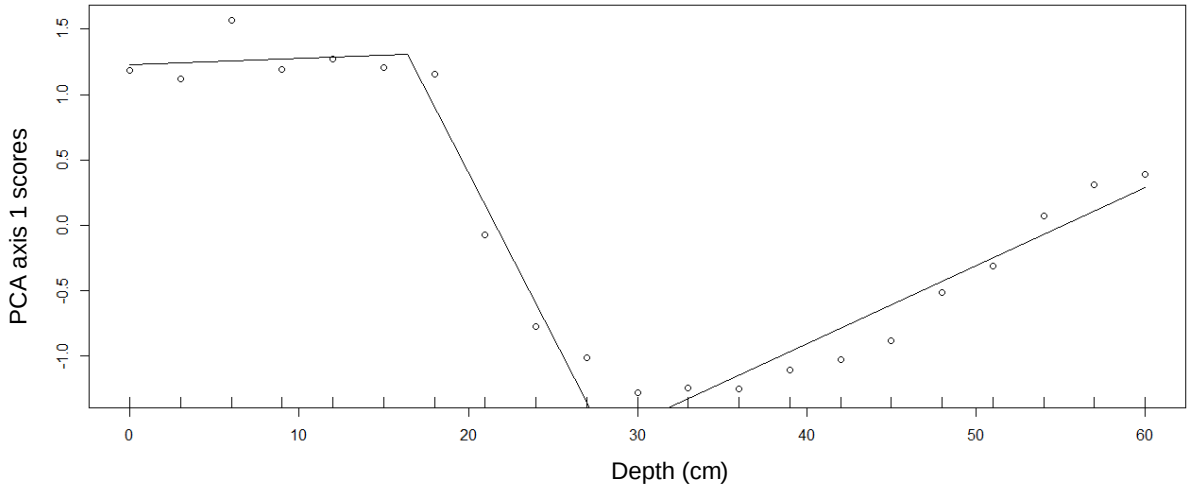

Figure 7.7. Breakpoint analysis of the SLNG05 macrofossil PCA axis 1 scores. Two significant ($p \leq 0.01$) points of change were identified, at 30 cm and 18 cm.

Macrofossil Zone 1: Early-19th century to c. 1970 (61 cm to 21 cm)

Early in Macrofossil Zone 1, dominant macrophyte remains include *Potamogeton* spp. leaves and seeds, *Callitriche hermaphroditica* seeds, and *Zanichellia palustris* seeds (Figure 7.3a). Both *Callitriche hermaphroditica* and *Zanichellia palustris* peak in the mid-19th century (c. 1860). *Callitriche hermaphroditica* and *Zanichellia palustris* remains declined in abundance late

in the 19th century, and implied shifts in submerged aquatic macrophyte community occurred, first with increased abundances and dominance of *Potamogeton* spp. remains, with *P. pectinatus* (PPECT), *P. pusillus/berchtoldii* (PPUS/PBER), *P. compressus* (PCOM), and *P. friesii* (PFRI) remains high in numbers pre-1930 (Figure 7.3a). *Potamogeton* spp. remains declined in numbers post-1930, occurring with increases in *Myriophyllum* spp. (MSIB, MSPIC), *Ceratophyllum demersum* (CDEM), *Chara* spp., Nymphaeaceae trichosclereids, and aquatic moss remains. These macrophyte remains peak between the mid-1920s and ~1960, followed by declines in most macrophytes beginning c. 1965 prior to the end of Macrofossil Zone 1 (Figure 7.3a). *Callitriche hermaphroditica* increased in abundance at the very end of Macrofossil Zone 1, with number of remains found similar to early Zone 1 numbers. Macrofossil richness increased through the first half of Macrofossil Zone 1 to peak at 75 c. 1900 (Figure 7.3b).

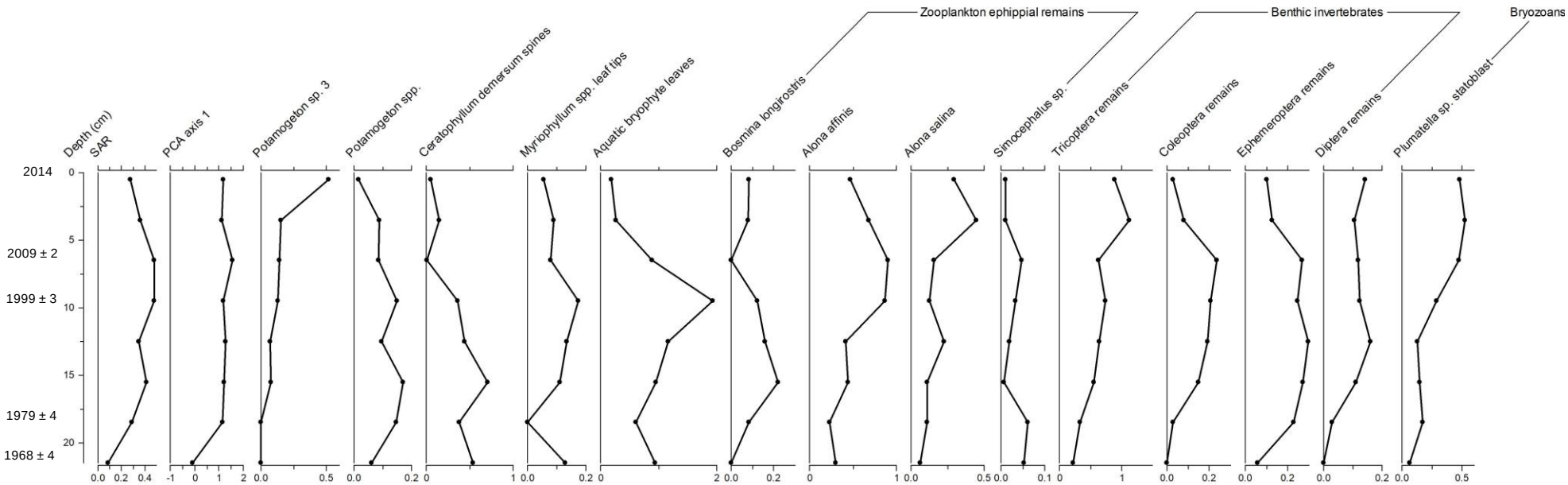

Figure 7.8. Macrofossil fluxes (no. count cm^{-2} yr^{-1}) of select remains from SLNG05 sediment core. Sediment accumulation rate (SAR; g cm^{-2} yr^{-1}) and PCA axis 1 scores since c. 1965 are included. Radioisotope-derived dates and related uncertainties are posted.

Early in Macrofossil Zone 1, ephippial remains from Daphniidae increased in abundance, primarily, *Ceriodaphnia* sp., *Simocephalus* sp., and *Daphnia pulex* (Figure 7.3b). In mid-Macrofossil Zone 1, *D. magna* ephippial remains increase in abundance, appearing in the record at ~1880, peaking in abundance ~1920. The decline in *Daphnia magna* occurred concurrently with the decline in *D. pulex* and *D. longispina*, and is followed by an increase in *Ceriodaphnia* sp. and *Alona* spp., which remained high in abundance until ~1970 (Figure 7.3b). Remains of Diptera and Coleoptera are present early in Macrofossil Zone 1, but declined in abundance and disappeared from the sediment record c. 1900. Trichoptera remains begin to increase in the late-19th century, and sustained high numbers of all Trichoptera remains, as well as increases in Ephemeroptera remains, coincided with declines in Diptera and Coleoptera remains (Figure 7.3c). High abundances of bryozoans occurred between the mid-19th century and c. 1960, at which time declines in the abundance of all bryozoan remains occurred (Figure 7.3c). Remains of fish (Percid and Cyprinid) were sparse and low in numbers in Macrofossil Zone 1.

Macrofossil Zone 2: c. 1980 to 2014 (18 cm to 0 cm)

A significant breakpoint was identified in the macrofossil PCA axis 1 scores around the transition from Macrofossil Zone 1 to Macrofossil Zone 2 (Figure 7.7), coinciding with declines in most aquatic macrophyte remains to very low abundances (Figure 7.3a). Macrofossil Zone 2 macrophyte remains were dominated by *Potamogeton* spp., including *Potamogeton compressus*, *Potamogeton pectinatus*, and *Potamogeton* sp. 3, which is an unidentified hybrid species. There is a decline in flux in recent years of most submerged macrophytes at SLNG05, with the exception of *Potamogeton* sp. 3, an unknown hybrid, which increases in concentration and flux, while sedimentation rates decline since c. 2005 (Figures 7.3a, 7.8). Small-bodied Chydoridae and Bosminidae cladocera dominate the zooplankton community in Macrofossil Zone 2, with high abundances of *Bosmina longispina*, *Alona* spp. and *Camptocercus rectirostris* ephippial remains found in this zone. Increasing abundances of *Alona* spp. ephippial remains were observed through Macrofossil Zone 2, with abundance peaks for this zone occurring in the most recent sample for both *Alona affinis* and *Alona salina* (Figure 7.3b). Declines in abundance of most benthic invertebrate remains occurred at the transition from Macrofossil Zone 1 to

Macrofossil Zone 2, including those of Trichoptera cases and Ephemeroptera abdominal gills (Figure 7.3c). Increases in remains of Coleoptera and Diptera occurred at the onset of Macrofossil Zone 2, and continued through most of the zone. Remains of Ephemeroptera remained fairly constant through most of Macrofossil Zone 2. Bryozoan remains, including statoblasts of *Cristatella mucedo* and an unknown bryozoan, were low in numbers and sparsely occurring through Macrofossil Zone 2, while numbers of *Plumatella* sp. statoblasts recovered through Macrofossil Zone 2 to peak in abundance in the most recent sample (Figure 7.3c). Fish scale remains (from both percid and cyprinid fish) were higher in abundance and more frequently occurring in Macrofossil Zone 2. Macrofossil richness was at the record minimum at the beginning of Macrofossil Zone 2, at 34, which is the lowest richness observed since the mid-19th century.

7.3.2 SLNG05 sedimentary diatom record

Taxa present at ≥ 5% at a single depth, and zones of change within the diatom record for SLNG05 are presented in the stratigraphy in Figure 7.9a-b. A total of 270 species from 45 genera were identified within SLNG05 diatom assemblages. Throughout the entire record, diatom concentrations ranged from approximately 7.56 x 10^6 valves g^{-1} dry weight (mid-19th century) to 2.64 x 10^5 valves g^{-1} dry weight (mid-1960s) (Figure 7.9a). Rarefacted species richness ranged from 35.6 (c. 1930) to 82.2 (c. 1980), and sample N2 ranged from 5.8 (c. 1950) to 40.1 (2008) (Figure 7.9b). PCA of the SLNG05 diatom record indicated 65.1% of diatom assemblage variation explained along axis 1, and an additional 16% of variation explained along PCA axis 2 (Table 7.2). In the ordination, many of the planktonic diatoms plotted positively along PCA axis 1, with high association with recent samples, while many of the larger benthic, small benthic Fragilarioids, and epiphytic diatoms had higher association with older samples (Figures 7.10). Two significant zones of diatom community composition were determined for the SLNG05 record through broken stick analysis (Figure 7.11), and cluster analysis indicated that the two significant diatom zones were from 1) Early-19th century to mid-1960s (61 cm to 24 cm), and 2) mid-1960s to 2014 (22 cm to 0 cm) (Figures 7.12). Breakpoint analysis indicated two significant ($p \leq 0.01$) points of change in the diatom PCA axis 1 scores in the mid- to late-1960s (24 to 20 cm) (Figure 7.13).

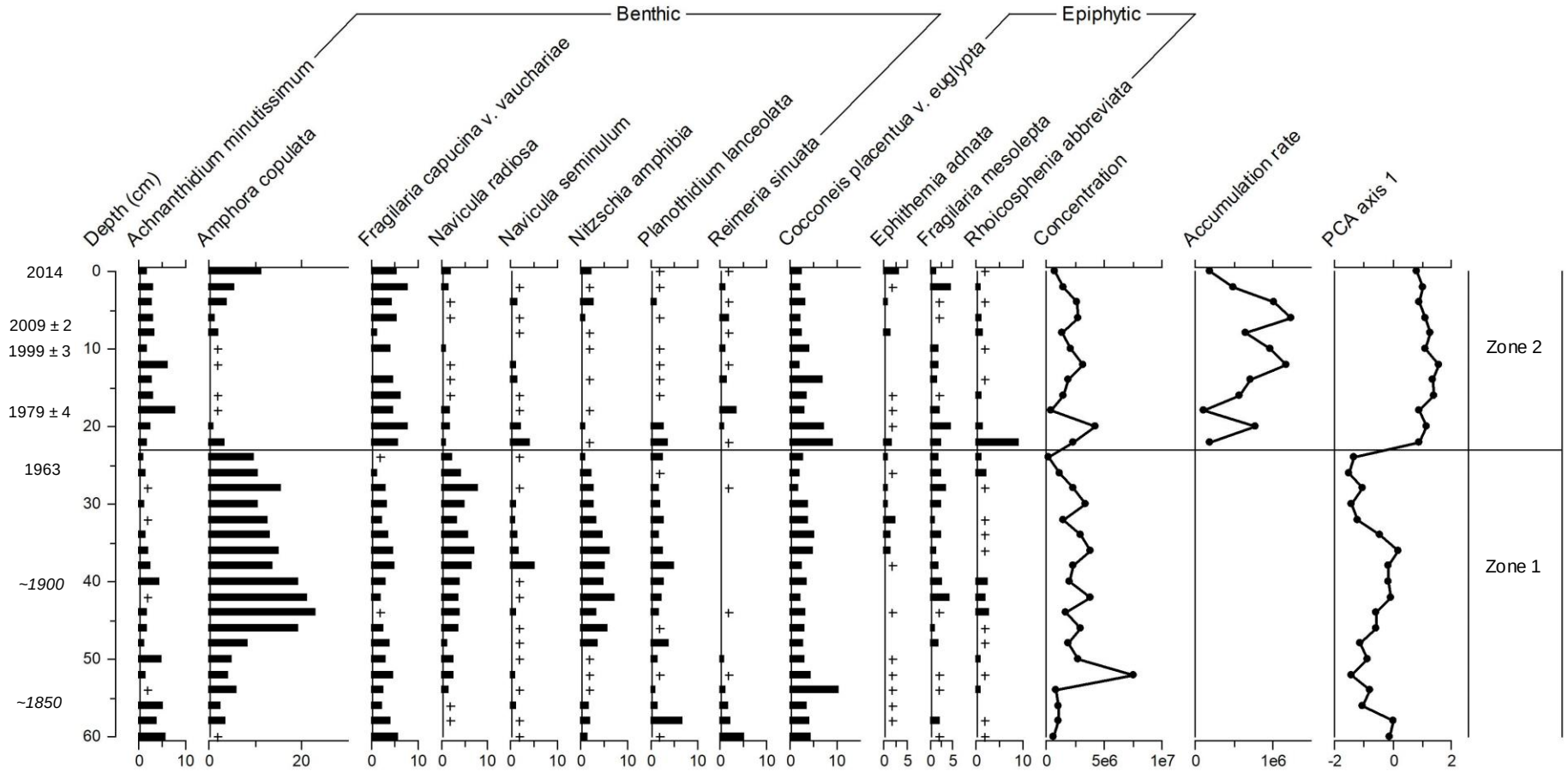

Figure 7.9a. Relative abundances (%) of benthic and epiphytic diatoms >5% from the SLNG05 sediment record. (+) indicates present in sample at <1% relative abundance. Diatom concentrations (no. valves g^{-1} dry weight) and diatom accumulation rates (no. valves cm^{-2} yr^{-1}) are plotted, as well as PCA axis 1 scores. Diatom Zones 1 and 2 indicated, based on broken stick and cluster analyses. Radioisotope-derived dates and confidence limits are highlighted on the y-axis. Italicized dates are extrapolated beyond ^{210}Pb radioisotope dating.

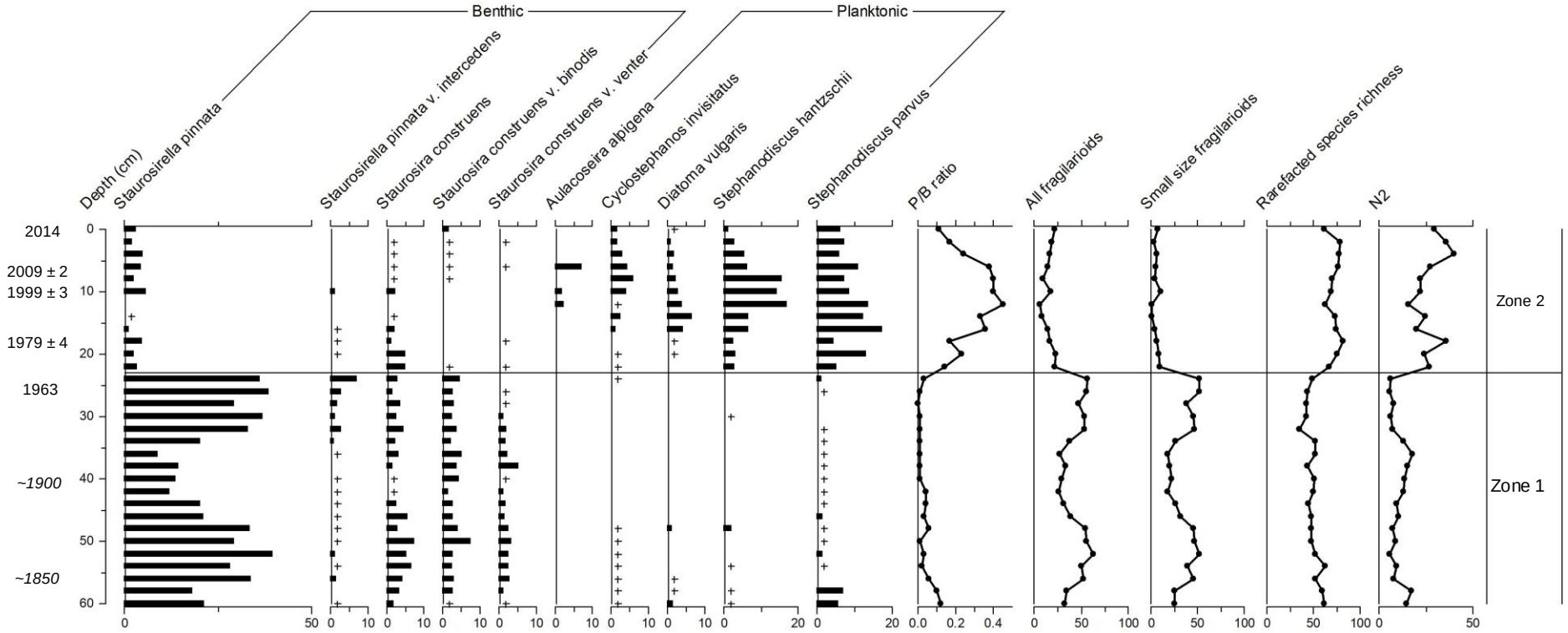

Figure 7.9b. Relative abundances (%) of small benthic fragilarioids and planktonic diatoms present at >5% in any one sample from the SLNG05 sediment record. Planktonic/Benthic (P/B) ratio, total sum all fragilarioids (%), total sum small fragilarioids of the SSP complex (%), rarefacted species richness (no. species), and Hill's N2 (no. species) measure of diversity. (+) indicates presence of species in sample at <1% relative abundance. Diatom Zones 1 and 2 indicated, based on broken stick and cluster analyses. Radioisotope-derived dates and confidence limits are highlighted on the y-axis. Italicized dates are extrapolated beyond ^{210}Pb radioisotope dating.

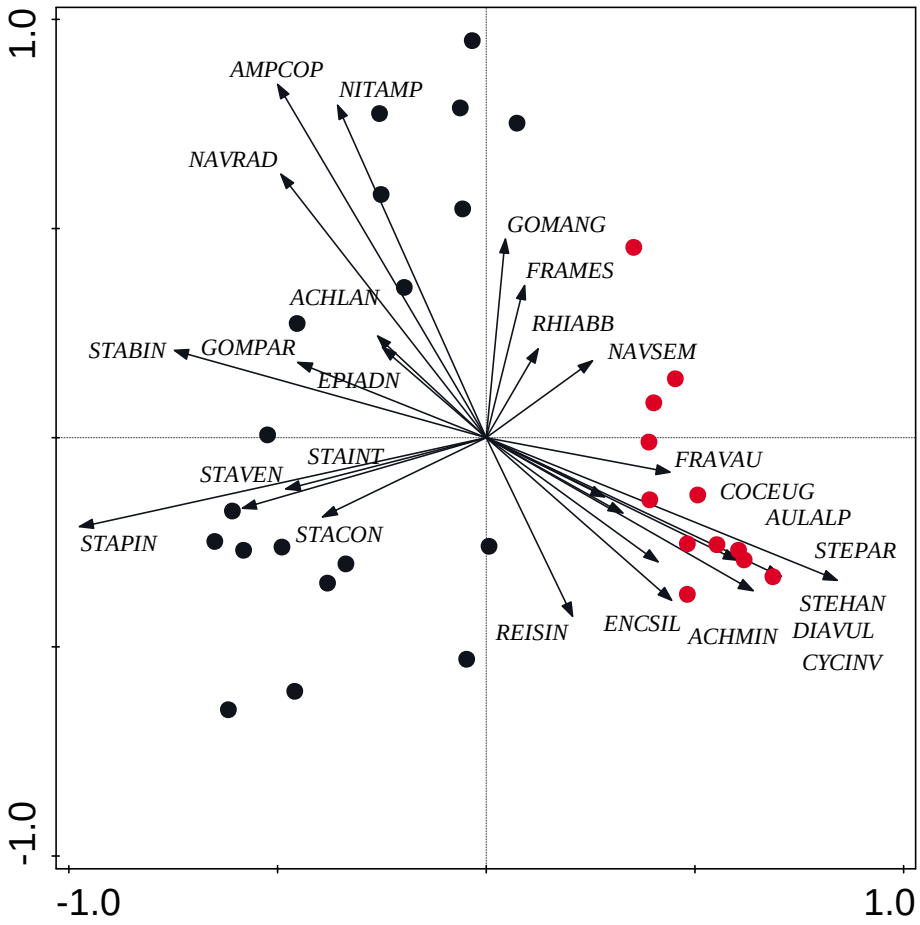

Figure 7.10. PCA biplot of diatom species and samples from SLNG05. Top 25 species are plotted according to relative abundance. Sample depths are colour-coded according to zone: Diatom Zone 1 (Early-19th century to mid-1960s) (black), Diatom Zone 2 (Mid-1960s to 2014) (red). Diatom species codes can be found in Appendix 6.

	Axis 1	***Axis 2***	***Axis 3***	***Axis 4***
Eigenvalues	0.6511	0.1605	0.0439	0.0231
Explained variation (cumulative)	65.1	81.2	85.6	87.9

Table 7.2. PCA summary table of the SLNG05 diatom assemblages. Eigenvalues and explained variation of the first four PCA axes indicated.

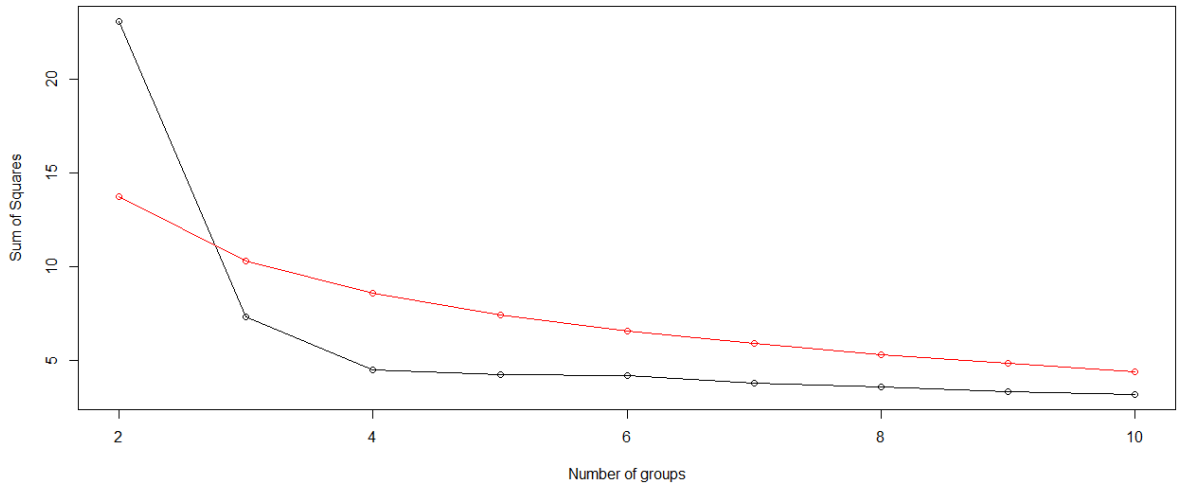

Figure 7.11. Broken stick of the SLNG05 diatom record. Two significant groupings of samples are indicated.

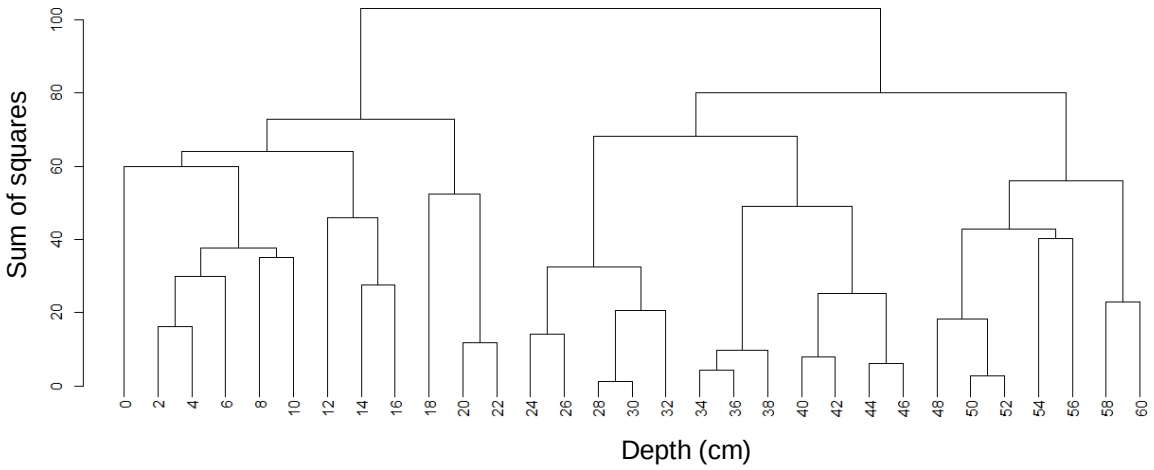

Figure 7.12. Cluster analysis of SLNG05 diatom samples. Sample depths are indicated (cm). Two significant groupings occur, as determined through broken stick analysis.

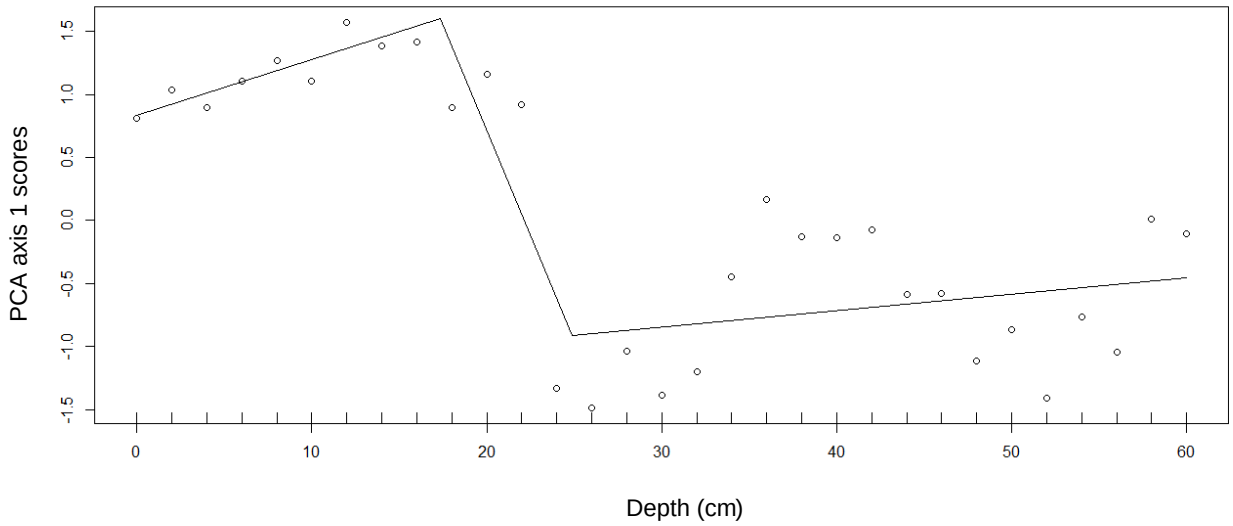

Figure 7.13. Breakpoint analysis of the SLNG05 diatom PCA axis 1 scores. Two significant ($p \leq 0.01$) points of change were identified between 24 cm to 20 cm.

Diatom Zone 1: Early 19th century to c. 1965 (60 cm to 24 cm)

Diatom Zone 1 was characterized by low rarefacted species richness and sample N2. Small benthic Fragilarioid species were more common in Diatom Zone 1, and *Staurosirella pinnata* dominated with relative abundances as high as 40%. Planktonic species were present at relatively higher abundances very early in Diatom Zone 1, but declined to very rare abundances (<1%) or disappeared from the record by the late-19th century (c. 1880) (Figure 7.9b). *Nitzschia amphibia, Navicula radiosa, Achnanthes lanceolata,* and *Amphora copulata* increased in relative abundances in the middle of Diatom Zone 1 when *Staurosirella pinnata* declined briefly between the late-19th century (c. 1880) and 1920. *S. pinnata* recovered post-1920 to relative abundances approaching 40% by the end of Diatom Zone 1 (Figure 7.9b).

Diatom Zone 2: c. 1965 to 2014 (22 cm to 0 cm)

Two significant breakpoints were identified in the diatom PCA axis 1 scores around the transition from Diatom Zone 1 to Diatom Zone 2 (Figure 7.13), coinciding with an abrupt decline in the relative abundance of *Staurosirella pinnata,* from 36% (24 cm) to 3% (22 cm) (Figure 7.9). Most species which were common or dominant in Diatom Zone 1 declined in abundance at the beginning of Diatom Zone 2, and were relatively rare through most of Diatom Zone 2. Planktonic species increased in abundance in Diatom Zone 2, along with increases in small benthic *Achnanthidium minutissimum,* and epiphytic *Cocconeis placentula* v. *euglytpa* and *Fragilaria* v.

capucina v. *vauchariae*. Zone 2 diatom assemblages were dominated by two planktonic species, *Stephanodiscus parvus* and *Stephanodiscus hantzschii* (Figure 7.9b). More recently, however, planktonic species appeared to be declining in abundance at SLNG05, and concurrent increases in *Amphora copulata* have occurred since 2005. Species richness and sample N2 are higher in Diatom Zone 2 than Diatom Zone 1, and single species relative abundances are lower overall. Diatom accumulation rates and concentrations since c. 1965 increase along with sedimentation accumulation rate for SLNG05 (Figure 7.9a).

7.3.3 SLNG05 sedimentary pigment record

Pigment concentrations found in the SLNG05 sedimentary record are detailed in Figure 7.14. Pigments representing total algae (Chl *a*, Chl *a* degradation products, and β-carotene), chlorophytes (Chl *b*, Chl *b* degradation product, and lutein), chromophytes (Chl *c*), total cyanobacteria (zeaxanthin), colonial cyanobacteria (canthaxanthin), siliceous algae (fucoxanthin), diatoms (diatoxanthin), and cryptophytes (alloxanthin), were identified in the record obtained from SLNG05. The first two PCA axes explained 97.9% of total pigment variability. PCA axis 1 explained 79.1% of total variability in the SLNG05 sedimentary pigment record, and PCA axis 2 explained an additional 19% (Table 7.3). In the ordination, all pigments plotted strongly and positively along PCA axis 1 (Figure 7.15). Broken stick analysis indicated five significant zones within the SLNG05 pigment record (Figure 7.16). Cluster analysis detected significant clustering of sample depths as follows: 1) Early- to mid-19th century (61 cm to 48 cm), 2) late-19th century to mid-1970s (47 cm to 20 cm), 3) late-1970s to early-1980s (19 cm to 17 cm), 4) mid-1980s to 2008 (16 cm to 4 cm), and 5) 2010 to 2014 (3 cm to 0 cm) (Figures 7.17). Breakpoint analysis of the SLNG05 pigment PCA axis 1 scores identified two significant ($p \leq 0.01$) shifts in the pigment assemblage, the first c.1900, and the second c. 2007 (Figure 7.18).

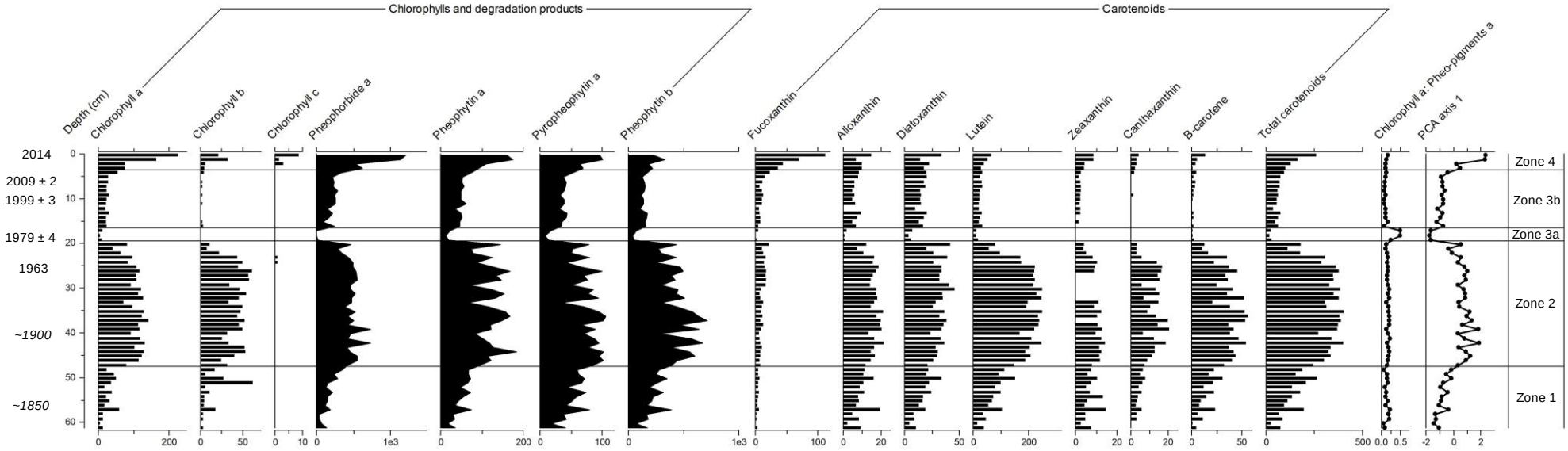

Figure 7.14. Pigment concentrations of chlorophylls, degradation products, and carotenoids for SLNG05, with indications of zones. Concentration units are in nmol g^{-1} organic matter. (+) indicates concentrations of <1 nmol/g organic matter dry weight. Pigment Zones 1 - 4 are indicated. Measure of preservation, ratio of Chl *a* : Chlorophyll *a* degradation products (Pheo *a*), indicated as well as PCA axis 1 scores. Radioisotope-derived dates and confidence limits are highlighted on the y-axis. Italicized dates are extrapolated beyond ^{210}Pb radioisotope dating.

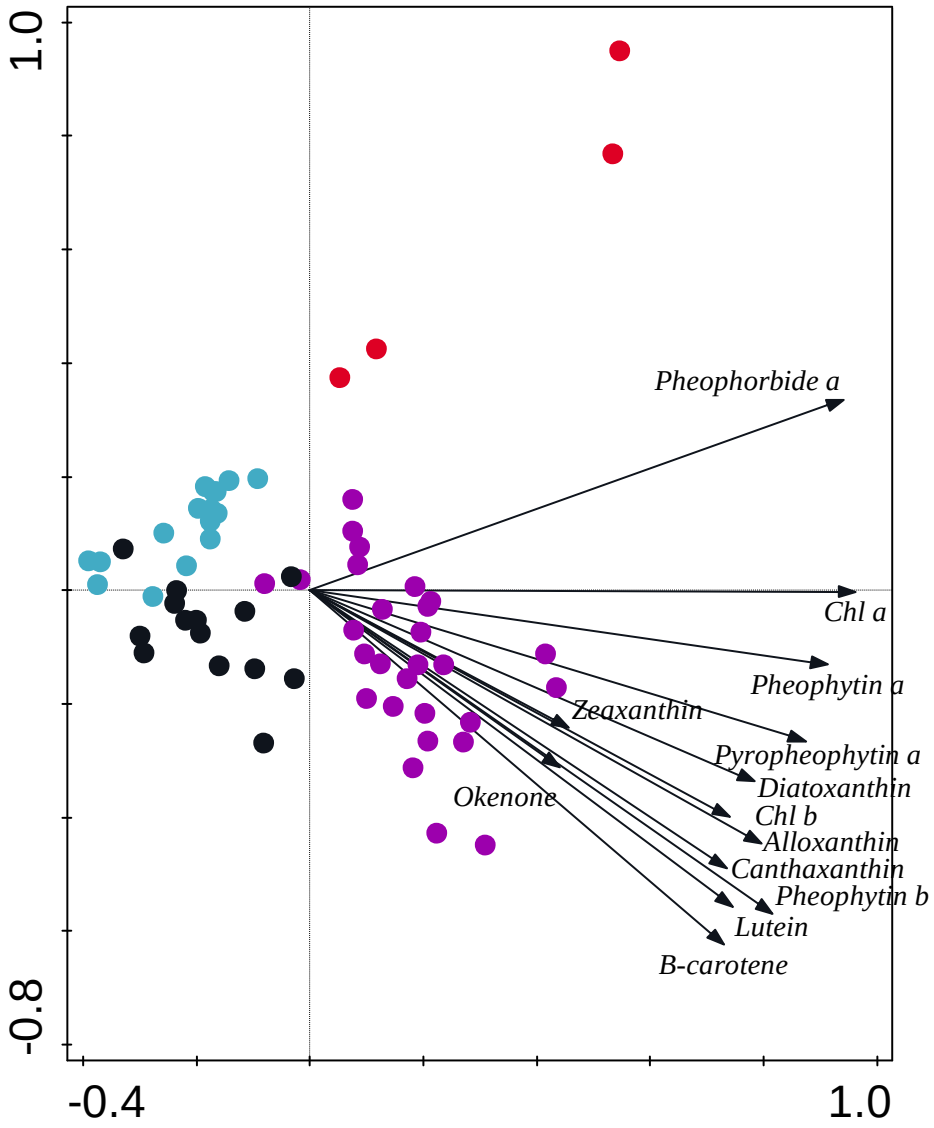

Figure 7.15. PCA biplot of pigments and sample depths from SLNG05. Sample depths are colour-coded according to zone: Pigment Zone 1 (Early to mid-19th century) (black), Pigment Zone 2 (Late-19th century to mid-1970s) (purple), Pigment Zone 3 (Late-1970s to 2008) (light blue), Pigment Zone 4 (2010 to 2014) (red).

	Axis 1	***Axis 2***	***Axis 3***	***Axis 4***
Eigenvalues	0.7914	0.1874	0.0137	0.0041
Explained variation (cumulative)	79.1	97.9	99.2	99.7

Table 7.3. PCA summary table of the SLNG05 pigment concentrations. Eigenvalues and explained variation of the first four PCA axes indicated.

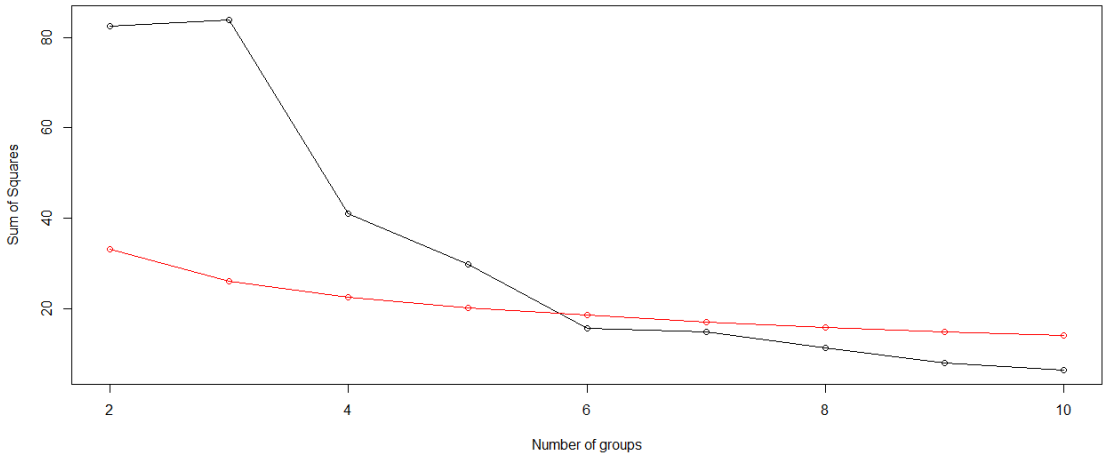

Figure 7.16. Broken stick of the SLNG05 pigment record. Five significant groupings of samples are indicated.

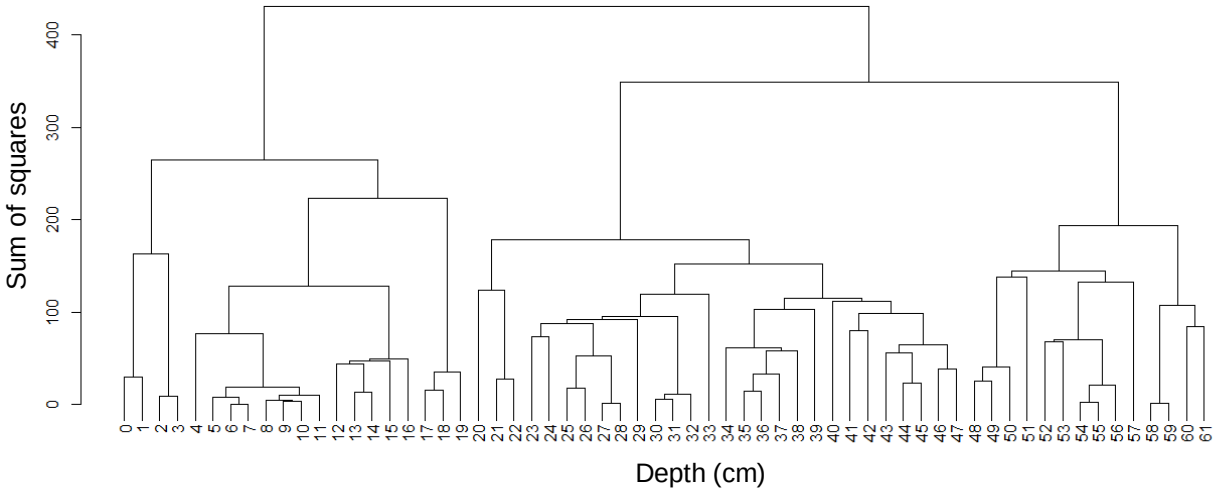

Figure 7.17. Cluster analysis of SLNG05 pigment samples. Sample depths are indicated (cm). Five significant groupings occur, as determined through broken stick analysis.

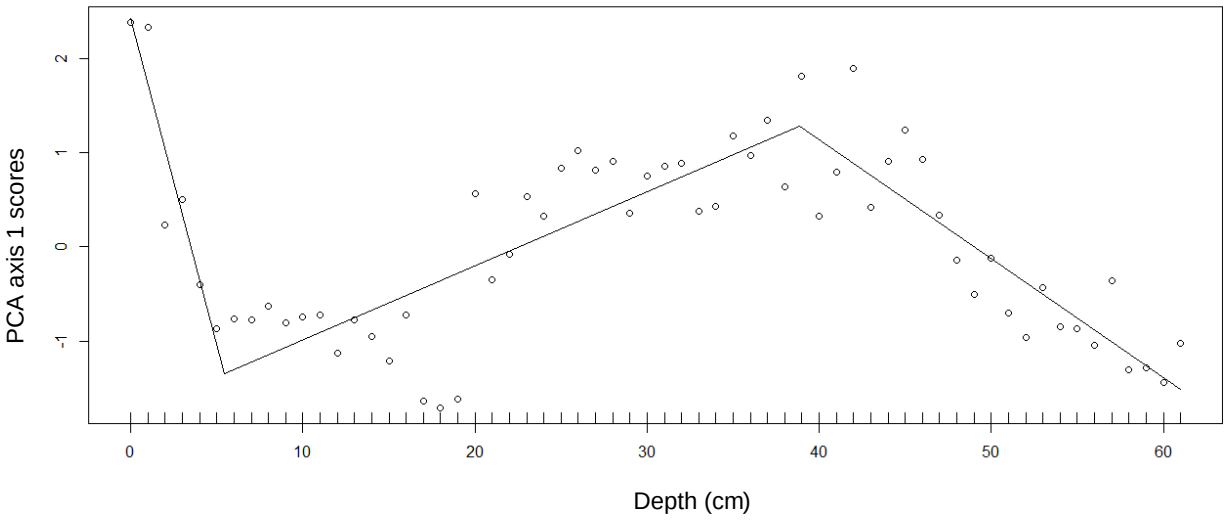

Figure 7.18. Breakpoint analysis of the SLNG05 pigment PCA axis 1 scores. Two significant ($p \leq 0.01$) points of change were identified, first c. 1900, and second c. 2007.

Pigment Zone 1: Mid-19th century (61 cm to 48 cm)

Concentrations of chlorophylls *a* and *b* were low through Pigment Zone 1, showing only minor increases towards the end of the zone. Carotenoids representing siliceous algae, chlorophytes, total and colonial cyanobacteria, and cryptophytes, were present through Pigment Zone 1. Concentrations of all carotenoids were low at the onset of Pigment Zone 1, but increased throughout the zone. The ratio of chlorophyll *a*/chlorophyll *a* degradation products remained relatively constant through Pigment Zone 1, indicating little change in preservation of pigments through the zone.

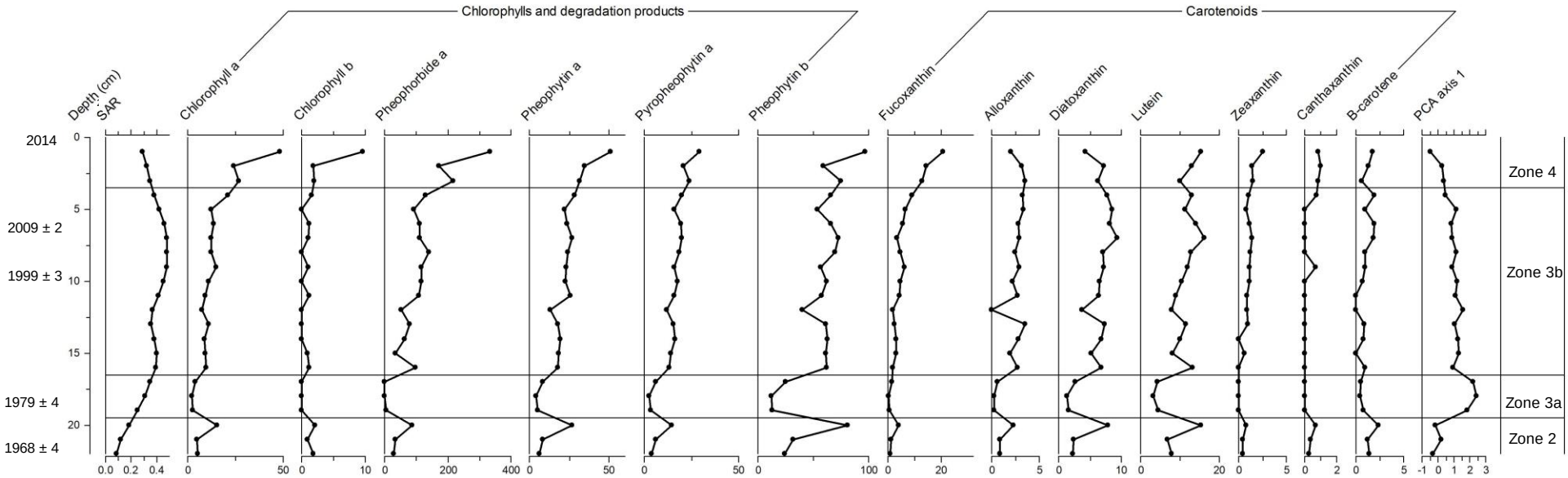

Figure 7.19. Fluxes of chlorophylls, degradation products, and carotenoids for SLNG05 from Pigment Zones 2 - 4. Units of fluxes are in nmol cm^{-2} yr^{-1}. Sedimentation accumulation rate (SAR; g cm^{-2} yr^{-1}) and PCA axis 1 scores since c. 1965 are shown.

Pigment Zone 2: Late-19th century to ~1975 (47 cm to 20 cm)

Concentrations of all pigments, including chlorophylls *a* and *b*, degradation products of chlorophylls *a* and *b*, and all carotenoids, increased early in Pigment Zone 2, to peak in the middle or late in the zone. Concentrations of indicators for total algae, Chl *a* and β-carotene, were high throughout the middle of Pigment Zone 2, between the late-19th century and ~1955. Total carotenoid concentration displayed a similar trend through Pigment Zone 2, and sustained high concentrations until the early-1960s (Figure 7.14). Indicators of siliceous algae, including fucoxanthin and diatoxanthin, remained high until the end of Pigment Zone 2, while indicators for chlorophytes (Chl *b* and lutein) and colonial cyanobacteria (canthaxanthin) displayed decreased concentrations by the mid-1960s. Zeaxanthin (total cyanobacteria) disappeared from the SLNG05 pigment recorded between ~1930 and 1950. Further, Chl *c* (chromophytes) appeared in the record briefly in the mid-1960s (Figure 7.14). The ratio of chlorophyll *a*/chlorophyll *a* degradation products remained relatively constant through Zone 2, indicating little change in preservation of pigments through the zone. Concentrations of total carotenoids and Chl *a* began to decline towards the end of Pigment Zone 2, in the mid-1960s (Figure 7.14).

Pigment Zone 3a: Late-1970s to early-1980s (19 cm to 17 cm)

This brief period at the beginning of Pigment Zone 3 was defined by a significant decrease in all chlorophyll, degradation product, and carotenoid concentrations (Figure 7.14). However, the ratio of chlorophyll *a*/chlorophyll *a* degradation products was high through this section of Pigment Zone 3, indicating increased preservation of pigments. There was a lack of Chl *b* (chlorophytes) and Chl *c* (chromophytes), and carotenoids zeaxanthin and canthaxanthin (total and colonial cyanobacteria), during this zone, low concentrations of all other carotenoids and Chl *a* and Chl *a* and Chl *b* degradation products.

Pigment Zone 3b: Mid-1980s to 2008 (16 cm to 4 cm)

Concentrations of all chlorophylls (except Chl *c*), degradation products, and carotenoids increased in the middle of Pigment Zone 3, but remained low. Concentrations remained similar to or lower than those of Pigment Zone 1. Further, there was an absence of canthaxanthin (colonial cyanobacteria) throughout most of Pigment sub-zone 3b, and chlorophyll *b* and β-

carotene are sparsely represented, indicating low concentrations of all algal groups at this time (Figure 7.14).

Pigment Zone 4: 2010 to 2014 (3 cm to 0 cm)

Increased concentrations of most chlorophylls, degradation products, and carotenoids occurred in Pigment Zone 4. However, many of the concentration increases did not surpass the high concentrations of pigments observed in Pigment Zone 2. Further, Chl *c* returned to the record in the uppermost 2 cm. There was potential for increased preservation of pigments in the uppermost sediments, particularly for fucoxanthin and Chl *c*, relative to further down the sediment record, however, the ratio of chlorophyll *a*/chlorophyll *a* degradation products remains relatively constant from Pigment Zone 3 to Pigment Zone 4, indicating little change in preservation of pigments in the uppermost sediments (Figure 7.14).

7.3.4 Community-level change: Comparisons of temporal variation between proxies

7.3.4.1 Diatom and pigment sedimentary records

The first two axes of the co-correspondence analysis (CoCA) very strongly capture the extent of cross-correlation between the two communities (Table 7.4), and the relation between the two communities is highly significant (Table 7.5). Species common to Diatom Zone 1, including fragilarioids, cluster to the left side of the ordination graph, and tend to co-occur with higher concentrations of zeaxanthin (total cyanobacteria), alloxanthin (chryptophytes), lutein and pheophytin *b* (chlorophytes) (Figure 7.20). Chlorophyll *a* (total algae) falls near zero on axis 1, but negative along axis 2, co-occurring with epiphytic diatoms *Fragilaria mesolepta, Epithemia adnata,* and *Rhoicosphenia abbreviata*, species most common towards the end of Diatom Zone 1, and early in Diatom Zone 2, but decline in abundance early in Diatom Zone 2. Planktonic diatoms, which are most common to Diatom Zone 2, fall to the far-right of the ordination graph, and do not fall out with any of the pigments, most likely due to the lower concentrations in Pigment Zone 2 (Figure 7.20, Figure 7.14).

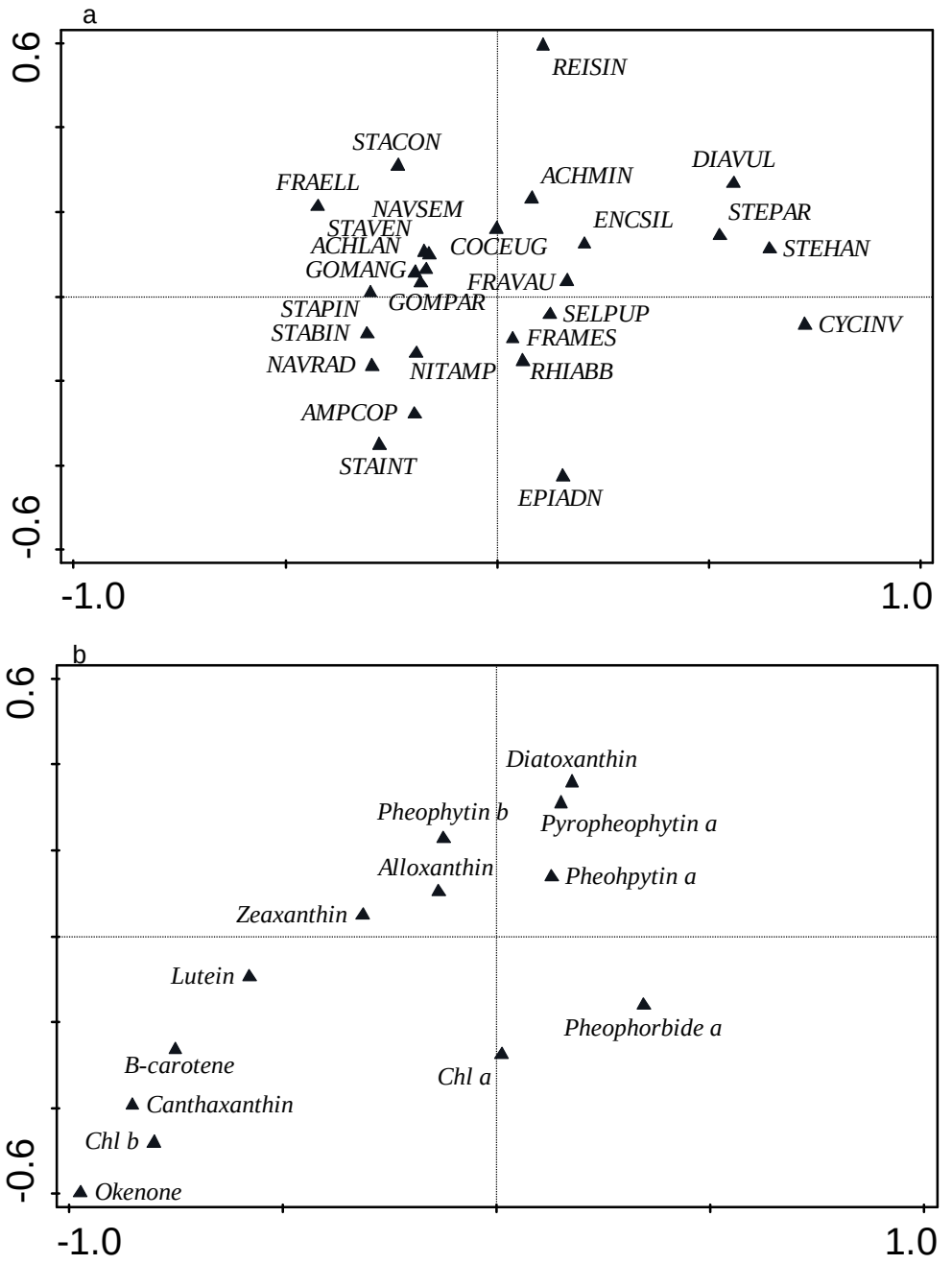

Figure 7.20. Diatom (a) and pigment (b) CoCA community biplots. Species falling in the same area across plots tend to co-occur in the proxy records. Diatom species codes can be found in Appendix 6.

Proxies	Axis 1	Axis 2	Axis 3	Axis 4
Diatom*Pigment	0.8809	0.7997	0.7945	0.7250
Pigment*Macrofossil	0.8602	0.8270	0.8127	0.7487
Diatom*Macrofossil	0.9436	0.9574	0.9712	0.9495

Table 7.4. Cross correlations between axes determined through co-correspondence analysis. High positive values indicate strong correlation between the first CoCA axes.

Proxies	Test on all axes (p-value)	Test on first axis (p-value)
Diatom*Pigment	0.002	0.002
Pigment*Macrofossil	0.002	0.002
Diatom*Macrofossil	0.006	0.006

Table 7.5. Tests for significance across axes for each analysis in CoCA. Significance $p \leq 0.01$.

7.3.4.2 Diatoms and macrofossil sedimentary records

The first two axes of the co-correspondence analysis (CoCA) very strongly capture the extent of cross-correlation between the two communities (Table 7.4), and the relation between the two communities is highly significant (Table 7.5). Species common to Diatom Zone 1, including small fragilarioids, epiphytics, and large benthic species, occurred on the left of the ordination graph, co-occurring with pelagic daphnids *Daphnia pulex,* and *D. longispina*, plant-associated bryozoan *Cristatella mucedo*, and most submerged and floating macrophyte remains, including *Ceratophylum demersum, Myriophyllum* spp., *Potamogeton* spp., and Nymphaeaceae trichosclereids (Figure 7.21). Species more common to Diatom Zone 2, including planktonic species and small benthic species, occurred to the right of the ordination plot, and co-occurred with small pelagic *Bosmina longispina*, benthic chydorids, most benthic invertebrates, and aquatic mosses (Figure 7.21).

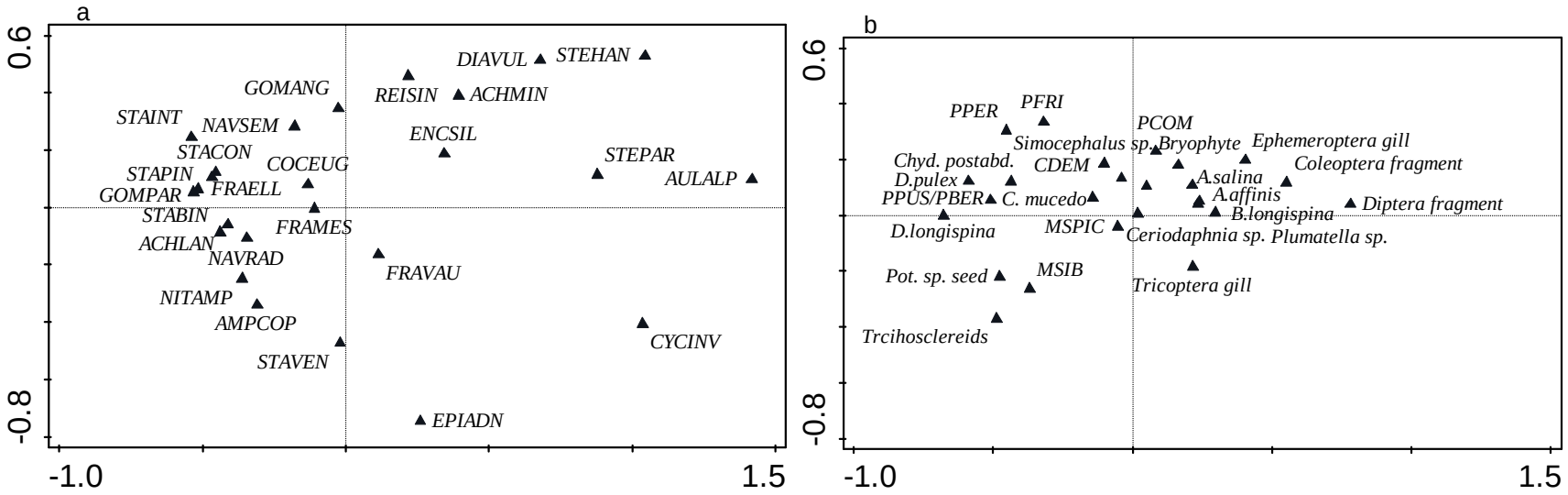

Figure 7.21. Diatom (a) and macrofossil (b) CoCA community biplots. Species falling in the same area across plots tend to co-occur in the proxy records. Diatom species codes can be found in Appendix 6. Macrofossil codes can be found in Appendix 5.

7.3.4.3 Pigment and macrofossil sedimentary records

The first two axes of the co-correspondence analysis (CoCA) very strongly capture the extent of cross-correlation between the two communities (Table 7.4), and the relation between the two communities is highly significant (Table 7.5). Biological remains more common in Macrofossil Zone 1, including daphnids (regardless of habitat preference), *Ceratophyllum demersum, Potamogeton* spp., and *Cristatella mucedo*, fell to the left of the ordination and tended to co-occur with alloxanthin (chryptophytes) and pheophytin *b* (chlorophytes). Diatoxanthin and chlorophyll *a* degradation product, pheophytin *a*, fell to the right of the ordination plot, and co-occurred with most benthic invertebrates, *Plumatella* sp. (Figure 7.22). Benthic chydorids and pelagic bosminids did not co-occur with high concentrations of pigments.

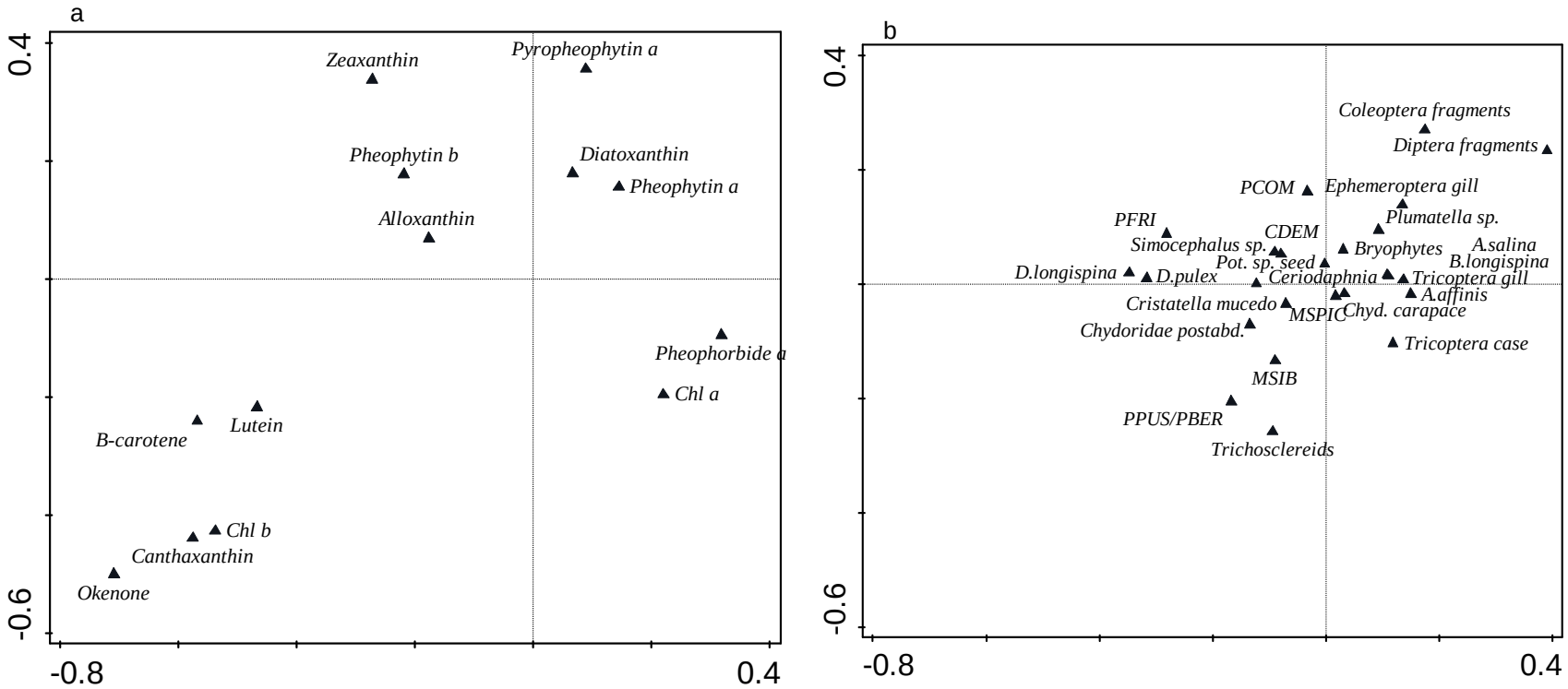

Figure 7.22. Pigment (a) and macrofossil (b) CoCA community biplots. Species falling in the same area across plots tend to co-occur in the proxy records. Macrofossil codes can be found in Appendix 5.

7.4 Discussion

7.4.1 Changes to lake structure and ecological function in the late-19th century

First signs of change to the aquatic ecosystem at SLNG05 occurred in the late-19th century. Increased algal biomass is indicated with increased concentrations of all pigments beginning in the late-19th century and persisting until the mid-20th century. Increased macrophyte abundance, indicated from increased concentrations of macrofossil remains, and an increase in organic matter at SLNG05 inferred through an increase in LOI_{550} (See 4.3.3, Figure 4.8) are further evidence for increasing productivity of SLNG05 at this time. Macrophyte increases are also implied through an increase in macrofossil richness, increasing from 31 species in the mid-19th century to 75 species by c. 1910. Increased primary production at SLNG05 would have resulted in increased carbonate content (Talling, 1976), which is also observed through an increase in LOI_{950} and calcite precipitate on macrofossil remains, such as macrophyte leaves and *Chara* sp. oospores. Increased productivity at SLNG05 beginning in the late-19th century may be due to increased nutrient influx which has been known to increase macrophyte density in lakes (Jeppesen *et al*., 2001; Randsalu-Wendrop *et al.*, 2014). Increases in nutrient flux to the Selenga River and delta could have been a result of the increasing development of agricultural practices beginning in the 19th century in the Selenga River basin in southeast Siberia (Bazhenova and Kobylkin, 2013), increasing population in the catchment resulting in an increase in sewage discharge (*ibid.)*. Alternatively, increase in productivity could be related to an increase in temperature with the termination of the Little Ice Age, evidence for which has been recorded in the region through diatom assemblage changes linked to decreasing seasonal ice cover (Mackay *et al*., 2012), expansion of Siberian pine into the mountain tundra belt of the Western Sayan Mountain range (Kharuk *et al*., 2008), and increased water tempratures (Hampton *et al*., 2008) and decreased ice thickness (Todd and Mackay, 2003) on Lake Baikal.

A second possibility that would give rise to increased macrophyte abundance, algal concentrations, and overall productivity, is the shallowing of SLNG05, possibly due to decreased connection with the Selenga River. Current maximum depth of SLNG05 is ~1.0 meters, and it is postulated that in the late-19th century, the depth declined from > 1 metre to < 1 metre. Macrofossil richness in shallow lakes of the Selenga River basin is significantly higher in

lakes with low connectivity with the Selenga River, and macrofossil richness increases in the early-20th century at SLNG05 to values similar to those of low-connectivity sites in the Selenga River basin (See Section 3.3.2, Table 3.15). Moreover, a strong negative spatial relationship was observed between surface area and macrophyte macrofossil richness in contemporary Selenga River basin lakes, with richness highest at smaller, low or intermittent connectivity sites (See Section 3.3.1.2, Figure 3.4). Similar observation between surface area, connectivity, and macrophyte richness were observed by Bailey and Guimond (2009). The decline in abundance of planktonic diatoms in the late-19th century, coinciding with the increase in abundance of large benthics and epiphytic diatoms (Figure 7.8), are similar to the assemblage characteristics observed in contemporary Selenga River basin lakes with minimal connectivity to the Selenga River (See Section 3.3.1.3, Figure 3.8). Moreover, Hay *et al*. (2000) also found that high-closure lakes in the Mackenzie Delta, Northwest Territories, Canada, were often dominated by epiphytic taxa or large naviculoids, such as *Navicula radiosa*, and *Nitzschia amphibia*, and had an absence of planktonic species. Decreasing size and depth of SLNG05 between the late-19th century and the mid-20th century is further supported through the increase in Ca/Ti ratios, decrease in Fe/Mn ratios, increasing LOI_{550}, and declines in magnetic susceptibility, indicating increased evaporative conditions in the lake, increased autochthonic calcite production, increasing organic matter accumulation and decomposition, and resulting reducing conditions through this period (Davies, 2015; See Sections 5.3.2, 4.4.3.5, 4.4.3.6). With decreased connection from the river, there is further potential for increased light conditions with less turbid water coming in from the river. Improved light conditions would lead to increased macrophyte density and increased benthic productivity. In northern shallow lakes with extensive submerged macrophyte coverage, extended periods of winter ice cover leads to increased macrophyte decomposition, and subsequent increases in reducing conditions in the surface sediments (Anema *et al*., 1990; Hay *et al*., 2000).

Summer precipitation amount is the most significant contributor to water levels and variations in runoff in southeast Siberia, as snowfall plays a minor role due to the semi-arid winters, characteristic of the region (Berezhnykh *et al.,* 2012). Low-water periods within the Selenga River basin are closely related to low July/August precipitation (Frolova *et al*., 2017), which is linked to the convergence of westerly winds over northeast Asia with the East Asian

Summer Monsoon (EASM), and the EASM intensity, and a decrease in circulation intensity is linked with decreased runoff from the Selenga River (Berezhnykh *et al.,* 2012). Further, much of the interannual variability in winter climate conditions are dictated by the Siberian High (SH) intensity (Gong and Ho, 2002). The presence of the SH leads to winters which are cold and dry (Lydolf, 1977). Low water periods for the Selenga River basin were reported during most of the 19th century as a result of the decreased circulation intensity of summertime air masses over continental southeast Siberia (Berezhnykh *et al*., 2012). Therefore, it is possible that changes in summer atmospheric circulation patterns, combined with the strong intensity of the Siberian High in winter, led to drier overall conditions in the late-19th century in the Selenga River basin, resulting in decreased connectivity between SLNG05 and the Selenga River.

Macrophyte expansion took place at SLNG05 in the late-19th and early-20th centuries, as a result of either increased nutrient flux, decreased depth of the lake, or a combination of the two. The increased macrophyte density may have facilitated the increase in large-bodied Daphniidae in the early-20th century, including *Daphnia magna, Simocephalus* sp., and *Daphnia pulex*, as a high abundance of submerged macrophytes may provide refugia for zooplankton and invertebrates, resulting in higher abundances even with fish presence. Increased abundance of *Daphnia magna* ephippial remains peaking c. 1920, provide evidence of decreased fish predation, either as a result of declined fish abundance in SLNG05 at this time, or increased submerged macrophyte abundance and refugia (Jeppesen *et al*., 1997; Cousyn and DeMeester, 1998; Burks *et al.,* 2001). However, issues exist with inferring past fish populations based directly on fish remains found in macrofossil samples, as these remains are often scarce, and very large amounts of sediment are required to obtain reliable data (Jeppesen *et al.,* 2001). However indirect methods, such as those deduced from zooplankton remains and related trophic interactions, provide insight (*ibid.*). Increased plant-cover likely also led to the increase in plant-associated daphnid, *Ceriodaphnia* sp., and several types of plant-associated invertebrate, bryozoans, beginning c. 1910 and persisting until ~1960. Increase in benthic chydorids, including *Alona* spp. is likely due to increasingly favourable benthic conditions due to increasing light availability with decreasing depth and turbidity. Most pelagic daphnids and bosminids decline in abundance beginning ~1940, possibly due to increasingly shallow waters (likely <1

metre depth) and increasing light conditions and plant density, favouring the benthic chydorids and plant-associated *Ceriodaphnia* sp.

Increases in macrophyte density would likely have led to high organic matter accumulation and plant decomposition in the sediment of SLNG05, and subsequent decreases in oxygen concentrations at the sediment-water interface, and an enhancement of reducing conditions at the sediment-water interface (Randsalu-Wendrop *et al*., 2014). Such conditions are evidenced at this time in SLNG05 through low Fe/Mn ratios (See Section 5.3.2, Figure 5.15). Conditions such as these may have implications for sample preservation, and it is possible that the increased concentrations of pigments between c. 1880 and 1960 are due to increasing organic matter in the sediments, low oxygen concentrations, and increased reducing conditions at SLNG05, which may lead to increased rates of preservation of pigments upon incorporation in the lake sediment (Leavitt, 1993; Bianchi *et al.,* 2000; Reuss *et al*., 2005). Further evidence for increased preservation rates of pigments in the early-20th century is the appearance of chl *c*, in two samples c. 1960. Chlorophyll *c* is a relatively unstable pigment, prone to post-depositional degradation. Further, the increase in concentration of macrophyte remains between the late-19th century and mid-1960s may be due to increased macrophyte expansion through SLNG05 owing to the decreased depth, but also may be the result of the coring location in 2014 in SLNG05 having occurred at what once was an intermediate depth, in a shallower littoral zone, which generally accumulates a higher concentration of macrofossils in the sediment record (Birks, 1973; Dieffenbacher-Krall and Halteman, 2000; Birks, 2012). Either scenario, however, infers a shallowing and shrinking of SLNG05 between the late-19th century and mid-20th century.

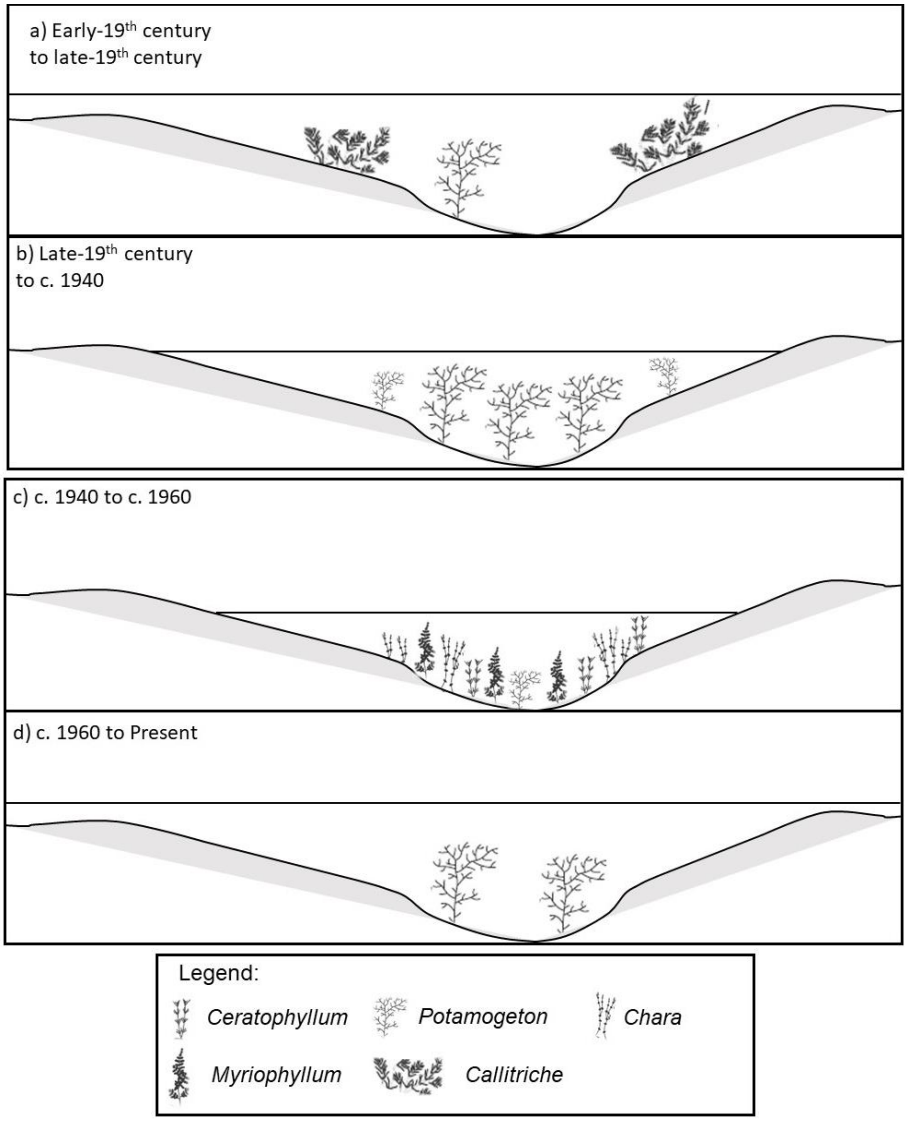

Figure 7.23. Conceptual diagram of water level, connectivity, and macrophyte community change at SLNG05 since the early-19th century. a) High connectivity lake with macrophyte community comprised of *Potamogeton-Callitriche-Zanichellia*, b) Decreased connectivity and shallower water levels, macrophyte community is primarily *Potamogeton*, c) Increasingly shallow water levels, and increased abundance and diversity of macrophyte community *Myriophyllum-Ceratophyllum-Chara* dominated, d) Increased connectivity and water levels, and decreased macrophyte diversity and abundance.

Species	Guild	Autecology	Authority	References
Amphora copulata	Benthic	Mainly occurring in alkaline waters, eutrophic, never or rarely occurring outside of water bodies	(Kütz.) Schoeman and R.E.M.Archibald 1986	Van Dam *et al*., 1994
Achnanthidium minutissimum	Benthic	Pioneer species, phosphorus specialist. Requires nearly continuous 100% oxygen saturation in water, pH circumneutral. Opportunistic species with wide tolerance of trophic state.	(Kütz.) Czarn. 1994	Cholnoky, 1968; Kuhn *et al*., 1981; Van Dam *et al.,* 1994; Reavie and Smol, 1998; Brown *et al*., 2008; Watchorn *et al*., 2008
Fragilaria capucina v. vaucheriae	Benthic	Mainly occurring in alkaline waters, eutrophic, can occur on moist/wet places.	(Kützing) Petersen 1938	Van Dam *et al*., 1994
Navicula radiosa	Benthic	Meso-eutrophic.	Kützing 1844	Van Dam *et al*., 1994
Nitzschia amphibia	Benthic	Neutral to alkaline waters, including subaerial habitats, eutrophic environments.	Grunow 1862	Van Dam *et al*., 1994
Planothidium lanceolata	Benthic	Eutrophic, neutral to alkaline waters.	(Brébisson) Lange-Bertalot 1999	Van Dam *et al*., 1994
Cocconeis placentula v. euglypta	Epiphytic	Mainly occurring in alkaline waters, eutrophic; C. placentula's preferred habitat is *Ceratophyllum demersum*.	Ehrenberg 1838	Van Dam *et al*., 1994
Epithemia adnata	Epiphytic	Exclusively occurring in alkaline pH waters, meso-eutrophic.	(Kützing) Brébisson 1838	Van Dam *et al*., 1994
Fragilaria mesolepta	Epiphytic	Alkaline, freshwater, tolerant of higher ionic content.	Rabenhorst 1861	Van Dam *et al*., 1994
Rhoicosphenia abbreviata	Epiphytic	Epiphyte of filamentous algae, non-motile, eutrophic, alkaline, pollution tolerant, freshwater with high ionic content.	(Agardh) Lange-Bertalot 1980	Van Dam *et al*., 1994
Staurosirella pinnata	Benthic	Prefers shallow, littoral habitats. Mesoeutrophic to eutrophic or oligotrophic to eutrophic. Requires highly oxygenated waters.	(Ehrenberg) Williams and Round 1987	Van Dam *et al*., 1994
Staurosira construens v. venter	Benthic	Prefers shallow, littoral habitats. Mesoeutrophic to eutrophic or oligotrophic to eutrophic. Requires highly oxygenated waters (nearly 100% saturation).	(Ehrenberg) Hamilton 1992	Patrick and Reimer, 1966; Bradbury, 1971; Van Dam *et al*., 1994; Metcalfe *et al*., 1997; Haberzettl *et al*., 2005

Staurosira construens v. binodis	Benthic	Prefers shallow, littoral habitats. Mesoeutrophic to eutrophic or oligotrophic to eutrophic. Littoral assemblage. Requires highly oxygenated waters, pollution intolerant.	(Ehrenberg) Hamilton 1992	Patrick and Reimer, 1966; Bradbury, 1971; Van Dam *et al*., 1994; Metcalfe *et al*., 1997; Haberzettl *et al*., 2005
Stephanodiscus parvus	Planktonic	Occurs exclusively in alkaline pH. Meso-eutrophic, high total phosphorus and moderate chloride concentration.	Stoermer & Håkansson 1984	Stoermer, 1978; Stoermer *et al*. 1978; Stoermer and Håkansson, 1984; Van Dam *et al*., 1994; Reavie and Kireta, 2015
Stephanodiscus hantzschii	Planktonic	Occurring exclusively at pH >7. A strong indicator of high phosphorus, indicator species dominant in eutrophic lakes.	Grunow in Cleve & Grunow 1880	Stoermer and Yang, 1969; Anderson, 1990; Hall and Smol, 1992; Van Dam *et al*., 1994; Reavie and Kireta, 2015.
Diatoma vulgaris	Planktonic	Occurs exclusively at pH > 7. Meso-eutrophic.	Bory 1824	Van Dam *et al*., 1994
Cyclostephanis invisitatus	Planktonic	Indicator of eutrophic conditions in rivers and shallow lakes; High total phosphorus optimum.	(Hohn and Hellermann) Theriot, Stoermer and Håkasson 1998	Yang *et al*., 2005; Edlund *et al*., 2009; Reavie and Kireta, 2015

Table 7.6. Summary of main ecological characteristics of dominant diatom species from SLNG05 sediment core.

7.4.2 Mid-twentieth century anthropogenic disturbances and regime shift

Structural ecosystem changes in the 1960s and 1970s were seen across all biological proxies at SLNG05, with significant shifts in macrophyte abundance and richness (Figure 7.3), invertebrate assemblages (Figure 7.3b), diatom assemblages (Figure 7.9), and pigment concentrations (Figure 7.14). Exceptional declines in macrophyte richness, and abundance of certain macrophyte remains in the 1960s and 1970s included those from *Ceratophyllum demersum*, *Myriophyllum* spp., aquatic mosses, and Nymphaeaceae trichosclereids. The decline in submerged macrophytes likely resulted in a decline in plant-associated bryozoans (Bennion *et al.,* 2015) as well as plant-associated *Ceriodaphnia* sp. Declines in pelagic zooplankton abundance at this time may be due to the disappearance of submerged macrophyte refugia, resulting in increased fish predation on the larger-bodied daphnids *Daphnia pulex, Daphnia magna,* and *Daphnia longispina*, and occurred in conjunction with increases in

pelagic, small-bodied *Bosmina longispina*, which often increases in abundance when fish predation on the larger daphnids increases (Mills *et al*., 1987; Jeppesen *et al*., 2001; Jeppesen *et al.,* 2011).

The ecosystem-wide ecological changes that occurred in the 1960s and 1970s at SLNG05 may be related to extensive flooding that occurred around Lake Baikal and the Selenga Delta at this time, due to the completion of the Irkutsk Dam on the Angara River in 1956. Filling of the associated reservoir began in 1956 and within seven years the reservoir was full and Lake Baikal was recorded as having risen by ~1.5 m depth (Bolgov *et al*., 2017). Subsequently, low-lying shorelines and delta environments of Lake Baikal were submerged and flooded, and over 350 km^2 of the Selenga River Delta was flooded (Pinegin *et al*., 1976). A corresponding increase in magnetic susceptibility is recorded at SLNG05, possibly indicating a change in source to the lake, representing increased connectivity with the Selenga River, and signalling an in-wash of sediments linked to a flood occurrence (See Section 4.3.3, Figure 4.8) (Guo *et al*., 2015; Gell *et al*., 2007). There is also a sharp and temporary increase in sedimentation rate in the early-1960s (~1963 ± 4 yrs), which corresponds with the timing of flooding (See Section 4.4.3. Figure 4.14), and a temporary increase in pigment preservation, possibly due to rapid burial (Figure 7.14) (Reuss *et al*., 2005). The increase in sedimentation rate in the early-1960s may have resulted in possible dilution of pigment concentrations, diatom concentrations, and macrofossil remains at this time.

Possible alternatives to increasing connectivity as the cause of ecosystem changes in the 1960s and 1970s include both the introduction of *E. canadensis*, and a change in trophic status on SLNG05. First, *E. canadensis* is not currently found in SLNG05, and it is therefore unlikely that the invasive waterweed became established in SLNG05 in the late-20th century. However, in the second instance, continued high nutrient levels at SLNG05 in the mid-20th century may have eventually led to an ecosystem shift from macrophyte dominated to algal dominated, and resulted in a decline in abundance and richness over a short period of time of most submerged macrophytes (Sayer *et al*., 2010a). Post-1960 increases in planktonic diatom species, and increasing relative abundances of *Stephanodiscus* spp., *Cyclostephanos* spp., and *Fragilaria capucina* v. *vaucheriae* likely indicate increases in nutrients, as these species are often found in mesotrophic-eutrophic freshwaters (Berthon *et al*., 2014; Lucas *et al*., 2015). However, the

macrophyte community composition pre-1970, which primarily consisted of *Potamogeton* spp., *Myriophyllum* spp., *Ceratophyllum demersum*, *Chara* sp., and aquatic mosses, was more typical of “stable lakes” with high macrophyte abundance, than lakes subject to high nutrients influxes and imminent population “crashes” (Sayer *et al.* 2010b). Total algal biomass underwent a significant decrease c. 1970, concurrent with the decrease in submerged macrophyte abundance (Figure 7.2a and 7.11), also captured by the CoCA between the pigment and macrofossil record, as most pigments co-occur with the submerged macrophytes (Figure 7.19). Moreover, pre-1960 diatom assemblages do not suggest progressively increasing nutrient levels, as the small, benthic fragilarioids which dominated the SLNG05 assemblages at this time are most commonly found in pre-anthropogenic impact sites, with lower nutrient levels and favourable light conditions (Bennion *et al*., 2015). Finally, continued high nutrient concentrations would have resulted in sustained increases in sediment accumulation rates, rather than the temporary increase observed in the 1960s (See Section 4.4.3. Figure 4.14; Rose *et al*., 2011). Therefore, the significant change observed in the three proxies over a relatively short period of time suggests a structural, rather than functional change at SLNG05, driving the ecological shifts.

Diatom species assemblage changes beginning in the mid-1960s indicate greater connectivity of SLNG05 with the Selenga River. Increasing abundance of planktonic diatoms, and dominance by *Stephanodiscus* spp., are probable indicators of increased river inoculation, and connection to the Selenga River, as analysis of contemporary SLNG diatom communities in Section 3.3.1.3 such planktonic species as *S. parvus* are strongly associated with increasing surface area in contemporary sites. Further, Genkal and Popovskaya (2008) observed high abundances of *Stephanodiscus* spp. and *Cyclotella* spp. in plankton samples from the Selenga River, while planktonic diatoms and *Stephanodiscus* sp. have been recorded as dominant in diatom assemblages from other northern river deltas (Hay *et al.,* 2000; Sokal *et al.,* 2008; Brock *et al*., 2011). Vologina *et al*. (2010) also observed a substantial decrease in abundance of small fragilarioids, primarily *Staurosirella pinnata* in Proval Bay sediments after the construction of the Irkutsk Dam, with a greater abundance of planktonic taxa replacing the small benthic fragilarioids. Sokal *et al.* (2008) also noted a greater diversity of guilds in no-closure systems in the Mackenzie River delta in northern Canada. Larger centric diatoms (e.g. *Cyclostephanos* sp.,

and *Aulacoseira* sp.) are common in recent diatom assemblages of SLNG05, and often require more silica for construction of the frustule. Increased silica availability may have increased at SLNG05 with increased sediment accumulation rates since 1980, potentially due to greater river influence (Hall *et al*., 2004; Wolfe *et al*., 2005).

Species richness and sample N2 are higher post-1965 than pre-1965, and single species relative abundances are lower overall. Diatom species richness and N2 from contemporary Selenga River basin lakes was highest in intermediate connectivity sites (See Section 3.3.1, Figure 3.5b), indicating the possibility that increase in species richness and N2 post-1965 at SLNG05 was related to increased connection with the Selenga River and increased disturbance. A relationship was observed amongst contemporary Selenga River basin lakes between connectivity and primary producer biomass, richness, and diversity, primarily related to the level of connectivity-related disturbance across sites (See Section 3.3.1, Figure 3.8). Low-connectivity lakes and ponds have minimal levels of disturbance from river intrusions, and often become dominated over time by a select few species, and have low species turnover rates (Hay *et al.,* 2000). Among lake comparisons conducted in Yellowstone National Park, U.S.A by Interlandi and Kilham (2001), indicated a significant negative relationship between species diversity and system productivity. A similar negative relationship is seen through the records from SLNG05, as pigment Chl *a* is higher when both species richness and Hill's N2 are lower in the diatom record. Flood stress and disturbance can be an important determinant of productivity and ecological structure in floodplain wetlands, as lakes with higher levels of river connectivity may be subject to persistent intrusions of cold, turbid waters, the negative impacts of which on plant productivity outweigh the concurrent increase in nutrients brought to lakes by river water (Robertson *et al*., 2001; Sokal *et al*., 2010). Bailey and Guimond (2009) observed that plant productivity in small lakes in Jasper National Park, Canada, was related to degree of flooding and related nutrient dynamics, and that flood disturbance, or degree of river connectivity, was a greater driver in determining plant production than resource availability.

Breakpoint analysis indicated significant points of change in both diatom and macrofossil PCA axis 1 scores in the 1960s and 1970s, with both records indicating the establishment of a new stable community structure c. 1980 (Figure 7.7 and Figure 7.13). Ecological regime shifts are abrupt changes in ecological structure and function, generally on several trophic levels,

resulting in a sudden swing to an alternative ecological state (Andersen et al., 2008; Randsalu-Wendrup et al., 2014). The ecological shifts at SLNG05 are observed across multiple biological records, at several trophic levels. The crossing of critical thresholds within an ecosystem will cause a regime shift and result in an alternative state from the original, with different ecological structures and functions. It is likely that between the late-19th century and mid-20th century, SLNG05 underwent intermittent connectivity with the Selenga River, and that the increased, permanent connection with the river which began in the mid-1960s led to structural changes which included decreased macrophyte abundance, shifts in diatom assemblages, and associated changes in invertebrate communities, and associated changes in ecosystem functioning, including decreased productivity. Water depth is a significant variable influencing diatom and macrophyte distributions in shallow wetland lakes, which may be related to changes in hydrological regimes (Moser et al., 2000; Michelutti et al., 2001). Moreover, small fluctuations in water levels in shallow lake systems may have a large influence on dilution/evapoconcentration and light penetration (Cobbaert et al., 2014). Brock et al. (2011) observed that following the construction of the Peace River hydroelectric dam, flood regimes were altered downstream along the Slave River, resulting in increased flood frequency and higher water levels in shallow lakes in the Slave River Delta, altering the macrophyte and diatom communities. Similarly, McGowan et al. (2011) observed increases in shallow lake primary productivity and algal biomass, through the investigation of photosynthetic pigments, related to increased macrophyte abundance during periods of low-water levels.

The ecological shifts observed in the 1960s and 1970s across all biological proxies is the greatest shift observed throughout the records, and the flooding of the Selenga Delta as a result of the construction of the hydroelectric Irkutsk Dam was the greatest disturbance to the system through the 19th and 20th centuries, and the ecological impacts outweighed those of the Tsagan earthquake of 1862, which was one of the strongest earthquakes recorded in eastern Siberia (Orlov, 1872; Vologina *et al*., 2010), and caused total subsidence of the eastern side of the Selenga Delta (See Section 1.4.2 for further discussion on the Tsagan earthquake). Moreover, little ecological response was observed in the biological records from SLNG05 around the time of the Tsagan earthquake. It could be concluded, therefore, that the largest ecological impact

on shallow lakes in the region was a result of regional anthropogenic development in the 20th century (Figure 7.7 and Figure 7.13).

7.5 Conclusions

Multi-proxy records from SLNG05 indicated shifts in ecosystem structure and function in the late-19th century. The most likely theory for the ecological changes that occurred is a change in connectivity between SLNG05 and the Selenga River, which incited a change in lake depth, and resulted in increased productivity of SLNG05, manifested as increased density of submerged macrophytes and increased algal biomass. Change in connectivity in the 19th century may be related to changes in atmospheric circulation patterns, which led to decreased precipitation and river runoff in the Selenga River basin. There is, however, potential that the pigment and macrofossil records could be implying increased nutrient influx to SLNG05 beginning in the late-19th century, as this timing coincides with increased agricultural presence in the Selenga River basin. However, the diatom records from this time do not indicate high nutrient levels, and an absence of planktonic species between the late-19th century and mid-20th century further supports the low-connectivity theory. Potential implications for increased pigment preservation in SLNG05 between the late-19th century and mid-20th century, as a result of increased macrophyte density and subsequent increases in organic matter and decaying plant material in the sediment, resulting in increasingly anoxic conditions at the sediment-water interface.

The largest ecological change in the biological records from SLNG05 occurred in the mid-20th century, with significant changes in ecological structure of the shallow lake observed. Exceptional declines in submerged macrophyte abundance and algal concentrations may have led to shifts in trophic interactions. Increased abundances of planktonic diatoms, which dominated the SLNG05 record post-1960s, indicated the most likely reason for the changes observed in the mid-20th century as increased connectivity to the Selenga River. The increased connection between the Selenga River and SLNG05 at this time is likely due to the extensive flooding that occurred around Lake Baikal and the Selenga Delta in the early to mid-1960s, as a result of the completion of the Irkutsk Dam along the Angara River, Lake Baikal's only outflow. The ecological changes observed at SLNG05 as a result of regional hydroelectric development were the greatest observed in the SLNG05 records, suggesting that the mid-20th century anthropogenic activities and resulting floods were of greater disturbance to the Selenga Delta

ecosystem than previous natural disturbances, including the 1862 catastrophic Tsagan earthquake. The mid-20th century flooding resulted in significant ecological shifts at SLNG05, and ecological variability in the ecosystem since that time, has been a factor of these anthropogenic events.

7.6 References

Anderson N.J. (1990) The biostratigraphy and taxonomy of small Stephanodiscus and Cyclostephanos species (Bacillariophyceae) in a eutrophic lake, and their ecological implications. *British Phycological Journal* **25**, 217-235.

Bailey S.E., & Guimond J.K. (2009) Aboveground biomass and nutrient limitation in relation to river connectivity in montane floodplain marshes. *Wetlands* **29,** 1243-1254.

Battarbee R.W. Jones V., Flower R., Cameron N., Bennion H., Carvalho L., & Juggins S. (2001) Diatoms. In Terrestrial, algal and siliceous indicators. Eds. J. Smol, H.J.B. Birks, and M. Last, Kluwer Academic Publishers, The Netherlands. pp. 155–202.

Bazhenova O.I., & Kobylkin D.V. (2013) The dynamics of soil degradation processes within the Selenga Basin at the agricultural period. *Geography and Natural Resources* **34,** 221-227.

Bennion H., Davidson T.A., Sayer C.D., Simpson G.L., Rose N.L., & Sadler J.P. (2015) Harnessing the potential of the multi-indicator palaeoecological approach: an assessment of the nature and causes of ecological change in a eutrophic shallow lake. *Freshwater Biology*, doi: 10.1111/fwb.12579.

Berezhnykha T.V., Marchenkoa O.Y., Abasova N.V., & Mordvinov V.I. (2012) Changes in the Summertime Atmospheric Circulation Over East Asia and Formation of Long-Lasting Low-Water Periods Within the Selenga River Basin. *Geography and Natural Resources* **33,** 223-229.

Berthon V., Alric B., Rimet F., & Perga M-E. (2014) Sensitivity and responses of diatoms to climate warming in lakes heavily influenced by humans. *Freshwater Biology*, doi:10.1111/fwb.12380.

Bianchi T.S., Johansson B., & Elmgren R. (2000) Breakdown of phytoplankton pigments in Baltic sediments: effects of anoxia and loss of deposit-feeding macrofauna. *Journal of Experimental Marine Biology and Ecology* **251**, 161– 183.

Birks H.H. (1973) Modern macrofossil assemblages in lake sediments in Minnesota. In: Birks H.J.B., Editor: R.G. West. Quaternary plant ecology. Blackwell Scientific Publications, Oxford, pp. 172–188.

Birks H.H. (2001) Plant macrofossils. In: Tracking Environmental Change Using Lake Sediments. Volume 3: Terrestrial, Algal, and Siliceous Indicators. Eds. J.P. Smol, H.J.B. Birks & W.M. Last, Kluwer Academic Publishers, Dordrecht, the Netherlands. pp. 49–74.

Birks H.J.B. (2012) Ecological palaeoecology and conservation biology: controversies, challenges, and compromises. *International Journal of Biodiversity Sciences and Ecosystem Services Management* **8**, 292–304.

Bolgov, M.V., Buber A.L., Korobkina E.A., Lyubushin A.A., & Filippova I.A. (2017) Lake Baikal: extreme level as a rare hydrological event. *Water Resources* **44,** 522-536.

Bradbury J.P. (1971) Paleolimnology of lake Texoco Mexico: Evidence from diatoms. *Limnology and Oceanography* **16,** 180-200.

Brock B.E., Martin M.E., Mongeon C.L., Sokal M.A., Wesche S.D., Armitage D., Wolfe B.B., Hall R.I., & Edwards T.W.D. (2011) Flood frequency variability during the past 80 years in the Slave River Delta, NWT, as determined from multi-proxy palaeolimnological analysis. *Canadian Water Resources Journal*, **35**, 281-300.

Brown L., May J. & Hunsaker C. (2008) Species composition and habitat associations of benthic algal assemblages in headwater streams of the Sierra Nevada, California. *Western North American Naturalist* **68**, 194-209.

Burks R.L., Jeppesen E., & Lodge D.M. (2001) Littoral zone structure as Dapnia refugia against fish predators. *Limnology and Oceanography* **46,** 230-237.

Cholonky B.J. (1968) Die Okologie der Diatomeen in Binnengewasser. J. Cramer, Lehre, 699 pp.

Cousyn C., & De Meester L. (1998) The vertical profile of resting egg banks in natural populations of the pond-dwelling cladoceran Daphnia magna Straus. *Archives of Hydrobiology Special Issues Advanced Limnology* **52**, 127–39.

Davies S. J. (2015) Micro-XRF core scanning in palaeolimnology: recent developments. In: Developments in Paleoenvironmental Research. Volume 17: Micro-XRF Studies of Sediment Cores: Applications of a Non-Destructive Tool for Environmental Sciences. Eds. I.W. Croudace, & R.G. Rothwell, Springer, the Netherlands. pp. 189-226.

Dieffenbacher-Krall A.C., & Halteman W. (2000) The relationship of modern plant remains to water depth in alkaline lakes in New England, USA. *Journal of Paleolimnology* **24**, 213–229.

Edlund M.B., Engstrom D.R., Triplett L.D., Lafrancois B.M., & Leavitt P.R. (2009) Twentieth century eutrophication of the St. Croix River (Minnesota-Wisconsin, USA) reconstructed from the sediments of its natural impoundment. *Journal of Paleolimnology* **41**, 641-657.10.1007/s10933-008-9296-1.

Frolova N.L., Belyakova P.A., Grigoriev V.Y., Sazonov A.A., Zotov L.V., & Jarsjo J. (2017) Runoff fluctuations in the Selenga River basin. *Regional Environmental Change*. DOI 10.1007/s10113-017-1199-0.

Gell P., Tibby J., Little F., Baldwin D., & Hancock G. (2007) The impact of regulation and salinization on floodplain lakes: the lower River Murray, Australia. *Hydrobiologia* **591**, 135-146.

Genkal S.I., & Popovskaya G.I. (2008) Centric datom algae of the Selenga River and its delta branches. *Inland Water Biology* **1**, 120-128.

Gong D. Y., & Ho C.H. (2002) The Siberian High and climate change over middle to high latitude Asia. *Theoretical and Applied Climatology* **72**, 1–9.

Guo W., Huo S., & Ding W. (2015) Historical record of human impact in a lake in northern China: Magnetic susceptibility, nutrients, heavy metals, and OCPs. *Ecological Indicators* **57**, 74-81.

Haberzettl T., Fey M., Lucke A., Maidana N., Mayr C., Ohlendorf C., Schabitz F., Schelser G.H., Wille M. and Zolitschka B. (2005) Climatically driven lake level changes during the last two millennia as reflected in sediments of Laguna Potrok Aike, southern Patagonia (Santa Cruz, Argentina). *Journal of Paleolimnology 33*, 283-302.

Hall R.I., & Smol J. (1992) A weighted—averaging regression and calibration model for inferring total phosphorus concentration from diatoms in British Columbia (Canada) lakes. *Freshwater Biology* **27**, 417-434.

Hall R.I., Wolfe B.B., Edwards T.W.D., Karst-Riddoch T.L., Vardy S.R., McGowan S., Sjunneskog C., Paterson A., Last W., English M., Sylvestre F., Leavitt P.R., Warner B.G., Boots B., Palmini R., Clogg-Wright K., Sokal M., Falcone M., van Driel P., & Asada T. (2004) A Multi-Century Flood, Climatic, and Ecological History of the Peace-Athabasca Delta, Northern Alberta, Canada. Final Report to BC Hydro, 163 pp + Appendices.

Hampton S.E., Izmest'eva L.R., Moore M.V., Katz S.L., Dennis B., & Silow E.A. (2008) Sixty years of environmental change in the world's largest freshwater lakeelake Baikal, Siberia. *Global Change Biology* **14**, 1947-1958.

Hay M.B., Michelutti N., & Smol J.P. (2000) Ecological patterns of diatom assemblages from Mackenzie Delta lakes, Northwest Territories, Canada. *Canadian Journal of Botany* **78**, 19-33.

Interlandi S.J., & Kilham S.S. (2001) Limiting resources and the regulation of diversity in phytoplankton communities. *Ecology* **82,** 1270-1282.

Jeppesen E., Jensen J.P., Sondergaard M., Lauridsen T., Pedersen L.J., & Jensen L. (1997) Top-down control in freshwater lakes: the role of nutrient state, submerged macrophytes, and water depth. *Hydrobiologia* **342/343,** 151-164.

Jeppesen E., Leavitt P., De Meester L., & Jensen J.P. (2001) Functional ecology and paleolimnology: using cladoceran remains to reconstruct anthropogenic impact. *Trends in Ecology and Evolution* **16,** 191-198.

Jeppesen E., Noges P., Davidson T.A., Haberman J., Noges T., Blank K., Lauridsen T.L., Sondergaard M., Sayer C., Laugaste R., Johansson L.S., Bjerring R., Amsinck S.L. (2011) Zooplankton as indicators in lakes: a scientific-based plea for including zooplankton in the ecological quality assessment of lakes according to the European Water Framework Directive (WFD). *Hydrobiologia* **676,** 279-297.

Juggins S. 2014. C2 data analysis, Version 1.7.6. University of Newcastle, United Kingdom.

Kharuk V.I., Dvinskaya M.L., Im S.T., & Ranson K.J. (2008) Tree vegetation of the forest-tundra ecotone in the Western Sayan Mountains and climatic trends. *Russian Journal of Ecology* **39**, 8-13.

Khazheeva Z.I., & Tulokhonov A.K. (2007) Distribution of metals in bottom deposits in the branches of Selenga River Delta. *Geochemistry International* **45,** 185-192.

Kuhn D.L., Plafkin J.L., Cairns J. & Lowe R.L. (1981) Quantitative characterisation of aquatic environments using diatom life-form strategies. *Transactions of the American Microscopial Society* **100**, 165-182.

Leavitt P.R. (1993) A review of factors that regulate carotenoid, and chlorophyll deposition, and fossil pigment abundance. *Journal of Paleolimnology* **9**, 109–127.

Lucas B.T., Liber K., & Doig L.E. (2015) Reconstructing diatom and chironomid assemblages to infer environmental spatiotemporal trends within Lake Diefenbaker, a narrow river-valley reservoir on the Canadian Prairies. *Journal of Great Lakes Research* **41,** 45-55.

Lydolf P. E. (1977) Climates of the Soviet Union, Elsevier. 443 pp.

Mackay A.W., Bezrukova E.V., Leng M.J., Meaney M., Nunes A., Piotrowska N., Self A., Shchetnikov A., Shilland E., Tarasov P., Wang L., & White D. (2012) Aquatic ecosystem responses to Holocene climate change and biome development in boreal, central Asia. *Quaternary Science Reviews* **41,** 119-131.

McGowan S., Leavitt P.R., Hall R.I., Wolfe B.B., Edwards T.W.D., Karst-Riddoch T., & Vardy S.R. (2011) Interdecadal declines in flood frequency increase primary production in lakes of a northern river delta. *Global Change Biology* **17,** 1212–1224.

McGowan S., Barker P., Haworth E.Y., Leavitt P.R., Maberly S.C., & Pates J. (2012) Humans and climate as drivers of algal community change in Windermere since 1850. *Freshwater Biology* **57**, 260-277.

Metcalfe S.E., Bimpson A., Courtice A.J., O'Hara S.L. and Taylor D.M. (1997) Climate change at the monsoon/Westerly boundary in northern Mexico. *Journal of Paleolimnology* **17**, 155-171.

Mills E.L., Green D.M., & Schiavone A.J. (1987) Use of zooplankton size to assess the community structure of fish populations in freshwater lakes. *North American Journal of Fisheries Management* **3,** 369-378.

Orlov A.P. (1872) General remarks on earthquakes, with special reference to South Siberia and Turkestan Region. *Proceedings of the Kazan University Society of Natural Sciences*, **3.**

Patrick R., & Reimer C.W. (1966) The diatoms of the United States. The Academy of Natural Sciences, Philadelphia.

Pinegin A.V., Rogozin A.A., Leshchikov F.N., Kulish L.Y., & Yakimov A.A. (1976) Shore dynamics of Lake Baikal at the new level regime. Nauka, Moscow.

R. v.3.2.4 R. 2016. The R Foundation, R Development Team. Vienna.

Randsalu-Wendrop L., Conley D.J., Carstensen J., Hansson L-A., Bronmark C., Fritz S.C., Choudhary P., Routh J., & Hammarlund D. (2014) Combining limnology and palaeolimnology to investigate recent regime shifts in a shallow, eutrophic lake. *Journal of Paleolimnology* **51**, 437-448.

Reavie E.D. & Smol J.P. (1998) Epilithic diatoms of the St. Lawrence river and their relationships to water quality. *Canadian Journal of Botany* **76**, 251-257.

Reavie E.D., & Kireta A.R. (2015) Centric, Araphid and Eunotioid Diatoms of the Coastal Laurentian Great Lakes. *Bibliotheca Diatomologica* **62,** 1-184.

Reuss N., Conley D.J., & Bianchi T.S. (2005) Preservation conditions and the use of sediment pigments as a tool for recent ecological reconstructions in four Northern Europe estuaries. *Marine Chemistry* **95,** 283-302.

Robertson A.I., Bacon P., & Heagney G. (2001) The responses of floodplain primary production to flood frequency and timing. *Journal of Applied Ecology* **38,** 126-136.

Rose N.L., Morley D., Appleby P.G., Battarbee R.W., Alliksaar T., Guilizzoni P., Jeppesen E., Korhola A., & Punning J-P. (2011) Sediment accumulation rates in European lakes since AD 1850: Trends, reference conditions and exceedence. *Journal of Paleolimnology* **45**, 447-468.

Round F.E. (1990) Diatom communities, their response to changes in acidity. *Philosophical Transactions of the Royal Society: Series B, Biological Sciences* **327,** 243-249.

Sayer C., Davidson T.A., Jones J.I., & Langdon P.G. (2010a) Combining contemporary ecology and paleolimnology to understand shallow lake ecosystem change. *Freshwater Biology* **55,** 487-499.

Sayer C., Davidson T.A., &b Jones J.I. (2010b) Seasonal dynamics of macrophytes and phytoplankton in shallow lakes: a eutrophication-driven pathway from plants to plankton. *Freshwater Biology* **55**, 500-513.

Sokal M. A., Hall R.I., & Wolfe B.B. (2008). Relationships between hydrological and limnological conditions in lakes of the Slave River Delta (NWT, Canada) and quantification of their roles on sedimentary diatom assemblages. *Journal of Paleolimnology* **39**, 533 ‐ 550.

Sokal M.A., Hall R.I., Wolfe B.B. (2010) The role of flooding on inter-annual and seasonal variability of lake water chemistry, phytoplankton diatom communities, and macrophyte biomass in the Slave River Delta (Northwest Territories, Canada). *Ecohydrology* **3,** 41-54.

Stoermer E.F. (1978). Phytoplankton as indicators of water quality in the Laurentian Great Lakes. *Transactions of the American Microscopical Society* **97,** 2-16.

Stoermer E.F., & Yang J.J. (1969) Plankton diatom assemblages in Lake Michigan. Univ. Michigan, Great Lakes Res. Div. Spec. Rep. No. 47, 168 pp.

Stoermer E.F., & Håkansson H. (1984) Stephanodiscus parvus: Validation of an enigmatic and widely misconstrued taxon. *Nova Hedwigia* **39,** 497-511.

Stoermer E.F., Ladewski B.G., & Schelske C.L. (1978) Population response of Lake Michigan phytoplankton to nitrogen and phosphorus enrichment. *Hydrobiolgia* **57,** 249-265.

Talling S.J. (1976) The depletion of carbon dioxide from lake water by phytoplankton. *Journal of Ecology* **64,** 79-121.

Ter Braak C.J.F. & Šmilauer P. (2012): Canoco reference manual and user's guide: software for ordination, version 5.0. Microcomputer Power, Ithaca, USA, 496 pp.

Todd M.C., & Mackay A.W. (2003) Large-scale climatic controls on lake Baikal ice cover. *Journal of Climate* **16**, 3186–3199.

Van Dam H., Mertens A., & Sinkeldam J. (1994) A coded checklist and ecological indicator values of freshwater diatoms from the Netherlands. *Netherlands Journal of Aquatic Ecology* **28,** 117-133.

Vologina E.G., Kalugin I.A., Osukhovskaya Y.N., Sturm M., Ignatova N.V., Radziminovich Y.B., Dar'in A.V., & Kuz'min M.I. (2010) Sedimentation in Proval Bay (Lake Baikal) after earthquake-induced subsidence of part of the Selenga River delta. *Russian Geology and Geophysics*, **51,** 1275-1284.

Watchorn M., Hamilton P., Anderson T., Roe H. and Patterson R.(2008) Diatoms and pollen as indicators of water quality and land-use change: a case study from the Oak Ridges Moraine, Southern Ontario, Canada. *Journal of Paleolimnology* **39**, 491-509.

Wolfe B.B., Karst-Riddoch T.L., Vardy S.R., Falcone M.D., Hall R.I., & Edwards T.W.D. (2005) Impacts of climate and river flooding on the hydro-ecology of a floodplain basin, Peace-Athabasca Delta, Canada since A.D. 1700. *Quaternary Science* **64,** 147-162.

Yang X., Dong X., Gao G., Pan H., & Wu J. (2005) Relationship between surface sediment diatoms and summer water quality in shallow lakes of the middle and lower reaches of the Yangtze River. *Journal of Integrative Plant Biology* **47**, 153–164. 10.1111/j.1744-7909.2005.00035.x.

Chapter 8: Sedimentary record of biological change in BRYT02

8.1 Introduction to Chernoe Ozero (Black Lake) and the Gusinoozersk region of the Selenga River basin

Gusinoozersk is the nearest town to Black Lake and is situated on the shores of Lake Gusinoye (Figure 8.1). It was first settled in 1939 for the purposes of expanding coal mining in the Gusinoye region (Pisarsky *et al.,* 2005). Increasing population and intensive anthropogenic development following World War II (WWII) gave the settlement "town" status in 1953. Increases in population in the 1950s and increased military installation in the area led to the construction of the Gusinoozersk State Regional Power Plant (SRPP) in the 1960s, a coal power plant on the shores of Lake Gusinoye, which began operations in 1976 (Pisarsky *et al.,* 2005). The increase in anthropogenic operations in the Gusinoye region of the Selenga River basin since the mid-20th century has the potential for great influence on pollution levels in the region, and high concentrations (2-3 times above regional background levels) of sulphur and trace metal contaminants have been measured in pine needles on the outskirts of Gusinoozersk (Afanas'yeva *et al*., 2007).

Figure 8.1. Location of Black Lake (BRYT) within the Gusinoye region of the Selenga River basin, in close proximity to Lake Gusinoye and the town of Gusinoozersk.

Uncertainties remain as to how the 20th century regional and local anthropogenic disturbances in southeast Siberia may impact the shallow lake environments of the area. The impact of various environmental stressors on the biological, chemical, and physical properties of these systems, can result in changes in ecological structure and function of a shallow lake (Andersen *et al*., 2008; Randsalu-Wendrup *et al*., 2014). It is likely that land development in watersheds exerts strong impacts on aquatic communities through stressors related to land conversion, such as pollution, nutrient loading or sediment discharge (Kovalenko *et al*., 2014; O'Dwyer *et al*., 2013). Nutrient enrichment and pollution increases could eventually lead to a shift in ecological functioning of the shallow lakes systems, with increased productivity of lakes and ponds and eventual eutrophication (O'Dwyer *et al*., 2013; Luoto *et al*., 2014). Water depth is a significant variable directly and indirectly influencing several trophic levels within the shallow lake ecosystem, including diatom, macrophyte and zooplankton distributions, with small fluctuations in water levels in shallow lake systems having a large influence on dilution/evapoconcentration and light penetration (Moser *et al*., 2000; Cobbaert *et al*., 2014). Such anthropogenic disturbances have potential for altering ecological structure and functioning of shallow lake ecosystems, and promote the crossing of critical thresholds, leading to a regime shift, and with potential to result in an alternative state from the original, with different ecological structures and functions.

Black Lake is a shallow lake (<3 metres maximum depth) located in close proximity to the town of Gusinoozersk in southeast Siberia, approximately 200 km upstream of the Selenga Delta along the Selenga River, and 80 km direct distance southeast of Lake Baikal (Figure 8.1). Black Lake was chosen to provide contrast to the lakes of the Selenga Delta (SLNG04 and SLNG05), as it is similar in physical characteristics, yet removed from the direct influences of the Selenga River, and is situated in a more heavily industrialized area. The aim of this chapter is to determine to what extent these aforementioned disturbances have impacted the ecological structure and functioning of Black Lake throughout the 20th century, and to assess the ecological impacts of stressors on a shallow lake without the direct influence of impact from the Selenga River and Lake Baikal (i.e. fluctuating water levels). Black Lake would, theoretically, be impacted by regional disturbances that may also impact SLNG04 and SLNG05, such as air pollution and agriculture, but will not be impacted by disturbances local to the Selenga Delta,

such as the Tsagan Earthquake of 1862, or the flooding that resulted from the construction of the Irkutsk Dam in the early to mid-1960s (See Section 1.4.2, Figure 1.3 for a detailed timeline of these events). However, there may be other local disturbances to the Gusinoye region that would not influence the Selenga Delta sites as greatly. Specific objectives have been chosen to address the aims of the chapter, and are as follows:

1) Changes in ecological structure since the late-19th century will be assessed by analyzing algal communities, including diatoms, from a sediment core extracted from Black Lake;
2) Changes in ecological functioning of Black Lake since the late 19th century will be assessed using sedimentary pigment and diatom records enumerated from a sediment core extracted from Black Lake;
3) Potential for regime shifts will be evaluated through the use of statistical analyses (e.g. breakpoint analysis)

a b

Figure 8.2. a) BRYT view from the eastern shore, facing northwest; b) BRYT view from the southeastern shore, facing west.

8.2 Methods

Details of coring method, sediment core extruding, and sediment core partitioning for analyses are described in Section 4.2.

8.2.1 Sedimentary diatoms

Subsamples at 2.0-cm intervals from sediment core BRYT02-C were analysed for diatom analysis according to standard procedures (Battarbee *et al.,* 2001). All diatom laboratory processing and slide preparation methods, enumeration, identification, and numerical analysis followed procedures outlined in Section 3.2.1.3. Species rarefaction for BRYT02 was set to 304

valves, which was the total number of valves enumerated at 30 cm depth, and the minimum number of valves counted in a single sample. Richness in all other samples was then assessed at 304 valves. Diatom accumulation rates were calculated using sedimentation accumulation rates of sediment core BRYT02-C since c. 1960 AD (See Section 4.4.3.3 for details of radioisotope dating of sediment core BRYT02-C).

8.2.2 Sedimentary diatom assemblage data analysis

For a detailed account of diatom data analytical procedures, see Section 6.2.4. BRYT02 unconstrained ordinations were performed on a condensed dataset which included only those species present at >2% relative abundance, which included 47 species. Stratigraphical plots of diatom community assemblage relative abundances were constructed, and included all species present at >5% at any one depth (22 species).

8.2.3 Sedimentary pigments

Pigments of photosynthetic organisms were analyzed from sediment samples from BRYT02-C following McGowan *et al.* (2012), and laboratory methods were followed as described in Section 3.2.1.4. Sediment was subsampled for pigment analysis at 1.0-cm intervals from BRYT02-C as described in Section 3.2.1.6. Pigment fluxes were calculated using sedimentation accumulation rates of BRYT02-C since c. 1960 AD (See Section 4.4.3.3 for details of radioisotope dating of BRYT02-C).

8.2.4 Sedimentary pigment data analysis

For detailed account of pigment data analytical procedures, see Section 6.2.6.

8.2.5 Data analysis of all biological proxies

For a detailed account of methods for co-correspondence analysis for diatoms and pigments data, see Section 6.2.7. Exploratory detrended correspondence analysis (DCA) indicated short gradient lengths (< 3.0 SD) for all sedimentary biological records, indicating the appropriateness of linear ordination techniques (Principal components analysis (PCA)).

8.3 Results

8.3.1 BRYT02 sedimentary diatom record

Taxa present at ≥ 5% at a single depth, and zones of change within the diatom record for BRYT02 are presented in the stratigraphy in Figures 8.3a-b. A total of 171 species from 45 genera were identified within BRYT02 diatom assemblages. Throughout the entire record, diatom concentration ranged from approximately 9.27 x 10^4 valves g^{-1} dry weight (late-19th century) to 4.12 x 10^6 valves g^{-1} dry weight (mid-1980s) (Figure 8.3a). Rarefacted species richness ranged from 19 (early-20th century) to 59 species (mid-1960s), and sample N2 ranged from 2.6 (late-19th century) to 18.7 species (mid-1970s) (Figure 8.3a). PCA of the BRYT02 diatom record indicated 55% of diatom assemblage variation explained along axis 1, and an additional 18.3% of variation explained along PCA axis 2 (Table 8.1). In the ordination, the oldest sample depths plotted negatively along PCA axis 1, while recent samples plotted positively along axis 1, with mid-range samples plotting around the origin (Figure 8.4). A greater degree of spread along PCA axis 2 is also seen in the older samples. Most of the small fragilarioid species plot negatively along PCA axes 1 and 2, with the exception of *Pseudostaurosira brevistriata,* which plots positively along PCA axis 2 (+0.6054) with several large benthic species (Figure 8.4). *Fragilaria berolinensis* plots very strongly and positively along PCA axis 1 (+0.9512), along with several planktonic and epiphytic species. Three significant zones of diatom community composition were determined for the BRYT02 record through broken stick analysis (Figure 8.5), and cluster analysis indicated that the three significant diatom zones were from 1) Late-19th century to mid-1950s (74 cm to 36 cm), 2) c. 1960 to late-1980s (34 cm to 18 cm), and 3) c. 1990 to 2014 (16 cm to 0 cm) (Figure 8.6). Breakpoint analysis indicated a significant ($p \leq 0.01$) change in the diatom PCA axis 1 scores in the late-1980s (Figure 8.7).

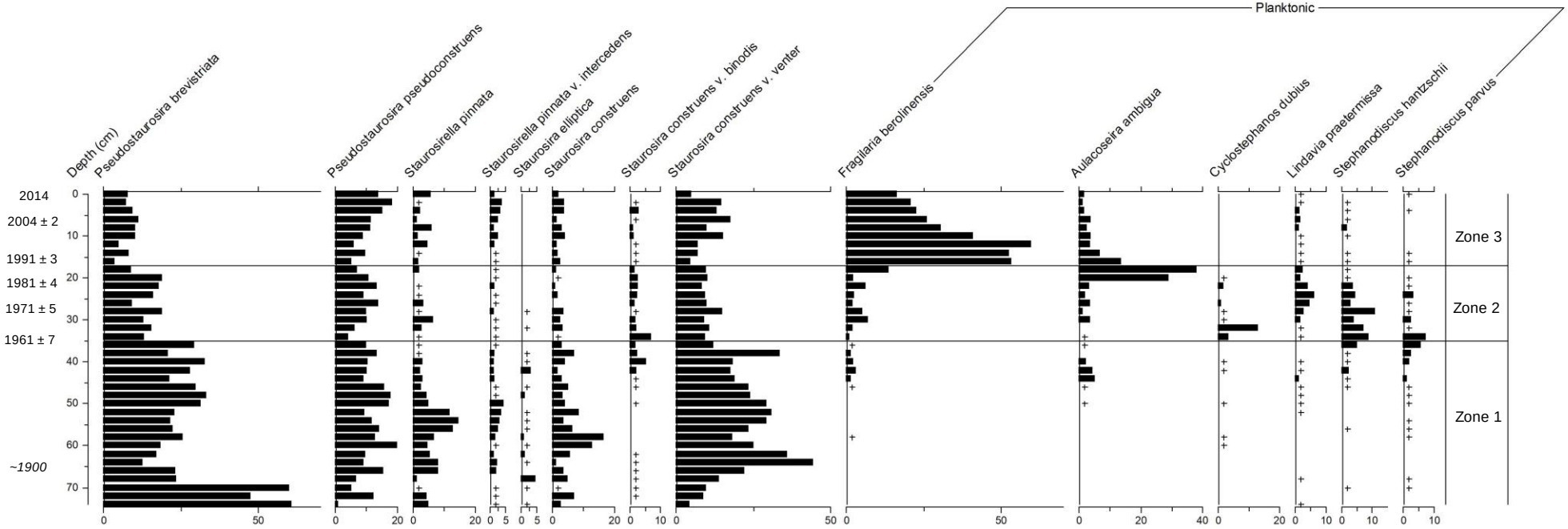

Figure 8.3a. Relative abundances (%) of small, periphytic fragilarioids of the *Staurosira-Staurosirella-Pseudostaurosira* (SSP) complex, and planktonic diatoms present at >5% in any one sample from the BRYT02 sediment record for Black Lake. (+) indicates presence of species in sample at <1% relative abundance. Diatom Zones 1 – 3 are indicated, based on broken stick and cluster analyses. Radioisotope-derived dates and confidence limits are highlighted on the y-axis. Italicized dates are extrapolated beyond ^{210}Pb radioisotope dating.

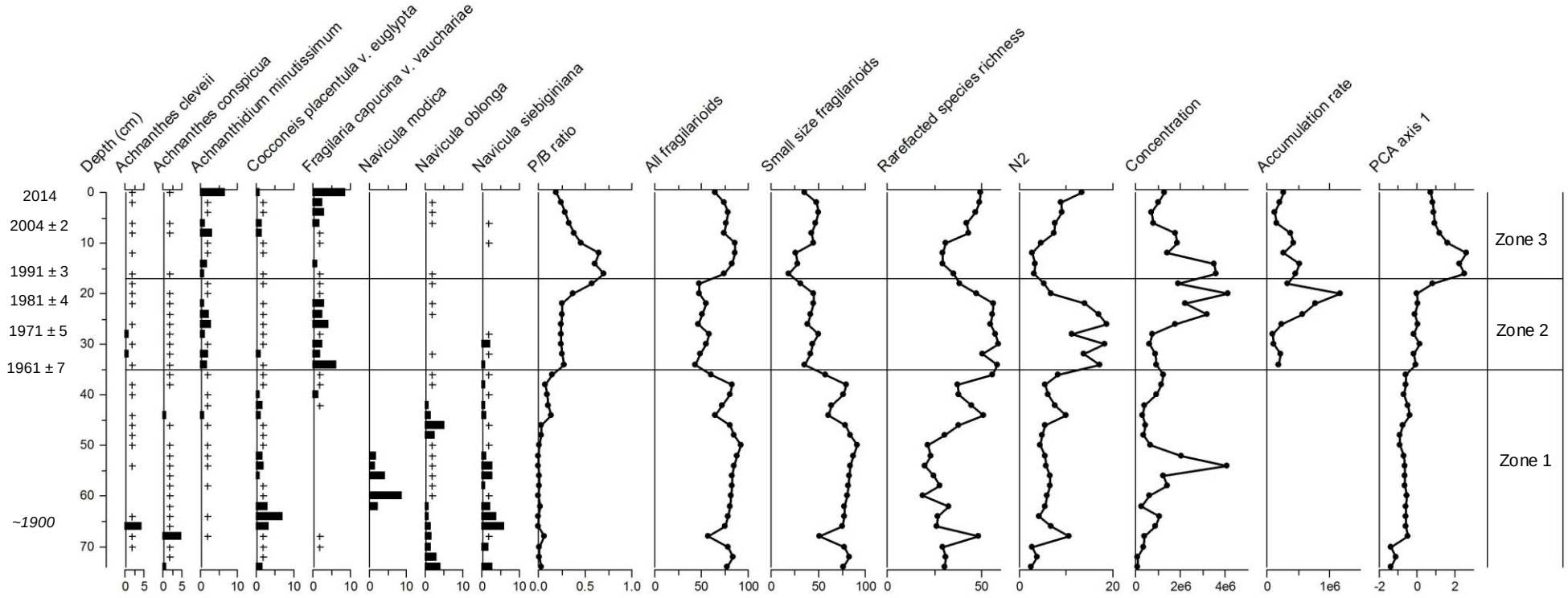

Figure 8.3b. Relative abundances (%) of periphytic diatoms >5% in any one sample from the BRYT02 sediment record for Black Lake. (+) indicates present in sample at <1% relative abundance. Planktonic/Benthic (P/B) ratio, total sum all fragilarioids (%), total sum small fragilarioids of the SSP complex (%), diatom rarefacted species richness (no. species), Hill's N2 (no. species) measure of diversity, concentrations (no. valves g^{-1} dry weight), diatom accumulation rates (no. valves cm^{-2} yr^{-1}), and PCA axis 1 scores are plotted. Diatom Zones 1 – 3 are indicated, based on broken stick and cluster analyses. Radioisotope-derived dates and confidence limits are highlighted on the y-axis. Italicized dates are extrapolated beyond ^{210}Pb radioisotope dating.

	Axis 1	Axis 2	Axis 3	Axis 4
Eigenvalues	0.5496	0.1827	0.1124	0.0652
Explained variation (cumulative)	55.0	73.2	84.5	91.0

Table 8.1. PCA summary table of the BRYT02 diatom assemblages. Eigenvalues and explained variation of the first four PCA axes indicated.

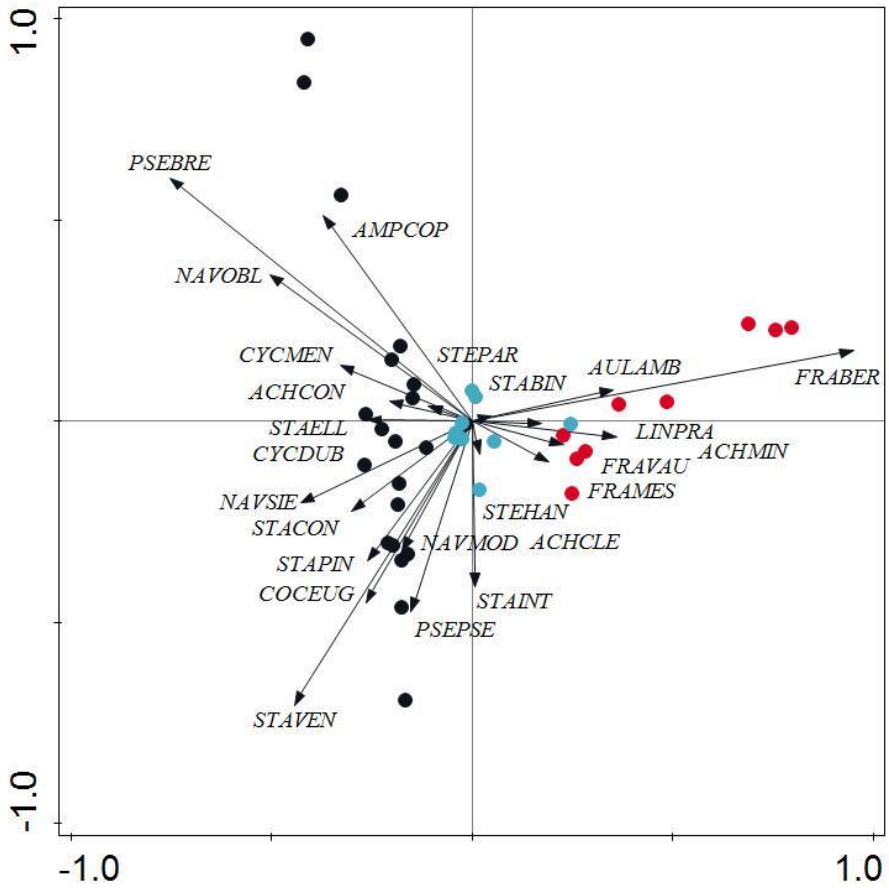

Figure 8.4. PCA biplot of diatom species and samples from BRYT02. Top 25 species based on relative abundances are plotted. Sample depths are colour-coded according to zone: Diatom Zone 1 (Late 19th century to mid-1950s) (black), Diatom Zone 2 (c. 1960 to late-1980s) (light blue), Diatom Zone 3 (c. 1990 to 2014) (red). Diatom species codes can be found in Appendix 6.

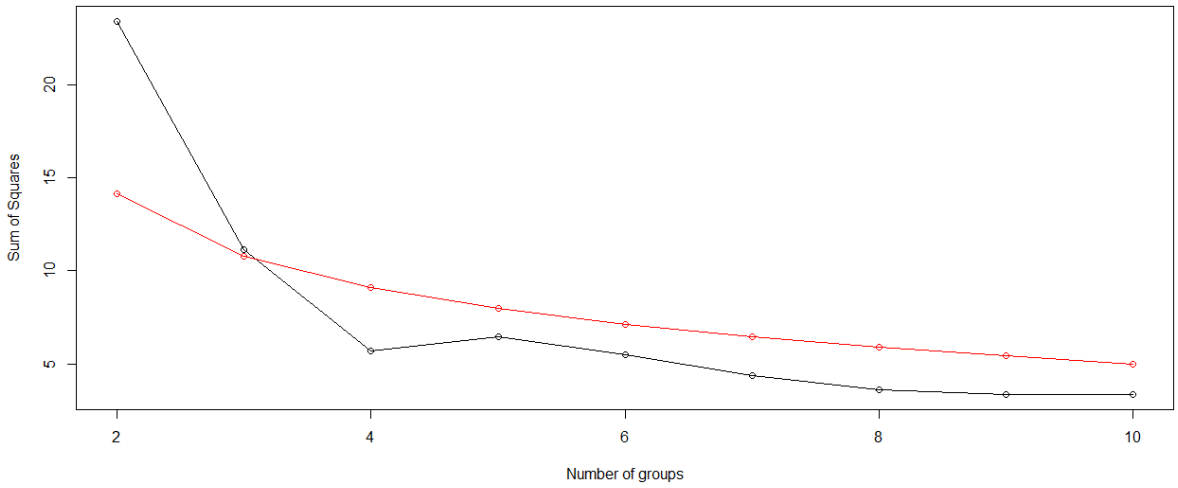

Figure 8.5. Broken stick of the BRYT02 diatom record. Three significant groupings of samples are indicated.

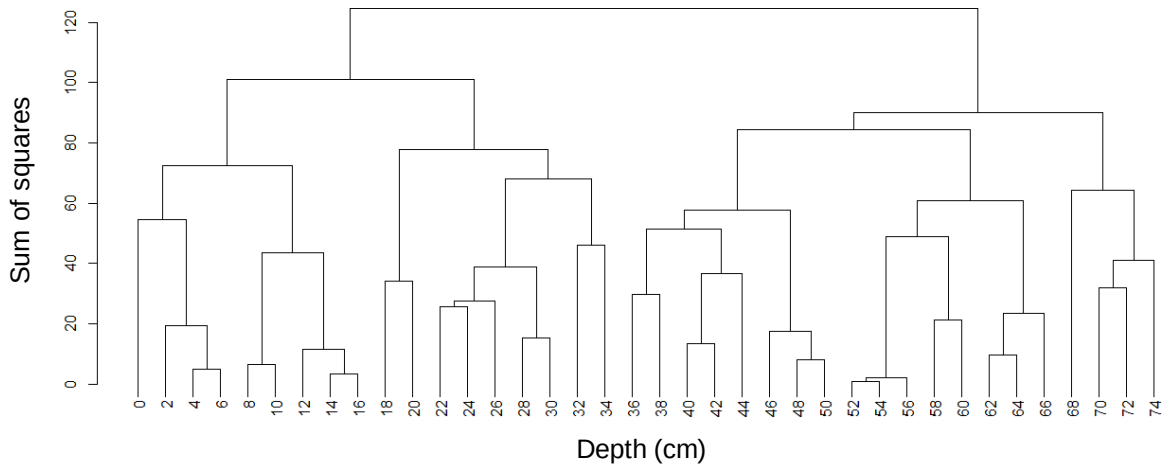

Figure 8.6. Cluster analysis of BRYT02 diatom samples. Sample depths are indicated (cm). Three significant groupings occur, as determined through broken stick analysis.

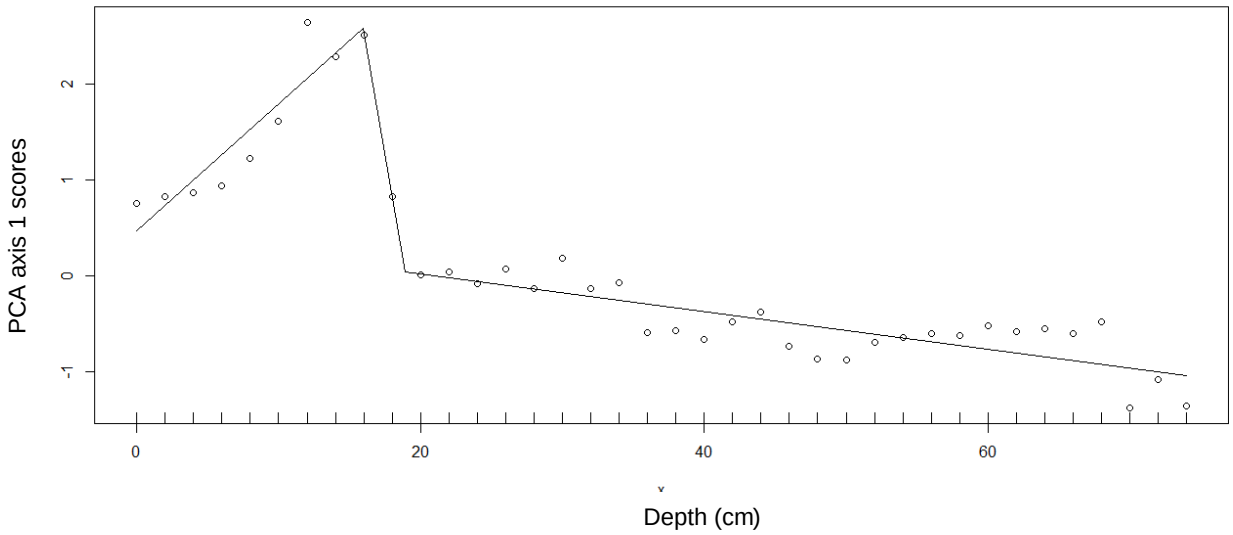

Figure 8.7. Breakpoint analysis of the BRYT02 diatom PCA axis 1 scores (y-axis). The break in axis scores between 20 cm and 16 cm was identified as significant ($p \leq 0.01$).

Diatom Zone 1: Late-19th century to mid-1950s (74 cm to 36 cm)

Species richness, sample N2, and diatom concentrations are low through Diatom Zone 1. Species richness increased late in Diatom Zone 1, c. 1930, and remained elevated for the remainder of the zone (Figure 8.3a). The assemblage early in Diatom Zone 1 is dominated by *Pseudostaurosira brevistriata*. However, by the onset of the 20th century, *P. brevistriata* declined in abundance, and was replaced as the dominant species by a different fragilarioid, *Staurosira construens* v. *venter* (Figure 8.3b). Diatom Zone 1 is dominated primarily by these small fragilarioids. Benthic naviculoids and small epiphytic species *Cocconeis placentula* v. *euglypta* are common through Diatom Zone 1. By the end of Diatom Zone 1, there was a decline in abundance of some fragilarioids, including *Staurosirella pinnata*, and the appearance of planktonic species at abundances greater than 1% (Figure 8.3b).

Diatom Zone 2: ~1960 to late-1980s (34 cm to 18 cm)

Diatom concentration began to increase c. 1975, and remained high through the remainder of Diatom Zone 2. Species richness and N2 were high through most of this zone, reaching richness values near 60 species per sample and N2 values near 20 species between ~1960 and 1980 (Figure 8.3a). Coinciding with the increased species richness early in Diatom Zone 2, was an increase in the planktonic/benthic (P/B) ratio c. 1960, with the decline in abundance of *Staurosira construens* v. *venter* and most other small fragilarioids, and increased abundance of

planktonic *Stephanodiscus* spp. and *Cyclostephanos dubius,* as well as epiphytic *Fragilaria capucina* v. *vaucharіae* (Figure 8.3a-b). Planktonic species continued to increase in abundance in Diatom Zone 2, with *Lindavia praetermissa* peaking c. 1975, followed by *Aulacoseira ambigua* rapidly increasing in abundance and peaking c. 1985. Both species richness and N2 declined towards the end of the zone.

Diatom Zone 3: ~1990 to 2014 (16 cm to 0 cm)

A significant breakpoint was identified in the diatom PCA axis 1 scores around the transition from Diatom Zone 2 and Diatom Zone 3 (Figure 8.7), coinciding with peak P/B ratios and minimum levels of the small fragilarioid species (Figure 8.3b). Diatom concentration remained elevated at the onset of Diatom Zone 3, but began to decline in the mid-1990s, and remained below 1975-1995 levels for the remainder of the record. Species richness and sample N2 were low in the 1990s, at the onset of Diatom Zone 3, likely due to the rapid increase in abundance by a single species: *Fragilaria berolinensis* (Figure 8.3b). *Fragilaria berolinensis* reached 60% relative abundance in the BRYT02 record by the late-1990s, then declined, steadying at ~20% relative abundance by 2014. With the decline in *Fragilaria berolinensis*, species richness increased at the onset of the 21st century, and continued to increase towards the surface. The decline in abundance of *Fragilaria berolinensis* occurred with an increase in other fragilarioids, including *Staurosira construens* v. *venter, Pseudostaurosira pseudoconstruens,* and *Fragilaria capucina* v. *vaucharіae*.

8.3.2 BRYT02 sedimentary pigment record

Pigment concentrations in BRYT02 are detailed in Figure 8.8. Pigments representing total algae (Chl *a*, Chl *a* degradation products, and β-carotene), chlorophytes (Chl *b*, Chl *b* degradation product, and lutein), chromophytes (Chl *c*), total cyanobacteria (zeaxanthin), colonial cyanobacteria (canthaxanthin), siliceous algae (fucoxanthin), diatoms (diatoxanthin), and cryptophytes (alloxanthin), were identified. The first two PCA axes explained 95.4% of total pigment variability. PCA axis 1 explained 87.7% of total variability in the BRYT02 sedimentary pigment record, and PCA axis 2 explained an additional 7.72% (Table 8.2). In the ordination, most older depths plotted negatively along PCA axis 1, while very recent depths plotted positively along PCA axis 1, and mid-core depths were spread across the PCA ordination space

(Figure 8.9). In the ordination, all pigments plotted positively along PCA axis 1, with stronger positive association between indicators for total algae (Chl *a,* Chl *a* degradation products), diatoms (diatoxanthin), and cryptophytes (alloxanthin) and recent samples. Chlorophyte pigments and β-carotene (total algae) plotted negatively along PCA axis 2, with stronger positive association with samples from Pigment Zones 2 and 3 (Figure 8.9). Broken stick analysis indicated four significant zones within the BRYT02 pigment record (Figure 8.10). Cluster analysis detected significant clustering of sample depths as follows: 1) Late-19th century to c. 1920 (74 cm to 55 cm), 2) c. 1920 to c. 1965 (54 cm to 30 cm), 3) c. 1965 to c. 2010 (29 cm to 4 cm), 4) c. 2010 - 2014 (3 cm to 0 cm) (Figure 8.11). Breakpoint analysis of the BRYT02 pigment PCA axis 1 scores identified a significant ($p \leq 0.01$) shift in the pigment assemblage c. 2005 (Figure 8.12).

	Axis 1	***Axis 2***	***Axis 3***	***Axis 4***
Eigenvalues	0.8767	0.0772	0.0297	0.0063
Explained variation (cumulative)	87.7	95.4	98.4	99.0

Table 8.2. PCA summary table of the BRYT02 pigment concentrations. Eigenvalues and explained variation of the first four PCA axes indicated.

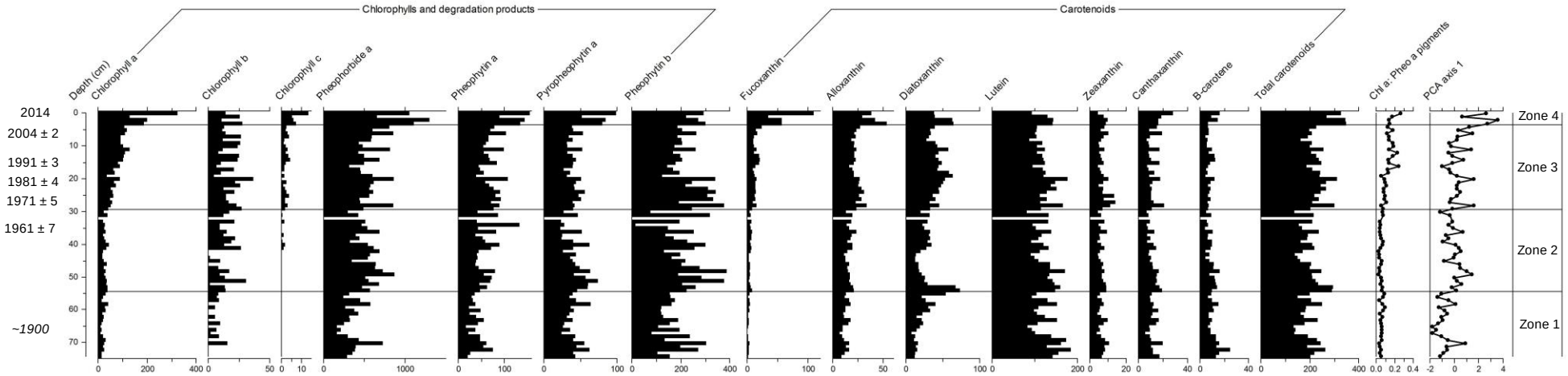

Figure 8.8. Pigment concentrations of chlorophylls, degradation products, and carotenoids for Black Lake, with indications of zones. Concentration units are in nmol g^{-1} organic matter. (+) indicates concentrations of <1 nmol/g organic matter dry weight. Pigment Zones 1-4 are indicated. Measure of preservation, ratio of Chl *a* : chlorophyll *a* degradation products (Pheo *a* pigments), indicated as well as PCA axis 1 scores. Radioisotope-derived dates and confidence limits are highlighted on the y-axis. Italicized dates are extrapolated beyond ^{210}Pb radioisotope dating.

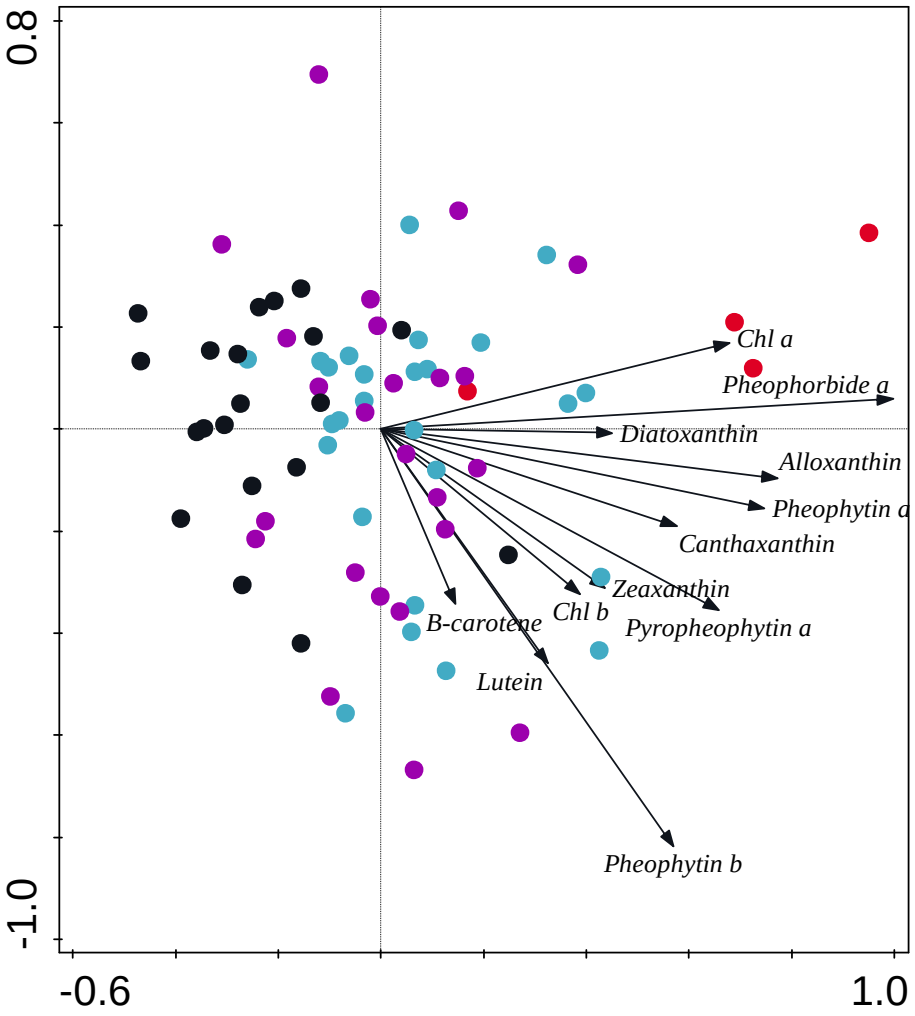

Figure 8.9. PCA biplot of pigments and sample depths from Black Lake. Sample depths are colour-coded according to zone: Pigment Zone 1 (Late 19th century to c. 1920) (black), Pigment Zone 2 (c. 1920 to c. 1965) (purple), Pigment Zone 3 c. 1965 to c. 2010) (light blue), Pigment Zone 4 (c. 2010 to 2014) (red).

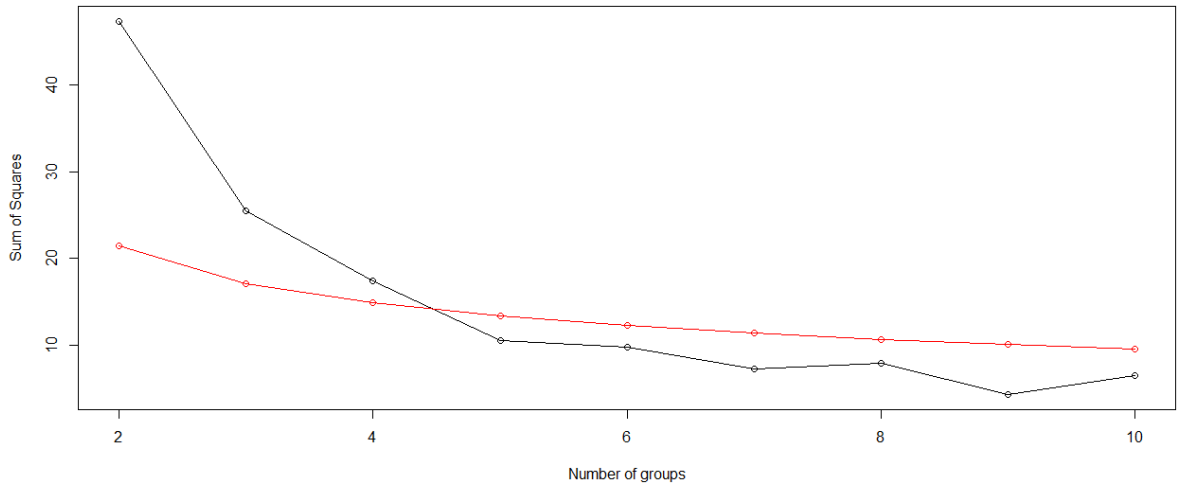

Figure 8.10. Broken stick of the BRYT02 pigment record. Four significant groupings of samples are indicated.

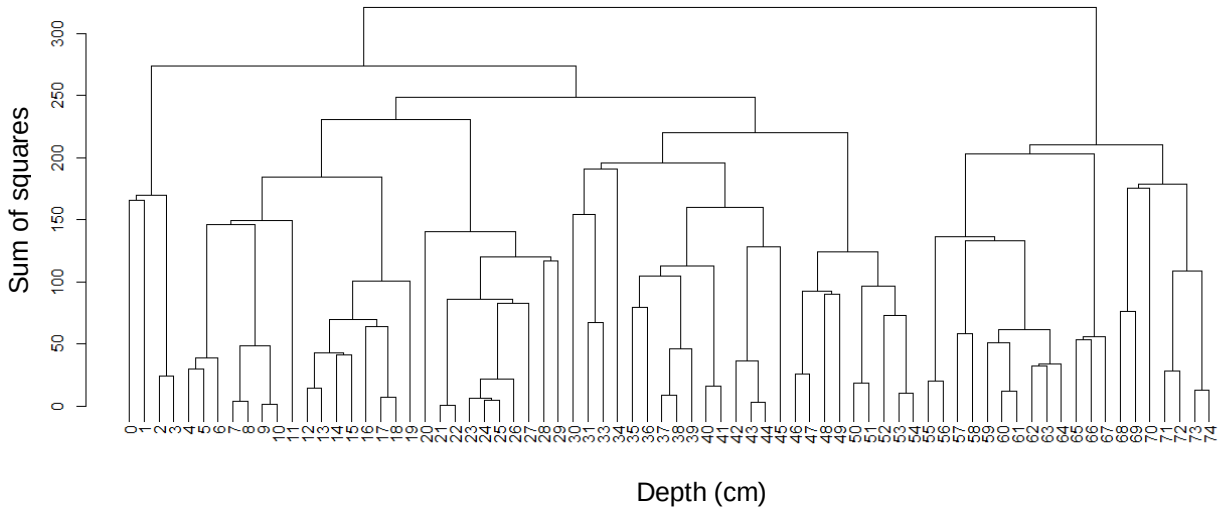

Figure 8.11. Cluster analysis of BRYT02 pigment samples. Sample depths are indicated (cm). Four significant groupings occur, as determined through broken stick analysis.

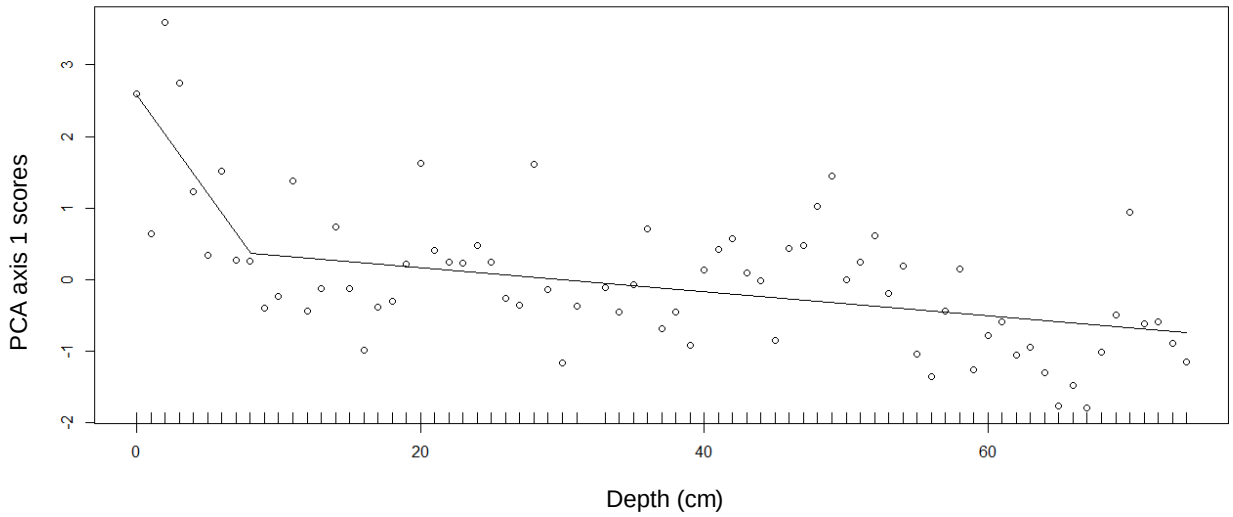

Figure 8.12. Breakpoint analysis of the BRYT02 pigment PCA axis 1 scores. A significant ($p \leq 0.01$) change is identified at ~6 cm.

Pigment Zone 1: Late 19th century to c. 1920 (74 cm to 55 cm)

From the late-19th century and into the early-20th century, the sediment record from BRYT02 indicated low concentrations of all algae (chlorophyll *a*) at the site (Figure 8.8). Further, most other algal group indicators were relatively constant in concentration through Pigment Zone 1, including pigments for cyanobacteria (total and colonial), chlorophytes, and siliceous algae.

Pigment Zone 2: c. 1920 to c. 1965 (54 cm to 30 cm)

Indicators for chlorophytes (Chl *b,* pheophytin *b*, lutein) increase in concentration into Pigment Zone 2, but remain relatively constant through the remainder of the record from BRYT02. Chlorophyll *c* (chromophytes) appeared in the pigment record c. 1945, but remained constant at low concentrations through the rest of this zone. Through Pigment Zones 1 and 2, chlorophyll *a* / Pheo *a* pigment ratios remained low and constant, indicating little fluctuation in preservation during the early record (Figure 8.8).

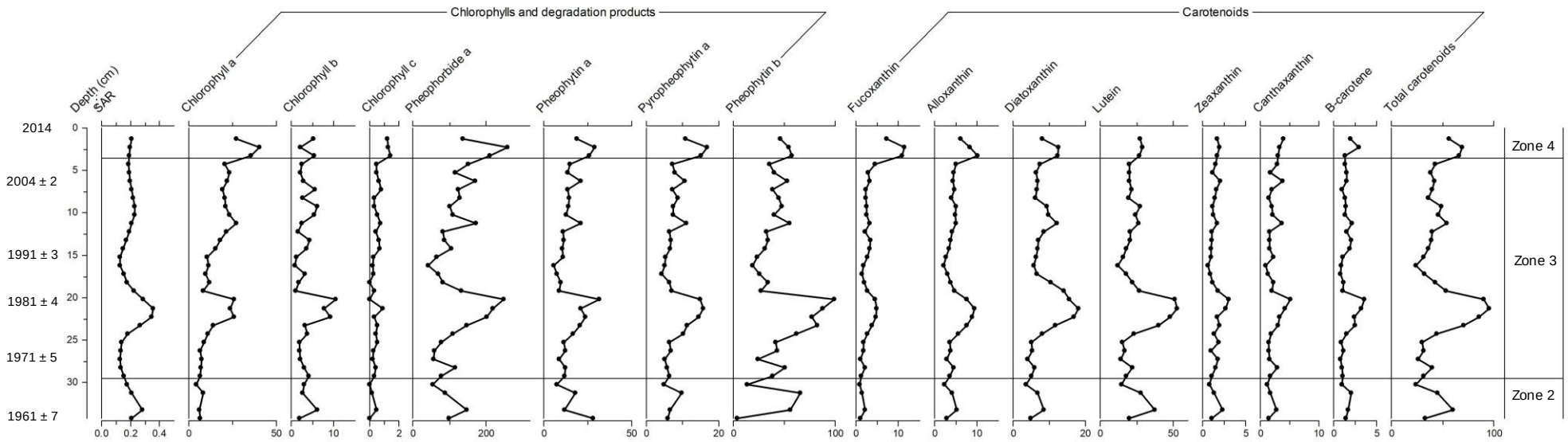

Figure 8.13. Fluxes of chlorophylls, degradation products, and carotenoids for Black Lake from Pigment Zones 2, 3, and 4. Units of fluxes are in nmol cm^{-2} yr^{-1}. Sedimentation accumulation rate (SAR; g cm^{-2} yr^{-1}) and PCA axis 1 scores since c. 1960 are shown.

Pigment Zone 3: c. 1965 to c. 2010 (29 cm to 4 cm)

Chlorophyll *a* concentrations increase through Pigment Zone 3, between c. 1965 and the late-1990s, before leveling off for the remainder of this zone (Figure 8.8). Chlorophyll *c* concentrations increase at the onset of Pigment Zone 3 and remains steady at the slightly elevated concentration through the zone. Pigments of siliceous algae (diatoxanthin and fucoxanthin) increase in concentration at the onset of Pigment Zone 3, and diatoxanthin continues to increase through the first half of Pigment Zone 3, peaking in concentration in the mid-1980s. Alloxanthin concentrations increase at the onset of Pigment Zone 3, with slightly higher concentrations concurrent with the concentrations peaks in diatoxanthin and Chl *a*. The ratio of chlorophyll *a* / Pheo *a* pigments in Pigment Zone 3 indicated potential for increased preservation through the zone relative to older sediments, particularly beginning in the mid-1980s, which is often observed when algal production increases (Leavitt, 1993; Figure 8.8). However, the increase in preservation may also be related to increased sedimentation rates beginning c. 1990 (See Section 4.4.3.3, Figure 4.16), which would result in more rapid burial of sediments and less oxidative degradation of pigments (Leavitt, 1993; Reuss *et al*., 2005). Near the end of Pigment Zone 3 (c. 2005), a significant breakpoint was identified in the pigment PCA axis 1 scores (Figure 8.12), which corresponds to increased concentrations in pigments (Figure 8.8). The shape of the breakpoint regression model, however, resembles that of a post-depositional degradation curve, likely indicating a close relationship between the PCA axis 1 scores, and pigment degradation upon burial in the sediments.

Pigment Zone 4: c. 2010 to 2014 (3 cm to 0 cm)

In the most recent sediment samples, there is an indication of increased concentrations of many algal groups, and overall increases in total algae at BRYT, as chlorophyll *a* and its degradation products, chlorophyll *c*, alloxanthin (cryptophytes), canthaxanthin (colonial cyanobacteria), fucoxanthin (siliceous algae), and β-carotene increase through Pigment Zone 4 (Figure 8.8). Increasing fluxes of most pigments were observed in the record since 2010 (Figure 8.13).

8.3.3 Community-level change: Comparisons of temporal variation between proxies

The first two axes of the co-correspondence analysis (CoCA) very strongly capture the extent of cross-correlation between the two communities (Table 8.3), and the relation between the two communities is highly significant (Table 8.4). Periphytic and small fragilarioid diatoms common to Diatom Zone 1, cluster to the lower-left side of the ordination graph, and tend to co-occur with zeaxanthin and canthaxanthin (cyanobacteria), lutein and pheophorbide *b* (chlorophytes), and β-carotene (total algae), as most of these pigments concentrations do not vary greatly throughout the record from BRYT02 (Figure 8.13). Planktonic diatoms most prevalent in Diatom Zone 2, including *S. parvus, S. hantzschii,* and *L. praetermissa*, tend to co-occur with pheophytin *a* (total algae), Chl *b* (chlorophytes), and alloxanthin (cryptophytes), as these pigments display greatest change concurrent with the planktonic diatoms. Lastly, *F. berolinensis* and *A. ambigua*, diatoms dominating the assemblages since c. 1980, late in Diatom Zone 2, fall to the lower-right of the ordination, with diatoxanthin (diatoms), and to a lesser extent, Chl *a* (total algae) (Figure 8.14).

Proxies	Axis 1	Axis 2	Axis 3	Axis 4
Diatom*Pigment	0.8971	0.7985	0.6413	0.6860

Table 8.3. Cross correlations between axes determined through co-correspondence analysis. High positive values indicate strong correlation between the first CoCA axes.

Proxies	Test on all axes (p-value)	Test on first axis (p-value)
Diatom*Pigment	0.002	0.002

Table 8.4. Tests for significance across axes for each analysis in CoCA. Significance $p \leq 0.01$.

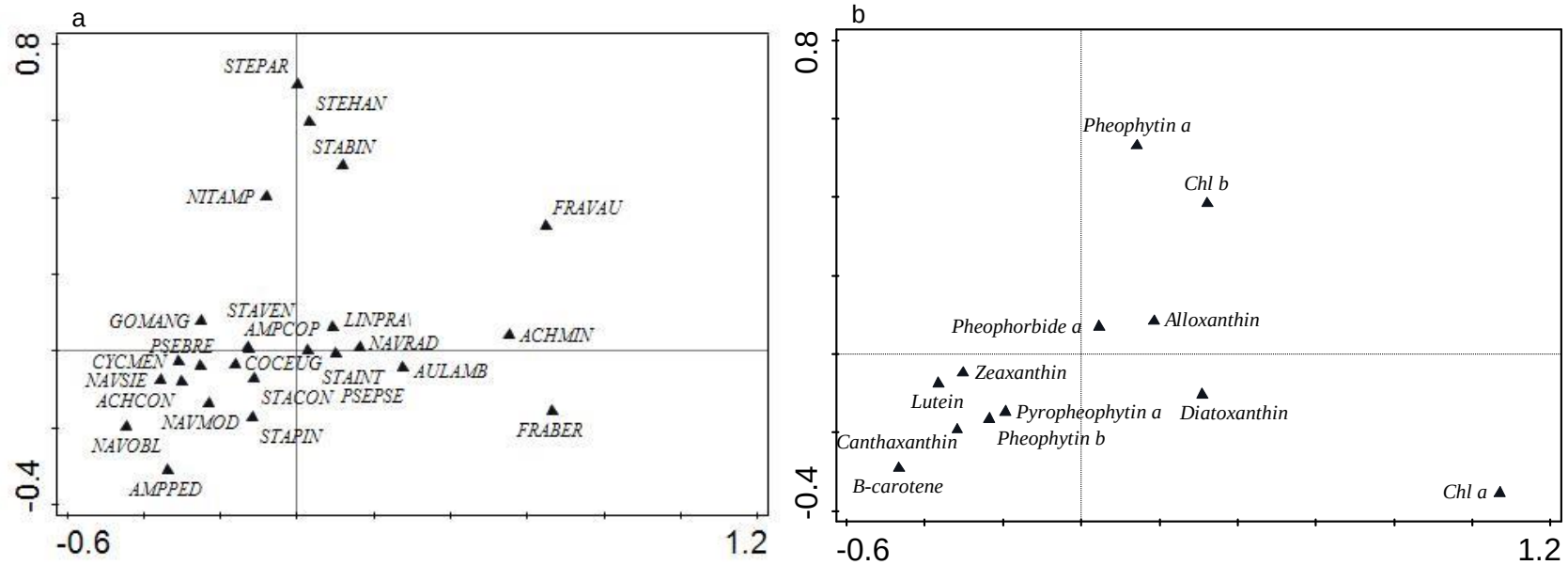

Figure 8.14. Diatom (a) and pigment (b) CoCA community biplots for Black Lake. Species falling in the same area across plots tend to co-occur in the proxy records. Diatom species codes can be found in Appendix 6.

8.4 Discussion

8.4.1 Signals of anthropogenic disturbance since the beginning of the mid-twentieth century

Pigment and diatom records from the late-19th and early-20th centuries are evidence of low productivity, characterized primarily by low algal concentrations and biomass. Diatom communities of the early record were comprised primarily of small fragilarioids and periphytic species, namely naviculoids. Fossil diatom assemblages dominated by the small fragilarioids are common of a wide variety of lake types, including those from small Canadian Arctic lakes and ponds (e.g. Douglas and Smol, 1995), shallow UK lakes (e.g. Bennion *et al.,* 2001; Sayer *et al.,* 2010), and European alpine lakes (e.g. Schmidt *et al.,* 2004). Such species are typically associated with hospitable benthic substrates, including submerged macrophytes, sand, and sediment, favourable light conditions, and have wide tolerances for nutrient conditions (Sayer*,* 2001; Bennion *et al.,* 2012). Fragilarioids are also often pioneer species, able to tolerate less hospitable conditions such as extended ice cover and high UV penetration (Douglas and Smol, 1995; Smol *et al*., 2008). Eftesum (2017) also found macrophyte communities of Black Lake in the late-19th and early-20th centuries were comprised predominantly by *Chara* spp, common in lower productivity, clear-water shallow lakes, with stable and diverse macrophyte communities (Bazarova and Itigilova, 2006; Sayer *et al*., 2010). It is likely that the early environment at Black Lake contained favourable light conditions, lower nutrient concentrations, and was dominated by benthic primary production.

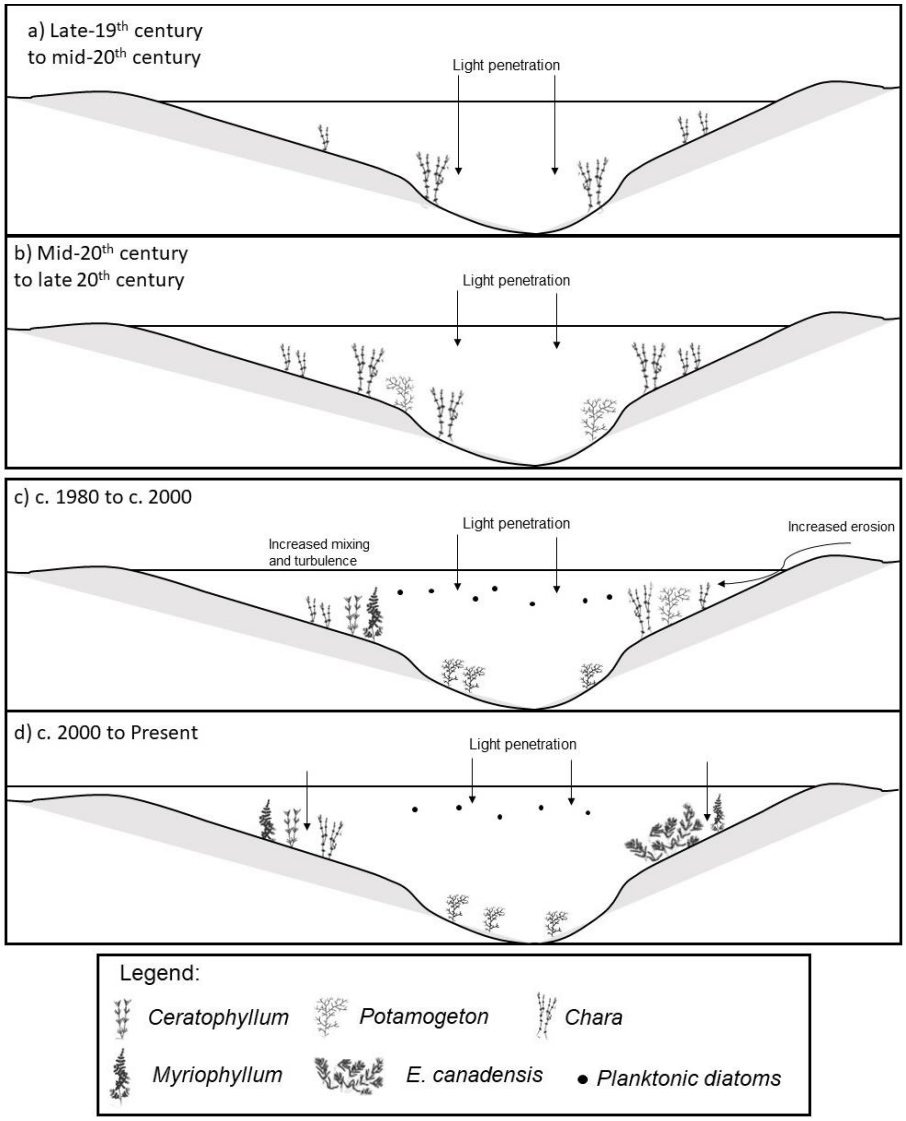

Figure 8.15. Conceptual diagram of water level, connectivity, and macrophyte community change at Black Lake since the late-19th century. a) High light penetration with mostly benthic communities, and macrophyte community comprised primarily of *Chara*. b) Decreased light penetration, increased diversity of submerged macrophytes, *Chara-Potamogeton*, c) Increased mixing and turbulence with increased light penetration, increased diversity of macrophyte community *Myriophyllum-Ceratophyllum-Chara-Potamogeton* dominated, d) Increased connectivity and water levels, and increased benthic producitivty and light penetration, pelagic macrophyte primarily *Potamogeton*, littoral macrophytes *Myriophyllum-Ceratophylum-Chara*.

Species	Guild	Autecology	Authority	References
Staurosirella pinnata	Benthic	Prefers shallow, littoral habitats. Mesoeutrophic to eutrophic or oligotrophic to eutrophic. Requires highly oxygenated waters.	(Ehrenberg) Williams and Round 1987	Van Dam *et al*., 1994
Staurosira construens v. venter	Benthic	Prefers shallow, littoral habitats. Mesoeutrophic to eutrophic or oligotrophic to eutrophic. Requires highly oxygenated waters.	(Ehrenberg) Hamilton 1992	Patrick and Reimer, 1966; Bradbury, 1971; Van Dam *et al*., 1994; Metcalfe *et al*., 1997; Haberzettl *et al*., 2005
Staurosira construens v. binodis	Benthic	Prefers shallow, littoral habitats. Mesoeutrophic to eutrophic or oligotrophic to eutrophic. Littoral assemblage. Requires highly oxygenated waters, pollution intolerant.	(Ehrenberg) Hamilton 1992	Patrick and Reimer, 1966; Bradbury, 1971; Van Dam *et al*., 1994; Metcalfe *et al*., 1997; Haberzettl *et al*., 2005
Pseudostaurosira pseudoconstruens	Benthic	Requires highly oxygenated waters. Meso-eutrophic.	(Marciniak) Williams and Round 1987	Van Dam *et al*., 1994
Pseudostaurosira brevistriata	Benthic	Mainly occurring in alkaline waters, requires nearly continuous 100% oxygen saturation in water, very low tolerance for pollution, wide range of trophic state tolerances.	(Grunow) Williams and Round 1987	Van Dam *et al*., 1994
Fragilaria berolinensis	Planktonic	Mainly occurring in alkaline waters, hypereutrophic.	(Lemmermann) Lange-Bertalot 1993	Van Dam and Mertens, 1993; Van Dam *et al*., 1994
Aulacoseira ambigua	Planktonic	Meso-eutrophic with high TP optima, although lower than other eutrophic centrics. High light requirements. Indicator of high turbulence in the water column. Late summer to autumn blooming diatom. Indicator of pelagic habitat. Preference for lakes with high silica concentrations, and may be an indicator of increase soil erosion or anthropogenic eutrophication.	(Grunow) Simonsen 1979	Bradbury, 1977; Kilham *et al*., 1986; Bradbury and Dieterich-Rurup, 1993; Brugam *et al*., 1998; Trifonova and Genkal, 2001; Bradbury *et al*., 2002, Baier *et al*., 2004

Cyclostephanos dubius	Planktonic	Occurs exclusively at pH >7. High abundance in eutrophic lakes with high conductivity; Found in shallow channels connecting wetlands.	(Fricke) Round in Theriot et al. 1987	Hickel and Håkansson, 1987; Van Dam *et al*., 1994.
Lindavia praetermissa	Planktonic	Oligotrophic/mesotrophic to eutrophic, has been found in the plankton and the littoral zone, alkaline lakes and ponds.	(Lund) T. Nakov et al. 2015	Tanaka, 2007; Houk *et al*., 2010
Stephanodiscus parvus	Planktonic	Occurs exclusively in alkaline pH. Meso-eutrophic, high total phosphorus and moderate chloride concentration.	Stoermer & Håkansson 1984	Stoermer, 1978; Stoermer *et al*. 1978; Stoermer and Håkansson, 1984; Van Dam *et al*., 1994; Reavie and Kireta, 2015
Stephanodiscus hantzschii	Planktonic	Occurring exclusively at pH >7. Can occur at low oxygen saturation (>30%). Strong indicator of high phosphorus, Dominant in eutrophic lakes.	Grunow in Cleve & Grunow 1880	Stoermer and Yang, 1969; Anderson, 1990; Hall and Smol, 1992; Van Dam *et al*., 1994.
Achnanthidium minutissimum	Benthic	Pioneer species, phosphorous specialist. Requires nearly continuous 100% oxygen saturation in water, pH circumneutral. Opportunistic species with wide tolerance of trophic state.	(Kütz.) Czarn. 1994	Cholnoky, 1968; Kuhn *et al*., 1981; Van Dam *et al.,* 1994; Reavie and Smol, 1998; Brown *et al*., 2008; Watchorn *et al*., 2008
Fragilaria capucina v. vaucheriae	Benthic	Mainly occurring in alkaline waters, eutrophic, can occur on moist/wet places.	(Kützing) Petersen 1938	Van Dam *et al*., 1994
Navicula oblonga	Benthic	Eutrophic, alkaline fresh waters with elevated concentrations of dissolved solids and nutrients.	(Kützing) Kützing 1844	Patrick and Reimer, 1966; Van Dam *et al*., 1994
Cocconeis placentula v. euglypta	Epiphytic	Mainly occurring in alkaline waters, eutrophic.	Ehrenberg 1838	Van Dam *et al*., 1994

Table 8.5. Summary of main ecological characteristics of dominant diatom species from BRYT02 sediment core.

A shift in both pigment concentration and diatom assemblage records occurred in the mid-20th century (c. 1960) at Black Lake (Figures 8.3 and 8.8). Total algal pigments (Chl *a* and pheophytin *a*) display the greatest change in the pigment record c. 1965, and likely reflect

increases in siliceous algae and cryptophytes beginning c. 1965. Chl *a* continued to increase into the 1970s, along with increases in diatom concentrations. The historically dominant small fragilarioids and periphytic diatoms underwent a decline in relative abundances c. 1960, with increases in relative abundances of several planktonic species, including *Aulacoseira ambigua, Cyclostephanos dubius, Lindavia praetermissa, Stephanodiscus parvus* and *S. hantzschii*, indicating an increase in pelagic productivity (Vadeboncoeur *et al.,* 2003). Declines in periphytic species and concurrent increases in planktonic species may be attributed to increases in nutrient-associated levels of turbidity, declines in light penetration, declines in submerged macrophyte abundances, and loss of associated habitats (Bennion *et al*., 2001; Sayer *et al.,* 2010). The increase in a larger fragilarioid species, *Fragilaria capucina* v. *vaucharіae*, which is typical of anthropogenically eutrophied systems, further indicates likely increases in nutrient levels at this time (Kravtsova *et al*., 2014). Increases in the proportion of planktonic species, and periphytic species typically found in higher nutrient environments, and concurrent with declines in small fragilarioid species and benthic species and increasing pigment concentrations, indicating increasing eutrophication, likely as a result of increasing nutrient fluxes (Battarbee *et al*., 2001; Sayer *et al.,* 2010) to Black Lake in the mid-20th century.

The initial enrichment observed at Black Lake in the mid-20th century was likely a result of the anthropogenic expansions in the Gusinoye region in the decades following World War II (WWII) (Pisarsky *et al.,* 2005). Industrial and population growth began in the 1940s, including mining applications, quickly followed by military installations, the constructions of the Trans-Mongolian Railroad and the Gusinoozersk State Regional Power Plant (SRPP), by the 1960s (Pisarsky *et al*., 2005). Agricultural expansion in the Selenga River basin occurred intensively post-WWII, and between the mid-1950s and mid-1970s, the total arable lands in southeast Siberia increased by almost 60% (Bazhenova and Kobylkin, 2013). Intensive increases in sheep population continued until c. 1990, which contributed to the increase in nutrient flux to soils, and increased sediment erosion within the Selenga River basin (Bazhenova and Kobylkin, 2013). Enrichment from increased populations and intensification of agricultural practices in the Selenga River basin post-WWII likely drove the observed changes in diatom assemblage and pigment concentration in the mid-20th century.

The diatom assemblage shifts observed in the 1980s were primarily a shift towards pelagic-dominated primary production (Figure 8.3). The transient increase in *Aulacoseira ambigua* in the 1980s may indicate a temporary disturbance to Black Lake during this decade. While *A. ambigua* has a high total phosphorus (TP) optima, with preference for meso- eutrophic habitats (Kauppila *et al*., 2003), and is considered to be an indicator of anthropogenically eutrophied systems (Kling, 1998), *A. ambigua* has a lower TP optima than *Stephanodiscus* spp. and *Cyclostephanos dubius* (See Table 8.5), and the progression from the *Stephanidiscus-Cyclostephanos* community to *Aulacoseira ambigua* dominated assemblage may indicate a temporary decline in nutrient concentrations (Bennion *et al*., 2012; Heathcote *et al.,* 2015). *Aulacoseira ambigua* is more heavily silicified than *Stephanodiscus*, with greater silica and mixing requirements (Kilham *et al.,* 1996), and it is possible that the increase in *A. ambigua* in the 1980s was due to increased turbulence and mixing, particularly in the late-summer and autumn (Bradbury, 1977), related to the increase in flow and runoff in the Selenga River basin in the 1980s due to increased summer precipitation between 1983 and 1995 (Berezhnykh *et al*., 2012; Kasimov *et al*., 2016). The increased precipitation may have resulted in increased transport of clastic minerals (including silica) to the lake, and *A. ambigua* has been associated with increases in soil erosion to shallow lakes (Bradbury *et al*., 2002), The changes in precipitation and mineral transport to the lake may have altered the mixing regime at Black Lake, initially favouring the proliferation of *A. ambigua*. However, the increase in *Fragilaria berolinensis*, a planktonic diatom with high TP optima, and decline in *A. ambigua* beginning c.1990, indicates continued increasing nutrient concentrations at Black Lake, as the planktonic fragilarioid is often found in eutrophic to hyper-eutrophic conditions (van Dam and Mertens, 1993; Round and Maidana, 2001; Solis *et al.,* 2009). The increase in relative abundance of *F. berolinensis* occurs with increases in pigment concentrations for total algae (Chl *a* and pheophytin *a*) c. 1990, giving further evidence for increasing nutrient status and algal production at Black Lake towards the end of the 20th century (Leavitt, 1993; McGowan *et al.,* 2012). Moreover, Eftesum (2017) recorded a shift in submerged macrophyte community from *Chara*-dominated to *Potamogeton*-dominated assemblage concurrent with the algal shifts, further suggesting increasing eutrophication at Black Lake (Sayer *et al*., 2010).

The overall increasing algal production and shift from primarily benthic to pelagic primary production in the 1980s at Black Lake may be considered a regime shift, as a significant change was observed through breakpoint analysis (Figure 8.7). The impact of environmental stressors, if large enough to result in changes in ecological structure and/or function of a lake i.e. from benthic to planktonic-dominated primary production, may be classified as a regime shift (Scheffer *et al*., 2001; Andersen *et al*., 2008). The shift from benthic to planktonic primary production is one of the most common forms of regime shift in shallow, freshwater lakes (Scheffer, 1997; Jackson, 2003; Folke *et al*., 2004), and is most often associated with increasing nutrient-loadings (O'Dywer *et al*., 2013). Although, unfortunately, this shift is only measured at the primary producer level, to classify this as a regime shift at the whole-lake level, it would be beneficial to assess if similar significant changes have occurred at higher trophic levels. A likely reason as to why a similar breakpoint is not observed in the pigment record is that the shift in diatoms did not occur as a result of increasing concentration or biomass, but rather a shift in ecological structure. Pigment records record both benthic and primary production, and so a shift in ecosystem function (i.e. productivity) would be recorded, but not necessarily a shift in ecosystem structure (i.e. from benthic to pelagic primary production). Rather than a sudden increase in production, a general, sustained increase in trophic status (seen through Chl *a* concentrations) has occurred through the years at Black Lake (Figure 8.8).

Increases in species richness and diatom assemblage N2 occurred between c.1955 and 1980, in the early stages of nutrient enrichment at Black Lake. A similar relationship was observed between ecosystem productivity and species richness by Korhonen *et al.* (2011), with phytoplankton biomass largely and positively related to resource availability. However, decreasing diatom assemblage N2 beginning in the early-1980s may be indicative of increasing eutrophication at this time, and is due to the increasing single species dominance in the diatom assemblages, first *A. ambigua* in the 1980s, followed by *F. berolinensis* from c.1990 until 2000 (Bennion *et al.,* 1996; Bennion *et al.,* 2000; Randsalu-Wendrop *et al.,* 2014). The low species richness and diatom assemblage N2 coincided with increasing diatom concentrations and Chl *a* concentrations in the sedimentary pigment record, indicating a negative relationship between diversity and algal biomass since c.1980. Interlandi and Kilham (2001) found a significant negative relationship between species diversity and system productivity among lakes in

Yellowstone National Park, U.S.A, with low phytoplankton biomass occurring with high species diversity. This relationship was also observed on both spatial and temporal scales, across Selenga River basin sites, described in Chapter 3, 6, and 7. Beginning c. 1950, diatom species richness and diatom concentrations have had an apparent negative relationship, with the increase in concentration observed post-1970 occurring concurrently with declines in species richness and diatom assemblage N2 (Figure 8.3a). Traditionally, biomass is driven by nutrient availability.

8.4.2 Indicators of recent recovery at BRYT

Declines in the relative abundance of some hyper-eutrophic and eutrophic diatom species began in c. 2000, including *F. berolinensis* and many of the centric planktonic species. Declines in planktonic, eutrophic indicators occurred concurrently with increasing relative abundances of pre-enrichment species, including small fragilarioids, *S. construens* v. *venter* and *Pseudostaurosira pseudoconstruens*, and indicate possible ecological recovery of Black Lake from nutrient enrichment. Recorded decreases in surface water flows and surface water levels in the Selenga River basin began in 1995, as a result of a weakening of atmospheric circulation and resulting declines in summer precipitation (Berezhnykh *et al*., 2012; Kasimov et al., 2016). An increase in abandoned agricultural fields and reduction in arable lands also occurred beginning c.1990, while increased intensification of reforestation efforts began in the 1990s (Bazhenova and Kobylkin, 2013). The co-occurrence of these events would have led to declines in nutrient fluxes to surface waters in the Selenga River basin, as well as declines in surface flow, erosion and sediment flux. The decline in relative abundance of nutrient-rich indicators, planktonic centrics and planktonic *F. berolinensis*, which began c. 2000, are likely a result of these climatic and economic changes in southeast Siberia.

The small *Staurosira-Staurosirella- Pseudostaurosira* fragilarioids have previously been found to be more sensitive to changes in habitat availability than nutrients, as they appear to have wide tolerances for nutrient concentrations (Bennion *et al*., 2001; Sayer, 2001). Decreased turbidity from runoff, soil erosion and sediment flux, increased light penetration and favourable light conditions, would have led to increased hospitable benthic habitats at Black Lake, and a subsequent rise in relative abundances of the small fragilarioids (Sayer, 2001). An extensive shallow littoral zone is currently present on the north side of the lake, with clear water conditions

and abundant submerged macrophytes. However, a relatively deeper pelagic zone through the centre and to the south end of the lake contains little evidence of submerged macrophyte presence. The recent increases in habitat availability and variety of habitat type present at Black Lake since c. 2000 AD would have likely led to the increases in species richness observed recently, and may be the reason for increased relative abundance of the small fragilarioids.

While diatom assemblages since the onset of the 21st century indicate some recovery, it does not appear to be as significant a shift as those observed c. 1960 or c. 1990, as neither broken stick nor breakpoint analysis indicates a significant change in diatom assemblages within the 21st century (Figures 8.5 and 8.6). Moreover, pigment records do not convey signs of ecological recovery, as was seen in the diatom assemblages. Many pigment concentrations, including Chl *a* and degradation products, indicate continued increases in total algal biomass at Black Lake until the present day (Figure 8.8). However, some pigments, such as Chl *a*, fucoxanthin, and Chl *c*, are labile, and prone to post-depositional degradation (Leavitt, 1993; McGowan *et al.,* 2005). Further, the only significant breakpoint identified in the pigment record was at 6 cm depth, while the rest of the record remained relatively unchanged (Figure 8.12). It is possible, therefore, that the sub-surface increase in pigment concentrations, and significant assemblage shift, is due to post-depositional degradation of some of the pigments. Moreover, there is no similar signal for increasing productivity in the diatom record, further indicating that the increase in sub-surface pigment concentrations are due to post-depositional degradation. The lack of recovery signal from the pigment record, along with a lack of statistically significant change in diatom assemblages in recent years, leads to the likely conclusion that while anthropogenic events may be in place to incite some degree of ecological recovery, it is less of an ecological response than both the mid-20th century onset of eutrophication, and the shift to hyper-eutrophic diatom community c. 1990.

While there may be a real decline in external nutrient loading to BRYT in recent years, it is possible that the effects of this could be confounded by climate change. Climate change-related changes in regional temperature and precipitation patterns may elicit algal responses that would mimic those of nutrient increases, including the continued increase in total algal abundance (Chl *a* and pheophytin *a*), and prevent total ecological recovery to pre-enrichment communities (Moss *et al.,* 2011; Battarbee *et al.,* 2012). Warmer and shorter winters may lead to delayed ice-

formation on shallow lakes of the Selenga River basin as well, translating to longer ice-free seasons and increased length of the growing season, which would lead to increased hospitable littoral habitat, and has been recorded as a primary response to climate change in remote, northern shallow lakes (Smol *et al.,* 2005). Air temperatures in the Selenga River basin warmed nearly twice as fast as the global average (a total increase of 1.6°C) for the period 1938 to 2009, with most of the warming occurring during the winter season (Törnqvist *et al*., 2014). Further, a lengthened ice-free season for Lake Baikal has been recorded over the past 137 years, primarily related to later ice onset (Magnuson *et al.,* 2000; Todd and Mackay, 2003). Therefore, the increased relative abundance of periphytic species in BRYT in the 21st century may be a response to indirect influence of temperature-related changes in the shallow lake. Therefore, while initial changes in the ecology of Black Lake was due to enrichment commencing in the mid-20th century, it is likely that any potential for ecological recovery from declines in nutrient inputs may be outweighed by responses to regional changes in climate in the 21st century.

8.5 Conclusion

Ecological records of algal groups from Black Lake indicate a pre-enrichment period of the lake prior to the mid-20th century, composed primarily of benthic primary production and low productivity. Increased population, transportation developments, and industrial expansion in the Gusinoye region of the Selenga River basin beginning in the 1940s and 1950s likely contribute to the enrichment of the study site beginning in the mid-20th century. Enrichment resulted in increases in total algal abundance (Chl *a*), and post-enrichment diatom communities were comprised primarily of planktonic centric and fragilarioid species, indicating a shift from benthic to planktonic primary production. Potential sensitivities of diatom communities to changes in atmospheric circulation patterns and summer precipitation trends caused a shift in dominant species in the 1980s, and resulted in declines in species richness and diversity, with concurrent increases in algal abundance. Diatom community changes in the 1980s may be indicative of an ecological regime shift at this time, due to increases in nutrient levels at Black Lake. However, it would be beneficial to measure temporal changes in other trophic levels (e.g. macrophyte and zooplankton communities) to assess if a whole-ecosystem regime shift occurred at this time, as a similarly significant change is not observed in the pigment record in the 1980s. While relative

abundances of eutrophic to hypereutrophic diatom species showed dominance until the 21st century, recent increases in small *Staurosira-Pseudostaurosira* fragilarioids may indicate improved light conditions and an increase in benthic habitat availability. Continued increases in total algal abundance (Chl *a*) to the present, combined with shifts in diatom relative abundances, may indicate that nutrient enrichment may be declining, but the may be being masked by algal community responses to climate change in the Selenga River basin. This demonstrates the sensitivity of shallow lake algal communities to multi-stressor environments, with ecological recovery to decades-long nutrient enrichment confounded by recent direct and indirect effects of a warming climate in southeast Siberia.

8.6 References

Afanas'yeva L.V., Kashin V.K., Mikhailova T.V., Berezhnaya N.S. Influence of aerotechnogenic pollution on the accumulation of heavy metals in Pinus sylvestris fir-needle. Chemistry for Sustainable Development, vol. 15 (1), 2007. P. 25-31. (In Russia)

Anderson N.J. (1990) The biostratigraphy and taxonomy of small Stephanodiscus and Cyclostephanos species (Bacillariophyceae) in a eutrophic lake, and their ecological implications. *British Phycological Journal* **25**, 217-235.

Baier J., Lucke A., Negendank J.F.W., Schleser G-H., & Zolitschka B. (2004) Diatom and geochemical evidence of mid- to late-Holocene climatic changes at Lake Holzmaar, West-Eifel (Germany). *Quaternary International* **113,** 81-96.

Battarbee R.W. Jones V., Flower R., Cameron N., Bennion H., Carvalho L., & Juggins S. (2001) Diatoms. In Terrestrial, algal and siliceous indicators. Eds. J. Smol, H.J.B. Birks, and M. Last, Kluwer Academic Publishers,The Netherlands. pp. 155–202.

Battarbee R.W., Anderson N.J., Bennion H., & Simspon G.L. (2012) Combining limnological and paleolimnological data to disentangle the effects of nutrient pollution and climate change on lake ecosystems: problems and potential. *Freshwater Biology* **57**, 2091-2106.

Bazarova B., & Itigilova M. (2006) Long-term production dynamics of aquatic vegetation in the Arakhlei Lake (Eastern Transbaikalia). *Biology Bulletin of the Russian Academy of Sciences* **33**, 68–75.

Bazhenova O.I., & Kobylkin D.V. (2013) The dynamics of soil degradation processes within the Selenga basin at the agricultural period. *Geography and Natural Resources* **34,** 221-227.

Bennion H., Juggins S., & Anderson N.J. (1996) Predicting epilimnetic phosphorus concentrations using an improved diatom-based transfer function and its application to Lake Eutrophication management. *Environmental Science and Technology* **30**, 2004–2007.

Bennion H., Monteith D., Appleby P.G. (2000) Temporal and geographical variation in lake trophic status in the English Lake District: evidence from (sub)fossil diatoms and aquatic macrophytes. *Freshwater Biology* **45,** 394-412.

Bennion H., Appleby P.G., & Phillips G.L. (2001) Reconstructing nutrient histories in the Norfolk Broads, UK: Implications for the role of diatom-total phosphorus transfer functions in shallow lake management. *Journal of Paleolimnology* **26,** 181-204.

Bennion H., Carvalho L., Sayer C.D., Simpson G.L., & Wischnewski J. (2012) Identifying from recent sediment records the effects of nutrients and climate on diatom dynamics of Loch Leven. *Freshwater Biology* **57,** 2015-2029.

Berezhnykh T.V., Marchenko O.Yu., Abasov N.V., Mordvinov V.I. Changes in the Summertime Atmospheric Circulation Over East Asia and Formation of Long-Lasting Low-Water Periods Within the Selenga River Basin. Geography and Natural Resources, 2012, vol. 33(3). P. 223-229.

Bradbury J.P. (1971) Paleolimnology of lake Texoco Mexico: Evidence from diatoms. *Limnology and Oceanography* **16,** 180-200.

Bradbury J.P., & Dieterich-Rurup K.V. (1993) Holocene diatom paleolimnology of Elk Lake, Minnesota. In: Elk Lake, Minnesota: Evidence for rapid climate change in the North-

Central United States. Eds. J.P. Bradbury & W.E. Dean. Geological Society of America, **276**, DOI: https://dx.doi.org/10.1130/SPE276-p215.

Bradbury P., Cumming B., & Laird K. (2002) A 1500-year record of climatic and environmental change in Elk Lake, Minnesota III: measures of past primary productivity. *Journal of Paleolimnology* **27,** 321-340.

Brown L., May J. & Hunsaker C. (2008) Species composition and habitat associations of benthic algal assemblages in headwater streams of the Sierra Nevada, California. *Western North American Naturalist* **68**, 194-209.

Brugam R.B., McKeever K., & Kolesa L. (1998) A diatom-inferred water depth reconstruction for an Upper Peninsula, Michigan, lake. *Journal of Palaeolimnology* **20,** 267-276.

Cholonky B.J. (1968) Die Okologie der Diatomeen in Binnengewasser. J. Cramer, Lehre, 699 pp.

Douglas M.S.V., & Smol J.P. (1995) Periphytic diatom assemblages from high arctic ponds. *Journal of Phycology* **31,** 60-69.

Eftesum E. (2017) Reconstructing shallow lake ecosystem dynamics in southeastern Siberia using macrofossil analysis. Unpublished MSc thesis, Department of Geography, University College London.

Haberzettl T., Fey M., Lucke A., Maidana N., Mayr C., Ohlendorf C., Schabitz F., Schelser G.H., Wille M. and Zolitschka B. (2005) Climatically driven lake level changes during the last two millennia as reflected in sediments of Laguna Potrok Aike, southern Patagonia (Santa Cruz, Argentina). *Journal of Paleolimnology 33*, 283-302.

Hall R.I., & Smol J. (1992) A weighted—averaging regression and calibration model for inferring total phosphorus concentration from diatoms in British Columbia (Canada) lakes. *Freshwater Biology* **27**, 417-434.

Heathcote A.J., Ramstack Hobbs J.M., Anderson N.J., Frings P., Engstrom D.R., & Downing J.A. (2015) Diatom floristic change and paleoproduction as evidence of recent eutrophication in shallow lakes of the midwestern USA. *Journal of Paleolimnology* **53,** 17-34.

Hickel B., & Håkansson H. (1987) Dimorphism in *Cyclostephanoc dusius* (Bacillariophyta) and the morphology of initial valves. *Diatom Research* **2,** 35-46.

Houk V., Klee R., & Tanaka H. (2010) Atlas of freshwater centric diatoms with a brief key and descriptions, Part III. Stephanodiscaceae A. Cyclotella, Tertiarius, Discostella. Fottea 10 (Supplement): 1-498.

Interlandi S.J., & Kilham S.S. (2001) Limiting resources and the regulation of diversity in phytoplankton communities. *Ecology* **82,** 1270-1282.

Juggins S. 2014. C2 data analysis, Version 1.7.6. University of Newcastle, United Kingdom.

Kasimov N.S., Lychagin M.Yu., Chalov S.R., Shinkareva G.L., Pashkina M.P., Romanchenko A.O., Promakhova E.V. Catchment based analysis of matter flows in the Selenga-Baikal system. Moscow university bulletin. Series 5. Geography. 2016. № 3. P. 67-81.

Kilham P., Kilham S.S., & Hecky R.E. (1986) Hypothesized resource relationships among African planktonic diatoms. *Limnology and Oceanography* **31**, 1169-1181.

Kilham S.S., Theriot E.C., & Fritz S.C. (1996) Linking planktonic diatoms and climate change in the large lakesof the Yellowstone ecosystem using resource theory. *Limnology and Oceanography* **41,** 1052-1062.

Korhonen J.J., Wang J., & Soininen J. (2011) Productivity-diversity relationships in lake plankton communities. *PLoS ONE* **6,** e22041. doi: 10.1371/journal.pone.0022041.

Kravtsova L.S., Izhboldina L.A., Khanaev I.V., Pomazkina G.V., Rodionova E.V., Domysheva V.M., Sakirko M.V., Tomberg I.V., Kostornova T.Y., Kravchenko O.S., & Kupchinsky A.B. (2014) Nearshore benthic blooms of filamentous green algae in Lake Baikal. *Journal of Great Lakes Research* **40,** 441-448.

Kuhn D.L., Plafkin J.L., Cairns J. & Lowe R.L. (1981) Quantitative characterisation of aquatic environments using diatom life-form strategies. *Transactions of the American Microscopial Society* **100**, 165-182.

Leavitt P.R. (1993) A review of factors that regulate carotenoid, and chlorophyll deposition, and fossil pigment abundance. *Journal of Paleolimnology* **9**, 109–127.

Magnuson J.J., Robertson D.M., Benson B.J., Wynne R.H., Livingstone D.M., Arai T., Assel R.A., Berry R.G., Card V., Kuusisto E., Granin N.G., Prowse T.D., Stewart K.M., & Vuglinski V.S. (2000) Historical trends in lake and river ice cover in the northern hemisphere. *Science* **289**, 1743–1746.

McGowan S., Leavitt P.R., Hall R.I., Anderson N.J., Jeppesen E., & Odgaard B.V. (2005) Controls on algal abundance and community composition during ecosystem state change. *Ecology* **86**, 2200-2211.

McGowan S., Barker P., Haworth E.Y., Leavitt P.R., Maberly S.C., & Pates J. (2012) Humans and climate as drivers of algal community change in Windermere since 1850. *Freshwater Biology* **57**, 260-277.

Metcalfe S.E., Bimpson A., Courtice A.J., O'Hara S.L. and Taylor D.M. (1997) Climate change at the monsoon/Westerly boundary in northern Mexico. *Journal of Paleolimnology* **17**, 155-171.

Moss B., Kosten S., Meerhoff M., Bttarbee R.W., Jeppesen E., Mazzeo N., Havens K., Lacerot G., Liu Z., De Meester L., Paerl H., & Scheffer M. (2011) Allied attack: climate change and eutrophication. *Inland Waters* **1,** 101-105.

Patrick R., & Reimer C.W. (1966) The diatoms of the United States. The Academy of Natural Sciences, Philadelphia.

Pisarsky B.I., Hardina A.M., & Naganawa H. (2005) Ecosystem evolution of Lake Gusinoe (Transbaikal Region, Russia). *Limnology*, **6**, 173-182.

R. v.3.2.4 R. 2016. The R Foundation, R Development Team. Vienna.

Randsalu-Wendrop L., Conley D.J., Carstensen J., Hansson L-A., Bronmark C., Fritz S.C., Choudhary P., Routh J., & Hammarlund D. (2014) Combining limnology and palaeolimnology to investigate recent regime shifts in a shallow, eutrophic lake. *Journal of Paleolimnology* **51**, 437-448.

Reavie E.D. & Smol J.P. (1998) Epilithic diatoms of the St. Lawrence river and their relationships to water quality. *Canadian Journal of Botany* **76**, 251-257.

Reavie E.D., & Kireta A.R. (2015) Centric, Araphid and Eunotioid Diatoms of the Coastal Laurentian Great Lakes. *Bibliotheca Diatomologica* **62,** 1-184.

Reuss N., Conley D.J., & Bianchi T.S. (2005) Preservation conditions and the use of sediment pigments as a tool for recent ecological reconstructions in four Northern Europe estuaries. *Marine Chemistry* **95,** 283-302.

Round F.E. (1990) Diatom communities, their response to changes in acidity. *Philosophical Transactions of the Royal Society: Series B, Biological Sciences* **327,** 243-249.

Round F.E., & Maidana N.I. (2001) Two problematic freshwater araphid taxa re-classified in new genera.

Sayer C.D. (2001) Problems with the application of diatom-total phosphorus transfer functions: examples from a shallow English lake. *Freshwater Biology* **46,** 743-757.

Sayer C.D., Burgess A., Kari K., Davidson T.A., Peglar S., Yang H., & Rose N. (2010) Long-term dynamics of submerged macrophytes and algae in a small and shallow, eutrophic lake: implications for the stability of macrophyte-dominance. *Freshwater Biology* **55,** 565-583.

Schmidt R., Kamenik C., Lange-Bertalot H., & Klee R. (2004) *Fragilaria* and *Staurosira* (Bacillariophyceae) from sediment surfaces of 40 lakes in the Austrian Alps in relation to environmental variables, and their potential for paleoclimatology. *Journal of Limnology* **63,** 171-189.

Smol, J. P., Wolfe A.P., Birks H.J.B., Douglas M.S.V., Jones V.J., Korhola A., Pienitz R., Rühland K., Sorvari S., Antoniades D., Brooks S.J., Fallu M-A., Hughes M., Keatley B.E., Laing T.E., Michelutti N., Nazarova L., Nyman M., Paterson A.M., Perren B., Quinlan R., Rautio M., Saulnier-Talbot E., Siitonen S., Solovieva N, & Weckström J. (2005) Climate-driven regime shifts in the biological communities of arctic lakes. *Proceedings of the National Academy of Sciences* **102**, 4397–4402.

Solis M., Poniewozik M., & Mencfel R. (2009) Bloom-forming cyanobacteria and other algae in selected anthropogenic reservoirs of the Leczna-Wlodawa Lakeland. *Oceanological and Hydrobiological studies* **38,** 71-78.

Stoermer E.F. (1978). Phytoplankton as indicators of water quality in the Laurentian Great Lakes. *Transactions of the American Microscopical Society* **97,** 2-16.

Stoermer E.F., & Yang J.J. (1969) Plankton diatom assemblages in Lake Michigan. Univ. Michigan, Great Lakes Res. Div. Spec. Rep. No. 47, 168 pp.

Stoermer E.F., & Håkansson H. (1984) Stephanodiscus parvus: Validation of an enigmatic and widely misconstrued taxon. *Nova Hedwigia* **39,** 497-511.

Stoermer E.F., Ladewski B.G., & Schelske C.L. (1978) Population response of Lake Michigan phytoplankton to nitrogen and phosphorus enrichment. *Hydrobiolgia* **57,** 249-265.

Tanaka H. (2007) Taxonomic studies of the genera Cyclotella (Kützing) Brébisson, Discostella Houk et Klee, and Puncticulata Håkanson in the family Stephanodiscaceae Glezer et Makarova (Bacilariophyta) in Japan. *Bibliotheca Diatomologica* **53**, 1-205.

Ter Braak C.J.F. & Šmilauer P. (2012): Canoco reference manual and user's guide: software for ordination, version 5.0. Microcomputer Power, Ithaca, USA, 496 pp.

Todd M.C., & Mackay A.W. (2003) Large-scale climatic controls on lake Baikal ice cover. *Journal of Climate* **16**, 3186–3199.

Törnqvist R., Jarsjö J., Pietron J., Bring A., Rogberg P., Asokan S.M., & Destouni G. (2014) Evolution of the hydro-climate system in the Lake Baikal system. *Journal of Hydrology* **519,** 1953-1962.

Trifonova I. & Genkal S. (2001) Species of the genus Aulacoseira Thwaites in lakes and rivers of north-western Russia-distribution and ecology. In *Proceedings of the 16th International Diatom Symposium, Athens and Aegean Islands* **25,** 315-322.

Vadeboncoeur Y., Jeppesen E., Vander Zanden M.J., Schierup H-H, Christoffersen K., & Lodge D.M. (2003) From Greenland to green lakes: Cultural eutrophication and the loss of benthic pathways in lakes. *Limnology and Oceanography* **48,** 1408-1418.

van Dam H., & Mertens A. (1993) Diatoms on herbarium macrophytes as indicators for water quality. *Hydrobiologia* **269/270,** 437-445.

Van Dam H., Mertens A., & Sinkeldam J. (1994) A coded checklist and ecological indicator values of freshwater diatoms from the Netherlands. *Netherlands Journal of Aquatic Ecology* **28,** 117-133.

Watchorn M., Hamilton P., Anderson T., Roe H. and Patterson R.(2008) Diatoms and pollen as indicators of water quality and land-use change: a case study from the Oak Ridges Moraine, Southern Ontario, Canada. *Journal of Paleolimnology* **39**, 491-509.

Chapter 9: Synthesis

9.1 Introduction

The shallow lake systems of the Selenga River basin provide critical function to maintaining the ecosystem health of Lake Baikal, a UNESCO World Heritage Site. However, intensifying anthropogenic disturbances since the 19th century, and the likely continued effects of climate change in the region, initiate a crucial need to identify the timing and rates of change of ecological impact of these systems, and the ecological sensitivity and response to perturbations. Therefore, the primary aims of this thesis were as follows:

1. To determine to what extent hydrological regime determines the ecological structure (biology) and functioning (e.g. productivity) of shallow lakes within floodplain delta wetlands.
2. Determine historical levels of anthropogenic contamination to shallow lakes of the Selenga River basin.
3. Assess the impact on shallow lakes from local vs. regional vs. long-range transport of contaminants, and spatial variations in contaminant records from lakes within a floodplain delta wetland and outside of a floodplain wetland.
4. Determine potential for ecological response within shallow lakes to natural and anthropogenic disturbances across several trophic levels, including assessments of sensitivity to local vs. regional disturbances, and primary drivers of ecological change across different temporal and spatial scales.

Contemporary analysis of ecological spatial variability revealed that connectivity, physical lake parameters, and trophic interactions were the main drivers determining ecological properties of shallow lakes within the Selenga River basin. How these key drivers varied in the past was investigated, and ecological response was analyzed through palaeoecological multi-proxy reconstructions. Further, the extent to which shallow lakes in the Selenga River basin have been subjected to long-range, regional, and local contamination was investigated. This final chapter goes further to bring a synthesis between findings in this study. Initially the most important changes from each lake are summarised, and commonalities or differences between records are discussed. Anthropogenic disturbances have been important drivers of ecological

change in the 20th century, inciting ecological shifts observed across multiple trophic levels, with implication for ecological regime shifts.

9.2 Ecological responses to anthropogenic and natural disturbances in Siberian shallow lake ecosystems

9.2.1 Multi-proxy reconstructions from individual lakes

9.2.1.1 SLNG04

Local events and hydrological changes since the 19th century have had the greatest influence on SLNG04 ecology. Hydrological changes resulted in geochemical shifts (organic matter and carbonate content, trace metal and element concentrations) at SLNG04, which are tied to ecological responses. The first ecological shift in the SLNG04 record is captured by all three biological proxies and several geochemical proxies in the mid-19th century (Figure 9.1). The ecological shift coincides with increases in organic matter content, carbonate content, Ca, Fe, Mn, and Ca/Ti ratios, declines in Fe/Mn ratios, and highly fluctuating magnetic susceptibility. The timing of these ecological and geochemical shifts coincides with the Tsagan earthquake (1862), the epicentre of which was just offshore of the northeast corner of the Selenga Delta, located in what is now Proval Bay (Figure 6.1; Vologina *et al*., 2010). The largest ecological shift in the 20th century was observed in the diatom community c. 1920, and manifested as an abrupt decline in diatom concentrations. Early- to mid-20th century contaminant increases in the sediment record at this time signals increases in regional and local development, including agricultural intensification and industrialization. The intensification of agricultural practices and increasing nutrient flux to SLNG04 likely led to increased diatom dissolution (and is the likely cause of the decline in diatom concentration), as a result of increased alkalinity and pH, which is hinted at with the increased carbonate content c. 1920 (Figure 9.1; Ryves *et al*., 2006). Breakpoint analysis of macrofossil ordination scores indicated significant point of change coinciding with increasing diatom concentrations, declining Ca/Ti ratios and carbonate content, and increasing Fe/Mn ratios in the 1960s. The ecological and geochemical changes coincide with the extensive flooding of the Selenga Delta and Lake Baikal as a result of the Irkutsk Dam construction on the Angara River (Pinegin *et al*., 1976). Therefore, early in the SLNG04 record, local, natural disturbances, such as the Tsagan earthquake of 1862, elicited major ecological response. Into the 20th century, anthropogenic disturbances had the greatest influence on

SLNG04 ecology, including the flooding of the Selenga Delta and Lake Baikal in the 1960s, which resulted in hydrological changes and caused geochemical shifts and ecological responses, and nutrient enrichment from agricultural intensification in the 20th century. Primarily, hydrological changes have resulted in geochemical shifts (organic matter and carbonate content, trace metal and element concentrations) at SLNG04, which are tied to ecological responses.

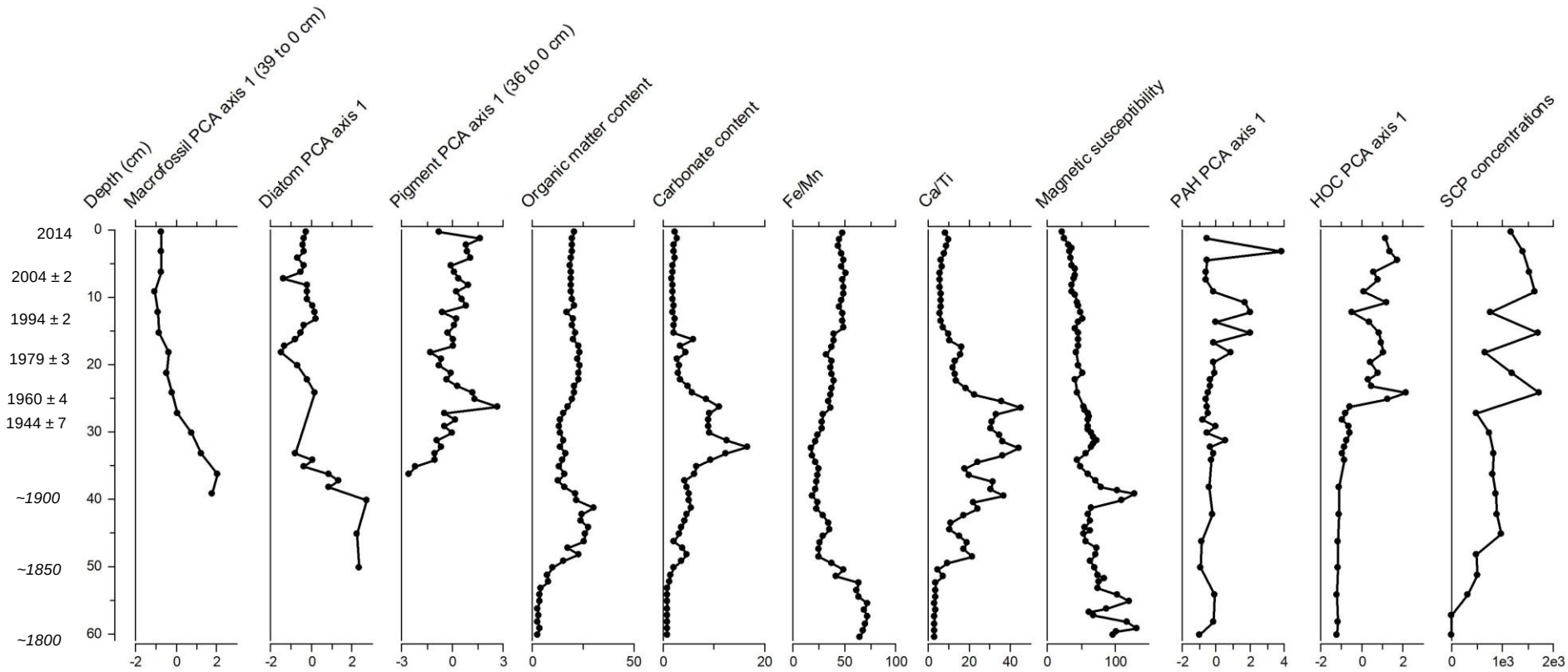

Figure 9.1. SLNG04 summary figure of key findings from the sediment cores collected from the lake. From left to right: Unconstrained ordination axis 1 scores for biological proxies (no units), organic matter content (from LOI_{550}; %), carbonate content (from LOI_{950}; %), trace element ratios, magnetic susceptibility (SI units), unconstrained ordination axis 1 scores for PAH and HOC concentrations (no units), and SCP concentrations (no. SCP g^{-1} dry mass).

9.2.1.2 SLNG05

Similar to SLNG04, local events and hydrological changes since the 19th century have had the greatest influence on SLNG05 ecology. Changes in trace and major elements, geochemical, and magnetic susceptibility records from SLNG05 likely depict hydrological variability of the shallow lake during the 19th and 20th centuries (Figure 9.2), particularly, a shallowing of the lake in the late-19th century and into the early-20th century, due to disconnection from the Selenga River. The shallowing of the lake also resulted in changes in all biological proxies, most notably declines in planktonic diatoms, increased pigment concentrations, and increased macrophyte abundance and density. A shift in all biological proxies at SLNG05 between 1960 and 1970 indicated possibility of an ecological regime shift (Figure 9.2), and coincided with changes in geochemical indicators. The widespread ecological and geochemical changes at SLNG05 were likely instigated by change in hydrological regime as a result of flooding following the construction of the Irkutsk Dam on the Angara River in the 1960s, and increased connectivity of SLNG05 with the Selenga River (Pinegin *et al*., 1976). Ecological changes include an increase in planktonic diatom species and concurrent decline in small benthic fragilarioids, declines in submerged macrophyte richness, abundance and density, decreased pigment concentrations, and increased diatom species richness (Figure 9.2). Therefore, the SLNG05 sedimentary records indicate the strong influence of hydrological changes on ecological and geochemical proxies through the 19th and 20th centuries.

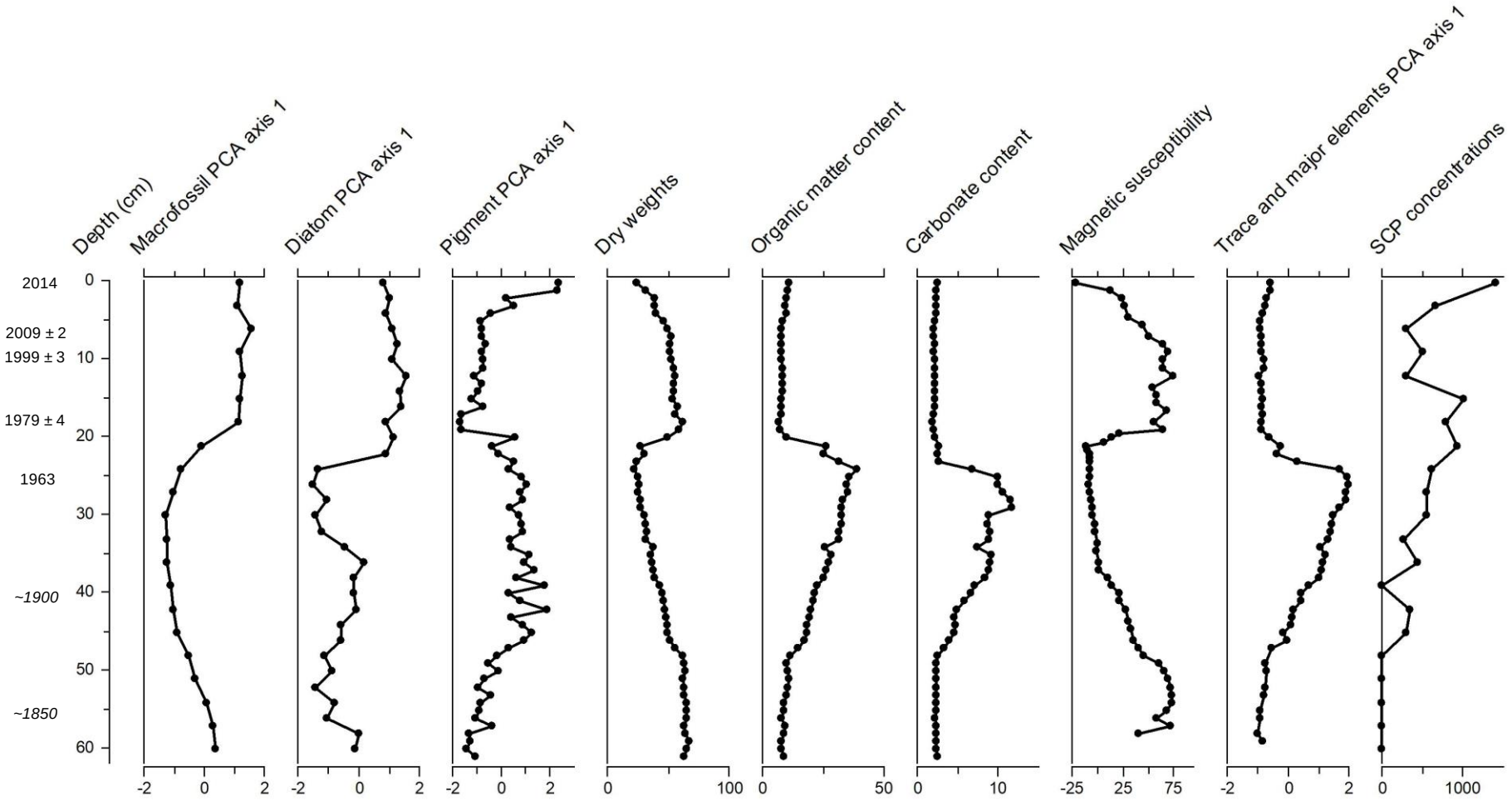

Figure 9.2. SLNG05 summary figure of key findings from the sediment cores collected from the lake. From left to right: Unconstrained ordination axis 1 scores for biological proxies (no units), dry weights (%), organic matter content (from LOI_{550}; %), carbonate content (from LOI_{950}; %), magnetic susceptibility (SI units), SCP concentrations (no. SCP g^{-1} dry mass).

9.2.1.3 BRYT02 (Black Lake)

Geochemical records (organic matter and carbonate content, and trace and major element concentrations) from Black Lake likely indicate that the increased development and industrialization near Lake Gusinoye and in close proximity to Black Lake in the 1940s and 1950s resulted in a change in source-water to the lake in the late-1940s (Figure 9.3; Pisarsky *et al.*, 2005). Ecological records indicate the most profound change at Black Lake occurred in the mid to late-20th century, first with increasing pelagic primary productivity post-1960 evidenced by the increase in planktonic diatoms, and eventual switch to primarily pelagic primary production, with a dominance by planktonic diatoms at Black Lake by 1980 (Figure 9.3). Increased local population, transportation developments, and industrial expansion in the Gusinoye region of the Selenga River basin in the 1940s-1960s were likely drivers of this change. While pigment concentrations may indicate continued increasing productivity in recent years, diatom assemblages indicate increases in benthic species, likely related to increasing littoral habitat availability. The more recent ecological changes may be tied to impacts from climate change in southeast Siberia observed in recent years, including lengthening of the ice-free season due to increased temperatures (Törnqvist *et al*., 2014).

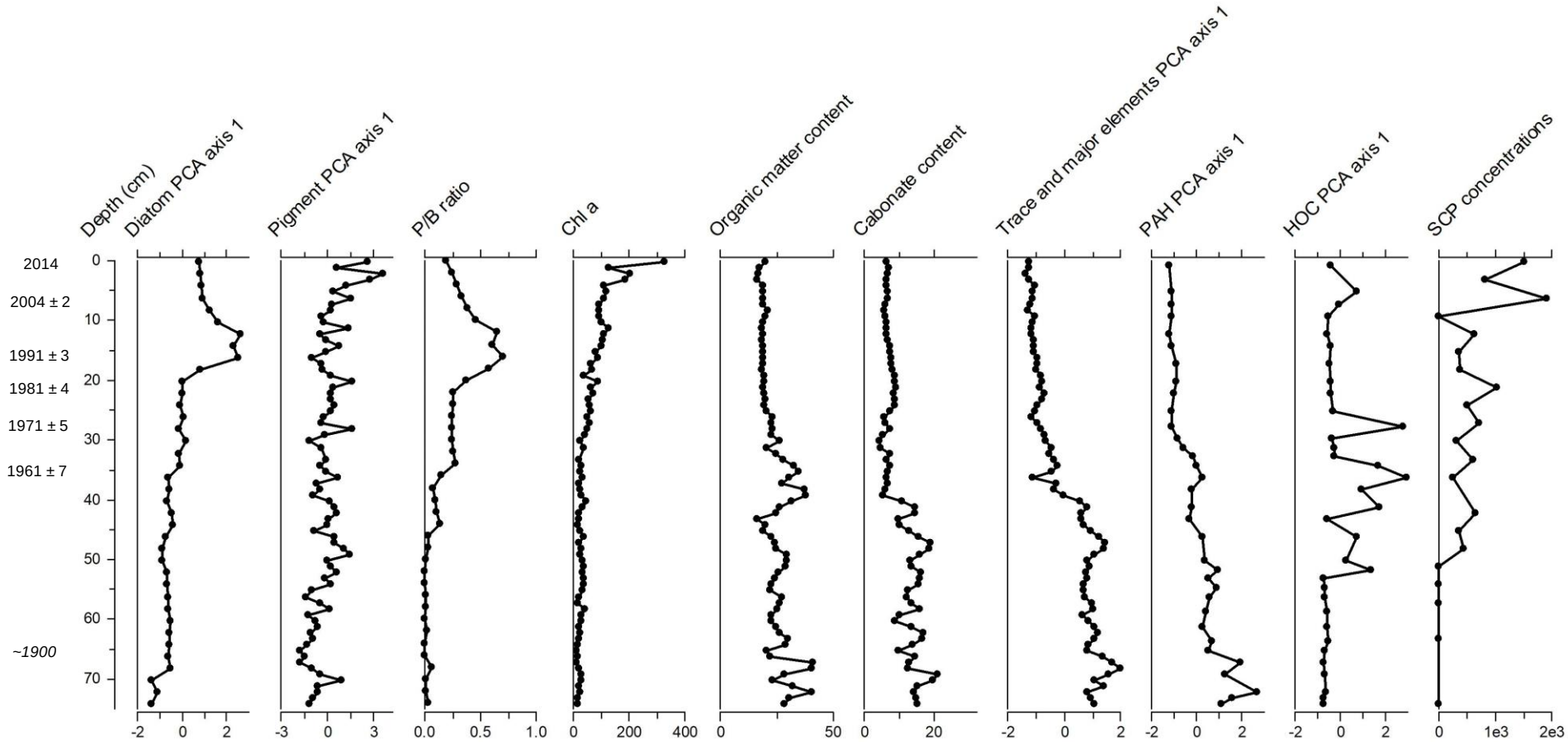

Figure 9.3. Black Lake summary figure of key findings from the sediment cores collected from the lake. From left to right: Unconstrained ordination axis 1 scores for biological proxies (no units), Planktonic/Benthic (P/B) ratio, Chl *a* concentration (nmol g^{-1} organic matter), organic matter content (from LOI_{550}; %), carbonate content (from LOI_{950}; %), and SCP concentrations (no. SCP g^{-1} dry mass).

9.2.2 Synthesizing recent trends across Selenga River basin shallow lakes

As the early SLNG04 sediment record indicates a pre-shallow lake, marshy environment, the ecological record would have been a hospitable habitat to different life forms of diatoms, with different macrophyte presence, and is, therefore, different from the early ecological records from SLNG05 and Black Lake, as these two sites were already fully formed shallow lake environments in the 19th century. Background diatom communities at SLNG05 and Black Lake were comprised of small, benthic fragilarioids, typically associated with hospitable benthic substrates, including submerged macrophytes, sand, and sediment, favourable light conditions, and have wide tolerances for nutrient conditions (Sayer, 2001; Bennion *et al.,* 2012). Fragilarioids are also often pioneer species, able to tolerate less hospitable conditions such as extended ice cover and high UV penetration (Douglas and Smol, 1995; Smol *et al*., 2008), and have been found to dominate other shallow lakes in Siberia (Laing *et al*., 1999; Westover *et al*., 2005; Mackay *et al*., 2012). Further, both SLNG05 and BRYT show increased pelagic primary production beginning mid- to late-20th century, and a corresponding decline in benthic primary production.

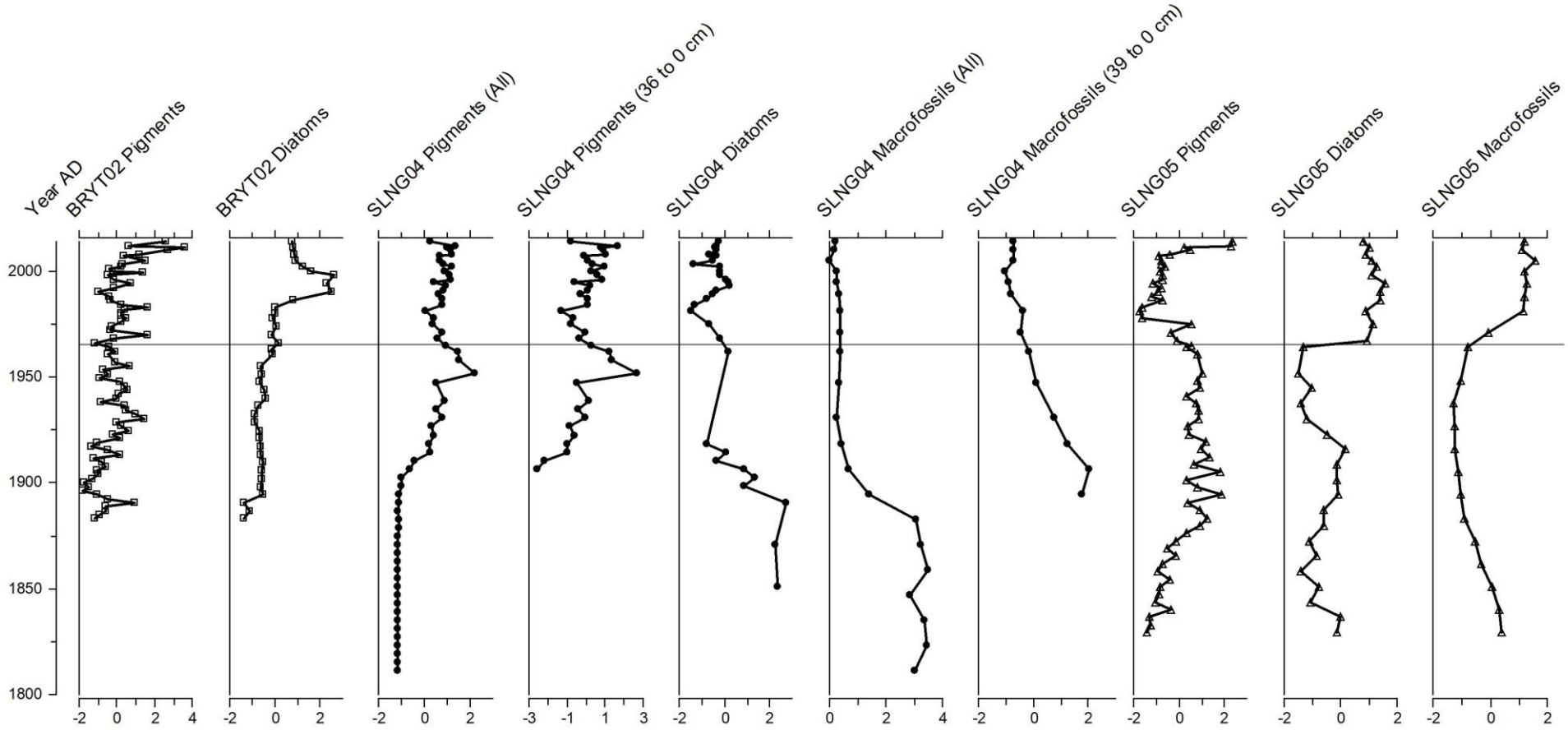

Figure 9.4. Ordination axes for all biological proxies from all three palaeolimnological study lakes in the Selenga River basin. Black Lake records are represented by open squares, SLNG04 records by closed circles, and SLNG05 records by open triangles. The horizontal grey line indicates 1965 AD, the timing around which the Selenga Delta was flooded due to the construction of the Irkutsk Dam.

The two Selenga Delta lake records (SLNG04 and SLNG05) extend back to the early-19th century, while the record from Black Lake (BRYT) extends only to the late-19th century (Figure 9.4). Within the period of overlap between the three records, the primary finding that is common between all records is the ecological response to evidence of increasing nutrient levels at the three lakes beginning in the early to mid-20th century (Aim 4). The evidence is observed as increasing macrophyte abundance and meso-eutrophic diatom communities at SLNG04 and SLNG05, increasing pelagic primary productivity at Black Lake, and increasing pigment concentrations at SLNG04 and Black Lake. The increase in inferred-nutrient levels is likely related to increasing regional anthropogenic development at this time in southeast Siberia, with agricultural intensification in the early-20th century, and economic and industrial intensification following World War II (Khanin, 2003; Pisarsky *et al*., 2005; Bazhenova and Kobylkin, 2013) (Aim 2 and Aim 3).

An important similarity between the two Selenga Delta lakes is the evidence for physical, chemical, and ecological change that occurred in both lakes in the mid-20th century, which affected the SLNG04 diatom record, and all biological proxies at SLNG05 (Figures 9.1 and 9.2). Both shallow lakes within the Selenga Delta show evidence of decreasing lake depth in the 1920s to 1950s, and change in connectivity level to either full disconnection or intermittent connectivity, with corresponding increases in submerged macrophyte abundance and alkalinity/pH (carbonate content; Figures 9.1 and 9.2). Both lakes then experienced an end to this period of lower connectivity levels c. 1960/1970, which was observed in the SLNG04 diatom record, and all SLNG05 biological proxies, as well as the sediment geochemical records from both lakes (Aim 1 and Aim 4) (Figures 9.1 and 9.2).

A finding that has consistently been observed across sedimentary palaeo-records from the three lakes is the similarity in timing of ecological changes between diatom and macrofossil records, with algal pigment records differing in timing of significant changes. This follows on the findings of Chapter 3, with the established similarities between environmental drivers (e.g. connectivity) of change in diatom and macrofossil records in contemporary Selenga River basin shallow lakes, and also the significant influence that variations in macrofossils has on variations in diatom assemblages (See Section 3.3.1.3). In Chapters 6 and 7, breakpoint analysis of

diatom and macrofossil axis 1 scores revealed similar timing of significant change between the ecological records, however breakpoint analysis of pigment assemblages differed. Total variations in pigment assemblages are primarily driven by total algal biomass (e.g. Chl *a*, Chl *a* degradation products), which is likely driven primarily by nutrient enrichment, than hydrological changes, which likely drive the major shifts in diatoms, macrophytes, and zooplankton (Aim 4).

The contaminant records from the three sites express some commonalities in timing of onset, increase, and decrease in contaminant concentrations in the Selenga River basin (See Section 5.4.2, Table 5.7). Primary, is the level of contamination across all three sites, which remains relatively low throughout the sedimentary records, without signs of high levels of toxicity. The earliest sign of contamination in the basin was recorded at the two Selenga Delta sites, SLNG04 and SLNG05, in the 19th century, with the start of the SCP records. This early onset recorded at both sites is likely the result of long-range atmospheric transport of SCPs to the Selenga River basin. The major period of increasing contamination in the Selenga River basin began in the mid-20th century, in the decades immediately following World War II, coinciding with much of the Northern Hemisphere post-war development, the Great Acceleration (Steffen *et al*., 2015), and the Russian economic growth plans of the 20th century (Khanin, 2003); all lake sediment records report increasing contamination in the mid-20th century, including SCP concentration increase at all lakes, and PAH and HOC concentrations at SLNG04 and Black Lake, and likely indicates the major period of regional and local increase in economic development. Declines in contaminant concentrations in the late-20th and early-21st centuries are likely due to declining industrialization in Russia following break-up of the former U.S.S.R. (Khanin, 2003) (Aim 2).

Temporal changes in trace element and metal concentrations at individual lakes are likely related to local influences, primarily hydrological changes and local anthropogenic disturbances. High concentrations of trace elements are most likely related to naturally high levels in the watershed, chemically-enhanced concentrations due to changing redox conditions, or allochthonic inputs from local human disturbances, including nearby agricultural practices and development. Arsenic appears to be the only trace element of possible concern across the Selenga Delta, as both SLNG04 and SLNG05 showed increased concentrations in the mid-20th century (Aim 1 and Aim 2).

9.3 Important drivers of ecological variability through the 19th to 21st centuries

Anthropogenic disturbances appear to currently be the primary threat to the ecology of the shallow lakes within the Selenga River basin, which must be considered in all future hydrological and economic development decisions. Hydrological changes and increased nutrients are the two most prominent factors affecting ecological change in these Siberian shallow lakes. Analysis of contemporary and palaeo-records of ecological variability in the Selenga River basin revealed that hydrological regime and level of connectivity appears to drive much of the ecological changes observed in Selenga Delta lakes. Contamination levels, while detectable, remain too low throughout the 19th and 20th centuries from all three shallow lakes to elicit ecological responses. The ecological impacts of nutrient increases are observed in all three lakes studied, and while nutrients appear to play a secondary role in ecological variability in lakes within the Selenga Delta, temporal changes in ecological structure at Black Lake imply a response primarily to nutrient enrichment throughout the 20th century. Within the Selenga Delta, known historical events impacting the hydrology and morphology of the wetland have had differing levels of impact on the ecosystem. The ecological impacts of the 1862 Tsagan earthquake (Vologina *et al*., 2010) were confined to the eastern side of the Selenga Delta, and the event, which resulted in the initial formation of the lake, and corresponding ecological response was observed in the SLNG04 sedimentary record. This event was not observed in the SLNG05 sedimentary record, despite extending back to the early-19th century. However, the extensive flooding that occurred as a result of hydroelectric development along the Angara River in early-1960s (Pinegin *et al*., 1976), had ecological ramifications across the Selenga Delta, as ecological responses to the flooding were recorded in sedimentary records from both SLNG04 and SLNG05.

Palaeoecological similarities and sensitivities between the two Selenga Delta lakes are greater than those between all three lakes, likely due to the primary influence of hydrological variability on sites within the Selenga Delta, and the influence of local disturbances. Hydrological regimes and flood dynamics are more important determinands for productivity and structure of wetlands than nutrient status (Boyd, 1971; Laitenen, 1990; Mitsch and Gosselink, 2007; Sokal *et* al., 2010). Moreover, flood disturbance and variability in connectivity are the primary drivers of productivity in highly connected (no-closure) lakes within wetland

environments, and macrophyte biomass may be significantly lower in flooded, highly connected systems due to inputs of cold, turbid river water, despite influxes of nutrients (Bailey and Guimond, 2009). Hydrological regime has been observed in other wetlands/river deltas around the world as being one of the most important factors in determining ecology, primarily macrophyte gradients and diatom assemblages (Hay *et al*., 2000; Arias *et al*., 2013). Because hydrological variability has been the primary driver of ecological variability in Selenga Delta lakes, such lakes are more sensitive to local and regional scale disturbances that directly impact the hydrological regime.

The findings of the current study carry direct ecological implications for anthropogenic disturbances in the Selenga River basin. Findings indicate that hydrological changes within the Selenga Delta will result in extreme ecological changes within shallow lake ecosystems. This has implications for future development in the region, both upstream of the Selenga Delta along the Selenga River and its tributaries, and within Lake Baikal and the Angara River. Currently, plans for two hydrological developments within the Mongolian Selenga River basin are being considered (The World Bank, 2017). The first is construction of the Shuren Hydropower Dam on the Selenga River in northern Mongolia. The project was first proposed in 2013 and would see the disruption of river flow in the Selenga River basin, resulting in downstream impacts in the Selenga Delta and Lake Baikal. The second development is the Orkhon-Gobi Water Diversion scheme, which would see the construction of a pipeline to transport water from the Orkhon River to the Gobi Desert for use in mining. The operation of either of these developments would lead to alterations in the hydrological regime in the Selenga River basin, reduction in water transported to the Selenga Delta and Lake Baikal, and reduction in water levels within the Delta. Results of this thesis have demonstrated the control that connectivity and hydrological status plays in determining ecological variability within shallow lakes, and the extreme ecological impact that has arisen in the past due to fluctuations in water levels within the Selenga Delta, and decreased connectivity for individual lakes. Findings that lakes with lower connectivity have higher levels of production and lower diversity will also have important implications for Lake Baikal as well, as the aquatic systems of the Selenga Delta are breeding ground for many of Baikal's endemic fish, and provide habitat for other endemic species.

Contamination records discussed in Chapter 5 provide evidence of low, but measurable contamination in the Selenga River basin during the 20th and 21st centuries, from local and regional sources. These records should act as baselines of contamination for future development in the basin, including industrial, commercial and agricultural development. Contamination records from the 20th century suggested rapid development in the region, likely reflecting the intensive economic growth plans of the former USSR between 1928 and 1991 (Dienes, 1987; Khanin, 2003), and expose the potential for environmental damage in the Selenga River basin if economic development in Siberia and Mongolia goes unhindered. As populations increase and larger centres of development encroach on what was once remote landscape, future contamination records are likely to reflect the increasing development. As future development in both Siberia and Mongolia has potential to impact the Selenga River basin, records of previous contamination in the region should be considered.

The Selenga River basin in southeast Siberia warmed nearly twice as fast as the global average (a total increase of 1.6°C) for the period 1938 to 2009, with most of the warming occurring during the winter season, and precipitation and evapotranspiration have increased through the 20th and 21st centuries (Törnqvist *et al*., 2014). Further, a lengthened ice-free season for Lake Baikal of approximately 16 days has been recorded over the past 137 years, primarily related to later ice onset (Magnuson *et al.,* 2000; Todd and Mackay, 2003). Warmer and shorter winters may lead to delayed ice-formation on shallow lakes of the Selenga River basin, translating to longer ice-free seasons and increased length of the growing season, which would lead to increased hospitable littoral habitat, which has been recorded as a primary response to climate change in remote, northern shallow lakes (Smol *et al.,* 2005). Recent diatom assemblage changes at Black Lake may be evidence for climate-related impacts on the shallow lake ecosystem. Increased relative abundances of periphytic species (including small benthic fragilarioids) at Black Lake in the 21st century may be due to increased habitat availability due to lengthening of the ice-free season of the lake. Ecological signals of climatic changes have not been observed at SLNG04 or SLNG05, and, at present, any impact of climate change may be outweighed by the impacts of hydrological changes in these systems. Therefore, the ecological influence of hydrology currently appears to override the influence of 20th and 21st century climate change on shallow lakes in the Selenga Delta. The climate of

southeast Siberia is predicted to continue to warm through the 21st century, with continued increases in overall temperatures, greater temperature increases during the winter than the summer, and increases in precipitation expected (Malsy *et al*., 2012; Törnqvist *et al*., 2014). These continued changes have potential for greater ecological impact, and potential for climate influences to become more important than current primary environmental drivers of ecological variability, such as hydrology, in floodplain delta wetlands.

The invasive Canadian waterweed, *E. canadensis*, is currently not widespread throughout the Selenga Delta, as the invasive waterweed was only observed at 3 out of 14 Selenga Delta sites, as well as in Black Lake. However, when *E. canadensis* was observed, it was either the dominant submerged macrophyte, or was found at high frequencies (Section 3.3.1, Table 3.4). Unfortunately, remains of *E. canadensis* do not preserve in the sedimentary record, however indirect evidence for the introduction and establishment of *E. canadensis* in the SLNG04 macrofossil record was observed, including decline in abundance of most submerged macrophytes and shift trophic structure at SLNG04 c. 1990. Such ecological events have been observed elsewhere as the result of *E. canadensis* establishment (Kravtsova *et al*., 2009; Mjelde *et al*., 2012). The continued spread of the already established invasive has implications for ecological structure, and maintenance of indigenous food-webs and trophic structure within Selenga River basin shallow lakes. Without proper attention, invasive species such as *E. canadensis* can easily become widely established throughout an ecosystem such as the Selenga Delta, by both natural spread due to high interconnectedness between lakes, and anthropogenic means, through transport from boating, angling, etc. Spread and establishment of invasive species such as *E. canadensis*, with the ability to drastically alter indigenous habitats and food-webs will have environmental, social, and economic ramifications.

9.4 Considerations for future work

The current study highlighted several important variables in determining the ecological structure and function across shallow lake ecosystems in the Selenga River basin, and those drivers which are most likely to result in significant shifts in aquatic ecology. Future work should, therefore, focus on expanding the knowledge gained herein, and aim to further investigate how these variables and drivers have in the past and may in the future have varied, and the potential ecological response. Several potential directions for future work include the following:

1. Further investigations into the extent and impact of anthropogenic disturbances in the Selenga River basin, including pollution, and connectivity changes in the Selenga Delta, and resulting ecological shifts in Selenga Delta lakes (SLNG04 and SLNG05). Particularly, work including isotopic analysis of carbon and nitrogen to determine changes in productivity, changes in the sources of carbon and nitrogen, nutrient enrichment and cycling in lakes.
2. To further investigate the nature of hydrological connectivity at these sites, through both surface and groundwater connections, contemporary and palaeolimnological oxygen isotope work should be undertaken. Contemporary river and lake water samples would be important for end member modelling. Analysis of sediment cores for oxygen isotope changes would indicate fluctuations in source water to the Selenga Delta shallow lakes through time, and highlight periods of changing connectivity.
3. Further work investigating the nature and extent of contemporary food-web interactions in these shallow lakes would be beneficial, as trophic interactions were shown to be an important driver of ecological variability across Selenga River basin shallow lakes. Contemporary analysis of food-web interactions could also help to inform on interpretations made from the macrofossil palaeo-record. Such work could be accomplished through isotope work, including $\delta^{13}C$ and $\delta^{15}N$.
4. Further work should be conducted to elucidate the role of climate change on ecological changes observed in Selenga River basin shallow lakes. Temperature and precipitation changes during the past century have potentially impacted shallow lake ecosystems studied herein, and possible impacts have been observed recently at Black Lake. However further work in this region may help to discern between recent changes in nutrient enrichment, and impacts from climate change.

9.5 Conclusions

1. Spatial variability and composition of contemporary ecological communities in Selenga River basin shallow lakes are determined by degree of connectivity, trophic interactions, and physical landscape parameters such as lake surface area and depth.

2. Contamination of shallow lakes in the Selenga River basin has been low to medium compared to globally contaminated sites, with detectable and distinct periods of anthropogenic pollution in the mid-20th century, extending until the late-20th century, and is closely linked with periods of increasing and decreasing economic development in Russia. The anthropogenic contamination record at this time consisted of increases in HOCs, PAHs, SCPs, and Hg, and indicated local to regional sources of pollution in the 20th century.
3. Shallow lakes of the Selenga River basin have undergone significant ecological shifts since the mid-19th century, with the most profound shifts occurring in the mid-20th century at SLNG04 (diatoms) and SLNG05 (macrofossils, diatoms, and pigments), and the late-20th century at Black Lake (diatoms).
4. Hydrological variability and nutrient pollution are primary drivers of ecological variability since the 19th century. Ecological changes were observed in the macrophyte, zooplankton, and algal communities at SLNG04 and SLNG05, resulting from physical (change in depth), chemical (increasing pH and alkalinity), and biological (increased macrophyte production; invasive species) shifts related to changes in connectivity and nutrient pollution. Nutrient pollution at Black Lake in the mid- to late-20th century resulted in algal community shifts, including a likely shift from benthic primary production to primarily pelagic primary production.
5. The mid-20th century flooding of Lake Baikal and the Selenga River Delta following construction of the Irkutsk Dam on the Angara River had more widespread ecological impacts than the Tsagan earthquake of 1862, which is the strongest earthquake recorded in southern Siberia. The earthquake was only recorded in the sediment record of SLNG04, while the impacts of the mid-20th century flooding was recorded in the sediment geochemical and ecological records of both SLNG04 and SLNG05.

This study has contributed to the need for increased research effort in southeast Siberia, in a region of international importance. The Selenga Delta is a Ramsar wetland of international importance due to the critical habitat it provides to waterfowl and endemic species, high levels of habitat heterogeneity and biodiversity, and the crucial function the delta provides for

maintaining the health and integrity of Lake Baikal, a UNESCO World Heritage Site. Moreover, the Selenga River basin comprises approximately 80% of the Lake Baikal watershed, making the health of the aquatic ecosystems within the Selenga River basin crucial to maintain. This study has indicated that levels of contemporary and historical contamination at shallow lakes within the basin have remained low to moderate through the 19th to 21st centuries. This study has also provided evidence of the primary drivers of contemporary ecological stability and variability across the Selenga River basin, as well as palaeolimnological records of the magnitude of ecological response to anthropogenic and natural disturbances through the 19th to 21st centuries, with a view to providing insight into the potential for ecological response to continued anthropogenic disturbance in the Selenga River basin in the future.

9.6 References

Arias M.E., Cochrane T.A., Norton D., Killeen T.J., & Khon P. (2013) The flood pulse as the underlying driver of vegetation in the largest wetland and fishery of the Mekong basin. *Ambio* **42,** 864-876.

Bailey S.E., & Guimond J.K. (2009) Aboveground biomass and nutrient limitation in relation to river connectivity in montane floodplain marshes. *Wetlands* **29,** 1243-1254.

Bazhenova O.I., & Kobylkin D.V. (2013) The dynamics of soil degradation processes within the Selenga Basin at the agricultural period. *Geography and Natural Resources* **34,** 221-227.

Bennion H., Carvalho L., Sayer C.D., Simpson G.L., & Wischnewski J. (2012) Identifying from recent sediment records the effects of nutrients and climate on diatom dynamics of Loch Leven. *Freshwater Biology* **57,** 2015-2029.

Boyd C.E. (1971) Further studies on productivity, nutrient, and pigment relationships in Typha latifolia populations. *Bulletin of the Torrey Botanical Club* **98,** 144–150.

Dienes L. (1987) The soviet oil industry in the twelfth five-year plan. *Soviet Geography* **28**, 617-655.

Douglas M.S.V., & Smol J.P. (1995) Periphytic diatom assemblages from high arctic ponds. *Journal of Phycology* **31,** 60-69.

Hay M.B., Michelutti N., & Smol J.P. (2000) Ecological patterns of diatom assemblages from Mackenzie Delta lakes, Northwest Territories, Canada. *Canadian Journal of Botany* **78**, 19-33.

Khanin G.I. (2003) The 1950s – the triumph of the Soviet economy. *Europe-Asia Studies* **55**, 1187-1212.

Kravtsova L.S., Izhboldina L.A., Mekhanikova I.V., Pomazkina G.V., & Belykh O.I. (2009) Naturalization of Elodea canadensis Mich. in Lake Baikal. Russian Journal of Biological Invasions, 1, 162-171.

Laing T.E., Rühland K.M., & Smol J.P. (1999) Past environmental and climatic changes related to tree-line shifts inferred from fossil diatoms from a lake near the Lena River Delta, Siberia. *The Holocene* **9,** 547-557.

Laitenen, J. (1990) Periodic moisture fluctuation as a factor affecting mire vegetation. *Aquilo Series Botanica* **28,** 45–55.

Mackay A.W., Bezrukova E.V., Leng M.J., Meaney M., Nunes A., Piotrowska N., Self A., Shchetnikov A., Shilland E., Tarasov P., Wang L., & White D. (2012) Aquatic ecosystem responses to Holocene climate change and biome development in boreal, central Asia. *Quaternary Science Reviews* **41,** 119-131.

Malsy M., Flörke M., Borchardt D. (2016) What drives the water quality changes in the Selenga Basin: climate change of socio-economic development. *Regional Environmental Change* DOI 10.1007/s10113-016-1005-4.

Mitsch W.J., & Gosselink J.G. (2007) Wetlands, 4th Edition. Wiley & Sons, United States of America.

Mjelde M., Lombardo P., Berge D., & Johansen S.W. (2012) Mass invasion of non-native *Elodea canadensis* Michx. In a large, clear-water, species-rich Norwegian lake – impact on macrophyte biodiversity. *International Journal of Limnology* **48,** 225-240.

Pinegin A.V., Rogozin A.A., Leshchikov F.N., Kulish L.Y., & Yakimov A.A. (1976) Shore dynamics of Lake Baikal at the new level regime. Nauka, Moscow.

Pisarsky B.I., Hardina A.M., & Naganawa H. (2005) Ecosystem evolution of Lake Gusinoe (Transbaikal Region, Russia). *Limnology*, **6**, 173-182.

Ryves D., Battarbee R., Juggins S., Fritz S., & Anderson N.J. (2006) Physical and chemical predictors of diatom dissolution in freshwater and saline lake sediments in North America and West Greenland. *Limnology and Oceanography* **51,** 1355–1368.

Sayer C.D. (2001) Problems with the application of diatom-total phosphorus transfer functions: examples from a shallow English lake. *Freshwater Biology* **46,** 743-757.

Smol, J. P., Wolfe A.P., Birks H.J.B., Douglas M.S.V., Jones V.J., Korhola A., Pienitz R., Rühland K., Sorvari S., Antoniades D., Brooks S.J., Fallu M-A., Hughes M., Keatley B.E., Laing T.E., Michelutti N., Nazarova L., Nyman M., Paterson A.M., Perren B., Quinlan R., Rautio M., Saulnier-Talbot E., Siitonen S., Solovieva N, & Weckström J. (2005) Climate-driven regime shifts in the biological communities of arctic lakes. *Proceedings of the National Academy of Sciences* **102**, 4397–4402.

Sokal M.A., Hall R.I., Wolfe B.B. (2010) The role of flooding on inter-annual and seasonal variability of lake water chemistry, phytoplankton diatom communities, and macrophyte biomass in the Slave River Delta (Northwest Territories, Canada). *Ecohydrology* **3,** 41-54.

Steffen W., Broadgate W., Deutsch L., Gaffney O., & Ludwig C. (2015) The trajectory of the Anthropocene: The Great Acceleration. *The Anthropocene Review* **2,** 81-98.

The World Bank. (2017) MN-Mining Infrastructure Investment Supp (P118109). [online] Available from: projects.worldbank.org/P118109/mn-mining-infrastructure-supp?lang=en$tab=overview. [Accessed: 23rd August, 2017].

Todd M.C., & Mackay A.W. (2003) Large-scale climatic controls on lake Baikal ice cover. *Journal of Climate* **16**, 3186–3199.

Törnqvist R., Jarsjö J., Pietron J., Bring A., Rogberg P., Asokan S.M., & Destouni G. (2014) Evolution of the hydro-climate system in the Lake Baikal system. *Journal of Hydrology* **519,** 1953-1962.

Vologina E.G., Kalugin I.A., Osukhovskaya Y.N., Sturm M., Ignatova N.V., Radziminovich Y.B., Dar'in A.V., & Kuz'min M.I. (2010) Sedimentation in Proval Bay (Lake Baikal) after earthquake-induced subsidence of part of the Selenga River delta. *Russian Geology and Geophysics*, **51,** 1275-1284.

Westover K.S., Fritz S.C., Blyakharchuk T.A., & Wright H.E. (2005) Diatom paleolimnological record of Holocene climatic and environmental change in the Altai Mountains, Siberia. *Journal of Paleolimnology* **35,** 519-541.

Appendices

Site	pH	Conductivity (µS/cm)	DO ($mg \cdot L^{-1}$)	Secchi depth (%)	TP ($\mu g \cdot L^{-1}$)	SRP ($\mu g \cdot L^{-1}$)	DOC ($mg \cdot L^{-1}$)	Chl a ($nmol \cdot L^{-1}$)	Hg ($ng \cdot L^{-1}$)
SLNG01	7.11	448	1.74	75	296.20	7.29	12.51	7.796	6.48
SLNG03	8.87	270	7.40	100	162.20	47.29	14.49	30.515	6.44
SLNG04	10.13	170.6	8.95	100	252.20	165.86	8.42	2.694	7.93
SLNG05	8.95	180.3	7.78	100	84.20	31.57	12.44	3.036	5.92
SLNG06	8.68	247	8.10	71	152.20	48.92	14.54	6.302	6.18
SLNG07	7.40	162.1	1.04	100	58.20	14.43	7.37	1.936	5.27
SLNG08	8.77	217.3	9.66	100	146.20	13.00	13.56	2.385	5.78
SLNG09	9.44	219.8	0.81	100	114.20	13.00	27.18	18.960	5.81
SLNG10	8.39	175.1	6.86	100	48.20	21.57	5.71	1.092	6.05
SLNG11	7.60	205.9	7.05	100	106.20	35.86	14.56	6.427	8.17
SLNG12	8.24	196.2	8.26	100	68.20	15.86	6.56	1.926	6.00
SLNG13	9.42	192.1	7.14	100	54.20	25.86	15.30	0.739	8.71
SLNG14	9.81	204.6	8.91	100	342.20	231.57	17.79	7.778	10.14
SLNG15	7.81	300	3.50	64	174.20	38.71	28.34	2.330	8.51
BRYT	10.17	280	9.06	18	74.20	23.00	15.99	17.044	4.16

Appendix 1a. Water chemistry data from the 15 study lakes. Results presented in Chapter 2.

Site	Al^{3+}	Ca^{2+}	Fe^{3+}	K^{+}	Mg^{2+}	Si^{4+}	Sr^{2+}	Cl^{-}	F^{-}	SO_4^{2-}	∑cations	∑anions	∑ions
SLNG01	0.0533	34.665	9.550	1.862	13.994	0.539	0.541	0.788	0.574	0.0810	3.556	0.0541	3.610
SLNG03	0.0071	16.370	0.628	4.305	10.149	0.486	0.248	6.282	0.551	0.0640	1.884	0.207	2.092
SLNG04	0.0063	11.426	0.147	0.0840	3.287	0.137	0.113	0.351	0.386	1.552	0.878	0.0625	0.941
SLNG05	0.128	16.428	0.556	1.356	6.292	0.489	0.176	0.802	0.404	2.838	1.499	0.103	1.602
SLNG06	0.0461	15.305	0.341	1.638	5.896	0.136	0.159	2.472	0.262	4.732	1.345	0.182	1.527
SLNG07	0.0070	8.359	0.937	0.228	2.366	0.170	0.0763	0.477	0.349	4.186	0.698	0.119	0.817
SLNG08	0.0112	13.557	0.640	0.842	4.887	0.130	0.134	1.328	0.532	0.528	1.164	0.0764	1.240
SLNG09	0.0317	12.189	0.502	1.636	7.402	0.216	0.153	0.589	0.560	0.212	1.333	0.0505	1.384
SLNG10	0.0104	15.082	0.274	0.881	4.384	0.165	0.146	1.091	0.289	6.216	1.185	0.176	1.360
SLNG11	0.0176	14.622	0.549	1.286	6.398	0.410	0.162	0.721	0.678	2.639	1.391	0.111	1.502
SLNG12	0.0112	17.334	0.463	1.069	5.327	0.240	0.172	1.173	0.332	5.844	1.402	0.172	1.575
SLNG13	0.0048	8.961	0.448	4.588	5.523	0.221	0.114	1.602	0.352	0.445	1.085	0.0729	1.158
SLNG14	0.0105	22.958	0.580	1.832	4.625	0.409	0.259	0.990	0.440	0.971	1.677	0.0713	1.748
SLNG15	0.0431	12.564	2.675	1.195	8.645	0.290	0.179	1.067	1.017	0.084	1.573	0.0853	1.659
BRYT	0.0409	5.176	0.0938	0.213	5.994	0.302	0.102	0.523	2.227	6.742	0.819	0.272	1.091

Appendix 1b. Major cation and anion concentrations, and ion balances for the 15 study lakes. Concentrations from Al^{3+} to SO_4^{2-} are recorded as $mg \cdot L^{-1}$. All ion balances are recorded as $meq \cdot L^{-1}$.Results presented in Chapter 2.

Site	Mg	Al	Si	P	S	K	Ca	Ti	Mn	Fe	Fe/Mn	Ca/Ti
SLNG01	1.116	4.318	16.520	0.188	0.228	1.302	8.984	0.312	0.411	6.162	14.982	28.758
SLNG03	0.450	0.557	10.130	0.373	0.562	0.162	20.530	0.075	0.545	4.981	9.143	274.465
SLNG04	1.012	4.109	18.850	0.362	0.374	1.345	3.016	0.323	0.195	8.534	43.719	9.352
SLNG05	1.529	6.759	25.380	0.161	0.187	2.089	1.729	0.468	0.096	5.250	54.745	3.698
SLNG06	1.642	7.075	24.520	0.165	0.189	2.137	2.179	0.466	0.159	5.353	33.646	4.678
SLNG07	0.813	3.085	15.120	0.250	0.793	1.018	4.223	0.230	0.198	7.133	36.080	18.385
SLNG08	1.206	6.089	24.110	0.145	0.515	1.897	2.144	0.412	0.166	5.094	30.761	5.209
SLNG09	1.215	4.907	20.360	0.173	0.750	1.537	4.389	0.326	0.250	5.312	21.223	13.451
SLNG10	0.759	4.018	23.550	0.134	1.541	1.419	1.858	0.296	0.059	4.225	71.976	6.273
SLNG11	1.298	6.181	24.300	0.158	0.380	1.951	1.763	0.430	0.143	5.581	39.028	4.099
SLNG12	1.305	6.465	25.040	0.169	0.221	1.987	2.072	0.437	0.181	5.693	31.384	4.746
SLNG13	1.202	6.315	23.230	0.158	0.646	2.019	2.675	0.420	0.183	5.266	28.729	6.374
SLNG14	1.350	6.749	24.710	0.127	0.351	2.090	2.822	0.433	0.126	4.994	39.635	6.514
SLNG15	1.104	5.084	21.890	0.208	0.616	1.596	3.162	0.328	0.222	5.159	23.228	9.637
BRYT	1.050	6.125	17.908	0.114	0.663	1.341	6.954	0.364	0.181	3.595	19.849	19.100

Appendix 2a. Lithogenic elements (%) and elemental ratio data from the 15 study lakes. Results presented in Chapter 3.

Site	Ni	Cu	Zn	As	Br	Pb	LOI_{550}	LOI_{950}
SLNG01	25.400	21.100	61.600	35.400	14.600	13.800	15.79	8.70
SLNG03	5.700	5.000	16.000	30.000	27.800	4.600	22.16	21.56
SLNG04	24.000	28.900	71.500	53.000	16.800	16.800	19.54	2.72
SLNG05	37.200	34.300	99.800	9.600	7.800	24.800	9.92	2.12
SLNG06	40.300	30.900	96.900	9.400	10.800	21.700	7.91	1.98
SLNG07	18.100	25.000	54.200	43.200	18.700	15.900	27.36	2.93
SLNG08	37.700	34.900	96.300	10.800	20.200	24.800	17.05	2.50
SLNG09	32.500	39.200	82.300	21.500	20.800	21.600	24.62	4.29
SLNG10	35.500	50.100	77.700	20.200	41.700	22.800	33.85	3.32
SLNG11	38.300	38.800	101.200	10.500	12.900	26.000	14.84	2.40
SLNG12	35.000	30.900	92.900	8.800	9.600	22.700	10.42	2.19
SLNG13	41.300	34.700	94.800	11.100	16.100	23.300	13.80	2.66
SLNG14	40.600	35.800	98.500	9.000	12.500	25.100	11.10	2.84
SLNG15	33.700	32.000	75.800	16.200	22.600	18.200	24.52	2.50
BRYT	16.460	17.840	81.020	9.260	15.380	19.860	18.12	6.63

Appendix 2b. Trace metals (µg g^{-1}), trace elements (µg g^{-1}), and loss-on-ignition (%) data from the 15 study lakes. Results presented in Chapter 3.

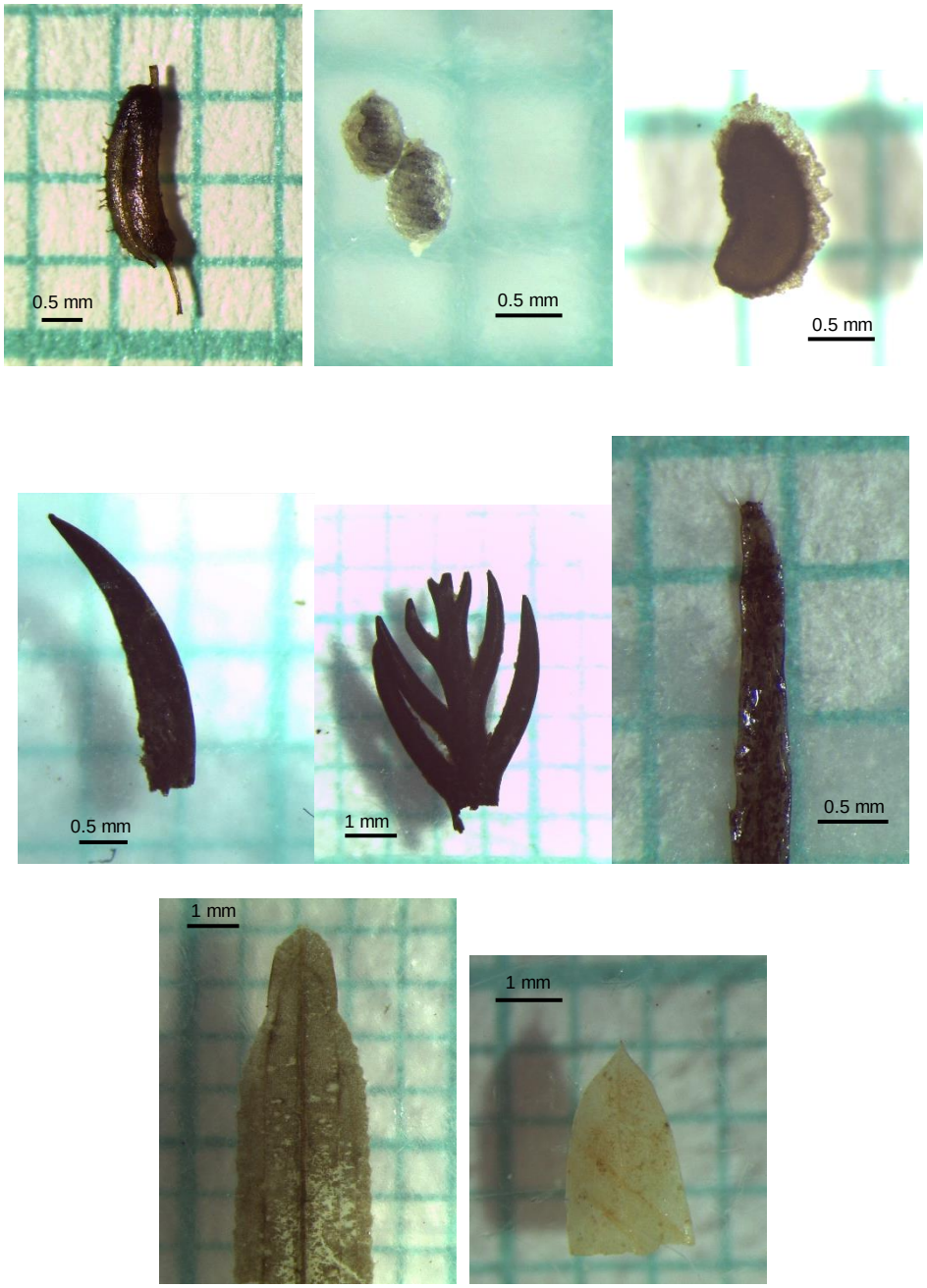

Appendix 3a. Common fossil macrophyte remains from Selenga River basin shallow lakes. Top row (L-R): *Zannichellia palustris* seed, calcified oospores of *Chara* sp., *Callitriche hermaphroditica* fruit, Second row (L-R) *Myripohyllum sibericum* leaf tip, *Myriophyllum spicatum* leaf tip cluster, *Ceratophyllum demersum* leaf tip, Third row (L-R): *Potamogeton* sp. 3 leaf tip (unknown hydbrid found only at SLNG05), *Potamogeton compressus* leaf tip.

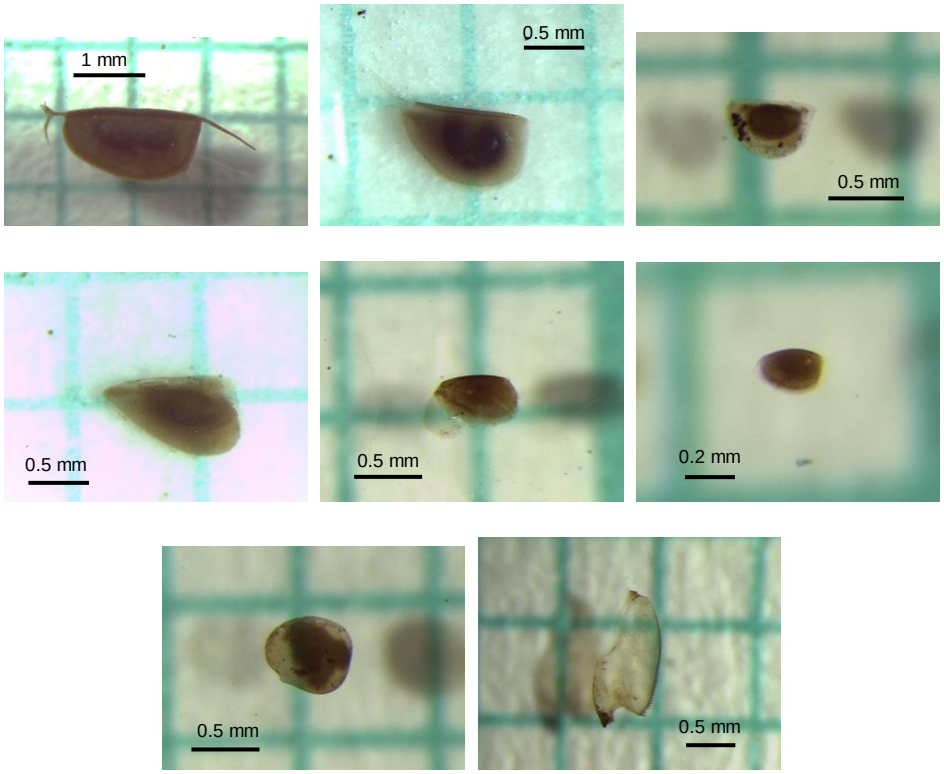

Appendix 3b. Common fossil zooplankton remains from Selenga River basin shallow lakes. Top row (L-R): Ephippial remains of *Daphnia magna*, *Daphnia pulex*, *Ceriodaphnia* sp., Second row (L-R): Ephippial remains of *Simocephalus* sp., *Alona affinis*, *Alona salina*, Third row (L-R): Chitinous remains of Chydoridae: carapace, post-abdomen.

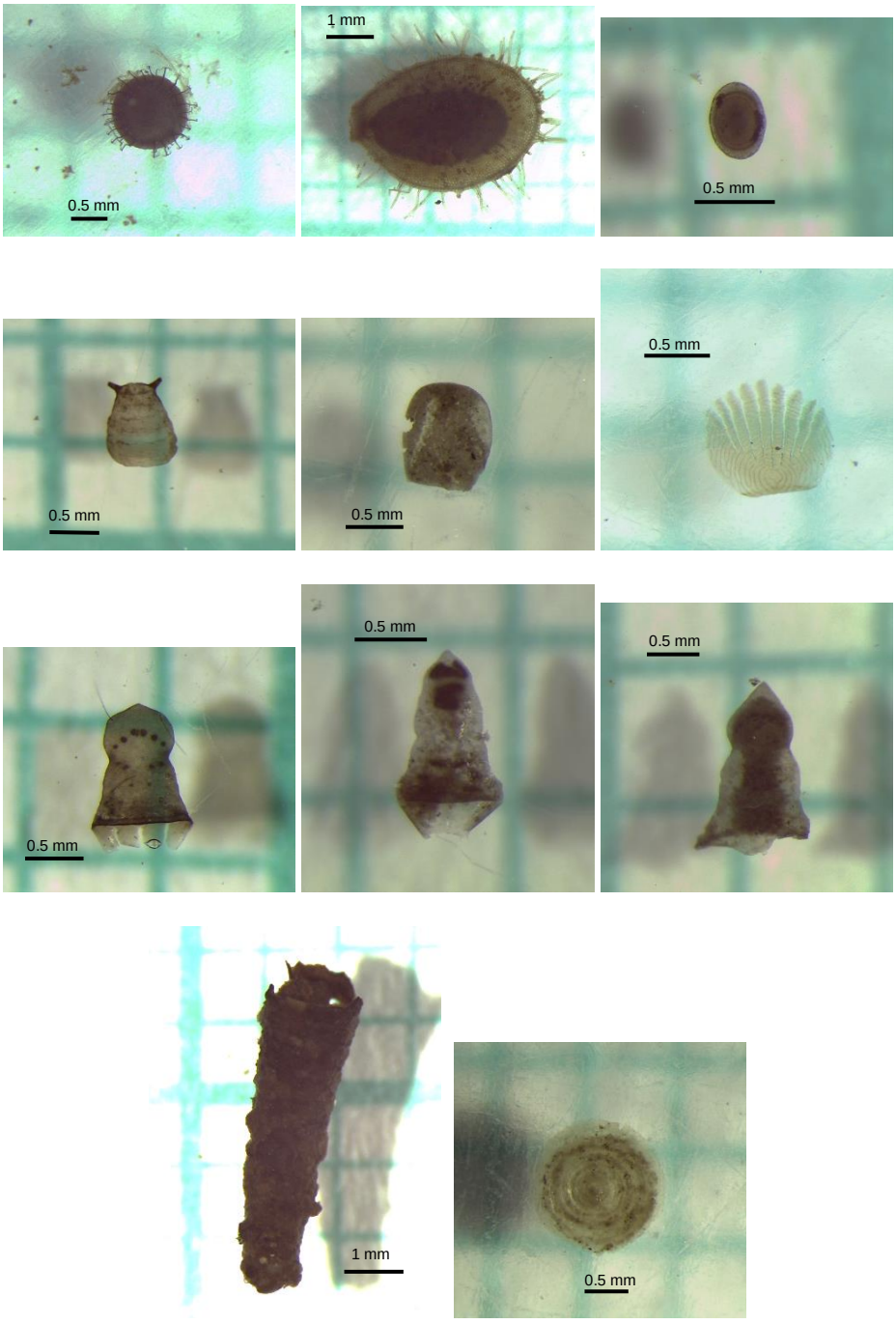

Appendix 3c. Common fossil invertebrate and fish remains from Selenga River basin shallow lakes. Top row (L-R): *Cristatella mucedo* statoblast, Unknown statoblast sp. 1, *Plumatella* sp. statoblast, Second row (L-R) Unidentified larval abdominal remain of Diptera sp., Ephemeroptera wing bud, Percid fish scale, Third row (L-R): larval frontoclypeal apotomes of *Cyrnus trimaculatus*, *Athripsodes* cf. *aterrimus, Phrangea* cf. *cipunctata*, Fourth row (L-R): larval case of Trichoptera, larval case lid of Trichoptera.

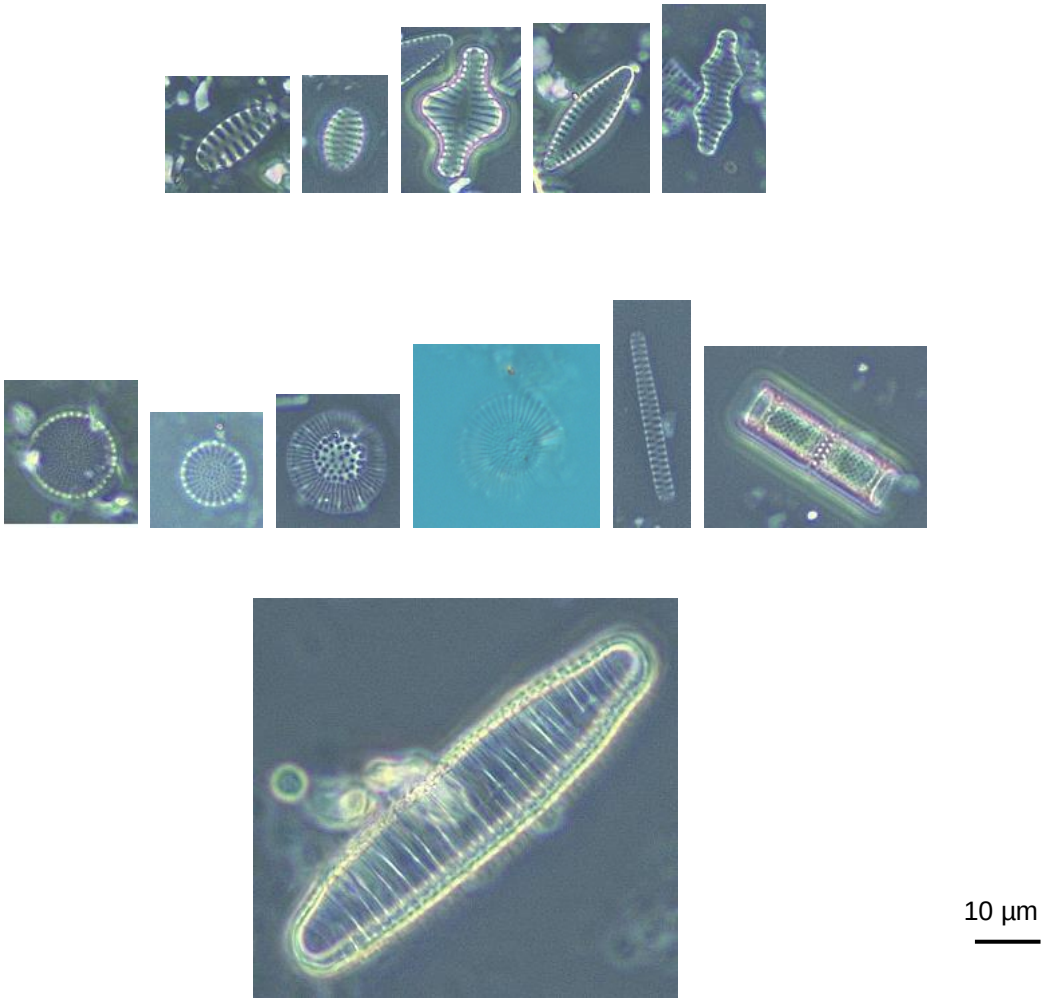

Appendix 4a. Magnification is 1000x. Common diatom species from Selenga River basin shallow lakes. Top row (L-R): Small benthic fragilarioids: *Staurosirella pinnata*, *Staurosira construens* v. *venter*, *Pseudostaurosira pseudoconstruens*, *Pseudostaurosira brevistriata*, and *Staurosira construens* v. *binodis*, Second row (L-R): Planktonics: *Stephanodiscus hantzschii*, *Stephanodiscus parvus*, *Lindavia praetermissa*, *cyclostephanos invisitatus*, *Fragilaria berolinensis*, *Aulacoseria ambigua*, Third row: Planktonic: *Diatoma vulgaris*.

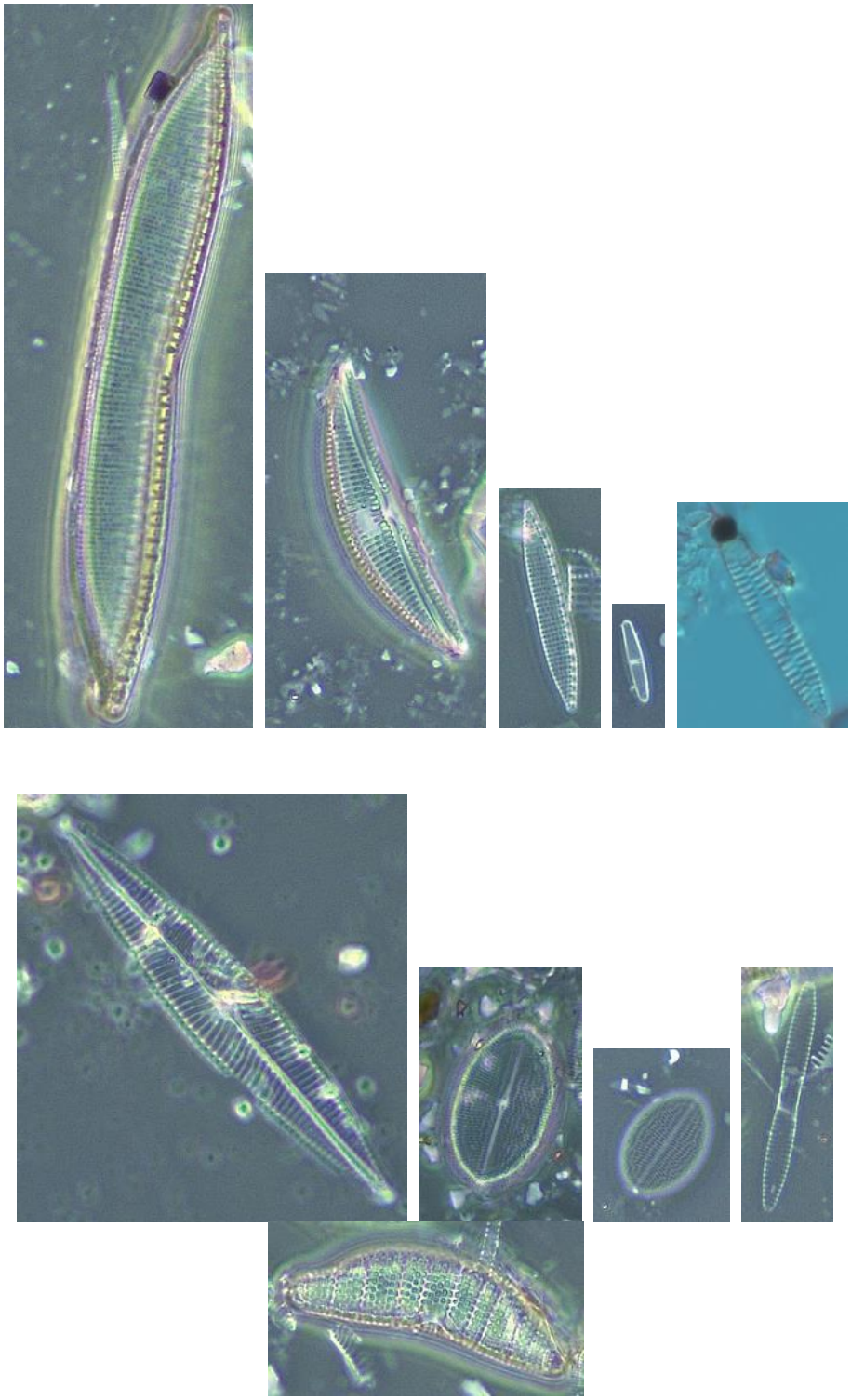

Appendix 4b. Magnification is 1000x. Common diatom species from Selenga River basin shallow lakes. Top row (L-R): Aerophilous *Hantzschia amphioxys*, Benthics: *Amphora copulata*, *Nitzschia amphiba*, *Achnanthidium minutissimum*, *Fragilaria capucina* v. *vaucheriae*, Second row (L-R): Benthic: *Navicula radiosa*, Epiphytics: *Cocconeis placentual* v. *euglypta* valve 1, *Cocconeis placentula* v. *euglypta* valve 2, *Fragilaria mesolepta*, *Epithemia adnate.*

Full Macrofossil Name	Macrofossil Code
Ceratophyllum demersum	CDEM
Myriophyllum sibericum	MSIB
Myriophyllum spicatum	MSPIC
Elodea canadensis	ECAN
Potamogeton pusillus	PPUS
Potamogeton berchtoldii	PBER
Utricularia vulgaris	UVUL
Lemna trisulca	LTRIS
Potamogeton perfoliatus	PPER
Callitriche hermaphroditica	CHERM
Potamogeton friesii	PFRI
Potamogeton crispus	PCRIS
Potamogeton pectinatus	PPECT
Potamogeton compressus	PCOM
Potamogeton sp. 3	PPOTSP3
Ephemeroptera wing bud	E. wing bud
Ephemeroptera abdominal gill	E. gill
Lemna Minor	LMIN

Appendix 5. Macrofossil names and corresponding codes used throughout the thesis.

Diatom Species	Diatom Code
Achnanthes cleveii	ACHCLE
Achnanthes conspicua	ACHCON
Achnanthidium lanceolata	ACHLAN
Achnanthidium minutissimum	ACHMIN
Amphora copulata	AMPCOP
Amphora montanii	AMPMON
Amphora pediculus	AMPPED
Aulacoseria ambigua	AULAMB
Aulacoseira alpigena	AULALP
Cocconeis placentua v. euglypta	COCEUG
Cyclotella meneghiniana	CYCMEN
Cyclotella pseudostelligera	CYCPSE
Cyclostephanos dubius	CYCDUB
Cyclostephanos invisitatus	CYCINV
Diatoma vulgaris	DIAVUL
Encyonema silesiacum	ENCSIL
Epithemia adnata	EPIADN
Epithemia sorex	EPISOR
Epithemia turgida	EPITUR
Eunotia bilunaris	EUNBIL
Fragilaria berolinensis	FRABER
Fragilaria bicapitata	FRABIC
Fragilaria capucina v. vauchariae	FRAVAU
Fragilaria mesolepta	FRAMES
Gomphonema angustum	GOMANG
Gomphonena parvulum	GOMPAR
Hantzschia amphioxys	HANAMP
Lindavia praetermissa	LINPRA
Navicula ignota	NAVIGN
Navicula menisculus	NAVMEN
Navicula cf. modica	NAVMOD
Navicula oblonga	NAVOBL
Navicula radiosa	NAVRAD
Navicula seibigiana	NAVSIE
Navicula seminulum	NAVSEM
Navicula trophicatrix	NAVTRO
Nitzschia amphibia	NITAMP
Nitzschia perminuta	NITPER
Nitzschia liebertruthii	NITLIB
Pseudostaurosira pseudoconstruens	PSEPSE
Pseudostaurosira brevistriata	PSEBRE
Reimeria sinuata	REISIN
Rhoicosphenia abbreviata	RHIABB
Rhopolodia gibba	RHOGIB
Sellaphora pupula	SELPUP
Staurosira construens	STACON
Staurosira construens v. venter	STAVEN
Staurosira construens f. binodis	STABIN
Staurosira elliptica	STAELL
Staurosirella pinnata	STAPIN
Staurosirella pinnata v. intercedens	STAINT
Staurosirella leptostauron	STALEP
Stephanodiscus hantzschii	STEHAN
Stephanodiscus parvus	STEPAR

Appendix 6. Diatom species names and corresponding codes used throughut the thesis.